Tectonic Evolution of the Marlborough Region, South Island, New Zealand

A thesis
submitted in fulfilment
of the requirements for the Degree
of
Doctor of Philosophy in Earth Sciences
at
The University of Waikato

by

Ming-Hung Kao

The University of Waikato

1998

Abstract

The tectonic evolution of the Marlborough region has been studied by application of fission track thermochronology and finite element (FE) methods. The region lying within the Australian-Pacific plate boundary zone is considered to have a transcurrent fault system, known as the Marlborough Faults System (MFS). The MFS is viewed as comprising secondary transforms connecting the Hikurangi subduction margin with the main Alpine Fault oblique-slip boundary. This fault system appears to have developed sequentially towards the southeast during the past 5 million years. Consequently, the subducted Pacific plate has extended beneath the region.

The FE modelling results reveal that the accommodation percentage of total displacements in Marlborough is about 85% of the total plate motion. The instantaneous displacements of the Marlborough faults show successively increase to the southeast away from the Wairau Fault. The contour of instantaneous displacements estimated by the FE modelling can be compared to the topography of Marlborough. According to the results of the FE modelling cases, the main conclusions drawn are: (1) A curved fault (the Alpine Fault) resulted from a change in the plate motion vector and is a manifestation of dextral tectonic rotation. (2) The development of the MFS reflects the continuation of tectonic rotations. (3) Three secondary faults (Awatere, Clarence, and Hope) may have developed within a short period of one another. This suggests that the change in plate motion has impacted in Marlborough. (4) Uplift movements of the Spenser Mountains and Kaikoura Ranges still continue. (5) Suggate's model (1979) of a pre-existing fault offset of the Alpine Fault is not a unique result in the FE modelling.

The extremely young fission track ages (<10 Ma) in the vicinity of the Alpine Fault bend and Seaward Kaikoura Range coincide with the recent rapid uplift/erosion in these areas. All the apatite ages are less than the corresponding depositional ages of the samples, which indicates that the host rocks in Marlborough have experienced exposure to elevated temperatures in the zone of partial annealing for apatite, some of them having been reset. Except for the samples in the Marlborough Sounds region, zircon fission track ages are older than 119 Ma, reflecting that the host rocks of the samples have not experienced temperatures in the zircon partial annealing zone since the mid Cretaceous. Apatite fission track ages and mean lengths indicate that there are two major cooling events: one occurring from the early Miocene (~20 Ma) and the other in the mid Cretaceous (~100 Ma). Modelled thermal

histories indicate that in the Wairau block the timing of the main Neogene uplift/erosion event is earlier (mid to late Miocene) than to the southeast in the Seaward Kaikoura Range (late Pliocene-Pleistocene). The greatest amount of cooling in Marlborough occurs along the Alpine Fault in the vicinity of the big bend, where rocks have cooled from temperatures above 240 ± 25°C (temperature at which fission tracks are reset in zircon). These samples derive from the Alpine Schist belt. Over wide parts of Marlborough the rocks now at the surface have cooled from lower levels of the apatite partial annealing zone (<110°C). Generally, the rocks have cooled from at least 50°C to surface temperatures (10-15°C).

The largest amount of rock uplift (~11.5 km) occurs in the area of the Alpine Fault bend. The amounts of rock uplift and denudation derived from the fission track parameters are in the range 0.7-11.5 km and 0.6-11.0 km, respectively. The amounts of rock uplift in the Inland and Seaward Kaikoura Ranges are about 2.4 and 4.8 km, respectively. The amount of denudation across Marlborough is generally higher in the Wairau block than elsewhere. In the Seaward Kaikoura Range, high elevation coincides with large amounts of denudation. Compared with the region of continent-continent convergence to the south in Canterbury, the amounts of rock uplift and denudation in Marlborough are relatively small, revealing the differences between a fully developed continent-continent collision zone and the continental transform setting in Marlborough.

The horizontal movements determined by the FE modelling can be converted into vertical movements. Both the FE modelling and fission track results show that the pattern of vertical deformation is consistent with the topography in Marlborough: the younger the fission track age, the more uplift/deformation there has been. The FE modelling and fission track results reveal the character of the tectonic evolution of Marlborough and are a step towards its quantification.

Acknowledgements

I would like to thank many people who have helped and encouraged me throughout the preparation of my D. Phil. thesis:

Primarily, my chief supervisor Associate Professor Peter Kamp for suggesting the Marlborough fission track project, and for the benefit of his guidance, advice, and discussion during the preparation of the thesis.

Secondly, Professor Campbell S. Nelson, as second supervisor, for his guidance and support during my study.

Special thanks to Frank Bailey in the Department of Earth Sciences for his kindness and all the help he gave me in integrating into the New Zealand setting.

The members of the Fission Track research group at the University of Waikato, Ian Whitehouse, H. B. Soenandar, Ganqing Xu, and Ivan Liddell for their support and suggestions in the field of fission track thermochronology.

Earth Sciences Department staff and graduate students, Assoc. Prof. Roger Briggs, Sydney Wright, Elaine Norton, Michael Vennard, Renat Radosinsky, Stephen Bergin, Laurence Gaylor, Bruce Parkinson, Tim Naish, Rob Lieffering, Tian Fenming, Joseph Mathew, and Steven Hood for their help and friendship.

My friends in Hamilton: Pat and Bob Sherson, Mary and Peter Gutmann, Mr. David Shin, Mr. Nan Zu, Mrs. and Mr. Liao, and Chih-Chieh Liou for their generosity and kindness.

My family in Taiwan: my parents, sisters, and brothers for their love and support when I studied in Taiwan and New Zealand.

Finally, my lovely wife, Ms. Ching-Lan Lin, for her love, understanding, and patience while I wrote the thesis.

Table of Contents

Chapter 1

Introduction

Chapter 1

Introduction

Fission track analysis is an innovative method for the investigation of the thermal and tectonic history of geological provinces. The aims of this study are to apply the fission track method and the finite element method to establish:

1. The amount of rock section eroded from the Marlborough region and its timing.
2. The uplift characteristics of the Marlborough region during the past 25 m.y., and especially the last 5 m.y.
3. The pattern of deformation in Marlborough modelled on rock mechanic principles and analyzed using finite element methods.
4. The evolution of the modern plate boundary in the Marlborough region.

1.1 Tectonic Setting

The Marlborough region, lying between the Alpine (Wairau) and Hope Faults, contains several dextral strike-slip to oblique faults (Figure 1.1). This region lies within the Australian-Pacific plate boundary zone at a critical position between the southern end of the Hikurangi margin (where the oceanic Pacific plate subducts beneath the continental Australia plate) and the Alpine Fault section (where the continental Pacific plate collides with continental Australia plate). The Marlborough faults have usually been explained as secondary transforms connecting the Hikurangi subduction margin with the main Alpine Fault oblique-slip boundary (Wellman, 1971; Christoffel, 1971). Stock and Molnar (1982) stated that a change in the direction of migration of the Australian-Pacific pole of rotation occurred about 9.8 Ma ago (at about anomaly 5). Scholz et al. (1973) concluded that the Awatere, Clarence and Hope transforms faults have developed successively to reflect a changing plate motion vector. Rynn and Scholz (1978) accepted the model of "a changing plate motion vector" and noted the abundance of seismic activity south of the Hope Fault. The subduction of the Pacific plate has probably propagated southwards during the Late Neogene, causing continuous activation of the Marlborough Faults (Carter and Carter, 1982). Several palaeomagnetic studies while documenting the occurrence of rotations of blocks between the faults also support this concept of successive propogation of faults during the

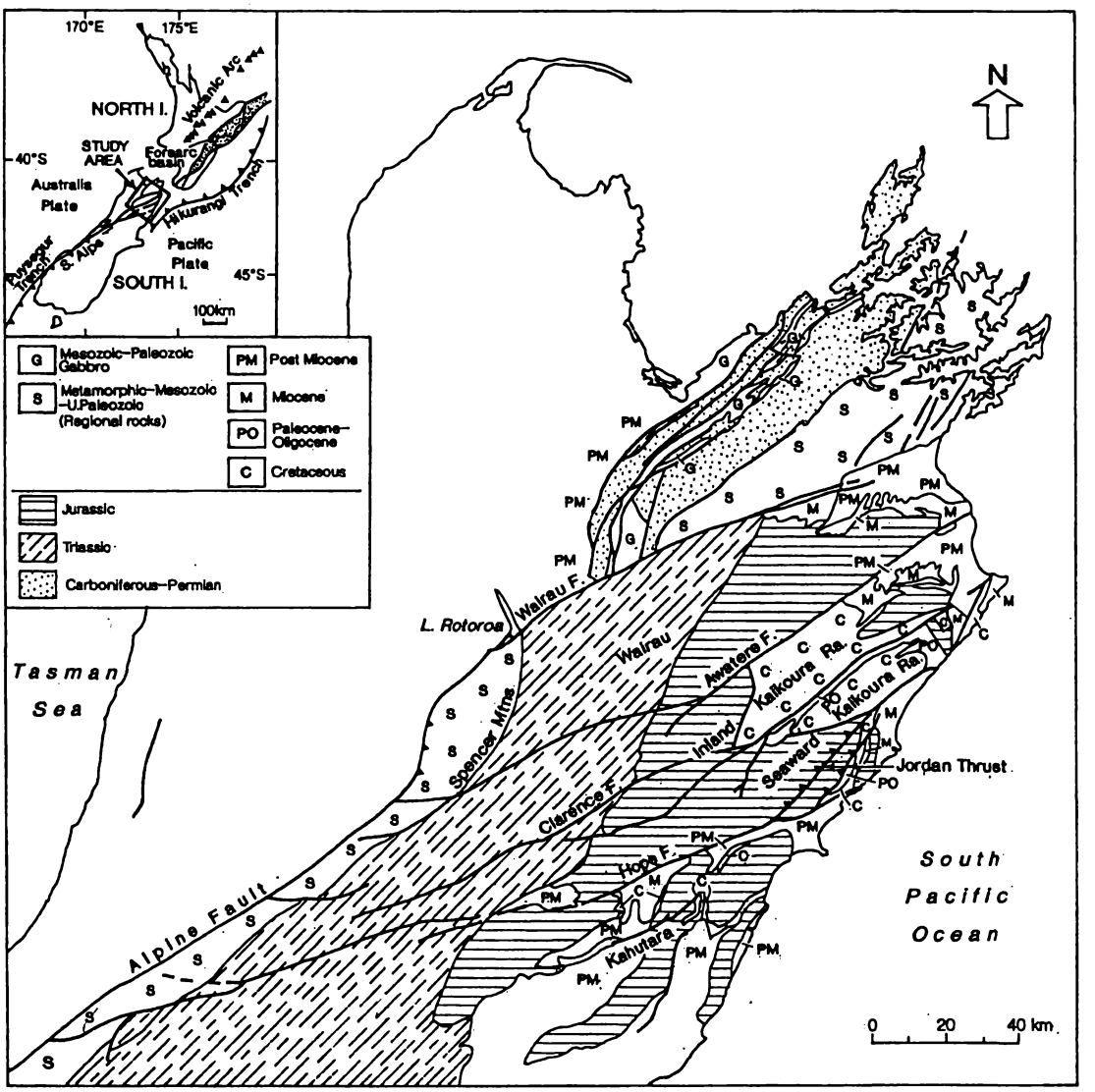

Figure 1.1 Tectonic and geological map of Marlborough, South Island, New Zealand.

Neogene (Walcott, 1978a; Lamb, 1988; Mumme et al., 1989; Roberts, 1992; Vickery and Lamb, 1995). They do not so much relate the rotations to changes in the Australia-Pacific pole positions, but to the kinematics of deformation between active strike-slip faults, and at the termination of these faults.

1.2 Geologic Setting

The Torlesse Supergroup constitutes the basement of the Marlborough region. Bradshaw et al. (1981) explained that the angular unconformity separating the Torlesse Supergroup from younger units, represents the stratigraphic expressions of the end of the early Cretaceous Rangitata Orogeny. These strata comprise sandstone, mudstone, conglomerate, rare chert, volcanic rocks, and limestone which are severely deformed. The age of basement rocks ranges from the Late Jurassic to Early Cretaceous (Pahau subterrane), with Triassic (Rakaia subterrane) successions in the far west. The Alpine Schist crops out adjacent to the Alpine Fault. Its exposure is a result partly of Cretaceous denudation (Suggate, 1978b) but mainly Neogene denudation, as is shown here. The depositional ages of cover strata range from Cretaceous to Quaternary. The stratigraphy of the Cretaceous section contains greywacke and argillite deformed in subduction prisms. These rocks are distributed in the Inland and Seaward Kaikoura Ranges (Figure 1.1). The Cretaceous/Tertiary boundary occurs between two lithostratigraphic units in the sedimentary cover: the Branch Sandstone and Mead Hill Formation. The Branch Sandstone represents a shallow marine environment; the Mead Hill Formation forms the basal unit of the Amuri Limestone (Laird, 1992). Early Cenozoic sequences accumulated during a tectonically quiet period when Marlborough was part of a passive margin environment. This was followed by the Kaikoura Orogeny, dating from the early Miocene, which reflects development of the modern Australia-Pacific plate boundary in the region (Browne, 1995).

In Marlborough, magmatism and extension occurred at about 100 Ma. After the initiation of extension and magmatism (~100 Ma), marine sedimentary sequences (greensands/limestone) accumulated and subsided through thermally controlled processes (Lensen, 1962). This tectonic quiescence lasted from 90 to 25 Ma (Baker and Seward, 1996). From the early Miocene onwards, crustal shortening and strike-slip faulting are considered to have become increasingly important in the Marlborough region (Carter and Norris, 1976; Suggate, 1978a; Baker and Seward, 1996).

1.3 Fission Track Analysis

Apatite and zircon fission track data provide not only information about numerical ages but also estimation of the paleotemperature history of host rocks. Fission tracks in U-bearing crystals such as apatite and zircon result from the spontaneous fission of ^{238}U, and can be applied to thermal and tectonic studies. The annealing of fission tracks is an important aspect of the fission track thermochronometer. Because of a kinetic understanding of annealing in apatite, thermal histories can be reconstructed from forward modelling of time-temperature histories and comparison of predicted and measured fission track ages and lengths. Different minerals have different "closure temperatures". "Closure temperature" is a concept that links the observed age to the temperature at which fission track age starts to accumulate (Dodson, 1973; Hodges, 1991). For example, the closure temperature for apatite ranges from 110°C to 125°C depending on apatite composition (Gleadow and Duddy, 1981; Green et al., 1989b); for zircon it is about 240 ± 25°C (Hurford, 1986). The closure temperature is dependent on the rate of cooling of rock successions, the faster the rate, the higher the closure temperature. Because of the annealing of fission tracks, the distribution of single-grain ages and track length distributions will indicate the thermal history of a specific sample. If the geothermal gradient and initial elevation of the land surface are known or assumed, a cooling history can be interpreted as an uplift-denudation history. Information about the amount, age and rate of rock uplift and denudation can then be developed for a sample host rock (Brown, 1990).

Fission track analysis has been used in many thermo-tectonic studies. Wagner and Reimer (1972) first applied fission track analysis to estimate uplift rates in the Central European Alps. Using this method, Naeser and McCulloh (1989) studied the depositional and thermal history of rocks in sedimentary basins; Gleadow et al. (1983) and Green et al. (1989a) applied several temperature-sensitive fission-track parameters to interpret the thermal history of the hydrocarbon-bearing Otway Basin in south-eastern Australia. Tippett and Kamp (1993) used reset and partial annealed fission track ages from the S. Alps, South Island, New Zealand and estimated the amount, timing, and rate (2-10 mm/yr) of rock uplift and denudation. Moore et al. (1986) studied the thermal evolution of the rifted continental margin in southeastern Australia by fission track analysis.

1.4 Finite Element Method

The finite element (FE) method is a numerical analysis technique for stress analysis and associated field problems. It has been used widely in mathematics, physics, rock mechanics, and other fields. For non-linear rock problems, the FE method is particularly powerful in the analysis of jointed rock structure. In this study, we assume that the Marlborough region is a single system; it is like a jointed rock and the faults can be assumed to be joints. The properties of the rock and joints are based on the laws of rock mechanics and experimental results. By these assumptions, the application of the FE method can improve our understanding of the tectonics of the Marlborough region.

The FE method is usually a step-by-step process. In a two-dimensional stress-deformation analysis, the FE method consists of the following eight steps (Desai, 1979):

Step 1. Discretize and select element configuration.
Step 2. Select approximation models or functions.
Step 3. Define strain (gradient)-displacement (unknown) and stress-strain (constitutive) relationships.
Step 4. Derive element equations.
Step 5. Assemble element equations to obtain global, or assemblage equations and introduce boundary conditions.
Step 6. Solve the primary unknowns.
Step 7. Solve for derived or secondary quantities.
Step 8. Interpretation of results.

These steps are followed in application of the FE method to analysis of the deformation patterns in Marlborough.

1.5 Thesis Format

This thesis consists of eight chapters, references, and data appendix. The eight chapters include:

Chapter 1. Introduction

Chapter 2. Principles of Fission Track Analysis

Chapter 3. Application of the Finite Element Method in Tectonics

Chapter 4. Geology and Deformation of the Marlborough Region

Chapter 5. FE Modelling Results

Chapter 6. Fission Track Results and their Interpretation

Chapter 7. Comparison between FE Modelling and Fission Track Results

Chapter 8. Summary

Chapter 2

Principles of Fission Track Analysis

Chapter 2

Principles of Fission Track Analysis

Fission track analysis is a very useful method in the study of the thermo-tectonic history of basement terranes and sedimentary basins. Fission track data can be applied as a dating technique, but its open-system behaviour also enable it to establish the thermal history of rock successions. Several parameters are used to assess the thermo-tectonic history of a specific region. These include mean fission track ages, the distribution of single grain ages, mean confined track length, and the distribution of confined fission tracks lengths within samples (Green et al., 1989a). Fission track analysis has been applied widely in thermal and tectonic studies. For example, Kamp et al. (1989) inferred the total amount of late Cenozoic uplift and erosion across the Southern Alps associated with continent-continent collision across the Alpine Fault, which was developed further by Tippett and Kamp (1993). In application to an extensional margin, Rohrman et al. (1994) explained the syn- and post-rift thermal evolution of the Oslo Rift of southeast Norway.

The principles, methodology, techniques, and application have been established in many papers, including Gleadow (1981), Green (1985), Green et al. (1986, 1989b), Laslett et al. (1987), Duddy et al. (1988), Hurford (1986), Kamp et al. (1989), Tagami et al. (1988), and Hasebe et al. (1992).

2.1 Origin of latent fission tracks

The Decay of heavy radioactive elements (e.q. ^{232}Th, ^{235}U, and ^{238}U) will cause heavy charged particles to pass through insulating materials and leave trails of radiation damage within them (Silk and Barnes, 1959; Price and Walker, 1962a). Price and Walker (1962b) discovered that the damage trails could become stable and enlarged by chemical etching until they could be observed under an ordinary optical microscope. Fleischer et al. (1965) defined that a latent track is a path of ionization-produced defects prevailed by vacancies and displaced atoms that reside in interstitial sites (Figure 2.1). The number of latent fission tracks (fossil tracks) in a uranium-bearing mineral depends on the mineral age and its uranium concentration. Because ^{235}U is less abundant than ^{238}U, $(^{235}U/^{238}U) \approx$

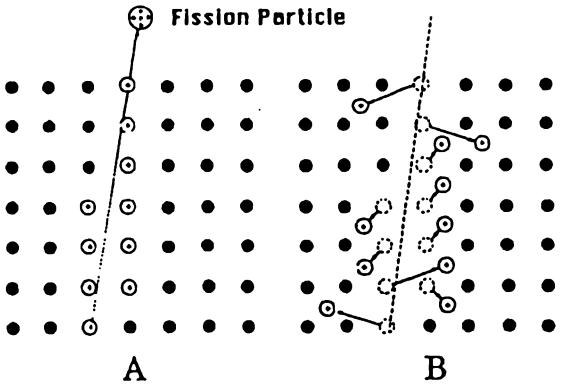

Figure 2.1 Ion explosion spike mechanism: track formation in a crystalline solid. In A the atoms are ionized by passage of a charged fission particle. In B, instability causes ions to eject into the lattice forming the fission track damage zone by mutual repulsion. From Naeser (1979), after Fleischer et al., (1965).

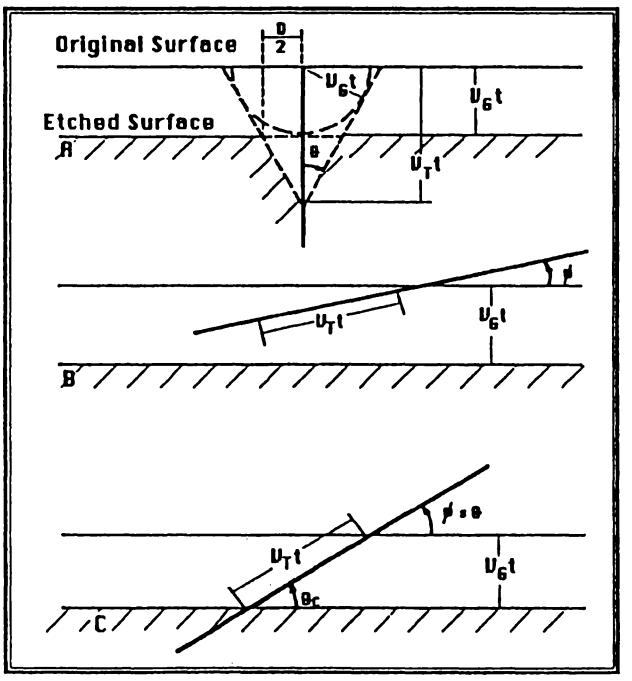

Figure 2.2 Track registration geometry: (A) track geometry is determined by the comparative rates of general attack V_G, and preferential attack, V_T along the track; (B) no track is registered if the angle of incidence is less than arcsin (V_G/ V_T), i.e. the general rate of etching is greater than the track etching rate; (C) arcsin (V_G/V_T) = θ and therefore the track just fails to be registered. Above this critical angle θ_c, tracks are able to be registered (from Fleischer et al., 1975). Note that t = etching time.

(1.3/137.8), latent fission tracks could be considered as resulting chiefly from the production of the spontaneous fission of ^{238}U.

2.2 Fission track etching

2.2.1 Etching principles

It is necessary to etch fossil tracks before they can be observed. The development of fission track etching depends on the rate of etching along the track, V_T; and the general etching rate of the surface, V_G. If V_T is much greater than V_G (i.e. $V_T >> V_G$) (Figure 2.2), the track will have an elongated shape (e.q. a cylindrical tube). When V_G and V_T are similar (but $V_T > V_G$), the track will reveal a shallow, conical etch pit. If V_T is smaller than V_G (i.e. $V_T < V_G$), the track will not be revealed (Fleischer and Price, 1963).

2.2.2 Etching conditions

In this study, 1M HNO (at 20 °C) was used to etch apatite crystals; the duration of etching was 25 seconds. A eutectic of KOH(62g)-NaOH(42g) were used to etch zircon crystals at about 200 °C - the etching time ranging from 3 to 50 hours.

2.2.3 Anisotropic etching

Fleischer et al. (1975) concluded that the general etching rate, V_G, is anisotropic for most crystals. The etching efficiency will still be high when the general etching rate is anisotropic (and $V_T >> V_G$, V_G is normal to the surface). The track cross-section will be dependent on variations in V_G in other directions. The anisotropy of V_G will decrease when the amounts of radiation damage from α-decay of U, and Th increase (Gleadow,1978). Usually, the higher etching shows that some crystallographic planes could have a much greater V_G normal to the surface and lower etching efficiency. The sharper the polishing scratches, the lower the bulk surface etching rate. Crystals exhibiting polishing scratches (<1.5 μm) could have the highest etching efficiency (~100%) (Gleadow, 1978,1981). These crystals are good for the determination of track density (dating) and the measurement of horizontally confined lengths.

2.3 Fission track dating

2.3.1 Identification of fission tracks

Differentiation between fission tracks and non-fission-tracks pits is very important in fission track dating. Fleischer and Price (1964) stated five key properties of etched fission tracks:

a. Etched fission tracks must be straight.
b. Etched fission tracks have a limited length;
   the maximum track length ranges between 10-20 μm.
c. Fission tracks should be randomly oriented,
   having no preferred relationship to a crystallographic direction.
d. Unetched fission tracks have limited thermal stability.
e. The distribution of spontaneous tracks should be statistically the same as
   that of induced tracks.

Fission tracks can be identified by these characteristics under microscopic observation.

2.3.2 Registration geometry

The spatial relationship between the track recording surface and the source of the tracks can be described by registration geometry. An internal surface where tracks are recorded from both sides has a 4π registration geometry; an external surface where tracks are recorded from one side only has 2π geometry. To adjust for the different registration efficiencies of the recording surfaces a correction factor must be applied to the ratio of track densities. In the external detector method, the geometry factor is 0.5; the population method's factor is 1 (Gleadow and Lovering, 1977; Green and Durrani, 1978).

2.3.3 Fission track age equation

The fission track age equation is similar to that for other radiometric dating techniques. The density of fission tracks in a random cut surface through apatite or zircon

depends on the uranium concentration of crystals, age and track length. When the thermal neutron fluence, spontaneous track density (ρ_s), and neutron-induced track density (ρ_i) are confirmed, a fission track age of a sample can be determined by the following age equation (Hurford and Green, 1983):

$$T = 1/\lambda_D \ln [1 + (\lambda_D \phi \sigma I G \sigma_s) / (\lambda_f \sigma_i)] \quad (2.1)$$

where

λ_D = total decay constant for ^{238}U; 1.55125 x10^{-10} yr^{-1} (Jaffrey et al., 1971).

λ_f = spontaneous fission decay constant of ^{238}U; two values: 7.03 x 10^{-17} or 8.42 x 10^{-17} (Spadavecchia and Hahn, 1967; Roberts et al., 1968).

I = isotopic ration ^{235}U / ^{238}U; 7.2527 x 10^{-3} (Conran and Adler, 1976).

ρ = thermal neutron cross-section for ^{235}U; 580.2 x 10^{-24} cm^2/atom (Hannah et al., 1969).

ϕ = thermal neutron fluence (neutrons cm^{-2}).

G = geometry factor (=1 for population dating method; 0.5 for external detector method).

ρ_s = spontaneous track density (tracks cm^{-2})

ρ_i = neutron-induced track density (tracks cm^{-2})

T = age in years

2.4 Dating methods

Several fission track dating methods were developed during the 1980s. The population method, external detector method (EDM) (Gleadow, 1981), re-etch methods (Fleischer et al., 1964b; Bigazzi, 1967; Welin et al., 1972), re-polish methods (Watanabe and Suzuki, 1969), and subtraction method (Wagner, 1966; Naeser et al., 1980) have often been applied in many studies (Huford and Green, 1982).

2.4.1 Procedures and techniques

In the determination of the fission track age, several dating procedures have been created and discussed in many publications (Fleischer et al, 1975; Naeser, 1979; Gleadow, 1981; Hurford and Green, 1982; Storzer and Wagner, 1982; Van den haute, 1986; Van den haute and Chambaudet, 1990).

2.4.2 Grain-population methods

The grain-population methods and grain-by-grain methods are widely applied in fission track geochronology. In grain-population methods, hundreds of grains (70-250 μm) are separated into two aliquots. The first one is used for the analysis of the spontaneous track density (ρ_s) and the second one for the analysis of the induced tracks density (ρ_i). The subtraction method and pre-irradiation annealing method are usually applied to obtain the spontaneous tracks density (ρ_s) and the induced tracks density (ρ_i). The subtraction method is used in the dating of glass shards (Wagner, 1966; Naeser et al, 1980). Grain-population methods can have highly reproducible results if samples are homogenous in uranium and show isotropically etched tracks (Van den haute and Chambaudet, 1990). It is not appropriate to apply grain-population methods for samples which show strong uranium heterogeneity or strong track etching anisotropy.

2.4.3 Grain-by-grain methods

In grain-by-grain methods, both the induced and the spontaneous tracks are analysed in the same grains. It is useful for grain-by-grain methods when a sample reveals strong uranium heterogeneity among grains or has grains of different age. The external detector method (EDM), re-etch method, and re-polish methods have been developed to determine the ρ_s / ρ_i ratio and fission track age. These methods are often applied in many studies (Hurford and Green, 1982). In the EDM, an external detector which is held in close contact with the grains mounted during irradiation is applied to measure the induced tracks. In this case, both the spontaneous and induced tracks are revealed and counted in different materials. For minerals with high α-radiation damage or grains with an inhomogeneous uranium

distribution, the ρ_s and ρ_I of these difficult samples can be measured by the EDM (Gleadow and Lovering, 1975). The EDM has been used to analyse all the data in this study.

2.5 Zeta calibration

The fission track age can be expressed by (Fleischer and Hart, 1972):

$$T = \zeta (\rho_s / \rho_i)\ \rho_d \qquad (2.2)$$

ρ_s = spontaneous track density (tracks/cm^2)

ρ_i = neutron-induced track density (tracks/cm^2)

ζ = a personal Zeta constant (year/cm^2)

A dating system based on the age standard approach was developed to overcome the dispute about the value of the decay constant for spontaneous fission within uranium (Fleischer and Hart, 1972; Fleischer et al, 1975). In the 1980s, this method was promoted by some geochronologists (Hurford and Green, 1982,1983).

The Zeta calibration system can be used to overcome the degree of uncertainty in the half- life for spontaneous fission of ^{238}U.

The Zeta calibration method includes two steps. At first, age standards are irradiated and analysed together with a standard glass (SRM, U, CN) for the purpose of establishing a calibration factor, ζ.

$$\zeta = [\, e^{\lambda d}\ T_{STD} - 1\ ]\ [\lambda_D (\rho_s / \rho_i)_{STD}\ \rho_d\ ] \qquad (2.3)$$

ρ_s = spontaneous track density (tracks/cm^2)

ρ_i = neutron-induced track density (tracks/cm^2)

ζ = a personal Zeta constant (year/cm^2)

After the ζ factor has been set up, the age of an unknown sample can be determined by the following equation:

$$T_{UN} = \ln [1 + \lambda_D \zeta (\rho_s / \rho_i) \rho_d] / \lambda_D \quad (2.4)$$

The ζ factor is not a constant, its value is personal. Based on a scale to SRM612, for apatite (age standards with SRM 612 glass), the ζ ranges from 310 to 360 for apatite; the overall weighted value is 381.8 ± 10.3 for zircon (Green, 1985; Tagami, 1987).

2.6 Statistical analysis

The counts of fission tracks is assumed to follow a Poisson distribution. The statistical analysis of the fission track dating by the EDM has been studied in many papers (Johnson et al., 1979; McGee and Johnson, 1979; Green, 1981a; Galbraith, 1981; Bardsley, 1983; Galbraith, 1984; and Galbraith and Laslett, 1985). For a Poisson distribution, the standard deviation SD of a track count can be defined by

$$SD = \sqrt{N} \quad (2.5)$$

where

SD is the standard deviation,
N is the total number of tracks counted.

The standard deviation of the fission track age can be determined by

$$SD_{FT} = T \sqrt{\frac{1}{N_s} + \frac{1}{N_i} + \frac{1}{N_d}} \quad (2.6)$$

where

T = the fission track age.

SD_{FT} = the standard deviation of the age,
N_s = the total number of tracks counted for spontaneous track densities.
N_i = the total number of tracks counted for induced track densities.
N_d = the total number of tracks counted for standard glass track densities.

It is possible that the distribution of fission tracks is actually non-poissonian. Galbraith (1981) stated that a χ^2 test can be used to detect whether a statistical analysis of fission track counts has Poisson statistics. If the fission track results pass the χ^2 test [the $p(\chi^2)$ value > 5%], then it is reasonable to assume that the fission track counts follow a Poisson distribution.

For the population method, the uncertainty will be underestimated when there is variation in uranium between grains. Errors calculated from the standard deviations of the actual grain counts are assumed to be normally distributed. The combined error can be calculated by (Gleadow, 1984):

$$SD_{FT} = T\sqrt{\left(\frac{M_{SD}}{m_s}\right)^2 + \left(\frac{M_{SD}}{m_i}\right)^2 + \frac{1}{N_d}} \qquad (2.7)$$

where

T = the fission track age.
M_{SD} = the standard error of the mean (i.e. $SD/\sqrt{N}$).
m_s = the mean count of spontaneous tracks.
m_i = the mean count of induced tracks.
N_d = the total number of tracks counted for standard glass track densities.

2.7 Fission track annealing

Price and Walker (1963) discovered the phenomena of track-fading and noticed that both the number and mean length of fission tracks were reduced by heating. The annealing of fission tracks is a valuable characteristic in geologic dating. Because of fission track annealing, thermal history can be reconstructed according to the information recorded in the

track lengths. In general, different minerals have different "closure temperature". For example, the temperature of totally annealed apatite fission tracks ranges from 105°C to 150°C (Naeser, 1981); the temperature of totally annealed zircon fission tracks lies around 240 ± 40°C (Hurford, 1986). In the following sections, the fission track annealing factors, processes, mechanism and thermal history models are discussed respectively.

2.7.1 Annealing factors

Fleischer et al. (1965) showed that track fading is essentially a function of temperature, with pressure, plastic deformation and highly ionizing radiation at upper crustal levels having little effect. It had been confirmed that a large dose of ionizing radiation has no effect on track annealing. Green et al. (1986) used confined fission track lengths to study the thermal annealing of induced fission tracks in a single fluorapatite crystal (Durango apatite). They concluded that the anisotropic characteristics of annealing, crystallographic orientation, chemical composition, and temperature are important factors in apatite fission track annealing. Clearly, the annealing process depends on temperature, chemical composition, and crystallographic orientation, and to a lesser extent.

a. Temperature

There is no doubt that temperature is the dominant control on fission-track annealing. Fleischer et al. (1965) studied track fading by using samples of tektite glass, zircon and olivine. They concluded that temperature is the most important factor in annealing. According to their experimental data, the relationship between temperature and time was a linear pattern in the Arrhenius plot. The influence of temperature has also been discussed in several other studies (e.g. Storzer and Wagner, 1969; Fleischer and Hart, 1972). Gleadow and Duddy (1981) showed that the temperature of apatite fission track annealing is significant between ~70° C and 125° C. Duddy et al. (1988) made use of the equivalent-time principle to study the variable temperature behaviour of fission track annealing. The fact that temperature is more influential than time is additionally described in their conclusions.

b. Chemical composition

Fission track annealing also depends on chemical composition. For example, fission tracks of Cl-apatite are more resistant to annealing than F-apatite (Green et al., 1985). The annealing rate of Cl-rich apatite is slower than F-rich apatite. Green et al. (1986) also suggested that fission- track annealing of a single apatite crystal is strongly influenced by the

chemical composition of the crystal, the Cl/F ratio. Crowley et al. (1990) studied the annealing of fission-track damage in F-, OH-, Cl-, and Sr-apatite to examine the effects of apatite composition. According to their experimental data, the pattern of resistance to annealing is Cl-apatite > Sr-F-apatite = F-apatite ~ OH-apatite. Therefore, it is necessary to note for thermal history studies that apatites of different composition have different annealing rates.

c. Crystallographic orientation

Generally, fission tracks parallel to the **c** axis are more resistant to annealing than tracks perpendicular to it. The anisotropy of fission track annealing had been proved by some experimental studies (i.e. Green and Durrani, 1977; Green, 1981; Green et al., 1986; Donelick et al., 1990; Crowley et al., 1991). Green et al. (1986b) observed "unetchable gaps" in their annealing experiment and suggested that the existence of unetchable gaps delays the annealing process. They used the gap model to describe anisotropic annealing. Because of unetchable gaps lying at small angles to the **c** axis, fission tracks at low angles to the **c** axis take a longer time to anneal.

d. Pressure

Temperature and pressure are usually dominant factors controlling the behaviour of materials. The influence of pressure in fission track annealing was demonstrated by Fleischer et al. (1965). They studied the behaviour of fission-track annealing in different samples at 1 atm, 10 kb, 30 kb, 60 kb and in compression tests at 2 kb. According to their experimental results, they concluded that the annealing curves of zircon and olivine have not been effected by hydrostatic pressure greater than 80 kb. When the pressure lies between 10 kb and 80 kb, the annealing curves are not linear in an Arrhenius plot. In other words, if the average value of a pressure gradient was 0.3 kb/km (Gutenberg, 1959), then the pressure lying from 3 km to 24 km would influence the annealing process. Meanwhile, an environment having greater hydrostatic pressure (>80 kb), below 24 km, has no influence on annealing curves.

e. Plastic deformation

Fleischer et al. (1965) studied the effect of shear stress in annealing by using the three compression test in mica crystals. They described how hydrostatic pressure alone does not cause the fission track annealing to happen, but shear deformations are able to shorten or erase tracks.

2.7.2 Annealing process

a. Qualitative description

Although the phenomenon of fission track annealing is easy to observe, the annealing processes are still unknown. The quantitative and kinetic studies of fission track annealing processes are discussed in the next section. Green et al. (1986) used confined fission track lengths of a single fluorapatite crystal (Durango apatite) to study the annealing processes. They found that the annealing of fission tracks in apatite appears to be characterised by two processes. Firstly, the dominant process, small degree of annealing, leads to a progressive shrinking of the tracks from each end and a length distribution showing a length reduction ($l/l_0 \sim 0.65$; l, current mean length; l_0, initial mean length.). Meanwhile, tracks parallel to the **c** axis shorten more slowly than those perpendicular to it. Secondly, as annealing becomes more extreme ($l/l_0 < 0.65$), the tracks break up into discontinuous portions. Furthermore, the existence of unetchable gaps may delay the annealing process.

b. Quantitative analysis

There are many studies about the annealing process of apatite fission track in an empirical mathematical analysis. Using the track densities (or projected track lengths) of Durango apatite, Mark et al. (1973) presented the following equation to describe the annealing behaviour:

$$p / p_o = \exp [- a (T) t] \qquad (2.8)$$

where

$a (T) = a_o \exp (-E_0 / kt)$; p is the track density after annealing; p_o is the original track density; T is the annealing temperature in Kelvin scale; t is the annealing time; k is Boltzmann's constant; E_o is an activation energy; and a_o is a constant. Equation (2.8) was generalised to:

$$p (t) = \sum_{j=1}^{n} p_j \exp (- a_j) \qquad (2.9)$$

Dakowski et al. (1974) showed another experimental formula for thermal fading of fission track in minerals and glasses:

$$\ln (t) - \ln (t_o) = (T^{-1} - T_o^{-1}) (a r^2 + b r + g) \qquad (2.10)$$

in which

$r = p/p_o$; a, b, and g are constants; and $\{ \ln (t_o), T_o \}$ is a point common to all track retention levels. For minerals, Equation (2.10) can be reduced to :

$$p (t) / p_o = a - b \ln (t) \qquad (2.11)$$

Afterwards, Burchart et al. (1979) made a comparison between Equation (2.11) and the following equation (Mantovani, 1974):

$$p (t) / p_o = a - b t \qquad (2.12)$$

They described that the statistical analysis of Equation (2.11) has the minimum mean squared deviation of data from the best fit straight line, but the others do not. However, Pellas and Perron (1984) studied the annealing of Durango apatite and concluded that the previous track formation models are not consistent with their experimental results.

In the experimental data of Fleischer et al. (1965), a linear relationship between the logarithm of annealing time and T^{-1} (the absolute temperature) was discovered. It is easy to assume the annealing process in this equation:

$$\ln (t) = A + B T^{-1} \qquad (2.13)$$

where A is a constant; and B is interpreted in terms of E/k, in which k is Boltzmann's constant and E is an activation energy. After investigating the published and experimental annealing data for apatite, Green et al. (1988) demonstrated that "fission track annealing cannot be described by first-order kinetics, and no convincing evidence to the contrary".

Analysing the laboratory annealing data of Green et al. (1986), Laslett et al. (1987) presented two mathematical models in order to describe the annealing process:

$$A(r) = \ln(t) - B\,T^{-1} \qquad \text{(Parallel Arrhenius Model)} \qquad (2.14)$$

$$\ln(t) = A(r) + B(r)\,T^{-1} \qquad \text{(Fanning Arrhenius Model)} \qquad (2.15)$$

where $r = l/l_0$ (l is tracks current mean length, l_0 is tracks initial mean length); T and t are the same as Equation (2.8); A(r) is an unknown function of r; and B is a constant. In their conclusion, both the parallel and fanning Arrhenius models can be used to construct the annealing process. In addition, the fanning model gives a better fit than the parallel model (98.0% to 96.7%).

2.7.3 Annealing mechanism and kinetics

Carlson's model

Carlson (1990) made use of a kinetic model based upon an atomic-scale and predicted that apatite fission track annealing is a two-stage annealing process. This kinetic model provides not only a physical explanation but also physical mechanisms. In his article, the two-stage annealing process includes: (1) axial shortening and (2) segmentation of tracks. The kinetics of the axial shortening depends on three parameters (n, Q, and A): n, a number which describes the shape of the initial radial defect distribution; Q, the activation energy for the atomic motions required to eliminate defects; and A, a rate constant which incorporates factors for the geometry of a conical track tip and for the defect density at the radial centre of the disrupted. The kinetics of the segmentation mechanism is determined by a single additional parameter that quantifies, as a function of the mean track length, the fraction of the total number of tracks that have been segmented.

However, Crowley (1993) presented a discussion paper to show that Carlson's model is not a defensible kinetic description of annealing. His reasons are: (1) the annealing mechanism is physically invalid; (2) the model does not provide adequate fits to laboratory data as previously published empirical models; and (3) the model does not provide reasonable predictions when extrapolated outside the range of the data. He concluded that Calson's model is based on the zero-order kinetics of topotactic transformations, and such kinetics do not apply to defect elimination. At the same time, he suggested that an empirical model should provide a good fit experimental data and be based on correct kinetic processes.

Corrigan (1993) used observed fission track data of Oligocene strata to test annealing models and concluded that the models of fission track annealing published lately predict significantly different mean track length vs. present temperature profiles of thermal histories. Meanwhile, he suggested that Carlson's model using an initial mean length of 15.8 μm instead of 16.6 μm, or the Crowley et al. model (1991) for track-length reduction down to ~11 μm can provide the best estimates.

2.7.4 Thermal history models

Generally, there are three models in the modelling of apatite thermal history: (1) the empirical model, (2) the forward model, and (3) the inverse model.

a. Empirical model

The Otway Group, deposited across 1000 km in Southern Australia during the early Cretaceous, consists of three main depositional areas: Otway, Gippsland, and Bass basins. Gleadow and Duddy (1981) described that the fission-track ages of sphene, zircon, and apatite in the outcrop section of the Otway Group were consistent and concluded that the outcrop section had a low-temperature thermal history environment below 70° C. The five fission track parameters (i.e. fission track age, variation of apparent fission track age with depth, distribution of single grain ages, variation of mean confined track length with depth, and distribution of confined fission track lengths.) observed from the Otway wells show that the temperature (depth) significantly depends on these parameters. In short, the data of the Otway wells are able to interpret paleotemperature not only in the Otway basin but also in other basins. However, the analysis of the Otway samples ignores the apatite composition. It should be noted that unknown samples need to have a similar spread of Cl-apatite when they are compared with those of the Otway Basin. Using the data of the Otway wells, Dumitru (1988) as well as Kamp et al. (1989) determined the thermal histories of rock sequences in the Great Valley forearc basin (in U. S. A.) and the Triassic sandstone and schist underlying the Southern Alps (in New Zealand).

b. Forward model

Green's model

According to the annealing data for Durango apatite, Green et al. (1989b) developed a forward model to predict fission track length, fission track age, and fission track distribution

from a given thermal history. Because of the annealing of fission tracks, the distribution of current fission tracks can reflect the thermal history. Therefore, the response of the Apatite Fission Track Analysis (AFTA) system is able to be simulated by a specific thermal history (Green, 1989b). Making use of the variable-temperature annealing description, given by Duddy et al. (1988), they predicted the final length of fission tracks formed during each time interval. Summation of the final lengths can also produce the net distribution of track lengths. Besides, they used the relationship for mono-composition apatite (Green, 1988), supposing that ages are normalized to a mean length of 15.5 μm, as observed in the age standards used, to calibrate the apatite fission track dating system (Green, 1985; Gleadow et al., 1986a). Testing this model by different geological data, fission track data from the Otway wells, Gleadow et al. (1986a) and Green et al. (1989b) stated that their model had made an agreement between the predicted and observed data. Corrigan (1991), however, argued that "forward modelling is unable to directly address the effect of data uncertainty on thermal history; and the nonuniqueness of thermal histories compatible with a given set of data can not be addressed (except by trial and error) with forward models".

c. Inverse model

(1) Lutz's model

Being different from the forward method, the inverse method uses fission track data to estimate thermal histories. Lutz and Omar (1991) applied an iterative approach to systematically modify a starting thermal history to achieve satisfactory statistical agreement between the predicted and observed fission track age and track length distribution. They defined an objective function, G (referring to their Appendix B):

$$G = g(\Delta FTA) + h(\Delta FTLD) \tag{2.16}$$

where

g(ΔFTA) is a function which predicts the difference between the measured and predicted fission track distribution and h(ΔFTLD) is a function predicting the difference between the measured and predicted fission track length distribution. The purpose of the inverse method is to reduce the value of G to establish possible thermal histories.

(2) Corrigan's model

Corrigan (1991) made use of a stochastic inversion technique, simulated annealing, to study the inversion of apatite fission track data for thermal history information. Simulated annealing, a hybrid Monte Carlo optimisation procedure (Kirkpatrick et al., 1983), has the ability to climb out of local minima in search of a global minimum state. He concluded that his approach allows determination of the range of thermal histories compatible with an observed confined track length distribution and associated fission track age, and it provides an estimate of the probability distribution of temperatures at a specific time. Using three synthetic data sets, generated from the forward model, Corrigan explained the inversion method and the thermal history information that can be recovered from apatite fission track data for various types of thermal histories.

2.7.5 Lengths of annealed fission tracks

Two approaches have been used in the measurement of the annealed fission tracks (Figure 2.3):

(1) To measure intersecting tracks exposed in an internal surface of a crystal:

(a) measurement of 'projected semi-track length' (Wagner and Storzer, 1972; Wagner, 1988; Wagner et al., 1989a; Dokowski, 1978); (b) measurement of 'semi-track length' (Bhandri et al., 1971; Dakowski, 1978).

(2) To measure confined tracks within the crystal, via another track ('Track In Track' or 'TINT') or via a fracture or cleavage ('Track In CLEage') or 'TINCLE': (a) measurement of dipping and horizontal tracks ('confined track length') (Lal et al., 1969; Bhandri et al., 1971); (b) measurement of only horizontal confined tracks ('horizontally confined track length') (Gleadow et al., 1983; Gleadow et al., 1986a, 1986b; Donelick, 1991; Green et al., 1986, 1989).

In this thesis all the track length measurements were of horizontally confined track lengths.

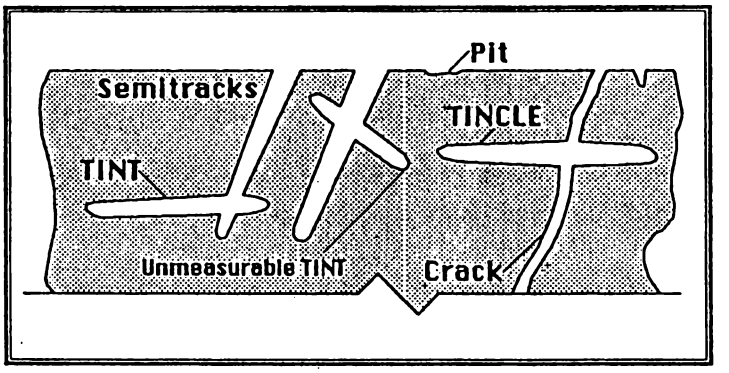

Figure 2.3 Fission track lengths: Schematic representation of a cross-section through the crystallographic c-axis showing measurable and unmeasurable confined tracks, and semi-tracks (modified from Lal et al., 1969).

2.8 Correction of track annealing

Due to natural annealing the fossils tracks in minerals and glasses are generally shorter in size than the induced fission tracks (Maurette et al., 1964; Fleischer et al., 1964a; Bigazzi, 1967). Maurette et al. (1964) and Berzina et al. (1967) found that annealing affects not only the track length but also the track density. Storzer and Wagner (1969) first achieved the use of length measurements for the correction of thermally lowered fission track ages caused by annealing. There are two techniques in the correction of track annealing: one is the track-size correction technique, the other is the plateau technique.

2.8.1 Track-size correction technique

The original pre-annealing track density can be determined by applying the correlation between track density and size reduction because of annealing. The correlation curves are called correction curves (Storzer and Wagner, 1969). The curves have been widely applied in the apatite fission track dating (Green, 1988; Mark et al., 1973; Nagpaul et al., 1974; Sharma et al., 1978; Wagner and Storzer, 1970, 1972; Watt and Durrani, 1985).

In the track-size correction technique, it is necessary to spend much time in determining the size measurements. Wagner and Storzer (1970, 1975) have used the track-size correction technique to apatite.

2.8.2 Plateau-correction technique

The plateau-correction technique has been studied in many papers (Storzer and Popeau, 1973; Burchart et al., 1975; Galazka and Burchart, 1976; Miller and Wagner, 1981; Westgate, 1989; Bigazzi et al., 1990). The fossil tracks usually have higher resistance against annealing than the freshly induced tracks. They can be annealed together by increasing temperature (isochronal plateau) or duration (isothermal plateau, Burchart et al., 1975) in the laboratory. The relationship of the annealing temperature and ratio of fossil to induced track densities plotted as a function of temperature (or time) shows a plateau value which means the annealing rates of fossil and induced tracks are equal. The partial track loss can be determined by the fission track age measured from the ratio within the plateau region. The plateau-correction technique has been applied in the apatite fission track dating (Storzer and Poupeau, 1973; Poupeau et al., 1980).

2.9 Application of fission track analysis in thermo-tectonic history

The application of the fission track data in the thermal-tectonic history has been discussed in many papers e.g. Gleadow et al., 1983; Green et al., 1989a; Kamp and Green, 1990; Tippett and Kamp, 1993; Kamp et al., 1996.

2.9.1 Closure temperature, cooling and uplift rates

In the fission track dating system, the temperature zone of partial track annealing (partial annealing zone, PAZ) is not easy to define, because it is known that tracks even at 20°C have a small degree of annealing. Generally, the low temperature end of the PAZ is taken as 60-70°C. The fission tracks usually begin to change their stability behaviour in this PAZ zone. The closure temperature (or effective retention temperature) is expressed as a discrete temperature threshold within the PAZ. At the closure temperature, the fission track system is theoretically closed and the fission tracks are considered to be retained (Wagner and Haute, 1992). Different minerals have different closure temperatures. "Closure temperature" is a concept that unites the observed age to the temperature at which fission track age starts to accumulate (Dodson 1973; Hodges, 1991). Several track-retention temperatures have been developed: 110 ± 20°C for apatite, 240 ± 50°C for zircon, 250 ± 40°C for sphene, (Naeser, 1979; Gleadow and Lovering, 1978; Gleadow and Duddy, 1981; Hammerschmidt et al., 1984; Harrison et al., 1979; Zaun and Wagner, 1985; Hurford, 1986). The closure temperature concept is useful where fossil partial annealing zones can not be reconstructed (against elevation) for a region. The cooling rates (R_c) can be defined as:

$$R_c = (T_m - T_{surface}) / t_m \qquad (2.17)$$

where

R_c = the cooling rates (°C/Ma).

T_m = the closure temperature (°C).

$T_{surface}$ = the ambient surface temperature (°C).

t_m = the fission track age (Ma).

If the regionally equal geothermal gradient (G) is assumed, the mean uplift rate (U_r) can be calculated by:

$$U_r = R_c / G \qquad (2.18)$$

where

U_r = the mean uplift rate (km/Ma).

R_c = the cooling rates (°C/Ma).

G = geothermal gradient (°C).

Koons (1987) stated that the assumption of the regionally equal geothermal gradient will fail if the uplift rate exceeds ~2 km/Ma.

2.9.2 Temperature-time paths and geologic environments

The variation of the horizontally confined fission track length distributions (Figure 2.4) reveal the different thermal histories (Gleadow et al., 1983, Gleadow et al., 1986a). Simple and progressive burial histories are shown in Figures 2.4A, 2.4B, and 2.4C. The confined fission track length distribution reflects heating through the partial annealing zone: the longer heating time the temperature-path has, the shorter confined track lengths the samples have. The bimodal distribution (Figure 2.4D) indicates that the sample experienced a component of heating within a partial annealing zone followed by an interval of residence at low temperature with minimum annealing. The skewed distribution (Figure 2.4E) shows that the temperature-time path has a slow cooling history through the annealing zone. A recent heating event will give samples a shortened length distribution (Figure 2.4F).

There are five fundamental shapes of the horizontally confined fission track length distributions as expressed by Gleadow et al. (1986a). The shapes can be divided into several geological environments:

	Mean Length (μm)	Standard Deviation (μm)

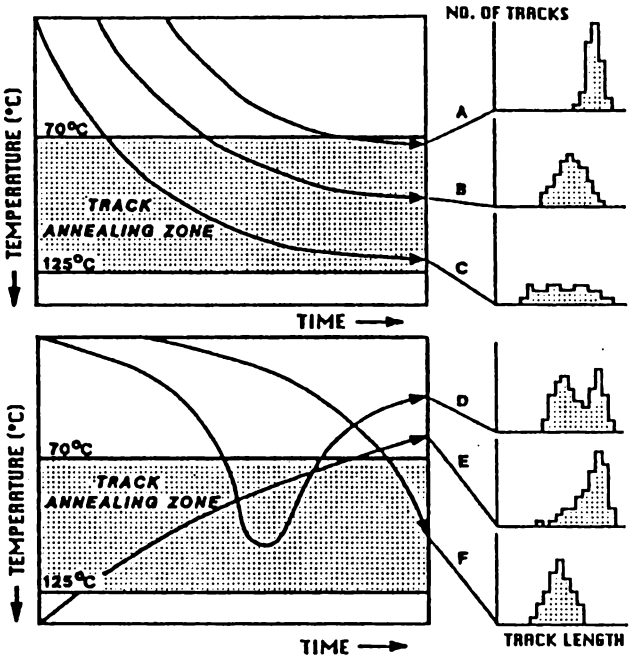

Figure 2.4 Temperature-time paths and the resulting apatite horizontally confined fission track length distributions for rocks of varying thermal history (from Gleadow et al., 1983).

Induced tracks	~16.3	0.9
Volcanic rocks	14.6 - 15	~1.0
Granitic basement terranes	~12 - 13	1.2 - 2
Bimodal tracks	5 - 15	>2
Mixed tracks	10.5 - 13.5	>1.3

Figure 2.5 shows the correlation between the mean track length and standard deviation for the five geological environments. The induced tracks have lower standard deviations, and the mixed/bimodal tracks have larger standard deviations.

2.9.3 Paleotemperature indicator

Apatite Fission Track Analysis is a useful tool for the study of thermal history analysis in sedimentary basins. Green et al. (1989b) stated five temperature-sensitive fission track parameters obtained in the Otway basin as the guide to the paleotemperature and thermal histories. The five temperature-sensitive parameters are: the fission track ages, variation of apparent fission track age with depth, distribution of single grain ages, variation of mean confined track length with depth, and distribution of confined fission track lengths:

(1) Fission track age: if the fission track age of a sample obtained in the Otway Basin is less than the stratigraphic age, then this evidence indicates that the sample has passed through or resided within the apatite partial annealing zone (70-125°C).

(2) Variation of apparent fission track age with depth (Figure 2.6a): the correlation of the fission track age profile with depth (temperature) shows that the samples have a simple thermal history. The fission track ages have no annealing effect in the plateau region (<70°C) and decrease gradually to zero below the plateau region (>70°C).

(3) Distribution of single grain ages (Figure 2.6b): the form of the distribution of single grain ages can reveal the temperature information for a sample. The peak of the smoothed function at the young age progressively falls toward the higher ages. In addition, the values of the $P(\chi^2)$ can be used to assess the probability that all grains are consistent with a single age (Galbraith, 1981). In the examples (Figure 2.6c), samples derived from

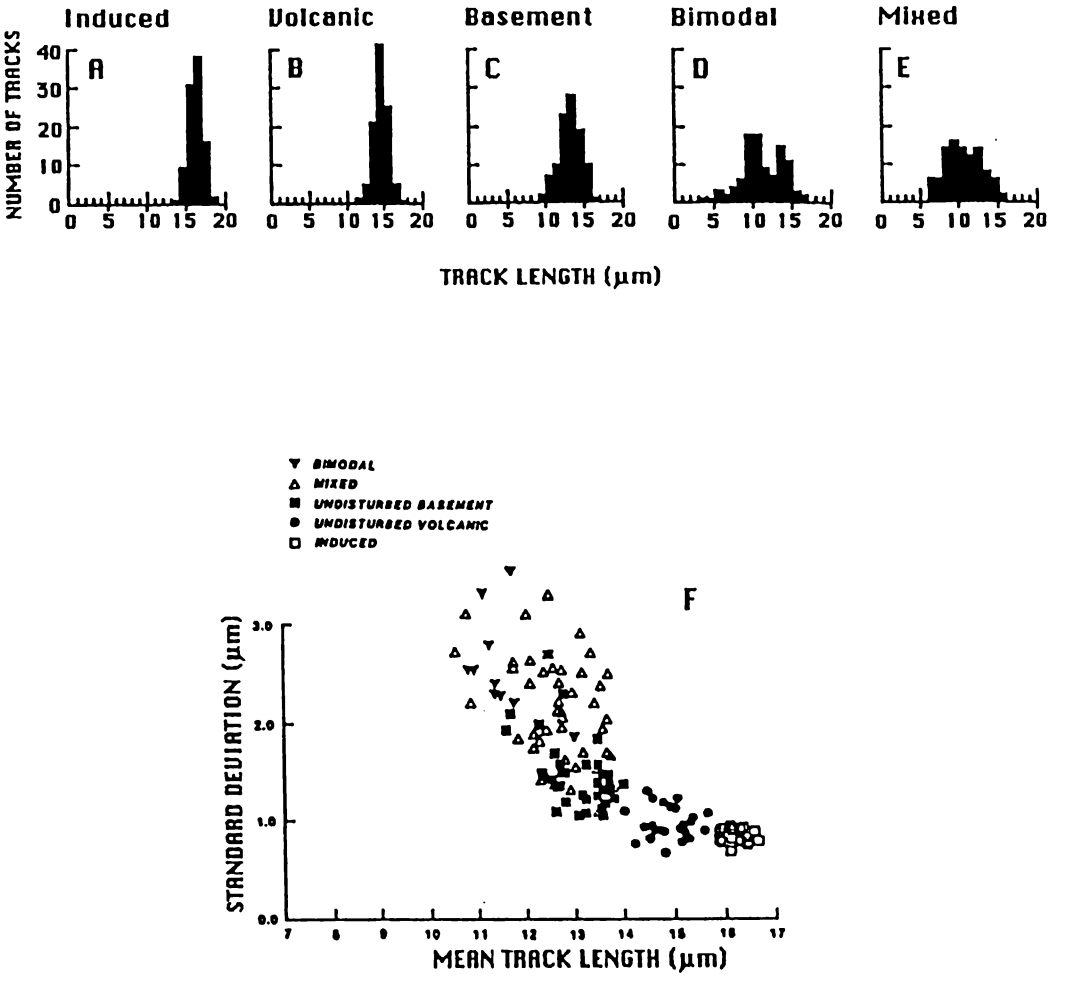

Figure 2.5 Fission track (horizontally confined) length data for characteristic geological environments (from Gleadow et al., 1986a).

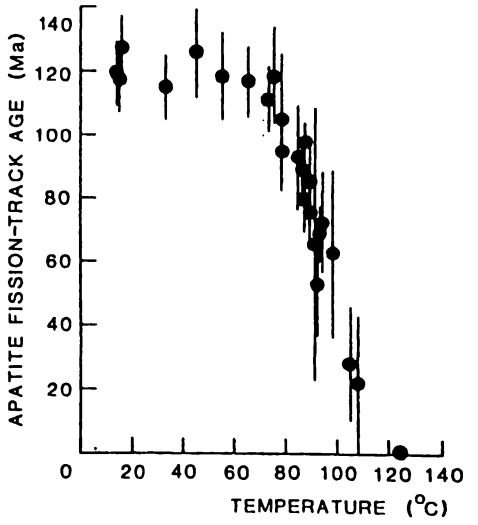

Figure 2.6a Variation of fission-track age of Otway Group samples with corrected present-day down-hole temperature in four Otway Basin wells. At the present time these samples are thought to be at their maximum temperatures. Error bars are shown at 2 sigma.

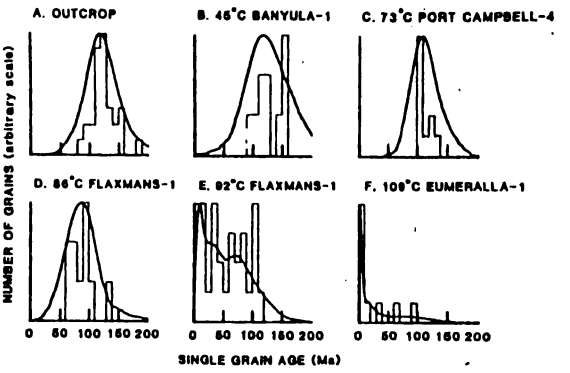

Figure 2.6b Distributions of single grain apatite ages from six Otway Group samples. The curve is the smoothed probability function obtained by the addition of Gaussian distributions representing each single grain age and its corresponding error. A, outcrop (composite); B, 45°C, Banyula-1; C, 73°C, Port Campbell-4; D, 86°C, Flaxman's-1; E, 92°C, Flaxman's-1; F, 109°C, Eumeralla-1. The distributions in E and F are characteristic of samples presently between 90° and 95°C and 105° and 110°C, respectively.

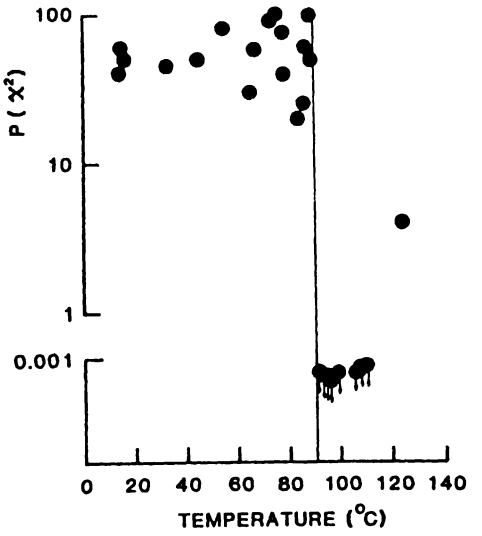

Figure 2.6c Variation of $P(\chi^2)$ (see text) with corrected present down-hole temperature in four Otway Basin wells. Below 90°C (which is indicated by the vertical line) all single grain ages agree with a single pooled age. Above this temperature the difference in annealing properties of individual apatite grains introduces a significant spread in ages, reflected in the extremely low values of $P(\chi^2)$, which are all less than 0.01%. At temperatures greater than 120°C, $P(\chi^2)$ rises again as an increasing proportion of grains are reduced to zero age.

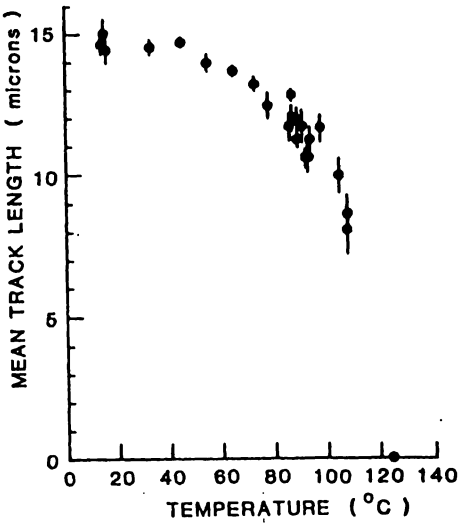

Figure 2.6d Variation of mean confined track length in Otway Group apatites with corrected present-day down-hole temperature. Error bars are shown at 2 sigma.

temperatures below 90°C, the values of the $P(\chi^2)$ are greater than 5%; at temperatures above 90°C, they are less than 5%.

(4) Variation of mean confined track length with depth (Figure 2.6d): The mean lengths of the samples at temperatures below 50°C are greater than 14 μm; at temperatures above 50°C they decrease steadily to zero at ~125°C. Therefore, the mean confined track length is a sensitive indicator of the paleotemperature.

(5) Distribution of confined fission track lengths: not only the mean confined track length but also the form of distribution of confined fission track lengths are sensitive to temperature. The distributions of the samples at temperatures below 50°C (Figure 2.6e) have narrow, symmetric forms. When the samples are above 50°C (the mean length < 13 μm), the distribution becomes broader. Moreover, the more annealed samples have larger standard deviations of the confined track length (Figure 2.6f).

The samples of the Otway Basin have experienced a simple thermal history and are near or at their maximum temperature. The patterns in the five fission tracks parameters obtained for the Otway Basin can be applied to other basins if the samples contain a similar spread of apatite compositions, and the basin has a similar (rift-passive margin) tectonic history.

2.10 Applications of fission track dating

Besides the applications in thermo-tectonic histories, fission track dating has been applied in other studies:

(a) Tephrochronlogy (Seward, 1974, 1975; Kohn, 1979).

(b) Post-Orogenic Uplift of Mountain Belts (Wagner and Reimer, 1972; White and Green, 1986; Kamp et al., 1989).

(c) Epeirogenic Uplift of Basements (Gleadow and Fitzgearld, 1987; Van den haute, 1986b).

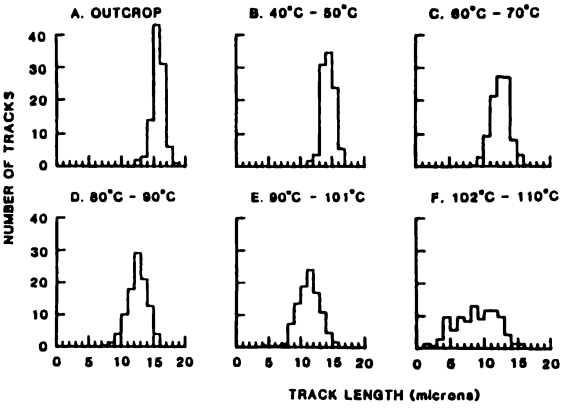

Figure 2.6e Distributions of confined fission-track lengths in Otway Group apatites. These are composite distributions (normalized to a total of 100 tracks) produced by summing results from samples in all four wells within the specified temperature limits. Within these limits all samples have essentially similar distributions. A, outcrop; B, 40° to 50°C; C, 60° to 70°C; D, 80° to 90°C; E, 90° to 101°C; F, 102° to 110°C. Both the mean track length and the form of the track length distribution are highly sensitive indicators of temperature. The flat distribution from lengths of 1 μm up to 16 μm shown in F is particularly diagnostic of temperatures in the range 102°C to 110°C.

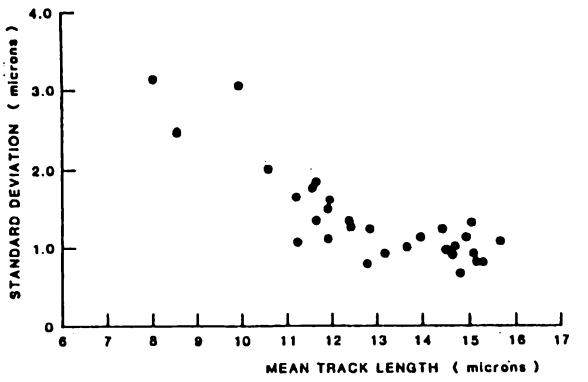

Figure 2.6f Relationship between standard deviation of the confined track length distribution and mean confined track length in Otway Group apatites from the four selected wells. The increase in standard deviation as mean length decreases emphasizes the increasing spread of lengths in more annealed samples as shown in Figure 2.6e.

(d) Age and Amount of Displacement along Faults (Zimmermann, 1980; Wagner et al., 1989b; Tagami et al., 1988).

(e) Meteoroid Impacts (Storzer and Wagner, 1977; Wagner, 1977).

(f) Sea-floor Spreading (Fleischer et al., 1968; Aumento, 1969; Storzer and Selo, 1976).

Chapter 3

Application of the Finite Element Method in Tectonics

Chapter 3

Application of the Finite Element Method in Tectonics

3.1 Introduction

The finite element (FE) method is a numerical technique for the analysis of stress fields. It has been applied in mathematics, physics, rock mechanics, and so on. For non-linear rock problems, the FE method is particularly powerful in the analysis of jointed rock structure. In this study, we assume that the Marlborough region is like a jointed rock and the faults are analogous to joints. The properties of rocks and joints are established by several laws of rock mechanics and experimental results. By these assumptions, the FE method may be applied to study the tectonics of this region.

3.2 Eight steps of the FE method

A natural system can usually be discretizing into smaller systems. A body is divided into a number of smaller regions, called finite elements (Turner et al., 1956; Clough, 1960). There are many parameters which influence a natural system. The FE method is used to discretize the system into small components/elements (finite elements). All the components are assembled by the laws of equilibrium and the physical condition of continuity at the junctions are enforced. The goals of the FE method are to unite the understanding about individual elements and to understand the wholeness or continuous nature of a system. The FE method is always a step-by-step process. Generally, the FE method consists of the following eight steps (Desai, 1979):

Step 1. Discretize and select element configuration

A body can be divided into many small bodies; these are called finite elements. The points where the sides of the elements intersect are called nodes or nodal points. For the Marlborough region, which is considered as a two-dimensional body, two types of elements (i.e. triangles and quadrilaterals) are used in the finite element configuration.

Step 2. Select approximation models or functions

In stress-deformation problems, the nodal points of the element are helpful for writing mathematical functions to express the shape of a distribution of the unknown quantity over the domain of the element. The polynomial interpolation function is usually the form of the mathematical functions. It can be defined as:

$$u = N_1u_1+N_2u_2+N_3u_3+ \ldots \ +N_mu_m \tag{3.1}$$

where

u is denoted as the unknown, the polynomial interpolation function;

$u_1, u_2, u_3, \ldots, u_m$ are the values of the unknowns at the nodal points;

$N_1, N_2, N_3, \ldots, N_m$ are the interpolation functions.

Step 3. Define strain (gradient) - displacement (unknown) and stress-strain (constitutive) Relationships

For the stress-deformation problems, the relationship of deformation and strain can be defined by:

$$\varepsilon_y = dv / dy \tag{3.2}$$

where

v is the deformation of the y direction; ε_y is the strain.

The relationship of stress and strain in a solid body can be defined by Hook's Law:

$$\sigma_y = E_y \varepsilon_y \tag{3.3}$$

where

σ_y is the stress in the vertical (y) direction; E_y is the Young's modulus of elasticity; ε_y is the strain.

Step 4. Derive element equations

The behaviour of the element is governed by equations set up by laws and principles. Generally, the equations are represented as

$$[\mathbf{k}]\{\mathbf{q}\}=\{\mathbf{Q}\} \tag{3.4}$$

where

$[\mathbf{k}]$ is the element property matrix, $\{\mathbf{q}\}$ is the vector of unknowns at the element nodes, and $\{\mathbf{Q}\}$ is the vector of element nodal forcing parameters.

Step 5. Assemble element equations to obtain global or assemblage equations and introduce boundary conditions

One of the finite element aims is to obtain equations for the entire body that define nearly the behaviour of the body. The vectors of all the elements in Step 4 can be added together in order to formulate the assemblage vector of nodal forcing parameters.

$$[\mathbf{K}]\{\mathbf{r}\}=\{\mathbf{R}\} \tag{3.5}$$

where

$[\mathbf{K}]$ is the assemblage property matrix; $\{\mathbf{r}\}$ is the assemblage vector of nodal unknowns; $\{\mathbf{R}\}$ is the assemblage vector of nodal forcing parameters. For the stress-deformation problems, $[\mathbf{K}]$ is the assemblage stiffness matrix, $\{\mathbf{r}\}$ is the nodal displacement vector, and $\{\mathbf{R}\}$ is the nodal load vector. The boundary conditions are expressed as the surroundings or the constraints. They will influence how the body will present.

Step 6. Solve the primary unknowns

Equation (3.5) is a set of linear (or non-linear) simultaneous algebraic equations, which can be written in the following form:

$$K_{11}\, r_1 + K_{12}\, r_2 + \ldots + K_{1n} r_n = R_1$$

$$K_{21}\, r_1 + K_{22}\, r_2 + \ldots + K_{2n} r_n = R_2$$

$$K_{n1} r_1 + K_{n2} r_2 + \ldots + K_{nn} r_n = R_n \qquad (3.6)$$

These equations can by solved by the Gaussian elimination or iterative methods. The primary unknowns (r_1 , r_2 , ... , r_n), the displacements, will finally be obtained.

Step 7. Solve for derived or secondary quantities

The primary quantities can be used to determine the secondary quantities by the stress-displacement and stress-strain relationships. The relationships of the strain, displacement, and stress in Step 3 can be used to find the secondary quantities.

Step 8. Interpretation of results

The final goal of the FE method is to interpret the results and to solve the modelling problem. If the interpretation of results is not consistent with the natural system, we probably need to adjust the input-data or change the assumptions in order to achieve better results for the interpretation.

3.3 Rock mechanics

3.3.1 Material properties

The properties of rocks and joints are listed in the following (Tables 3.1 and 3.2) (Goodman, 1976; Jumikis, 1983):

Table 3.1 Rock properties

Rock (High strength sandstone)

Linear, transversely isotropic solid. The rock elements may denote uniformly bedded or flat rock. The rock elements have no failure.

Properties

Uniaxial compressive strength σ_c	220	MN/m^2
Young's modulus of elasticity E	4.41 - 5.10	MN/m^2
Poisson's ratio υ	0.21 - 0.24	

Shear modulus $G = \dfrac{1}{2 \bullet (1+\upsilon)/E + (k_s \bullet h)^{-1}}$

Table 3.2 Joints properties

Properties		
Unconfined compressive strength q_u	49.0 - 98	MN/m^2
Joint shear stiffness k_s	500	
B_0 the ratio of the residual to peak strength at low normal stress		
V_{mc} the maximum amount a joint can close (positive)		
ζ the seating load for measuring (negative)		
ϕ_u the friction angle for a smooth joint		
I_0 the dilatancy angle at zero normal pressure		

*a. Asperities follow Fairhurst's failure criterion, composed of a parabolic envelope conformed to Mohr circles for the unconfined compression and tension tests (Fairhurst, 1964); b. Peak shear strength τ_p is given by Ladanyi and Archambault's equation with the transition pressure $\sigma_T = q_u$ of the wall rock; c. Dilatancy v and area of contact vary with normal pressure as given by Ladanyi and Archambault, with $\sigma_T = q_u$; d. Residual shear strength $\tau = B(\sigma)\,\tau_p$ where decreases linearly from B_o at $\sigma = 0$ to 1 at $\sigma = q_u$; e. The ratio of peak to residual displacement, M, measured in a test beginning from $\tau = 0$, equals 4; f. Dilatancy does not happen when the shear deformation goes beyond the residual value.

3.3.2 Triaxial testing of joints

Some results of triaxial tests on joints had been stated by Lane and Heck (1964), Handin and Stearns (1964), Raliegh and Paterson (1965), Byerlee (1967), Rosengren (1968), Heuze and Goodman (1967), Goodman and Ohnishi (1973), among others.

A specimen with a joint inclined at ψ with the long axis (Figure 3.1) has the following relationships,

$$\sigma = \sigma_3 + (\sigma_1 - \sigma_3)\sin^2\psi \qquad (3.7)$$

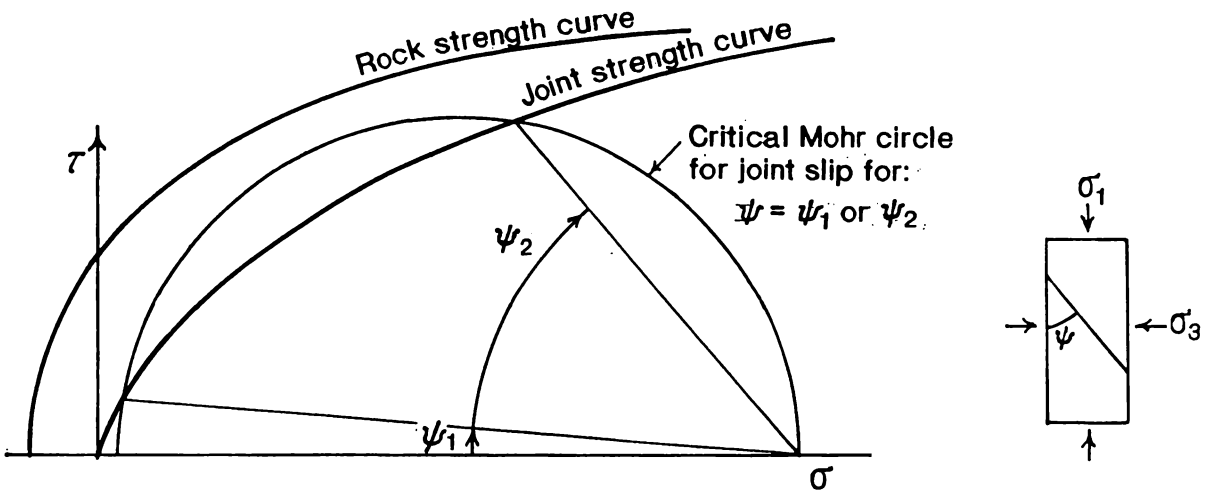

Figure 3.1 Mohr's Circle (from Goodman, 1976).

$$\tau = (\sigma_1 - \sigma_3) \sin \psi \cos \psi \qquad (3.8)$$

$$\tau = (\sigma - \sigma_3) \text{ cotan } \psi \qquad (3.9)$$

The relation between the residual shear strength and normal stress could be approximated by the Coulomb equation:

$$S = C_J + \sigma \tan (\phi_r) \qquad (3.10)$$

where

S = the residual shear strength.
C_J = the cohesion; for undisturbed jointed rock masses, it ranges from 20 to 30 kg/cm^2 or 280 - 420 psi.
σ = the normal stress.
ϕ_r = the residual friction angle.

3.4 Mechanical properties of discontinuities

3.4.1 Normal deformation of joints

The normal deformation in joints has two physical constraints. First, an open joint has no tensile strength. Secondly, a maximum possible closure, V_{mc}, must be less than the thickness of the joint. Based on these two conditions, a relationship between the normal deformation and the compression was set up by Goodman (1976),

$$\frac{\rho - \xi}{\xi} = A \left\{ \frac{\Delta v}{V_{mc} - \Delta v} \right\}^t \quad (\Delta v < V_{mc}) \qquad (3.11)$$

where

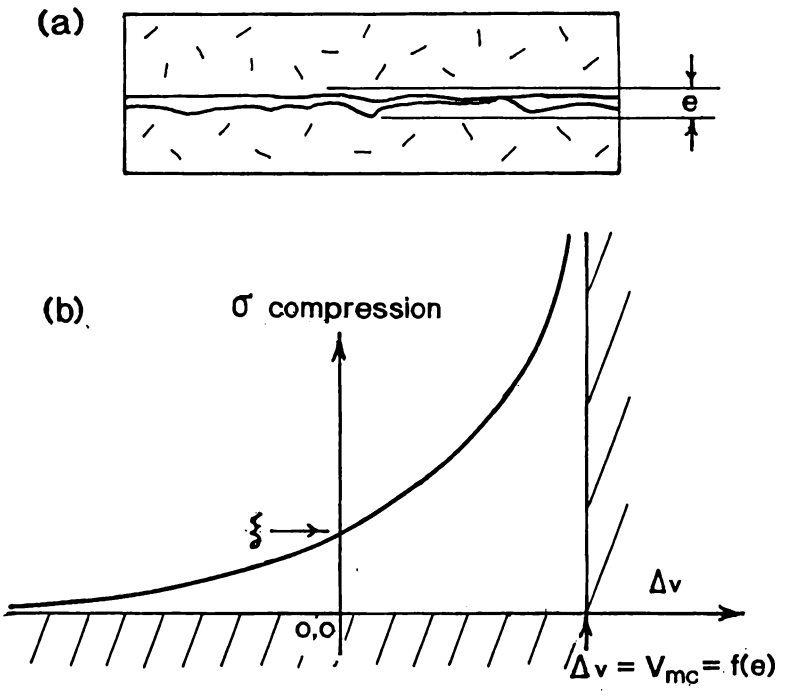

Figure 3.2 (a) Idealization of a joint. (b) Behaviour of a joint in comperession. ξ is the seating load.

σ = the normal pressure.

ξ = the seating pressure.

Δv = the normal deformation;

A and t are constants.

A hyperbolic compression curve (Figure 3.2) shows this normal behaviour.

3.4.2 Shear deformation of joints

Shear deformation in joints had been discussed in several papers [Krsmanovic and Langof (1964), Hoek and Pentz (1968), Rosengren (1968), Goodman (1970) and Coulson (1972)]. At constant confining pressure, the shear deformation curve can be shown in Figure 3.3, where τ_p is the peak stress, u_p is the shear deformation at τ_p , τ_r is the post-peak stress, u_r is the shear deformation at τ_r, and k_s is the unit shear stiffness (Goodman et al., 1968).

The changes in normal stress will influence all of the parameters of the joint shear behaviour. There are two models to describe the variation of peak shear displacement and shear stiffness: one is the constant stiffness model, the other is the constant displacement model. A bilinear relationship (Figure 3.4) between the peak shear strength and the normal stresses was found by Patton (1966).

$$\tau_p = \sigma \tan (\phi_u+i) \qquad (\sigma < \sigma_T) \qquad (3.12)$$

$$\tau_p = C_J + \sigma \tan (\phi_u+i) \qquad (\sigma > \sigma_T) \qquad (3.13)$$

where

$$\sigma_T = C_J / (\tan (\phi_u+i)$$

Dilatancy

Under the confining pressure, dilatancy is one of the brittle rock deformations. It describes the joint thickening, the normal displacement caused by shear.

Ladanyi and Archambault's equation

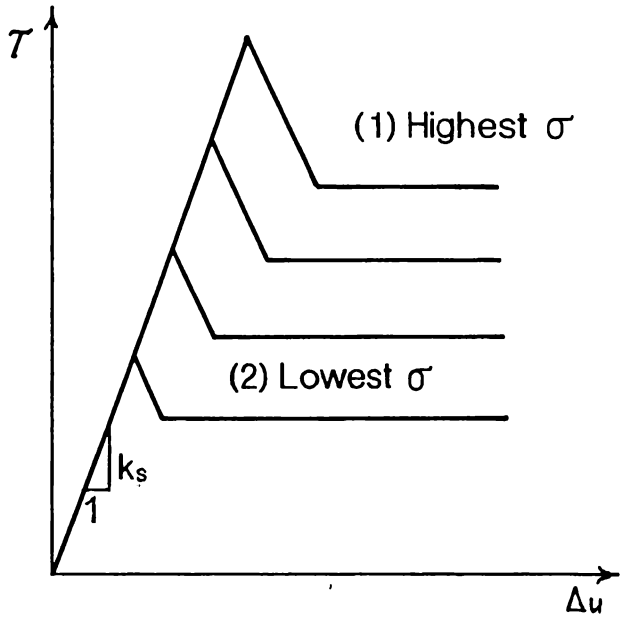

Figure 3.3 Constant stiffness model (from Goodman, 1976).

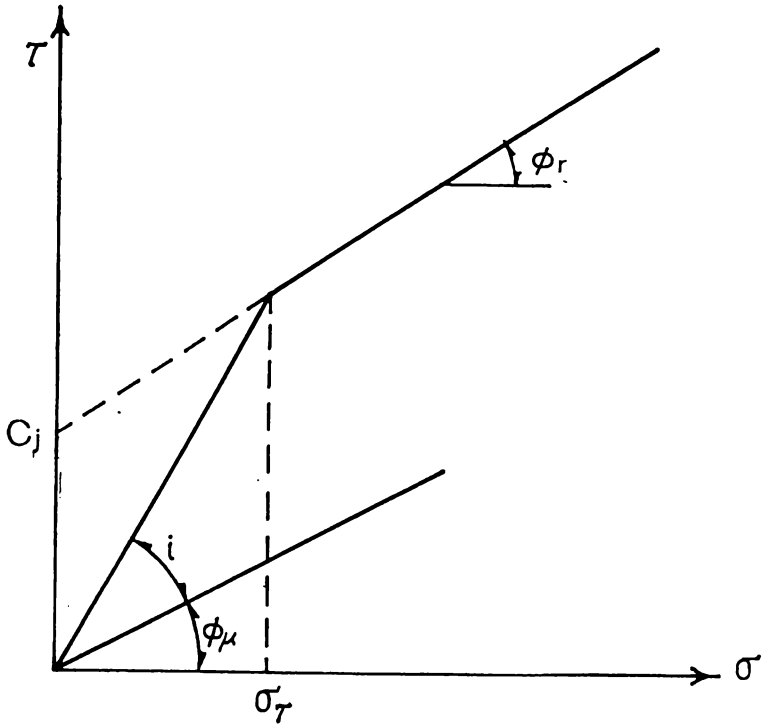

Figure 3.4 Patton's bilinear criterion for shear strength of joints.

Ladanyi and Archambault (1970) developed a strength equation for discontinuities which consists of the friction, dilatancy, and interlock contributions to the peak shear strength (Equation 3.14).

$$\tau_p = \frac{\sigma \bullet (1 - a_s) \bullet (v + \tan\phi_u) + a_s \bullet s_R}{1 - (1 - a_s) \bullet v \bullet \tan\phi_u} \tag{3.14}$$

where

σ = the normal stress.

a_s = the proportion of the joint area sheared through the asperities.

v = the dilation rate at the peak shear stress $\Delta v\ (\tau_p) / \Delta u\ (\tau_p)$.

ϕ_u = the friction angle for a joint.

s_R = the shear strength of the rock composing the asperities.

$$a_s = 1 - \left(1 - \frac{\sigma}{\sigma_T}\right)^{3/2} \qquad \text{for} \quad \sigma < \sigma_T \tag{3.15}$$

$$a_s = 1 \qquad \text{for} \quad \sigma \geq \sigma_T$$

$$v = \left(1 - \frac{\sigma}{\sigma_T}\right)^4 \tan i \qquad \text{for} \quad \sigma < \sigma_T$$

$$v = 0 \qquad \text{for} \quad \sigma \geq \sigma_T$$

σ_T is the transition pressure (Figure 3.4).

$$s_R = q_u \frac{(1+n)^{1/2} - 1}{n} \bullet (1 + n/q_u)^{1/2} \tag{3.16}$$

where

q_u = the unconfined compressive strength.

n = the ratio of compressive to tensile strength of the rock comprising the asperities.

3.5 Application in tectonic studies

The application of the finite element method in tectonic studies depends on the natural features of the Marlborough region, geodetic data, and several assumptions. For a modelling program, it is necessary to compare the modelling results with the observed data. Some modelling results and interpretations will be discussed in Chapter 5.

3.5.1 General features of the Marlborough faults

There are several features of the Marlborough faults (Figure 1.1):

(1) The shear zone consists of several dextral strike-slip faults: the Alpine (Wairau), Awatere, Clarence, Hope, and other faults (Lensen, 1962). Based on differences in structure, Lamb (1988) defined the Marlborough Fault System as consisting of two domains. In the southern domain, the major faults are pure strike-slip faults. In the northern domain, the major faults have a significant component of oblique thrusting, which is related to the rapid uplift of the Kaikoura Ranges.

(2) The Inland Kaikoura and Seaward Kaikoura Ranges, lying in the SE Marlborough region, are separated by the Awatere, Clarence, and Hope Faults.

(3) The 2000 m contour of the South Island shows that the southern domain in Marlborough has higher elevations, which is consistent with the distribution of the Kaikoura Ranges.

(4) During the Quaternary, the slip rate along these faults has increased with distance southeast of the Alpine (Wairau) Fault (Dissen and Yeats, 1991; Knuepfer, 1992).

(5) The Alpine Fault bend occurring at the southwest end of the Wairau Block is bounded by the Alpine Fault and Wairau Fault.

(6) The widening north of the Awatere Fault, of the chlorite subzone 2, makes up the greater part of the chlorite zone near the Alpine Fault bend (Suggate, 1979).

(7) The lines of the dextral strike-slip faults are not straight. The direction of the ENE-trending Marlborough Faults ranges from 055° to 075°. The trend of the Marlborough Faults is from about 070° in the south-west to 055° in the north-east (Lamb, 1988).

3.5.2 Two-dimensional modelling

By the principles of rock mechanics and the finite element method, a two-dimensional modelling computer program was written to study the tectonics of the Marlborough region.

Some fundamental information will be discussed in this section.

(1) Nodes, elements, and material properties

(a) Nodes: All the nodes in the elements configuration are located at the same scale as the Geological Map of New Zealand 1: 250,000. (b) Joint elements: A joint element consists of four nodes. All the joint elements are quadrilaterals. In consequence of the connection of joint elements, a discontinuity regarded as a fault can be modelled by them. (c) Solid elements: Because all of the study region is assumed to be a linear, transversely isotropic solid, solid elements may therefore be used to cover the region except the discontinuities. The shape of each solid element is a triangle.

(2) Element configuration of Marlborough

The element configuration (Figure 3.5a) of the Marlborough region, based on the structural geology, is set up for the numerical modelling. There are 256 nodes and 363 elements in the figure, including 280 solid elements and 83 joint elements. The original figure before the stress is applied shows the position of each node. Several assumed stress data have been used for testing the modelling program (Jetty) in order to find the best input parameters for modelling. This original figure (shape) will be deformed when the input stress (load) acts on the modelling area. According to the present plate motion and the trial-and-error modelling, the best input parameters will be found by the modelling results. They will be applied in other modelling cases.

(3) Initial and boundary conditions

a. Initial stress

Several initial stress conditions will be assumed in each case study. For example, some cases have been simulated under different initial conditions. If a case is a fail test (i.e. the input load is higher than the critical stress), then the elements configuration will be out of

order. The initial stress data are consistent with the crustal strain of the Marlborough region which is a dextral shear zone. The input stress data include σ_x (normal stress parallel Y-direction), σ_y (stress parallel Y-direction), and τ_{xy} (shear stress). The relation between the shear strength and normal stress could be approximated by the Coulomb equation.

b. Boundary conditions

Seven nodes located in the north-west corner of Figure 3.5A are fixed in order to represent the fixed Australian plate relative to the Pacific plate. It means that the displacements after deformation are relative to the Australian plate. The others nodes are not constrained and are free to move in both X- and Y- directions.

c. Material properties

The stress-stain relationship for the modelling program (Jetty), is assumed to be elastic. The modulus of elasticity is 5000; the Poisson's ratio is 0.2; the shear modulus is 417.

(4) Assumptions

There are some assumptions applied in the tectonic modelling:

(a) The tectonic movements may be expressed by the principles of rock mechanics.

(b) The Marlborough Faults System consists of five major faults [the Alpine (Wairau), Awatere, Clarence, Kekerengu, and Hope] and other secondary faults.

(c) The Marlborough region is assumed to be the same as a single rock which is analogous to a geological unit.

(d) The Marlborough faults lying in the region are considered as discontinuities (joints).

3.5.3 Modelling program --- "Jetty"

The **"Jetty"** program was written by Dr. Christopher St. John and Richard E. Goodman (1976). It is a Fortran program for analysis of jointed rock structures. Based on the principles of rock mechanics and the finite element method, the **"Jetty"** program could be applied to model the tectonic evolution of the Marlborough faults system.

Steps of the finite element analysis program:

1. Input data

The input data are: nodal points data; element data; rock and joint properties; initial stresses; residual stress data; boundary constraint data.

2. Form solid element stiffness matrix, (K), for each type, orientation, and shape of solid element.

3. Form joint element stiffness matrix ($K_{s,n}$) for each type, length, and orientation of joint element (the local directions s and n are respectively parallel and perpendicular to the original orientation of the joint walls).

4. Assemble structural stiffness matrix (**K**).

5. Assemble residual stress contributions to the load vector.

6. Invert the structural stiffness (**K**) and retain $(\mathbf{K})^{-1}$.

7. Determine displacements by matrix multiplication.

$\{u\} = (K)^{-1} \{F\}_i$

8. Form modified joint element stiffness and initial forces and relative displacements Δv_i and Δu_i.

9. Determine normal force $\{F_n\}_i$ and shear force $\{F_s\}_i$ in each modified joint element.

10. Update $F_{n,0}$ and $F_{s,0}$; rotate to global coordinates and update $\{F\}_i$.

$F_{n,0}$ is the initial normal force; $F_{s,0}$ is the initial shear force

11. i = i+1 go to step 7 (if i equals the last iteration, the program will end).

3.5.4 Modelling cases

There are several cases for the study of tectonic modelling:

In each case seven nodes located in the north-west corner of the elements figure are fixed in order to represent the fixed Australian plate. The displacements after deformation will be relative to the Australian plate.

(1) Case A

This case can be compared to the present movements of the Marlborough faults. The elements configuration (Figure 3.5A) is the same as the Marlborough fault system.

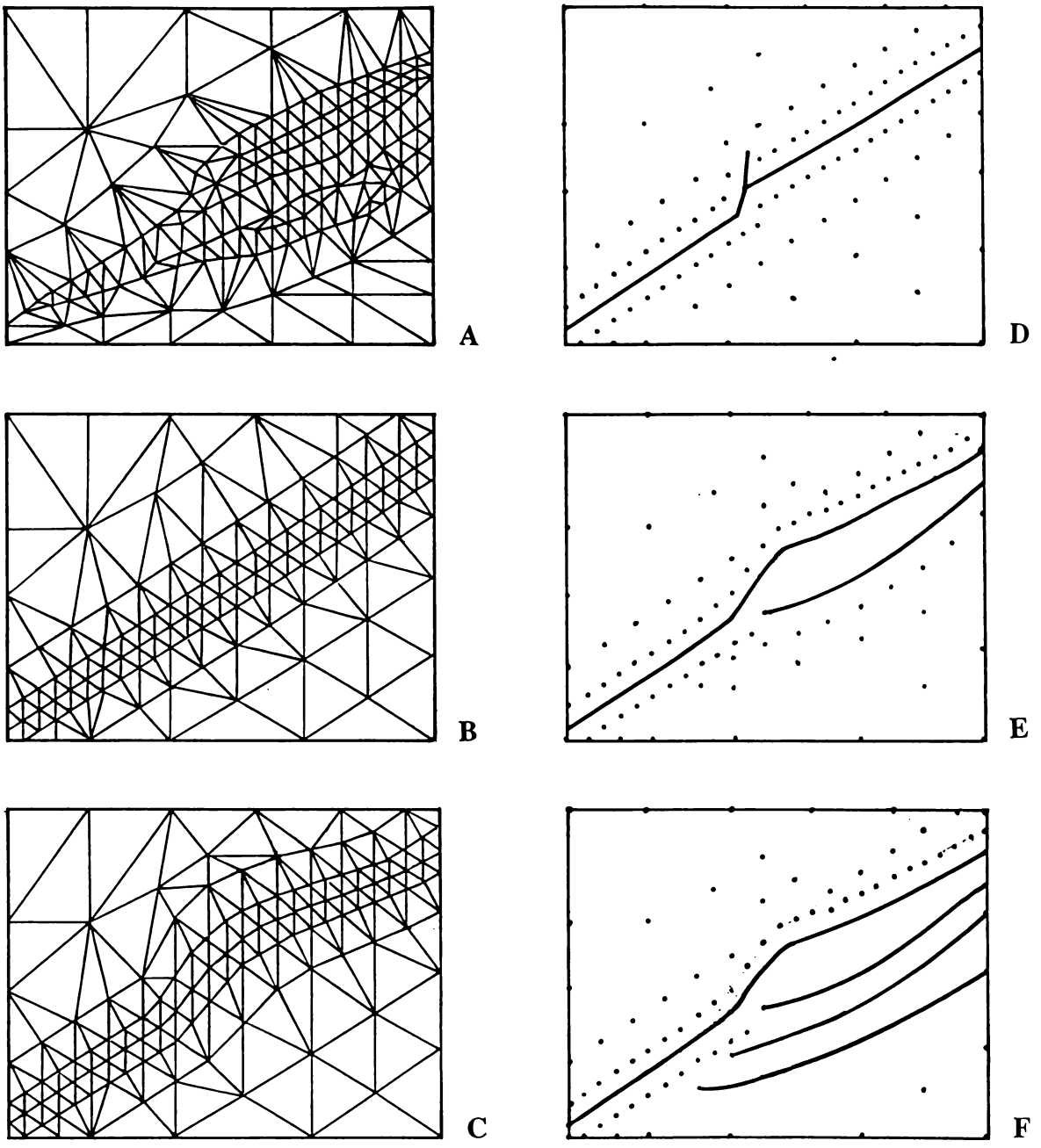

Figure 3.5 Modelling Cases A-F.

(2) Case B

The elements configuration (Figure 3.5B) is considered as a straight fault which represents the Alpine Fault.

(3) Case C

The elements configuration (Figure 3.5C) is established as a curved fault.

(4) Case D

The elements configuration (Figure 3.5D) represents that of a single fault displaced along a pre-existing fault. This elements configuration is similar to the figure which was suggested by Suggate (1979; Figure 4c).

(5) Case E

The elements configuration (Figure 3.5E) shows that a major fault (the Alpine) and two secondary faults (the Awatere and Clarence) co-exist.

(6) Case F

The elements configuration (Figure 3.5F) indicates that a major fault (the Alpine) and three secondary faults (the Awatere, Clarence, and Hope) have occurred.

The modelling results will be discussed further in chapter 5.

Chapter 4

Geology and Deformation of the Marlborough Region

Chapter 4

Geology and Deformation of the Marlborough Region

The Marlborough region lies between the Cook Straight and Seaward Kaikoura Range. It contains several major dextral faults, in particular those between the Alpine (Wairau) and Hope Faults, known as the Marlborough Fault System. According to geological evidence, this region experienced magmatism and extension at about 100 Ma. Later, a long period (~60 Myr) of tectonic quiescence and slow thermal subsidence followed. From the early Miocene (~22 or 24 Ma), the region has experienced compressive tectonism associated with development of the modern plate boundary. The initiation of the Marlborough Fault System (MFS) may be as young as 5 to 6 Ma and related to a change in the position of the Australian-Pacific finite pole of rotation. Because the region is located within the Australian-Pacific plate boundary zone, its geology and history of deformation are somewhat complicated. In this chapter the absolute ages of biostratigraphic Stage boundaries are those shown in Figure 4.6.

4.1 Basement geology

The basement of Marlborough comprises Torlesse Supergroup (Figure 4.1). During the Permian to early Cretaceous, the Torlesse rocks were accreted onto the Pacific margin of Gondwana along a southwesterly-dipping subduction zone (Bradshaw et al., 1981; Bradshaw, 1989). The Torlesse Supergroup can be separated into three terranes: the Esk Head, Pahau, and Rakaia Terranes (Bradshaw et al., 1981). The Esk Head Terrane is really a major melange zone and includes late Triassic to Jurassic rocks. The Pahau Terrane comprises late Jurassic to early Cretaceous sediments, and the Rakia Terrane comprises late Carboniferous to late Triassic sediments. In addition to sandstones and mudstones, the strata include conglomerates, rare cherts, volcanics, and limestones, which are extremely deformed. Bradshaw et al. (1981) explained that the angular unconformity, separating the Pahau Terrane from young units, represents the stratigraphic expression of the end of the early Cretaceous Rangitata II Orogeny. This angular unconformity shows that the tectonics of Marlborough changed significantly from compression to extension during the mid Cretaceous. Bradshaw (1989) stated that the convergent tectonics of the Rangitata II Orogeny was caused by collision and subduction of the Phoenix/Pacific Ridge along the

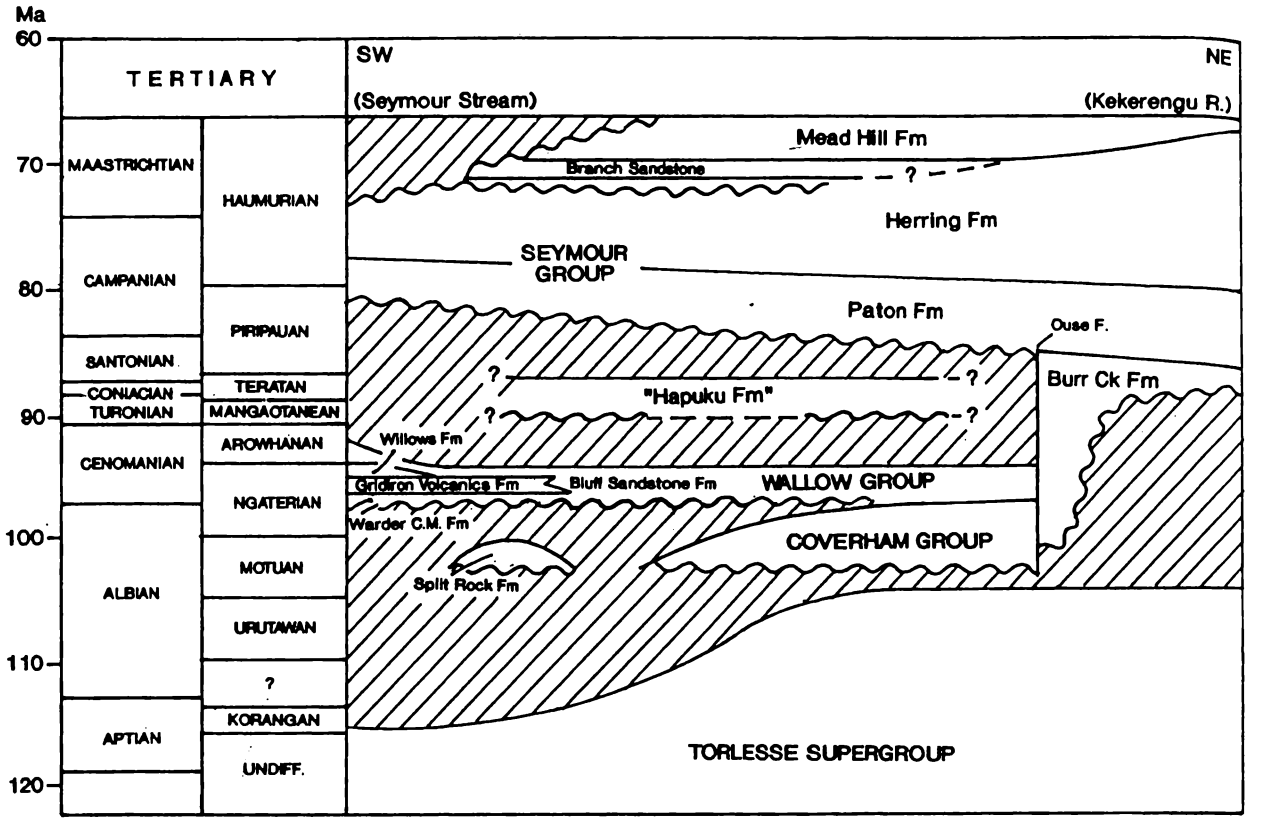

Figure 4.1a Chronostratigraphic chart showing relationships of Cretaceous rocks. Correlation of local with international stages is based on the Time Scale of Edwards et al. (1988). From Laird (1992).

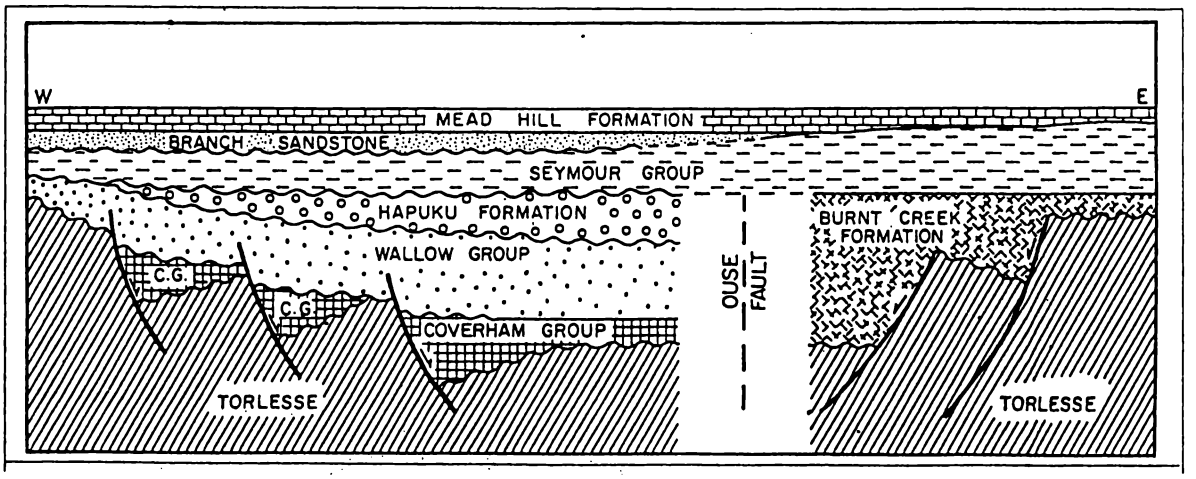

Figure 4.1b Oblique section across Marlborough showing basin framework and relationship of Cretaceous sedimentary units. Vertical scale arbitrary. From Laird (1992).

active margin in the east of New Zealand. The deformation and uplift of the Torlesse rocks as a whole, including all three terranes, resulted from this orogeny. The folded and eroded Motuan Stage (Albian, 100-105 Ma) fossils of Torlesse rocks reveal that the peak of the orogeny did not occur until the early Motuan (Laird, 1992).

4.2 Cover rock succession

The stratigraphy of cover rocks in Marlborough ranges from Cretaceous to Quaternary in age. Laird (1992) demonstrated that the major Cretaceous lithostratigraphic units in this region include the Coverham Group, Wallow Group, Hapuku Formation (new name), Burnt Creek Formation, and Seymour Group, Branch Sandstone, and Mead Hill Formation (Figure 4.1). Reay (1993) suggested that the Tertiary rocks in Marlborough can be organised into two major groups: the Muzzle and Motunau Groups. Browne (1995) demonstrated that Neogene units in Marlborough had two main depositional areas: stratigraphic units (early Miocene) of southern Marlborough include the Spy Glass Formation, Weka Pass Stone, and Whale Black Limestone; stratigraphic units (late Miocene to Pliocene) of northern Marlborough consist of the Medway, Upton, and Starborough Formations (Figure 4.2).

4.2.1 Cretaceous strata

The Torlesse rocks, the basement of Marlborough, were accreted during the Permian to early Cretaceous. The deposition of basement sediments were halted by an intra-Motuan (Albian) tectonic event considered to represent the termination of subduction (Laird et al., 1994). Following this event, the Coverham Group, Wallow Group, and Hapuku Formation were deposited across a regional unconformity (Figures 4.1a,b). In the north east, the Burnt Creek Formation occupies this stratigraphic position.

a. Mid to late Cretaceous strata

Coverham Group

The accumulation of the Coverham Group overlying Torelesse rocks was associated with block faulting during the late Motuan to early Ngaterian Stages. The widespread formation of half grabens during this period has been interpreted in terms of crustal extension, which is also the case at this time in other parts of New Zealand (Laird, 1992).

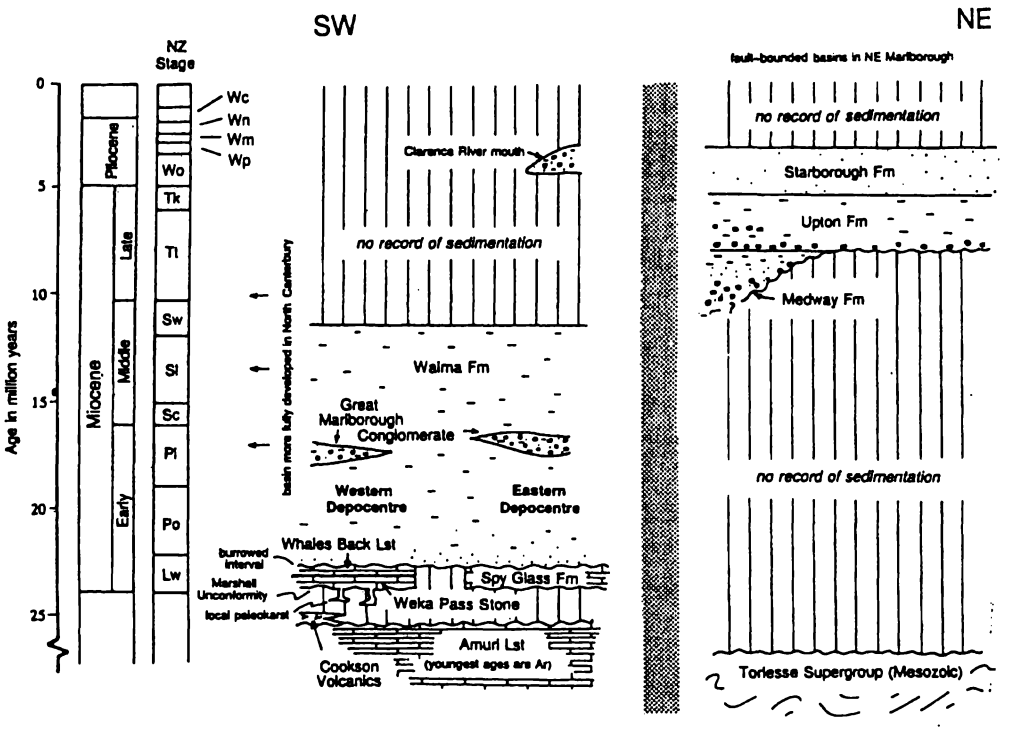

Figure 4.2 Cenozoic stratigraphic units in Marlborough. From Browne (1995).

Lensen (1978) defined the Coverham Group and included within it "shelf faces deposits (Split Rock Formation) in western and southern Marlborough, and deeper water siltones and graded-bedded sequences in northern and eastern Marlborough" of mid-late Cretaceous age.

Wallow Group

During the Ngaterian Stage the Wallow Group accumulated unconformably across basement and much but not all of the Coverham Group. This group shows deposition of marine and non-marine conglomerates, sandstones, and mudstones of late Ngaterian and, locally, of Arowhanan age. In the east, strata may be conformable with sediments of the Coverham Group (Laird, 1992). The Bluff Sandstone Formation is dominant in the western and southern successions (Lensen, 1978), inserted within, or overlain by, the basaltic Gridiron Volcanics Formation (Reay, 1993) (Figure 4.1a).

Hapuku Formation

The Hapuku Formation overlies the Wallow Group unconformably, but without angular discordance, and consists of siltstone, fine-grained sandstone, and glauconite. In addition, the lithology has a characteristic in common which is the highly burrowed nature of the deposits, indicating that the Hapuku Formation accumulated in a shallow marine environment. The age of the Hapuku Formation ranges from Mangaotanean to Teratan (Laird, 1992).

Burnt Creek Formation

The Burnt Creek Formation unconformably overlies Torlesse Supergroup rocks east of Ouse Stream and has an age range from Motuan to Teratan (Hall, 1964; Laird, 1992). The formation comprises massive basal conglomerate consisting of sub-rounded pebbles and boulders in a sandstone matrix, followed by alternations of thin conglomerate layers, and increasingly thick mudstone towards the top. The northeast trending Ouse Fault separates the Burnt Creek Formation from Torlesse Supergroup and the Split Rock Formation (Laird, 1992). Ritchie and Bradshaw (1985) stated that the Paton Formation overlying the Burnt Creek Formation is the oldest late Cretaceous unit on both sides of the Ouse Fault (Figure 4.1a).

b. Late Cretaceous strata

During Piripauan times a major transgression occurred throughout the whole of Marlborough, resulting in the deposition of the **Seymour Group** (Reay, 1993). This group

includes three formations: the Paton and Herring Formations (Webb, 1971), and the Claverley Sandstone (Warren and Speden, 1978).

Paton Formation

The Paton Formation, consisting of glauconite fine to medium-grained sandstone lies conformably on the Burnt Creek Formation in the east and unconformably upon older units to the west of the Ouse Fault (Ritchie and Bradshaw, 1985; Laird, 1992). The age of the Paton Formation is mainly Piripauan, but it may be Haumurian (late Cretaceous) in the southwest (Laird, 1992). The Paton Formation probably accumulated in a shallow marine environment (Reay, 1993).

Herring Formation

The Herring Formation and Woolshed Formation conformably overlie the Paton Formation, and form the most widespread late Cretaceous units in Marlborough. These two formations were grouped together by Laird (1992). The Herring Formation consists of muddy siltstone and interbedded white, fine sandstone (Reay, 1993). The age of the Herring Formation is restricted to the Haumurian (Laird, 1992).

Claverley Sandstone

The Claverley Sandstone conformably overlies the Herring Formation, is a yellow-brown and grey, poorly sorted, very fine-grained sandstone. The poorly-sorted deposits combined by burrowing organisms reveal that the Claverley Sandstone probably accumulated in a shallow marine environment. The age of the Claverley Sandstone ranges within the Haumurian (Laird, 1992).

c. Late Cretaceous/Tertiary units

A succession formed by two lithostratigraphic units, the Branch Sandstone and Mead Hill Formation, lying close to the Cretaceous/Tertiary boundary extends from the late Cretaceous into the early Tertiary (Reay and Strong, 1992; Webb, 1971). The Branch Sandstone, which is Haumurian in age, unconformably overlies the Herring Formation. Being a massive fine-grained, well-sorted sandstone, the Branch Sandstone probably accumulated in a shallow marine shelf environment. The Mead Hill Formation overlies it unconformably in the west and conformably in the northeast (Figure 4.1a). The Mead Hill Formation comprises chert-rich micritic limestone forming the basal unit of the Amuri Limestone. The age of its lower part is late Haumurian (Laird, 1992).

4.2.2 Paleocene to Eocene strata

Tertiary rocks of Marlborough can be divided into two groups: the Muzzle and Motunau Groups. The Muzzle Group overlies the Seymour Group and comprises a sequence of calcareous, glauconitic, clastic, and igneous lithologies (Reay, 1993). Browne and Field (1985) stated that the Motunau Group shows "a period of largely marine sedimentation that culminated in late Miocene to Pleistocene regression". This group consists of the Amuri Limestone, Grasseed Volcanics, and Fells Greensand. The Motunau Group comprises Cookson Volcanics, Weka Pass Stone, Waima, and Great Marlborough Conglomerate formations (Reay, 1993).

Amuri Limestone

The Amuri Limestone consists of muddy siliceous calcareous ooze limestone, dark siltstone, fine sandstone, and galuconite. The age of the Amuri Limestone ranges from late Paleocene to late Eocene (Reay, 1993). It represents a bathyal continental margin/slope to basin deposit.

Grasseed Volcanics

The Grasseed Volcanics, intercalated with the upper part of the Amuri Limestone, consists of basic dikes, sills, lava flows, and associated sedimentary rocks. The extrusive part of the Grasseed Volcanics is equivalent to "tuff within the Amuri Limestone" (Suggate, 1958p.406). Foraminifera ages and potassium-argon ages indicate that the age of Grasseed Volcanics ranges from middle to late Eocene (Reay, 1993).

Fells Greensand

Fells Greensand, interbeded with the upper limestone and upper marl lithotypes of the Amuri Limestone, was defined by Hall (1964) as "massive, finely laminated, hard rock". Reay (1993) introduced it as an upper member of the Amuri Limestone Formation.

Cookson Volcanics

Rocks of the Cookson Volcanics unconformably overlie the Amuri Limestone, or locally Fell Greensand and Grasseed Volcanics. This unconformity is part of the Marshall Unconformity of Carter (1988). Cookson Volcanics consist of a basalt plug, flows, sills, dikes, breccia, volcarenite, and calcareous sediments. Foraminifera reveal a Whaingaroan (early Oligocene) age; the age of the basalt plug dated by the potassium-argon dating is 27.6

± 1.1 Ma, which is equivalent to the early part of the Duntroonian Stage (late Oligocene) (Reay, 1993).

4.2.3 Oligocene to early Miocene strata

In southern Marlborough, the Waitakian Stage calcareous lithologies consist of three units: the Spy Glass Formation lying in the eastern depocentre; the Weka Pass Stone and Whales Back Limestone lying in the western depocentre (Browne, 1995) (Figure 4.2).

Spy Glass Formation

The Spy Glass Formation resting on the Marshall Unconformity is a cream, centimetre- to decimetre-bedded wackestone (Browne and Field, 1985). Its thickness reaches ~100 m in eastern central Marlborough. In the formation bioclasts are dominated by densely packed planktonic foraminifera (Browne 1995).

Weka Pass Stone

The Weka Pass Stone, unconformably overlying the Amuri Limestone or resting conformably on Cookson Volcanics, is a glauconitic, sandy calcarenite (Reay, 1993). The unconformity beneath the Weka Pass Stone may be considered as the Marshall Unconformity of Carter (1988). Foraminifera show that the age of the Weka Pass Stone ranges from latest Whaingaraoan (Early Oligocene) to early Otaian (Early Miocene) (Reay, 1993).

Whales Back Limestone

The Whales Back Limestone, resting disconformably on older Teritary strata or conformably on the Weka Pass Stone, is an interbedded glauconic wackstone and mudstone. Its thickness reaches 90 m in the north. Foraminifera reveal lower Waitakian ages for this formation (Browne, 1995).

Waima Formation

Waima Formation, forming the background sediment of the Great Marlborough Conglomerate, was introduced by Hall (1964) for blue-grey calcareous siltstone of Waitakian-Altonian (late Oligocene-early Miocene) age. This Formation conformably overlies Weka Pass Stone, but disconformably rests on the Amuri Limestone. The age of the Waima Formation indicated by foraminifera ranges from Otaian to Lillburnian (early to middle Miocene).

Great Marlborough Conglomerate

Thomson (1913) named the Lower Miocene conglomerate in the northeastern part of the South Island as Great Marlborough Conglomerate (GMC). The background sediment of the GMC is the Waima Formation. The GMC consists of channelised cohesive debris flow deposits. The age of the GMC ranges from Otaian (early Miocene) at its base to Altonian (middle Miocene) at the top (Reay, 1993).

4.2.4 Middle Miocene strata

The deposition of Waima Formation and Great Marlborough Conglomerate continued into the Clifdenian Stage. In northern Marlborough, there is no pre-Waiauan Neogene record (Browne, 1995).

4.2.5 Late Miocene-Pliocene strata

In northern Marlborough, the Neogene succession is made up of three stratigraphic units: the Medway (oldest), Upton, and Starborough (youngest) formations (Maxwell, 1990; Roberts and Wilson, 1992).

Medway Formation

The Medway Formation consists of fine sandy mudstone, conglomerate, and interbedded sandstone (Melhuish, 1988; Maxwell, 1990). Foraminifera from the lower part of the succession are early Tongaporutuan or possibly Waiauan in age. The formation is considered as to have accumulated in an inner shelf setting (Browne, 1995).

Upton Formation

The sediment type of the Upton Formation is similar to that of the upper Medway formation. The Upton Formation consists of fine-grained sandy siltstone, with interbedded sandstone and conglomerate. The beds range in age between late Tongaporutuan and Opoitian (Roberts and Wilson, 1992). A rich foraminferal fauna reveals deposition in bathyal settings (Kennett, 1966; Morgans, 1980).

Starborough Formation

The Starborough Formation consists of fine to coarse sandstone and very fine sandy siltstone. The depositional age ranges from Opoitian to Waipipian (Morgans, 1980; Beu and

Maxwell, 1990). This formation is interpreted as having accumulated in an inner to middle shelf settings. Some parts of the formation were deposited in deeper-water environment (Browne, 1995).

4.3 Geological history

In Marlborough, magmatism and extension occurred from about 100 Ma, following a long interval of subduction accretion. The mid-Cretaceous extension is indicated by: (1) the occurrence of ultramafic-gabbro-syenite plutonic complexes (Baker et al., 1994; Grapes, 1975) associated with radial dike swarms; (2) the development of metamorphic core complexes in Westland (Tulloch and Kimbrough, 1989; Spell and McDougall, 1994), the opening of the Bounty Trough (Davy, 1984), and extensive mid to upper Cretaceous volcanism in the Chatham Rise sedimentary sequences; (3) a Rb-Sr isochron age of 97 $\pm$ 0.5 Ma for the alkaline Mandamus Igneous Complex, lying 80 km to the south of the volcanics in the Clarence Valley (Weaver and Pankhurst, 1991) and (4) the Rb-Sr and fission track ages for the Tapuaenuku Plutonic Complex, which range from 105 to 93 Ma (Baker and Seward, 1996).

The Split Rock Formation is of Motuan age (105-100 Ma) and comprise the oldest deposits that accumulated within the mid to late Cretaceous extensional grabens. It is considered to be a marine fan delta sequence (Reay, 1993). The terrestrial sediments of the Warder Formation (Ngaterian, 100-94 Ma), overlying the Split Rock Formation, represent the end of a regressive phase.

After the cessation of active extension and magmatism during the early-late Cretaceous, a marine sedimentary sequence of Piripauan to late Oligocene age accumulated, reflecting a long interval of thermal relaxation and subsidence (Lensen, 1962). This tectonic quiescence lasted from 85 to 25 Ma. The deposition particularly of greensands and marine limestone reflects this quiescence (Baker and Seward, 1996). During the early Miocene (25-22 Ma), thrusting and shortening activities became dominant in the Marlborough region (Carter and Norris, 1976; Suggate, 1978a; Baker and Seward, 1996). The Great Marlborough Conglomerate is a dramatic lithological expression of rapid uplift and erosion.

In brief, the Marlborough region experienced magmatism and extension from about 100 Ma. Later, a long period (~60 Myr) of tectonic quiescence and slow thermal subsidence followed. From the early Miocene (~22 or 24 Ma), the region has experienced compressive tectonism associated with development of the modern plate boundary.

4.4 Deformation of the Marlborough region

Earth deformation usually has certain relationships with the movements of plates. The earth deformation studies in the New Zealand region relative to plate tectonics have been discussed by several geologists (Walcott 1978a, 1978b, 1979; Reyners, 1980; Lensen, 1981; Bibby and Walcott, 1984; Holt and Haines, 1995). The Marlborough region is located at the southern end of the Hikurangi Trough, which is the southern continuation of the Kermadec Trench. According to seismic evidence, gravity anomalies, and geodetic data, the Hikurangi Margin is defined as an active continental margin where the Pacific Plate subducts beneath the North Island and northern South Island. Transform basins in the Marlborough region are related to the change in the plate motion from being focussed on the subduction thrust of the Hikurangi margin to strike-slip movement within continental crust (Carter and Carter , 1982). Bibby et al. (1986) stated that the uplift of the Kaikoura Ranges and the strike slip motions of the Marlborough faults reflect the termination of the subduction occurring in the Marlborough region. The age (early to middle Miocene) of the Great Marlborough Conglomerate indicates the beginning of deformation in the Marlborough region (Lensen, 1962; Freund, 1971).

4.4.1 Paleomagnetic data

Paleomagnetic data can generally be used to study tectonic rotations. Using the paleomagnetic method, Roberts (1992) concluded that rapid tectonic rotation of 7-8°/Ma occurred in the northern Marlborough domain at ~4 Ma. Moreover, Wright and Walcott (1986) concluded that in the past 5 Ma the large rotation of part of New Zealand could be related to a change in position of the Euler poles for the Pacific-Australia plates. The beginning of NNE-trending folding in Marlborough is related to a change in the motion of the Pacific plate relative to the Australian plate. Vickery and Lamb (1995) stated that large tectonic rotations have occurred in the convergent plate-boundary zone since the early Miocene. During the last 4 Ma, the MFS has resulted in a regional ~20° clockwise rotation. In the northern Marlborough domain, the Wairau block is rotating at 8°± 5° /Ma relative to

Figure 4.3 Map of South Island, New Zealand showing estimated uplift rates in mm/yr (from Wellman , 1979).

the Australian plate and the Awatere block at 7°± 4° /Ma. The rotation in the northern Marlborough domain probably does not occur in the southern Marlborough domain (Lamb, 1988). The paleomagnetic studies reveal that tectonic rotations in the Marlborough region have occurred since the early Miocene, and most markedly during the past 5 Ma.

4.4.2 Geophysical data

Geodetic measurements across plate boundary zones are generally consistent with long-term rates of plate motion (Argus and Gordon, 1990; Ward, 1990; Holt and Haines, 1995).

The convergence rate of the Pacific plate relative to the Australian plate in the boundary zone is about 42 mm/year at 255° (Demets et al., 1990). Geodetic studies have proved that the current plate motion is accommodated onshore in the (MSF) (Bibby, 1981; Walcott, 1984). Bibby (1981) suggested that about 80% of the relative plate motion occurred across the Marlborough system during the last 100 years.

Vertical deformation

Because post-glacial reversal of the upthrown side had been found at several faults, the vertical rates of faulting in Marlborough are difficult to determine (Berryman, 1979). The tilt rates associated with the Awatere and Clarence Faults are 0.2 ± 0.1 μrad/year, and 0.3 ± 0.1 μrad/year, respectively (Wood and Blick, 1986). Rates of vertical deformation in Marlborough lie between +5 and -5 mm/year. The uplift map for the South Island of New Zealand (Wellman, 1979) shows that the uplift rates in Marlborough lie between 0.0 and 10.0 mm/year (Figure 4.3). The Seaward Kaikoura Range in the southern Marlborough region currently is considered to have the greatest uplift rate.

Horizontal deformation

During the Late Quaternary, the horizontal movement of the Marlborough region has been dominantly right lateral. This region and eastern North Island are defined as a shear zone which is one of the five tectonic zones lying in New Zealand. The shear rate in the southern shear zone, 0.35 x 10^{-6} rad/year, is the greatest (Lensen, 1975).

Strain rate

The distribution of the average shear strain rate ($5x10^{-7}$/y) shows a 100 km wide zone (Bibby, 1976). According to the geologic and geodetic data, the rate of displacement of the major faults in Marlborough only reveal one third of the total shear strain rate (Lensen, 1975; Bibby, 1976,1981). Walcott (1984) estimated the shear strain rate of New Zealand from survey data and found that non-uniform distribution of strain occurs in the northern part of the South Island, the Australia-Pacific plate boundary zone. The most rapid rate (6×10^{-7}/yr) happens in the southern part of the Marlborough region. By the analysis of geological strain rates, Holt and Haines (1995) stated that the strike-slip structures within the Marlborough region have accommodated 80-100% of the total plate motion between the Australia and Pacific plates.

Principal horizontal shortening directions

The direction of the Principal Horizontal Shortening (PHS) is derived from the ratio of horizontal (H) to vertical (V) fault displacements:

$$H / V = \tan(2\alpha) \qquad (4.1)$$

where α is the angle between the PHS direction and the strike of the fault (Lensen, 1958). For normal faulting, α is zero; for reverse faulting α is 90°. The PHS directions in Marlborough lie between 100°-115° (Berryman, 1979), and can be compared with the first-motion data of microearthquakes (Arabasz and Robinson, 1976) and geodetic studies (Bibby, 1976), which reveal strike-slip mechanisms with ENE-strike in this area. Berryman (1979) stated that the PHS directions of fifteen faults in the South Island show that the Alpine and Marlborough Faults accommodate the most rapid faulting.

4.5 Late Quaternary deformation

The rate of horizontal deformation of Marlborough , -0.35 mm/km/year, is greatest in the shear zone. Rates of vertical deformation in Marlborough lie between +5 and -5 mm/year. The uplift map for the South Island of New Zealand (Figure 4.3; Wellman, 1979) shows that the uplift rates in Marlborough lie between 0.0 and 10.0 mm/year. In addition, the Seaward Kaikoura Range in southern Marlborough region has the greatest uplift rate.

Slip vectors

The slip vectors of the focal mechanisms indicate that their horizontal projections had the trend of paralleling the relative velocity vectors of the Pacific plate relative to the Indian plate (Arabasz and Robinson, 1976; Robinson and Arabasz, 1975; Scholz et al., 1973). The slip vectors of the major faults reveals that the strike-slip rates range from 4 to 15 mm a^{-1} for the last 10 Ka (Berryman, 1979; Kieckhefer, 1979; Wellman, 1983; Grapes and Wellman, 1986). Dissen and Yeats (1991) suggested that the late Quaternary slip rates for the Marlborough faults range from 4 to 25 mm/yr.

Seismicity

During the last 150 years, seven earthquakes with magnitudes ≥ 7 have occurred in the northern South Island (Smith and Berryman, 1986). The Marlborough earthquake (1848), Glynn Wye earthquake (1888), and Arthurs's Pass earthquake (1929) showed that strike-slip displacements were dominant (Pearson, 1993; Cowan, 1990; Mckay, 1890; Yang, 1989, 1992).

Microseismicity

Arabasz and Robinson (1976) used the results of a microearthquake survey to study the structure of the northern South Island and concluded that (a) the regional compression is along an axis trending NW to WNW. (b) the Clarence and Awatere Faults are the most seismically active breaks in the region. The area near the Wairau Fault has very low seismic activity. (c) The strike-slip and thrust mechanisms are related to the regional geology.

Seismogenic stress conditions

In central New Zealand, three provinces with differing stress regimes can be defined by the earthquake first-motions data. The greatest principal stress of the south-west province which includes the Marlborough region, is consistent with the directions of plate convergence and subduction (Evison and Webber, 1986).

Rate of co-seismic strain release

Pearson (1993) calculated the rates of co-seismic strain release for the large earthquakes over the last 150 years in the northern South Island, and concluded that (1) the rate of seismic activity accommodates about 70% of the relative motions; (2) the Marlborough faults have accommodated about 60% of these plate movements.

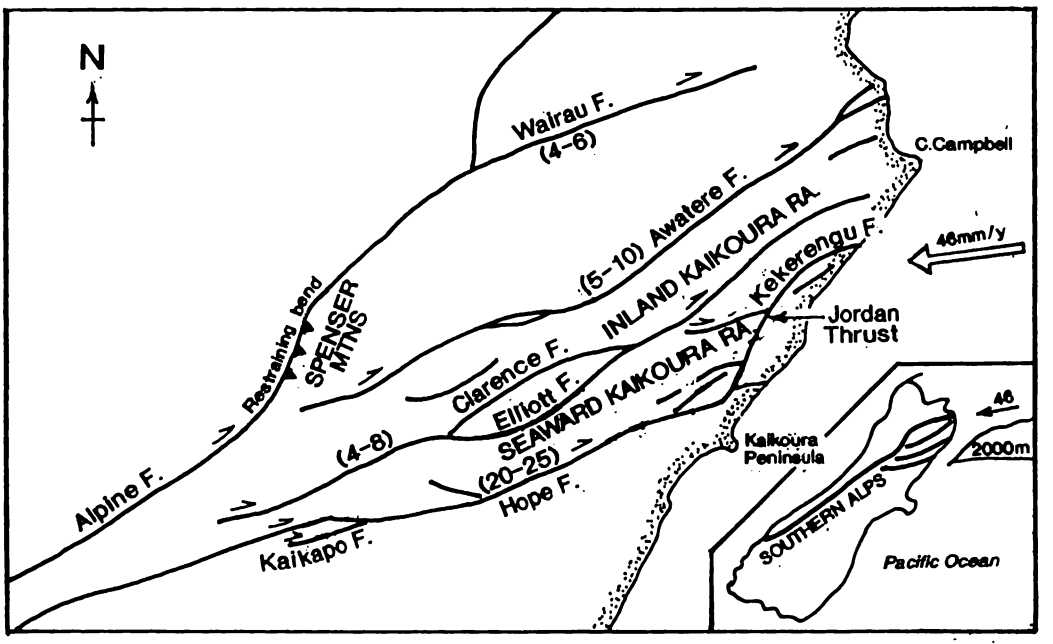

Figure 4.4 The Marlborough Fault System (from Dissen and Yeats, 1991).

Gravity

Isostactic gravity anomalies are generally related to the regional geology. The pattern of gravity anomalies of New Zealand has been studied by Reilly (1965). The gravity data for the South Island has been established by several geologists (Reilly and Whiteford, 1979; Davy and Watts, 1983). Both the Bouger and isostatic anomalies indicate crustal uplift in the Southern Alps and Kaikoura Ranges. The values of the Bouger anomalies in the Marlborough region range from -25 to -50 mgal ($1mgal=1x10^{-5}$ m/s^2); the isostaic anomalies from 0 to -75 mgal. The negative gravity anomalies reflect thickened continental crust.

4.6 Marlborough Fault System

4.6.1 General

The MFS (Figure 4.4) comprises the Wairau (Alpine), Awatere, Clarence, Kekerengu, and Hope Faults (Lensen, 1962). Suggate (1978b) defined the Marlborough region, lying between the Hope and Alpine Faults, as part of the Marlborough-Wellington Shear-Fault Zone. Lamb (1988) suggested the Marlborough fault system consists of two domains: (a) a southern domain and (b) a northern domain underlain by a Benioff zone (Anderson et al., 1993; Ansell and Adams, 1986). Carter and Carter (1982) stated that the Porters Pass, Ashley, and Motunau Faults further to the south should be included in the Marlborough Fault System. The evidence of these dextral faults had been discussed in several studies. Lensen (1962) demonstrated that a twelve-mile transcurrent drag occurred along the Awatere Fault during the Quaternary. In addition, Freund (1971) concluded that a 12 mile movement occurred on the Hope Fault during the Kaikoura Orogeny (Neogene). The average strike-slip rates range from 4 to 15 mm/year (Berryman, 1979; Kieckhefer, 1979; Wellman, 1983; Grapes and Wellman, 1986). The continuity of Middle Miocene to Pliocene sedimentary sequences reveals that the latest phase of deformation happened in the last 4 Ma (Lensen, 1962; Kennett, 1966).

4.6.2 Marlborough Fault System and plate motion

The Marlborough faults were usually explained as secondary transforms, connecting the Hikurangi subduction margin with the main Alpine Fault oblique-slip boundary (Wellman, 1971; Christoffel, 1971). However, Freund (1971) demonstrated that the

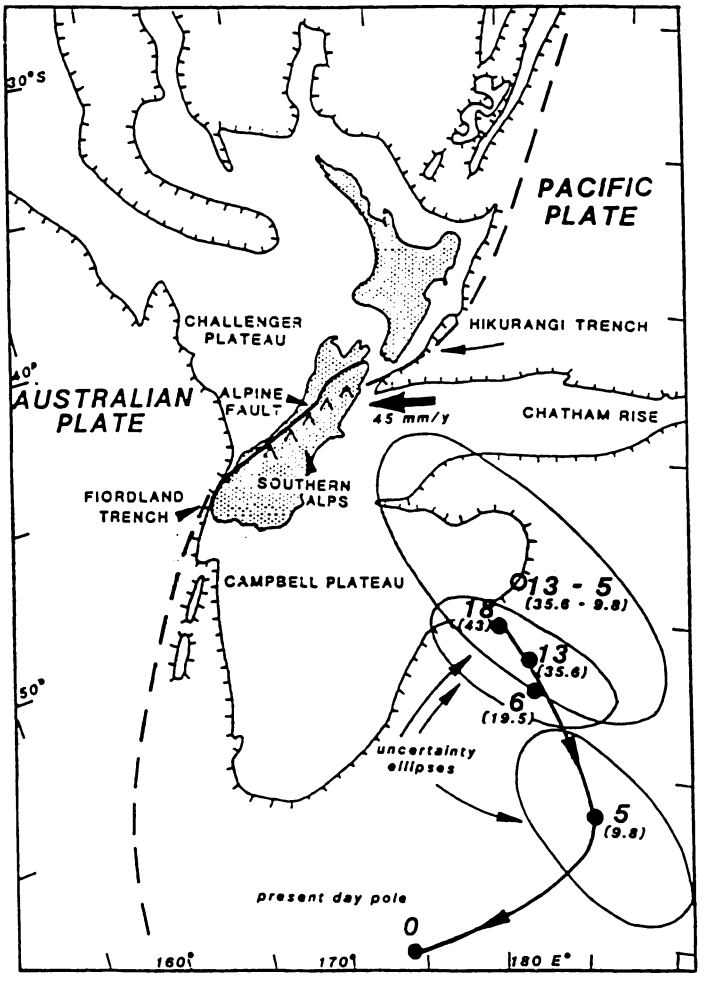

Figure 4.5 The Pacific-Australian plate boundary adjacent to New Zealand, showing finite pole positions during the last 43 m.y. (since anomaly 18). The poles and the uncertainty areas for anomalies 13 and 5 are from Stock and Molnar (1982). Refer to text for discussion on the 35.6 to 9.8 m.y. finite difference pole. The arrow shows the present day velocity of the pacific plate relative to the Australian plate. From Allis (1986).

Marlborough faults do not really link with the Alpine Fault. Scholz et al. (1973) stated that the Awatere, Clarence and Hope transforms faults have developed successively to reflect a changing plate motion vector. Rynn and Scholz (1978) accepted the model of "a changing plate motion vector" and noted the abundance of seismic activity south of the Hope Fault. They stated that "the Arthurs Pass region is a developing shear zone, since no through-going faults have been observed geologically in the region". According to the geologic and geophysical data, Carter and Carter (1982) suggested that "the subduction of the Pacific plate may have propagated southwards during the Late Neogene, causing successive activation of the Marlborough fault". Therefore, the formation of the MFS may have a relationship with the changing plate motion vector, i.e. the rotation of the Pacific-Australian pole (Figure 4.5; Allis, 1986). According to several geological studies (Lensen, 1975; Bibby, 1981; Pearson, 1993; Holt and Haines, 1995), the Marlborough region has accommodated 80-100% of the total plate motion between the Australia and Pacific plates in northern South Island.

4.7 Comment on Walcott (1998) and implications for interpretation of fission track data for Marlborough

Walcott (1998) applied a two-dimensional model to explain the meaning of "rock uplift" parameters applied by Tippett and Kamp (1993) to fission track data for the Southern Alps. He stated that the geologic location of the rocks in an absolute framework can be different at the start and end of cooling, indicating that the true pathway of the sample host rocks probably contain a significant horizontal component, as suggested also by relative plate motions.

In the two-dimensional model of Walcott (1998), rock uplift may comprise the horizontal and vertical components. In the earlier one-dimensional model of Brown (1991) applied by Tippett and Kamp (1993), rock uplift represents only the vertical component which a sample host rock follows from its initial depth to the surface. If rock uplift of the sample consists of a horizontal component, then the uplift defined by a one-dimensional model is not equivalent to the real movement. Therefore, Walcott (1998) argued that the meaning of "rock uplift" parameters of Tippett and Kamp (1993) should be modified to include two-dimensional deformation. Their estimates of denudation determined from fission track data seem to be lower than those based on simple mass balance calculations (Walcott, 1998). Tippett and Kamp (1993) drew maps of cooling/erosion based on the final/present locations of samples. If viewed from the Pacific plate their approach is reasonable as

thermochronological data cannot establish the amount of absolute motion experienced by host rocks. The degree of erosion of the leading edge of the Pacific plate cannot be established from thermochronology of the remaining crustal section of the Pacific plate.

The Marlborough region lies within the Australian-Pacific plate boundary zone. The Marlborough faults have been recognised as secondary transforms connecting the Hikurangi subduction margin with the main Alpine Fault oblique-slip boundary (Wellman, 1971; Christoffel, 1971). A change in the direction of migration of the Australian-Pacific pole of rotation occurred at about 9.8 m.y. ago (Stock and Molnar, 1982). The Awatere, Clarence and Hope faults have developed successively as transform faults to reflect the changing plate motion vector (Scholz et al., 1973). Compared with the Southern Alps (the continent-continent collision zone), rock uplift of the Marlborough region is relatively smaller. Because a fully developed continent-continent collision zone occurs to the south, the Marlborough region is more of a continental transform setting.

In brief, the Marlborough region has undergone less convergence and regional erosion than the Southern Alps. For this region, the amounts of rock uplift and denudation estimated by fission track data may be consistent with the "backstacking" approach of Brown (1991). The point of Walcott's analysis does not apply to Marlborough to the same extent in the convergence direction, as it does in the region south of Arthur's Pass, where the Hope Fault converges with the Alpine Fault, because the relative plate motion is distributed across four major faults rather than the one fault zone. An implication that still stands however is the fact of relative motion between blocks in Marlborough, which suggests that any contouring of uplift/erosion data should not cross the major fault zones.

4.8 Summary

The Marlborough region experienced magmatism and extension from about 100 Ma. Later, a long period (~60 Myr) of tectonic quiescence and slow thermal subsidence followed. From the early Miocene (~22 or 24 Ma) the region has experienced compressive tectonism associated with development of the modern plate boundary. Today, about 80-100% of the total plate motion between the Australia and Pacific plates in northern South Island is accommodated in this region. The Marlborough Fault System may have developed to the south through time and have a relationship with changes in the positions of the Pacific-Australia-Pacific poles of rotation, as shown by Allis (1986) (Figure 4.5).

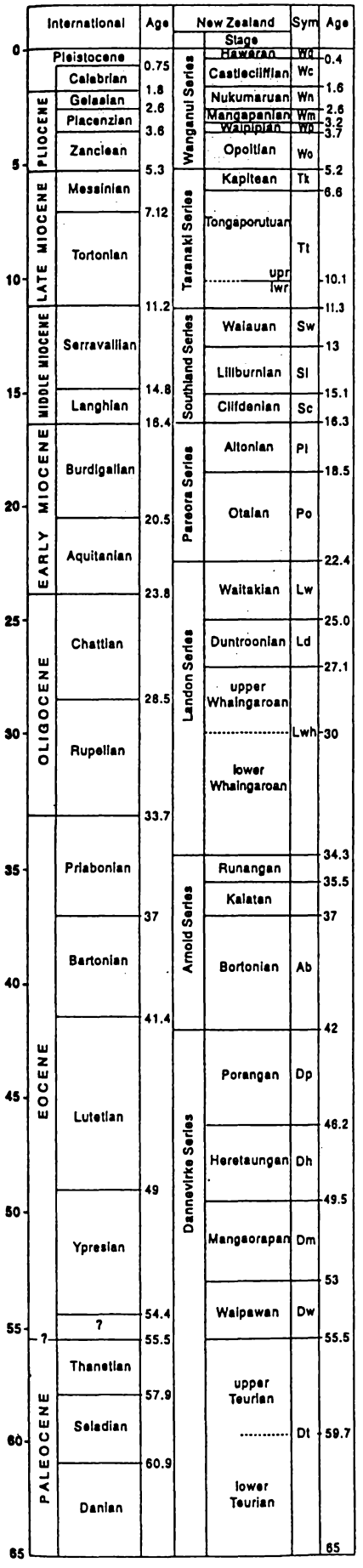

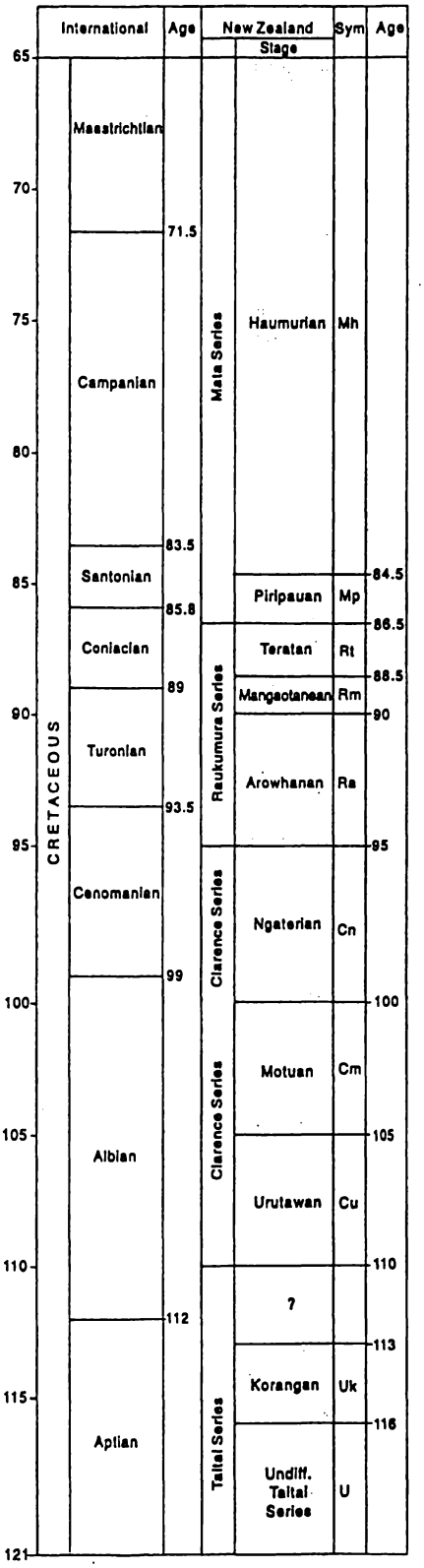

Figure 4.6 Interim New Zealand Geological Timesacle from Crampton et al. (1995).

Chapter 5

FE Modelling Results

Chapter 5

FE Modelling Results

The principles and application of the finite element (FE) method in tectonics have been discussed in Chapter 3. In this chapter, the FE modelling is applied to: (1) establish appropriate modelling parameters (Case A, Figure 3.5A) describing the present displacements within the Marlborough Fault System (MFS), and (2) apply these parameters in Cases B-F to establish constraints on the evolution of the MFS.

5.1 Introduction

It is necessary to use some assumptions for modelling studies, which for this study are as follows:

a. The crust of the Marlborough region is a single geological unit.
b. The crust of the Marlborough region is assigned to be a linear, isotropic solid.
c. The Marlborough Fault System (MFS) consists of four major faults: the Alpine (Wairau), Awatere, Clarence, and Hope Faults.
d. The Marlborough faults are recognized as having horizontal displacements. The faults are analogous to joints in a rock mechanic sense.

Based on these assumptions and the principles of rock mechanics, a computer program of the finite element method was applied to study the tectonic evolution of the MFS and uplift patterns in the Marlborough region. Some modelling results related to the evolution of the MFS will be discussed in this chapter.

5.2 Modelling parameters

There are several main parameters which influence the modelling results: (1) E - modulus of elasticity, (2) G - shear modulus, (3) γ - Poisson's ratio, (4) stresses (σ_x , σ_y , τ_{xy}), (5) U_c - the unconfined compressive strength of the asperities, (6) T_c - the ratio of tensile

to compressive strength, (7) R_p - the ratio of residual to peak strength at low normal stress, (8) the maximum amount (V_{mc}) a joint can close from the load, (9) L - the load for measuring V_{mc}, (10) ϕ - the friction angle for a smooth joint/fault, and (11) K_s - shear stiffness.

5.2.1 Young's modulus and Poisson's ratio

Young's modulus of sedimentary rocks varies within 0.49 x 10^4 and 9.30 x 10^4 MN/m^2 (Jumikis, 1983). Young's modulus for sandstone ranges from 0.49 x 10^4 to 8.43 x 10^4 MN/m^2 (U.S. Bureau of Reclamation, 1954). Poisson's ratio of sedimentary rocks lies from 0.04 to 0.62 (Jumikis, 1983). For sandstone, the Poisson's ratio ranges from 0.066 to 0.62 (Johnson, 1970; U.S. Bureau of Reclamation, 1954). Young's modulus of metamorphic rocks lies between 1.42 x 10^4 and 10.0 x 10^4 MN/m^2; Poisson's ratio of metamorphic rocks ranges with from 0.01 to 0.44 (Jumikis, 1983). The Marlborough region consists of both sedimentary and metamorphic rocks. It is reasonable to assume the average values of these two parameters in modelling cases. Except for Case 10, Young's modulus is taken to range from 1.0 x 10^4 to 5.0 x 10^4 MN/m^2 and Poisson's ratio is assumed to be 0.2.

5.2.2 Shear modulus

The shear modulus in modelling cases ranges from 0.4166 x 10^4 to 4.1666 x 10^4 MN/m^2. The value of 2.0 x 10^4 MN/m^2 was assumed to be similar to that of sandstone rocks and the other value of 4.1666 x 10^4 MN/m^2 is close to the shear modulus of metamorphic rocks.

5.2.3 Shear stiffness

The relationship of shear deformation and shear stress is demonstrated in Figure 3.3. The slope is defined as the unit shear stiffness (Goodman et al., 1968). Because the values of shear stiffness for different classes of discontinuities are still unknown, it is necessary to assume a value in analysis (Goodman, 1976). Except for two subcases of Case A, the shear stiffness was assigned to 500 in other cases.

5.2.4 U_c strength and ratio of T_c

The unconfined compressive strength (U_c) is defined as a measure of the strength of a material under a directed, uniaxial stress. The unconfined compressive strength of sedimentary rocks generally ranges from 3.9 to 245.0 MN/m^2 (Jumikis, 1983). For sandstone, it ranges from 49.0 to 98.0 MN/m^2 (Farmer, 1968) or from 19.6 to 167.0 MN/m^2 (Szechy, 1966). The tensile strength of sedimentary rocks lies between 1.0 and 24.5 MN/m^2 (Jumikis, 1983). The tensile strength of sandstone ranges from 1.0 to 24.5 MN/m^2 (Szechy, 1966; Farmer, 1968). Therefore, the ratio of tensile to compressive strength (T_c) may lie between 0.1 and 0.6. The unconfined compressive strength of metamorphic rocks has the same range as that for sedimentary rocks (3.9 to 245.0 MN/m^2; Jumikis, 1983). The tensile strength of metamorphic rocks lies between 2.9 and 13.6 MN/m^2 (Szechy, 1966; Farmer, 1968). In these data, the ratio of tensile to compressive strength of metamorphic rocks could range from 0.1 to 0.3. The U_c value of modelling cases may range from 73.8 to 137.0 MN/m^2 ; the T_c value ranges from 0.26 to 0.6.

5.2.5 B_0 ratio

The B_0 ratio is defined as the ratio of residual to peak strength at low normal stress. It is one of the input parameters for the modelling program. The B_0 value ranges from 0.0 to 1.0, providing the modelling studies for the behaviour of brittle and plastic joints (Goodman, 1976).

5.2.6 Maximum closure

A maximum possible closure of a joint, V_{mc}, is another important factor in modelling studies. The relationship of the V_{mc} and joint deformation is still unknown (Goodman, 1976). However, a simple formula (Equation 3.11) was applied in the modelling programme. For Cases 1 - 16, the value ranges from 0.005 to 0.5.

5.2.7 Variation of modelling parameters in Case A

There are sixteen sub-cases in Case A (Figure 3.5a). It is necessary to study these sub-cases in order to obtain appropriate modelling parameters for Cases B, C, D, E, and F, discussed in Section 3.5.4. Modelling parameters of Cases 1-15 can be compared with those of Case 16 (Table 5.1):

Table 5.1

No. of Case	E (N/m2)	G (N/m2)	P's Ratio	Uc Strength (MN/m2)	T-C Ratio	R-P Ratio	Mc (m)	Load (MN/m2)	Phi (degree)	Ks
1	50000	20000	0.2	137.00	0.26	0.60	0.05	0.10	30	500
2	50000	20000	0.2	73.80	0.60	0.60	0.005	0.10	30	500
3	50000	20000	0.2	73.80	0.60	0.60	0.05	0.10	30	500
4	50000	20000	0.2	73.80	0.26	0.10	0.05	0.10	30	500
5	50000	20000	0.2	73.80	0.26	1.00	0.05	0.10	30	500
6	50000	20000	0.2	73.80	0.26	1.00	0.05	1.00	30	500
7	50000	20000	0.2	73.80	0.26	0.60	0.05	1.00	30	500
8	41650	17354	0.1	137.00	0.26	0.60	0.05	0.10	30	500
9	10000	4166	0.2	73.80	0.26	0.60	0.05	0.10	30	500
10	100000	41666	0.2	73.80	0.26	0.60	0.05	0.10	30	500
11	50000	20000	0.2	73.80	0.26	0.60	0.05	0.10	30	100
12	50000	20000	0.2	73.80	0.26	0.60	0.05	0.10	30	1000
13	50000	20000	0.2	73.80	0.26	0.60	0.05	0.10	80	500
14	50000	20000	0.2	73.80	0.26	0.60	0.005	0.10	30	500
15	50000	20000	0.2	73.80	0.26	0.60	0.05	0.50	30	500
16	50000	20000	0.2	73.80	0.26	0.60	0.05	0.10	30	500

* E - modulus of elasticity; G - shear modulus; P's ratio- Poisson's ratio; Uc - the unconfined compressive strength of the asperisities; Tc - the ratio of tensile to compressive strength of wall rock; Rp - the ratio of residual to peak strength at low normal stress; Mc - the maximum amount a joint can close from the load; L - the load for measuring Mc; Phi (ϕ) - the friction angle for a smooth joint.

Case 1 - Unconfined strength (U_c) was increased to 137.0.

Case 2 - Ratio of tensile to compressive strength (T_c) ratio assumed to be 0.6, and the maximum amount a joint can close from the load (V_{mc}) equalled 0.01.

Case 3 - T_c ratio assumed to be 0.6, and V_{mc} equalled 0.005.

Case 4 - The ratio of residual to peak strength at low normal stress (R_p) assumed to be 0.1.

Case 5 - R_p ratio assumed to be 1.0.

Case 6 - R_p ratio assumed 1.0, and L (load for measuring V_{mc}) equalled 1.0.

Case 7 - L (load) equalled 1.0.

Case 8 - Parameters related to metamorphic rocks.

Case 9 - Both Young's (E) and shear modulus (G) reduced to 1.0×10^4 and 0.4166×10^4 MN/m^2 respectively.

Case 10 - Young's (E) and shear modulus (G) increased to 10×10^4 to 4.1666×10^4 MN/m^2 respectively.

Case 11 - Shear stiffness (K_s) value assumed to be 100.

Case 12 - Shear stiffness (K_s) value assumed to be 1000.

Case 13 - Friction angle (assumed 80°).

Case 14 - V_{mc} equalled 0.005.

Case 15 - L equalled 0.5

Case 16 - $E = 5.0 \times 10^4$ MN/m^2, $G = 2.0 \times 10^4$ MN/m^2, $\gamma = 0.2$, $U_c = 73.8$ MN/m^2, $T_c = 0.26$, $R_p = 0.6$, $V_{mc} = 0.05$, $L = 0.1$, $\phi = 30°$, $K_s = 500$.

The initial stresses (σ_x , σ_y , τ_{xy}) were assigned by the Coulomb equation, Equation (3.10). Because the values of Cohesion and friction angle were assumed to equal 0.3 MN/m^2 and 30° respectively, initial stresses were obtained as follows:

$\sigma_x = 1.0$ MN/m^2

$\sigma_y = 9.0$ MN/m^2

$\tau_{xy} = 5.49$ MN/m^2

where

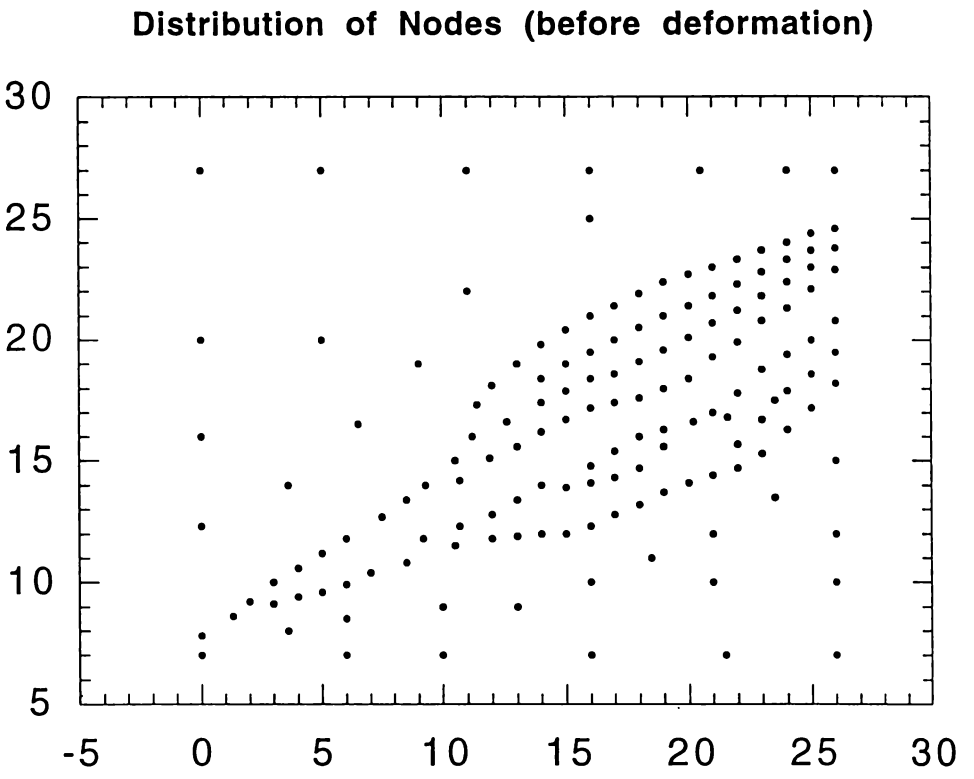

Figure 5.1a: Distribution of initial nodes (Figure 5.1a, before deformation) in Cases 1-16.

σ_x = a stress component acts in the X-direction.

σ_y = a stress component acts in the Y-direction.

τ_{xy} = shear stress.

For the comparison of modelling results, all modelling cases were assumed to be under these same stress conditions, (σ_x , σ_y , and τ_{xy} were fixed).

5.3 Presentation of results

The modelling results are illustrated in several types of figures for each case: distribution of the original configuration of nodes, distribution of nodes after deformation, the displacement field, and contours of displacement.

5.3.1 Original configuration of nodes

Figure 5.1a displays the original positions of nodes before deformation occurs. It can be used to compare the positions of nodes after deformation. Moreover, all the elements in modelling studies were established by these nodes.

5.3.2 Distribution of nodes after deformation

Except for some special fixed nodes, the positions of other nodes might be changed after deformation in each modelling case. For example, Figure 5.17 shows the positions of nodes in Case 17 which presents a failure modelling case. However, displacements of some cases are too small to be represented. In Case 16 the values of non-zero displacements range from 0.0000215 to 0.0898 (Figures 5.16a,b). It is necessary to enlarge the displacements of each case in order to show the trend of deformation. The displacements in Figure 5.16a are 100 times larger than those of the original deformation. Under initial stresses (σ_x = - 210.0 MN/m^2, σ_y = - 387.0 MN/m^2, τ_{xy} = - 330.0 MN/m^2), the south-east part of the MFS of Case 17 is extremely deformed and its deformation is larger than for other areas (Figure 5.17).

Table 5.2

No. of Case	Wairau Fault	Awatere Fault	Clarence Fault	Hope Fault	Maximum	Total
1	0.262	0.627	0.689	0.468	0.202	2.885
2	0.31	0.601	0.645	0.4838	0.183	2.85
3	0.11	0.368	1.035	1.021	0.199	3.829
4	0.598	0.843	1.049	1.006	0.208	5.439
5	0.418	0.668	1.278	1.099	0.303	5.031
6	1.281	4.602	10.73	22.1	1.282	65.03
7	1.337	4.552	10.65	22.097	1.254	62.42
8	0.466	0.768	0.8197	1.252	0.232	5.777
9	0.351	0.616	1.027	1.507	0.122	5.613
10	0.734	1.13	1.91	1.888	0.243	8.214
11	0.452	0.758	2.46	1.706	0.791	9.109
12	0.177	0.382	0.903	1.086	0.139	4.137
13	0.332	0.515	1.064	0.978	0.215	4.215
14	0.314	0.605	0.652	0.474	0.184	2.845
15	1.615	4.967	9.051	13.06	0.649	43.79
16	0.358	0.508	0.943	0.951	0.159	4.438

* Table 5.2 - displacements along four major faults of sixteen subcases of Case A.

* Total - total displacement in Marlborough; Maximum - a maximum displacement along a fault.

* Displacement unit - metre.

5.3.3 Displacement field

A figure of the displacement field shows the displacements of all nodes. An arrow of a node represents both its direction and magnitude of displacement. A node located in a discontinuity has two arrows which show the different movement of the two sides of the node.

5.3.4 Contours of displacement

Contours of displacement for each case can be used to display the variation of the displacement field. The values of displacement in a case have been normalized and range from 0.0 to 1000.0. This type of figure generally shows the trend of deformation for each case. A region with a high density of contour lines represents a high deformation area.

5.4 Results of cases

There are six major cases discussed in this section: Cases A, B, C, D, E, and F. All the cases present the same initial stress conditions. Case A includes seventeen sub-cases (Cases 1-16 and 17) which are related to the MFS. From these sub-cases, appropriate modelling parameters can be derived and applied in the other five modelling cases (Cases B-F). Table 5.1 lists modelling parameters for Cases 1-16. Table 5.2 lists all displacement data displayed by the same unit (metre). Case 17 is a special example to show a failure case. Critical conditions put the distribution of nodes out of order which represents a distorted fault system (Figure 5.17).

5.4.1 Case A

The aim of Case A was to establish appropriate modelling parameters. The modelling results of Case 16 were assumed to have an average variation in order to be compared with the subsequent cases.

Case 1

The individual model displacements of Case 1 range from 0.0 to 0.202, the total displacement across the MFS being 2.885. The Awatere Fault and Clarence Fault have large displacements being 0.627 and 0.689 respectively. However, the Wairau and Hope Faults

have smaller displacements which are 0.262 and 0.648, respectively. For Case 1, these modelling results suggest that the Awatere and Clarence Faults have a higher rate of deformation than the other faults (Figure 5.1b). In the figure showing the modelled displacement field (Figure 5.1c) two extremely large and anomalous displacements exist on the Awatere and Clarence Faults. Moreover, displacements of all the nodes are not consistent with the tectonic geology, which has dominantly dextral fault displacements. The contours of displacement (Figure 5.1d) are different from the uplift pattern of the Marlborough region.

Case 2

The individual model displacements in Case 2 range from 0.0 to 0.183, there being a total displacement of 2.850. The displacement data of the four major faults are very similar to those of Case 1. They are modelled as 0.310, 0.601, 0.648 and 0.484 for the Wairau, Awatere, Clarence, and Hope Faults, respectively. Figures 5.2a-c show that both Case 2 and Case 1 have the same patterns of nodal distribution, displacement field, and displacement contours.

Case 3

The individual model displacements in Case 3 range from 0.0 to 0.199, the total displacement being 3.829. Model displacements along the southeastern margins of the Kaikoura Ranges suggest that this area displays stronger deformation than other areas (Figure 5.3a). Larger displacements occur between the Clarence and Hope Faults, suggesting that greater deformation occurs in the vicinity of these two faults. Displacements modelled along the four major faults are 0.110, 0.368, 1.035 and 1.021, respectively. The modelled displacement field (Figure 5.3b) and the contours of displacement (Figure 5.3c) show that two significant peaked "uplifts" occur near the Alpine Fault bend and the Kaikoura Ranges.

Case 4

The individual model displacements in Case 4 range from 0.0 to 0.208 with a total displacement of 5.439. Displacements along the four major faults are modelled as 0.598, 0.843, 1.049 and 1.006, respectively. The pattern in the modelled displacement field (Figure 5.4b) and the contours of displacement (Figure 5.4c) are the same as those for Case 3. However, displacements near the Alpine Fault bend show that this area has stronger deformation than that in Case 3.

Case 5

The individual model displacements in Case 5 range from 0.0 to 0.303, the total displacement being 5.031. Displacements modelled along the four major faults are 0.418, 0.668, 1.278 and 1.099, respectively. The Clarence Fault displays more modelled deformation than the other faults. Figures 5.5a-c represent the results of Case 5. Generally, Cases 3, 4, and 5 have similar patterns in the modelled displacement field and the contours of displacement. The significant peaks of Cases 3 and 5 reveal that Case 4 has higher deformation than Case 3 and 5.

Case 6

The individual model displacements in Case 6 range from 0.0 to 1.282 with a total displacement of 65.03. This extremely high total displacement results from the greater input load (L), which is used for measuring a maximum possible closure of a joint. Extensional deformation is modelled to exist along the Hope Fault (Figure 5.6a) in this case. Displacements along the four major faults are modelled as 1.281, 4.602, 10.73 and 22.10, respectively. Displacements along the Hope Fault are significantly larger than those of the other major faults. The unusual displacements of these faults reveal that Case 6 failed to model the deformation of fault movements. The patterns in the modelled displacement field (Figure 5.6b) and the contours of displacement (Figure 5.6c) show no correlation with the displacement character history on the MFS and the regional uplift patterns.

Case 7

The individual model displacements in Case 7 range from 0.0 to 1.254, the total displacement being 62.42. The total displacement is close to that of Case 6. The greater the input load, the higher the total displacement. High rates of extensional deformation also exist along the Hope Fault (Figure 5.7a). Displacements modelled along the four major faults are 1.337, 4.552, 10.65 and 22.10, respectively. Because the patterns in the modelled displacement field (Figure 5.7b) and the contours of displacement (Figure 5.8c) are similar to those of Case 6, this case is another failure case.

Case 8

The individual model displacements in Case 8 range from 0.0 to 0.232 with a total displacement of 5.777. As with Cases 4 and 5, larger deformation occurs near both the Alpine Fault bend and the Kaikoura Ranges (Figure 5.8a). Displacements along the four major faults are modelled as 0.466, 0.768, 0.820 and 1.252, respectively. The patterns in

the modelled displacement field (Figure 5.8b) and the contours of displacement (Figure 5.8c) are very similar to those of Cases 3, 4, and 5.

Case 9

The individual model displacements in Case 9 range from 0.0 to 0.122, the total displacement being 5.613. Apart from the Wairau Fault, the other main faults exhibit larger deformation (Figure 5.9a). Displacements modelled along the four major faults are 0.351, 0.616, 1.027 and 1.507, respectively. The pattern in the modelled displacement field (Figure 5.9b) is different from those of Cases 6 and 7 (Figures 5.6b and 5.7b). However, they all exhibit a similar pattern of the contours of displacement (Figures 5.6c, 5.7c, and 5.9c). This case can be considered as a failure case.

Case 10

The individual model displacements in Case 10 range from 0.0 to 0.243 with a total displacement of 8.214. As with Cases 4, 5 and 8, higher deformation occurs near both the Alpine Fault bend and the Kaikoura Ranges (Figure 5.10a). Displacements along the four major faults are modelled as 0.734, 1.130, 1.910 and 1.888, respectively. The pattern of the modelled displacement field (Figure 5.10b) and the contours of displacement (Figure 5.10c) follow the same pattern as those in Cases 3, 4, 5 and 8.

Case 11

The individual model displacements in Case 11 range from 0.0 to 0.243, the total displacement being 8.214. No significant deformation occurs in the vicinity of the Alpine Fault bend or the Kaikoura Ranges, but higher deformation exists in the eastern parts of the Marlborough Faults System (Figure 5.11a). Displacements modelled along the major faults are 0.452, 0.758, 2.460 and 1.706, respectively. The pattern of the modelled displacements field (Figure 5.11b) and the contours of displacement (Figure 5.11c) show that strong deformation occurs only in the eastern area. Based on these results, Case 11 fails to adequately model all the surface uplift movements in the Marlborough region.

Case 12

The individual model displacements in Case 12 range from 0.0 to 0.139 with a total displacement of 4.137. Significant deformation occurs in most parts of the Marlborough region, but in contrast with Cases 4, 5, and 8, larger deformation exists in the eastern MFS (Figure 5.12a). Displacements along the four major faults are modelled as 0.177, 0.382, 0.903 and 1.086, respectively. The pattern of the modelled displacement field (Figure 5.12b)

and the contours of displacement (Figure 5.12c) show that strong deformation occurs chiefly in the eastern MFS. Case 12 also fails to model the surface uplift movements in the Marlborough region.

Case 13

The individual model displacements in Case 13 range from 0.0 to 0.215, the total displacement being 4.215. No significant deformation occurs in the Alpine Fault bend region, but in contrast with Cases 4, 5 and 8, larger deformation exists in the eastern MFS (Figure 5.13a). Displacements modelled along the four major faults are 0.332, 0.515, 1.064 and 0.978, respectively. The pattern of the modelled displacement field (Figure 5.13b) and the contours of displacement (Figure 5.13c) show that strong deformation only occurs in the eastern MFS. Case 13 as with Case 12 models the eastern deformation, but fails in the west.

Case 14

The individual model displacements in Case 14 range from 0.0 to 0.184 with a total displacement of 2.845. The modelled displacement data for the four major faults are also similar to those in Cases 1 and 2. They are modelled as 0.314, 0.605, 0.652 and 0.474, respectively. Figures 5.14a-c show that Case 14 has the same patterns as those of Cases 1 and 2.

Case 15

The individual model displacements in Case 15 range from 0.0 to 0.649, the total displacement being 43.79. Extensional deformation is modelled along the Hope Fault (Figure 5.15a). Displacements along the four major faults are modelled as 1.615, 4.967, 9.051 and 13.06, respectively. Because the pattern of the modelled displacement field (Figure 5.15b) and the contours of displacement (Figure 5.15c) are similar to those of Cases 6, and 7, Case 15 is another failure case.

Case 16

The individual model displacements in Case 16 range from 0.0 to 0.159 with a total displacement of 4.438. Significant deformation is modelled to occur in both the vicinity of the Alpine Fault bend and the Kaikoura Ranges (Figure 5.16a). Displacements modelled along the four major faults are 0.358, 0.508, 0.943 and 0.951, respectively. The variation within the modelled displacement field (Figure 5.16b) shows the trend of deformation in the Marlborough region. In addition, the contours of displacement (Figure 5.16c) are similar to

Table 5.3

No. of Case	Wairau Fault	Awatere Fault	Clarence Fault	Hope Fault	Marlborough	Total	Accommodation (%)
1	9.2	21.7	22.8	16.2	2.694	2.885	93.3
2	10.9	21.1	22.6	16.9	2.645	2.85	92.8
3	2.9	9.6	27	26.7	3.195	3.829	83.4
4	11	15.5	19.3	18.3	4.92	5.439	90.5
5	8.3	13.3	25.4	21.8	4.57	5.031	90.8
6	1.9	7.1	16.5	34.5	46.88	65.03	72.1
7	2.1	7.2	17.1	35.4	46.03	62.42	73.8
8	8.1	13.3	25.4	21.7	5.171	5.777	89.5
9	6.3	11	18.3	26.8	4.656	5.613	82.9
10	8.9	13.8	23.2	23	7.409	8.214	90.2
11	4.9	8.3	27	18.7	7.991	9.109	87.7
12	4.3	24.2	21.8	26.2	3.396	4.137	82.1
13	7.9	12.2	25.2	23.2	3.718	4.215	88.2
14	11	21.3	22.9	16.7	2.656	2.845	93.3
15	3.6	11.1	20.2	29.2	35.319	43.79	80.6
16	7.6	11.4	21.2	21.4	3.769	4.438	84.9

* Table 5.3 - percentage of displacement along four major faults of sixteen subcases of Case A.
* Total - total displacement in Marlborough; Maximum - a maximum displacement along a fault.
* Marlborough - total displacements in the Marlborough Fault System (MFS).
* Accommodation = Marlborough / Total.

the modern pattern of uplift rates (Figure 4.7 , Wellman, 1979). Case 16 is considered to be a successful one in modelling studies.

Except for Case 17 (a failure modelling case, Figure 5.17), all the results and modelling parameters are listed in Table 5.1 and 5.2. The displacement percentage of the four major faults in each case is defined by:

$$P_{fault} = D_{fault} / T_{total} \times 100\% \quad (5.1)$$

where

P_{fault} = the displacement percentage of a fault.
D_{fault} = total displacement along a fault.
T_{total} = total displacement of a case.

The accommodation percentage of the MFS in each case is defined by:

$$P_{MFS} = D_{MFS} / T_{total} \times 100\% \quad (5.2)$$

where

P_{MFS} = the accommodation percentage of the MFS.
D_{MFS} = total displacement of the MFS.
T_{total} = same as (5.1).

By the definitions of Equations 5.1 and 5.2, some results relating to the Marlborough faults were obtained (Table 5.3). For Cases 1-16, the P_{fault} value of the Wairau Fault ranges from 1.9 to 11.0%; the Awatere Fault from 7.1 to 24.2%; the Clarence Fault from 16.5 to 25.4%; and the Hope Fault from 16.2 to 35.4%. The values of P_{MFS} range from 72.1 to 93.3%. For Case 16, the value of P_{MFS} lies about the mean value of all subcases. These data reveal that the MFS has accommodated ~72 to ~93% of the total displacement. This is consistent with other geological studies which reveal that the Marlborough region has accommodated 80-100% of the total plate motion (Lensen, 1975; Bibby, 1981; Pearson, 1993; Holt and Haines, 1995).

The results presented so far show that Case 16 is the best model describing the current deformation within the Marlborough Fault System. The accommodation percentage of total displacement in Marlborough in this case is about 85%. The Wairau, Awatere, Clarence, and Hope Faults are modelled to have accommodated 7.6%, 11.4%, 21.2%, and 21.4% of the instantaneous displacement, respectively (Figure 5.18).

Modelling parameters of Case 16 are as follows:

E - modulus of elasticity = 5×10^4 MN/m^2.
G - shear modulus = 2×10^4 MN/m^2.
γ - Poisson's ratio = 0.2.
U_c - the unconfined compressive strength of the asperisities = 73.8 MN/m^2.
T_c - the ratio of tensile to compressive strength of wall rock = 0.26.
R_p - the ratio of residual to peak strength at low normal stress = 0.6
V_{mc} - the maximum amount a joint can close from the load = 0.05 m.
L - the load for measuring V_{mc} = 0.1 MN/m^2.
ϕ - the friction angle for a smooth joint = 30°.

Because material properties were assumed to be the same for all cases, these parameters can be applied in the following Sections 5.4.2-6 in which the FE modelling is applied to better understand the evolution of the MFS. The development of the MFS will be discussed by using the results for Cases B-F.

5.4.2 Case B

By studies of Case A, several appropriate parameters were obtained and used in the following modelling cases (Cases B-F). The initial conditions of Case B are the same as those for Case A. A single discontinuity represents a straight fault (Wairau) which is the initiation of the MFS. Under the same initial stresses (σ_x = - 1.0 MN/m^2, σ_y = - 9.0 MN/m^2, τ_{xy} = - 5.49 MN/m^2), the original configuration of nodes (Figure 5.19a, before deformation) was deformed into another form (Figure 5.19b).

The initiation of strike-slip displacement on the Alpine Fault occurred during the earliest Miocene (~23Ma) (Carter and Norris, 1976; Kamp, 1986). It is reasonable to assume

that the MFS evolved from a straight fault (the Alpine Fault). Under the modern conditions of plate motion, the results of Case B reveal that the horizontal displacements (or deformation) in the NE part of the straight fault are always larger than those in the SW part. The "opening" of the straight fault can be considered as an initiation of the MFS. The development of three secondary faults, the Awatere, Clarence, and Hope Faults may have a relationship with this "opening".

5.4.3 Case C

In this case a curved initial fault (Wairau) was assumed in order to model the possible evolution of the MFS. The original configuration of nodes (Figure 5.20a) shows the locations of nodes before deformation. There are two sub-cases discussed in this section.

Case C-1

Under initial stresses (σ_x = - 1.0 MN/m^2, σ_y = - 9.0 MN/m^2, τ_{xy} = - 5.49 MN/m^2), the configuration of nodes was transformed into a dislocated form (Figure 5.20b). This configuration shows that dextral movements are dominant along the curved fault. Moreover, a great amount of deformation has converged near the curved region, the Alpine Fault bend (Figure 5.20c).

Case C-2

When initial stresses were changed (σ_x = - 1.0 MN/m^2, σ_y = - 2.0 MN/m^2, τ_{xy} = - 1.4 MN/m^2), another deformed configuration of nodes was obtained (Figure 5.20d). Besides dextral movements, the configuration also reveals that a larger "opening" occurs in the upper part of the curved fault. This can be considered to be a dextral rotation.

The values of input stress ratio (σ_x/σ_y) in Cases C-1 and C-2 are 0.11 and 0.50, respectively. Modelling results of these cases imply that the increase in the ratio will cause more "opening" of the upper part of the curved fault. The plate boundary zone has accumulated large tectonic rotations since the early Miocene. These modelled results suggest that the development of the MFS probably started from a curved fault influenced by a dextral tectonic rotation.

5.4.4 Case D

Suggate (1979) suggested that a possible origin of the prominent Alpine fault bend involved offset of a pre-existing straight fault. In Case D, based by his suggestion, an original configuration of nodes (Figure 5.21a) was established for modelling studies. Figure 5.21b shows that the trend of deformation converges near the Alpine Fault bend. Moreover, the displacement field reveals that the pre-existing fault causes possible "uplift" movements across the Alpine Fault in the vicinity of the bend (Figure 5.21c), as a convergence of the strike of the fault offsetting the Alpine Fault.

5.4.5 Case E

It has been stated that a change in plate motion vector was responsible for the development of the MFS (Christoffel, 1971; Wellman 1971; Arabasz & Robinson, 1976; Scholz et al., 1973; Rynn & Scholz, 1978). An original configuration of nodes (Figure 5.22a) assumes that the Alpine (Wairau) and Awatere Faults occurred at the beginning. After deformation, the Wairau Fault has a trend of "closing" deformation (Figure 5.22b). Along the Awatere Fault, displacements are complicated and have no significant pattern (Figure 5.22c). These results may imply that three secondary faults, the Awatere, Clarence and Hope Faults, developed within a short period, not necessarily in sequence.

5.4.6 Case F

In this case three secondary faults (the Awatere, Clarence, and Hope) were assumed to have co-existed before the formation of the Marlborough faults. An original configuration of nodes (Figure 5.23a) assumes that the Alpine and three secondary faults initially existed together. After deformation, the northeastern part of Alpine Fault shows extensional deformation (Figure 5.23b). In addition, "overthrust" movements are dominant in southern Marlborough (Figure 5.23c). These "overthrust" movements may be compared to the formation of the Kaikoura Ranges.

5.5 Geological comparisons

For a modelling study, it is necessary to make a comparison between the modelled and measured data. The geological observations and studies of horizontal deformation in the Marlborough Fault System have been reported in several papers (Yeats and Berryman, 1987; Cowan, 1990; Dissen and Yeats, 1991; Berryman et al., 1992; Knuepfer, 1992; Little et al., 1998).

The calculated displacement percentages (CDP) obtained from the FE modelling will be compared with measured fault slip rates (Table 5.4). Slip-rate measurements in the Marlborough Faults are determined from the age of offsets based on either the time of the Last Glacial Maximum (Cowan, 1990) or the weathering-rind calibration curve (Knuepfer, 1984, 1992). Because the calculated displacements were assumed to be "instantaneous displacements ", the CDP values may have a good correlation with the slip rates. Both the CDP values and slip rates are appropriate factors for comparison (Figure 5.24). Except for the Clarence Fault, the CDP values and slip rates of three major faults (Wairau, Awatere, and Hope Faults) show an increasing trend away form the Wairau Fault. In the FE modelling, the Clarence Fault was recognizd as a major fault which is composed of other secondary faults. The CDP values of the Clarence Fault were derived from the major and secondary faults. This is probably the reason why the modelled and measured data of the Clarence Fault show a significant difference. Although the difference may have caused some errors, the modelling parameters of Case 16 (in Section 5.4.1) can be considered as the best model parameters for the other cases (Cases B-F).

The modelled results of Cases B and C can be compared to palaeomagnetic studies (Walcott, 1987; Lamb, 1988; Mumme et. al., 1989; Roberts, 1992; Vickery and Lamb, 1995), which reveal large tectonic rotations in the New Zealand plate-boundary zone since the early Miocene. Cases A, E and F show the modelled results in agreement with the formation of the Kaikoura Ranges and Spenser Mountains. However, Case D is a possible assumption for uplift movements across the Alpine Fault in the vicinity of the bend, and is not a unique model.

Table 5.4 Measured fault slip rates and calculated displacement percentages (CDP)

Fault	CDP (%)	Slip rates (mm/yr)	Ref.
Wairau	7.6	4 ± 1	Berryman et al. (1992)
		3.7-10.7	Knuepfer (1992)
		4-6	Dissen and Yeats (1991)
Awatere	11.4	5-7	Knuepfer (1992)
		5-10	Dissen and Yeats (1991)
		6-7	Little et al. (1998)
Clarence	21.2	1-8	Knuepfer (1992)
		4-8	Dissen and Yeats (1991)
Hope	21.4	19 ± 5	Knuepfer (1984)
		11-17	Cowan (1990)
		20-25	Dissen and Yeats (1991)

* Slip-rate measurements in the Marlborough Faults are determined from the age of offsets based on either the time of the Last Glacial Maximum (Cowan, 1990) or the weathering-rind calibration curve (Knuepfer, 1984, 1992).

5.6 Summary

According to the modelled results of Cases A-F, the development of the MFS can be recognized by the following characteristics:

a. The Alpine Fault was curved as a result of a change in the plate motion vector.

b. The continuation of tectonic rotations was responsible for the development of the MFS.

c. Three secondary faults (the Awatere, Clarence, and Hope Faults) have developed within a short period of one another.

d. Although the formation of MFS has now been completed, uplift movements of Spenser Mountains and Kaikoura Ranges still continue.

e. Suggate's model of a pre-existing fault offset of the Alpine Fault can cause possible "uplift" movements across the Alpine Fault in the vicinity of the big bend. In addition, the model of a curved fault also shows a similar "uplift" trend. Suggate's model does not give a unique result in the modelling undertaken here.

Because all of the modelled results were based on several assumptions, it is necessary to compare the results with other geological data. For example, fission track data about denudation and the topography of the Marlborough region. Comparison of the model with information about the topography and denudation is undertaken in Chapter 7.

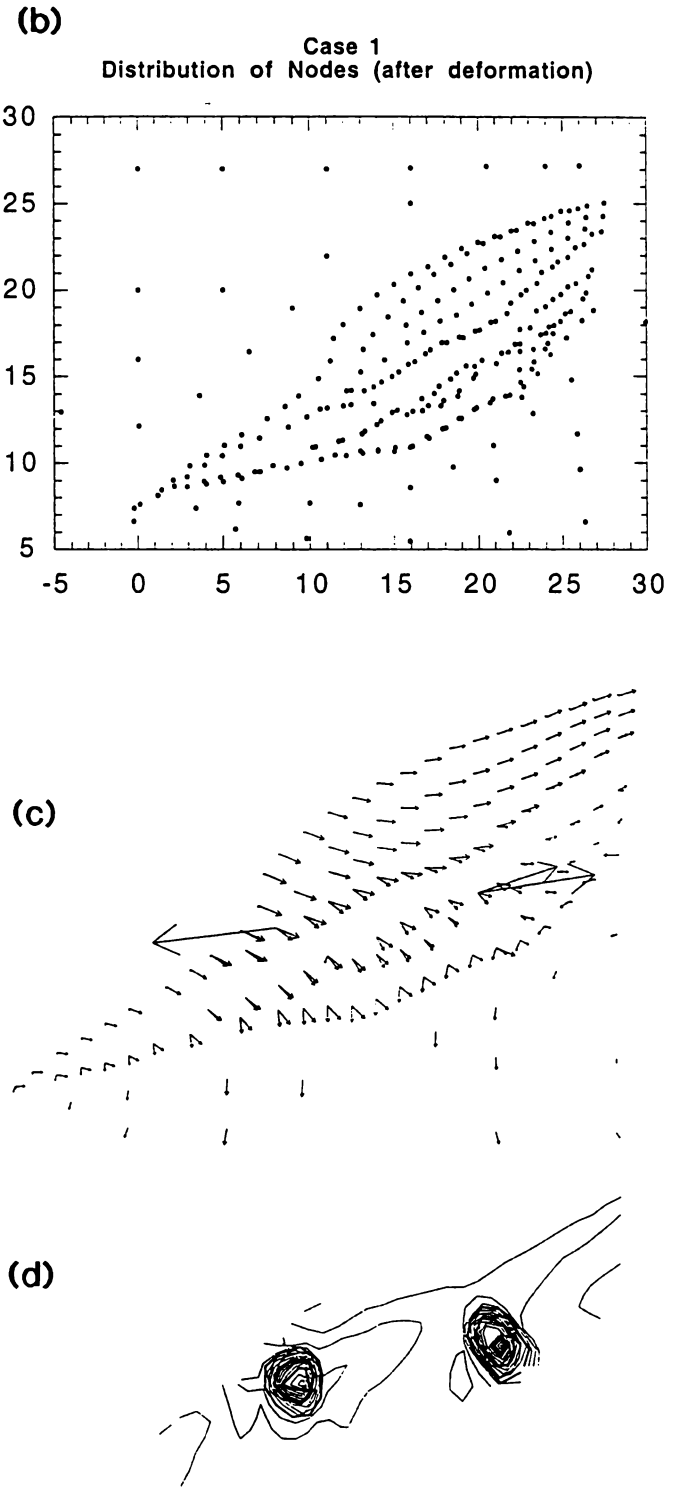

Figures 5.1b-d: Distribution of nodes (Figure 5.1b), displacement field (Figure 5.1c), and contour of displacements (Figure 5.1d) for Case 1.

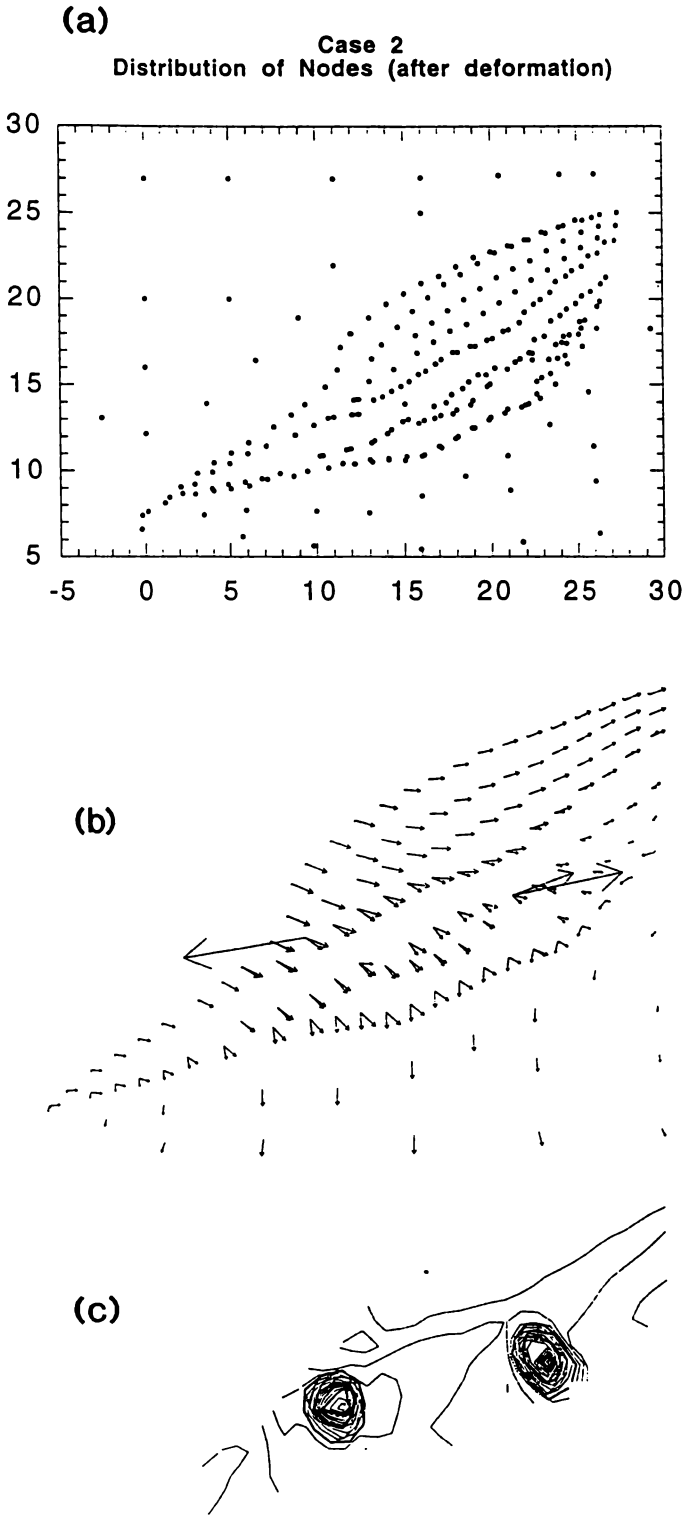

Figure 5.2: Distribution of nodes (Figure 5.2a), displacement field (Figure 5.2b), and contour of displacements (Figure 5.2c) for Case 2.

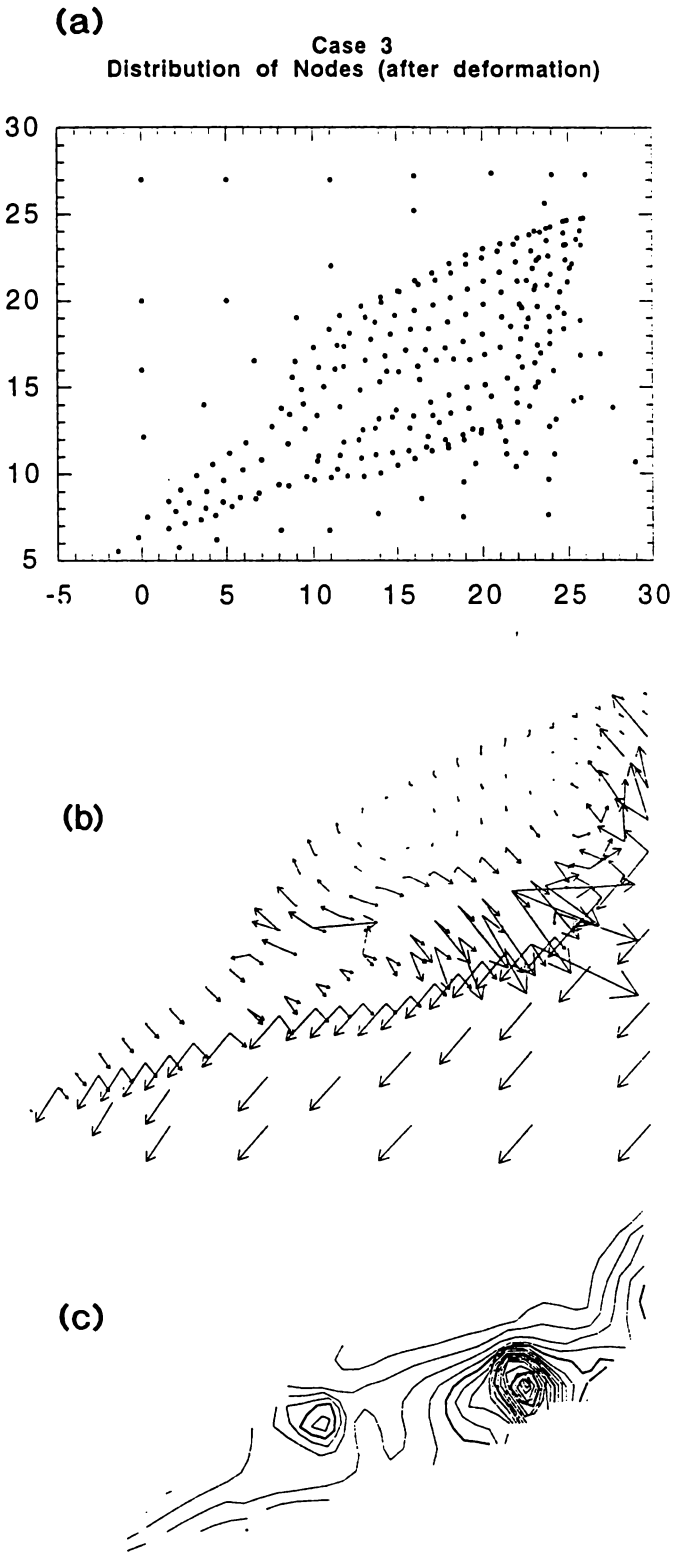

Figure 5.3: Distribution of nodes (Figure 5.3a), displacement field (Figure 5.3b), and contour of displacements (Figure 5.3c) for Case 3.

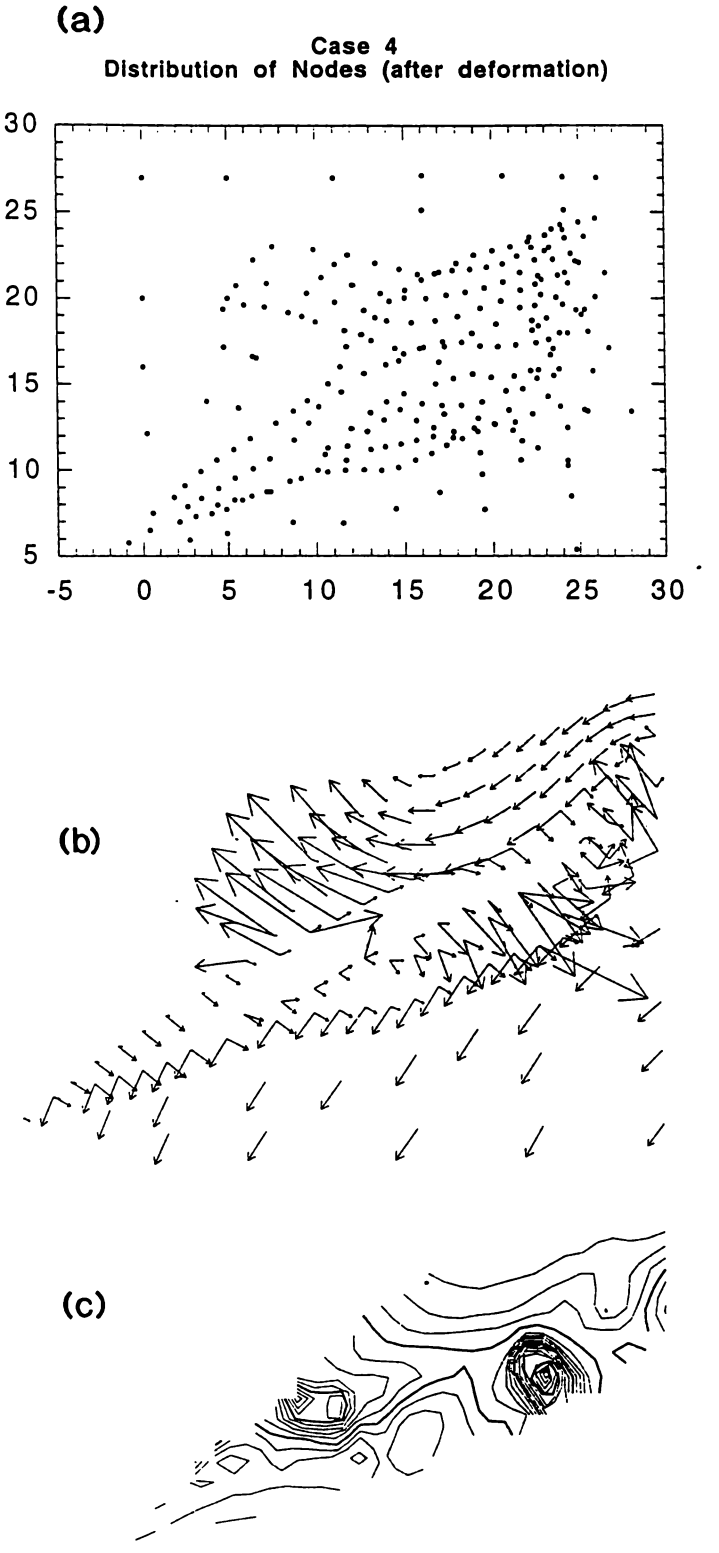

Figure 5.4: Distribution of nodes (Figure 5.4a), displacement field (Figure 5.4b), and contour of displacements (Figure 5.4c) for Case 4.

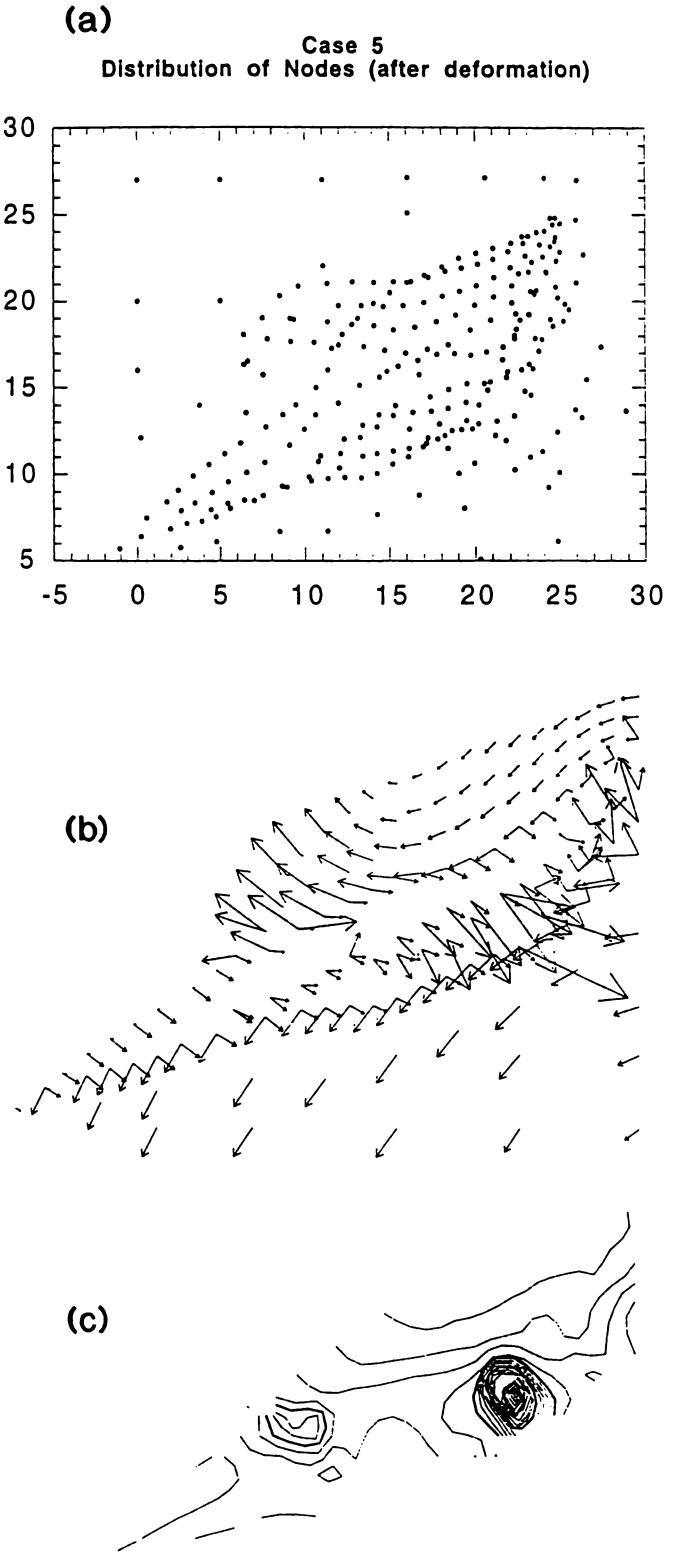

Figure 5.5: Distribution of nodes (Figure 5.5a), displacement field (Figure 5.5b), and contour of displacements (Figure 5.5c) for Case 5.

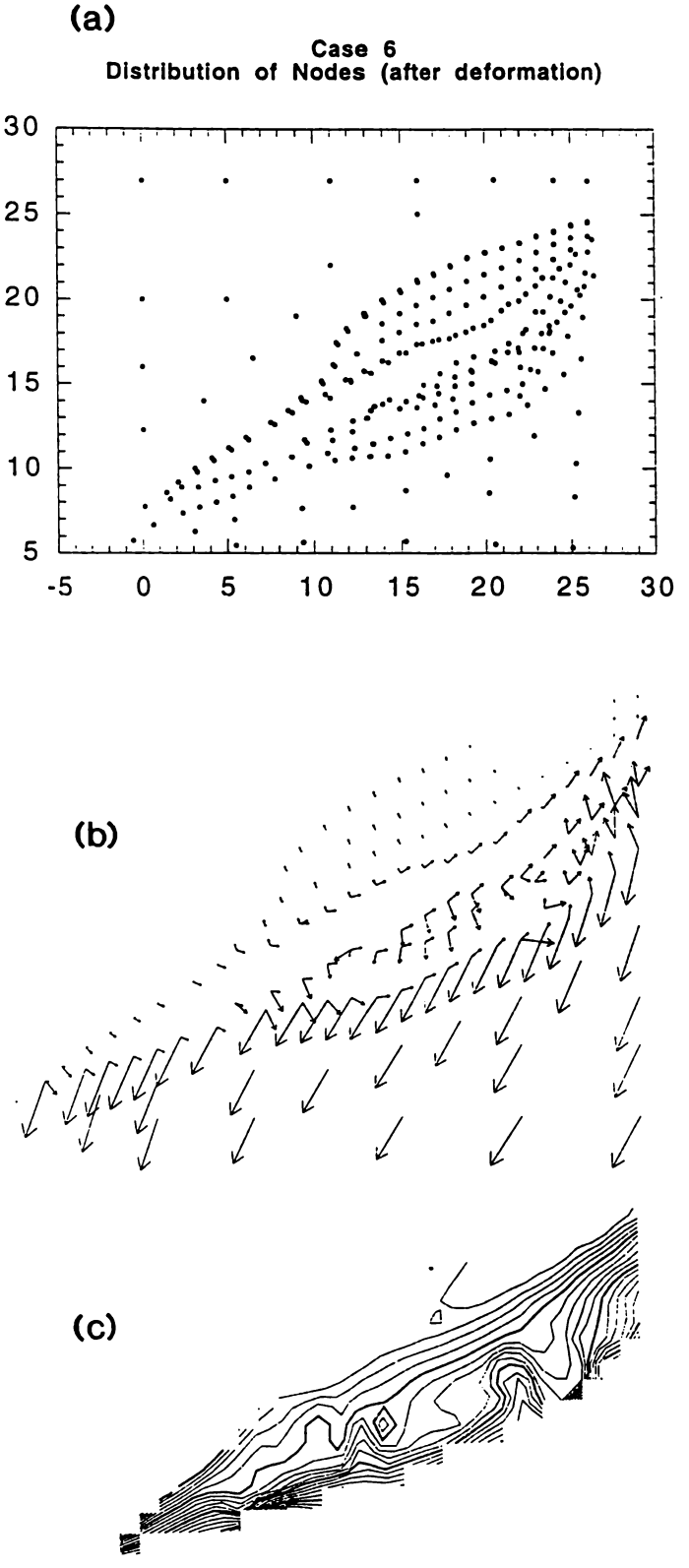

Figure 5.6: Distribution of nodes (Figure 5.6a), displacement field (Figure 5.6b), and contour of displacements (Figure 5.6c) for Case 6.

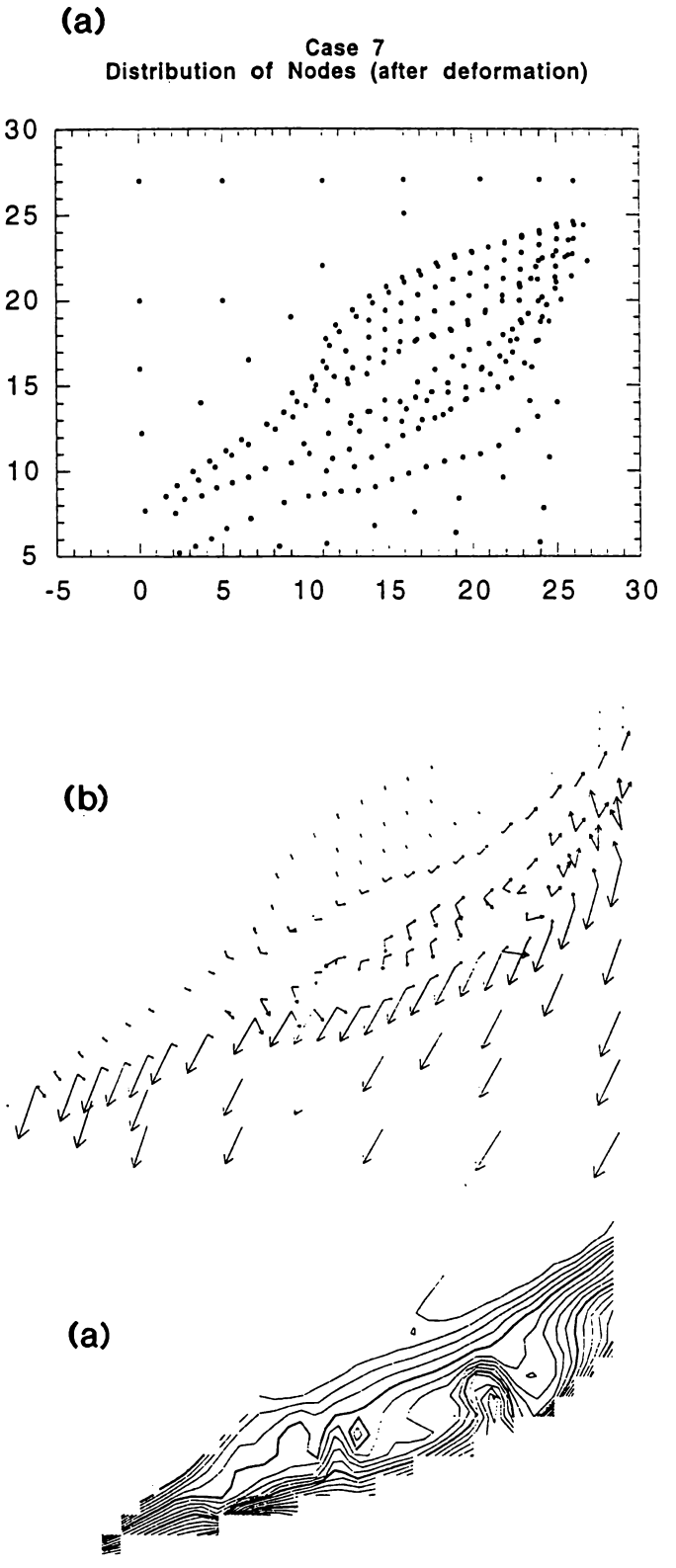

Figure 5.7: Distribution of nodes (Figure 5.7a), displacement field (Figure 5.7b), and contour of displacements (Figure 5.7c) for Case 7.

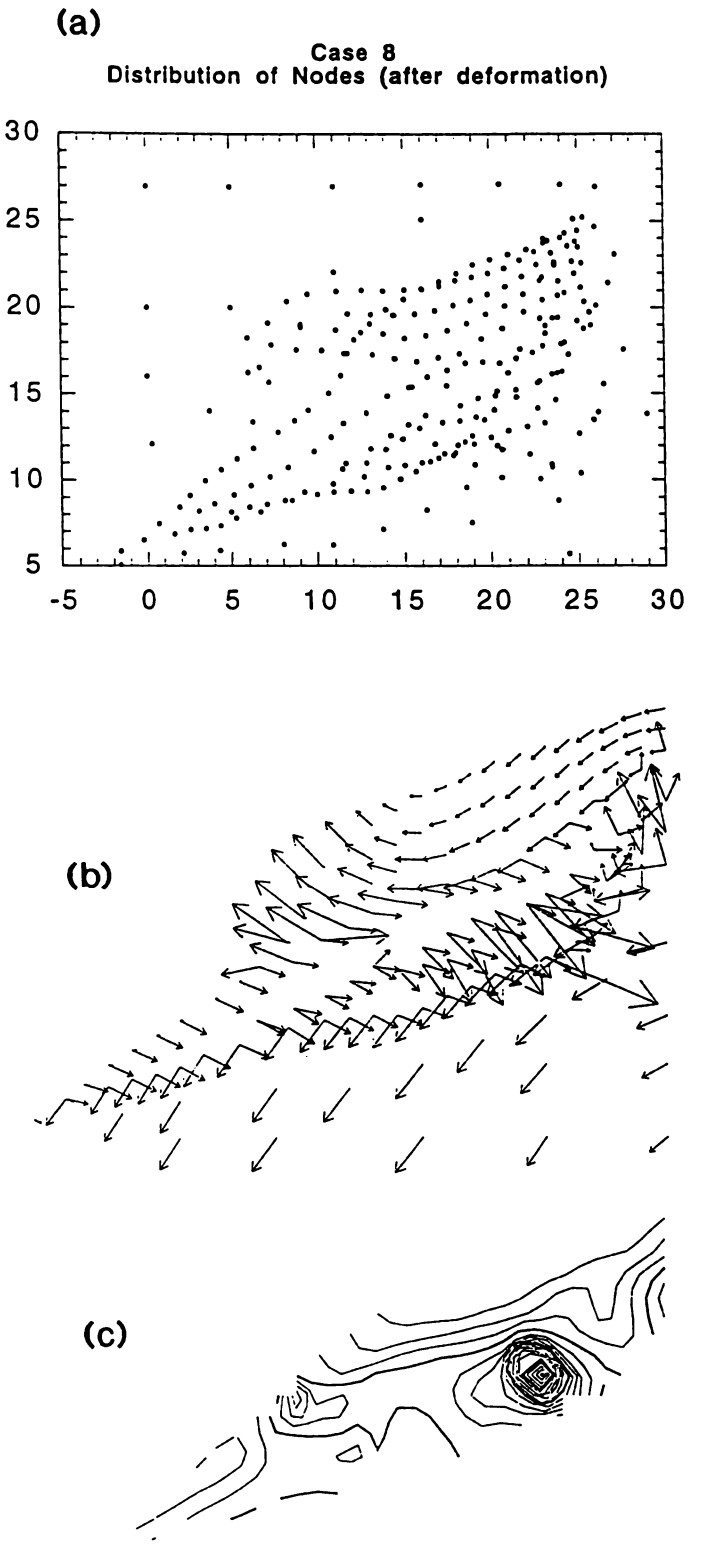

Figure 5.8: Distribution of nodes (Figure 5.8a), displacement field (Figure 5.8b), and contour of displacements (Figure 5.8c) for Case 8.

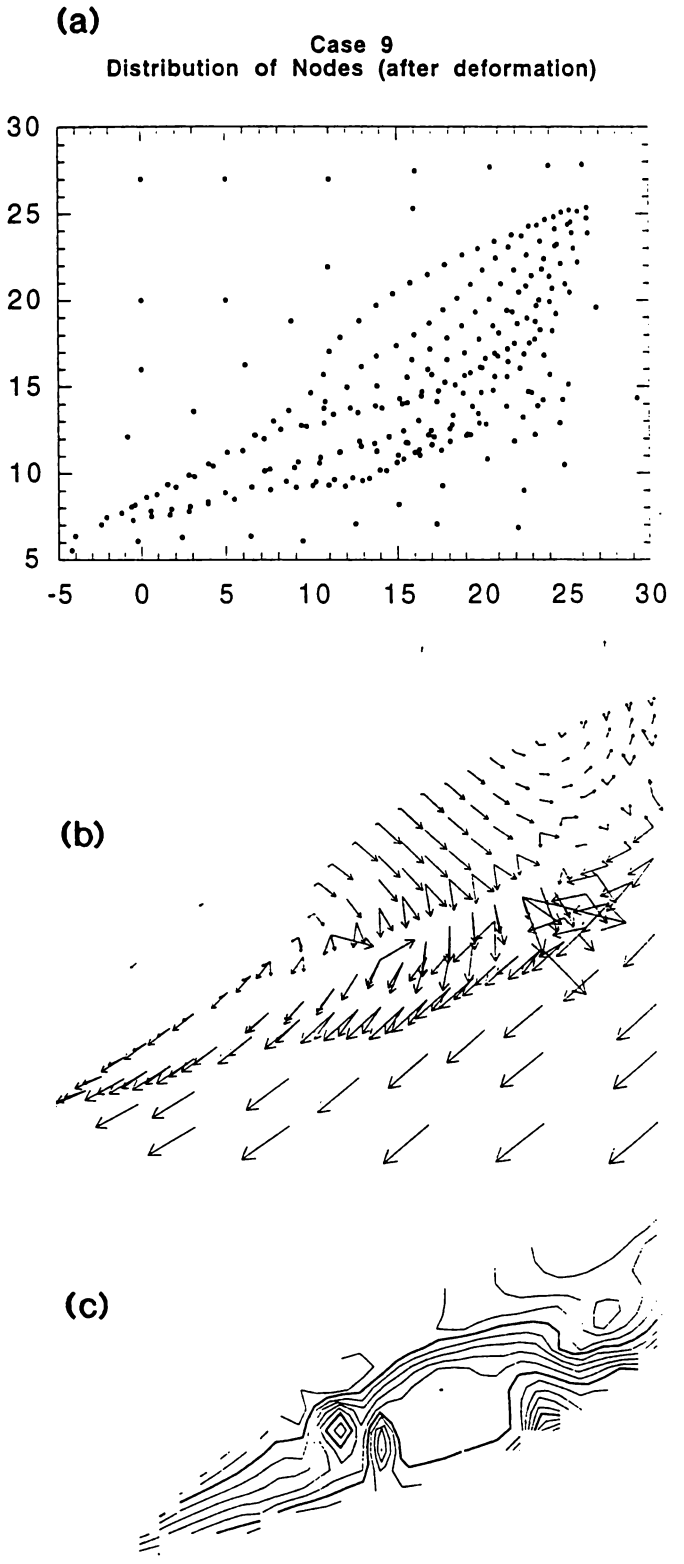

Figure 5.9: Distribution of nodes (Figure 5.9a), displacement field (Figure 5.9b), and contour of displacements (Figure 5.9c) for Case 9.

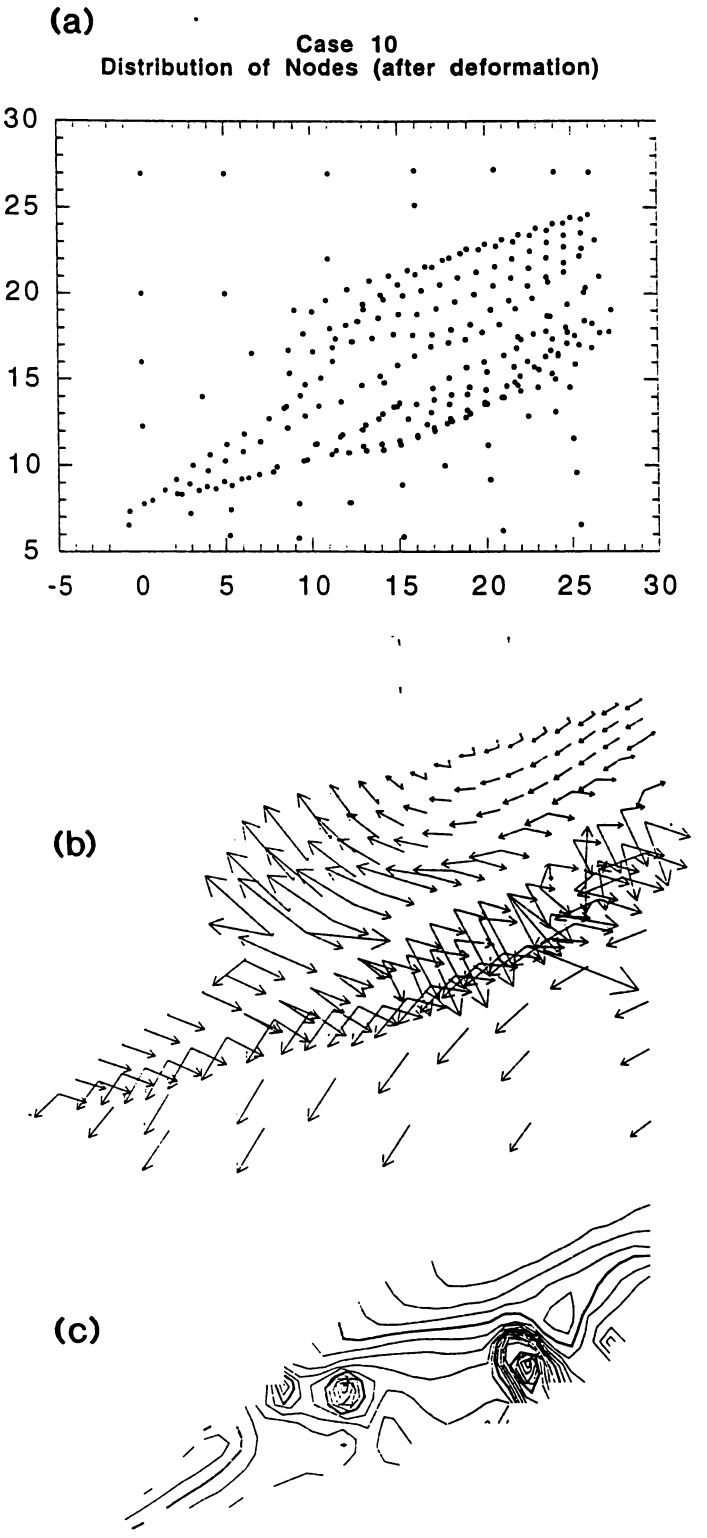

Figure 5.10: Distribution of nodes (Figure 5.10a), displacement field (Figure 5.10b), and contour of displacements (Figure 5.10c) for Case 10.

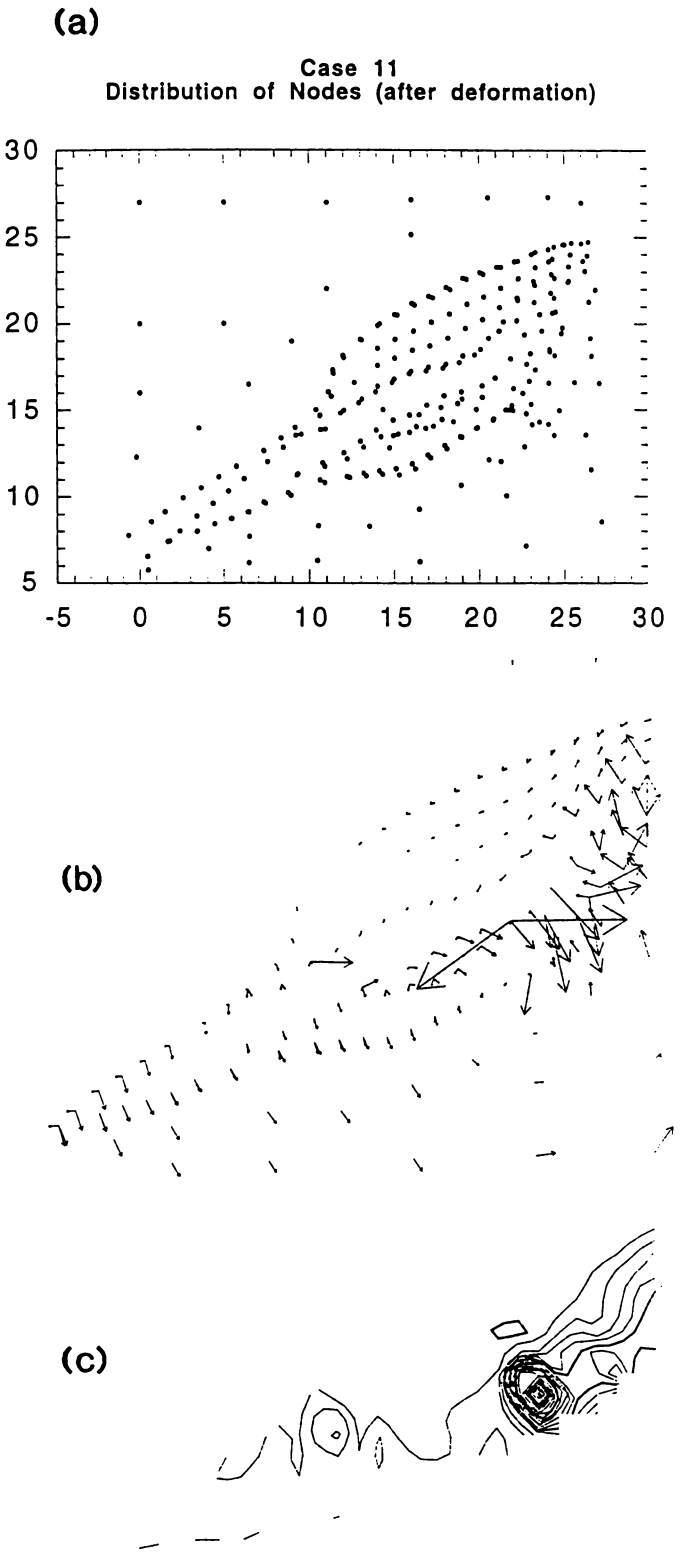

Figure 5.11: Distribution of nodes (Figure 5.11a), displacement field (Figure 5.11b), and contour of displacements (Figure 5.11c) for Case 11.

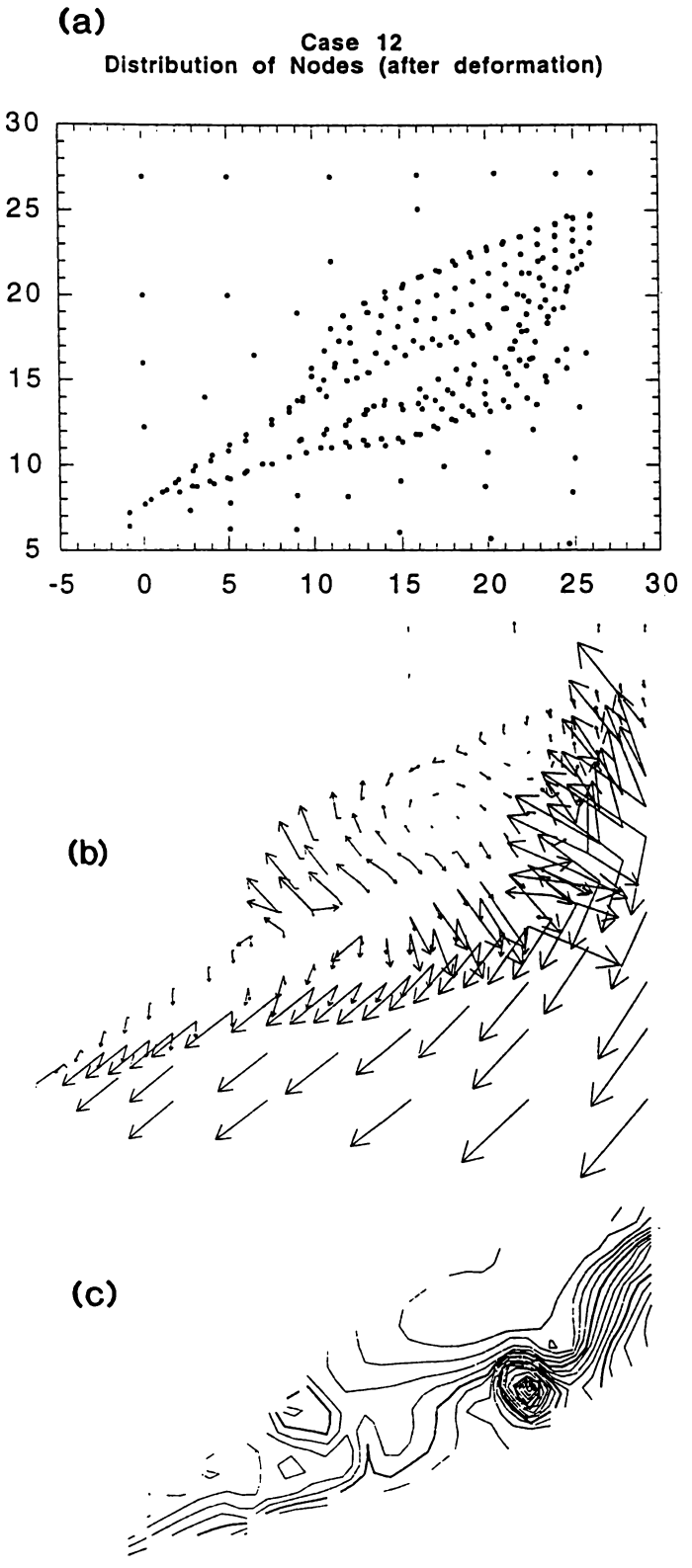

Figure 5.12: Distribution of nodes (Figure 5.12a), displacement field (Figure 5.12b), and contour of displacements (Figure 5.12c) for Case 12.

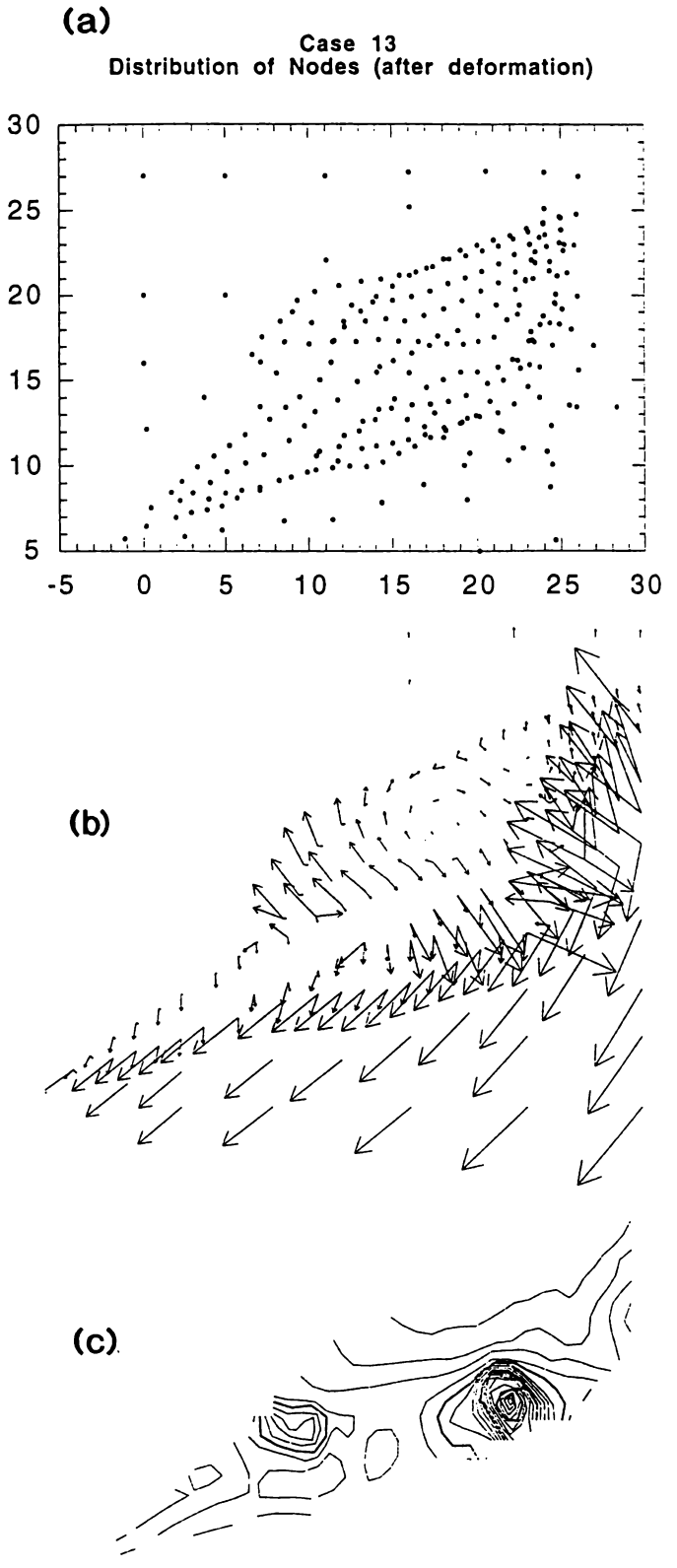

Figure 5.13: Distribution of nodes (Figure 5.13a), displacement field (Figure 5.13b), and contour of displacements (Figure 5.13c) for Case 13.

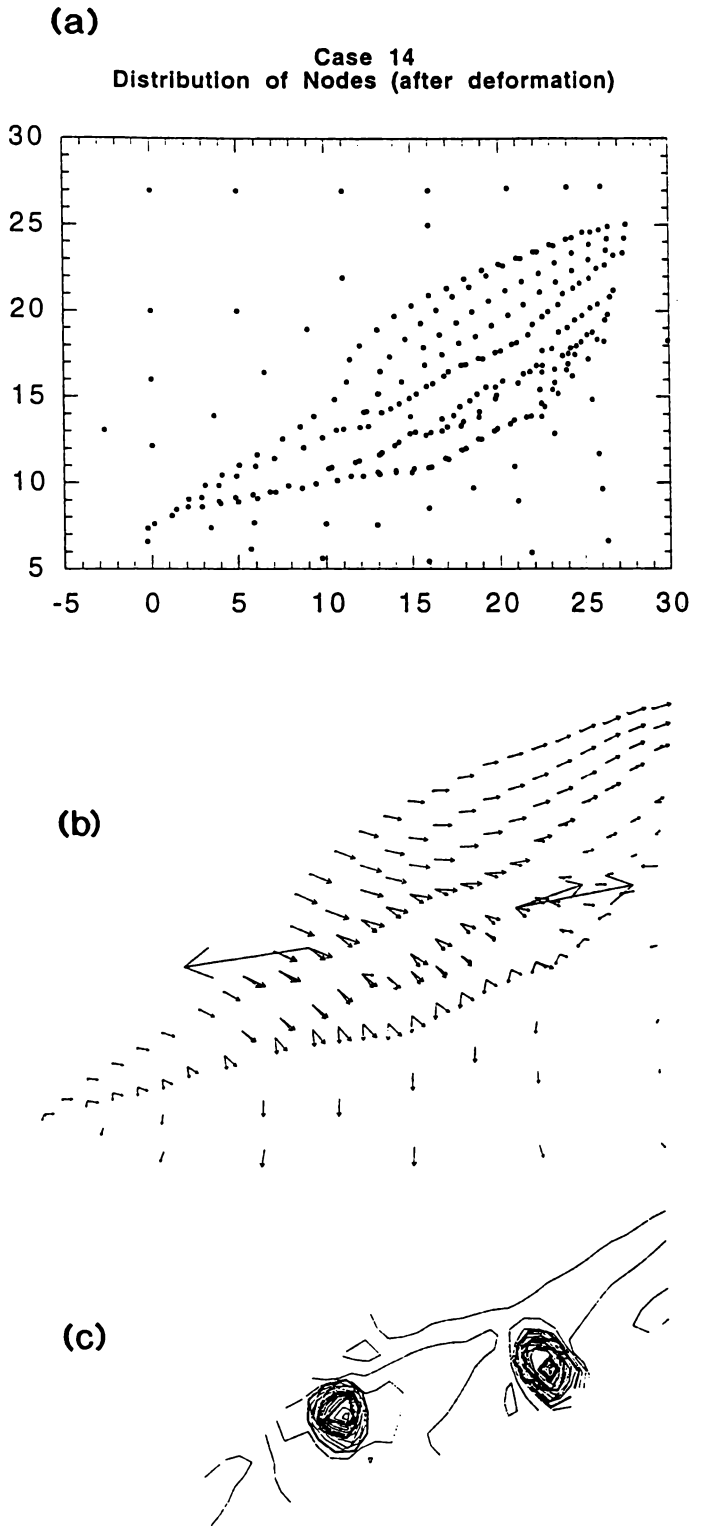

Figure 5.14: Distribution of nodes (Figure 5.14a), displacement field (Figure 5.14b), and contour of displacements (Figure 5.14c) for Case 14.

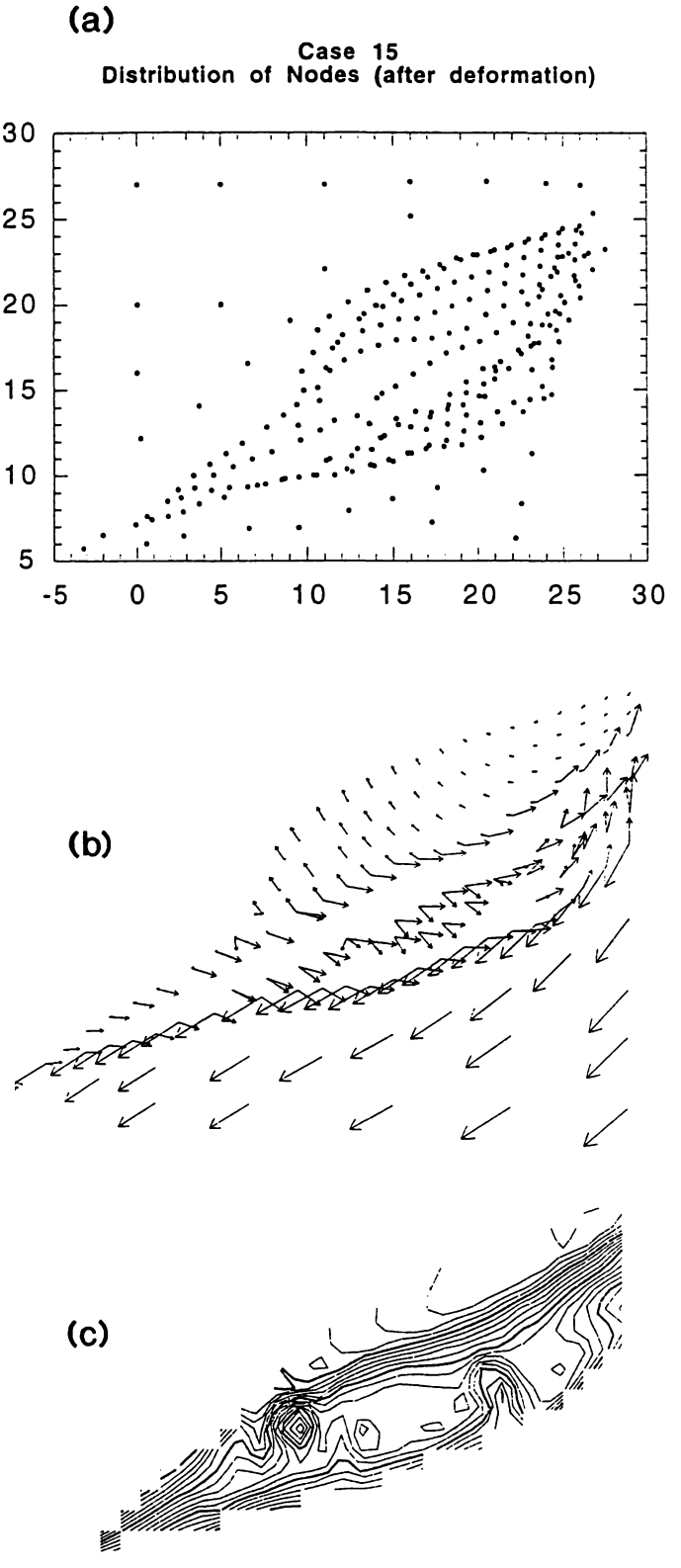

Figure 5.15: Distribution of nodes (Figure 5.15a), displacement field (Figure 5.15b), and contour of displacements (Figure 5.15c) for Case 15.

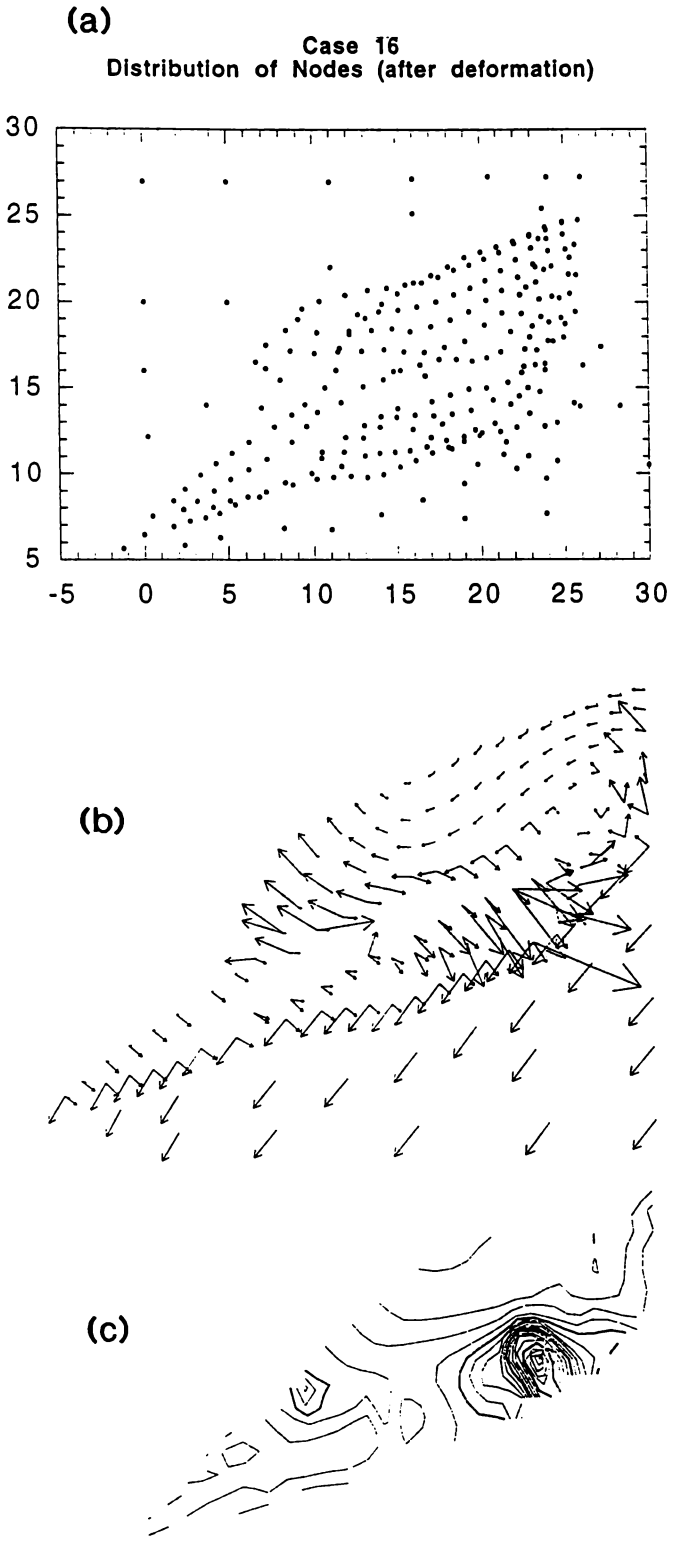

Figure 5.16: Distribution of nodes (Figure 5.16a), displacement field (Figure 5.16b), and contour of displacements (Figure 5.16c) for Case 16.

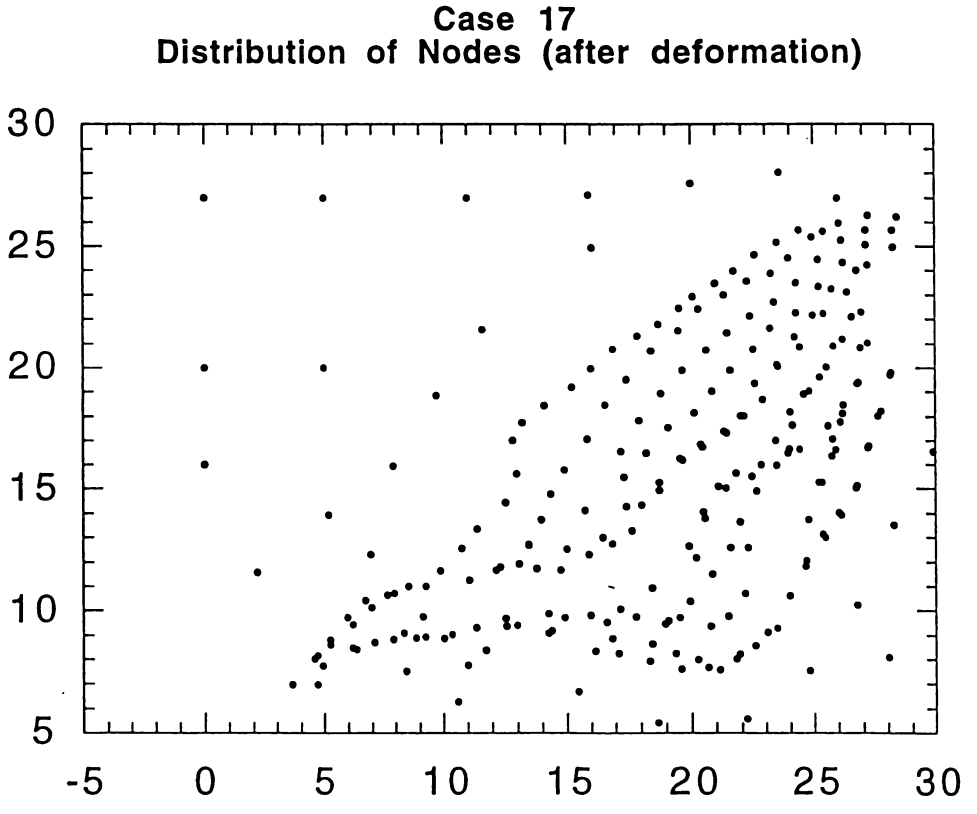

Figure 5.17: Distribution of nodes (after deformation) for Case 17.

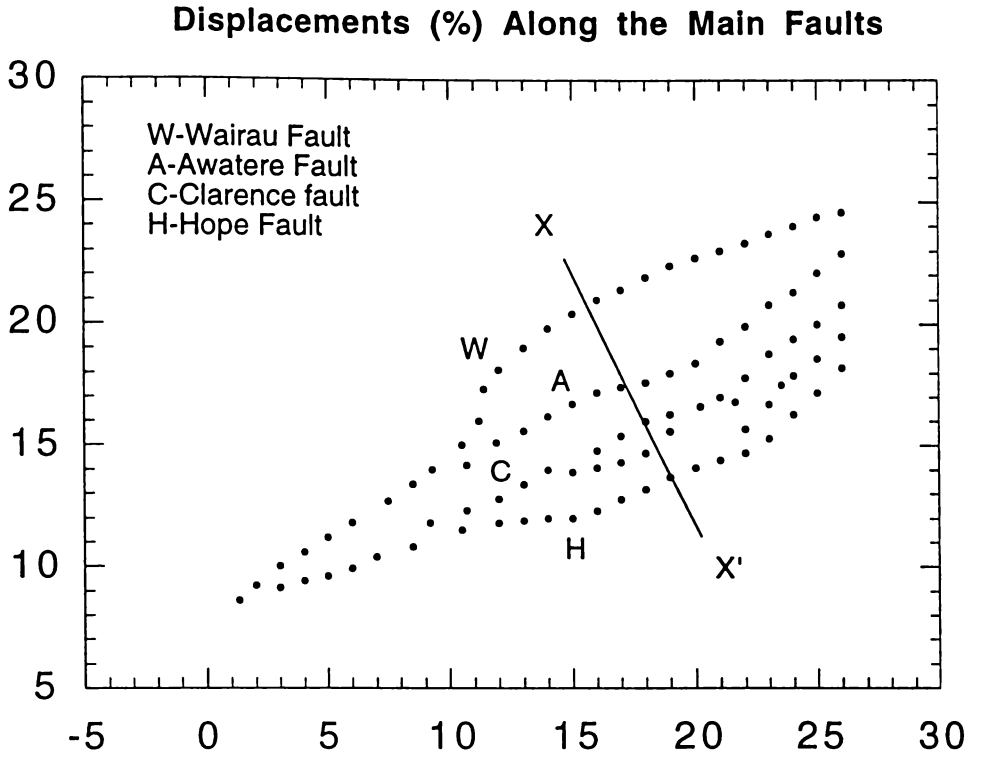

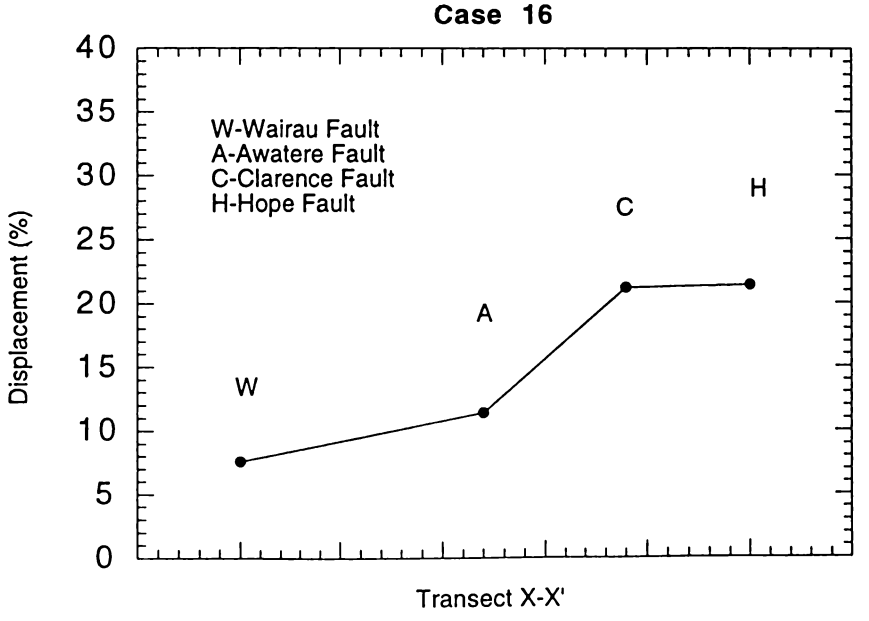

Figures 5.18: (a) Transect XX', (b) Current displacement (%) of the Marlborough Faults.

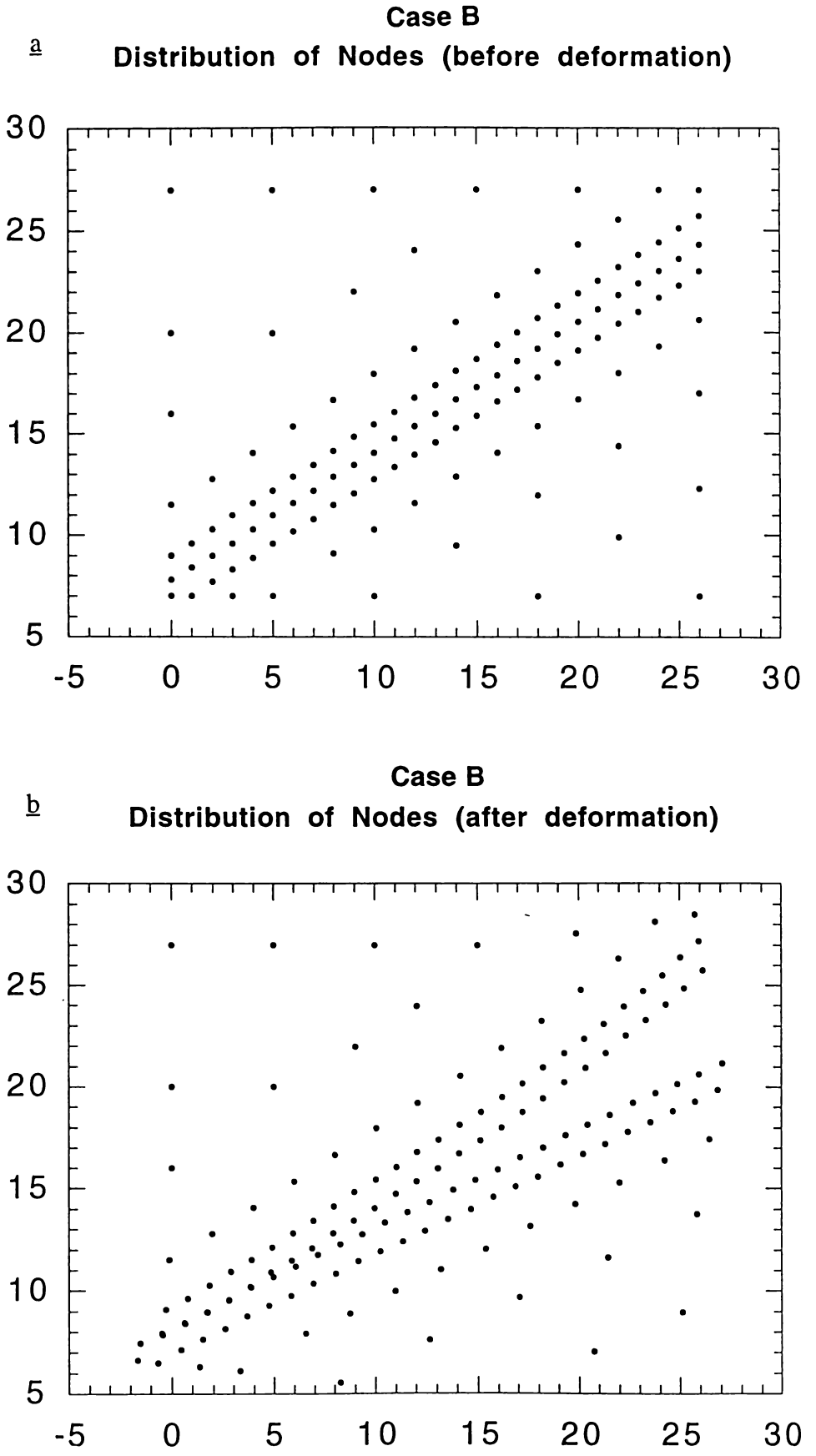

Figure 5.19: Distribution of nodes (Figure 5.19a, before deformation), and distribution of nodes (Figure 5.19b, after deformation) for Case B.

Case C
Distribution of Nodes (before deformation)

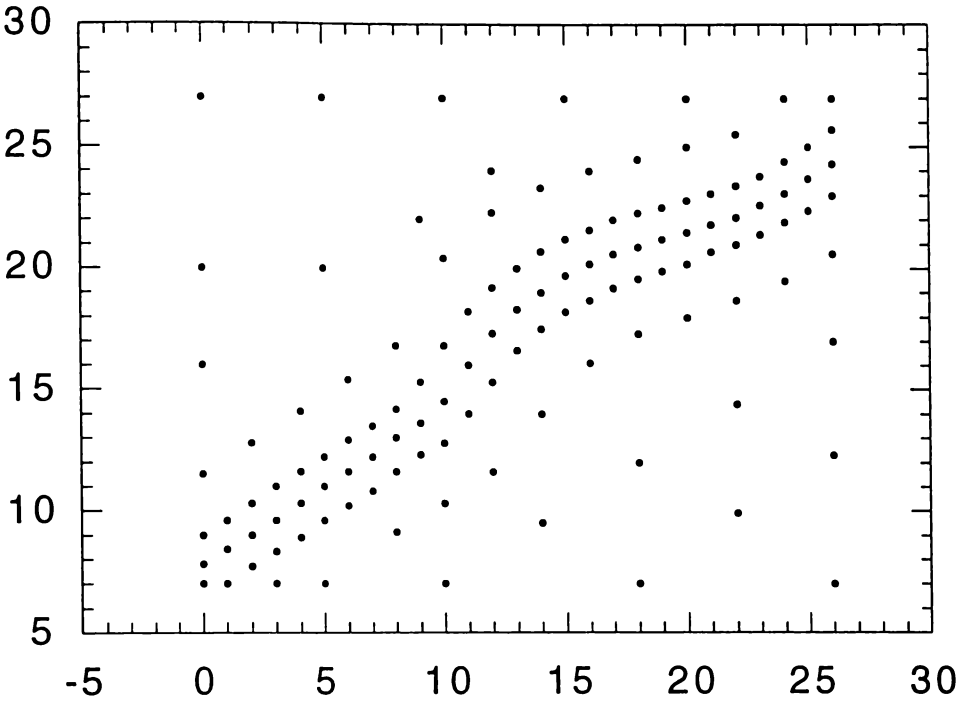

Fig 5.20a

Case C-1
Distribution of Nodes (after deformation)

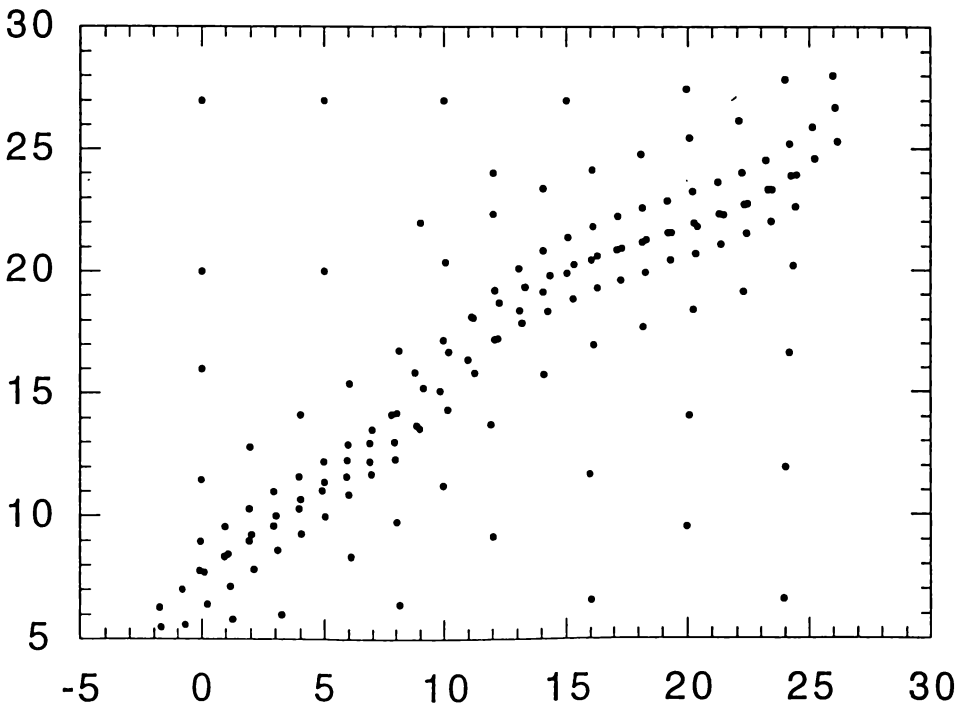

Fig. 5.20b

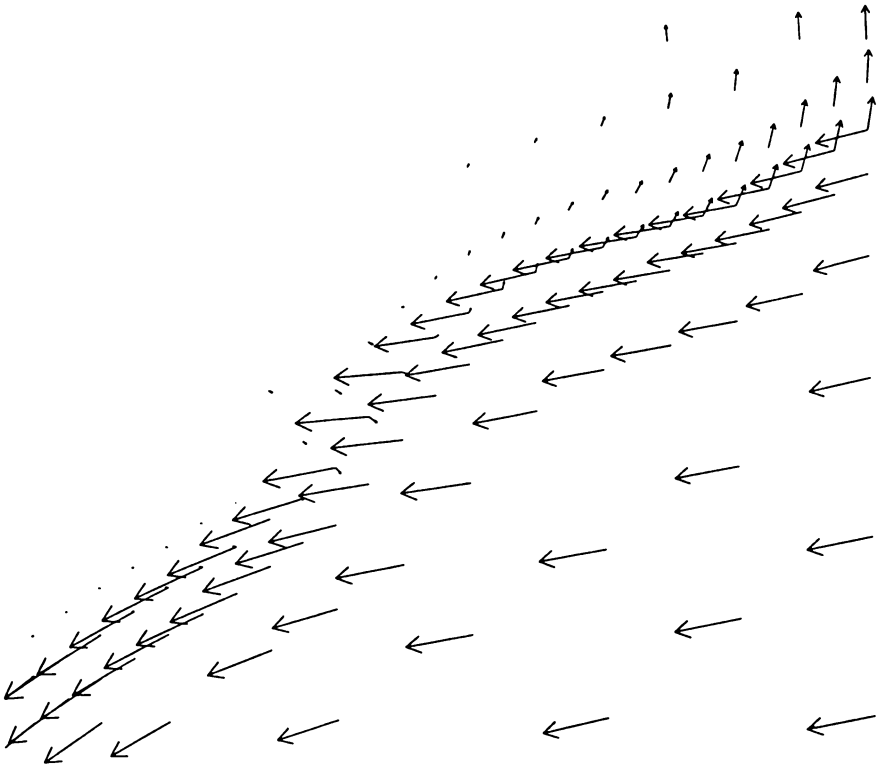

Fig. 5.20c

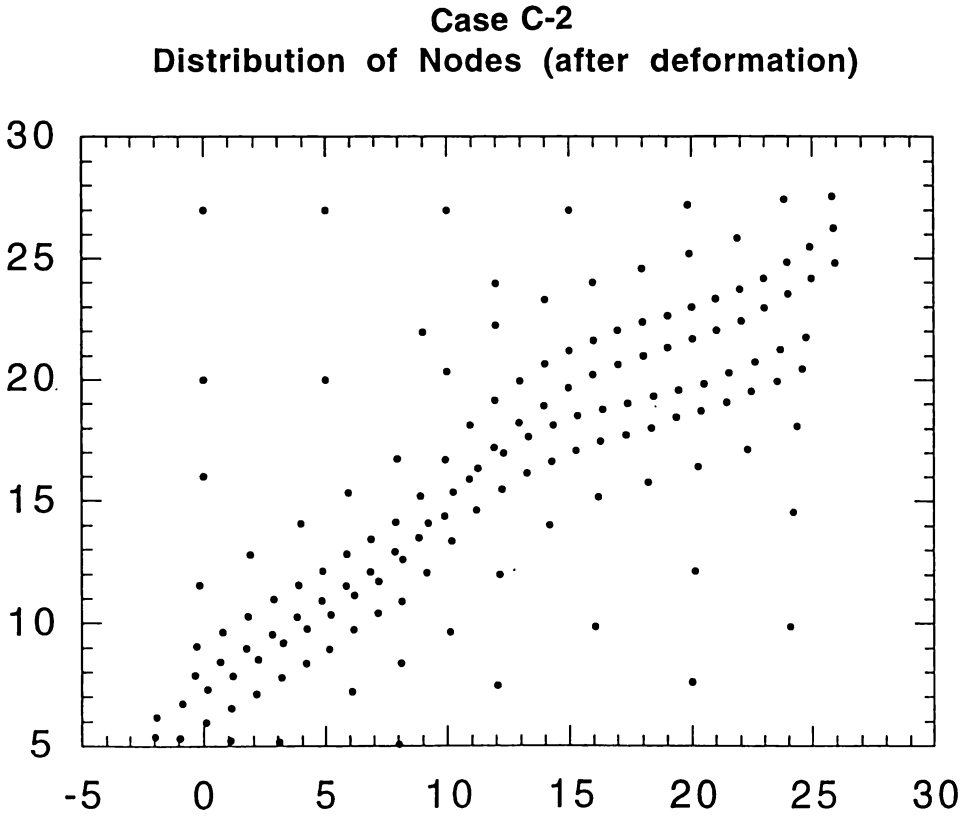

Fig. 5.20d

Figure 5.20: Distribution of nodes (Figure 5.20a, before deformation), displacement field for Case C-1 (Figure 5.20c), and distribution of nodes (Figures 5.20b,d, after deformation) for Case C.

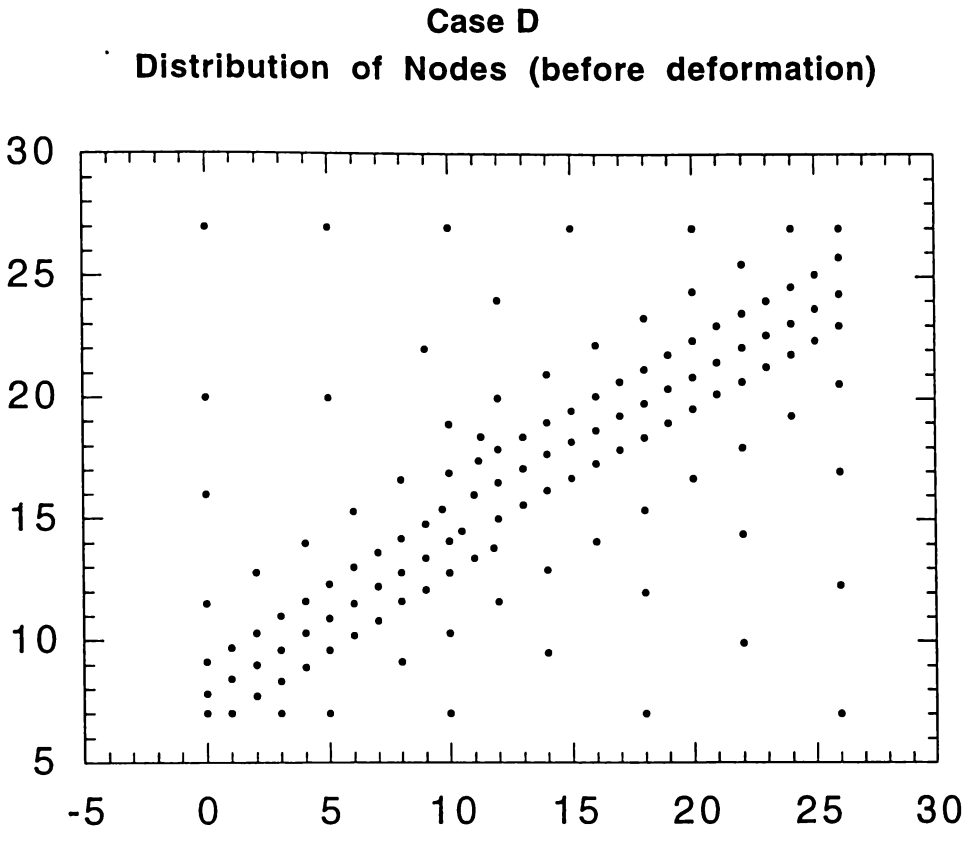

Fig 5.21a

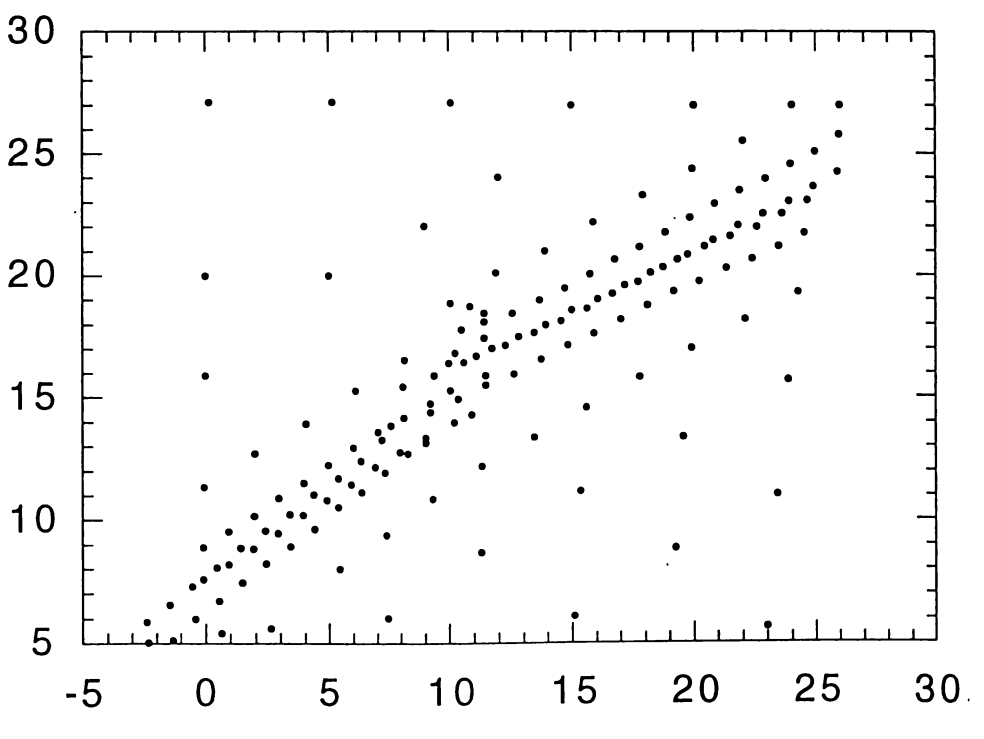

Fig. 5.21b

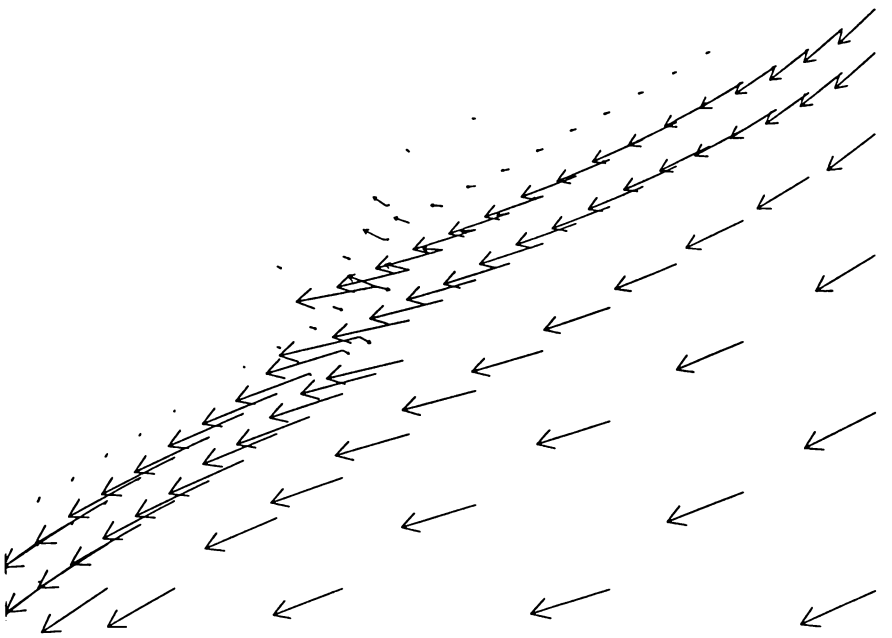

Fig. 5.21c

Figure 5.21: Distribution of nodes (Figure 5.21a, before deformation), displacement field (Figure 5.21c), and distribution of nodes (Figure 5.21b, after deformation) for Case D.

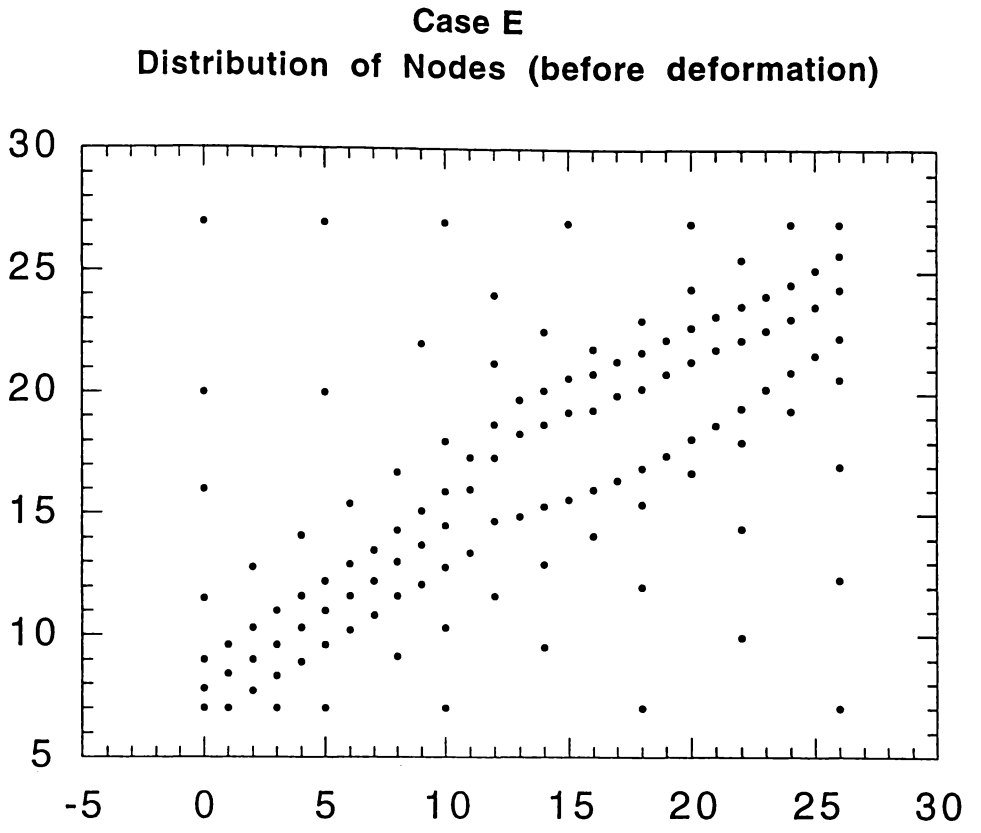

Fig 5.22a

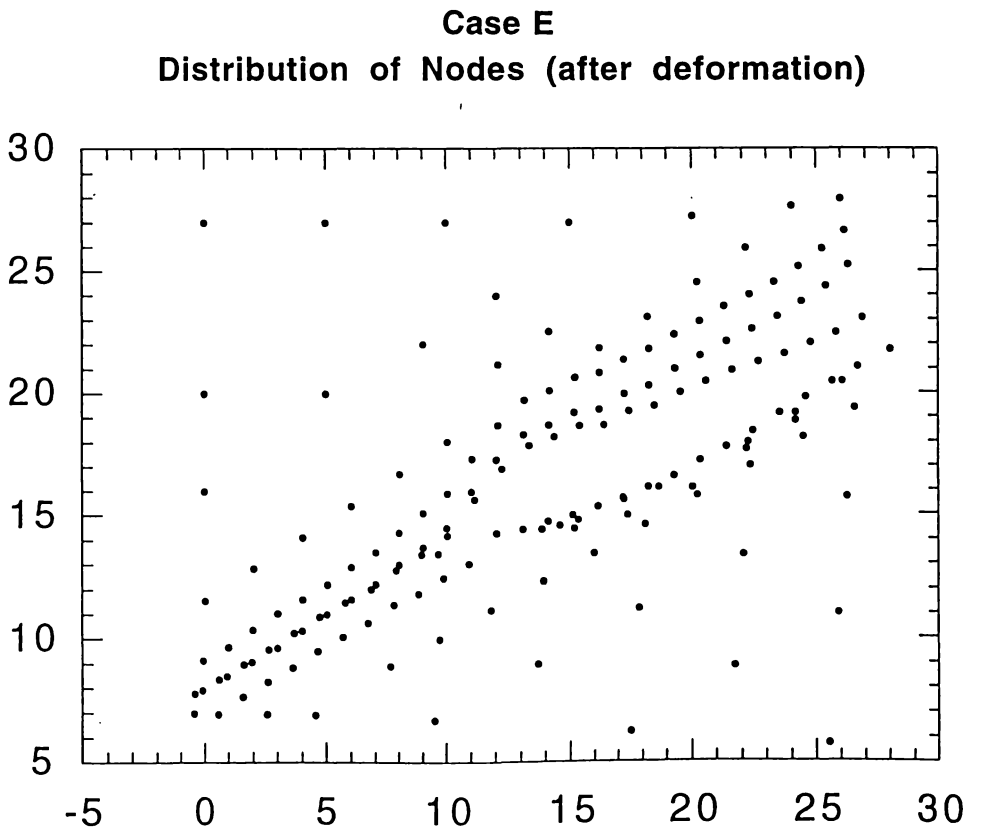

Fig. 5.22b

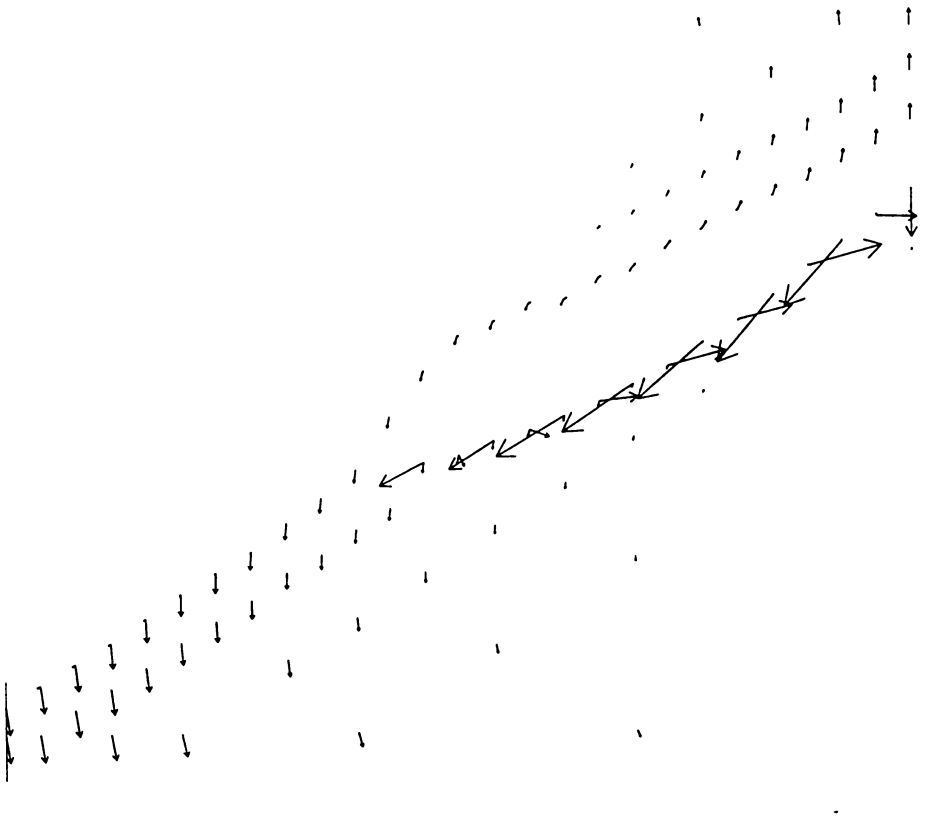

Fig. 5.22c

Figure 5.22: Distribution of nodes (Figure 5.22a, before deformation), displacement field (Figure 5.22c), and distribution of nodes (Figure 5.22b, after deformation) for Case E.

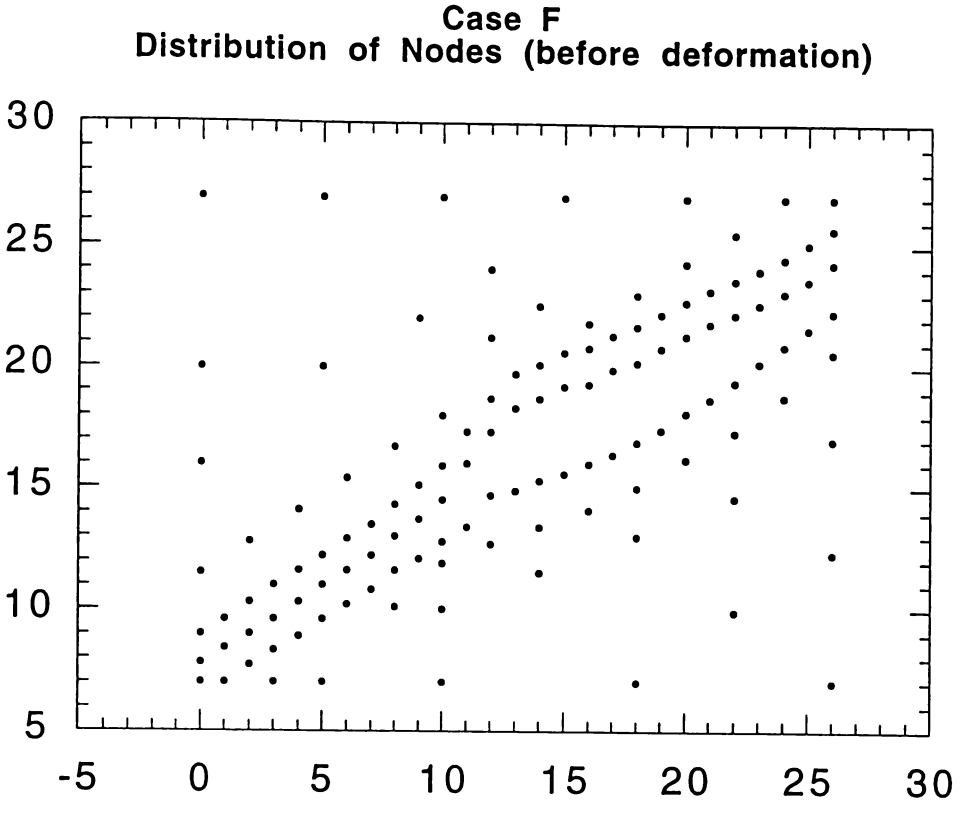

Fig 5.23a

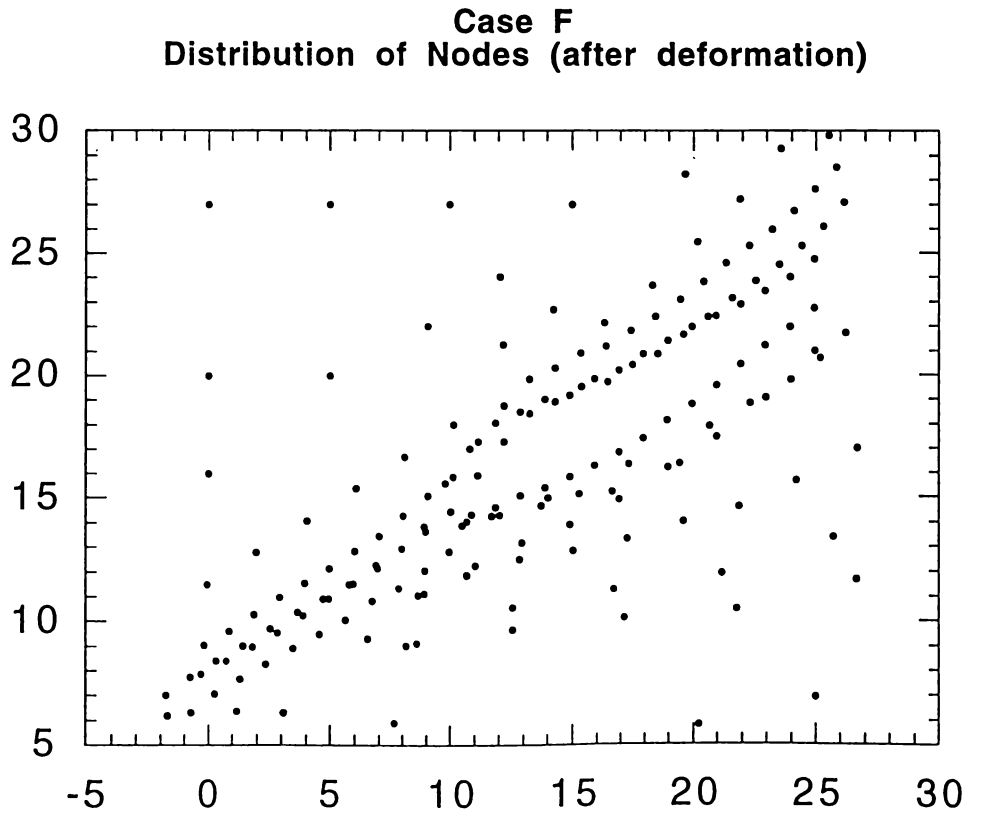

Fig. 5.23b

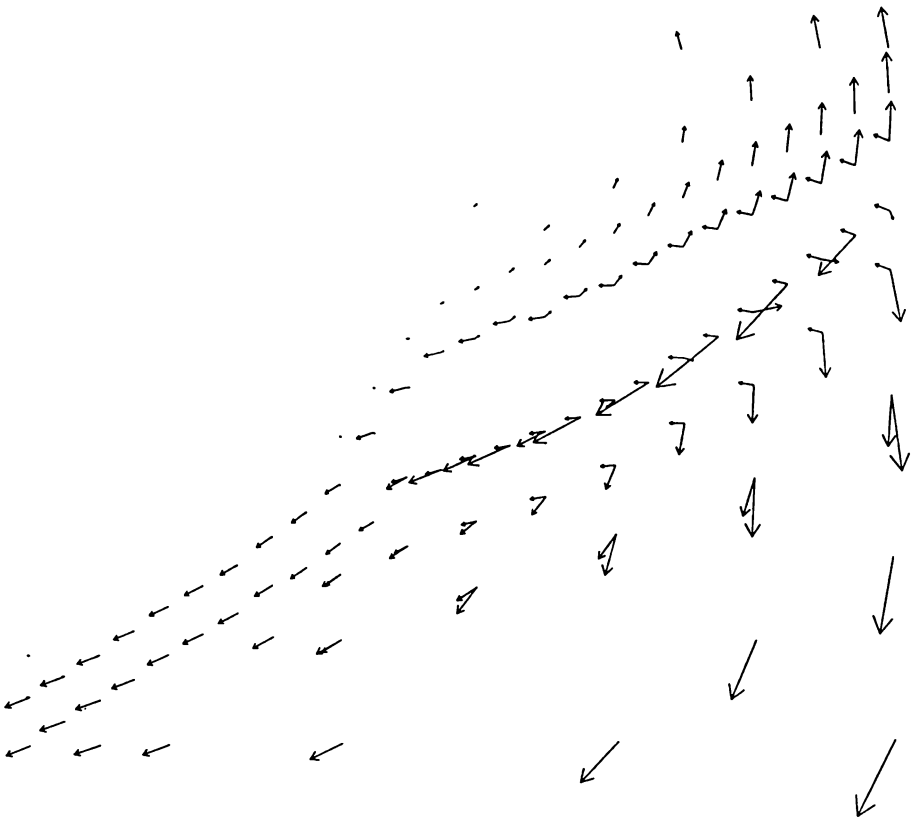

Fig. 5.23c

Figure 5.23: Distribution of nodes (Figure 5.23a, before deformation), displacement field (Figure 5.23c), and distribution of nodes (Figure 5.23b, after deformation) for Case F.

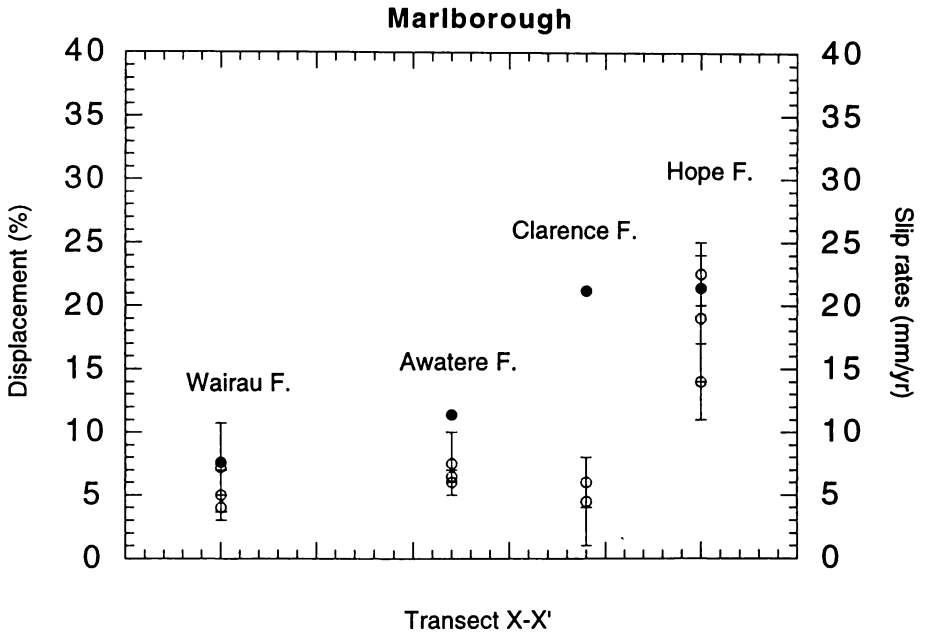

Figure 5.24 Current displacement (close circle) and slip rates (open circle), which are listed in Table 5.4.

Chapter 6

Fission Track Results and their Interpretation

Chapter 6

Fission Track Results and their Interpretation

6.1 Introduction

Apatite fission track thermochronology is a powerful method for establishing low-temperature thermal histories of rock successions (Naeser, 1979b; Laslett et al., 1987; Green et al., 1989b). In this chapter, application of fission track analysis is applied to assess the thermal and tectonic history of basement in Marlborough. The results of apatite and zircon fission track data will be discussed in several geological blocks and transects. Additionally, the fission track thermal history modelling software (Monte Trax), developed by Gallagher (1995), is applied to reconstruct the thermal histories of selected samples with good track length data. Maximum paleotemperatures and hence the amounts of denudation can be obtained by this modelling approach. For those samples for which there is insufficient length data to enable Monte Trax modelling to be undertaken, maximum temperatures are estimated from an apatite fission track age verus maximum temperature relationship established for samples that could be modelled sucessfully. Maximum temperatures are converted into amount of denudation by assuming a paleothermal gradient value of 20°C/km (Kamp, 1997).

6.2 Sampling strategy and experimental procedures

6.2.1 Sampling strategy

One hundred and twelve samples (9414-1 to -112) were collected from outcrops along roads throughout Marlborough, or by helicopter from the Seaward Kaikoura Range. Except for the twenty-four samples (9414-89 to -112) located in the Marlborough Sounds region, most of the samples were taken from within the Marlborough Fault System and the region of the Alpine Fault bend. They can be divided into five sub-regions and nine transects for this study (Figure 6.1). The five sub-regions are: the Wairau, Inland Kaikoura, Seaward Kaikoura , Kahutara, and Marlborough Sounds blocks. The five transects along the blocks are: the Wairau (T1), Inland Kaikoura (T2), Seaward Kaikoura (T3), Kahutara (T4), and the Marlborough Sounds transects (IJ). The four transects crossing the Marlborough Fault

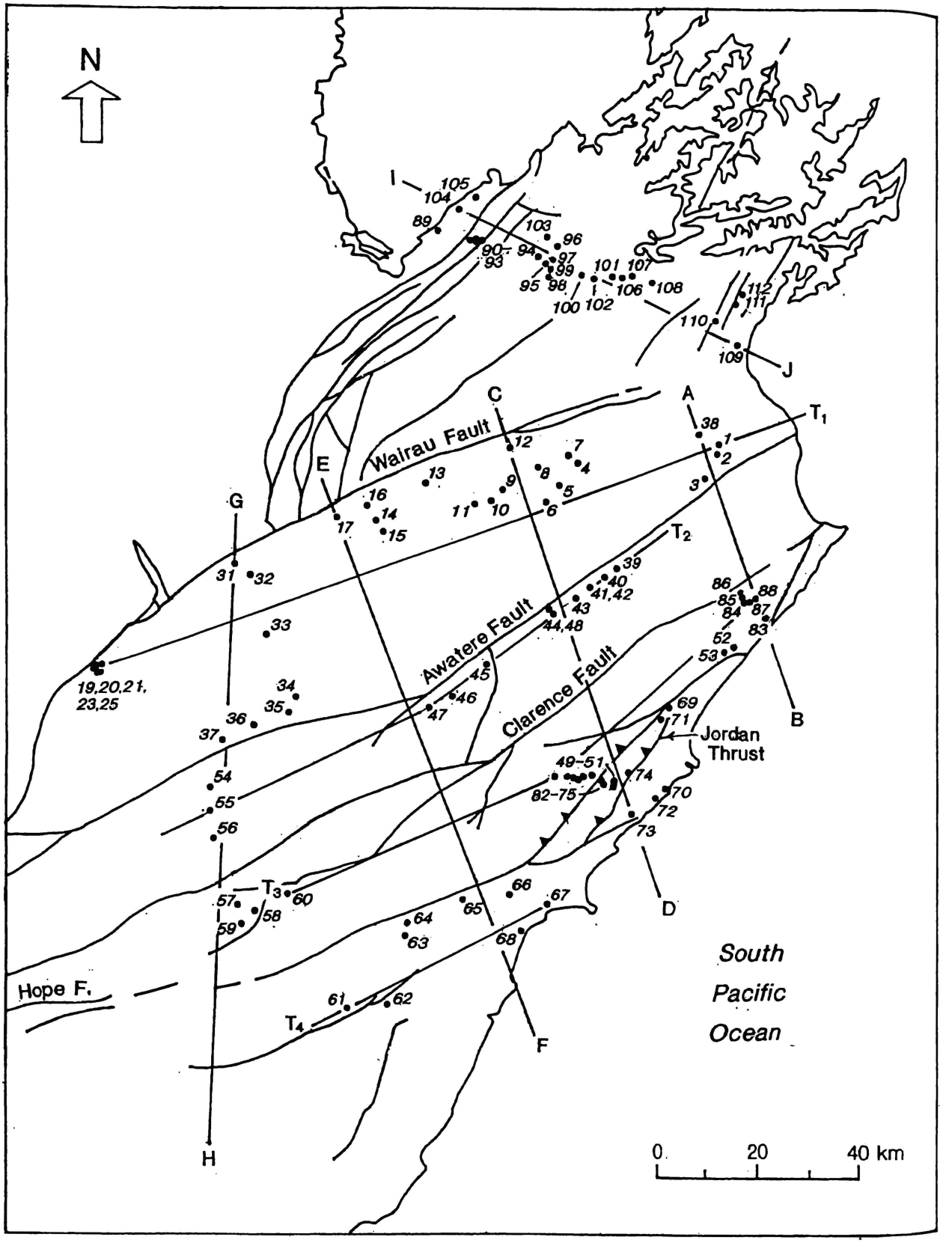

Figure 6.1 Locations of samples, transects, and sub-regions used in this study.

System are: the Blenheim (AB), Kaikoura-1 (CD), Kaikoura-2 (EF), and Spenser Mountains (GH) transects.

6.2.2 Experimental procedures

The experiment procedures applied in this study were followed using the methods described in the papers of Green (1986), Kamp et al. (1989), and Tippett and Kamp (1993). Apatite and zircon concentrates separated from rock samples (~3 to 4 kg) were obtained by various methods, including standard magnetic and heavy liquid techniques. The apatite concentrates were mounted in Petropoxy™ resin at ~140°C on glass slides and ground with silicon carbide paper to disclose internal crystal surfaces. After polishing with a slurry of alumina powder, the crystals were then etched in 5 M HNO_3 for 20s at ~24°C.

Zircon concentrates were mounted in FEP Teflon™ at ~ 300°C and ground to reveal internal surfaces. Once ground, zircon separates were polished with alumina slurry and then 1- μm diamond paste. The zircons mounts were etched in molten KOH-NaOH eutectic at ~ 205°C. The time of etching ranged from 16 to 56 hours. Finally, zircon mounts were cleaned by placing them in dilute HF for 1 hour.

The following procedures were followed: (a) all mounts were cut to 1 x 1.5 cm and cleaned with detergent and alcohol, (b) low-uranium mica external detectors were sealed directly in contact with the mounts by using envelopes of heat-shrink plastic, (c) pinpricks were made at the corners of each mount-mica sandwich for subsequent location, (d) all mounts were stacked vertically with dosimeter glass standards (SRM 612 for apatites, CN1 for zircons) placed at the top and bottom of each stack for irradiation. Each dosimeter was also mounted with a mica detector. Afterwards, all stacks were packed into canisters and irradiated in the X-7 facility of the HIFAR reactor, New South Wales, Australia. The nominal fluences of thermal neutrons were: 1 x 10^{16} neutrons cm^{-2} to 5 x 10^{16} neutrons cm^{-2} for apatites, and 3 x 10^{-15} neutrons cm^{-2} for zircons.

In this study, the external detector method described by Gleadow (1981) was applied in the dating. The fission track ages were determined by using the zeta calibration method (Hurford and Green 1982; Green, 1985). The measurement of fission track lengths was followed by using the recommendations of Laslett et al. (1982). A chi-square statistic was

used to determine the probability of grains counted in a sample belonging to a single population of ages (Galbraith, 1981). The results of weighted mean zetas are reported in Table 6.1: apatite weighted mean ζ = 348.4 ± 5.8 (SRM 612), zircon weighted mean ζ = 140.2 ± 3.6 (CN1). The results of calibration of horizontally confined track length determinations on apatite are listed in Table 6.2.

6.3 Fission track results and interpretation

Both apatite and zircon fission track results reveal that the fission track data are strongly influenced by the regional tectonics. The fission track data for Marlborough samples are shown in Table 6.3. The distribution of apatite fission track ages is illustrated in Figure 6.2. The distributions of apatite single-grain fission track ages and track lengths are shown in Figures 6.3 and 6.4. Uncertainties of fission track ages are reported at the 1σ level. The distributions of zircon fission track ages for samples are illustrated in Figure 6.5.

6.3.1 Apatite fission track age versus mean track length

Figure 6.6 is a plot of mean track length versus apatite age for samples originating in Marlborough from south of the Wairau Fault. It is useful to examine the data together in this plot before considering the data in transects, because it should reveal broad patterns about the occurrences of annealing zones and the timing of significant cooling events (e.g. Green, 1986).

A general boomerang trend is evident in the data, although there are complexities in the pattern for samples with 90 million years or more of age. Samples with very young (<10 Ma) ages have long lengths (>15 μm), reflecting very recent and rapid cooling of the host rocks from temperatures exceeding the closure temperature of fission tracks in apatite (taken as 110 °C). The decrease in mean track length with increasing age from 10 Ma to around 67 Ma is due to a change of the proportion of shorter tracks, annealed during burial (heating) of the basement leading up to a late Cenozoic regional cooling event, versus longer tracks formed during the late Cenozoic cooling phases and contributing to the total mean length. This component of the boomerang originates through different samples experiencing increasing levels of partial annealing as the age decreases and length increases. There is a

Table 6.1 Results of calibration of fssion track age determinations by the zeta apporoah.

Age Standard and Irradiation No.	Mineral (No. of crystals)	Spontaneous ρ_s	Spontaneous N_s	Induced ρ_i	Induced N_i	$P(\chi^2)$ %	Glass	Dosimeter ρ	Dosimeter N_d	$\zeta \pm 1\ \sigma$
Durango wk043	Apatite (20)	0.182	536	0.866	2548	90.6	SRM 612	0.9260	4581	323.2 ± 16.9
Durango wk044	Apatite (20)	0.186	496	0.915	2433	100	SRM 612	0.9151	4525	337.4 ± 18.2
Fish Canyon pt836	Apatite (20)	0.181	339	1.309	2452	100	SRM 612	1.1260	5570	359.2 ± 23.2
Fish Canyon pt836	Apatite (20)	0.224	209	1.456	1359	99.1	SRM 612	1.1260	5570	322.9 ± 25.7
Fish Canyon pt836	Apatite (20)	0.213	199	1.374	1281	99.0	SRM 612	1.1260	5570	319.7 ± 26.0
Fish Canyon wk043	Apatite (20)	0.186	237	1.129	1440	98.2	SRM 612	0.9151	4525	371.3 ± 28.2
Fish Canyon wk044	Apatite (20)	0.203	326	1.218	1953	73.2	SRM 612	0.9260	4581	361.8 ± 24.1
Mt Dromedary pt836	Apatite (20)	0.765	1040	1.552	2111	96.3	SRM 612	1.1260	5570	358.6 ± 14.6
Mt Dromedary pt836	Apatite (20)	0.786	1555	1.564	3094	100	SRM 612	1.1260	5570	351.5 ± 12.1
Mt Dromedary pt836	Apatite (20)	0.996	1902	1.996	3809	99.9	SRM 612	1.1260	5570	357.3 ± 7.6
Mt Dromedary pt836	Apatite (20)	0.931	1366	1.897	2784	98.5	SRM 612	1.1260	5570	360.0 ± 13.0
Mt Dromedary wk043	Apatite (20)	0.957	1528	1.465	2338	46.6	SRM 612	0.9151	4525	332.6 ± 12.2
Mt Dromedary wk044	Apatite (20)	0.624	995	1.112	1772	64.6	SRM 612	0.9260	4581	382.6 ± 16.3
									Apatite Mean ζ	348.4 ± 5.8
Buluk wk029	Zircon (20)	0.712	169	2.208	524	100	CN1	0.8772	2169	114.7 ± 10.5
Buluk pt845	Zircon (20)	1.181	369	1.757	549	100	U 3	0.4926	1218	98.0 ± 7.3
Tardree wk029	Zircon (20)	5.168	782	4.818	729	100	CN1	0.8772	2193	123.9 ± 7.3
Tardree wk029	Zircon (20)	5.192	914	5.003	886	100	CN1	0.8972	2218	127.4 ± 70.0
Tardree pt845	Zircon (20)	5.411	869	2.208	524	100	CN1	0.8772	2169	114.7 ± 10.5
Mt Dromedary wk029	Zircon (13)	12.843	724	6.652	375	99	CN1	0.9072	2240	113.6 ± 7.6
Mt Dromedary wk029	Zircon (17)	14.264	1058	8.170	606	100	CN1	0.9172	2264	124.2 ± 6.9
Mt Dromedary pt845	Zircon (10)	11. 994	949	2.958	234	100	U3	0.4926	1218	99.6 ± 7.8
Mt Dromedary pt845	Zircon (10)	12.354	672	2.978	162	100	U3	0.4926	1218	97.3 ± 9.0
Mt Dromedary pt846	Zircon (15)	13.891	1154	3.479	289	100	U3	0.4930	1219	101.0 ± 7.3
Mt Dromedary pt846	Zircon (15)	14.720	1252	3.692	314	100	U3	0.4930	1219	101.2 ± 7.0
Mt Dromedary pt846	Zircon (20)	12.464	1319	3.071	325	100	U3	0.4930	1219	99.4 ± 6.8
Fish Canyon wk029	Zircon (20)	4.067	739	9.597	1739	99.7	CN1	0.9272	2291	141.8 ± 5.4
Fish Canyon pt845	Zircon (20)	4.112	1822	3.631	1609	32.4	U3	0.4926	1218	99.9 ± 5.1
Fish Canyon pt845	Zircon (20)	5.023	2126	4.536	1920	100	U3	0.4926	1218	102. 2 ± 5.1
Fish Canyon pt846	Zircon (13)	4.135	773	3.713	649	100	U3	0.4930	1219	101.5 ± 6.6

Table 6.1 (continued)

Age Standard and Irradiation No.	Mineral (No. of crystals)	Spontaneous ρ_s	Spontaneous N_s	Induced ρ_i	Induced N_i	$P(\chi^2)$ %	Glass	Dosimeter ρ	Dosimeter N_d	$\zeta \pm 1\ \sigma$
Mt Warning wk029	Zircon (10)	3.198	272	8.595	731	98.8	CN1	0.9672	2387	126.9 ± 9.8
Mt Warning pt845	Zircon (20)	4.382	910	4.227	878	97.1	U3	0.4926	1218	89.5 ± 5.3
Mt Warning pt845	Zircon (13)	5.009	426	4.327	368	97.1	U3	0.4926	1218	80.1 ± 6.4
Mt Warning pt846	Zircon (13)	4.065	595	4.024	589	100	U3	0.4930	1219	91.7 ± 3.6
									Zircon Mean ζ	140.2 ± 3.6

Analyses of apatite and zircon age standards are by external detector method; track densities (ρ) are (x106 cm^{-2}); N is number of tracks counted. $P(\chi^2)$ is the probability of obtaining χ^2 value for ν degrees of freedom where ν = (Number of crystals-1) [Galbraith, 1981]; pooled ρ_s/ρ_i ratio used to calculate ζ and uncertainty where $P(\chi^2)>5\%$; mean ρ_s/ρ_i ratio used to calculate ζ and uncertainty where $P(\chi^2)>5\%$ [Green, 1981]. Standard ages used are Fish Canyon Tuff 27.8 ± 0.7 Ma, Tardree Rhyolite 58.7 ± 1.1 Ma [Hurford and Green, 1983]; Durango apatite 31.4± 0.5, Mount Dromedary Igneous Complex 98.7 ± 0.6 Ma, Lake Mountain Rhyodacite 367.6 ± 1.5 Ma, Mount Warning Complex 22.8 ± 0.5 Ma [Green, 1985]; Buluk Member tuff 16.2 ± 0.2 Ma [Hurford and Watkins, 1987]. An uncertainty component from the independent age is included in the error on each ζ value; apatite/zircon mean ζ and its error weighted according to uncertainties on individual ζ values. Apatite and zircon ζ determinations fulfill the requirements proposed by Hurford[1990]. Zircon mean ζ calculated for CN1, with U3 sample determinations being converted to CN1 terms by using the factor of Green [1985].

Table 6.2 Results of calibration of horizontally confined track length determinations on apatite.

Standard	Sample	Number of Tracks	Mean length ± 1σ, μm	Standard Deviation σ, μm
Durango	8794-1	44	14.10 ± 0.10	0.69
Durango	Sample maen	44	14.10 ± 0.10	
Fish Canyon	8794-5	27	15.20 ± 0.20	1.01
Fish Canyon	8794-23	52	14.86 ± 0.11	0.77
Fish Canyon	Sample mean		15.03 ± 0.11	
Mt Dromedary	8794-6	50	14.41 ± 0.13	0.89
Mt Dromedary	8794-7	67	14.01 ± 0.11	0.88
Mt Dromedary	8794-8	61	13.92 ± 0.12	0.90
Mt Dromedary	Sample mean		14.11 ± 0.07	

Table 6.3 Fission track data for Marlborough samples.

Sample Number	Location Easting	Northing	Ele. (m)	Mineral	No of Cry.	Spontaneous ρ_s	N_s	Induced ρ_i	N_i	$P(\chi^2)$ %	Mean ratio ρ_s/ρ_i	ρ_d (E+6)	N_d	Age (Ma) ± 1σ	Mean Track Length ± 1σ (μm)	SD (μm)	No. of Lengths	Transect
9414-01	2591300	5955000	220	apatite	20	0.066	15	0.710	161	78.0		1.156	2859	18.5 ± 5.0	14.72 ± 0.10	0.10	2	T1
				zircon	15	17.353	2008	4.062	470	<0.1	4.724 ± 0.419	1.191	2711	336.2 ± 45.3				
9414-02	2590500	5952900	300	apatite	20	0.310	133	2.402	1031	0.3	0.150 ± 0.020	1.120	2768	26.3 ± 3.6	12.89 ± 0.71	2.00	9	T1
				zircon	16	10.299	171	4.801	793	<0.1	2.198 ± 0.141	1.201	2760	177.0 ± 12.4				
9414-03	2587700	5946200	480	apatite	3	1.661	23	1.661	23	32.3		1.120	2768	25.4 ± 15.6				T1
				zircon	5	27.555	549	12.791	253	0.2	2.392 ± 0.411	1.206	2784	182.9 ± 26.7				
9414-04	2564500	5949400	120	apatite	2	0.369	9	2.286	52	76.9		1.156	2859	34.3 ± 12.4				T1
				zircon	20	13.098	2254	4.219	726	23.2		1.211	2809	258.3 ± 13.8				
9414-05	2560300	5943900	300	apatite	20	0.212	80	0.594	224	18.6		1.156	2859	70.5 ± 9.3	11.43 ± 0.47	2.40	27	T1
				zircon	20	12.745	2395	3.550	667	60.2		1.216	2834	299.0 ± 16.2				
9414-06	2557700	5938500	500	apatite	20	0.159	50	1.971	618	3.2	0.119 ± 0.030	1.156	2859	16.5 ± 2.7	12.80 ± 0.56	1.95	13	T1
				zircon	20	10.866	1612	3.424	508	1.8	3.220 ± 0.185	1.221	2859	261.5 ± 18.3				T1
9414-07	2563200	5951800	220	zircon	20	12.639	1600	3.926	497	66.3		1.226	2883	270.9 ± 16.4				
9414-08	2557500	5949300	300	apatite	2	0.316	15	1.622	77	65.7		1.156	2859	38.6 ± 10.9				T1
				zircon	20	13.298	1999	3.985	599	9.7		1.231	2908	281.7 ± 15.9				
9414-09	2550700	5944900	320	apatite	20	0.109	34	1.242	388	90.4		1.156	2859	17.4 ± 3.1	13.56 ± 0.90	2.02	6	T1
				zircon	20	12.176	2023	5.302	881	<0.1	2.485 ± 0.177	1.236	2932	197.0 ± 24.5				
9414-10	2545200	5941400	420	apatite	2	0.393	7	2.078	37	16.1		1.156	2859	36.8 ± 15.2				T1
				zircon	20	9.428	1725	4.515	826	<0.1	2.344 ± 0.225	1.241	2957	179.7 ± 14.7				
9414-11	2548200	5941600	400	apatite	20	0.213	62	1.785	519	< 0.1	0.097 ± 0.028	1.156	2859	20.0 ± 5.8	13.93 ± 0.55	1.65	10	T1
				zircon	20	11.337	1581	5.760	804	<0.1	2.133 ± 0.168	1.251	3006	171.7 ± 12.6				
9414-12	2553000	5956000	240	apatite	4	0.142	9	1.296	82	86.1		1.156	2859	21.8 ± 7.7				T1
				zircon	6	14.075	362	5.756	148	41.6		1.256	3031	211.8 ± 21.7				
9414-13	2536800	5950000	340	apatite	3	0.126	4	4.645	147	61.6		1.156	2859	5.4 ± 2.7				T1
9414-14	2526800	5940500	480	apatite	2	0.056	4	2.907	23	53.4		1.156	2859	33.8 ± 18.4				T1
				zircon	20	15.161	2489	5.452	895	21.7		1.266	3080	242.2 ± 12.1				T1
9414-15	2528200	5936900	520	zircon	12	15.416	1174	6.264	477	<0.1	2.604 ± 0.237	1.271	3105	215.6 ± 20.9				T1
9414-16	2525700	5945400	420	zircon	20	13.083	1695	4.801	622	8.6		1.276	3129	239.3 ± 13.5				T1

Table 6.3 (continued)

Sample Number	Location Easting	Northing	Ele. (m)	Min-eral	No of Cry.	Spontaneous ρ_s	N_s	Induced ρ_i	N_i	$P(\chi^2)$ %	Mean ratio ρ_s/ρ_i	ρ_d (E+6)	N_d	Age (Ma) ± 1σ	Mean Track Length ± 1σ (μm)	SD (μm)	No. of Lengths	Transect
9414-17	2519600	5943900	380	zircon	12	11.910	695	4.524	264	54.3		1.281	3154	232.2 ± 18.3				T1
9414-19	2470900	5908200	460	apatite	10	0.026	2	1.685	187	94		1.120	2768	2.1 ± 1.5				
				zircon	20	2.146	348	11.310	1835	<0.1	0.193 ± 0.002	0.756	1870	10.0 ± 0.9				T1
9414-20	2470600	5908200	440	apatite	9	0.101	6	3.741	222	92.3		1.120	2768	5.3 ± 2.2				T1
				zircon	20	1.575	282	11.876	2126	6.2		0.783	1939	7.3 ± 0.5				
9414-21	2470600	5908200	440	apatite	2	0.101	1	2.326	23	60		1.256	3105	6.1 ± 6.1				T1
				zircon	20	1.583	252	13.580	2162	32		0.836	2070	6.8 ± 0.5				
9414-23	2470200	5909700	420	apatite	11	0.069	15	3.788	823	92.4		1.196	2958	3.8 ± 1.0				T1
9414-25	2469800	5909300	540	apatite	4	0.144	3	4.093	85	45.4		1.291	3193	7.9 ± 4.7				T1
				zircon	20	1.846	336	11.730	2134	77.9		0.826	2136	9.5 ± 0.6				
9414-31	2498800	5933600	700	apatite	7	0.550	74	4.334	583	2.4	0.107 ± 0.033	1.233	3048	24.7 ± 5.5	14.43 ± 0.70	0.99	3	T1
				zircon	10	23.782	1176	7.098	351	11.1		1.076	2662	247.9 ± 17.1				
9414-32	2504400	5932500	620	zircon	10	13.298	1039	5.747	449	7.5		1.102	2728	176.3 ± 11.4				T1
9414-33	2500900	5914700	800	apatite	8	0.069	11	1.517	243	60.1		1.251	3093	9.7 ± 3.0	15.19 ± 0.66	1.15	4	T1
				zircon	20	12.471	1739	5.844	815	61.5		1.129	2794	166.7 ± 8.9				
9414-34	2504300	5904400	980	apatite	4	0.433	12	4.189	116	67.8		1.335	3303	24.0 ± 7.3				
				zircon	15	14.853	1087	7.474	547	6.4		1.155	2860	158.9 ± 9.7				
9414-35	2503300	5902500	940	apatite	10	0.469	76	3.280	532	36.9		1.344	3325	33.4 ± 4.2	13.15 ± 0.95	1.34	3	
				zircon	11	15.281	1073	5.597	393	47.2		1.182	2926	222.3 ± 14.9				
9414-36	2496800	5895800	920	apatite	5	0.327	11	1.487	50	79.1		1.353	3347	51.6 ± 17.2				
				zircon	11	17.331	857	5.865	290	<0.1	3.562 ± 0.556	1.209	2992	246.6 ± 39.7				
9414-37	2491500	5890700	1040	apatite	3	0.506	7	2.889	40	14.3		1.362	3369	41.4 ± 17.0				
				zircon	5	12.032	238	5.662	112	0.2	2.815 ± 0.749	1.235	3057	192.6 ± 42.5				
9414-38	2587700	5959100	60	apatite	5	0.715	57	2.710	216	<0.1	0.315 ± 0.106	1.29	3206	63.2 ± 22.4				T1
				zircon	20	10.291	1693	5.630	941	<0.1	2.101 ± 0.207	1.262	3120	162.8 ± 14.8				
9414-39	2573400	5931600	400	apatite	9	0.693	111	1.361	218	96.3		1.306	3229	113.2 ± 13.4	11.43 ± 1.11	2.22	5	T2
				zircon	18	10.580	1444	4.968	678	<0.1	2.359 ± 0.224	1.108	2738	162.0 ± 14.9				

Table 6.3 (continued)

Sample Number	Location Easting	Northing	Ele. (m)	Min-eral	No of Cry.	Spontaneous ρ_s	N_s	Induced ρ_i	N_i	$P(\chi^2)$ %	Mean ratio ρ_s/ρ_i	ρ_d (E+6)	N_d	Age (Ma) ± 1σ	Mean Track Length ± 1σ (μm)	SD (μm)	No. of Lengths	Transect
9414-40	2570800	5929800	400	apatite	12	0.207	48	0.808	187	21.6		1.315	3251	57.7 ± 9.4	12.69 ± 1.12	2.75	7	T2
				zircon	6	9.645	372	3.526	136	20.1		1.117	2761	210.7 ± 22.2				
9414-41	2567600	5927700	400	apatite	18	0.972	148	2.298	350	100		1.406	3479	102.7 ± 10.4				T2
				zircon	10	10.900	636	4.182	244	0.3	2.746 ± 0.296	1.127	2785	196.3 ± 24.5				
9414-42	2567700	5927600	400	apatite	10	0.890	139	2.137	334	18		1.333	3296	94.6 ± 9.8	10.62 ± 0.93	2.28	7	T2
				zircon	20	8.558	1515	5.005	886	<0.1	1.900 ± 0.161	1.136	2809	136.7 ± 9.9				
9414-43	2564700	5925500	400	apatite	20	1.395	400	3.183	913	17.1		1.342	3319	100.2 ± 6.4	12.43 ± 0.46	1.97	19	T2
				zircon	10	8.241	595	3.837	277	<0.1	2.410 ± 0.286	1.146	2833	169.4 ± 23.3				
9414-44	2558900	5923500	510	apatite	7	1.377	177	2.466	317	41.5		1.351	3341	128.3 ± 12.4	11.34 ± 0.86	2.28	8	T2
				zircon	20	8.740	994	4.836	550	43.2		1.156	2856	144.8 ± 9.0				
9414-45	2544900	5911900	1280	apatite	20	1.220	379	2.270	705	58.0		1.170	2894	107.1 ± 7.2	12.84 ± 0.24	1.46	37	T2
				zircon	20	8.905	1418	5.024	800	<0.1	1.904 ± 0.183	1.166	2880	141.3 ± 11.5				
9414-46	2537400	5905100	840	apatite	8	0.548	104	1.159	220	38.2		1.179	2914	95.0 ± 11.5	14.12 ± 0.26	1.09	18	T2
9414-47	2532300	5903300	900	apatite	11	1.268	130	2.390	245	58.8		1.187	2934	107.3 ± 11.9	12.02 ± 0.62	1.53	7	T2
				zircon	20	11.698	995	7.160	609	<0.1	1.715 ± 0.202	1.185	2927	132.5 ± 13.1				
9414-48	2559100	5923500	500	zircon	12	10.066	667	4.376	290	<0.1	2.101 ± 0.207	1.195	2951	192.6 ± 30.4				T2
9414-49	2570200	5886800	620	apatite	6	0.929	34	2.842	104	99.9		1.249	2536	70.7 ± 14.1				T3
				zircon	20	8.426	75	5.370	887	<0.1	2.343 ± 0.229	1.205	2974	172.7 ± 13.0				
9414-50	2570300	5886300	640	apatite	4	0.046	2	1.695	74	89.8		1.211	2995	5.6 ± 4.0				T3
				zircon	20	10.203	1675	5.774	948	<0.1	1.931 ± 0.187	1.215	2998	147.5 ± 13.4				
9414-51	2570400	5885700	460	apatite	9	0.283	97	1.873	640	<0.1	0.086 ± 0.033	1.219	3015	23.2 ± 7.0	9.89 ± 1.17	2.02	4	T3
				zircon	20	10.100	1738	5.645	973	0.3	1.891 ± 0.125	1.224	3022	152.2 ± 9.2				
9414-52	2591800	5914600	70	apatite	20	0.871	131	2.102	316	100		1.279	2720	91.7 ± 9.8				T3
				zircon	7	6.320	361	5.176	215	55.6		1.234	3046	143.6 ± 13.2				
9414-53	2591600	5915000	120	apatite	17	0.180	87	0.563	273	17.9		1.236	3055	67.3 ± 8.4	10.89 ± 0.81	1.40	4	T3
				zircon	10	8.999	712	4.386	347	<0.1	2.450 ± 0.443	1.243	3070	176.3 ± 25.1				

Table 6.3 (continued)

Sample Number	Location Easting	Northing	Ele. (m)	Min-eral	No of Cry.	Spontaneous ρ_s	N_s	Induced ρ_i	N_i	$P(\chi^2)$ %	Mean ratio ρ_s/ρ_i	ρ_d (E+6)	N_d	Age (Ma) ± 1σ	Mean Track Length ± 1σ (μm)	SD (μm)	No. of Lengths	Transect
9414-54	2491200	5879500	1040	apatite	2	0.169	6	3.707	132	87.5		1.244	3075	9.7 ± 4.1				T2
				zircon	16	13.104	1620	5.080	628	0.2	2.748 ± 0.241	1.253	3093	221.8 ± 16.5				
9414-55	2492300	5873100	900	apatite	11	0.093	21	2.408	543	84.3		1.252	3095	8.3 ± 1.9				T2
				zircon	13	11.096	1284	3.820	442	3.6	3.143 ± 0.225	1.263	3117	255.7 ± 19.3				
9414-56	2493100	5865100	840	apatite	11	0.038	17	0.742	328	87.0		1.260	3115	11.2 ± 2.8				T2
				zircon	10	8.922	803	4.578	412	0.7	2.177 ± 0.231	1.272	3141	175.4 ± 16.7				
9414-57	2498200	5861600	800	zircon	10	10.245	922	6.600	594	11.0		1.280	3165	137.8 ± 8.4				T3
9414-58	2500000	5856400	700	apatite	3	0.404	48	1.424	169	<0.1	0.187 ± 0.140	1.276	3155	36.7 ± 25.2				T3
				zircon	16	8.243	1125	3.488	476	<0.1	2.491 ± 0.256	1.050	2595	166.0 ± 15.6				
9414-59	2502500	5861100	760	zircon	18	6.962	1267	3.116	567	<0.1	2.588 ± 0.348	1.054	2605	157.5 ± 17.9				T3
9414-60	2505800	5867300	780	apatite	17	0.028	11	1.274	499	81.3		1.293	3196	4.9 ± 1.5	14.43 ± 0.76	1.08	3	T3
				zircon	16	11.177	1647	4.954	730	<0.1	2.416 ± 0.199	1.058	2615	165.5 ± 13.2				
9414-61	2520200	5839900	110	apatite	20	0.466	342	1.087	798	1.7	0.497 ± 0.031	1.369	3274	110.2 ± 9.6	14.62 ± 0.14	1.28	86	T4
				zircon	20	10.384	1941	5.692	1064	<0.1	1.960 ± 0.207	1.062	2624	129.0 ± 12.0				
9414-62	2527900	5840000	140	apatite	20	0.847	372	2.046	899	11.6		1.309	3236	92.4 ± 6.0	14.56 ± 0.17	0.87	28	T4
				zircon	10	13.016	1210	3.399	316	0.2	3.933 ± 0.512	1.066	2634	267.9 ± 28.4				
9414-63	2532400	5860500	360	apatite	20	0.298	233	0.590	461	41.7		1.317	3256	113.3 ± 9.4	14.17 ± 0.19	1.15	36	T4
				zircon	20	9.786	1684	3.789	652	<0.1	2.700 ± 0.252	1.070	2644	181.6 ± 16.1				
9414-64	2503100	5863000	400	apatite	6	0.471	118	1.465	367	0.8	0.357 ± 0.071	1.325	3276	73.6 ± 14.0	12.26 ± 1.15	2.00	4	T4
				zircon	20	8.572	1526	3.910	696	0.3	2.423 ± 0.175	1.073	2654	165.5 ± 11.5				
9414-65	2543600	5868300	280	apatite	7	0.057	16	0.577	161	<0.1	0.079 ± 0.062	1.165	2880	14.2 ± 9.9				T4
				zircon	20	11.463	2120	4.099	758	<0.1	3.065 ± 0.262	1.077	2664	217.0 ± 18.5				
9414-66	2551700	5867700	100	apatite	21	0.191	120	0.847	533	8.3		1.173	2900	45.2 ± 4.7				T4
				zircon	20	8.245	1476	4.665	835	54.4		1.081	2674	132.6 ± 7.1				
9414-67	2558400	5863300	20	apatite	20	0.276	162	0.722	424	<0.1	0.337 ± 0.065	1.181	2920	64.1 ± 12.1	12.17 ± 0.38	1.38	14	T4
				zircon	20	11.603	2100	5.951	1077	<0.1	2.100 ± 1.910	1.085	2683	144.9 ± 11.3				
9414-68	2553400	5858000	20	apatite	3	0.232	14	2.039	123	4.9	0.115 ± 0.076	1.189	2940	24.2 ± 10.2				T4
				zircon	15	12.329	1573	6.474	826	14.8		1 .089	2693	143.8 ± 7.7				

Table 6.3 (continued)

Sample Number	Location Easting	Northing	Ele. (m)	Min-eral	No of Cry.	Spontaneous ρ_s	N_s	Induced ρ_i	N_i	$P(\chi^2)$ %	Mean ratio ρ_s/ρ_i	ρ_d (E+6)	N_d	Age (Ma) ± 1σ	Mean Track Length ± 1σ (μm)	SD (μm)	No. of Lengths	Transect
9414-69	2578500	5902200	150	apatite	10	1.243	166	2.809	375	100		1.282	3169	98.1 ± 9.5				T3
				zircon	20	11.022	1875	5.743	977	<0.1	1.991 ± 0.148	1.093	2703	144.0 ± 9.1				
9414-70	2580700	5886600	20	apatite	15	0.467	168	0.881	317	12.6		1.205	2980	108.8 ± 10.7	13.01 ± 0.57	1.39	7	T3
				zircon	15	10.514	1331	5.158	653	<0.1	2.038 ± 0.097	1.097	2713	150.6 ± 14.7				
9414-71	2578200	5902200	150	zircon	3	13.145	221	4.580	77	0.4	3.328 ± 1.048	1.101	2723	217.3 ± 55.1				T3
9414-72	2578600	5884200	40	apatite	20	0.275	125	2.031	924	<0.1	0.099 ± 0.025	1.221	3020	19.4 ± 4.5	11.74 ± 0.67	2.52	15	T3
				zircon	20	12.48	2086	5.666	947	<0.1	2.402 ± 0.206	1.105	2732	167.2 ± 14.2				
9414-73	2573500	5880600	40	apatite	20	0.350	194	1.116	618	0.8	0.302 ± 0.043	1.230	3040	63.5 ± 7.9	11.74 ± 0.42	2.09	26	T3
				zircon	20	9.218	1951	5.339	1130	<0.1	1.861 ± 0.124	1.109	2742	134.6 ± 8.3				
9414-74	2573000	5889500	420	apatite	4	0.624	45	1.456	105	27.5		1.283	3060	93.8 ± 16.8				T3
				zircon	15	9.214	1048	5.231	595	11.3		1.112	2752	135.9 ± 8.2				
9414-75	2568600	5886500	1200	apatite	4	0.569	9	1.769	28	92		1.368	3383	76.1 ± 29.2				T3
				zircon	20	13.067	2184	6.767	1131	<0.1	0.256 ± 0.240	1.116	2762	150.6 ± 15.9				
9414-76	2567700	5886800	1560	apatite	6	0.453	13	3.277	94	74.3		1.382	3419	33.2 ± 9.9				T3
				zircon	20	13.739	2473	5.833	1050	<0.1	2.475 ± 0.189	1.120	2772	178.3 ± 13.7				
9414-77	2566300	5888100	2200	apatite	3	0.055	3	3.343	184	58.7	0.133 ± 0.056	1.261	3119	3.5 ± 2.1				T3
				zircon	12	15.293	1452	8.816	837	<0.1	2.134 ± 0.294	1.125	2781	158.4 ± 27.4				
9414-78	2564500	5887600	2300	apatite	3	0.070	6	4.063	347	87.3		1.270	3139	3.8 ± 1.6				T3
				zircon	20	9.870	1845	3.649	682	<0.1	2.828 ± 0.228	0.988	2443	181.5 ± 13.1				
9414-79	2563800	5886800	2200	apatite	4	0.026	4	1.099	170	62.6		1.278	3159	5.2 ± 2.6				T3
				zircon	5	9.509	442	5.099	237	30.8		1.001	2476	129.6 ± 11.3				
9414-80	2562800	5886900	2400	zircon	17	10.097	1408	4.977	694	<0.1	2.120 ± 0.199	1.014	2508	141.9 ± 12.3				T3
9414-81	2561200	5887100	2600	apatite	10	0.071	12	1.744	293	94.4		1.294	3199	9.1 ± 2.7	15.70 ± 0.33	0.46	3	T3
				zircon	20	9.578	1885	5.594	1101	<0.1	1.897 ± 0.165	1.027	2541	124.3 ± 7.6				
9414-82	2558700	5887000	1780	apatite	13	0.013	4	0.843	256	68.9		1.302	3129	3.5 ± 1.8				T3
				zircon	12	11.043	1114	4.590	463	19.6		1.041	2574	173.2 ± 11.1				

Table 6.3 (continued)

Sample Number	Location Easting	Northing	Ele. (m)	Min-eral	No of Cry.	Spontaneous ρ_s	N_s	Induced ρ_i	N_i	$P(\chi^2)$ %	Mean ratio ρ_s/ρ_i	ρ_d (E+6)	N_d	Age (Ma) ± 1σ	Mean Track Length ± 1σ (μm)	SD (μm)	No. of Lengths	Transect
9414-83	2600100	5924000	60	apatite	20	0.558	171	1.526	468	51.4		1.310	3239	81.7 ± 7.5	12.31 ± 0.42	1.78	19	T3
				zircon	7	9.878	508	5.483	282	9.2		1.054	2607	131.7 ± 10.7				
9414-84	2599000	5928900	160	apatite	20	0.748	285	1.300	495	98.4		1.318	3259	129.0 ± 10.0	12.98 ± 0.18	1.25	46	T3
				zircon	20	14.315	1345	4.406	414	25.2		1.067	2639	238.5 ± 15.5				
9414-85	2596500	5928800	220	zircon	20	10.410	1884	4.857	879	<0.1	2.301 ± 0.179	1.080	2672	159.3 ± 12.9				T3
9414-86	2596400	5930300	300	apatite	7	0.150	35	2.117	490	1.5	0.111 ± 0.038	1.231	3043	19.5 ± 5.3				T3
				zircon	20	15.386	2602	7.900	1336	<0.1	2.181 ± 0.252	1.093	2705	143.8 ± 14.3				
9414-87	2597700	5928600	380	apatite	20	0.203	126	0.816	507	43.2		1.235	3053	52.5 ± 5.4	12.40 ± 0.11	0.22	5	T3
				zircon	10	10.473	935	6.182	538	<0.1	1.875 ± 0.197	1.107	2737	134.7 ± 13.9				
9414-88	2598700	5928700	260	apatite	8	0.789	89	2.138	241	74.8		1.239	3063	78.1 ± 9.8	12.70 ± 1.01	2.68	8	T3
				zircon	10	9.284	686	4.314	320	0.1	2.297 ± 0.230	1.120	2770	165.7 ± 19.2				
9414-89	2537100	5998100	3	zircon	2	17.034	219	6.845	88	<0.1	2.236 ± 1.236	1.133	2803	143.3 ± 61.1				T3
9414-90	2543500	5997500	130	apatite	5	0.046	9	0.674	133	78.8		1.243	3074	14.4 ± 5.0				IJ
				zircon	5	17.100	575	6.394	215	9.8		1.146	2835	211.3 ± 18.2				
9414-91	2544300	5997700	80	apatite	20	0.040	26	0.336	219	95.8		1.247	3084	25.4 ± 5.3				IJ
				zircon	13	12.123	1127	4.765	443	0.6	2.692 ± 0.256	1.159	2868	202.0 ± 17.4				
9414-92	2544400	5997300	120	apatite	5	0.354	7	0.809	16	98.6		1.4 00	3461	105.8 ± 48.0				IJ
				zircon	20	7.983	1966	3.24	798	8.8		1.173	2900	199.5 ± 20.5				
9414-93	2545500	5997500	260	apatite	7	0.447	19	0.870	37	100		1.403	3469	124.3 ± 35.2				IJ
				zircon	14	13.385	1337	4.825	482	0.1	2.913 ± 0.270	1.186	2933	223.3 ± 19.2				
9414-94	2555500	5994900	80	apatite	10	0.447	23	1.167	60	99.9		1.407	3486	93.3 ± 23.0				IJ
				zircon	5	9.256	357	2.826	109	12.8		1.212	2999	272.4 ± 31.0				
9414-95	2557100	5993300	150	apatite	3	0.556	11	1.264	25	91.2		1.410	3486	107.2 ± 38.9				IJ
				zircon	3	8.612	247	3.591	103	29.4		1.239	3064	205.0 ± 24.9				
9414-96	2559100	5998600	60	apatite	5	0.397	76	1.372	263	14.3		1.268	3135	62.6 ± 8.3	11.37 ± 0.42	0.84	5	IJ
				zircon	10	9.873	869	3.340	294	2.2	2.988 ± 0.287	1.112	2749	220.4 ± 21.6				
9414-97	2558300	5994500	80	apatite	3	0.098	8	0.392	32	64.5		1.272	3145	54.4 ± 21.5				IJ
				zircon	20	10.263	1959	3.337	637	<0.1	3.210 ± 0.258	1.127	2787	235.0 ± 16.9				

Table 6.3 (continued)

Sample Number	Location Easting	Northing	Ele. (m)	Min-eral	No of Cry.	Spontaneous ρ_s	Spontaneous N_s	Induced ρ_i	Induced N_i	$P(\chi^2)$ %	Mean ratio ρ_s/ρ_i	ρ_d (E+6)	N_d	Age (Ma) ± 1σ	Mean Track Length ± 1σ (μm)	SD (μm)	No. of Lengths	Transect
9414-98	2557900	5989700	30	apatite	2	0.937	48	3.005	154	72.2		1.276	3155	67.9 ± 11.3	14.27 ± 0.88	0.88	2	IJ
9414-99	2558000	5992700	40	apatite	9	0.155	39	0.581	146	72.2		1.280	3165	58.5 ± 10.6	13.22 ± 0.37	0.37	2	IJ
				zircon	3	13.650	162	4.719	56	71.1		1.152	2848	229.5 ± 36.3				
9414-100	2563800	5991200	50	apatite	4	0.076	11	0.284	41	78.6		1.284	3175	58.9 ± 20.0				IJ
				zircon	20	7.461	1498	2.695	541	69.5		1.162	2873	221.7 ± 13.2				
9414-101	2569700	5991100	5	apatite	3	0.301	18	1.104	66	29.7		1.288	3185	60.0 ± 16.0				IJ
				zircon	15	7.431	1580	3.560	757	11.4		1.172	2897	169.2 ± 9.2				
9414-102	2566400	5990300	5	zircon	10	9.718	692	3.988	284	99.4		1.182	2922	198.8 ± 15.4				IJ
9414-103	2557100	6000500	140	zircon	12	8.598	1114	3.002	389	17.1		1.192	2947	235.0 ± 15.7				IJ
9414-104	2541000	6003300	0	apatite	20	0.019	12	0.530	338	95.1		1.301	3216	7.9 ± 2.3	14.01 ± 1.01	1.01	2	IJ
				zircon	9	10.000	811	7.016	569	24.3		1.202	2971	119.0 ± 7.5				
9414-105	2544200	6005500	0	apatite	20	0.050	29	0.503	292	15.4		1.305	3226	22.2 ± 4.4				IJ
				zircon	2	10.516	52	5.865	29	67.2		1.212	2996	150.6 ± 35.2				
9414-107	2573100	5992200	40	apatite	3	0.674	8	5.645	67	2.0	0.167 ± 0.083	1.239	3065	30.0 ± 16.3				IJ
				zircon	11	9.703	950	6.626	355	<0.1	2.830 ± 0.412	1.222	3021	213.7 ± 25.5				
9414-108	2577000	5991300	40	zircon	7	10.852	601	6.608	366	29.6		1.232	3045	140.3 ± 10.3				IJ
9414-109	2593900	5976600	0	zircon	10	8.865	754	4.303	366	12.1		1.242	3070	176.9 ± 12.6				IJ
9414-110	2589800	5982800	20	zircon	20	10.498	2170	4.852	1003	0.1	2.440 ± 0.286	1.252	3095	190.2 ± 12.5				IJ
9414-111	2593100	5988500	2	apatite	2	1.618	16	5.561	55	68.7		1.281	3167	64.6 ± 18.4				IJ
				zircon	20	7.091	1613	3.543	806	25.8		1.262	3120	174.7 ± 9.3				
9414-112	2594100	5991100	5	apatite	3	0.593	17	2.754	79	65.6		1.291	3193	48.2 ± 12.9				IJ
				zircon	10	7.752	552	3.792	270	27.4		1.272	3144	179.8 ± 14.5				

Easting and northing refer to New Zealand Map Series 260. Track densities (ρ) are $x10^6$ tracks cm^{-2}. All analyses are by external detector method using 0.5 for the $4\pi/2\pi$ geometry correction factor. Apatite ages calculated using dosimeter glass SRM 612 and zeta-612 = 348.4 ± 5.8 (1σ); zircon ages calculated using dosimeter glass CN1 and zeta-CN1 = 140.2 ± 3.6 (1σ). $P(\chi^2)$ is probability of obtaining χ^2 value for ν degrees of freedom (where ν is number of crystals - 1) [Galbraith, 1981]; pooled ρ_s/ρ_i ration is used to calculate age and uncertainty where $P(\chi^2)>5\%$; mean ρ_s/ρ_i ration is used to calculate age and uncertainty where $P(\chi^2)<5\%$ [Green, 1981]. Ele.: elevation (m); Cry.: crystals.

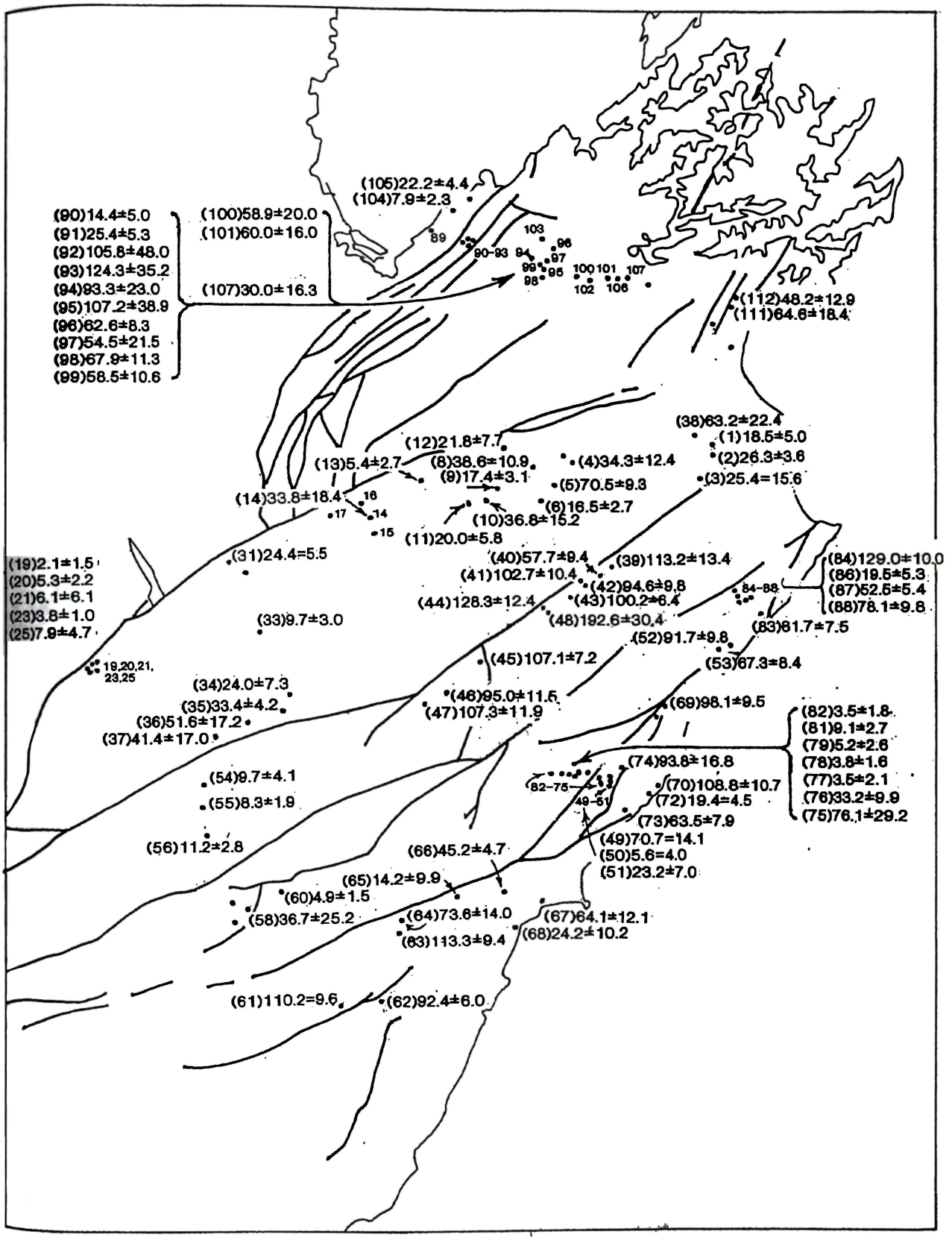

Figure 6.2 Distribution of apatite fission track ages in Marlborough.

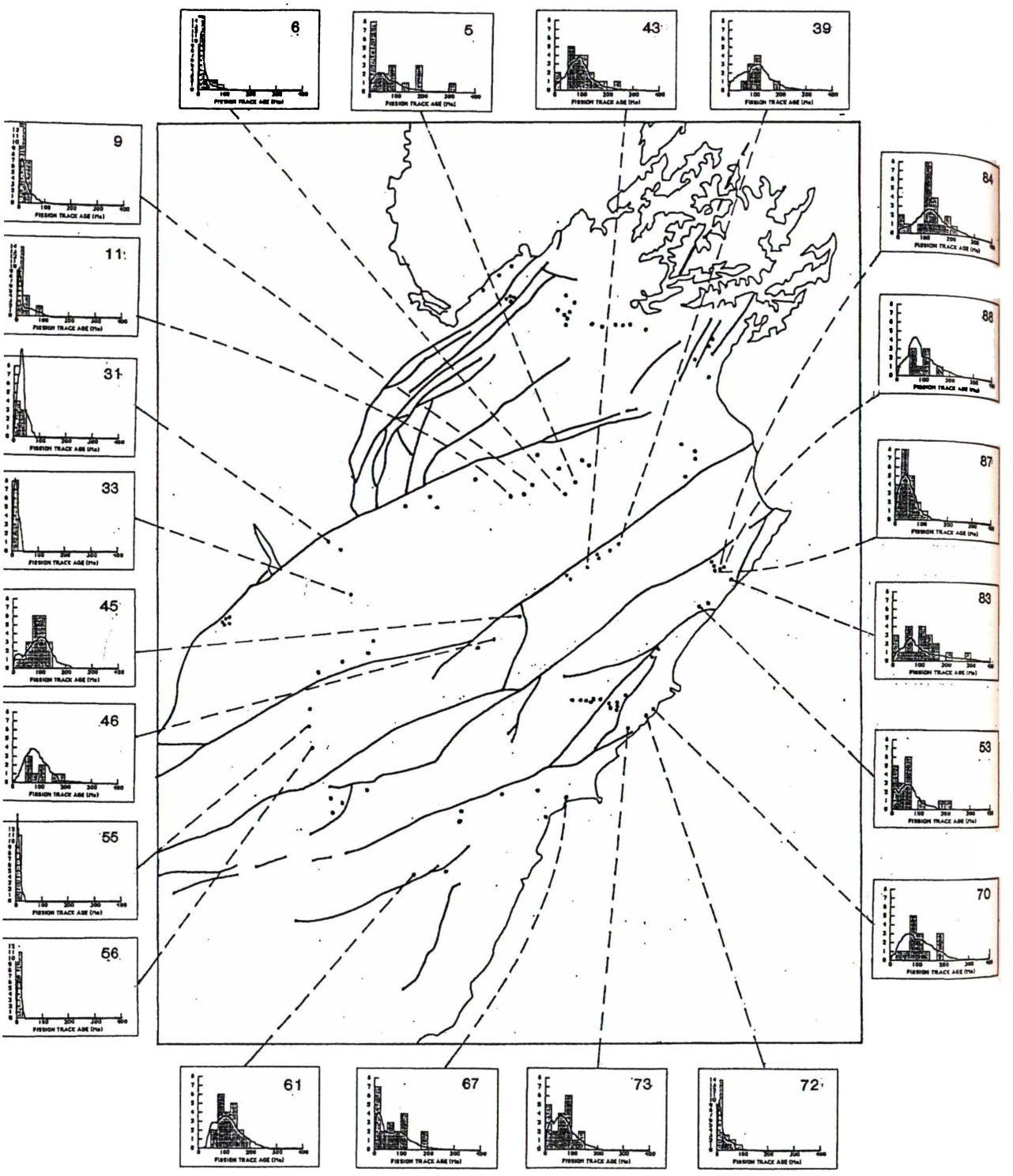

Figure 6.3 Distribution of apatite single-grain fission track ages in the Marlborough Fault System.

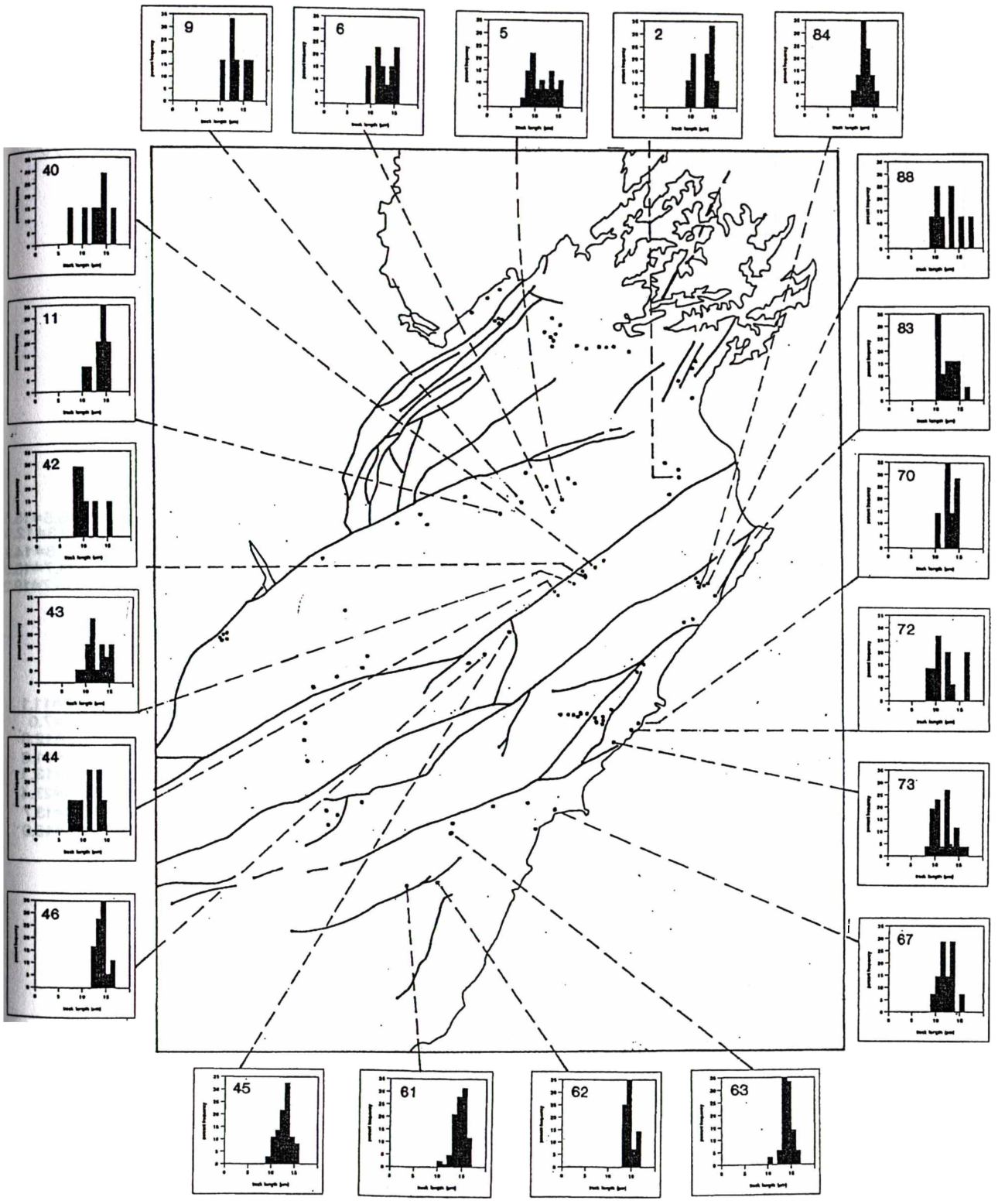

Figure 6.4 Apatite fission track length histograms for the samples of the Marlborough Fault System.

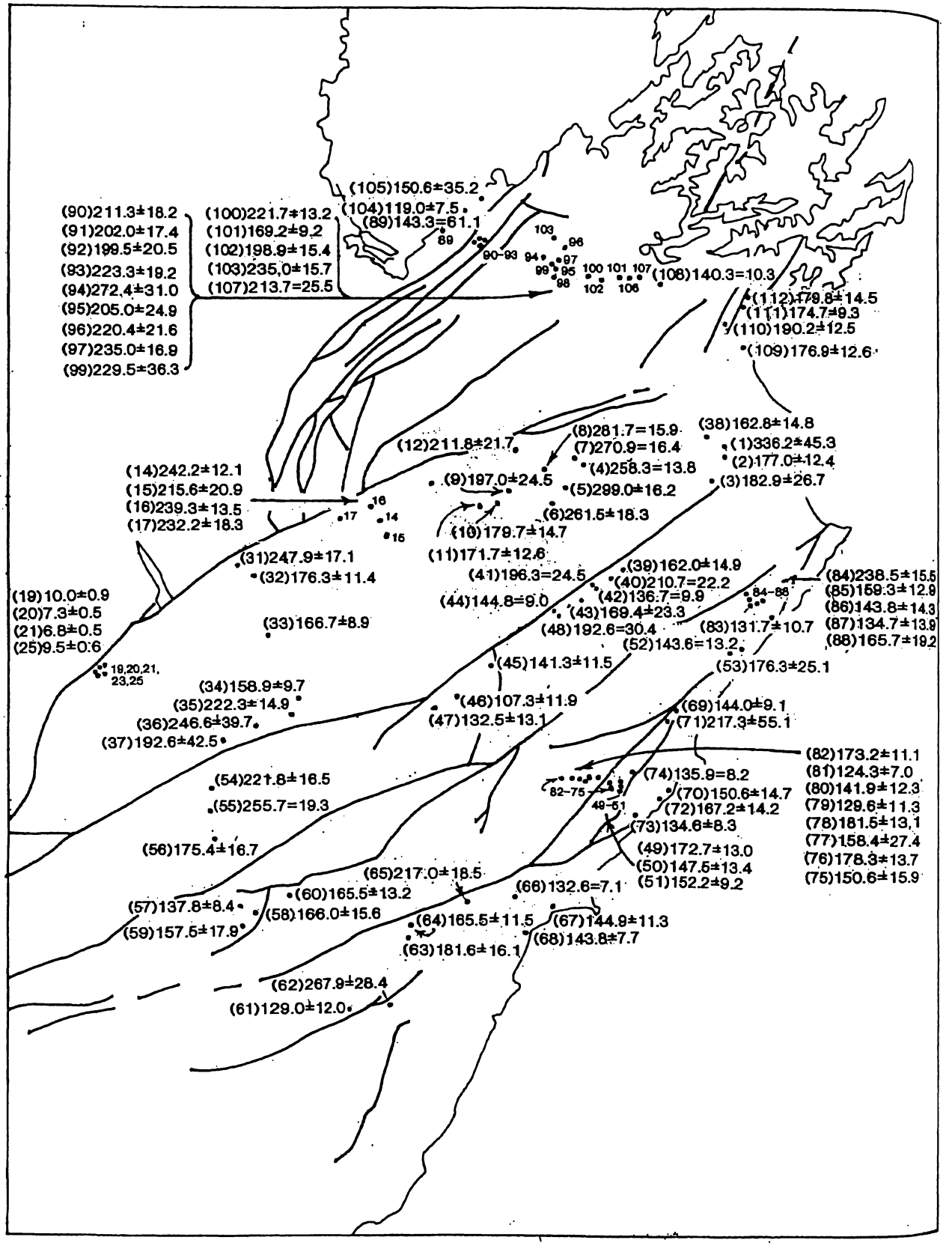

Figure 6.5 Distribution of zircon fission track ages in Marlborough.

trend in the plot (Figure 6.6) for some samples to then increase in mean length with an increase in apatite fission track age from 67 to about 100 Ma. This corresponds to decreasing levels of partial annealing for those samples that have more apparent age. The sample with around 100 Ma of age and long lengths cooled rapidly at around that time, and have remained at low temperatures since then in order to have retained the long mean lengths.

There are eight samples with ages of 90 Ma or more, but lengths of 13 μm or less. These samples and their host rocks have probably experienced two or more phases of partial annealing, one leading up to the mid Cretaceous, and a second phase during the Cenozoic, with cooling from elevated temperatures possibly around 100 Ma and 10 Ma.

In summary, the plot can be broken up into four parts: (i) Samples-33, -60 and -81 are reset. (iii) Samples on the plot between 9414-1 and -53 are heavily partially annealed and are inferred to have experienced the lower levels of a partial annealing zone prior to late Cenozoic cooling. (iii) Samples between 9414-5 and -61, and possibly -63, experienced the upper part of a partial annealing zone prior to late Cenozoic cooling. (iv) Samples 9414-39, -42, -43, -44, -45, -47, -70 and -84 have the most complicated thermal history, and either retain a provenance record, or experienced partial annealing in Marlborough during two intervals. These qualitative interpretations, although general, provide a useful basis to describe and interpret the same data in the spatial content of transects.

The length-age plot is similar to the patterns established previously for Canterbury involving rocks of similar character and age (Tippett and Kamp, 1993; Kamp, 1997). The main differences are that for Marlborough the minimum in the mean track lengths occur at about 67 Ma instead of about 30 Ma, and that many apatite samples exist with 100 Ma or more of age, whereas in Canterbury the apatite ages are mostly less than 95 Ma. These features probably reflect overall lower levels of partial annealing and correspondingly less total denudation in Marlborough, compared with Canterbury, where the basement is part of a well developed continent-continent collision zone.

6.3.2 Apatite results described for transects

Apatite fission track ages obtained in Marlborough (Table 6.3) range between 2.1 ± 1.5 Ma and 129.0 ± 10.0 Ma. The mean confined track lengths of the samples range

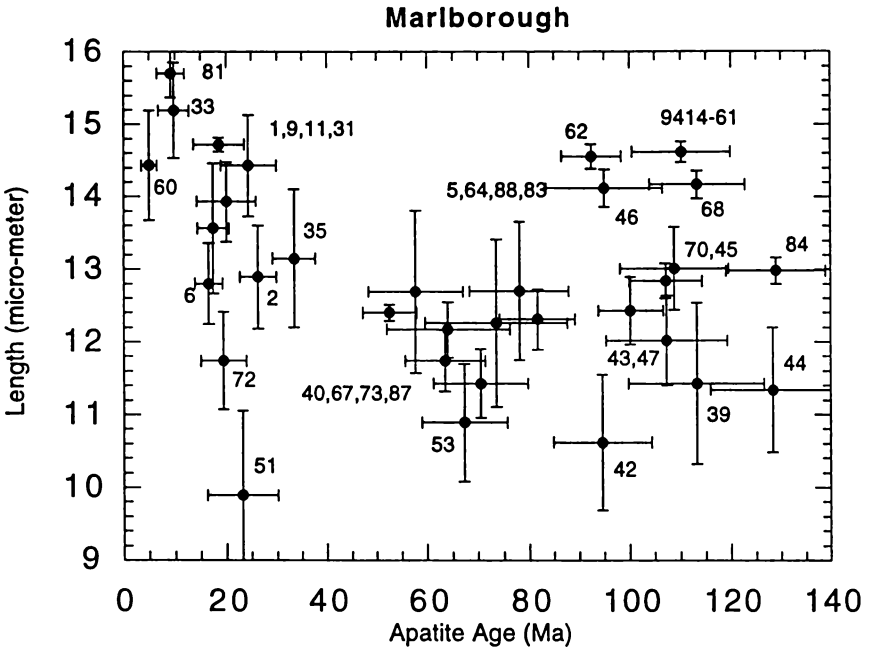

Figure 6.6 Mean fission track lengths versus apatite fission track ages for Marlborough samples. Uncertainties are at the 1σ level.

between 10.16 ± 0.67 (1σ) μm and 15.70 ± 0.33 μm, with standard deviation between 0.10 and 2.75 μm. Generally, younger apatite ages (<25 Ma) were obtained from the samples in the vicinity of the Alpine (Wairau) Fault, or close to the Jordan Thrust (Seaward Kaikoura Range).

Wairau Transect (T1)

The Wairau transect is oriented perpendicular to the Alpine Fault, but parallel to the Wairau Fault (Figure 6.1). The pooled/central ages and mean lengths are plotted with respect to distance from the Wairau Fault in Figure 6.7a. The ages increase away from the Alpine Fault. Samples from the Alpine Schist (9414-19, -20, -23 and -25) have ages of 2.1 ± 1.5 , 5.3 ± 2.2, 2.8 ± 1.0 and 7.9 ± 4.7 Ma, respectively, and are considered as reset fission track parameters, even through track lengths were not able to be measured because of the low track densities. This interpretation is supported by the similar apatite fission track ages obtained from Alpine Schist measured at Arthur's Pass and Lewis Pass by Tippett and Kamp (1993). The measured ages are close to recording the time when the host rocks cooled through the closure temperature of 110°C.

Samples 9414-33 and -13 also have ages less than 10 Ma, and are inferred to be reset or very close it. Sample 9414-31, -6, -9, -11, -12, -1 and -3 have early Miocene fission track ages, with lengths between 12.8 and 14.7 μm. These ages cannot be interpreted simply as being reset, and probably indicate that the host rocks have cooled from lowermost levels of a partial annealing zone (90-100°C) during the late Cenozoic. These samples are close to others (9414-4, -5 and -8) with apatite ages ranging between 34 and 70 Ma (Table 6.3), which will probably have experienced lower maximum temperatures, in the range 70-90°C. These older ages could reflect higher Cl contents in the apatites, which are more retentive of latent fission tracks, or alternatively, offsets by late Cenozoic faults between localities involving displacement and differential denudation of up to 1 km for a geothermal of 20°C /km. The differences in elevation between sample sites cannot explain on its own the difference in apatite fission track ages in this part of the transect.

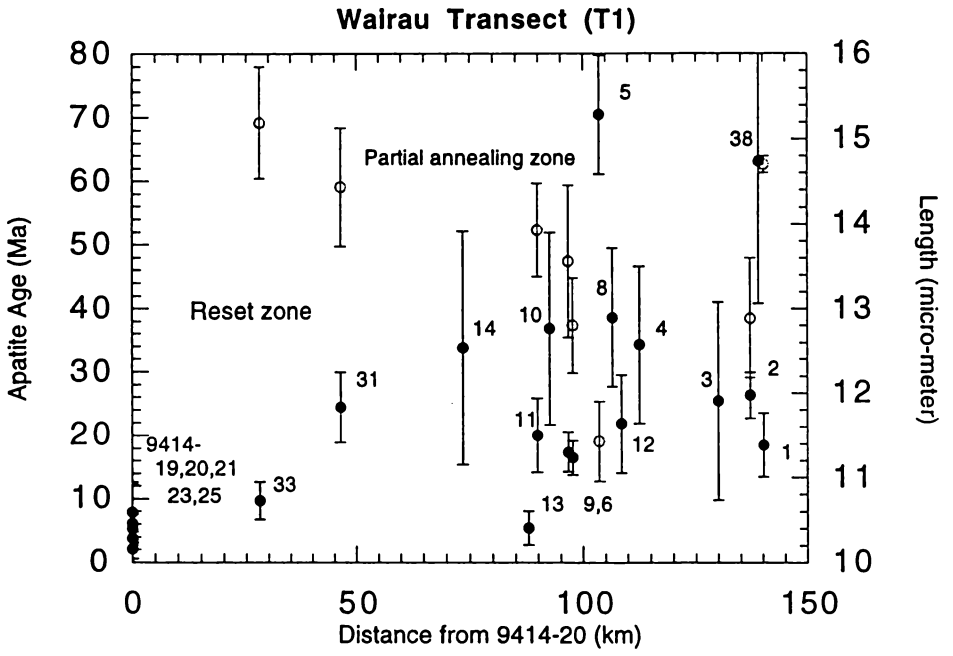

Figure 6.7a Apatite fission track age (close circle) and length (open circle) versus distance from Sample 9414-20.

Inland Kaikoura Transect (T2)

This transect incorporates samples obtained from the Inland Kaikoura Block between the Awatere and Clarence Faults (Figure 6.1). Samples 9414-54, -55 and -56 (Figure 6.7b) were obtained from Triassic sandstone and have apatite ages of 9.7 ± 4.1, 8.3 ± 1.9 and 11.2 ± 2.8 Ma. These samples give a weighted mean age of 9.3 ± 0.9 Ma, which in the absence of length data, but with reference to fission track ages further south in the Southern Alps, can be interpreted as reset or close to being reset. All of the rest of the samples, excluding 9414-40, are in the range of 94.6 ± 9.8 to 113.2 ± 13.4 Ma, giving a weighted mean age of 102.3 ± 2.5 Ma. The meaning of this age is unclear as the mean lengths are variable and suggest that the fission tracks were not even reset in the mid Cretaceous. These samples have probably experienced maximum paleotemperature of less than 60°C during the Cenozoic, which limits the amount of cooling, probably via erosion, associated with the modern plate boundary deformation. Sample 9414-40 is located within the Awatere Fault zone, and its younger apatite age (57.7 ± 9.4 Ma) may reflect uplift and denudation within it relative to the basement downthrown on the southeastern side of the fault where the neighbouring samples were obtained.

Seaward Kaikoura Transect (T3)

This transect lies within the block between the Clarence and Hope faults and includes a transect of samples taken up the face of the Seaward Kaikoura Range (Figures 6.1 and 6.7c). Sample 9414-58 contained only three datable grains, and gave a poorly constrained age of 36.7 ± 25.2 Ma. Neighbouring Sample 9414-60 has, however, a tightly constrained age of 4.9 ± 1.5 Ma indicating that it has been reset by late Cenozoic denudation. Samples 9414-76 to 82 from the southeastern faulted face of the Seaward Kaikoura Range have very young ages of 3.5 to 9.1 Ma. These are regarded as reset ages indicating up to 4 km of erosion from the southeastern face of the range. Samples from sites to the southeast of Jordan Thrust (9414-74 and -76) located at the foot of the Seaward Kaikoura Range, and those located close to the coastline (9414-70, -73 and -77). have fission track parameters suggesting that the host rocks have been annealed to variable but limited extents. Some of these samples have mid to late Cretaceous ages and will have experienced less than 60°C of cooling since then. Samples 9414-52 and -53 come from sites at the northern end of the Seaward Kaikoura Range. Their late Cretaceous ages are indicative of the lesser amounts of

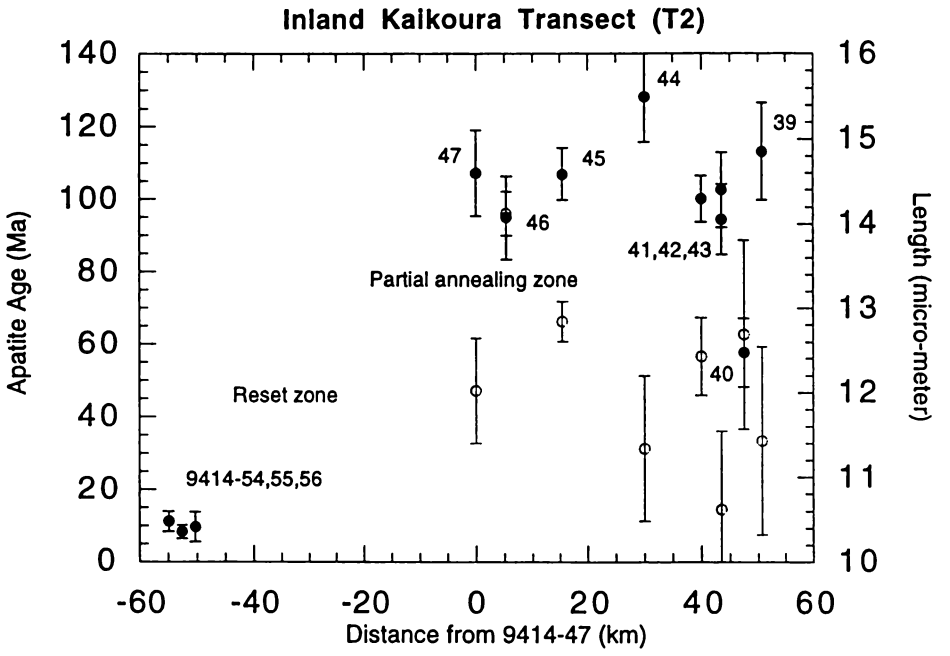

Figure 6.7b Apatite fission track age (close circle) and length (open circle) versus distance from Sample 9414-47.

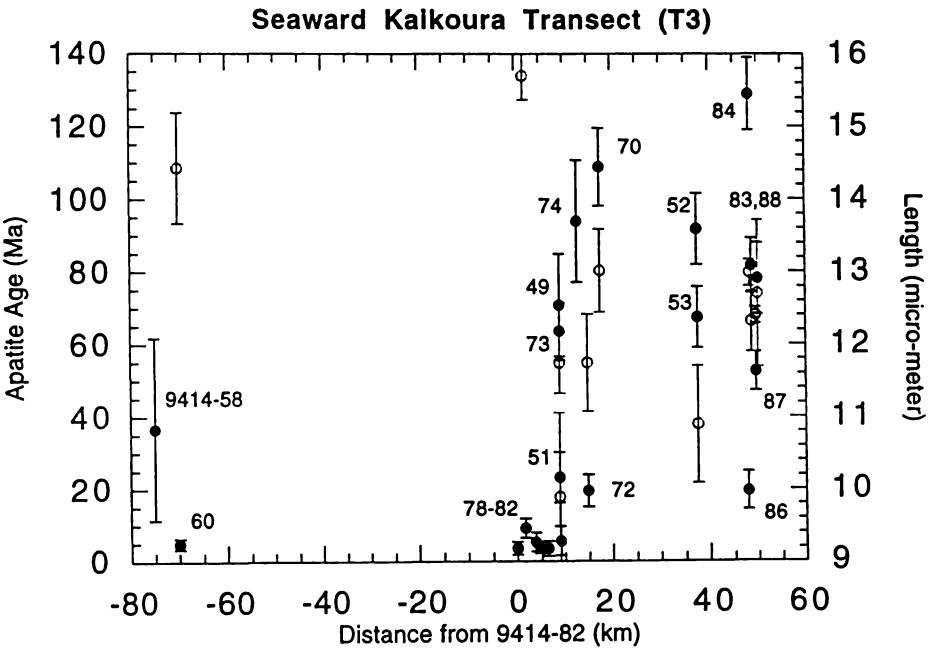

Figure 6.7c Apatite fission track age (close circle) and length (open circle) versus distance from Sample 9414-82.

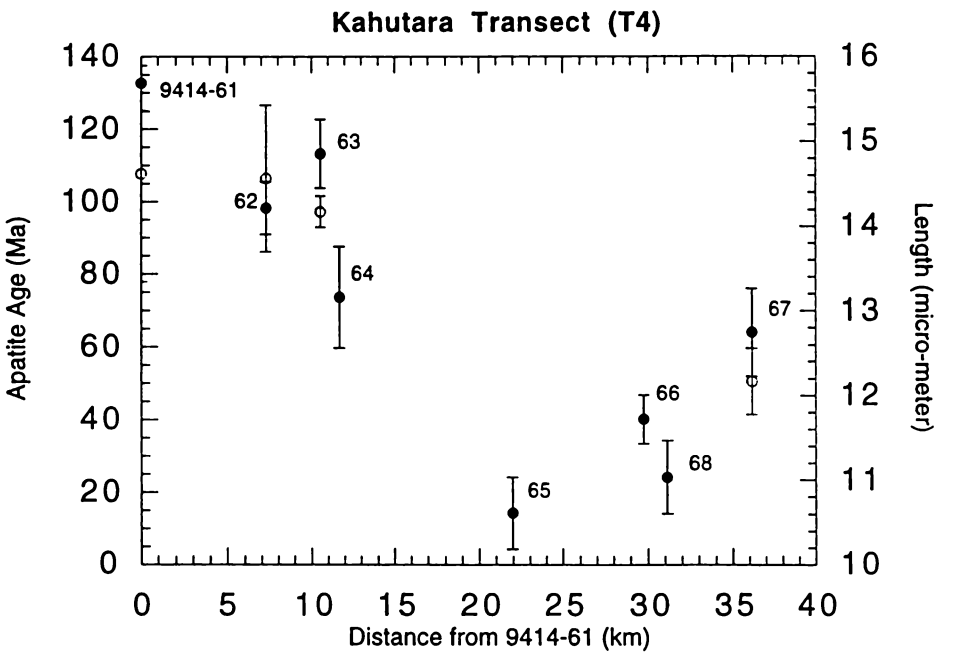

Figure 6.7d Apatite fission track age (close circle) and length (open circle) versus distance from Sample 9414-61.

late Cenozoic erosion from the more northern compared with the more central parts of the Seaward Kaikoura Range. The same interpretations apply to the samples (9414-83 to -88) at the northeastern end of the transect, which mostly have late Cretaceous ages. Exceptions are Sample 9414-84 with an age of 129 ± 10.0 Ma, and Sample 9414-86, which has an age of 19.5 ± 5.3 Ma, and comes from a locality on the upthrown side of the Inland Kaikoura block, where there has evidently been substantial denudation.

Kahutara Transect (T4)

Samples included in this transect all originate from Jurassic rocks lying to the south of the Hope Fault, in northern Canterbury (Figures 1.1, 6.1, and 6.7d). There seems to be a systematic change northeastward along the transect with a reduction in age to a minimum at Sample 9414-65 (14.2 ± 9.9 Ma), after which ages increase. This pattern indicates that the rocks have been heated in the past to variable levels in a partial annealing zone. As this area lies outside of the parts of Marlborough where substantial topography has developed, the cooling from the different levels of partial annealing cannot readily be explained by significant and variable amounts of erosion of basement. It is probably due to erosion of sedimentary section contained formerly in a late Cretaceous-Cenozonic basin, which has now been mostly inverted and eroded. The 1:250,000 geological map of northern Canterbury (Gregg, 1964) shows remnants of late Cretaceous and Cenozoic section all around the basement range that was sampled.

Marlborough Sounds Transect (IJ)

This transect lying north of the Wairau Fault consists of the samples taken from the Marlborough Sounds region. The depositional ages of the host rocks range from Carboniferous to Permian. The samples can be separated into two groups in this transect (Figures 6.1 and 6.7e): an older age group (~30-68 Ma) and a younger age group (~8-25 Ma). The different ages of these two groups may result from vertical movement on the Waimea Fault. The reset apatite age (7.9 ± 2.3 Ma) of Sample 9414-104 with long mean track lengths (14.27 ± 0.60 μm) indicates that the host rocks cooled through the closure temperature of 110°C during the late Cenozoic. For Samples 9414-90, -91 and -105, the apatite ages (~14-25 Ma) indicate they resided in the lower parts of a partial annealing zone (90-100°C) prior to the start of uplift and erosion. The fission track ages and lengths of

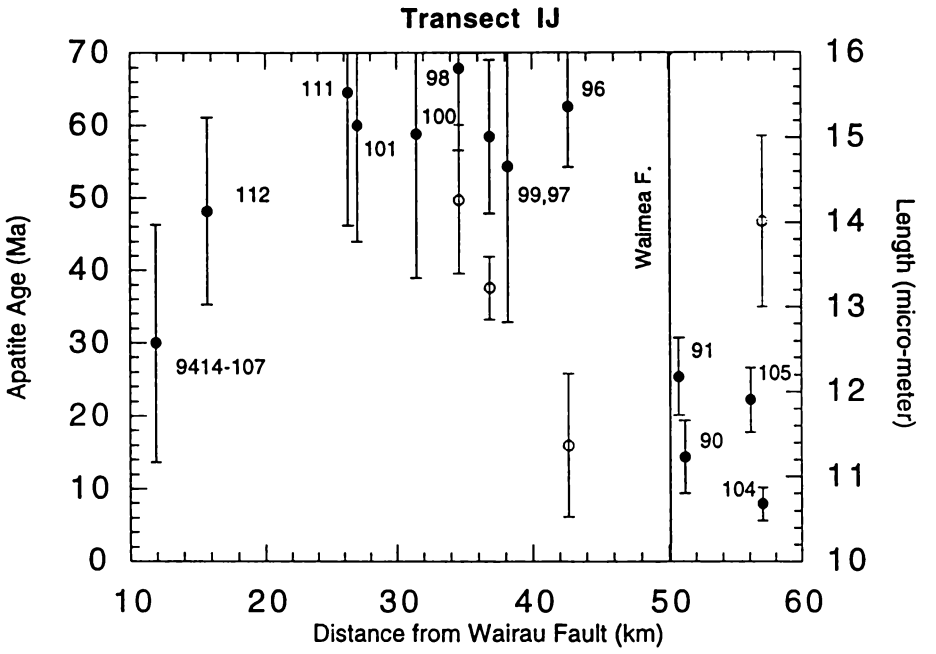

Figure 6.7e Apatite fission track age (close circle) and length (open circle) versus distance from Wairau Fault for samples in the Marlborough Sounds (IJ) transect.

9414-96, -97, -98, -99, -100, -101 and -111 show that they resided in the upper parts of a partial annealing zone (70-90°C) prior to uplift and erosion during the late Cenozoic.

Transects AB, CD, EF, and GH

The apatite fission track age and length data have also been plotted with respect to distance from the Wairau Fault (Figures 6.8a,b,c,d). The transects are oriented normal to the main Cenozoic faults. Most of the data points have been discussed in some detail above, and only general features are highlighted here. In Transect GH the apatite ages decrease south of the Wairau Fault and reach a plateau of 5-10 Ma across about 60 km of Triassic sandstone (Samples 9414-55 to 60) without showing offset corresponding to the major faults. The ages south of the Hope Fault are much greater, indicating much less late Cenozoic denudation. Samples 9414-34, -35 and -36 are not plotted on Transect GH as they occur further to the northeast. They have ages between 24.0 ± 7.3 and 51.6 ± 17.2 Ma, and were heavily partially annealed prior to cooling in the late Cenozoic. These samples are useful in reconstructing the extent of a high uplift/denudation zone surrounding the Spenser Mountains.

Transect EF shows significant younger ages in the block between the Wairau and Awatere Faults, than between the Awatere and Clarence Faults, suggestive of big differences across the Awatere Fault in the level of denudation. This pattern is also present in Transect CD, but not as marked. Another notable feature in Transect CD is the young ages between the Hope and Clarence Faults associated with denudation of the Seaward Kaikoura Range.

For Transect AB, fission track ages reveal a wide range from 18 to 129 Ma, implying that the host rocks of the samples have experienced variable levels of a partial annealing zone. Although there are not many mean track lengths in this transect, the early Miocene event can be determined by the reset samples (9414-1, -2 and -86). The apatite ages of samples (9414-3, -38, -83, -87 and -88) range from 25 to 84 Ma. The host rocks of Samples 9414-3, -38 and 87 experienced the lower parts of a partial annealing zone during the late Cenozoic; Samples 9414-87 and -88 cooled through the upper part. The host rocks of Sample 9414-84 may have experienced partial annealing during the late Cretaceous.

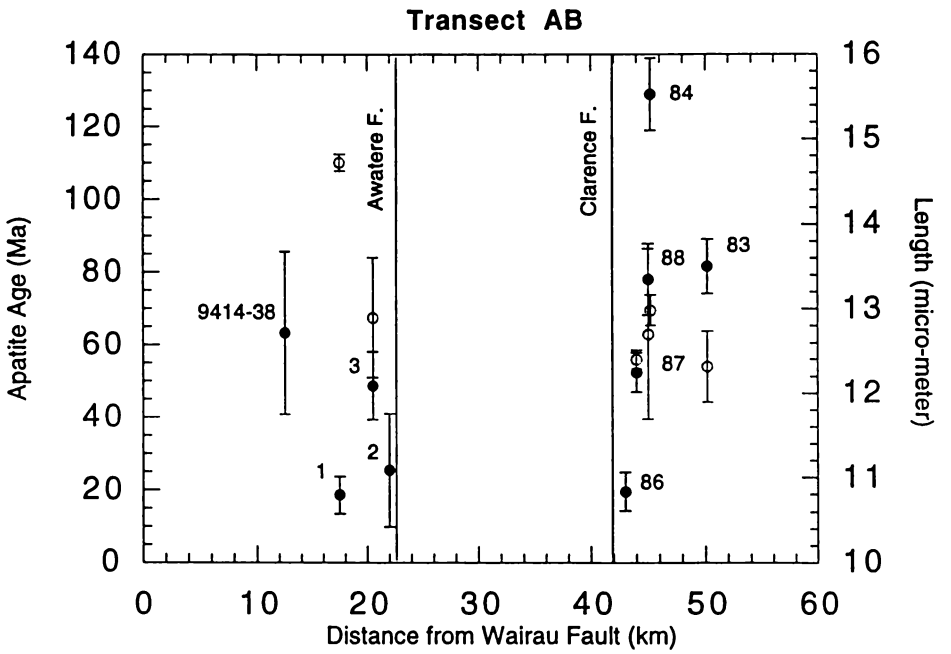

Figure 6.8a Apatite fission track age (close circle) and length (open circle) versus distance from Wairau Fault for samples in the Blenheim (AB) transect.

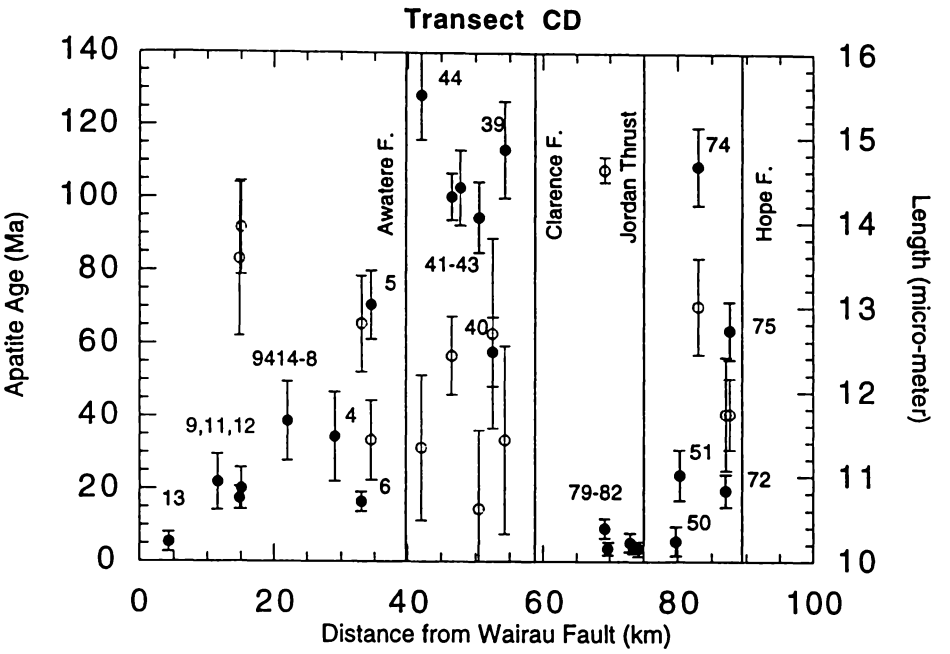

Figure 6.8b Apatite fission track age (close circle) and length (open circle) versus distance from Wairau Fault for samples in the Kaikoura-1 (CD) transect.

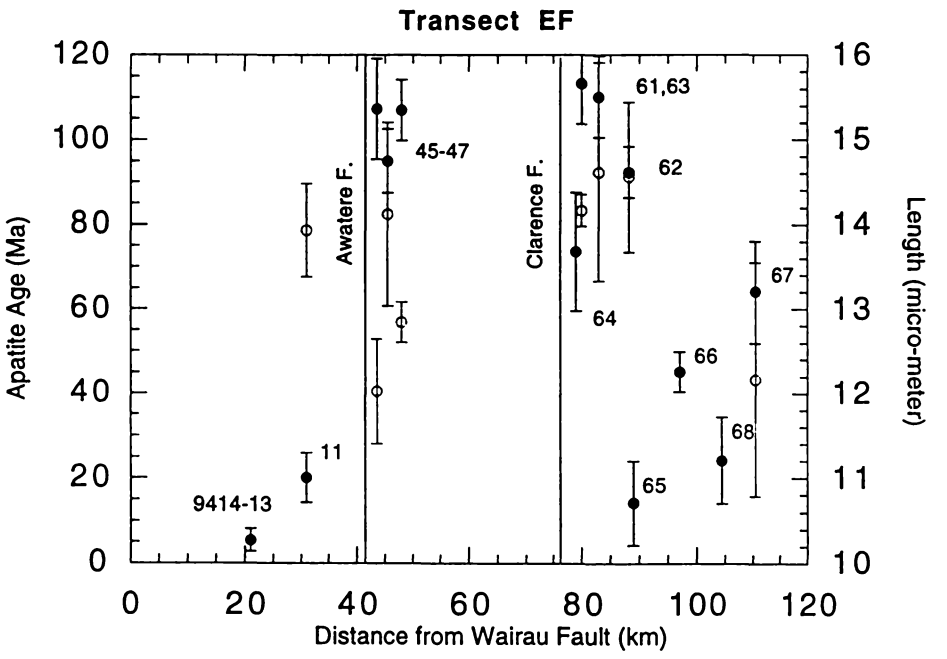

Figure 6.8c Apatite fission track age (close circle) and length (open circle) versus distance from Wairau Fault for samples in the Kaikoura-2 (EF) transect.

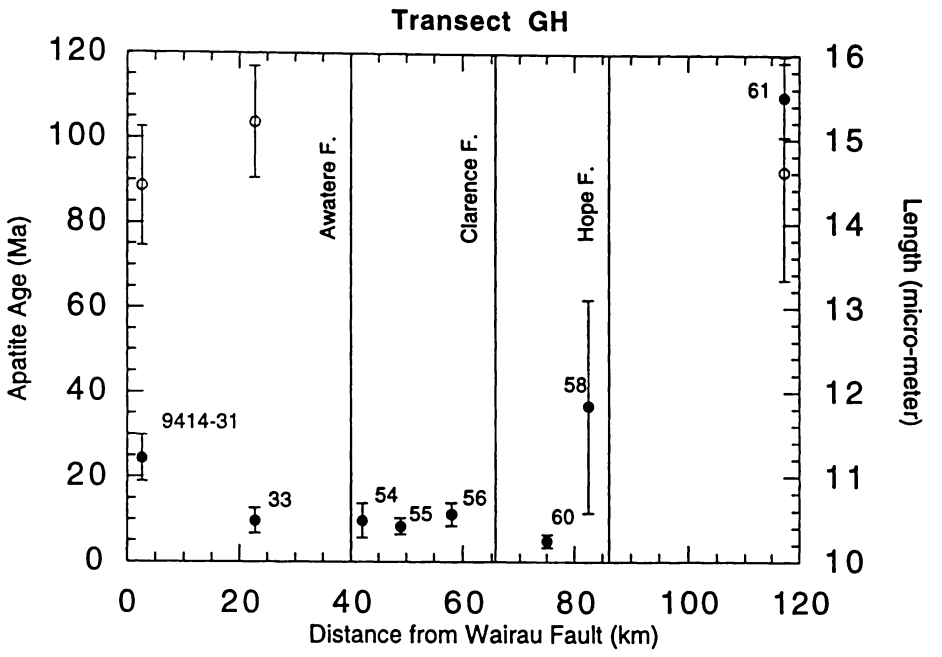

Figure 6.8d Apatite fission track age (close circle) and length (open circle) versus distance from Wairau Fault for samples in the Spenser Mountain (GH) transect.

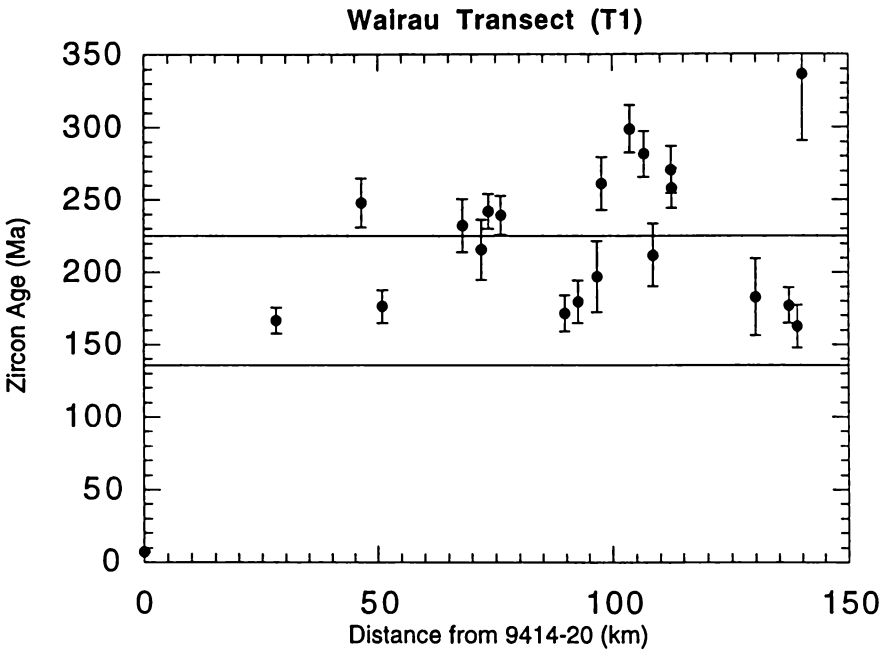

Figure 6.9a Transect T1: Zircon fission track age versus distance from Sample 9414-20; the area between two lines is the depositional age (from Triassic to Jurassic).

6.3.3 Zircon fission track results

All the zircon fission track data are reported in Table 6.3. Zircon ages of the samples range from 6.8 ± 0.5 Ma to 336.2 ± 45.3 Ma. However, despite this range, most of the pooled mean ages are greater than early Cretaceous ages and are related to the provenance of the grains, perhaps in some cases with a degree of partial overprinting prior to Cretaceous cooling. The zircon data are useful in helping to evaluate the degree of denudation where the apatites were totally overprinted. Hence the examination here of the data emphasised the search for zircons with reset late Cenozoic ages, or partial annealing zones cooled by late Cenozoic denudation. The provenance information contained in the zircon fission track ages is not explored in this thesis.

There is no significant pattern for zircon ages in each transect (Figures 6.9a-d and Figure 6.10). The extremely young ages (~6.8-10.0 Ma) of samples (9414-19, -20, -21 and -25) lying in the vicinity of the Alpine Fault bend indicate that the fission tracks had been reset during the recent rapid uplift and experienced cooling from temperatures of ~240°C. Except for the reset samples and some samples in the Marlborough Sounds region, most of the zircon ages are consistent with the stratigraphic ages, revealing that the samples have not been severely annealed since deposition. For Transect IJ, zircon ages are younger than the depositional ages (from Carboniferous to Permian), indicating that the host rocks of the samples had cooled through or from within a partial annealing zone. Sample 9414-104 has the youngest age (~119 Ma) which can be considered as a reset age, revealing that the host rocks of that sample had experienced temperatures of 240°C or higher during Mesozoic burial.

6.4 Timing of cooling

The timing of cooling events can be identified from the apatite fission track data and geological evidence.

6.4.1 Geological data

In Marlborough a magmatic and extension event occurred at ~100 Ma, as shown by the following evidence: (a) the Rb-Sr and fission track ages of the Tapuaenuku Plutonic

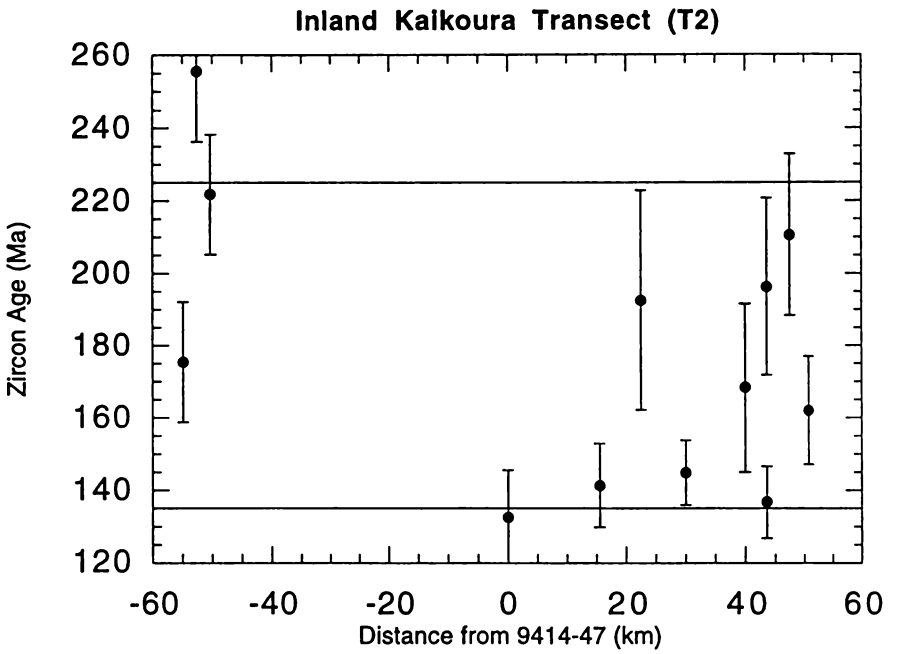

Figure 6.9b Transect T2: Zircon fission track age versus distance from Sample 9414-47; the area between two lines is the depositional age (from Triassic to Jurassic).

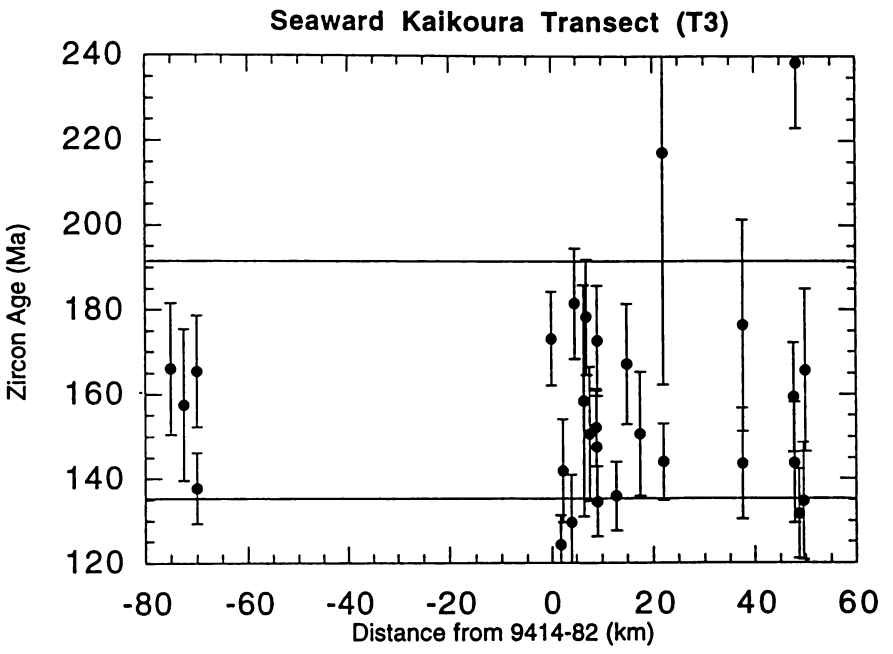

Figure 6.9c Transect T3: Zircon fission track age versus distance from Sample 9414-82; the area between two lines is the depositional age (from Triassic to Jurassic).

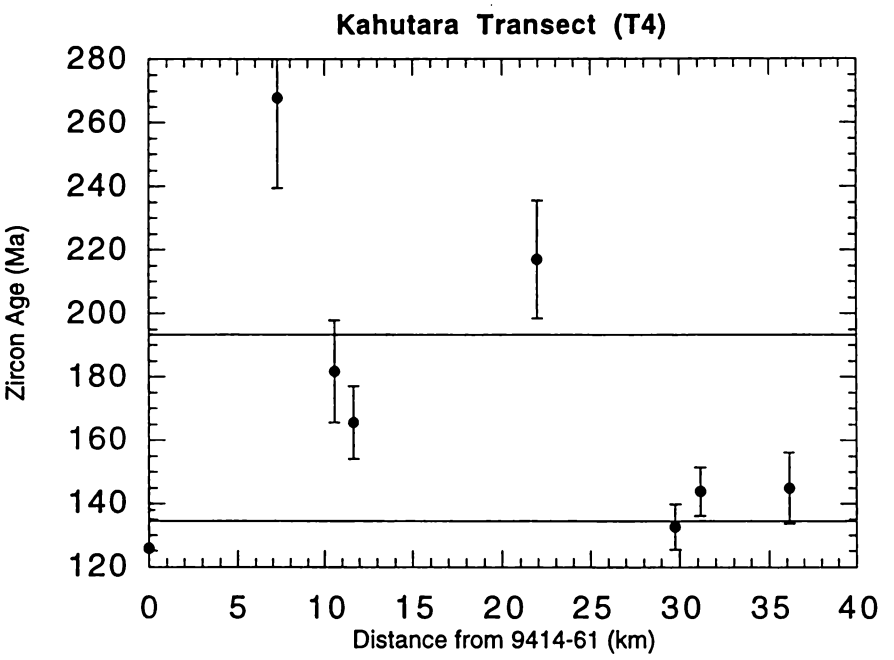

Figure 6.9d Transect T4: Zircon fission track age versus distance from Sample 9414-61; the area between two lines is the depositional age (Jurassic).

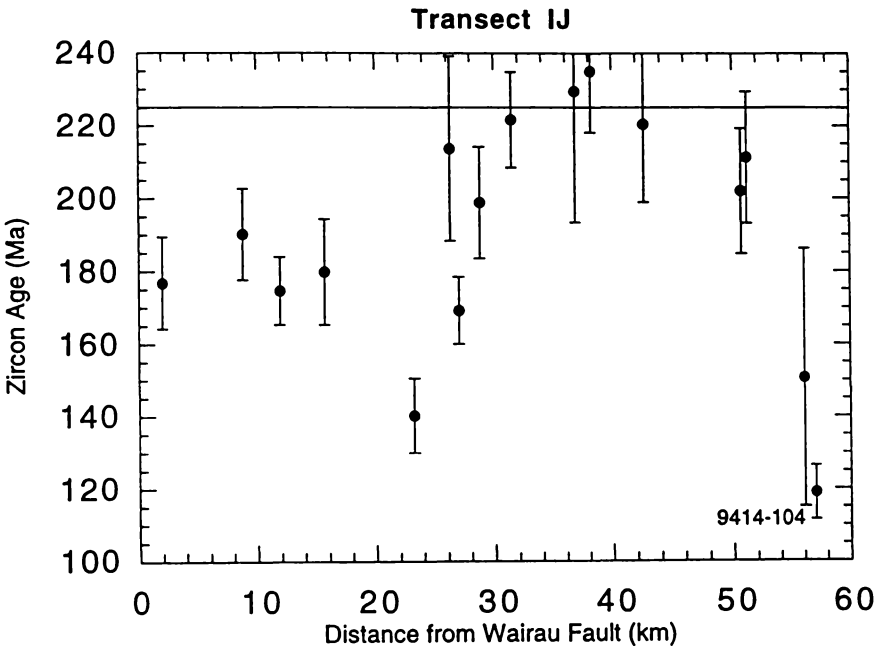

Figure 6.10 Transect IJ: Zircon fission track age versus distance from Wairau Fault; the area above the line is the depositional age (from Carboniferous to Permian).

Complex: range from 105 to 93 Ma (Baker and Seward, 1996); (b) the Split Rock Formation, belonging to Motuan age (105-100 Ma) unconformably overlies Torlesse basement (Reay, 1993); (c) the terrestrial sediments of the Warder Formation (Ngaterian, 100-94) overlying the Split Rock Formation represent the minimum age of a therrmal/tectonic event.

After the mid Cretaceous extension, tectonic quiescence occurred from 90 to 25 Ma. The deposition of greensands and marine limestone reflects this quiescence (Baker and Seward, 1996). During the late early Miocene, the Great Marlborough Conglomerate indicates rapid uplift and erosion. Thrusting and shortening deformation became dominant during the late Cenozoic Kaikoura Orogeny.

6.4.2 Apatite fission track data

Based on the pattern of mean fission track lengths versus apatite fission track ages (Figure 6.6), the reset samples (9414-1, -31, -46, -61, -62 and -63) reveal two major cooling events, occurring in the Miocene and mid Cretaceous (~100 Ma). Samples 9414-33 and -81 reflect the continuing of the cooling event from Pliocene to the present.

Although the samples in Transect AB (Figure 6.8a) have few mean lengths, three samples (9414-1, -2 and -86) reveal the cooling event during the early to mid Miocene. For Transect CD-(Kaikoura-1) (Figure 6.8b), the recent cooling event (from Pliocene to the present) can be identified by several reset samples (9414-13, -50, -78, -79, -80, -81 and -82); the partial annealing zone in the late Cenozoic is represented by several samples (9414-4, -5, -6, -8, -9, -11, -12, -40, -51, -72 and -75); Samples 9414-41, -42 and -43 were heavily annealed, but not reset in the late Cretaceous; Samples 9414-39, -44, and -74 experienced partial annealing in the late Cretaceous. The apatite fission track ages for the samples between the Wairau and Awatere Faults increase away from the Wairau Fault.

To summarise, fission track data and geological evidence indicate that two cooling events have occurred since the mid-late Cretaceous: one event started at about 20 Ma (the early Miocene) and continues to the present and the other started at about 100 Ma (late Cretaceous) and possibly continued for about 10 m.y.

6.4.3 Modelled thermal histories

Fission track thermal history modelling software, known as "Monte Trax", has been developed by Gallagher (1995) and can be applied to define the thermal histories consistent with observed fission track parameters. This programme assumes necessarily that the apatites have a uniform composition. We know however from the compositional data reported by Tippett and Kamp (1993) that the apatites in the Triassic sandstones, at least, have variable chlorine contents. No new composition data were obtained in this study, and therefore we are forced to assume that the temperature of total annealing in Marlborough apatites is similar to that of Durango apatite (~110°C). Monte Trax modelling was undertaken on eleven samples obtained from Marlborough (Table 6.4). These are the samples for which there were reasonable length data. The results of the modelling, which incorporated stratigraphic constraints, where those were available, are shown in Figures 6.11a-k for the eleven samples.

Samples 9414-2, -5 and -11 lie between the Wairau and Awatere Faults and were collected from the NE Wairau block. The basement in this block comprises mainly upper Triassic-Jurassic sandstone (greywacke). Cover strata are of late Miocene and late Quaternary ages. There is no record of Cretaceous to mid-Miocene stratigraphic units, but deposition during this interval cannot be ruled out. The three sample sites may have had similar thermal histories based on their position on the length-age plot (Figure 6.6). They will differ however in the maximum temperatures experienced, with the order of increasing paleotemperatures being 9414-11 > 9414-2 > 9414-5, as judged from the positions on the length-age plot (Figure 6.6).

The modelling of Sample 9414-5 requires a two stage cooling history. The first phase of cooling is required during the mid-Cretaceous, which brought the rocks sampled into the annealing zone. This ended at about 91 Ma. There may have been a slight amount of heating from 91-15 Ma, followed by rapid late-early to late Miocene cooling. This phase of cooling achieved through uplift and erosion would have removed the stratigraphic evidence for any sedimentation during the late Cretaceous-Miocene. The modelling is not really sensitive to the late Miocene sedimentation. The lack of a good match between the predicted and observed length distributions possibly reflects the difficulty of measuring good numbers of lengths in the apatites we had to work with.

Table 6.4 Paleotemperatures, rock uplift, and denudation amounts estimated by the forward modelling.

Sample Number	Area	Elevation (km)	Mineral	Age (Ma)	Mean Track Length ± 1σ (μm)	Pre-uplift Paleotemp. (°C)	Amount of Uplift (km)	Denudation (km)	Uplift Age (Ma)
9414-2	Wairau Block	0.3	apatite	26.3 ± 3.6	12.89 ± 0.71	104.0 ± 10.0	4.7 ± 1.2	4.4 ± 1.2	13.0 ± 2.0
			zircon	177.0 ± 12.4					
9414-5	Wairau Block	0.3	apatite	70.5 ± 9.3	11.43 ± 0.47	92.0 ± 10.0	4.1 ± 1.1	3.8 ± 1.1	15.0 ± 2.0
			zircon	299.0 ± 16.2					
9414-11	Wairau Block	0.4	apatite	20.0 ± 5.8	13.93 ± 0.55	106.0 ± 10.0	4.8 ± 1.2	4.4 ± 1.2	14.0 ± 2.0
			zircon	171.7 ± 12.6					
9414-43	Inland Kaikoura Range	0.4	apatite	100.2 ± 6.4	12.43 ± 0.46	59.0 ± 5.0	2.5 ± 0.6	2.1 ± 0.6	2.0 ± 1.0
			zircon	169.4 ± 23.3					
9414-45	Inland Kaikoura Range	1.28	apatite	107.1 ± 7.2	12.84 ± 0.24	55.0 ± 5.0	2.3 ± 0.5	1.0 ± 0.6	2.0 ± 2.0
			zircon	141.3 ± 11.5					
9414-61	Kahutara River	0.11	apatite	110.2 ± 9.6	14.62 ± 0.14	45.0 ± 5.0	1.8 ± 0.5	1.6 ± 0.5	3.0 ± 1.0
			zircon	129.0 ± 12.0					
9414-62	Kahutara River	0.14	apatite	92.4 ± 6.0	14.56 ± 0.17	50.0 ± 5.0	2.0 ± 0.5	1.9 ± 0.5	1.0 ± 0.5
			zircon	267.9 ± 28.4					
9414-63	Kahutara River	0.36	apatite	113.3 ± 9.4	14.17 ± 0.19	50.0 ± 5.0	2.0 ± 0.5	1.6 ± 0.5	1.0 ± 0.5
			zircon	181.6 ± 16.1					
9414-73	Seaward Kaikoura Range	0.04	apatite	63.5 ± 7.9	11.74 ± 0.42	85.0 ± 5.0	3.8 ± 0.8	3.7 ± 0.8	2.5 ± 1.0
			zircon	134.6 ± 8.3					
9414-83	Seaward Kaikoura Range	0.06	apatite	81.7 ± 7.5	12.31 ± 0.42	82.0 ± 5.0	3.6 ± 1.0	3.5 ± 1.0	2.0 ± 1.0
			zircon	131.7 ± 10.7					
9414-88	Seaward Kaikoura Range	0.26	apatite	78.1 ± 9.8	12.70 ± 0.1	85.0 ± 5.0	3.8 ± 1.0	3.5 ± 1.0	2.0 ± 1.0
			zircon	165.7 ± 19.2					
9414-19	Alpine Fault Bends	0.46	apatite	2.1 ± 1.5		~240.0	11.5 ± 1.8	11.0 ± 1.7	~5.0
			zircon	10.0 ± 0.9					
9414-20	Alpine Fault Bends	0.44	apatite	5.3 ± 2.2		~240.0	11.5± 1.8	11.0 ± 1.7	~5.0
			zircon	7.3 ± 0.5					
9414-21	Alpine Fault Bends	0.44	apatite	6.1 ± 6.1		~240.0	11.5 ± 1.8	11.0 ± 1.7	~5.0
			zircon	6.8 ± 0.5					
9414-23	Alpine Fault Bends	0.42	apatite	3.8 ± 1.0		~240.0	11.5 ± 1.8	11.0 ± 1.7	~5.0
9414-25	Alpine Fault Bends	0.54	apatite	7.9 ± 4.7		~240.0	11.5 ± 1.8	11.0 ± 1.7	~5.0
			zircon	9.5 ± 0.6					

Samples 9414-2 and -11 show very similar modelled histories to that for Sample 9414-5 (compare Figures 6.11a , b and c). They also show mid-Cretaceous cooling, but to higher temperatures in a partial annealing zone, meaning that fewer track lengths corresponding to that part of the thermal history are retained. Because rocks at the surface were sampled, the amount of late-early to mid Miocene cooling is much greater than that for Sample 9414-5.

Samples 9414-43 and -45 taken from the Inland Kaikoura Range lie between the Awatere and Clarence Faults. The stratigraphic components of the basement in the Inland Kaikoura block are similar to those of the Wairau block. The depositional ages of cover strata range from Cretaceous to Quaternary. The cover strata occur in the central to north-east parts of the Inland Kaikoura Range. The late Miocene and Quaternary rocks are limited to the north-easternmost end of the Awatere Valley. The hosts rocks of Sample 9414-43 are of mid Cretaceous age. The modelled thermal history of this sample (Figure 6.11d) indicates that apatites cooled rapidly in the source area during the mid Cretaceous, were deposited at about 100 Ma (Motuan) and probably reached maximum temperature (78°C) at the end of the Oligocene. There may have been some uplift/cooling during the early Miocene, followed by the further Pliocene uplift and erosion. Sample 9414-45 comprises Jurassic basement and shows a similar thermal history to Sample 9414-43 (Figure 6.11e), but with only minor late Cretaceous-Oligocene burial. Maximum temperature prior to Neogene cooling was about 65°C.

Samples 9414-73, -83 and -88 were collected from the Seaward Kaikoura block (Figure 6.1). These samples were difficult to model, that is, to get all predicted and observed parameters to match. However, the modelling was sufficient to estimate the maximum temperatures prior to Neogene inversion and erosion. Sample 9414-73 comprises Jurassic basement. It evidently cooled via uplift and erosion during the mid-Cretaceous, which uplifted the sample rocks into the zone of partial annealing (Figure 6.11f). There was minor heating during the late Cretaceous-Oligocene, with maximum temperatures of around 85°C prior to late Pliocene exhumation. Sample 9414-83 is a Motuan (Albian) sandstone. Modelling shows that this sample has probably been heated to a maximum temperature of about 82°C (Figure 6.11g). The apatites seem to have cooled during the early Cretaceous, were deposited in the basin with about 20 m.y. of inherited age, experienced some cooling during the early-late Cretaceous, and heating through burial during the late Cretaceous-

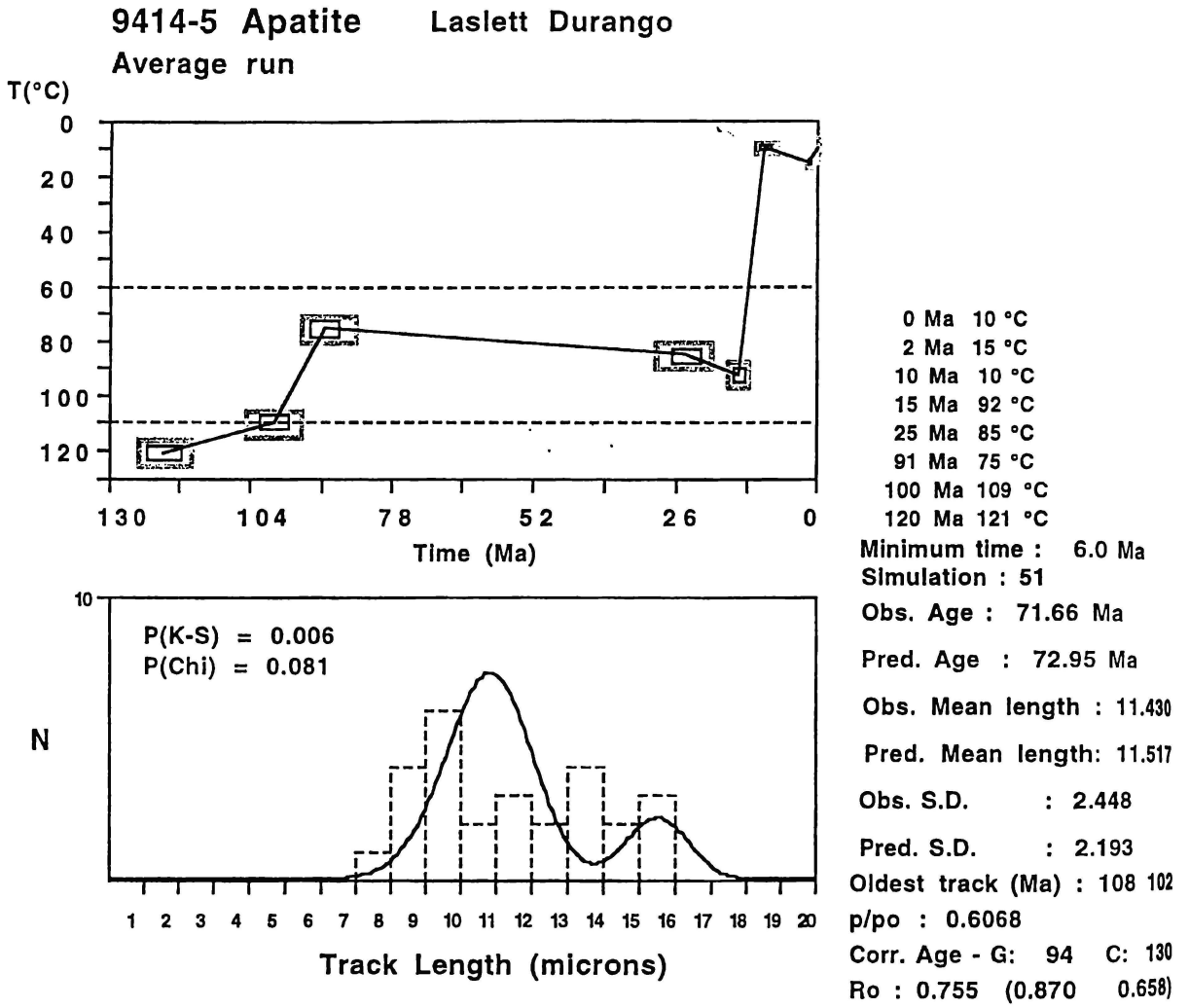

Figure 6.11a The observed and predicted fission track parameters, and modelled thermal history for Sample 9414-5, collected from the Wairau block.

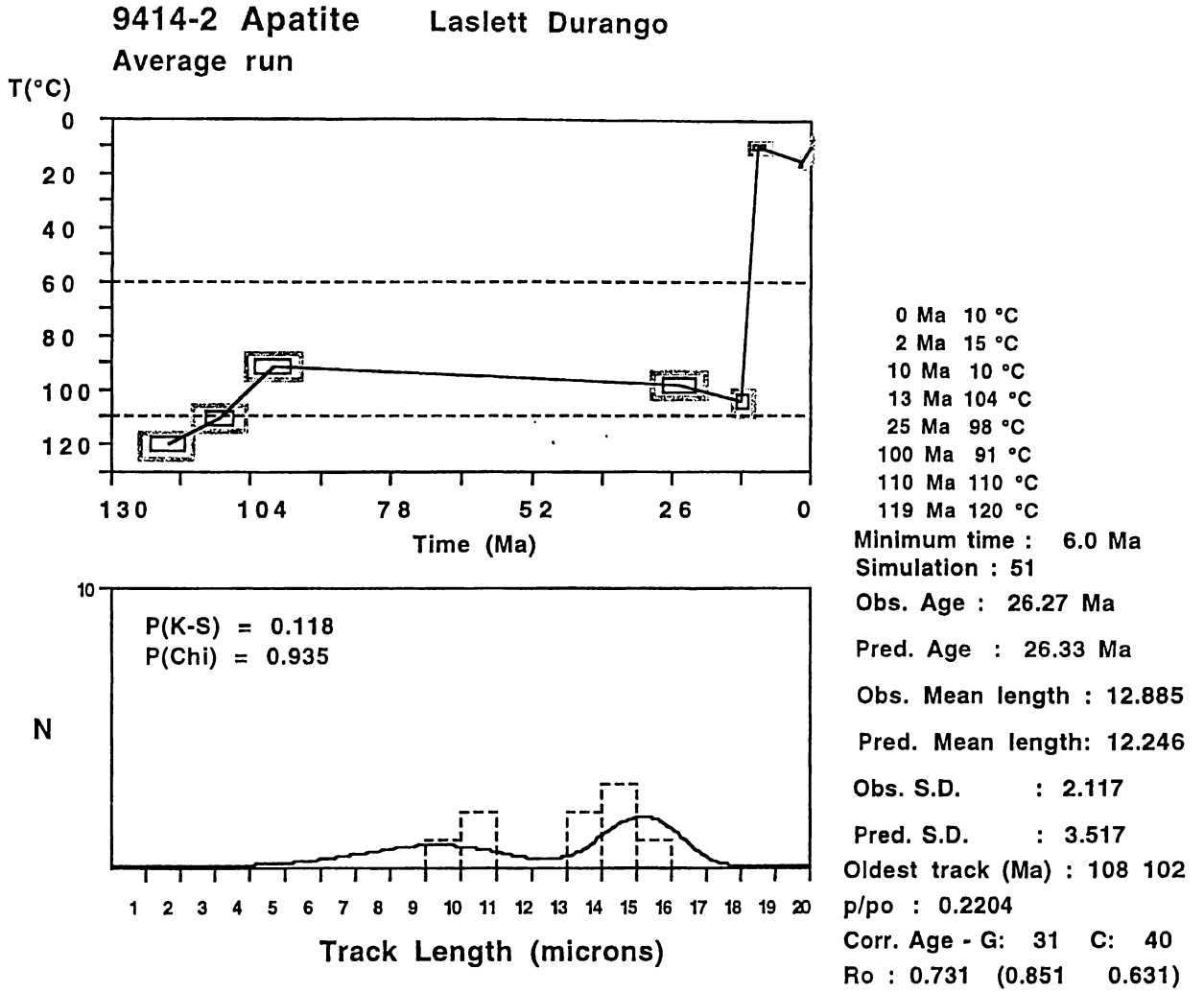

Figure 6.11b The observed and predicted fission track parameters, and modelled thermal history for Sample 9414-2, collected from the Wairau block.

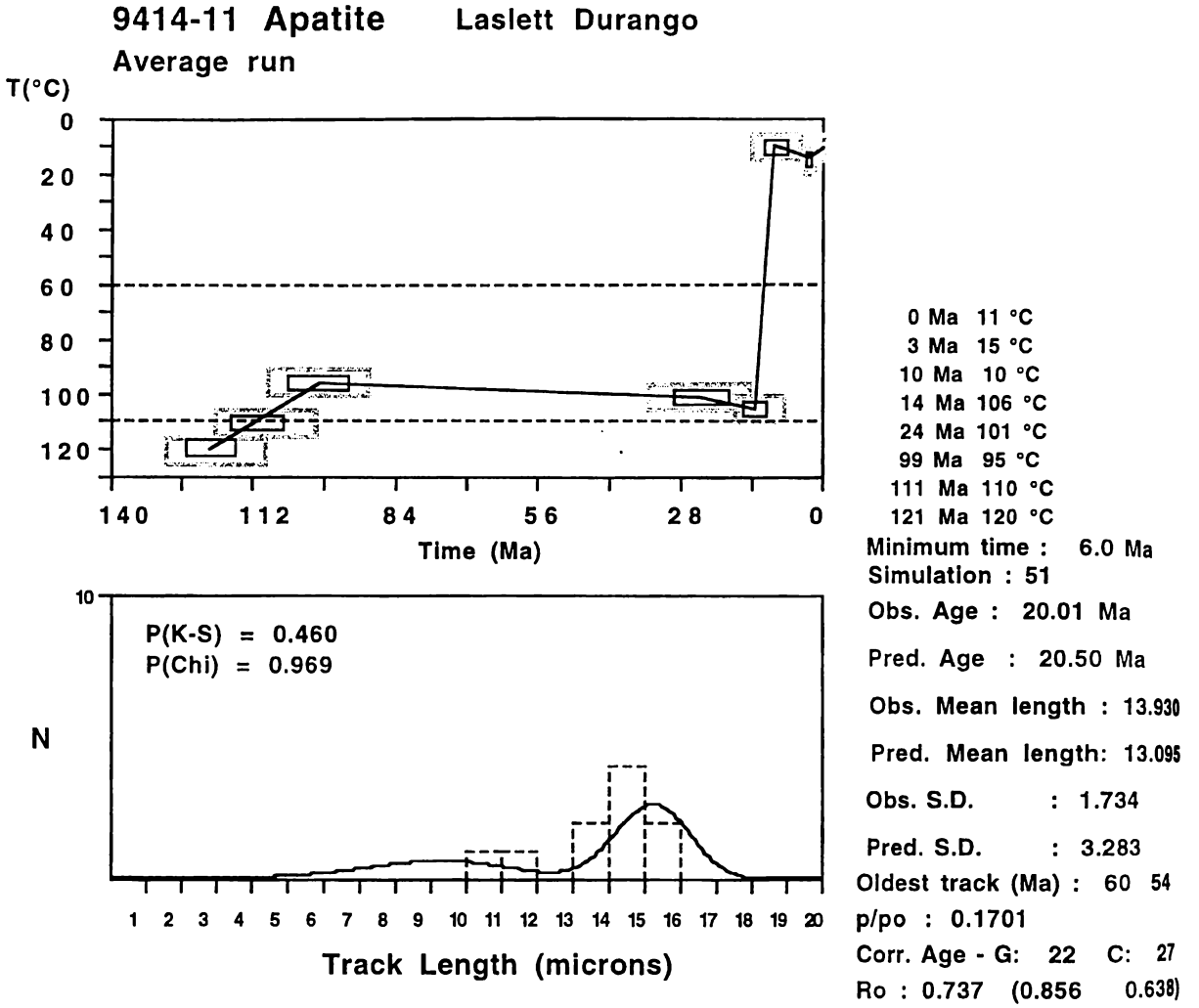

Figure 6.11c The observed and predicted fission track parameters, and modelled thermal history for Sample 9414-11, collected from the Wairau block.

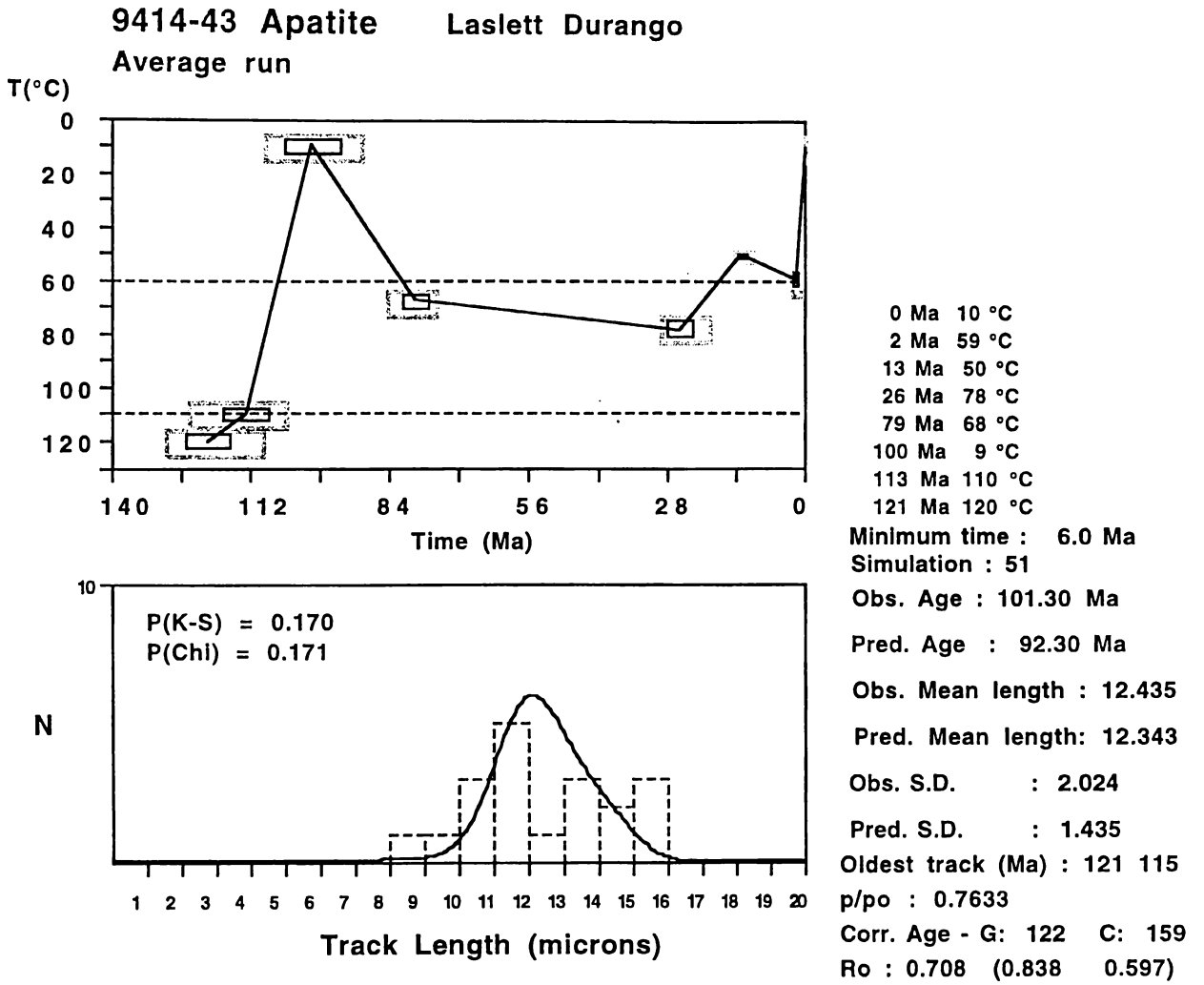

Figure 6.11d The observed and predicted fission track parameters, and modelled thermal history for Sample 9414-43, collected from the Inland Kaikoura block.

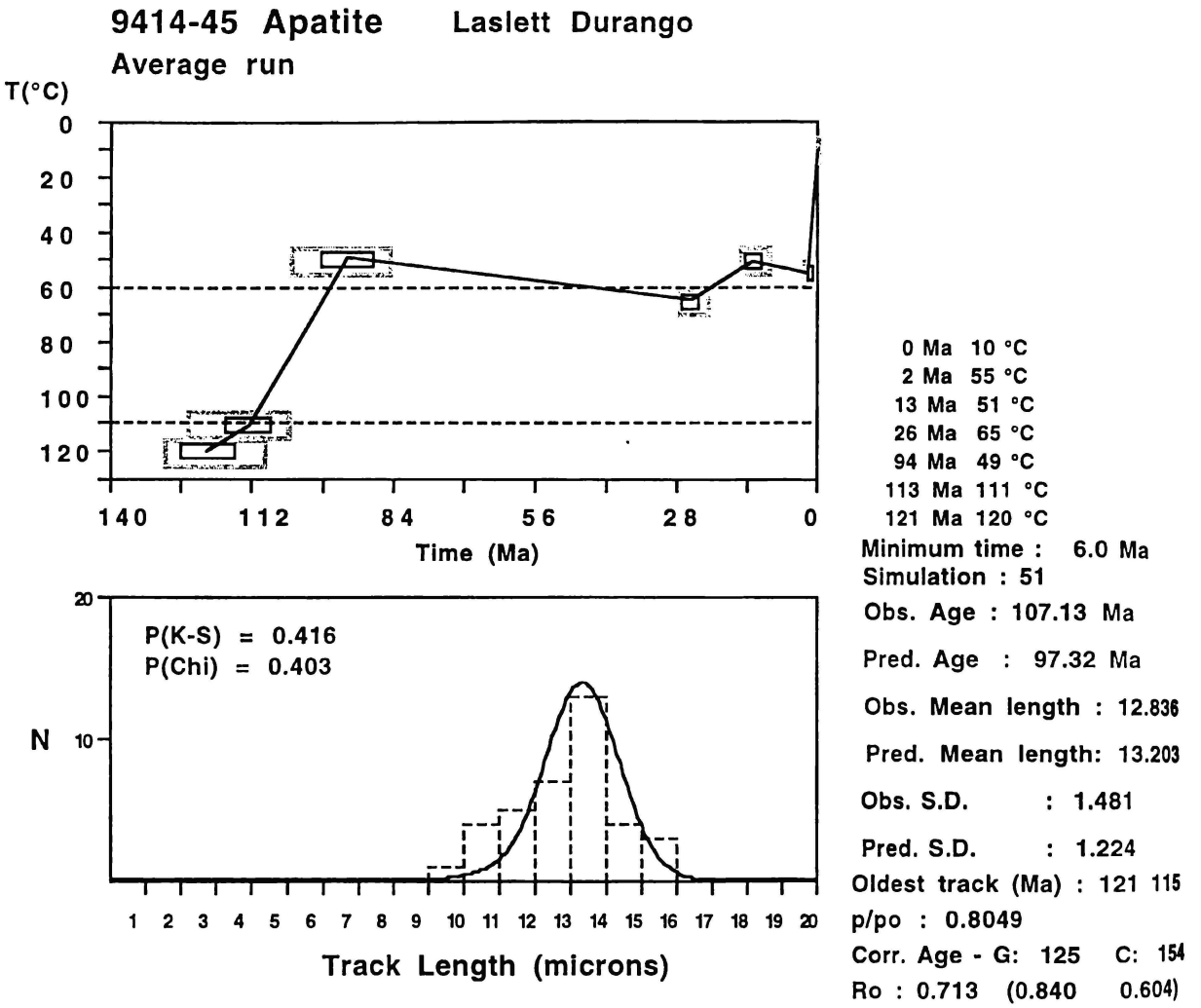

Figure 6.11e The observed and predicted fission track parameters, and modelled thermal history for Sample 9414-45, collected from the Inland Kaikoura block.

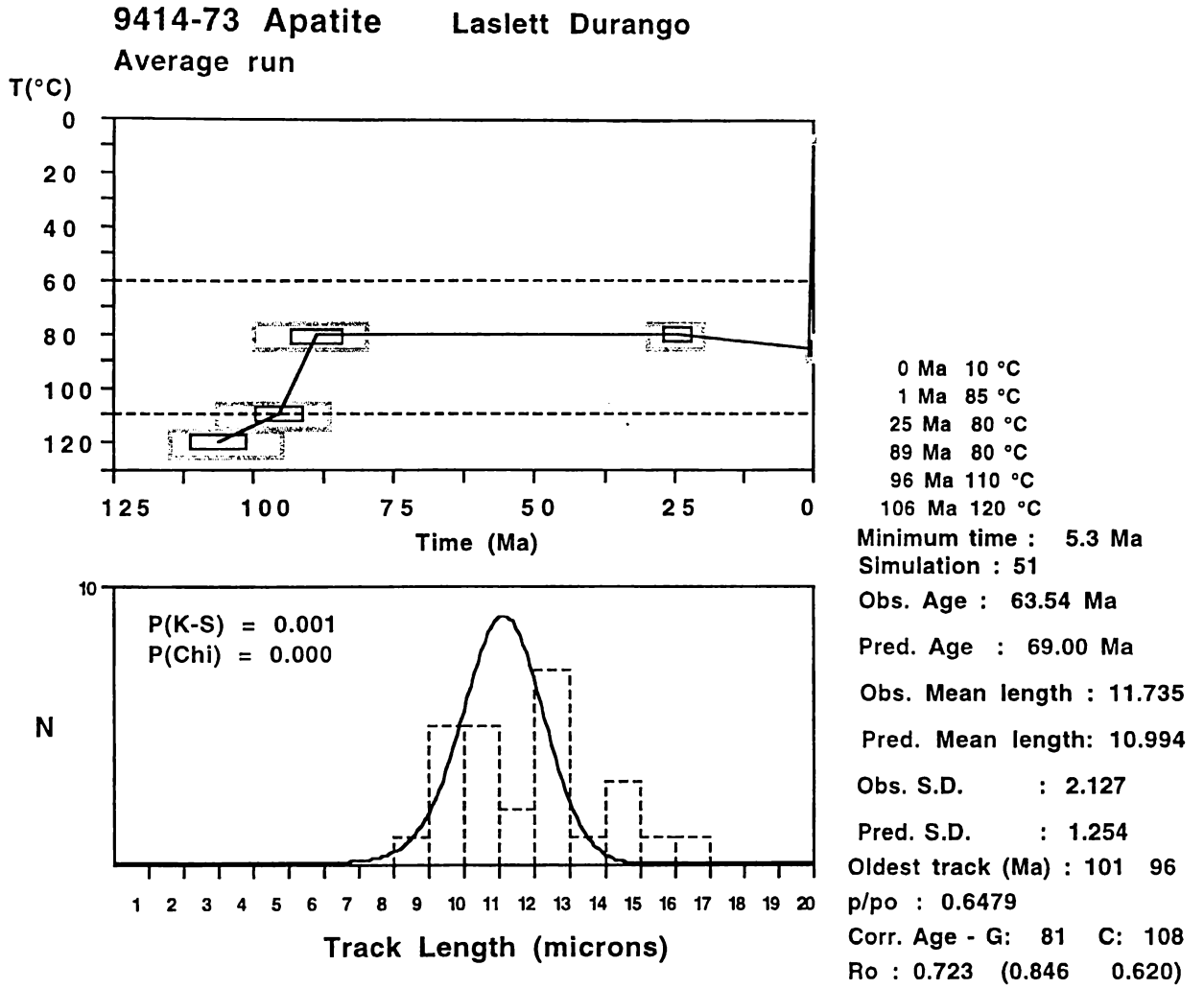

Figure 6.11f The observed and predicted fission track parameters, and modelled thermal history for Sample 9414-73, collected from the Seaward Kaikoura block.

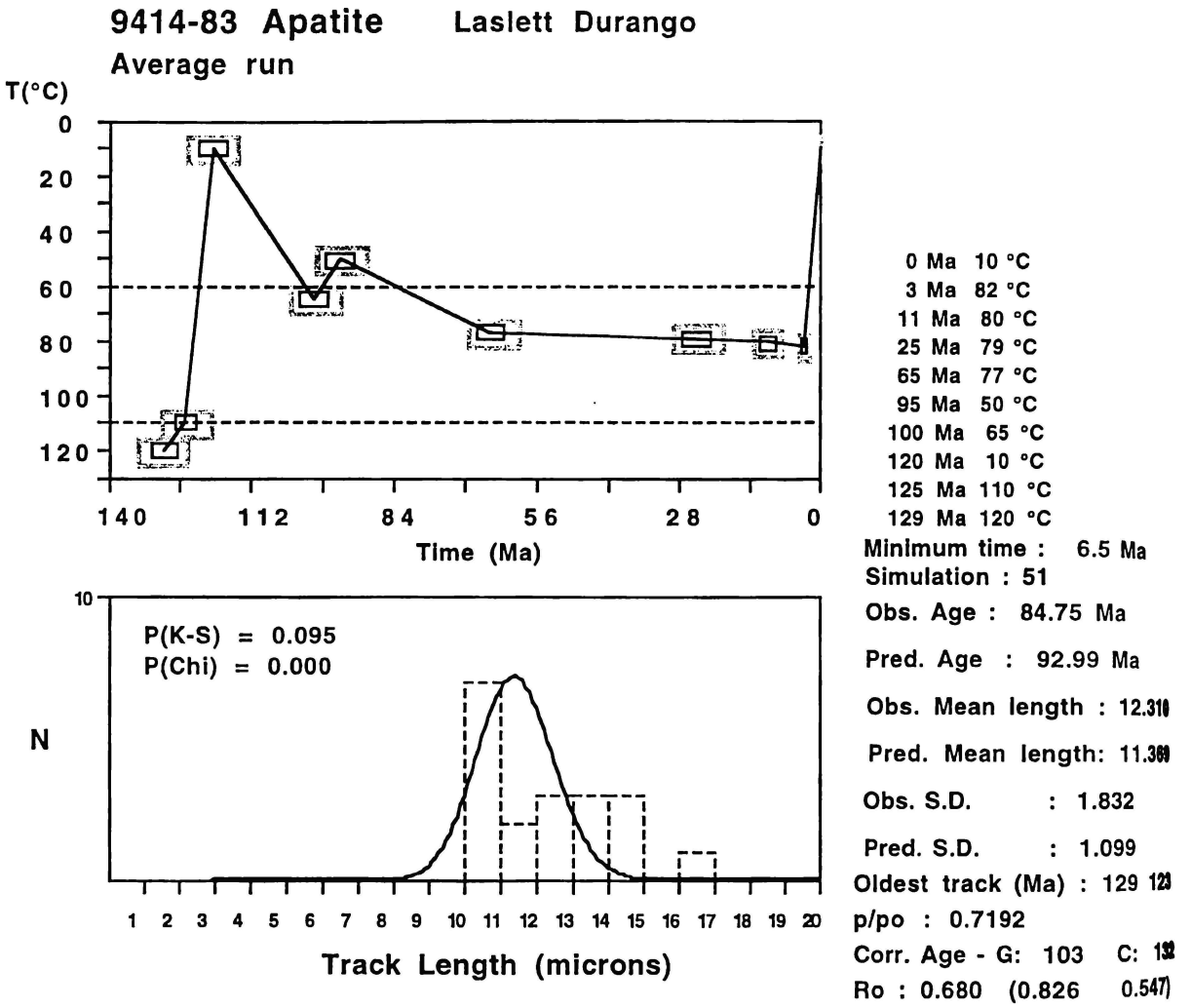

Figure 6.11g The observed and predicted fission track parameters, and modelled thermal history for Sample 9414-83, collected from the Seaward Kaikoura block.

Miocene. Sample 9414-88 is a lower Cretaceous sandstone, which appears to have cooled rapidly during the mid-Cretaceous, followed by rapid Motuan (Albian) burial and further slow late Cretaceous-Cenozoic burial and heating (Figure 6.11h). Maximum temperatures of about 85°C were experienced prior to cooling through uplift and erosion after 3 Ma.

Samples 9414-61, -62 and -63 come from sites south of the Hope Fault (Figure 6.1), and have Jurassic depositional ages. On Figure 6.6 these samples have long mean lengths and comparatively old ages. The modelling results are moderately successful (Figures 6.11i, j and k). All three samples show a strong mid-Cretaceous cooling phase that brought the host rocks up to near the surface. This was followed by late Cretaceous-Cenozoic heating through burial and accommodation of cover strata, followed by late Pliocene-Pleistocene uplift and erosion of that cover succession. Maximum temperatures achieved prior to the latest phase of uplift and erosion are in the ranges of 45-50°C.

In this section samples with good length data have been selected for modelling of the thermal histories. The sample were selected to sample all parts of the length-age plot (Figure 6.6). What has emerged is that all samples modelled retain same evidence for a mid Cretaceous cooling event, even where there has been major late Cenozoic cooling. (Samples with very young ages and long lengths have not been modelled because of the inadequacy of the length data, but these would not see back to the mid-Cretaceous event because they were totally reset by the recent uplift and denudation). The Jurassic rocks modelled (from more western parts of Marlborough) tend to show the cooling event as having occurred during the Motuan (Albian), whereas Motuan rocks annealed show a slightly later phase of uplift (94-90 Ma) and retain a provenance signal that "sees" back to the early Cretaceous. In all cases the modelling is consistent with late Cretaceous-Oligocene burial/heating, but this can be minor in the more western parts of Marlborough where these rocks are not present. The timing of the main Neogene uplift/erosion event varies, being earlier (mid to late Miocene) in the north (Wairau block) and later (late Pliocene-Pleistocene) in the southeast (Seaward Kaikoura Range). The samples in Figure 6-6 that have older ages (>90 Ma) but intermediate lengths (11-13 μm) appear to be from host rocks that were uplifted during the mid-Cretaceous into lower parts of a partial annealing zone, and experienced some subsequent late Cretaceous-Cenozoic burial. The consequence of spending considerable time in the zone of partial annealing, and only recent uplift, has been retention of age relative to length.

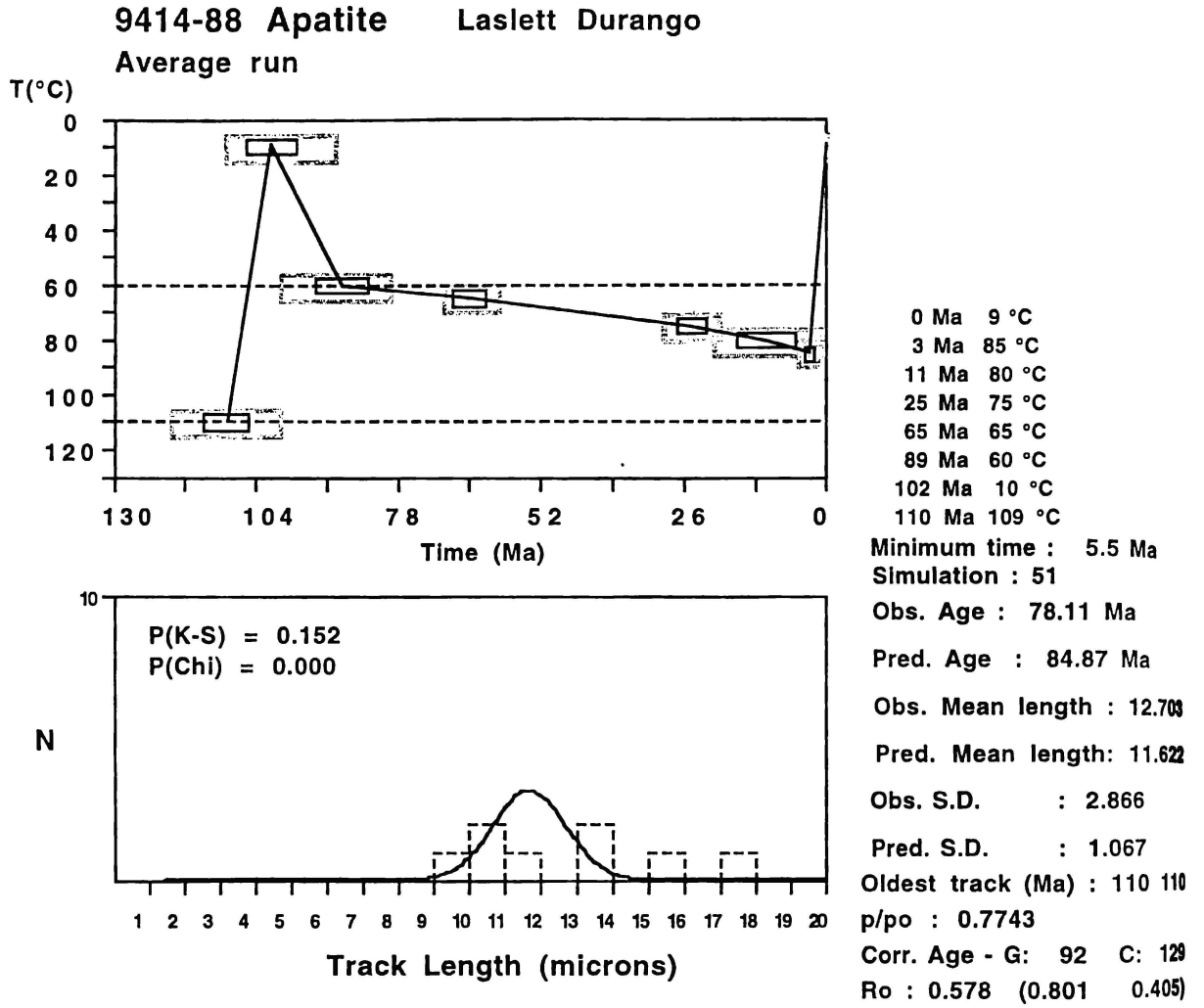

Figure 6.11h The observed and predicted fission track parameters, and modelled thermal history for Sample 9414-88, collected from the Seaward Kaikoura block.

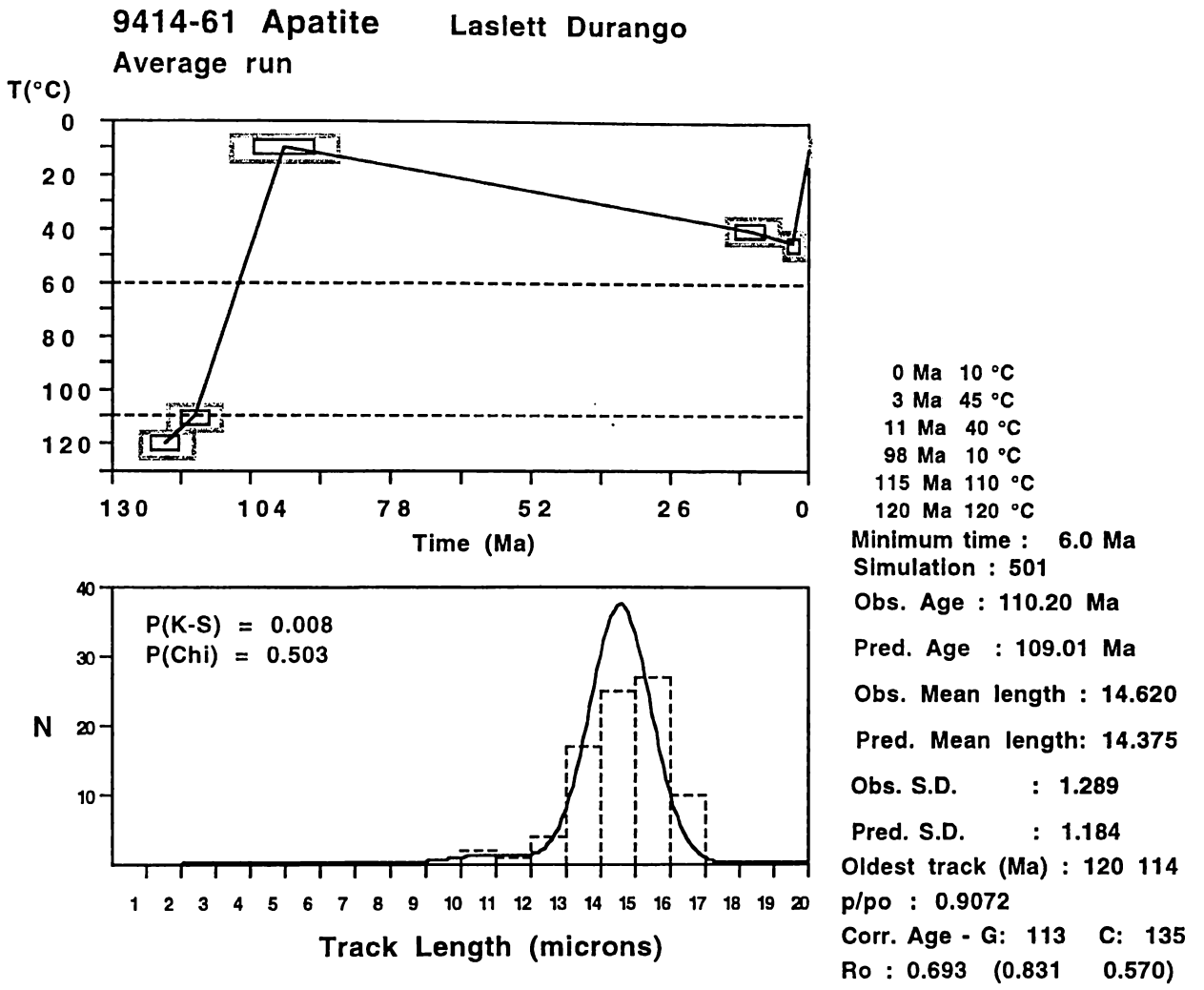

Figure 6.11i The observed and predicted fission track parameters, and modelled thermal history for Sample 9414-61, collected from the Kahutara block.

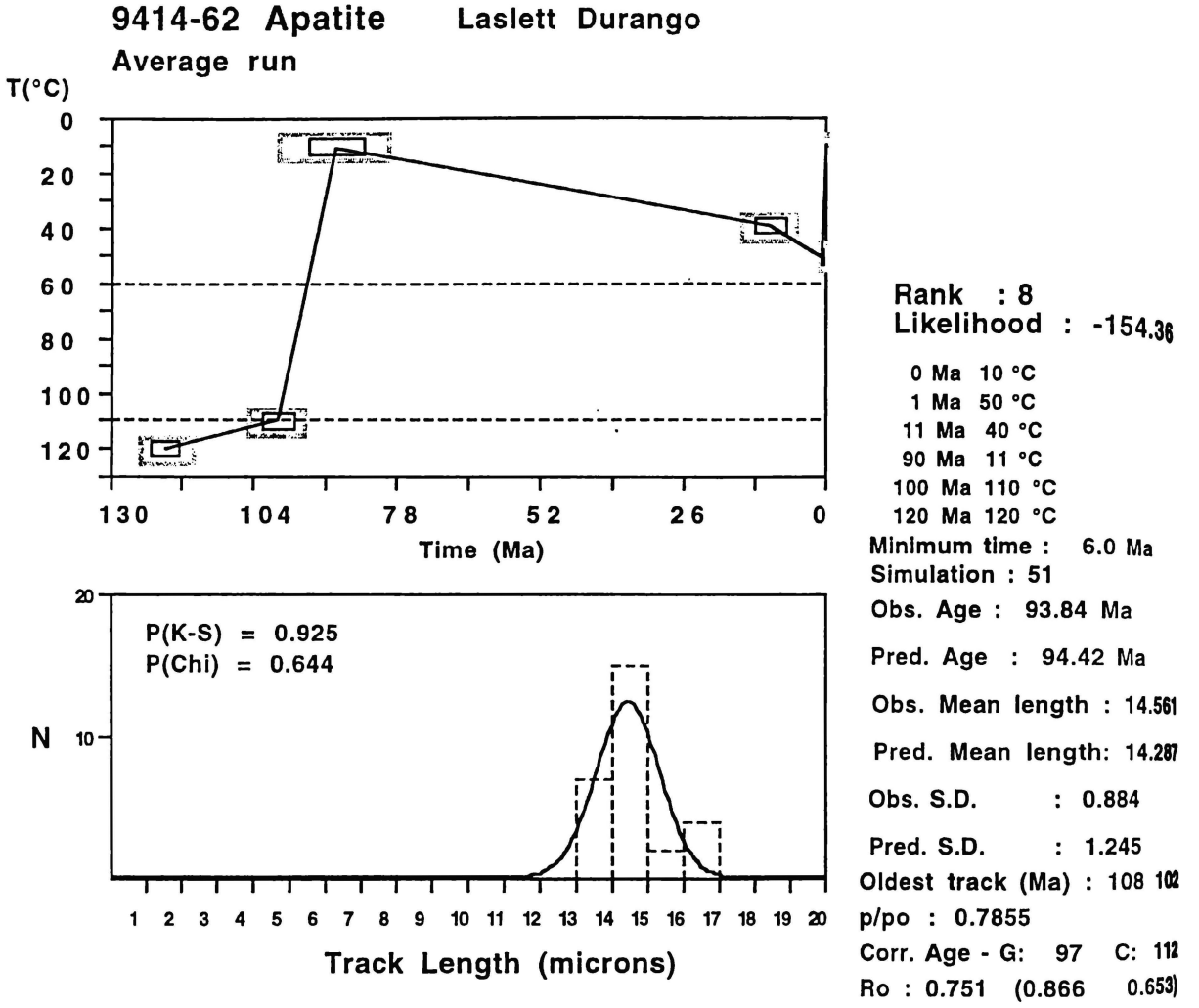

Figure 6.11j The observed and predicted fission track parameters, and modelled thermal history for Sample 9414-62, collected from the Kahutara block.

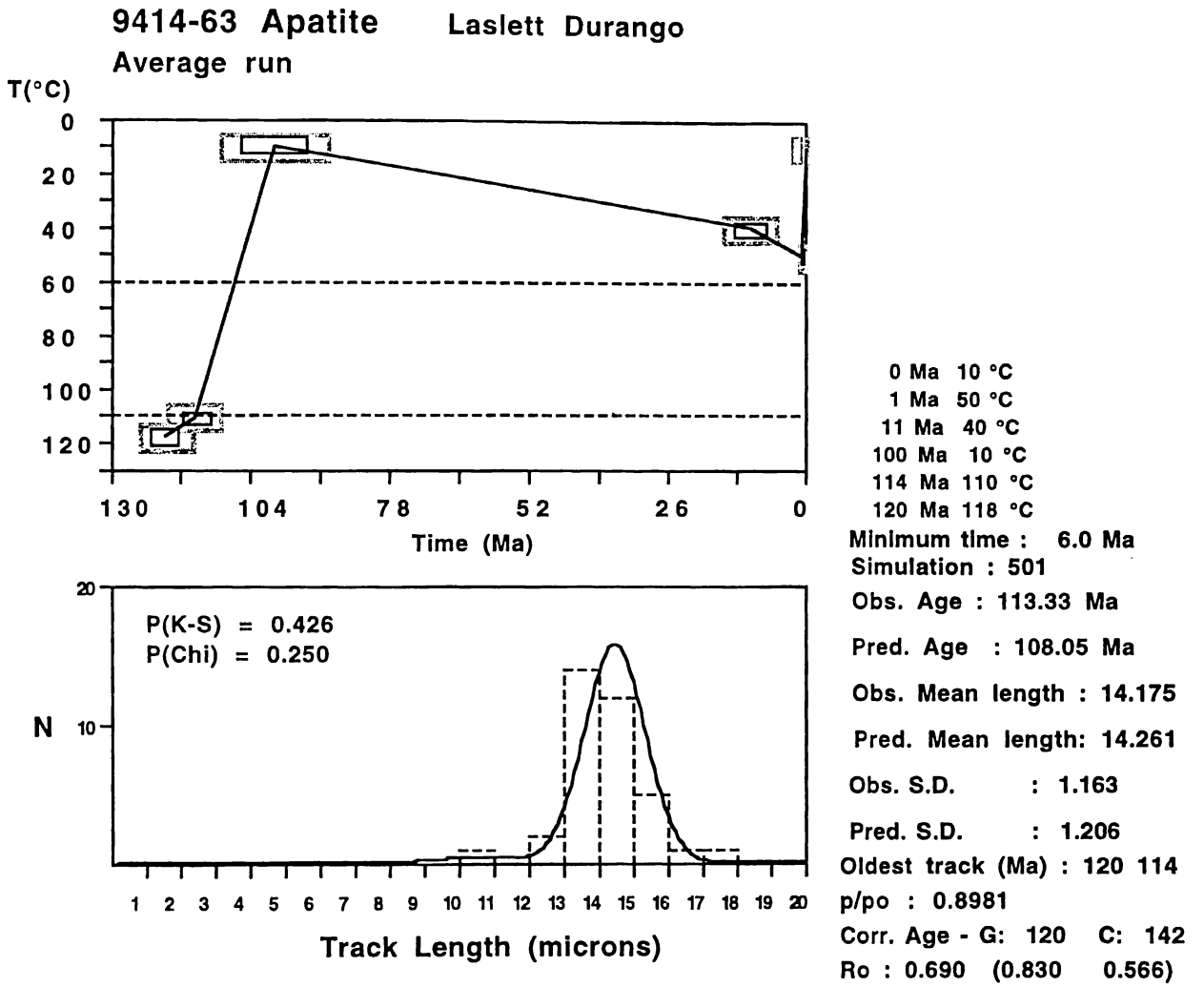

Figure 6.11k The observed and predicted fission track parameters, and modelled thermal history for Sample 9414-63, collected from the Kahutara block.

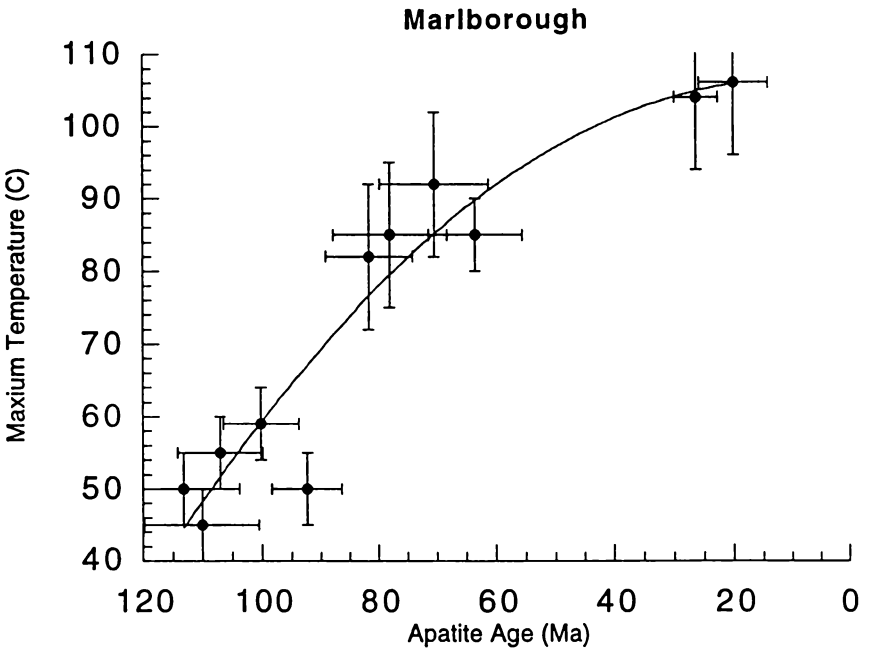

Figure 6.12 Maximum paleotemperature versus apatite fission track age for the samples, selected from the Marlborough region.

6.5 Estimation of maximum paleotemperatures, rock uplift, and denudation

6.5.1 Maximum paleotemperatures

The modelling of selected samples shows that the modelled thermal histories are consistent with the stratigraphic record preserved in parts of Marlborough. In particular, because of the long interval (late Cretaceous-Oligocene) of uninterrupted subsidence and heating, the fission track parameters carry a strong signal about the maximum paleotemperatures prior to late Neogene cooling. Given that the length data are not adequate for modelling of most of the samples, but most samples have measured apatite ages, an empirical relationship has been established (Figure 6.12) between apatite fission track age and maximum paleotemperature for the samples that have been modelled (Figures 6.11a-k). This relationship enables all samples with apatite fission track age to have an estimated maximum paleotemperature assigned to them. The resulting maximum temperatures are illustrated in Figure 6.13 and recorded in Table 6.5. Uncertainties are quoted at the 1σ level.

The greatest amount of cooling in Marlborough occurs along the Alpine Fault in the vicinity of the Alpine Fault bend, where rocks now at the surface have cooled from temperatures above 240 ± 25°C where fission tracks in zircon are reset. These samples correspond with exposure of Alpine Schist. Over wide parts of Marlborough the rocks now at the surface have cooled from lower levels of the apatite partial annealing zone, that is, from less than about 110°C. Generally, the rocks cooled at least from 50°C to surface temperatures (10-15°C). Across major faults (e.g. Hope Fault), the contracts in maximum temperatures can be marked, with the amount of cooling being greater on the upthrown side.

6.5.2 Rock uplift

Estimation of the total amount of rock uplift can be determined by the following relationship (from Brown, 1991; Tippett and Kamp, 1993):

$$U = (T_p - T_s) / G + E_s - E_{im} + \Delta E_{mst} \qquad (6.1)$$

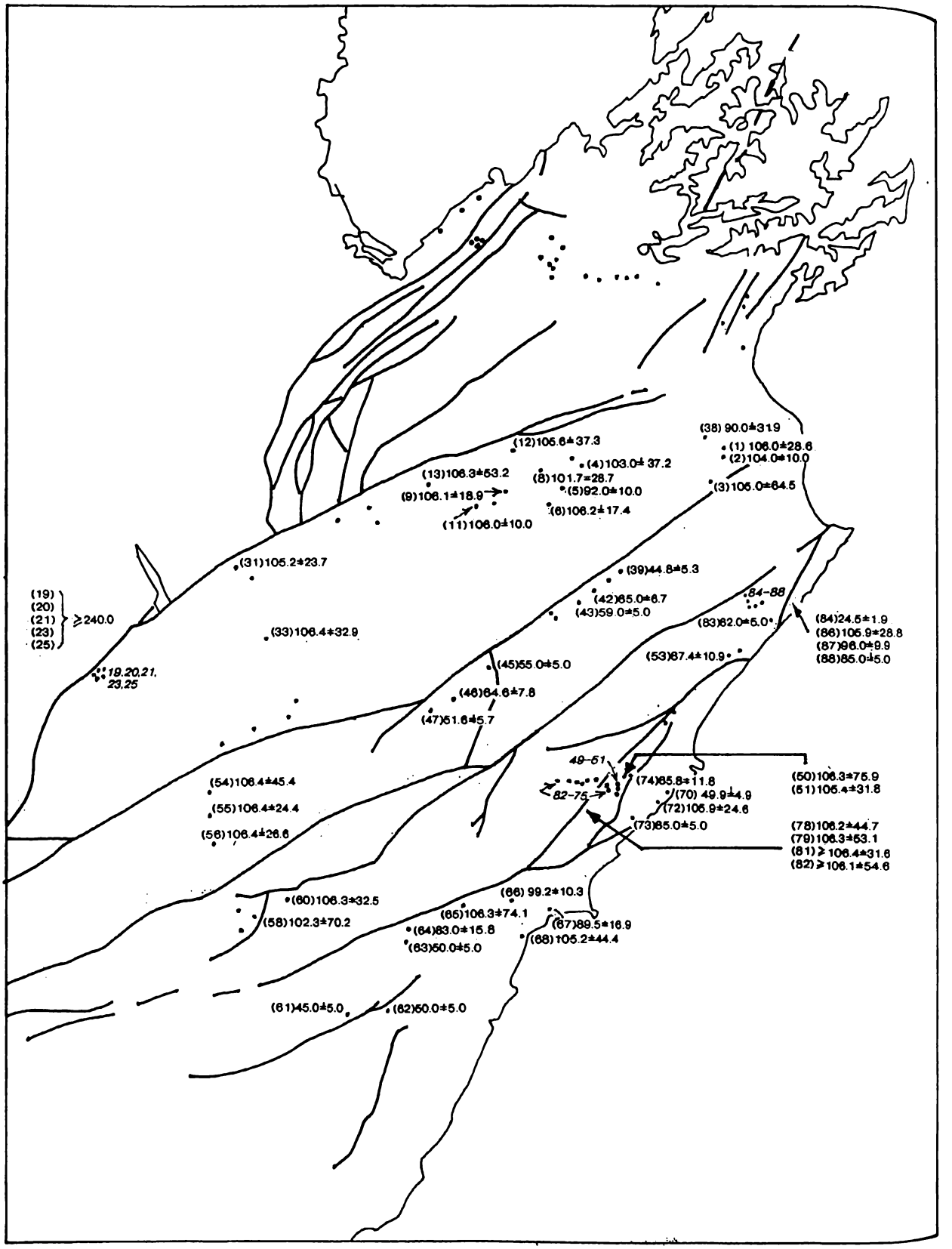

Figure 6.13 Distribution of maximum paleotemperatures prior to late Cenozoic inversion/cooling for sample sites from the Marlborough region.

Table 6.5 Paleotemperatures, rock uplift, and denudation amounts, estimated by Table 6.4.

Sample Number	Area	Distance from a Fixed Point (km)	Mineral	Age (Ma)	Mean Track Length ± 1σ (μm)	Pre-uplift Paleotemp. (°C)	Amount of Uplift (km)	Denudation (km)	Transect
9414-1	Wairau Block	140.1	apatite	18.5 ± 5.0	14.72 ± 0.10	106.0 ± 28.6	4.8 ± 2.0	4.6 ± 2.0	T1
			zircon	336.2 ± 45.3					
9414-3	Wairau Block	112.5	apatite	25.4 ± 15.6		105.0 ± 64.5	4.8 ± 3.6	4.3 ± 3.6	T1
			zircon	182.9 ± 26.7					
9414-4	Wairau Block	112.5	apatite	34.3 ± 12.4		103.0 ± 37.2	4.6 ± 2.4	4.5 ± 2.4	T1
			zircon	258.3 ± 13.8					
9414-6	Wairau Block	97.7	apatite	16.5 ± 2.7	12.80 ± 0.56	106.2 ± 17.4	4.8 ± 1.5	4.3 ± 1.5	T1
			zircon	261.5 ± 18.3					
9414-8	Wairau Block	106.7	apatite	38.6 ± 10.9		101.7 ± 28.7	4.6 ± 2.0	4.3 ± 2.0	T1
			zircon	281.7 ± 15.9					
9414-9	Wairau Block	96.7	apatite	17.4 ± 3.1	13.56 ± 0.90	106.1 ± 18.9	4.8 ± 1.6	4.5 ± 1.6	T1
			zircon	197.0 ± 24.5					
9414-12	Wairau Block	108.6	apatite	21.8 ± 7.7		105.6 ± 37.3	4.8 ± 2.4	4.5 ± 2.4	T1
			zircon	211.8 ± 21.7					
9414-13	Wairau Block	89.8	apatite	5.4 ± 2.7		106.3 ± 53.2	4.8 ± 3.1	4.5 ± 3.1	T1
9414-20	Wairau Block	0.0	apatite	5.3 ± 2.2		~240	11.5 ± 1.8	11.0 ± 1.7	T1
			zircon	7.3 ± 0.5					
9414-31	Wairau Block	46.4	apatite	24.4 ± 5.5	14.43 ± 0.70	105.2 ± 23.7	4.8 ± 1.8	4.1 ± 1.8	T1
			zircon	247.9 ± 17.1					
9414-33	Wairau Block	31.6	apatite	9.7 ± 3.0	15.19 ± 0.66	106.4 ± 32.9	4.8 ± 2.2	4.0 ± 2.2	T1
			zircon	166.7 ± 8.9					
9414-38	Wairau Block	139.0	apatite	63.2 ± 22.4		90.0 ± 31.9	4.0 ± 2.0	3.9 ± 2.0	T1
			zircon	166.7 ± 8.9					
9414-39	Inland Kaikoura Range	50.8	apatite	113.2 ± 13.4	11.43 ± 1.11	44.8 ± 5.3	1.7 ± 0.5	1.3 ± 0.5	T2
			zircon	162.0 ± 14.9					
9414-42	Inland Kaikoura Range	43.4	apatite	94.6 ± 9.8	10.62 ± 0.93	65.0 ± 6.7	2.8 ± 0.7	2.4 ± 0.7	T2
			zircon	136.7 ± 9.9					
9414-46	Inland Kaikoura Range	5.4	apatite	95.0 ± 11.5	14.12 ± 0.26	64.6 ± 7.8	2.7 ± 0.7	1.9 ± 0.8	T2

Table 6.5 (continued)

Sample Number	Area	Distance from a Fixed Point (km)	Mineral	Age (Ma)	Mean Track Length ± 1σ (μm)	Pre-uplift Paleotemp. (°C)	Amount of Uplift (km)	Denudation (km)	Transect
9414-47	Inland Kaikoura Range	0.0	apatite	107.3 ± 11.9	12.02 ± 0.62	51.6 ± 5.7	2.1 ± 0.5	1.2 ± 0.6	T2
			zircon	132.5 ± 13.1					
9414-54	Inland Kaikoura Range	-50.3	apatite	9.7 ± 4.1		106.4 ± 45.0	4.8 ± 2.8	3.8 ± 2.8	T2
			zircon	221.8 ± 16.5					
9414-55	Inland Kaikoura Range	-52.6	apatite	8.3 ± 1.9		106.4 ± 24.4	4.8 ± 1.8	3.9 ± 1.8	T2
			zircon	225.7 ± 19.3					
9414-56	Inland Kaikoura Range	-54.9	apatite	11.2 ± 2.8		106.4 ± 26.6	4.8 ± 1.9	4.0 ± 1.9	T2
			zircon	175.4 ± 16.7					
9414-50	Seaward Kaikoura Range	9.0	apatite	5.6 ± 4.0		106.3 ± 75.9	4.8 ± 4.2	4.2 ± 4.2	T3
			zircon	147.5 ± 13.4					
9414-51	Seaward Kaikoura Range	8.9	apatite	23.2 ± 7.0	9.89 ± 1.17	105.4 ± 31.8	4.8 ± 2.2	4.3 ± 2.2	T3
			zircon	152.2 ± 9.2					
9414-53	Seaward Kaikoura Range	37.6	apatite	67.3 ± 8.4	10.89 ± 0.81	87.4 ± 10.9	3.9 ± 1.1	3.8 ± 1.1	T3
			zircon	176.3 ± 25.1					
9414-58	Seaward Kaikoura Range	-75.0	apatite	36.7 ± 25.2		102.3 ± 70.2	4.6 ± 3.9	3.9 ± 3.9	T3
			zircon	147.5 ± 13.4					
9414-60	Seaward Kaikoura Range	-70.0	apatite	4.9 ± 1.5		106.3 ± 32.5	4.8 ± 2.2	4.0 ± 2.2	T3
			zircon	165.5 ± 13.2					
9414-70	Seaward Kaikoura Range	17.5	apatite	108.8 ± 10.7	13.01 ± 0.57	49.9 ± 4.9	2.0 ± 0.5	2.0 ± 0.5	T3
			zircon	150.6 ± 14.7					
9414-72	Seaward Kaikoura Range	15.0	apatite	19.4 ± 4.5	11.74 ± 0.67	105.9 ± 24.6	4.8 ± 1.8	4.8 ± 1.8	T3
			zircon	167.2 ± 14.2					
9414-74	Seaward Kaikoura Range	12.9	apatite	93.8 ± 16.8		65.8 ± 11.8	2.9 ± 0.9	2.4 ± 0.9	T3
			zircon	135.9 ± 8.2					
9414-78	Seaward Kaikoura Range	4.7	apatite	3.8 ± 1.6		106.2 ± 44.7	4.8 ± 2.7	2.5 ± 2.5	T3
			zircon	181.5 ± 13.1					
9414-79	Seaward Kaikoura Range	3.9	apatite	5.2 ± 2.6		106.3 ± 53.1	4.8 ± 3.1	2.6 ± 2.6	T3
			zircon	80.5 ± 11.4					
9414-81	Seaward Kaikoura Range	9.1	apatite	9.1 ± 2.7	15.70 ± 0.33	106.4 ± 31.6	4.8 ± 2.2	2.2 ± 2.2	T3
			zircon	124.3 ± 7.0					

Table 6.5 (continued)

Sample Number	Area	Distance from a Fixed Point (km)	Mineral	Age (Ma)	Mean Track Length ± 1σ (μm)	Pre-uplift Paleotemp. (°C)	Amount of Uplift (km)	Denudation (km)	Transect
9414-82	Seaward Kaikoura Range	3.5	apatite	3.5 ± 1.8		106.1 ± 54.6	4.8 ± 3.2	3.0 ± 3.0	T3
			zircon	173.2 ± 11.1					
9414-84	Seaward Kaikoura Range	48.7	apatite	129.0 ± 10.0	12.98 ± 0.18	24.5 ± 1.9	0. 7 ± 0.2	0.6 ± 0.2	T3
			zircon	238.5 ± 15.5					
9414-86	Seaward Kaikoura Range	47.8	apatite	19.5 ± 5.3		105.9 ± 28.8	4.8 ± 2.0	4.5 ± 2.0	T3
			zircon	143.8 ± 14.3					
9414-87	Seaward Kaikoura Range	49.6	apatite	52.5 ± 5.4	12.40 ± 0.11	96.0 ± 9.9	4.3 ± 1.1	3.9 ± 1.1	T3
			zircon	134.7 ± 13.9					
9414-61	Kahutara River	0.0	apatite	110.2 ± 9.6		45.0 ± 5.0	1.8 ± 0.5	1.6 ± 0.5	T4
			zircon	129.0 ± 12.0					
9414-64	Kahutara River	11.7	apatite	73.6 ± 14.0	12.26 ± 0. 10	83.0 ± 15.8	3.7 ± 1.2	3.3 ± 1.3	T4
			zircon	165.5 ± 15.5					
9414-65	Kahutara River	22.0	apatite	14.2 ± 9.9		106.3 ± 74.1	4.8 ± 4.1	4.5 ± 4.1	T4
			zircon	217.0 ± 18.5					
9414-66	Kahutara River	29.8	apatite	45.2 ± 4.7	10.16 ± 0.67	99.2 ± 10.3	4.5 ± 1.1	4.4 ± 1.1	T4
			zircon	132.6 ± 7.1					
9414-67	Kahutara River	36.1	apatite	64.1 ± 12.1	12.17 ± 0.38	89.5 ± 16.9	4.0 ± 1.3	4.0 ± 1.4	T4
			zircon	144.9 ± 11.3					
9414-68	Kahutara River	31.1	apatite	24.2 ± 10.2		105.2 ± 44.4	4.8 ± 2.7	4.7 ± 2.7	T4
			zircon	143.8 ± 7.7					

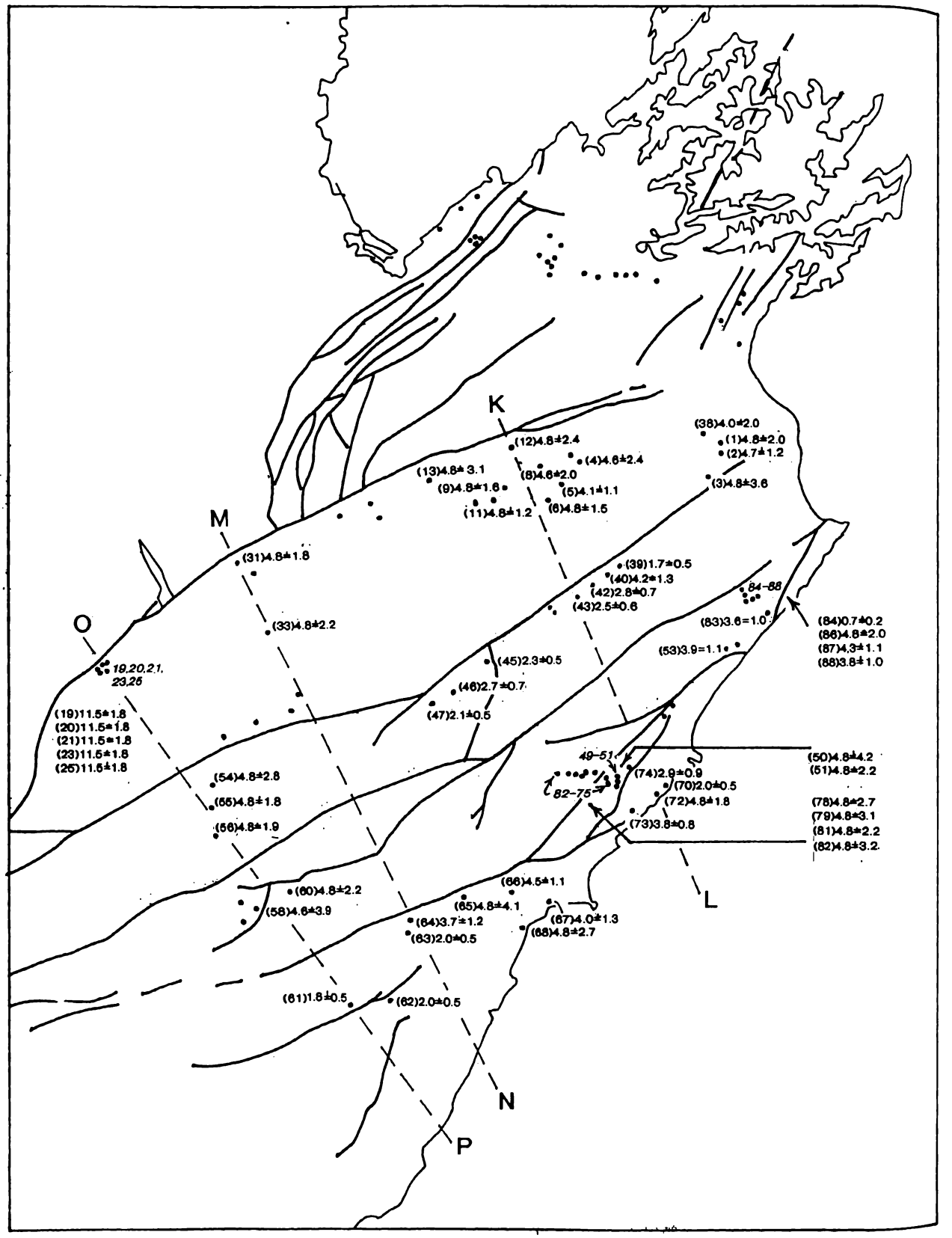

Figure 6.14 Distribution of amount of rock uplift for samples from Marlborough. The pre-uplift geothermal gradient assumed in converting paleotemperature to amount of rock uplift is 20.0°C/km.

where

U is amount of rock uplift (km).

T_p is pre-uplift paleotemperature (°C).

T_s is pre-uplift surface temperature (assume = 10°C).

G is pre-uplift geothermal gradient [assume = 20.0 ± 3.0°C (σ), after Kamp (1997)].

E_s is present sample elevation above mean sea level (km).

E_{im} is initial mean elevation of land surface (assume = 0 km).

ΔE_{msl} is difference between pre-uplift mean sea level and present-day mean sea level (assume = 0 km).

The pre-uplift geothermal gradient (G) is assumed to be 20.0 ± 3.0°C, following determination of this value in the Southern Alps (Kamp, 1997). Because the mean sea level of the present day is similar to that of the time from 25 to 10 Ma (Haq et al., 1987), ΔE_{msl} is assumed to be zero. The ΔE_{msl} is taken as zero for all samples, following the arguments given in Kamp and Tippett (1993). The estimates of rock uplift are listed in Tables 6.4 and 6.5. Uncertainties of rock uplift are given at the 1σ level. The map of the amount of rock uplift achieved during the late Miocene to Quaternary (Figure 6.14) shows that there is not a simple pattern. The greater amount of rock uplift has occurred in the vicinity of the big bend adjacent to the Alpine Fault. This amounts to 11.5 ± 1.8 km. The amounts of rock uplift in the Inland and Seaward Kaikoura Ranges are about 2.4 and 4.8 km, respectively. There is a wide variation in the amounts of rock uplift in the Kahutara block, there being less uplift for samples that have late Crteacous-Cenozoic sediments nearby.

6.5.3 Denudation

Denudation is a fundamental parameter in terms of the interpretation of fission track thermo-chronological data, because it is denudation which causes the cooling that influences the fission track parameters. Estimation of the amount of denudation can be determined by the following relationship (Brown, 1991):

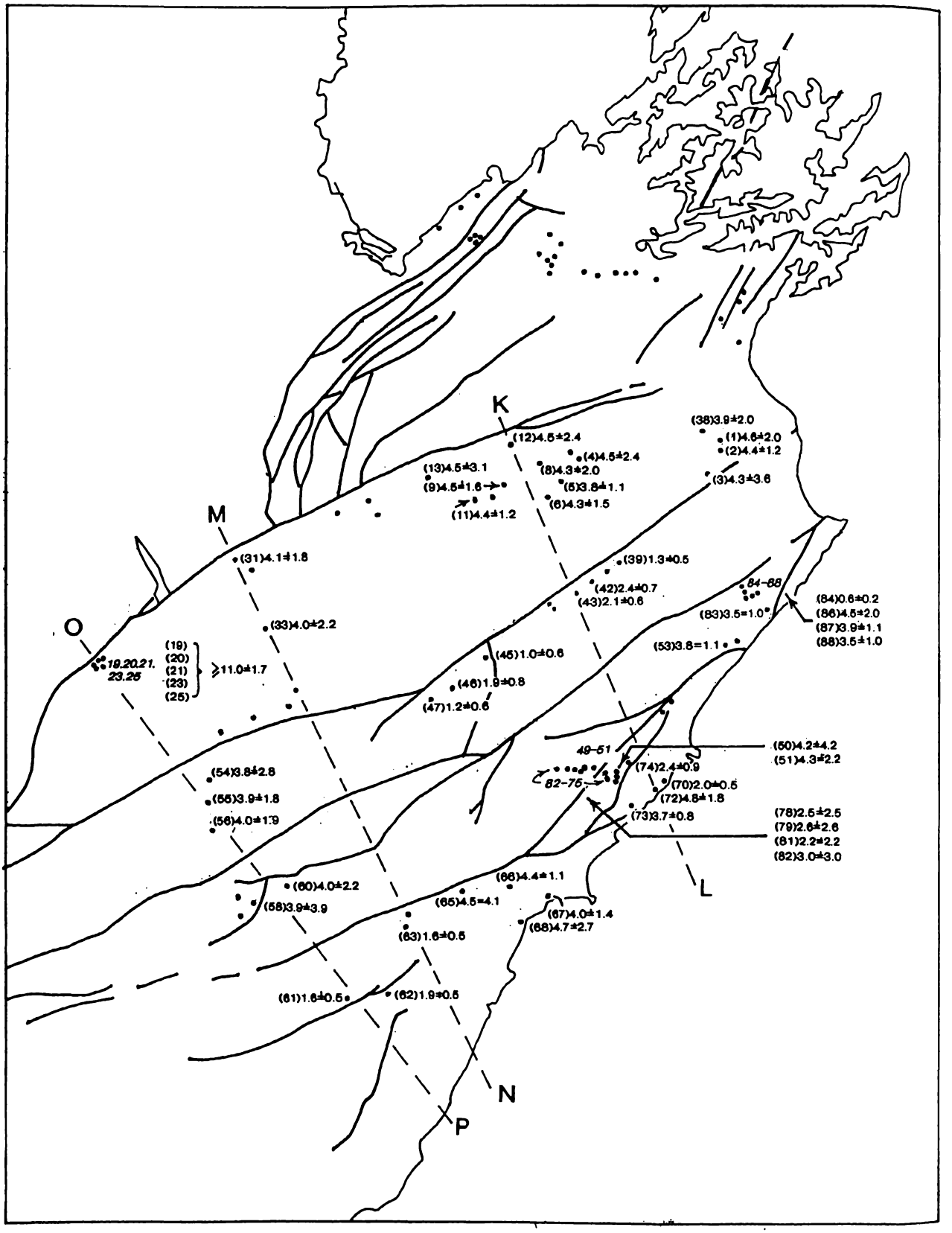

Figure 6.15 Distribution of the amount of denudation for samples from the Marlborough region.

$$D = (T_p - T_s) / G + d \qquad (6.2)$$

where

D is amount of denudation (km).

T_p is pre-uplift paleotemperature (°C).

T_s is pre-uplift surface temperature (assume = 10°C).

G is pre-uplift geothermal gradient [assume = 20.0 ± 3.0°C (σ)].

d is the difference between sample elevation and the present mean surface elevation (km). (d is negative when mean surface elevation > sample elevation).

The amounts of denudation estimated for the samples are given in Tables 6.4 and 6.5. Uncertainties are quoted at the 1σ level. The amount of denudation across Marlborough for the late Miocene to Quaternary is illustrated in Figure 6.15, and have a similar pattern to that for rock uplift. The largest amounts of denudation (~11.0 km) lie in the area of the Alpine Fault bend where Alpine Schist is exposed. Elsewhere the amount of denudation varies from one to four kilometres.

The distributions of rock uplift and denudation are shown in three transects in Figures 6.16a-c (line of sections shown on Figure 6.14). All transects are oriented normal to the strike of the major faults. Transect OP (Figure 6.16a) shows adjacent to the Alpine Fault the high amounts of rock uplift and denudation referred to above. Between the Awatere and Clarence Faults the values are around 4 km, and close to about 2 km southeast of the Hope Fault. In Transect MN (Figure 6.16b), the uplift and denudation are greater in the Wairau block than further to the southeast. In Transect KL (Figure 6.16c), the uplift/denudation values are around 4 km in the Awatere valley where the late Miocene-Quaternary beds are preserved. Values of 4 km are recorded over the Seaward Kaiakoura Range, where the sample sites presently have considerable elevation.

Across Marlborough the amount of denudation is generally higher in the Wairau block than elsewhere. It increases in amount southwestward between the Awatere and Clarence Faults. In the Seaward Kaikoura Range the amount of denudation is correlated with elevation, there being more denudation at higher elevations over the range. Compared with

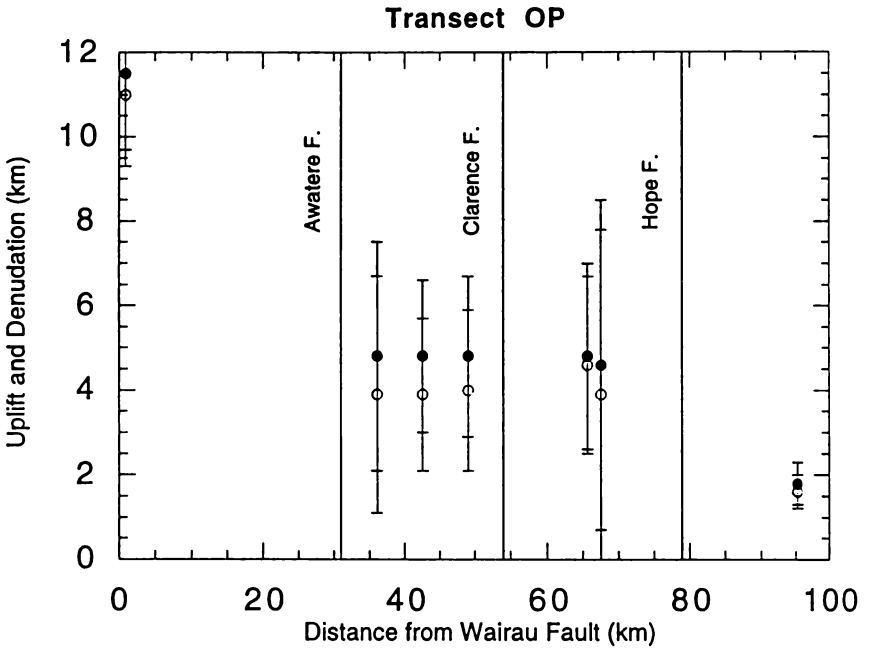

Figure 6.16a Transect OP: amounts of uplift (close circle) and denudation (open circle) versus distance from Wairau Fault.

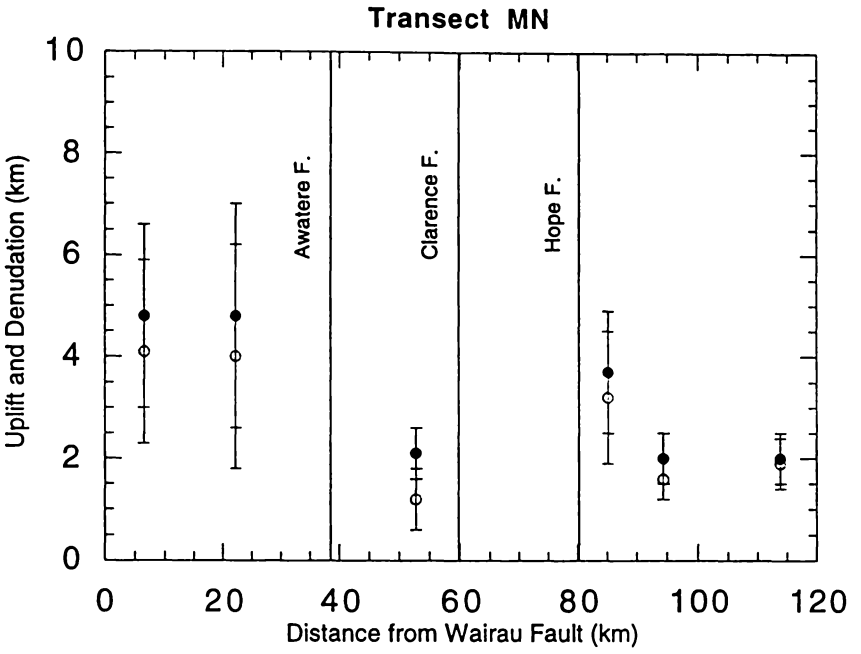

Figure 6.16b Transect MN: amounts of uplift (close circle) and denudation (open circle) versus distance from Wairau Fault.

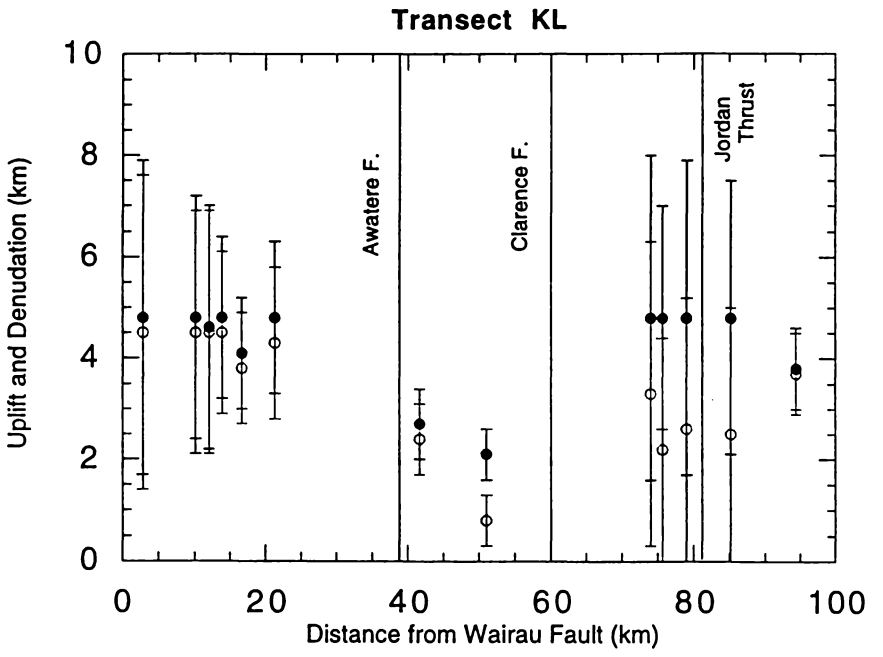

Figure 6.16c Transect KL: amounts of uplift (close circle) and denudation (open circle) versus distance from Wairau Fault.

the Southern Alps further to the south in South Island, the amount of denudation in Marlborough is much less than it is over the main part of the Alps (Kamp et al., 1989; Tippett and Kamp, 1993). This is due to the fact that a fully developed continent-continent collision zone occurs to the south, whereas Marlborough is more of a continental transform setting.

6.5.4 Alternative estimation of rock uplift for a zircon fission track closure temperature of 310°C

It is clear that the thermochronological estimation of rock uplift depends on the closure temperatures of the zircon and apatite fission track systems. The higher closure temperature a system has, the larger the amount of rock uplift it reveals for a given age estimate. The closure temperature of the zircon fission track system has been discussed by several geologists (Harrison et al., 1979; Zaun and Wagner, 1985; Hurford, 1986; Tagami et al., 1996). According to their conclusions, the closure temperature for fission tracks in zircon may range from 175°C to 310°C.

In this chapter, the closure temperature of zircon has been assumed to be 240 ± 50°C after Hurford (1986). This value is lower than the possible 310°C estimate made by Tagami et al. (1996). The difference between these two estimates will impact by way of under estimation of rock uplift by 30%. The effect is, that near the Alpine Fault where there are reset zircon ages, the amount of cooling in the last 10 m.y. will be greater than the amounts recorded in this thesis, resulting possibly in a greater amount of erosion by 30%. However, we have made calculations of uplift amounts for only a few samples in the Spenser Mountains. A compensating factor in the estimates made in the thesis of rock uplift is that this uplift advects the isotherms closer to the surface than would be the case if rocks were cooling from 240°C, giving a higher near-surface geothermal gradient. The greater the amount of rock uplift the greater the amount of advection of isotherms, which correspondingly reduces the amount of uplift for reset samples.

6.5.5 Relationship of the Great Marlborough Conglomerate and possible source areas based on apatite fission track ages

The Great Marlborough Conglomerate (GMC) is a well known and sedimentologically distinctive unit of late-early Miocene age in Marlborough. The area over

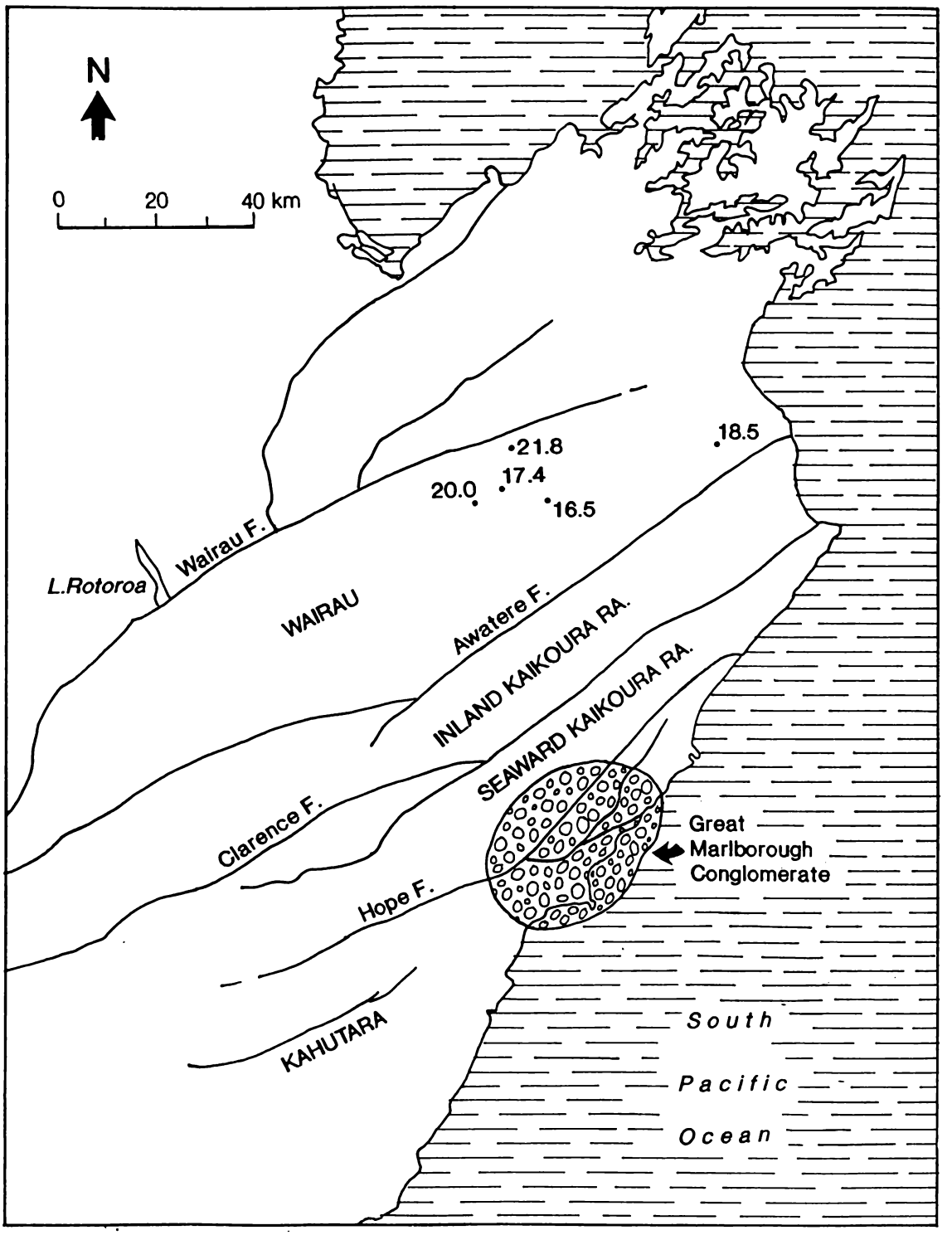

Figure 6.17 Paleographic extent of the Great Marlborough Conglomerate (Field et al., 1997) and its possible source area in the block between the Wairau and Awatere Faults determined by fission track ages.

which it is inferred to have been deposited (Field et al., 1997) is shown on Figure 6.17. The GMC consists of angular to well-rounded clasts of greywacke derived from the Torlesse Supergroup, with lesser proportions of Amuri Limestone, basalt and contemporaneous sandstone and siltstone clasts. The GMC is enclosed by the Waima Formation of Altonian age (late-early Miocene) comprising bathyal siltstone. The GMC has been inferred to record the sediment supply response to initial movements of the Marlborough Fault System (Field et al., 1997). The question arises therefore as to whether the fission track ages reported in this thesis can identify the source area of the greywacke clasts in the GMC.

Apatite fission track ages of Altonian age (18-16 Ma) on their own do not necessarily indicate areas of late-early Miocene uplift and erosion. The related track length distributions need to be considered to establish whether or not samples with the appropriate ages are reset. This is usually evaluated in the context of thermal history modelling. Fission track modelled of thermal histories of Samples 9414-2, -5 and -11 (Figures 6.11a-c) reveal that the basement in the NE Wairau block has experienced a two stage cooling history. The first phase of cooling occurred during the mid-Cretaceous. From the late-early to late Miocene, a second rapid cooling phase occurred that could have contributed sediment to the GMC. Samples not modelled because of a shortage of track lengths, but with appropriate ages (16-20 Ma) include Samples 9414-1, -6, -9, -11 and -12 (Figure 6.17). These indicate that a possible source area for the GMC lay in the block between the Wairau and Awatere Faults.

6.6 Summary

(1). The extremely young ages (<10 Ma) of zircon and apatite in the vicinity of the Alpine Fault bend and Seaward Kaikoura Range, are consistent with the recent rapid uplift/erosion in these areas. Most of the apatite ages are younger than depositional ages, indicating that the host rocks in Marlborough have experienced exposure to temperatures in the zone of partial annealing for apatite. In addition, apatite ages obtained along the Wairau Fault are always younger than those of other areas. Excluding the samples in the Marlborough Sounds region, most of zircon fission track ages are older than 119 Ma and are consistent with the depositional ages, implying that the host rocks of the samples in Marlborough have not experienced temperatures in the zircon partial annealing zone since the mid Cretaceous

(2) Apatite fission track ages and mean lengths show that there are two major cooling events, one occurring from the early Miocene (~20 Ma) and the other in the mid Cretaceous (~100 Ma). Modelled thermal histories of eleven samples selected from Marlborough samples are consistent with the stratigraphic record and reflect that in the Wairau block the timing of the main Neogene uplift/erosion event is earlier (mid to late Miocene) than to the southeast in the Seaward Kaikoura Range (late Pliocene-Pleistocene).

(3) The greatest amount of cooling in Marlborough occurs along the Alpine Fault in the vicinity of the Alpine Fault bend, where rocks now at the surface have cooled from temperatures above 240 ± 25°C where fission tracks in zircon are reset. These samples correspond to exposure of Alpine Schist. Over wide parts of Marlborough the rocks now at the surface have cooled from lower levels of the apatite partial annealing zone, that is, from less than about 110°C. Generally, the rocks at least cooled from 50°C to surface temperatures (10-15°C).

(4) Based on fission track ages and modelled thermal histories, estimation of rock uplift indicate that the largest uplift movements have occurred along the Alpine Fault and in the vicinity of the Seaward Kaikoura Range. The largest amount of rock uplift (~11.5 km) occurs in the area of the Alpine Fault bend. The amounts of rock uplift in the Inland and Seaward Kaikoura Ranges are about 2.4 and 4.8 km, respectively. There is a wide variation in the amounts of rock uplift in the Kahutara block, there being less uplift for samples that have late Crteacous-Cenozoic sediments nearby.

(5) Generally, across Marlborough the amount of denudation is higher in the Wairau block than elsewhere. It increases in amount southwestward between the Awatere and Clarence Faults. In the Seaward Kaikoura Range the amount of denudation can be related to elevation, there being more denudation at higher elevations over the range.

(6) In Marlborough the amounts of rock uplift and denudation derived from the fission track parameters are at the ranges of 0.7-11.5 km and 0.6-11.0 km, respectively. Compared with the Southern Alps and Canterbury (the continent-continent convergence), these amounts are relatively smaller. This is due to the fact that a fully developed continent-continent collision zone occurs to the south, whereas Marlborough is more of a continental transform setting.

Chapter 7

Comparison between FE Modelling and Fission Track Results

Chapter 7

Comparison between Fission Track and FE Modelling Results

7.1 Introduction

In this chapter, the results of the finite element (FE) modelling and fission track analysis will be compared with the topography and structure of the Marlborough region. FE modelling results, discussed in Chapter 5, were obtained by the FE method and principles of rock mechanics. On the other hand, fission track results discussed in Chapter 6 were established by experimental methods. Both the FE and fission track results may have some relationship to the topography and structure of Marlborough. The modelling results have been displayed here for the best FE deformation case to show the amount and distribution of rock uplift. Fission track results reflect the amount of cooling, which can be converted into the amount of rock uplift and denudation by assuming a pre-uplift geothermal gradient and using the relationships by Brown (1991), as discussed in Chapter 6. The topography is the difference between rock uplift and denudation.

7.2 Topography of the Marlborough region

Surface form is produced by the interaction of various geological processes. Land forms may reveal the relation between topography and geology. Some mountains and ranges in the NE South Island result from the movements of the Kaikoura Orogeny.

The dominant landforms of Marlborough consist of several ranges that result from crustal shortening on oblique-slip faults. The major landforms include the Spenser Mountains, Inland Kaikoura, and Seaward Kaikoura Ranges (Figure 7.1). The Spenser Mountains, reaching a height of 2338 m, are related to the Alpine uplift during the Kaikoura Orogeny. The altitude of the Kaikoura Ranges is over 2000 m; they are rugged and rapidly eroding. The Inland Kaikoura Range reaches a height of 2885 m at Mount Tapuaenuku. In the Seaward Kaikoura Range, Mountain Manakau is the hightest point at 2610 m. Fault-

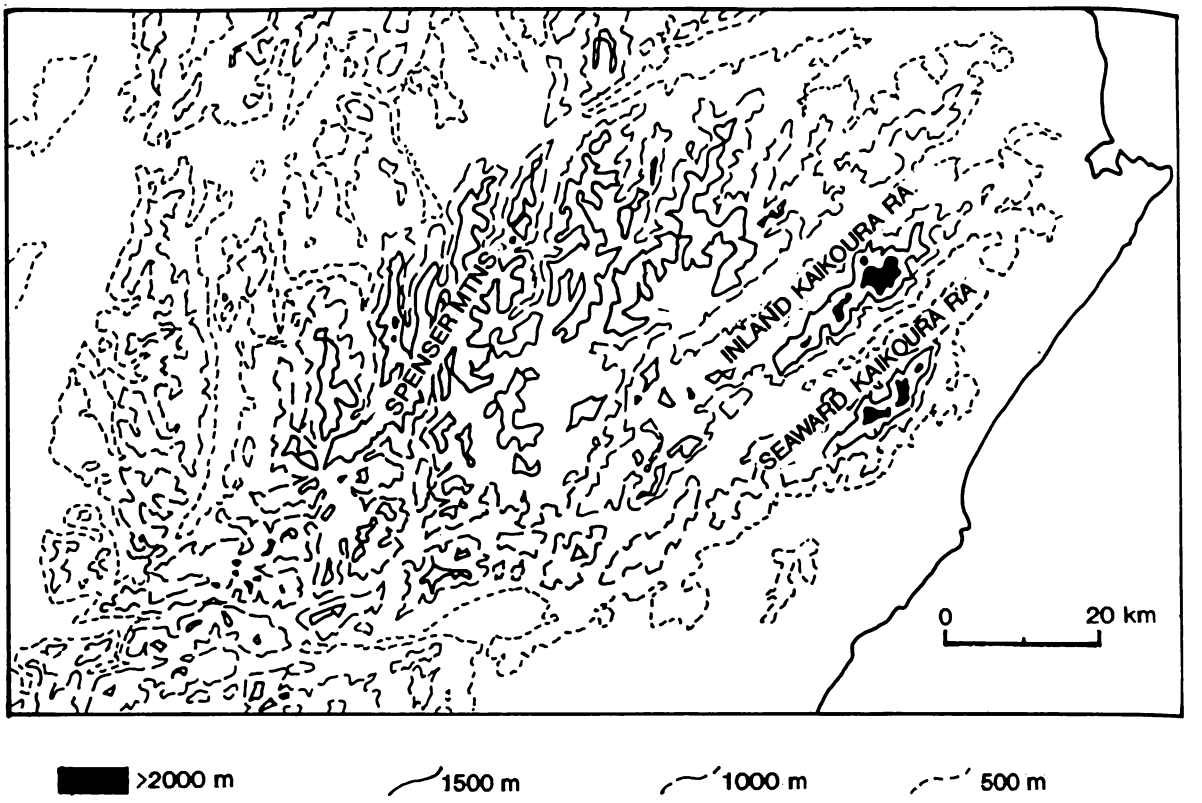

Figure 7.1 Topography of Marlborough.

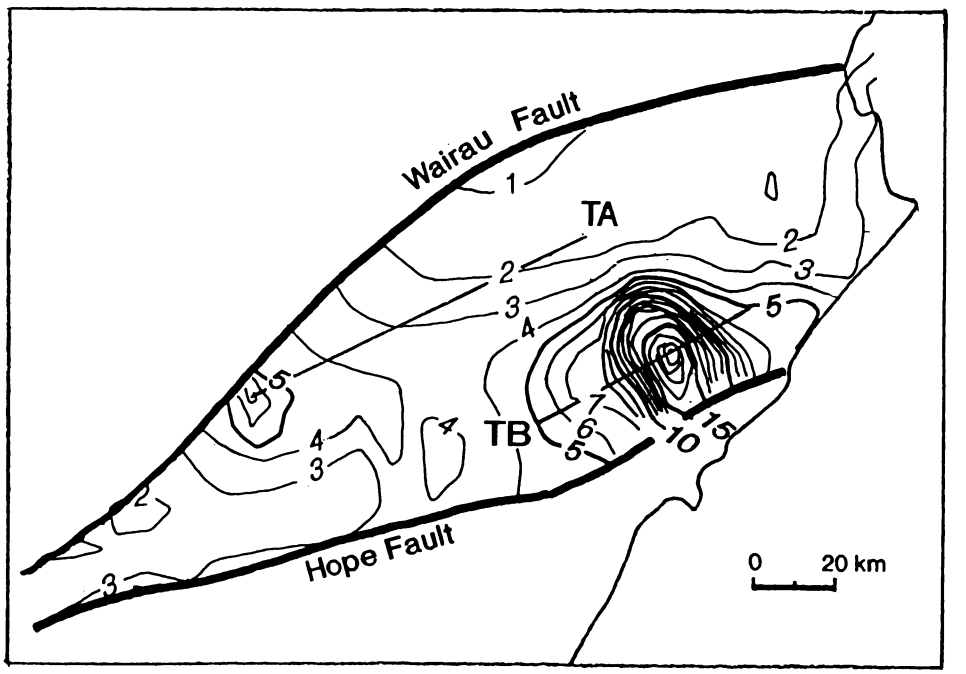

Figure 7.2 Contour of rock uplift, determined from the FE modelling results of the best model.

angle depressions between the ranges are occupied by valleys. Lowland areas are confined to the coast in the north-east region of Marlborough (Campbell and Johnston, 1982).

Figure 7.1 shows the topography of Marlborough. Most of the land lies 1000 m above sea level. In the Wairau block the highland (>1500 m) consists of the Spencer Mountains, St. Arnaud, and the Raglan Ranges. The Inland and Seaward Kaikoura Ranges, lying between the Awatere and Hope Faults, are clearly represented by the 1500 m contour.

Suggate (1978b) suggested that the locations of the crests of the highest ranges can be compared with the trends of the major South Island faults (the Awatere, Clarence, and Hope Faults). The crests of the Inland and Seaward Kaikoura Ranges lie to the NW of major bounding strike-slip faults. In addition, the crests of the Spenser Mountains show a wide distribution in the SW Wairau block.

7.3 FE modelling results and predictions

The Marlborough Fault System (MFS) is the primary (main) structure in Marlborough. For this reason, the FE modelling results will be limited to this system for further discussion.

7.3.1 Results of the best FE model

In Chapter 5, the FE modelling results of Case 16, considered to be the best model, show that there are two elongated "domes" (higher deformation) areas in the MFS (Figure 5.16). These two areas can be clearly compared to the Kaikoura Ranges and several other ranges (the Spenser Mountains, St. Arnaud, and the Raglan Ranges) which lie along the Alpine (Wairau) Fault. Although the patterns of the displacement field and contour of displacements (Figures 5.16b,c) only show the trend of horizontal movements, these results can be converted into vertical movements for comparison with the amounts of rock uplift and denudation which are estimated from fission track data.

A simplified contour of displacements of Case 16 (Figure 7.2) has been created from Figure 5.16c for further discussion. This figure will be recognized as the pattern of vertical movements of the MFS and compared with the pattern in topography, rock uplift, and denudation.

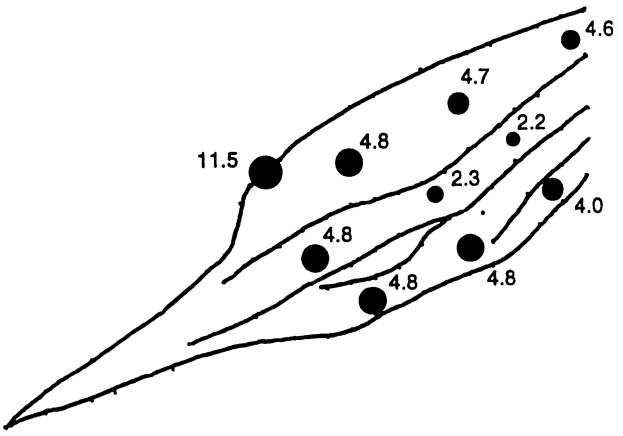

Figure 7.3a Distribution of the weighted mean amounts of rock uplift within the Marlborough Fault System (from the mid Miocene to present).

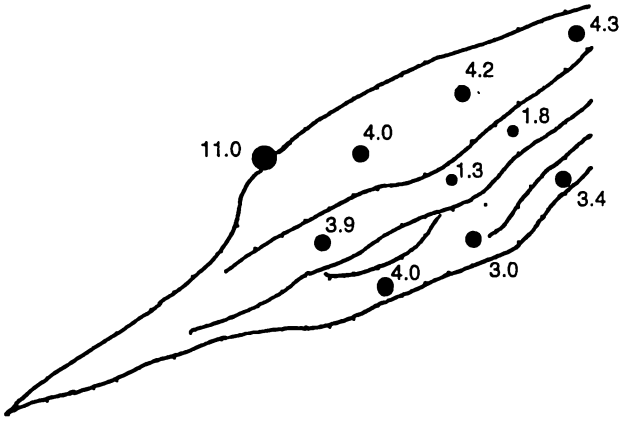

Figure 7.3b Distribution of the weighted mean amounts of denudation within the Marlborough Fault System (from the mid Miocene to present).

7.3.2 Predictions

Because the initiation of the MFS may be as young as 5 to 6 Ma, the FE modelling results of the best model (Figure 7.2) can be used to predict a period (<5 Ma) of vertical deformation. The pattern of Figure 7.2 will be recognized as the trend of vertical movements of the MFS and compared with the topography, rock uplift, and denudation. Each contour line has a deformation value (DV, non-unit) to represent the degree of vertical movements. The higher DV an area has, the more its deformation.

The DV values of the ranges along the Alpine Fault bend range from 2 to 7. On the other hand, the DV values of the Kaikoura Ranges are in the range of 4 to 21. Based on this distribution of the DV values, the FE modelling predicts that vertical movements of the Kaikoura Ranges are nearly three time larger than those of the ranges which are located in the vicinity of the Spenser Mountains. Meanwhile, the area lying in the NE Wairau block shows a simple "flat" (low deformation). The DV values of the NE Wairau block range from 0 to 3, indicating that there are less vertical movements in the region.

On the whole, the FE modelling results reveal that there are two high deformation areas in the Marlborough Fault System: the highest one is in the Kaikoura Ranges, and the second in the Spenser Mountains. Meanwhile, the other parts of the system show low deformation.

7.4 Fission track results

The development of the Marlborough Fault System (MFS) probably started at about 5 Ma (Little and Roberts, 1997). The amounts of rock uplift and denudation inferred from fission track results to have ocurred during the last 5 Ma can be used for comparison with the FE modelling results.

7.4.1 Rock uplift and denudation

There appears to be no simple pattern in the distribution of rock uplift and denudation (Figures 6.14, and 6.15) derived for Marlborough from fission track data. This arises because the fission track data in most samples reflect a thermal/tectonic history that extends

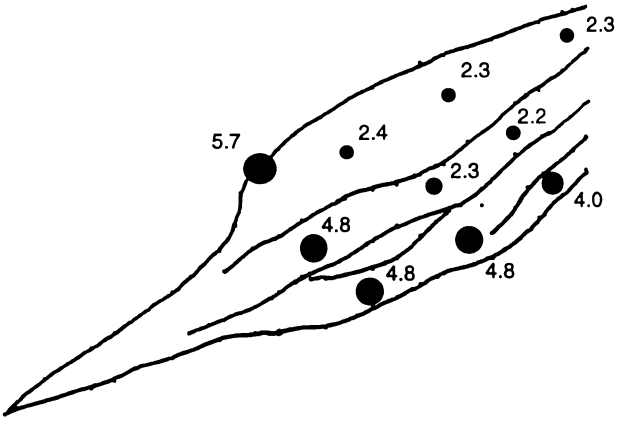

Figure 7.4 Weighted mean amounts of rock uplift within the Marlborough Fault System (from ~5 Ma to the present).

over a longer period than the development of the MFS. Generally, larger amounts of rock uplift and denudation occur in the Seaward Kaikoura Range (2.0-4.8 km) and along the vicinity of the Wairau Fault (3.8-11.0 km). For the central and northeastern parts of Marlborough, the amounts (1.0-2.8 km) of rock uplift and denudation are comparatively small. The weighted mean amounts of rock uplift and denudation within the MFS (Figures 7.3a and 7.3b) are estimated from the amounts which are derived from fission track data.

7.4.2 Rock uplift (<5 Ma)

Fission track data for the samples lying in the vicinity of the Alpine Fault bend and Wairau Fault indicate that the rock uplift and denudation have occurred over an interval of 10-12 m.y. In the Wairau block, thermal history modelling shows that most of the samples have experienced cooling, uplift, and erosion over a period since the mid Miocene. Hence, the amounts of rock uplift and denudation in Marlborough during the past 5 m.y. need to be isolated from the total Neogene vertical movements in order to compare validly the FE modelling results with empirical data. Some areas, for example the Seaward Kaikoura Range yield fission track information that carries exclusively a <5 Ma signal, which can be compared directly with the FE modelling results for the evolution of the MFS.

During the past 5 m.y., the amounts of rock uplift in the Wairau block appear to be about half of the total Neogene vertical movements. Under this assumption, the weighted mean amounts of rock uplift within the MFS (<5 Ma) can be obtained (Figure 7.4). Larger weighted mean amounts of rock uplift (4.8-5.7 km) occur in the vicinity of the Alpine Fault bend and Seaward Kaikoura Range. In NE Marlborough, the weighted mean amounts of rock uplift range from 2.2 to 2.4 km.

7.5 Comparison

7.5.1 FE modelling results and topography

Two transects (TA and TB) located in the Wairau block and Kaikoura Ranges are selected for comparison between FE modelling results and topography in Marlborough (Figure 7.2). Transect TB lying across the Kaikoura Ranges is used to represent the comparison in this region. Figure 7.5 shows that the elevation data and FE modelling results have a very good correlation. The patterns clearly coincide with each other.

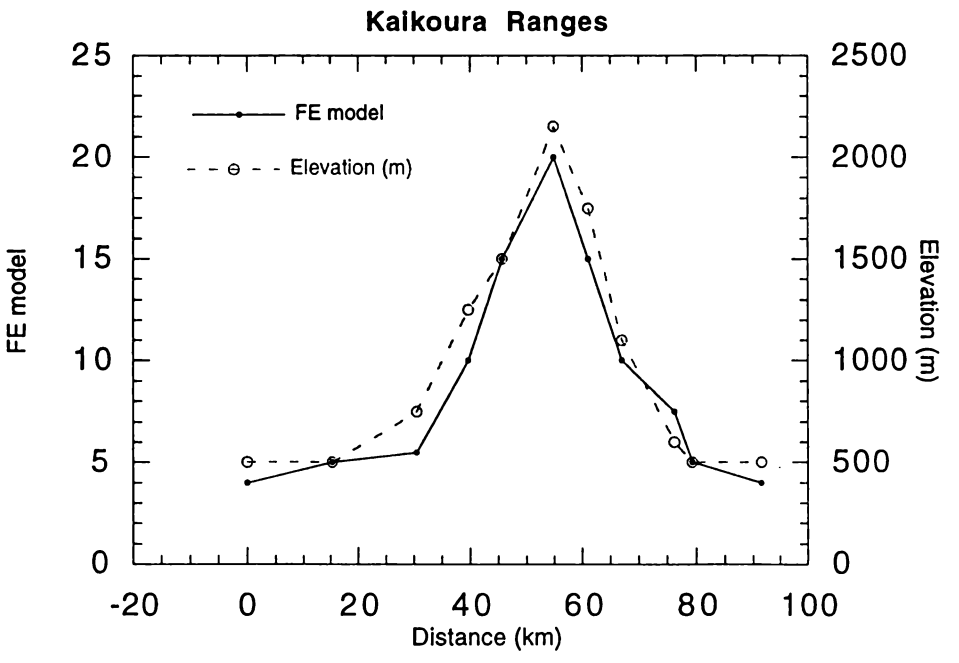

Figure 7.5 Comparison of the FE modelling results and topography of Kaikoura Ranges.

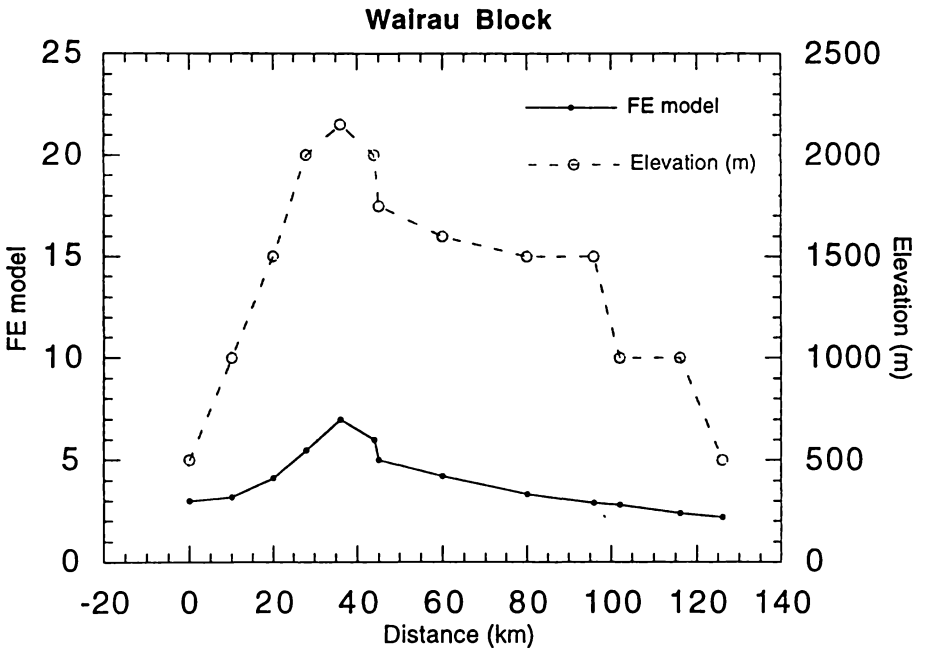

Figure 7.6 Comparison of the FE modelling results and topography of Wairau block.

For Transect TA across the Wairau block, the elevation data and FE modelling results have a similar trend, but different magnitudes (Figure 7.6). The uplift age in the Spenser Mountains is considered to be longer than 5 Ma. Meanwhile, the FE modelling results only reveal a limited period (<5 Ma) of deformation. Therefore, the topography of the Wairau block cannot have a good correlation with the FE modelling results.

7.5.2 FE modelling and fission track results

Although there is no simple pattern of rock uplift and denudaton within the MFS, the Kaikoura Ranges and Spenser Mountains are the main ranges of this region and can be recognized as having some relationship with the evolution of the MFS.

During the last 5 m.y., the pattern of rock uplift in Marlborough (Figure 7.4) estimated from fission track data is considered to have some relationship with the pattern obtained from the FE modelling results (Figure 7.2). Although these two patterns have a magnitude difference, they indicate several results: (a) larger amounts of rock uplift occur in the vicinity of the Alpine Fault bend and Seaward Kaikoura Range. (b) The amounts of rock uplift in NE Marlborough are comparatively small. (c) In the Wairau block, the amounts of rock uplift show a decreasing trend away from the Alpine Fault bend.

In brief, the evolution of the MFS has been recorded in fission track data. The FE modelling results can be compared amounts of rock uplift from fission track data where the initiation of uplift has occurred mainly after 5 Ma. It is reasonable to convert the FE horizontal deformation into vertical deformation in order to compare it with fission track data.

7.6 Summary

(1) Considering the timing of the formation of the MFS and the occurrence of rock uplift, the FE modelling results have very good correlation with the topography data. The results of the FE modelling reveal that the pattern of vertical deformation (uplift) is consistent with the topography in Marlborough.

(2) The pattern of deformation developed by the FE modelling clearly shows two high deformation areas which can be related to the crests of the Spenser Mountains and

Kaikoura Ranges. There is lower deformation in the NE Wairau block, indicating that vertical movements have not been dominant in this area during the past few million years.

(3) In the Kaikoura Ranges, the amounts of uplift and denudation assessed by fission track analysis coincide with the results of the FE modelling. However, the comparison in the Spenser Mountains fails to show a good correlation. Probably, fission track data in this area reflect a longer tectonic history (>5 Ma) of uplift and erosion.

(4) Except for the Alpine Fault bend, the highest amounts of rock uplift and denudation occur in the central part of the Seaward Kaikoura Range. This area is consistent with that of the FE modelling. The higher amounts of uplift and denudation, the more deformation (DV value) there has been.

(5) Comparison between the data derived from fission track ages and FE modelling, and topography shows that the assumptions and the principles of rock mechanics stated in Chapter 5 are reasonable for modelling the development of the Marlborough Fault System.

Chapter 8

Summary

Chapter 8

Summary

Fission track dating and finite element methods have been applied in this thesis in order to study the thermo-tectonic evolution of the Marlborough region. The results assessed by these two methods are supported and combined with the evidence of tectonics and geology in this region.

8.1 Tectonics

The Marlborough region lies within the Australian-Pacific plate boundary zone at a critical position between the southern end of the Hikurangi margin (where the Oceanic Pacific plate subducts beneath the Continental Australia plate) and the Alpine Fault section (where the continental Pacific plate collides with continental Australia plate). The Marlborough faults have been explained as secondary transforms connecting the Hikurangi subduction margin with the main Alpine Fault oblique-slip boundary. The development of the Awatere, Clarence and Hope faults reflects a changing plate motion vector. During the late Neogene, the subduction of the Pacific plate has probably propagated southwards and caused continuous activation of the Marlborough faults.

8.2 Geology

The basement of the Marlborough region is composed of the Torlesse Supergroup. This basement and younger units are separated by an angular unconformity, which represents the stratigraphic expressions of the end of the early Cretaceous Rangitata Orogeny. The age of basement rocks ranges from the late Jurassic to early Cretaceous, with Triassic successions in the far west. The Alpine Schist crops out adjacent to the Alpine fault. The depositional ages of cover strata range from Cretaceous to Quaternary. Cretaceous rocks are distributed in the Inland and Seaward Kaikoura Ranges. Early Cenozoic sequences accumulated during a tectonically quiet period when Marlborough was part of a passive margin environment. The quiet period was followed by the Kaikoura Orogeny, dating from

the Miocene, which reflects development of the modern Australia-Pacific plate boundary in the region.

At about 100 Ma, magmatism and extension occurred in Marlborough. After the cessation of extension and magmatism (~80 Ma), marine sedimentary sequences accumulated and subsided through thermally controlled processes. This tectonic quiescence lasted from 80 to 25 Ma. From the early Miocene onwards, crustal shortening and strike-slip faulting have become increasingly important in the Marlborough region.

8.3 FE modelling

Finite element (FE) modelling results indicate that tectonic movements in Marlborough may be expressed by the principles of rock mechanics.

The results of the best FE model reveal that the accommodation percentage of total displacements in Marlborough is about 85% of the total plate motion. The Wairau, Awatere, Clarence, and Hope Faults are modelled to have accommodated 7.6%, 11.4%, 21.2%, and 21.4% of the instantaneous displacement respectively. The contour of displacements determined by the FE modelling shows that there are two "domes" (higher deformation) areas in the Marlborough Fault System. The pattern can be compared to the topography of Marlborough. The two domes coincide with the Spenser Mountains and Kaikoura Ranges.

The FE method was then applied for further studies in several modelling cases (Cases B-F) to establish the development of the Marlborough Fault System (MFS). The main conclusions drawn are:

— A curved fault (the Alpine Fault) occurred as a result of a change in the plate motion vector. This curved fault is a manifestation of dextral tectonic rotation.

— the development of the MFS reflects the continuation of tectonic rotations.

— Three secondary faults (the Awatere, Clarence, and Hope Faults) have developed within a short period of one another. These faults reflect that a change in plate motion has occurred in Marlborough.

— Uplift movements of the Spenser Mountains and Kaikoura Ranges still continue, though the formation of the MFS has now been completed.

— Suggate's model (1979) of a pre-existing fault offset of the Alpine Fault can cause possible "uplift" movements across the Alpine Fault in the vicinity of the big bend. However, the model of a curved fault indicates a similar "uplift" trend. Suggate's model is not a unique result in the FE modelling.

In addition, the pattern of the displacement field and contour of displacements of the best FE model indicate the trend of horizontal movements can be converted into vertical movements for comparison with the amounts of rock uplift which are estimated from fission track data.

8.4 Fission track analysis

Apatite fission track ages of the samples collected from Marlborough range between 2.1 ± 1.5 Ma and 129.0 ± 10.0 Ma. The mean confined track lengths of the samples range between 10.16 ± 0.67 μm and 15.70 ± 0.33 μm, with standard deviation between 0.10 and 2.75 μm. Zircon fission track ages of the samples range from 6.8 ± 0.5 Ma to 336.2 ± 45.3 Ma. Based on fission track analysis, several conclusions can be drawn:

— The extremely young ages (<10 Ma) of zircon and apatite in the vicinity of the Alpine Fault bend and Seaward Kaikoura Range, coincide with the recent rapid uplift/erosion in these areas. All the apatite fission track ages are less than the corresponding depositional ages of the samples, revealing that the host rocks in Marlborough have experienced exposure to temperatures in the zone of partial to total annealing for apatite. Excluding the samples in the Marlborough Sounds region, most of the zircon fission track ages are older than 119 Ma and are consistent with or close to the depositional ages of the samples, indicating that the host rocks in Marlborough have not experienced temperatures of zircon partial annealing.

Apatite fission track ages and mean lengths show that there were two major cooling events, one occurring from the mid Cretaceous (~100 Ma) and the other in the early Miocene (~20 Ma). Modelled thermal histories of eleven samples selected from the Marlborough

samples are consistent with the stratigraphic record and reflect that in the Wairau block the timing of the main Neogene uplift/erosion event is earlier (mid to late Miocene) than to the southeast in the Seaward Kaikoura Range (late Pliocene-Pleistocene).

— The greatest amount of cooling in Marlborough occurs along the Alpine Fault in the vicinity of the Alpine Fault bend, where rocks now at the surface have cooled from temperatures above 240 ± 25°C where fission tracks in zircon are reset. These samples correspond to exposure via denudation of Alpine Schist. Over wide parts of Marlborough the rocks now at the surface have cooled from lower levels of the apatite partial annealing zone, that is, from less about 110°C. Generally, the rocks at least cooled from 50°C to surface temperatures (10-15°C).

— Based on fission track ages and modelled thermal histories, estimation of rock uplift indicate that the largest uplift movements have occurred along the Alpine Fault and in the vicinity of the Seaward Kaikoura Range. The largest amount of rock uplift (~11.5 km) occurs in the area of the Alpine Fault bend. The amounts of rock uplift in the Inland and Seaward Kaikoura Ranges are about 2.4 and 4.8 km, respectively. There is wide variation in the amounts of rock uplift in the Kahutara block, there being less uplift for samples that have late Crteacous-Cenozoic sediments nearby.

— Across Marlborough the amount of denudation is generally higher in the Wairau block than elsewhere. It increases in amount southwestward between the Awatere and Clarence Faults. In the Seaward Kaikoura Range the amount of denudation can be related to elevation, there being more denudation at higher elevations over the range.

— In Marlborough the amounts of rock uplift and denudation derived from the fission track parameters are at the ranges of 0.7-11.5 km and 0.6-11.0 km, respectively. Compared with the Southern Alps and Canterbury (the Continent-Continent convergence), these amounts are relatively smaller. This is due to the fact that a fully developed continent-continent collision zone occurs to the south, whereas Marlborough is more of a continental transform setting.

8.5 Conclusions

In this study, both fission track dating and finite element (FE) methods have been applied to established constraints on the tectonic evolution of Marlborough. The main conclusions are:

(1) The amounts of rock uplift and denudation in Marlborough are relatively less than those of the Southern Alps and Canterbury, reflecting the transform characteristics of the Australian-Pacific plate boundary zone in Marlborough compared with the continental-continental collision in the Southern Alps to the south.

(2) The evolution of the Marlborough Fault System may have followed the principles of rock mechanics and is related to its tectonic history.

(3) The uplift characteristics of Marlborough during the last 5 m.y. can be determined by the FE modelling and fission track dating methods. Considering the timing of rock uplift, the FE modelling results have a good correlation with fission track results.

(4) According to the FE modelling results, a great percentage (~85%) of the total horizontal plate motion has been accommodated in Marlborough.

(5) Both the fission track data and FE modelling results are consistent with the topography of Marlborough. The younger fission track age a host rock has, the more uplift/deformation it has experienced. This trend is supported by two high ranges, the Seaward Kaikoura Range and Spenser Mountains.

References

References

Allis, R.G., 1986. Mode of crustal shortening adjacent to the Alpine fault, New Zealand, Tectonics, 5(1): 15-32.

Anderson, H., Webb, T., and Jackson, J., 1993. Focal mechanisms of large earthquakes in the South Island of New Zealand: Implications for the accommodation of Pacific-Australia plate motion, Geophys. J. Int., 115: 1032-1054.

Ansell, J., and Adams, D., 1986. Unfolding the Wadati-Benioff zone in the Kermadec New Zealand region, Phys. Earth Planet. Inter., 44: 274-280.

Arabasz, W.J., Robinson, R., 1976. Microseismicity and geologic structure in the Marlborough region, New Zealand. New Zealand Journal of Geology and Geophysics, 19: 569-601.

Argus, D.F., and Gordon, R.G., 1990. Pacific-North America plate motion from very long baseline interferometry compared with that determined from magnetic anomalies, transform faults, and earthquake slip vectors, Journal of Geophysical Research, 95: 17315-17324.

Aumento, F., 1969. The Mid-Atlantic ridge near 45°N, Fission track and ferro-manganese chronology, Canad. J. Earth Sci, 6: 1431-1440.

Baker, J.A., Gamble, J.A., and Graham, I.G., 1994. Geology of the Tapuaenuku Igneous Complex, Marlborough, New Zealand, New Zealand Journal of Geology and Geophysics, 37: 249-268.

Baker, J., and Seward, D., 1996. Timing of Cretaceous extension and Miocene compression in northeast South Island, New Zealand: Constraints from Rb-Sr and fission-track dating of an igneous pluton, Tectonics, 15, 5: 976-983.

Bardsley, W. E., 1983. Confidence limits for fission-track dating, Mathematical Geology, 15/6: 649-658.

Berryman, Kelvin., 1979. Active faulting and derived PHS directions in the South Island, New Zealand, Bulletin Royal Society of New Zealand, 18: 29-34.

Berryman, K.R., Beanland, S., Cooper, A.F., Cooper, Cutten, H.N., Norris, R.J., and Wood, P.R., 1992. The Alpine fault, New Zealand: Variation in Quaternary structural style and geomorphic expression, in Major Active Faults of the World; Results of IGP Project 206, edited by Buckman, R.C., and Hancock, P.C., Hancock, Ann. Tectonicae, 6, suppl., 126-163.

Berzine, I.G., Vorob'eva, I.V., Geguzin, Ya.E., and Zlotova, I.M., 1967. Annealing of tracks of fragments from spontaneous fission of uranium in glasses and mica crystals, Soviet Phys. Dokl., 11: 1105-1107.

Beu, A.G., Maxwell, P.A., 1990. Cenozoic mollusca of New Zealand. New Zealand Geological Survey Paleontological Bulletin, 58, 518p.

Bhandari, N., .Bhat, S.G., Rajagopalana, D.Lal., Tamhare, A.S., and Venkatavardam, V.S., 1971. Fission track lengths in apatite: recordable track lengths, Earth and Planetary Science Letters, 13: 191-199.

Bibby, H.M., 1976. Crystal strain across the Marlborough faults, New Zealand. New Zealand, Journal of Geology and Geophysics, 19: 407-425.

Bibby, H.M., 1981. Geodetically determined strain across the Southern end of the Tonga-Kermadec-Hikurangi Subduction Zone, Geophys. J. Roy. astr. Soc., 66: 513-533.

Bibby, H. M., Haines, A. J., and Walcott, R. I., 1986. Geodetic strain and the present day plate boundary zone through New Zealand: Royal Society of New Zealand Bulletin, 24: 427-438.

Bibby, H.M., Walcott, R.I., 1984. Strain analysis using geodetic data, in An introduction to the recent crustal movements of New Zealand, Royal Society [New Zealand] Miscellaneous Series, 7: 61-68.

Bigazzi, G., 1967. Length of fission tracks and age of muscovite samples, Earth and Planetary Science Letters, 3: 434-438.

Bigazzi, G., Marton, P., Norelli, P., and Rozloznik, L., 1990. Fission track dating of Carpathian obsidians and provenance identification, Nucl. Tracks Radiat. Meas., 17: 391-396.

Bradshaw, J.D., 1989. Cretaceous geotectonic patterns in the New Zealand region. Tectonics, 8: 803-820.

Bradshaw, J.D., and Adams, C.J.D., 1980. Carboniferous to Cretaceous on the Pacific margin of Gondwana: the Rangitata phase of New Zealand. In: CRESSWELL, M. M. & VELLA, P. (eds) Gondwana Five. A. A. Balkema, Rotterdam: 217-221.

Bradshaw, J.D., Adams, C.J., and Andrews, P.B., 1981. Carboniferous to Cretaceous in the Pacific margin of Gondwana: the Rangitata phase of New Zealand, 217-212, In Cresswell, M.M., Vella, P. (eds), Gondwana Five.

Brown, R.W., 1991. Backstacking apatite fission-track "stratigraphy" : A method for resolving the erosional and isostatic rebound components of tectonic uplift histories, Geology, 19: 74-77.

Browne, G.H., 1995. Sedimentation patterns during the Neogene in Marlborough, New Zealand, Journal of The Royal Society of New Zealand, 25, No. 4: 459-483.

Browne, G.H., and Field, B.D., 1985. The lithostratigraphy of Late Cretaceous to Early Pleistocene rocks of northern Canterbury, New Zealand, New Zealand Geological Survey Record, 6: 63p.

Burchart, J., Dakowski, M., and Galazka, J., 1975. A technique to determine extremely high fission track densities, Bull. Acad. Polon. Sci., Ser. Sci. Terre, 23: 1-7.

Burchart, J., Butkiewicz, T., Dakowski, M., and Galazka-Friedman, J., 1979. Fission track retention in minerals as a function of heating time during isothermal experiments—a discussion. Nuclear Tracks, 3: 109-117.

Byerlee, J. D., 1967. Frictional characteristics of granite under high confining pressure, Journal of Geology and Geophysics, 72: 3639.

Campbell, I.B., and Johnston, M.R., 1982. In Soons, J.M., and Selby, M.J. (Eds), Nelson and Marlborough, 285-298, Chapter 15, Land Forms of New Zealand.

Carlson, W.D., 1990. Mechanisms and kinetics of apatite fission-track annealing, American Mineralogist, 75: 1120-1139.

Carter, L., 1988. Post-breakup stratigraphy of Kaikoura Synthem (Cretaceous-Cenozoic), continental margin, southeastern New Zealand, New Zealand Journal of Geology and Geophysics, 31: 405-429.

Carter, R.M., and Carter, L., 1982. The Motunau Fault and other structures at the southern edge of the Australia-Pacific plate boundary, offshore Marlborough, New Zealand, Tectonophysics, 88: 133-159.

Carter, R.M., and Norris, R.J., 1976. Cainozoic history of Southern New Zealand: An accord between geological observations and plate tectonic predictions, Earth and Planetary Science Letters, 31: 85-94.

Christoffel, D.A., 1971. Motion of the New Zealand Alpine Fault deduced from the sea-floor spreading, Bull. R. Soc. N.Z., 9: 25-30.

Clough, R. W., 1960. The Finite Element Method in Plane Stress Analysis, in Proc. 2nd Conf. on Electronic Computation, ASCE, Pittsburgh.

Conran, G.A., and Adler, H.H., 1976. The variability of the natural abundance of ^{235}U, Geochimica et Cosmochimica Acta, 40: 1487-1490.

Corrigan, J., 1991. Inversion of apatite fission track data for thermal history information, Journal of Geophysical Research, 96/B6: 10347-10360.

Corrigan, J.D., 1993. Apatite fission-track analysis of Oligocene strata in South Texas, U.S.A.: Testing annealing models, Chem. Geol. (Isot. Geosci. Sect.), 104: 227-249.

Coulson, J. H., 1972. Shear strength of flat surfaces in rock proc. 13th Symp. on Rock Mech. (A S C E) p77.

Cowan, H.A., 1990. Late Quaternary displacements on the Hope Fault at Glynn Wye, North Canterbury, New Zealand Journal of Geology and Geophysics, 33: 285-293.

Crowley, K.D., 1993. Mechanisms and kinetics of apatite fission-track annealing — Discussion, American Mineralogist, 78: 210-212.

Crampton, J.S., Beu, A.G., Campbell, H.J., Cooper, R.A., Morgans, H.E.G., Raine, J.I., Scott, G.H., Stevens, G.R., Strong, C.P., and Wilson, G.J., 1995. An interim New Zealand geological time scale. Institute of Geological & Nuclear Sciences science report 95/9.

Crowley, K.D., Cameron, M., and McPherson, B.J., 1990. Annealing of etchable fission-track damage in F-, OH-, Cl-, and Sr-apatite: 1. Systematics and preliminary interpretations, Nuclear Tracks, 17: 409-410.

Crowley, K.D., Cameron, M., and Schaeffer, R.L., 1991. Experimental studies of annealing of etched fission tracks in fluorapatite, Geochimica et Cosmochimica Acta, 55: 1449-1465.

Dakowski, M., 1978. Length distribution in thick crystals, Nuclear Tracks, 2: 181-189.

Dakowski, M., Burchart, J., and Galazka, J., 1974. Experimental formula for thermal for thermal fading of fission tracks in minerals and natural glasses, Bull. Acad. Pol. Sci., Ser. Sci. Terre, 22: 11-19.

Davey, F.J., and Watts, A.B., 1983. Gravity field of the southwest Pacific ocean: New Zealand region, Geol. Soc. Am. Map Chart Ser., 48.

Davy, B.W., 1984. Bounty Trough, in Geological Society of New Zealand Annual Conference Abstrsct, Misc.Publ. Geol. Soc. N.Z., 31A: 41.

Demets, C., Gordon, R.G., Argus, D.F., and Stein, S., 1990. Current plate motions. Geophysical Journal International, 101: 425-478.

Desai, C. S., 1979. Elementary finite element method. Prentice-Hall Inc., USA.

Dissen, R.V., and Yeats, R.S., 1991. Hope fault , Jordan thrust, and uplift of the Seaward Kaikoura Range, New Zealand, Geology, 19: 393-396.

Donelick, R.A., 1991. Crystallographic orientation dependence of mean etchable fission track length in apatite: an empirical model and experimental observations, American Mineralogist, 76: 83-91.

Donelick, R.A., Rowden, M.K., Mooers, J.D., Carpenter, B.S., and Miler, D.S., 1990. Etchable length reduction of induced fission tracks in apatite at room temperature (~23^{o} C): crystallographic orientation effects and "initial" mean lengths, Nuclear Tracks, 17/3: 261-265.

Dodson, M.H., 1973. Closure temperature in cooling geochronological and petrological systems, Contrib. Mineral. Petrol., 40: 259-274.

Duddy, I.R., Green, P.F. and Laslett, G.M., 1988. Thermal annealing of fission tracks in apatite 3. Variable temperature behaviour, Chem. Geol. (Isot. Geosci. Sect.), 73: 25-38.

Dumitru, T.A., 1988. Subnormal geothermal gradients in the great valley forearc basin, Califorina, during Franciscan subduction: a fission track study, Tectonics, 7/6: 1201-1211.

Evison, F.F., and Webber, S.J., 1986. Seismogenic stress conditions in Central New Zealand, Royal Society of New Zealand Bulletin, 24: 553-565.

Farmer, I. W., 1968. Engineering Properties of Rocks, London: E. & F. N. Spon Ltd.

Fairhurst, C., 1964. On the validity of the Brazilian test for brittle materials, IJRM & MS, V1, p535.

Field, B.D., Uruski, C.I., and others, 1997. Cretaceous-Cenozoic geology and petroleum systems of the East Coast Region, New Zealand, Institute of Geologic and Nuclear Sciences monograph 19.

Fleischer, R.L., and Price, P.B., 1963. Charged particle tracks in glass, Journal of Applied Physics., 34: 2903-2904.

Fleischer, R.L., and Price, P.B., 1964. Techniques for geological dating of minerals by chemical etching of fission fragment tracks, Geochim. Cosmochim. Acta, 28: 1705-1714.

Fleischer, R.L., Price, P.B., and Walker, R.M., 1964a. Fission track ages of zircons, Journal of Geophysical Research, 69: 4885-4888.

Fleischer, R,L., Price, P.B., Walker, R.M., and Hubbard, E.L., 1964b. Track registration in various solid-state nuclear track detectors, Phys. Rev., 133-5A: 1433-1449.

Fleischer, R.L., Price, P.B., and Walker, R.M., 1965. Effections of temperature, pressure, and ionization on the formation and stability of fission tracks in mineral and glasses, Journal of Geophysical Research, 70: 1497-1502.

Fleischer, R.L., and Hart, H.R., 1972. Fission track dating: Techniques and problems. In W.W. Bishop, Miller, D.A., and Cole S. (Editors), Calibration of hominoid evolution, Scottish Academic Press, Edinburgh: 135-170.

Fleischer, R.L., Price, P.B., and Walker, R.M., 1975. Nuclear tracks in solids, University of California Press, 605 pp.

Fleischer, R.L., Viertl, J.R.M., Price, P.B., and Aumento, F., 1968. Mid-atlantic ridge: age and spreading rates, Science, 161: 1339-1342.

Freund, R.,1971. The Hope Fault - a strike slip fault in New Zealand, N.Z. Geological Survey 86, 47pp.

Galazka, J. and Burchart, J., 1976. Cumulative isothermal heating (CIH) as a method to correct thermally lowered fission track ages. I. Mathematical models, Bull. Acad. Polon. Sci., Ser. Sci. Terre, 25: 1-7.

Galbraith, R. F., 1981. On statistical models for fission track counts, Mathematical Geology, 13: 471-478.

Galbraith, R. F., 1984. On statistical models in fission track dating, Mathematical Geology, 16/7: 653-669.

Galbraith, R. F., and Laslett, G. M., 1985. Some remarks on statistical estimation in fission track dating, Nuclear Tracks, 10: 361-363.

Gallagher, K., 1995. Monte Track - A fission track thermal history modelling program for the Macintosh. Dept. of Earth Sciences, The Open University, Milton Keynes and Dept. of Geological Sciences, UCL, London.

Gleadow, A.J.W., 1978. Comparison of fission track dating methods: effects of anisotropic etching and accumulated α-damage, U.S. Geol. Surv. Open-File Report 78-701: 143-145.

Gleadow, A.J.W., 1981. Fission track dating methods: What are the real alternatives?, Nuclear Tracks, 5: 3-14.

Gleadow, A.J.W., 1984. Fission track dating methods-II: A manual of principles and techniques, James Cook University, Townsville.

Gleadow, A.J.W., and Duddy, I.R., 1981. A natural long-term annealing experiment for apatite, Nuclear Tracks, 5: 169-174.

Gleadow, A.J., and Lovering, J.F., 1975. Fission track dating methods, Dept. of Geology, School of Earth Sciences, University of Melbourne, Publication No. 3.

Gleadow, A.J., and Lovering, J.F., 1978. Thermal history of granitic rocks from Western Victoria: A fission-track dating study, J. Geol. Soc. Austral., 25: 323-340.

Gleadow, A.J.W., and Duddy, I.R., 1981. A natural long-term track annealing experiment for apatite, Nucl. Tracks 5: 169-174.

Gleadow, A.J.W., Duddy, I.R., and Lovering, K.A., 1983. Fission track analysis: a new tool for the evaluation of thermal histories and hydrocarbon potential, Petrol. Explor. Assoc. Aust. J., 23: 93-102.

Gleadow, A.J.W., Duddy, I.R., Green., P.F., and Lovering, J.F., 1986a. Confined fission track lengths in apatite: a diagnostic tool for thermal history analysis, Contrib. Mineral. Petrol., 94: 405-415.

Gleadow, A.J.W., Duddy, I.R., Green, P.F., and Hegarty, K.A., 1986b. Fission track lengths in the apatite annealing zone and the interpretation of mixed ages, Earth and Planetary Science Letters, 78: 245-254.

Gleadow, A. J. W., and Fitzgerald, P. G., 1987. Uplift history and structure of the Transantarctic Mountains: new evidence from fission track dating of basement apatites in the Dry Valleys area, southern Victoria Land, Earth and Planetary Science Letters, 82: 1-14.

Gleadow, A.J.W., and Lovering, K.A., 1977. Geometry factor for external detectors in fission track dating, Nuclear Tracks, 1: 99-106.

Goodman, R. E., 1970. The deformability of joints, in Determination of the In-situ Modulus of Deformation of Rock - A. S. T. M. STP 477: p174.

Goodman, R. E., 1976. Methods of Geological Engineering in Discontinuous Rocks, West Publishing CO., USA.

Goodman, R. E., Taylor, R. L., and Brekke, T. L., 1968. A model for the mechanics of jointed rock, J. SMFD ASCE, 94: p637.

Goodman, R. E., and Ohneishi, Y., 1973. Undrained shear testing of jointed rock, Rock Mechanics, 5: p129.

Green, P.F., 1981a. A new look at statistics in fission track dating, Nuclear Tracks, 5: 77-86.

Green, P.F., 1981b. Track-in-track length measurements in annealed apatites, Nuclear Tracks, 5: 121-128.

Green, P.F., 1985. Comparison of zeta calibration baselines for fission track dating of apatite, zircon and sphene, Chemical Geology, 58: 1-22.

Green, P.F., 1986. On the thermo-tectonic evolution of Northern England: Evidence from fission track analysis, Geol. Mag., 123: 493-506.

Green, P.F., 1988. The relationship between track shortening and fission track age reduction in apatite: combined influences of inherent instability, annealing anisotropy, length bias and system calibration, Earth and Planetary Science Letters, 89: 335-352.

Green, P.F., and Durrani, S.A., 1977. Annealing studies of tracks in crystals, Nuclear Tracks, 1: 33-39.

Green, P.F., and Durrani, S.A., 1978. A Quantitative assessment of geometry factors for use in fission track studies, Nuclear Tracks, 2: 207-213.

Green, P.F., Duddy, I.R., Gleadow, A.J.W., and Tingate, P.R., 1985. Fission-track annealing in apatites: track length measurements and the form of the Arrhenius plot, Nuclear Tracks, 10 : 323-328.

Green, P.F., Duddy, I.R., and Laslett, G.M., 1988. Can fission track annealing in apatites be described by first-order kinetics? Earth and Planetary Science Letters, 87: 216-228.

Green, P.F., Duddy, I.R., Laslett, G.M., Hegarty, K.A., Gleadow, A.J.W., and Lovering, J.F., 1989a. Thermal annealing of fission tracks in apatites 4. Quantitative modelling techniques and extension to geological time scales, Chem. Geol. (Isot. Geosci. Sect.), 79: 155-182.

Green, P.F., Duddy, I.R., Gleadow, A.J.W., and Lovering, J.F., 1989b. Apatite fission track analysis as a paleotemperature indicator for hydrocarbon exploration, in Thermal history of sedimentary basins, editors N.D. Naeser, and T.H. McCulloch, Springer-Verlag, New York.

Green, P.F., Duddy, I.R., Gleadow, A.J.W., Tingate, P.R. and Laslett, G.M., 1986. Thermal annealing of fission tracks in apatite, 1. A qualitative description, Chem. Geol. (Isot. Geosci. Sect.), 59: 237-253.

Gregg, D.R., 1964. Sheet 18, Hurunui (1st Ed.). Geological Map of New Zealand 1:250,000, Department of Scientific and Industrial Research, Wellington, New Zealand.

Grindley, G.W., 1978. The Rangitata Orogeny-Metamorphism. In: SUGGATE, R. P., TEPUNGA, M. T. & STEVENS, G. R. (eds) The Geology of New Zealand. Government Printer, Wellington, 333-42.

Grapes, R. H., 1975. Petrology of the Blue Mountain Igneous Complex, Marlborough, New Zealand, J. Petrol., 16: 371-428.

Grapes, R.H., and Wellman, H.W., 1986. The north-east end of the Wairau Fault, Marlborough, New Zealand, J. R. Soc. N. Z., 16: 254-250.

Gutenberg, B., 1959. Physics of the Earth's Interior, Academic Press, New York.

Hall, W.D.M., 1964. Geology of Coverham and upper Waima valley, Marlborough, Unpublished M.Sc. thesis, lodged in the Library, Victoria University of Wellington.

Hammerschmidt, K., Wagner, G.A., and Wagner, M., 1984. Radiometric dating on research drill core Urach III: a contribution to its geothermal history, J. Geophys., 54: 97-105.

Handin, J., and Stearns, D. W., 1964. Sliding friction of rock, Trans. Amer. Geophysical Union, 45: p103.

Hannah, G.C., Wescott, C.H., Lemmel, H.D., Leonard, B.R., Story, J.S., and Attree, P.M., 1969. Revision of values for the 2200 m/s neutron constants for four fissile nuclides, Gen. Elec. Co. Atomic Energy Rev., 7: 3-92.

Haq, B.U., Hardenbol, J., and Vail, P.R., 1987. The chronology of fluctuating sea level since the Triassic, Science, 235: 1156-1167.

Harrison, T.M., Armstrong, R.L., Naeser, C.W., and Harakal, J.E., 1979. Geochronology and thermal history of the Coast Plutonic Complex, Near Prince Rupert, British Columbia. Canadian Journal of Earth Sciences, 16: 400-410.

Hasebe, N., Tagami, T., and Nishimura, S., 1992. Evolution of the Shimanto Accretionary Complex: A fission-track Thermochronologic study. In Underwood M.B. ed., Thermal Evolution of the Tertiary Shimanto Belt, Southwest Japan, Geological Society of America, Special Paper, 273: 121-136.

Heuze, F. E., and Goodman, F. E., 1967. Mechanical properties and in-situ behaviour of the Chino limestone, Crestmore mine, Riverside Cal., Proc. 9th Symp. on Rock Mechanics, (AIME).

Hodges, K.V., 1991. Pressure-Temperature-Time Paths, Annual Reviews of Earth and Planetary Science Letters, 19: 207-236.

Hoek, E., and Pentz, D. L., 1968. The stability of open pit mines, Rock Mech. Res. n5, Imperial College, London.

Holt, William E., and Haines, A.J., 1995. The kinematics of northern South Island, New Zealand, determined from geologic strain rates, Journal of Geophysical Research, 100, B9: 17991-18010.

Hurford, A.J., 1985. On the closure temperature for fission tracks in zircon (abstract), Nuclear Tracks, 10: 415.

Hurford, A.J., 1986. Cooling and uplift patterns in the Lepontine Alps South Central Switzerland and age of vertical movement on the Insubric fault line, Contrib. Mineral. Petrol., 92: 413-427.

Hurford, A.J., 1990. International union of geological sciences subcommission on geochronology: Recommedation for the standardization of fission track dating calibration and data reporting, Nucl. Tracks, 17: 233-236.

Hurford, A. J., and Green, P. F., 1982. A users' guide to fission track dating calibration, Earth and Planetary Science Letters, 59: 343-354.

Hurford, A. J., and Green, P. F., 1983. The zeta age calibration of fission track dating, Isotope Geosci, 1: 285-317.

Hurford, A,J., and Watkins, R.T., 1987. Fission track age of the tuffs of the Buluk Member, Bakate Formation, northern Kenya: A suitable fission track age standard, Chem. Geol., 66: 209-216.

Jaffey, A.H., Flynn, K.F., Glendenin, L.E., Bentley, W.C., and Essling, A.M., 1971. Precision measurements of the half-lives and specific activities of ^{235}U and ^{238}U, Phys. Rev., 4: 1889-1906.

Johnson, A. M., 1970. Physical Processes in Geology, San Francisco, Calif.: Freeman, Cooper and Company, p202.

Johnson, N. M., McGee, V. E. and Naeser, C. W., 1979. A practical method of estimating standard error of age in the fission track dating method, Nuclear Tracks, 3: 93-99.

Jumikis, A. R., 1983. Rock mechanics, second edition. Trans Tech Publication, Germany and USA.

Kamp, P.J.J, 1986. Late Cretaceous-Cenozoic tectonic development of the southwest Pacific region, Tectonophysics, 121: 225-251.

Kamp, P.J.J., 1997. Paleogeothermal gradient and deformation style, Pacific front of the Southern Alps Orogen: Constraints from fission track thermochronolgy, Tectonophysics, 271: 37-58.

Kamp, P.J.J., and Green, P.F., 1990. Thermal and Tectonic History of Selected Taranaki Basin (New Zealand) Wells Assessed by Apatite Fission Track Analysis, The American Association of Petroleum Geologists Bulletin, 74, 9: 1401-1419.

Kamp, P.J.J., Green, P.F., and White, S.H., 1989. Fission track analysis reveals character of collisional tectonics in New Zealand, Tectonics, 8: 169-195.

Kamp, P.J.J., and Takemura, Keiji., 1993. Thermo-tectonic history of Ryoke Basement in Hohi volcanic zone, northeast Kyushu, Japan: Constraints from fission track thermochronology, The Island Are, 2: 213-227.

Kamp, P.J.J. and Tippett, J.M., 1993. Dynamics of Pacific Crust in South Island (New Zealand) Zone of Oblique Continent-Continent Convergence, Journal of Geophysical Research, 98, B9: 16105-16118.

Kennett, J.P., 1966. Faunal Succession in Two Upper Miocene-Lower Pliocene Sections, Marlborough, New Zealand, Trans. R. Soc. N. Z. Geol., 3: 197-213.

Kieckhefer, R.M., 1979. Sheets M31D, N31A, N31C, and parts of M32A and M32B Leader Dale (1st edn), Sheets N31B and N31D Dillon (1st edn) Late Quaternary Tectonic Map of New Zealand 1:50,000, Department of Scientific and Industrial Research, Wellington, New Zealand.

Kirpatrick, S., Gelatt, C.D., Jr., and Vecchi, M.P., 1983. Optimization by simulated annealing, Sciences, 220: 671-680.

Knuepfer, P.L.K., 1984. Tectonic geomorphology and present-day tectonics of the Alpine shear system, South Island, New Zealand, 509pp., Ph.D thesis, Univ. of Ariz., Tucson.

Knuepfer, P.L.K., 1992. Temporal variations in latest Quaternary slip across the Australian-Pacific plate boundary, northeastern South Island, New Zealand, Tectonics, 11(3): 449-464.

Kohn, B. P., 1979. Identification and significance of a Late Pleistocene Tephra in Canterbury District, South Island, New Zealand, Quaternary Research 11: 78-92.

Koons, P.O., 1987. Some thermal and mechanical consequences of rapid uplift: an example from the Southern Alps, New Zealand, Earth and Planetary Science Letters, 86: 307-319.

Krsmanovic, D., and Langof, Z., 1964. Large scale laboratory tests of shear strength of rocky material, Rock Mech. and Eng. Geol. Supplement II: p20.

Ladanyi, B., and Archambault, G., 1970. Simulation of shear behaviour of a jointed rock mass, Proc. 11th Symp. on Rock Mechanics, (AIME): p105.

Laird, M.G., 1992. Cretaceous stratigraphy and evolution of the Marlborough segment of the east coast region, 1991 New Zealand Oil Exploration Conference Proceedings Ministry of Commerce (1992).

Laird, M.G., Mazengarb, C., Crampton, J.S., 1994. Mid and Late Cretaceous Basin Development in the East Coast Region, New Zealand. 1994 New Zealand Oil Exploration Conference Proceedings Ministry of Commerce (1994).

Lal, D., Rajan, R.S., and Tamhane, A.S., 1969. Chemical composition of nuclei of Z>22 in cosmic rays using meteoritic minerals and detectors, Nature, 221: 33-37.

Lamb, S. H., 1988. Tectonic rotations about vertical axes during the last 4 Ma in part of the New Zealand plate-boundary zone, Journal of Structural Geology, 10: 875-893.

Lane, K. S., and Heck, W. J., 1964. Triaxial testing for strength of rock joints, Proc. 6th Symp. on Rock Mech., Univ. of Missouri: p98.

Laslett, G.M., Green, P.F., Duddy, I.R., and Gleadow, A.J.W., 1987. Thermal annealing of fission tracks in apatite, 2. A quantitative analysis, Chem. Geol. (Isot. Geosci Sect.), 65: 1-13.

Laslett, G.M., Kendall, W.S., Gleadow, A.J.W. and Duddy, I.R., 1982. Bias in the measurement of fission tracks length distributions, Nucl. Tracks, 6: 79-85.

Lensen, G.J., 1958. Rationalised fault interpretation, New Zealand Journal of Geology and Geophysics, 1: 307-317.

Lensen, G.J., 1962. Sheet 16, Kaikoura (1st Edn). Geological Map of New Zealand 1:250,000, Department of Scientific and Industrial Research, Wellington, New Zealand.

Lensen, G.J., 1975. Earth-deformation studies in New Zealand, Tectonphysics, 29: 541-551.

Lensen, G.J., 1978. Marlborough. Pp. 383-390. In Suggate, R.P.; Stevens, G.R., Te Punga, M.T. (eds). The Late Mobile phase: Cretaceous. Chapter 6, The geology of New Zealand.

Lensen, G.J., 1981. Tectonic strain and drift, Tectonphysics, 71: 173-188.

Little, T.A., Grapes, R.H., and Berger, G.W., 1998. Late Quaternary strike-slip on the eastern part of the Awatere Fault, South Island, New Zealand, Geol. Soc. Am. Bull., 110: 2-23.

Little, T.A., and Roberts, A.P., 1997. Distribution and mechanism of Neogene to Present-day vertical-axis rotations, Pacific-Australia plate bounday zone, South Island, New Zealand, J. Geophys. Res., 102: 20,447-20,468.

Lowry, D.C., and Longley, I.M., 1991. A new model for the mid-Cretaceous structural history of the northern Gippsland Basin, The Apea Journal, 31(1): 143-153.

Lutz, T.M., and Omar, G., 1991. An inverse method of modelling thermal history from apatite fission track data, Earth and Planetary Science Letters, 104: 181-195.

Maxwell, F.A., 1990. Late Miocene to recent evolution of the Awatere basin, Medway and middle Awatere valleys, Marlborough, Unpublished M.Sc. thesis, lodged in the Library , Victoria University of Wellington, Wellington, 56p.

Mantovani, M.S.M., 1974. Variations of characteristics of fission tracks in muscovites by thermal effections, Earth and Planetary Science Letters, 2: 311-315.

Märk, E., Pahl, M., Purtscheller, F. and Märk, T.D., 1973. Thermische Ausheilung von Uran-Spatlspuren in Apatiten, Alterskorrekturen und Beiträge zur Geotherochronologie, Tshermaks Mineral. Petrogr. Mitt., 20: 131-154.

Maureatte, M., Pellas, P., and Walker, R.M., 1964. Etude des traces de fission fossiles dans le mica, Bull. Soc. Franç. Minér. Crist., 87: 6-17.

Maxwell, F.A., 1990. Late Miocene to recent evolution of the Awatere basin, Medway and middle Awatere valleys, Marlborough, Unpublished M.Sc. thesis, lodged in the Library , Victoria University of Wellington, Wellington, 56p.

McGee, V. E., and Johnson, N. M., 1979. Statistical treatment on experimental errors in the fission track dating method, Mathematical Geology, 11: 255-268.

Mckay, A., 1890. On the earthquakes of September 1988 in the Amuri and Marlborough districts of the South Island, New Zealand, Geological Survey report of geological exploration, 1888-1889, 20: 1-16.

Melhuish, A., 1988. Synsedimentary faulting in the lower Medway River area, Awatere valley, Marlborough, Unpublished M.Sc. (Hons.) thesis, lodged in the Library, Victoria University of Wellington, Wellington, 56p.

Merzer, A.M., and Freund, R., 1974. Transcurrent faults, beam theory and the Marlborough fault system, New Zealand, Geophys. J. R. Soc., 38: 553-562.

Merzer, A.M., and Freund, R., 1975. Buckling of strike-slip faults—in a model and in nature, Geophys. J. R. Soc., 4: 517-530.

Miller, D.S., and Wagner, G.A., 1981. Fission-track ages applied to obsidian artifacts from South America using the plateau-annealing and the track-size age-correction techniques, Nuclear Tracks, 5: 147-155.

Moore, M. E., Gleadow, A.J.W., and Lovering, J.F., 1986. Thermal evolution of rifted continental margins: New evidence from fission tracks in basement apatites from southeastern Australia, Earth Planetary Sciences Letters, 78: 255-270.

Morgans, H.E.G., 1980. Stratigraphy of the Neogene sequence at Blind river, Marlborough, New Zealand Geological Survey Report, Pal 36: 18p.

Mumme, T. C., Lamb, S. H., and Walcott, R. I., 1989. The Raukumara palaeomagnetic domain : constraints on the tectonic rotation of the east, North Island, New Zealand, from palaeo-magnetic data, New Zealand Journal of Geology and Geophysics, 32: 317-326.

Naeser, C.W., 1979a. Fission-track dating and geologic annealing of fission tracks, in E. Jäger and J. C. Hunziker (eds), Lectures in Isotope Geology, Springer-Verlag, Heidelberg, pp. 154-169.

Naeser, C.W., 1979b. Thermal history of sedimentary basins in fission track dating of subsurface rocks, Spec. Publ. Soc. econ. Paleont. Miner., 26: 109-112.

Naeser, C.W., 1981. The fading of fission-tracks in the geologic environment - data from deep drill holes (abstract), Nuclear Tracks, 5: 248-250.

Naeser, C.W., Izett, G.A., and Obradovich, J.D., 1980. Fission-track and K-Ar ages of natural glasses, U.S. Geol. Surv. Bull., 1489: 1-31.

Naeser, N. D., and McCulloh (eds), 1989. Thermal History of Sedimentary Basins, Springer-Verlag, New York: 157-180.

Nagpaul, K.K., Mehta, P.P., and Gupta, M.L., 1974. Annealing studies on radiation damages in biotite, apatite and sphene and corrections to fission track ages, Pure Appl. Geophys., 112: 131-139.

Nelson, C.S., 1978. Temperate shelf carbonate sediments in the Cenozoic of New Zealand, Sedimentology, 25: 125-166.

Nelson, C.S., 1990. Overview of New Zealand Cenozoic shelf limestones, Pp.5-7 in: Recent development in New Zealand basin studies, Lower Hutt, Department of Scientific and Industrial Research Geology and Geophysics, 50p.

Patton, F. D., 1966. Multiple modes of shear failure in rock, Proc. 1st Con. ISRM, Lisbon, 1: p509.

Pearson, C., 1993. Rate of co-seismic strain release in the northern South Island, New Zealand, Zealand Journal of Geology and Geophysics, 36: 161-166.

Pellas, P. and Perron, C., 1984. Track formation models: a short review. Nucl. Instrum. Methods, B1: 387-393.

Poupeau, G., Carpena, J., Chambaudet, A., and Romary, Ph., 1980. Fission track plateau-age dating, in H. Franxcois et al. (eds), Solid State Nuclear Track Detectors, Pergamon Press, Oxford, pp. 966-977.

Price, P.B., and Walker, R.M., 1962a. A new detector for heavy particle studies, Phys. Lett., 3: 113-115.

Price, P.B., and Walker, R.M., 1962b. Observations of charged-particle tracks in solids, J. Appl. Phys., 33: 3400-3406.

Price, P.B., and Walker, R.M., 1963. Fossil tracks of charged particles in mica and the age of minerals, Journal of Geophysical Research, 68: 4847-4862.

Raliegh, C. B., and Patersons, M. N., 1965. Experimental deformation of serpentine and its tectonic implications, Journal of Geology and Geophysics, 70: p3965.

Reay, M.B., 1993. Geology of the Middle Clarence Valey, Institute of Geological and Nuclear Sciences geological map 10, 1 sheet + 144p, Institute of Geological and Nuclear Sciences Ltd., Lower Hutt, New Zealand.

Reay, M.B., and Strong, C.P., 1992. The Branch sandstone, Clarence valley, and implications for latest Cretaceous paleoenvironments and geological history of central Marlborough, P. 43-49 in: Research notes 1991, New Zealand Geological Survey record 44.

Reilly, W.I., 1965. "Gravity Map of New Zealand 1: 4,000,000, Bouguer and Isostatic Anomalies" (1st ed.), DSIR, Wellington.

Reilly, W.I., and Whiteford, C.M., 1979. South Island Gravity Map of New Zealand, (1st Ed.), 1: 1,000,000, Bouguer Anomalies, New Zealand Department of Scientific and Industrial Research, Wellington.

Reyners, M., 1980. A microearthquake study of the plate boundary, North Island, New Zealand, Geophysical Journal of the Royal Astronomical Society, 63: 1-22.

Ritchie, D.D., and Bradshaw, J.D., 1985. Clarence-Kekerengu faults trip, Marlborough; Field trip guides, Geological Society of New Zealand, Christchurch Conference, Miscellaneous publication, 32B: 1-11.

Roberts, A.P., 1992. Paleomagnetic constraints on the tectonic rotation of the Southern Hikurangi Margin, New Zealand, New Zealand Journal of Geology and Geophysics, 35: 311-323.

Roberts, A.P., and Wilson, G.S., 1992. Stratigraphy of the Awatere Group, Marlborough, New Zealand, Journal of The Royal Society of New Zealand, 22: 187-204.

Robinson, R. and Arabasz, W.J., 1975. Microearthquakes in the north-west Nelson region, New Zealand Journal of Geology and Geophysics, 18: 83-91.

Roberts, J.H., Gold, R., and Armani, R.J., 1968. Spontaneous fission decay constant of ^{238}U, Phys. Rev., 174: 1482-1484.

Rohrman, M., Beek, P. van der, nas Andriessen, P., 1994. Syn-rift thermal structure ans post-fift evolution of the Oslo rift (southeast Norway): New Constraints from fission track thermochronology, Earth and Planetary Science Letters, 127: 39-54.

Rosengren, K. J., 1968. Rock mechanics of the Black Star open cut, Mount Isa PhD Thesis, Australian National Univ., Canberra.

Rynn, J.M.W., and Scholz, C.H., 1978. Seismotectonics of the Arthurs Pass region, New Zealand, Geol. Soc. Am. Bull., 89: 1373-1388.

Scholz, C.H., Rynn, J.M.W., Weed, R.W., and Frohlich, C., 1973. Detailed seismicity of the Alpine fault zone and Fiordland region, New Zealand, Geol. Soc. Am. Bull., 84: 3297-3316.

Seward, D., 1974. Age of New Zealand Pleistocene substages by fission track dating of glass shards from tephra horizons. Earth and Planetary Science Letters, 24: 242-248.

Seward, D., 1975. fission track ages of some tephras from Cape Kidnappers, Hawke's Bay, New Zealand. New Zealand Journal of Geology and Geophysics, 18: 507-510.

Sharma, K.K., Saini, H.S., and Nagpaul, K.K., 1978. Fission track annealing, ages of apatites from Mandi granite and their application to tectonic problems, Himalayan Geology, 8: 296-312.

Silk, E.C.H., and Barnes, R.S., 1959. Examination of fission fragment tracks with an electron microscope, Philos. Mag., 4: 970-972.

Smith, W. D., and Berryman, K. R., 1986. Earthquake hazard in New Zealand: inferences for seismology and geology. Royal Society of New Zealand Bulletin, 24: 223-243.

Soons, J.M., and Selby, M.J., 1982. The Stability of Hillslopes, 46-47, Chapter 3, Land Forms of New Zealand.

Spadavecchia, A., and Hahn, B., 1967. Die Rotationskammer und einige Anwendungen, Helv. Phys. Acta., 40: 1063-1079.

Spell, T.L., and McDougall, I., 1994. Thermochronology of a metamorphic core complex associated with the break up of Gondwana: The Paparoa Range, South Island, New Zealand, in Abstracts Eight International Conference on Geochronology, Cosmochronology and Isotope Geology, Berkeley, California, U.S. Geol. Surv. Circ., 1107: 300.

Stock, J., and Molnar,P., 1982. Uncertainties in the relative positions of the Australia, Antarctica, Lord Howe, and Pacific plates since the Late Cretaceous, Journal of Geophysical Research, 87B: 4697-4714.

Storzer, D., and Poupeau, G., 1973. Géochronologie.-Ages-plateaux de minéraux et verres par la méthode des traces de fission, Compt. Rend. Acad. Sci., Paris D276: 137-139.

Storzer, D., and Sélo, M., 1976. Uranium contents and fission track ages of some basalts from the FAMOUS area, Bull. Soc. Geol. Fr., 18: 807-810.

Storzer, D., and Wanger, G.A., 1969. Correction of thermally lowered fission track ages of tektites, Earth and Planetary Science Letters, 5: 463-468.

Storzer, D., and Wanger, G.A., 1977. Fission track dating of meteorite impacts, Meteoritics, 12: 368-369.

Storzer, D., and Wagner, G.A., 1982. The application of fission track dating in stratigraphy: a critical review, in G. S. Odin (ed.), Numerical Dating in Stratigaphy, Wiley, Chichester, pp. 199-221.

Suggate, R.P., 1958. The geology of the Clarence Valley from Gore Stream to Bluff Hill, Transactions of the Royal Society of New Zealand, 85 (3): 397-408.

Suggate, R.P., 1978a. In Suggate, R.P.; Stevens, G.R., Te Punga, M.T. (eds). The Kaikoura Orogeny, 672-673, Chapter 10, The geology of New Zealand.

Suggate, R.P., 1978b. In Suggate, R.P.; Stevens, G.R., Te Punga, M.T. (eds). The Kaikoura Orogeny, 680-682, Chapter 10, The geology of New Zealand.

Suggate, R.P., 1979. The Alpine Fault Bends and the Marlborough Faults, The Royal Society of New Zealand, 18: 67-72.

Suggate, R.P., and Grindley, G.W., 1972. South Island (1st Edn). Geological Map of New Zealand 1:1,000,000, Department of Scientific and Industrial Research, Wellington, New Zealand.

SzÉchy, K., 1966. The Art of Tunnelling, Budapest: Akadémiai Kiadó, p. 76.

Tagami, T.,1987. Determination of zeta calibration constant for fission track dating, Nucl. Tracks Radiat. Meas., 13: 127-130.

Tagami, T., Lal, N., Sorkhabi, R. B., and Nishimura, S., 1988. Fission track thermochronologic analysis of the Ryoke Belt and the Median Tectonic Line, Southwest Japan, Journal of Geophysical Research, 93: 705-713.

Tagami, T., Carter, A., and Hurford, A.J., 1996. Natural long-term annealing of the zircon fission-track system in Vienna Basin deep hole samples: constraints upon the partial annealing zone and closure temperature, Chem. Geol. (Isot. Geosci. Sect.) 130: 147-157.

Thomson, J.A., 1913. Results of field-work, New Zealand Geological Survey. 7th annual report: 122-123.

Tippett, J.M., 1992. Uplift history and geomorphic development of the Southern Alps, New Zealand, assessed by the fission track analysis, (Unpublished) Ph.D., University of Waikato.

Tippett, J.M., and Kamp, P.J.J., 1993. Fission Track Analysis of the Late Cenozoic Vertical Kinematics of Continental Pacific Crust, South Island, New Zealand, Journal of Geophysical Research, 98: 16119-16148.

Tulloch, A.J., and Kimbrough, D.L., 1989. The Paparoa Metamorphic Core Complex, South Island, New Zealand: Cretaceous extension associated with the fragmentation of the Pacific margin of Gondwana, Tectonics, 8: 1217-1234.

Turner, M. J., Clough, R. W., Martin, H. C., and Topp, L. C., 1956. Stiffness and Deflection Analysis of Complex Structures, J. Aero. Sci., 23: 9.

U. S. Bureau of Reclamation, 1954. Physical Properties of Typical Foundation Rocks, Concrete Laboratory Report SP 39.

Van Den haute, P., 1986a. Sphene fission-track dating of a precambrian alkaline pluton in Burundi (Central Africa), Terra Cognita, 6: 165.

Van Den haute, P., 1986b. Apatite fission-track dating applied to precambrian terranes, Chem. Geol., 57: 155-165.

Van den haute, P., and Chambaudet, A., 1990. Results of an interlaboratory experiment for the 1988 fission track workshop on a putative apatite standard for internal calibration, Nucl. Tracks Radiat. Meas., 17: 247-252.

Vickery, S., Lamb, S., 1995. Large tectonic rotations since the Early Miocene in a convergent plate-boundary zone, South Island, New Zealand. Earth and Planetary Science Letters, 136: 43-59.

Wagner, G.A., 1966. Altersbestimmungen an Tektiten und anderen natürlichen Gläsern mittels Spuren der spontanen Kernspaltung des Uran^{238} ("fission-track"-Methode), Z. Naturforschung 21a, 733-745.

Wagner, G.A., 1977. Spaltspurendatierung an Apatit und Titanit aus dem Ries: Ein Beitrag zum Alter und zur Warmegeschichte, Geol. Bavarica, 75: 349-354.

Wagner, G.A., 1988. Apatite fission-track geochrono-thermometer to 60°C : projected length studies, Chemical Geology (Isotope Geoscience Section), 72: 145-153.

Wagner, G. A., Gleadow, A. J. W., and Fitzgerald, P. G., 1989a. The significance of the partial annealing zone in apatite fission-track analysis: projected track lenght measurements and uplift chronology of the Transantarctic Mountains, Chem. Geol. (Isot. Geosci. Sect.), 79: 295-305.

Wagner, G.A., and Haute, P. V. D., 1992. Fission-Track Dating, Ferdinand Enke Verlag., Germany.

Wagner, G. A., Michalski, I., and Zaun, P., 1989b. Apatite fission track dating of the Central European Basement: Post-Variscan thermo-tectonic evolution, The German Continental Deep Dril-ling Program (KTB), Springer-Verlag, Heidelberg: 481-500.

Wagner, G. A., and Reimer, M., 1972. Fission track tectonics: the tectonic interpretation of fission track apatite ages, Earth and Planetary Science Letters, 14: 263-268.

Wagner, G.A., and Storzer, D., 1970. Die Interpretation von Spaltspurenaltern (fission track ages) am Beispiel von natürlichen Gläsern, Apatiten und Zirkonen, Ecologae Geol. Helv., 63/1: 335-344.

Wagner, G.A., and Storzer, D., 1972. Fission track length reductions in minerals and the thermal histories of rocks, Trans. Amer. Nucl. Soc., 15: 127-128.

Wagner, G.A., and Storzer, D., 1975. Spaltspuren und ihre Bedeutung für die thermische Geschichte des Odenwaldes, Aufschluss, 27: 79-85.

Wagner , G, A., and Reimer, M., 1972. Fission track tectonics: the tectonic interpretation of fission track apatite ages, Earth and Planetary Science Letters, 14: 263-268.

Walcott, R.I., 1978a. Present tectonics and Late Cenozoic evolution of New Zealand, Geophys. J. Roy. astr. Soc., 52: 137-164.

Walcott, R.I., 1978b. Geodetic strains and large earthquakes in the axial tectonic belt of North Island, New Zealand, Journal of Geophysical Research, 83: 4419-4429.

Walcott, R.I., 1979. Plate motion and shear rates in the vicinity of the Southern Alps, The Royal Society of New Zealand, 18: 5-12.

Walcott, R.I., 1984. Kinematics of the Plate Boundary Zone through New Zealand: A comparison of short and long term deformation, Geophys. J. Roy. astr. Soc., 79: 613-633.

Walcott, R.I., 1987. Geodetic strain and the deformational history of New Zealand during the late Cainozoic, Phil. Trans. R.Soc. Lond., A321: 163-181.

Walcott, R.I., 1998. Modes of oblique compression: late Cenozoic tectonics of the South Island of New Zealand, Reviews of Geophysics, 36, 1: 1-26.

Watanabe, N., and Suzuki, M., 1969. Fission track dating of archaeological glass materials from Japan, Nature, 222: 1057-1058.

Watt, S., and Durrani, S.A., 1985. Thermal stability of fission tracks in apatite and sphene: using confined track length measurements, Nucl. Tracks, 10: 349-357.

Ward, S.N., 1990. Pacific-North America plate motions: New results from very long baseline interferometry, Journal of Geophysical Research, 95: 21,965-21,981.

Warren, G., and Speden, I.G., 1978. The Piripauan and Haumurian stratotypes (Mata Series, Upper Cretaceous) and correlative sequences in the Haumuri Bluff district, south Marlborough (S56), New Zealand Geological Survey Bulletin 92, Wellington, Department of Scientific and Industrial Research, 60p.

Weaver, S.D., and Pankhurst, R.J., 1991. A precise Rb-Sr age for the Mandamus Igneous Complex, North Canterbury, and regional tectonic implications, New Zealand Journal of Geology and Geophysics, 34: 341-347.

Webb, P.N., 1971. New Zealand Late Cretaceous (Haumurian) foraminifera and stratigraphy: a summary, New Zealand Journal of Geology and Geophysics, 14: 795-828.

Welin, E., Lundström, I., and Aberg, G., 1972. Fission track studies on hornblende, biotite and phlogopite from Sweden, Bull. Geol. Soc. Finland, 44: 35-46.

Wellman, H.W., 1971. Reference lines, fault classification, transform systems, and ocean-floor spreading, Tectonophysics, 12: 199-209.

Wellman, H.W., 1979. An uplift map for the South Island of New Zealand, and a model for uplift for the Southern Alps, in Walcott, R.I., Cresswell, M.M. (Eds)., The origin of the Southern Alps, Royal Society of New Zealand Bulletin, 18: 13-20.

Wellman, H.W., 1983. New Zealand horizontal kinematics. In: Geodynamics of the Western Pacific-Indonesian Region (edited by Hilde, T. W. C., and Uyeda, S.), Am. Geophys. Un. Geodynamic Series, 11: 423-457.

Westgate, J.A., 1989. Isothermal plateau fission-track ages of hydrated glass shards from silicic tephra beds, Earth and Planetary Science Letters, 95: 226-234.

White, S. H., and Green, P. F., 1986. Tectonic development of the Alpine fault zone, New Zealand: a fission track study, Geology 14: 124-127.

Wood, P.R., and Blick, G.H., 1986. Some results of geodetic fault monitoring in South Island, New Zealand, Royal Society of New Zealand Bulletin, 18: 39-45.

Wright, I.G., and Walcott, R.I., 1986. Large tectonic rotation of part of New Zealand in the last 5 Ma, Earth and Planetary Science Letters, 80: 348-352.

Yang, J.S., 1989. Seismotectonic study of the central Alpine Fault region, South Island, New Zealand. Unpublished Ph. D. thesis, lodged in the Library, Victoria University of Wellington, Wellington, New Zealand.

Yang, J.S., 1992. Landslide and major earthquakes on the Kakapo Fault, South Island, New Zealand, Journal of The Royal Society of New Zealand, 22: 205-212.

Yeats, R.S., and Berryman, K.R., 1987. South Island, new Zealand, and Transverse Ranges, California: A seismotectonic comparison: Tectonics, 6: 363-376.

Zaun, P.E., and Wagner, G.A., 1985. Fission-track stability in zircons under geological conditions, Nucl. Tracks., 10: 303-307.

Zimmerman, R. A., 1980. Patterns of post-Triassic uplift and inferred Fall Line zone faulting in the eastern United States, GSA Abstracts, 12: 554.

Data Appendix:

Apatite single grain fission track age data
Apatite horizontally confined fission track length data
Zircon single grain fission track age data

Data Appendix:

Apatite single grain fission track age data
Apatite horizontally confined fission track length data
Zircon single grain fission track age data

9414-01 Apatite

IRRADIATION wk140-01 COUNTED BY: Kao

No.	Ns	Ni	Na	RATIO	U(ppm)	RHOs	RHOi	F.T.AGE(Ma)
1	0	3	6	0.000	5.6	0.000E+00	5.269E+05	0.0 ± 0.0
2	1	29	18	0.034	18.1	5.854E+04	1.698E+06	6.8 ± 7.0
3	0	1	4	0.000	2.8	0.000E+00	2.634E+05	0.0 ± 0.0
4	7	82	8	0.085	114.9	9.220E+05	1.080E+07	16.9 ± 6.7
5	1	2	12	0.500	1.9	8.781E+04	1.756E+05	98.5 ±120.7
6	0	1	18	0.000	0.6	0.000E+00	5.854E+04	0.0 ± 0.0
7	0	3	4	0.000	8.4	0.000E+00	7.903E+05	0.0 ± 0.0
8	0	2	8	0.000	2.8	0.000E+00	2.634E+05	0.0 ± 0.0
9	0	1	8	0.000	1.4	0.000E+00	1.317E+05	0.0 ± 0.0
10	0	1	3	0.000	3.7	0.000E+00	3.512E+05	0.0 ± 0.0
11	1	5	12	0.200	4.7	8.781E+04	4.391E+05	39.6 ± 43.4
12	0	2	6	0.000	3.7	0.000E+00	3.512E+05	0.0 ± 0.0
13	0	2	12	0.000	1.9	0.000E+00	1.756E+05	0.0 ± 0.0
14	0	1	6	0.000	1.9	0.000E+00	1.756E+05	0.0 ± 0.0
15	1	4	16	0.250	2.8	6.586E+04	2.634E+05	49.4 ± 55.3
16	1	4	12	0.250	3.7	8.781E+04	3.512E+05	49.4 ± 55.3
17	2	3	16	0.667	2.1	1.317E+05	1.976E+05	131.0 ±119.6
18	0	3	18	0.000	1.9	0.000E+00	1.756E+05	0.0 ± 0.0
19	0	2	12	0.000	1.9	0.000E+00	1.756E+05	0.0 ± 0.0
20	1	10	40	0.100	2.8	2.634E+04	2.634E+05	19.8 ± 20.8
	15	161			7.6	6.613E+04	7.098E+05	

Area of basic unit = 9.49E-07 cm-2

CHI SQUARED = 7.031454 WITH 19 DEGREES OF FREEDOM
P(chi squared) = 78.0 %
CORRELATION COEFFICIENT = 0.922
VARIANCE OF SQR(Ns) = .5231503
VARIANCE OF SQR(Ni) = 3.644452

Ns/Ni = 0.093 ± 0.025
MEAN RATIO = 0.104 ± 0.042

Pooled Age = 18.5 ± 5.0 Ma
Mean Age = 20.7 ± 8.3 Ma
Central Age = 18.5 ± 5.0Ma
% Rel. Error = 0.06
Ages calculated using a zeta of 348.4 ± 5.8 for SRM 612 glass
RHO D = 1.156E+06cm-2; ND = 2859

9414-2 Apatite

IRRADIATION WK140-2 COUNTED BY: KAO

No.	Ns	Ni	Na	RATIO	U(ppm)	RHOs	RHOi	F.T.AGE(Ma)
1	4	62	21	0.065	32.8	1.926E+05	2.985E+06	12.6 ± 6.5
2	4	56	9	0.071	69.1	4.494E+05	6.291E+06	13.9 ± 7.2
3	20	64	12	0.312	59.2	1.685E+06	5.393E+06	60.7 ± 15.6
4	3	14	12	0.214	13.0	2.528E+05	1.180E+06	41.7 ± 26.5
5	8	24	16	0.333	16.7	5.056E+05	1.517E+06	64.7 ± 26.5
6	18	213	70	0.084	33.8	2.600E+05	3.077E+06	16.5 ± 4.1
7	6	41	8	0.146	56.9	7.583E+05	5.182E+06	28.5 ± 12.5
8	20	80	18	0.250	49.4	1.123E+06	4.494E+06	48.6 ± 12.2
9	7	65	21	0.108	34.4	3.370E+05	3.130E+06	21.0 ± 8.4
10	3	31	12	0.097	28.7	2.528E+05	2.612E+06	18.9 ± 11.4
11	2	22	15	0.091	16.3	1.348E+05	1.483E+06	17.7 ± 13.1
12	6	57	21	0.105	30.1	2.889E+05	2.744E+06	20.5 ± 8.8
13	5	21	16	0.238	14.6	3.160E+05	1.327E+06	46.3 ± 23.1
14	7	81	28	0.086	32.1	2.528E+05	2.925E+06	16.8 ± 6.6
15	5	57	24	0.088	26.4	2.106E+05	2.401E+06	17.1 ± 8.0
16	4	48	40	0.083	13.3	1.011E+05	1.213E+06	16.2 ± 8.5
17	3	41	48	0.073	9.5	6.320E+04	8.637E+05	14.3 ± 8.5
18	3	10	15	0.300	7.4	2.022E+05	6.741E+05	58.3 ± 38.4
19	2	12	16	0.167	8.3	1.264E+05	7.583E+05	32.4 ± 24.8
20	3	32	12	0.094	29.6	2.528E+05	2.696E+06	18.3 ± 11.0
	133	1031			26.4	3.099E+05	2.402E+06	

Area of basic unit = 9.89E-07 cm-2

CHI SQUARED = 20.37718 WITH 19 DEGREES OF FREEDOM
P(chi squared) = 0.260 %
CORRELATION COEFFICIENT = 0.662
VARIANCE OF SQR(Ns) = .8946694
VARIANCE OF SQR(Ni) = 6.616808

Ns/Ni = 0.129 ± 0.012
MEAN RATIO = 0.150 ± 0.020

Pooled Age = 25.1 ± 2.4 Ma
Mean Age = 29.3 ± 4.0 Ma
Central Age = 26.3 ± 3.6Ma
% Rel. Error = 41.00
Ages calculated using a zeta of 348.4 ± 5.8 for SRM 612 glass
RHO D = 1.120E+06cm-2; ND = 2768

9414-3 APATITE MARLBOROUGH

IRRADIATION WK140-3
SLIDE NUMBER 3
COUNTED BY: KAO

No.	Ns	Ni	Na	RATIO	U (ppm)	RHOs (E+06)	RHOi (E+06)	F.T.AGE (Ma)
1	1	12	4	0.083	35.5	0.253	3.033	16.2 ± 16.9
2	2	6	4	0.333	17.7	0.506	1.517	64.7 ± 52.9
3	0	5	6	0.000	9.9	0.000	0.843	0.0 ± 0.0
	3	23			19.4	0.217	1.661	

AREA OF BASIC UNIT = 9.89E-07 cm
CHI SQUARED = 2.26087 WITH 2 DEGREES OF FREEDOM
P(chi squared) = 32.3 %
CORRELATION COEFFICIENT = 0.132
VARIANCE OF SQR(Ns) = 0.53
VARIANCE OF SQR(Ni) = 0.43

Ns/Ni = 0.130 ± 0.080
MEAN RATIO = 0.139 ± 0.100

Ages calculated using a zeta of 348.4 ± 5.8 for SRM612 glass
RHO D = 1.120E+06 ; ND = 2768

POOLED AGE = 25.4 ± 15.6 Ma
MEAN AGE = 27.0 ± 19.5 Ma

9414-04 APATITE Apatite

IRRADIATION FT:WK140
SLIDE NUMBER 4
COUNTED BY: Kao

No.	Ns	Ni	Na	RATIO	U (ppm)	RHOs (E+06)	RHOi (E+06)	F.T.AGE (Ma)
1	3	20	8	0.150	28.6	0.379	2.528	29.7 ± 18.4
2	6	32	15	0.188	24.4	0.404	2.157	37.1 ± 16.5
	9	52			25.9	0.396	2.286	

AREA OF BASIC UNIT = 9.89E-07 cm
CHI SQUARED = 8.590037E-02 WITH 1 DEGREES OF FREEDOM
P(chi squared) = 76.9 %
CORRELATION COEFFICIENT = 1.000
VARIANCE OF SQR(Ns) = 0.26
VARIANCE OF SQR(Ni) = 0.70

Ns/Ni = 0.173 ± 0.062
MEAN RATIO = 0.169 ± 0.019

Ages calculated using a zeta of 348.4 ± 5.8 for SRM612 glass
RHO D = 1.156E+06 ; ND = 2859

POOLED AGE = 34.3 ± 12.4 Ma
MEAN AGE = 33.4 ± 3.8 Ma

9414-05 APATITE Apatite

IRRADIATION WK140
SLIDE NUMBER 5
COUNTED BY: Kao

No.	Ns	Ni	Na	RATIO	U (ppm)	RHOs (E+06)	RHOi (E+06)	F.T.AGE (Ma)
1	5	17	6	0.294	32.5	0.843	2.865	58.1 ± 29.6
2	0	1	12	0.000	1.0	0.000	0.084	0.0 ± 0.0
3	5	18	18	0.278	11.5	0.281	1.011	54.9 ± 27.8
4	8	8	24	1.000	3.8	0.337	0.337	195.5 ± 97.9
5	1	10	8	0.100	14.3	0.126	1.264	19.8 ± 20.8
6	15	63	25	0.238	28.9	0.607	2.548	47.1 ± 13.6
7	4	6	12	0.667	5.7	0.337	0.506	131.0 ± 84.6
8	0	1	24	0.000	0.5	0.000	0.042	0.0 ± 0.0
9	2	17	12	0.118	16.2	0.169	1.432	23.3 ± 17.4
10	0	4	20	0.000	2.3	0.000	0.202	0.0 ± 0.0
11	1	1	12	1.000	1.0	0.084	0.084	195.5 ± 276.6
12	1	5	20	0.200	2.9	0.051	0.253	39.6 ± 43.4
13	24	49	18	0.490	31.2	1.348	2.752	96.5 ± 24.1
14	0	1	60	0.000	0.2	0.000	0.017	0.0 ± 0.0
15	1	1	9	1.000	1.3	0.112	0.112	195.5 ± 276.6
16	0	1	36	0.000	0.3	0.000	0.028	0.0 ± 0.0
17	0	1	16	0.000	0.7	0.000	0.063	0.0 ± 0.0
18	5	3	25	1.667	1.4	0.202	0.121	322.7 ± 235.8
19	3	7	12	0.429	6.7	0.253	0.590	84.5 ± 58.4
20	5	10	12	0.500	9.5	0.421	0.843	98.5 ± 54.0
	80	224			6.7	0.212	0.594	

AREA OF BASIC UNIT = 9.89E-07 cm
CHI SQUARED = 24.26685 WITH 19 DEGREES OF FREEDOM
P(chi squared) = 18.6 %
CORRELATION COEFFICIENT = 0.868
VARIANCE OF SQR(Ns) = 1.89
VARIANCE OF SQR(Ni) = 3.93

Ns/Ni = 0.357 ± 0.047
MEAN RATIO = 0.399 ± 0.103

Ages calculated using a zeta of 348.4 ± 5.8 for SRM612 glass
RHO D = 1.156E+06 ; ND = 2859

POOLED AGE = 70.5 ± 9.3 Ma
MEAN AGE = 78.7 ± 20.3 Ma

9414-6 Apatite

IRRADIATION wk140-6 COUNTED BY: Kao

No.	Ns	Ni	Na	RATIO	U(ppm)	RHOs	RHOi	F.T.AGE(Ma)
1	5	80	30	0.062	28.7	1.685E+05	2.696E+06	12.4 ± 5.7
2	6	73	18	0.082	43.6	3.370E+05	4.101E+06	16.3 ± 6.9
3	2	35	8	0.057	47.1	2.528E+05	4.424E+06	11.3 ± 8.2
4	2	4	12	0.500	3.6	1.685E+05	3.370E+05	98.5 ± 85.3
5	1	15	24	0.067	6.7	4.213E+04	6.320E+05	13.2 ± 13.7
6	1	13	12	0.077	11.7	8.426E+04	1.095E+06	15.3 ± 15.8
7	6	20	16	0.300	13.4	3.792E+05	1.264E+06	59.3 ± 27.6
8	2	36	24	0.056	16.1	8.426E+04	1.517E+06	11.0 ± 8.0
9	1	11	12	0.091	9.9	8.426E+04	9.269E+05	18.0 ± 18.8
10	0	15	6	0.000	26.9	0.000E+00	2.528E+06	0.0 ± 0.0
11	3	62	15	0.048	44.5	2.022E+05	4.179E+06	9.6 ± 5.7
12	3	28	10	0.107	30.1	3.033E+05	2.831E+06	21.2 ± 12.9
13	1	31	18	0.032	18.5	5.617E+04	1.741E+06	6.4 ± 6.5
14	3	8	9	0.375	9.6	3.370E+05	8.988E+05	74.0 ± 50.1
15	0	23	20	0.000	12.4	0.000E+00	1.163E+06	0.0 ± 0.0
16	2	9	9	0.222	10.8	2.247E+05	1.011E+06	44.0 ± 34.4
17	3	74	12	0.041	66.3	2.528E+05	6.235E+06	8.0 ± 4.7
18	0	2	4	0.000	5.4	0.000E+00	5.056E+05	0.0 ± 0.0
19	6	61	18	0.098	36.5	3.370E+05	3.427E+06	19.5 ± 8.4
20	3	18	30	0.167	6.5	1.011E+05	6.067E+05	33.0 ± 20.6
	50	618			21.7	1.647E+05	2.035E+06	

Area of basic unit = 9.89E-07 cm-2

CHI SQUARED = 15.98489 WITH 19 DEGREES OF FREEDOM
P(chi squared) = 3.2 %
CORRELATION COEFFICIENT = 0.625
VARIANCE OF SQR(Ns) = .5828899
VARIANCE OF SQR(Ni) = 5.162617

Ns/Ni = 0.081 ± 0.012
MEAN RATIO = 0.119 ± 0.030

Pooled Age = 16.0 ± 2.4 Ma
Mean Age = 23.6 ± 5.9 Ma
Central Age = 16.5 ± 2.7Ma
% Rel. Error = 25.44
Ages calculated using a zeta of 348.4 ± 5.8 for SRM 612 glass
RHO D = 1.156E+06cm-2; ND = 2859

9414-08 APATITE Apatite

IRRADIATION FT:WK140
SLIDE NUMBER 9
COUNTED BY: Kao

No.	Ns	Ni	Na	RATIO	U (ppm)	RHOs (E+06)	RHOi (E+06)	F.T.AGE (Ma)
1	0	1	24	0.000	0.5	0.000	0.042	0.0 ± 0.0
2	15	76	24	0.197	36.3	0.632	3.202	39.1 ± 11.1
	15	77			18.4	0.316	1.622	

AREA OF BASIC UNIT = 9.89E-07 cm
CHI SQUARED = .1969459 WITH 1 DEGREES OF FREEDOM
P(chi squared) = 65.7 %
CORRELATION COEFFICIENT = 1.000
VARIANCE OF SQR(Ns) = 7.50
VARIANCE OF SQR(Ni) = 29.78

Ns/Ni = 0.195 ± 0.055
MEAN RATIO = 0.099 ± 0.099

Ages calculated using a zeta of 348.4 ± 5.8 for SRM612 glass
RHO D = 1.156E+06 ; ND = 2859

POOLED AGE = 38.6 ± 10.9 Ma
MEAN AGE = 19.6 ± 19.6 Ma

9414-09 APATITE Apatite

IRRADIATION WK140
SLIDE NUMBER 10
COUNTED BY: Kao

No.	Ns	Ni	Na	RATIO	U (ppm)	RHOs (E+06)	RHOi (E+06)	F.T.AGE (Ma)
1	0	5	9	0.000	6.4	0.000	0.562	0.0 ± 0.0
2	4	20	9	0.200	25.5	0.449	2.247	39.6 ± 21.7
3	1	5	6	0.200	9.5	0.169	0.843	39.6 ± 43.4
4	0	3	18	0.000	1.9	0.000	0.169	0.0 ± 0.0
5	6	79	12	0.076	75.4	0.506	6.657	15.1 ± 6.4
6	4	34	28	0.118	13.9	0.144	1.228	23.3 ± 12.3
7	1	7	12	0.143	6.7	0.084	0.590	28.3 ± 30.3
8	0	12	15	0.000	9.2	0.000	0.809	0.0 ± 0.0
9	1	5	16	0.200	3.6	0.063	0.316	39.6 ± 43.4
10	2	25	18	0.080	15.9	0.112	1.404	15.9 ± 11.7
11	3	34	12	0.088	32.5	0.253	2.865	17.5 ± 10.5
12	2	15	10	0.133	17.2	0.202	1.517	26.4 ± 19.9
13	1	22	20	0.045	12.6	0.051	1.112	9.0 ± 9.2
14	3	48	24	0.062	22.9	0.126	2.022	12.4 ± 7.4
15	1	36	12	0.028	34.4	0.084	3.033	5.5 ± 5.6
16	0	4	36	0.000	1.3	0.000	0.112	0.0 ± 0.0
17	0	1	9	0.000	1.3	0.000	0.112	0.0 ± 0.0
18	4	25	8	0.160	35.8	0.506	3.160	31.7 ± 17.1
19	1	4	12	0.250	3.8	0.084	0.337	49.4 ± 55.3
20	0	4	30	0.000	1.5	0.000	0.135	0.0 ± 0.0
	34	388			14.1	0.109	1.242	

AREA OF BASIC UNIT = 9.89E-07 cm
CHI SQUARED = 11.5505 WITH 19 DEGREES OF FREEDOM
P(chi squared) = 90.4 %
CORRELATION COEFFICIENT = 0.821
VARIANCE OF SQR(Ns) = 0.66
VARIANCE OF SQR(Ni) = 4.38

Ns/Ni = 0.088 ± 0.016
MEAN RATIO = 0.089 ± 0.018

Ages calculated using a zeta of 348.4 ± 5.8 for SRM612 glass
RHO D = 1.156E+06 ; ND = 2859

POOLED AGE = 17.4 ± 3.1 Ma
MEAN AGE = 17.7 ± 3.7 Ma

9414-10 APATITE MARLBOROUGH

IRRADIATION WK140
SLIDE NUMBER 10
COUNTED BY: KAO

No.	Ns	Ni	Na	RATIO	U (ppm)	RHOs (E+06)	RHOi (E+06)	F.T.AGE (Ma)
1	4	11	8	0.364	16.3	0.506	1.390	70.6 ± 41.2
2	3	26	10	0.115	30.7	0.303	2.629	22.5 ± 13.7
	7	37			24.3	0.393	2.078	

AREA OF BASIC UNIT = 9.89E-07 cm
CHI SQUARED = 1.968704 WITH 1 DEGREES OF FREEDOM
P(chi squared) = 16.1 %
CORRELATION COEFFICIENT = -1.000
VARIANCE OF SQR(Ns) = 0.04
VARIANCE OF SQR(Ni) = 1.59

Ns/Ni = 0.189 ± 0.078
MEAN RATIO = 0.240 ± 0.124

Ages calculated using a zeta of 348.4 ± 5.8 for SRM612 glass
RHO D = 1.120E+06 ; ND = 2768

POOLED AGE = 36.8 ± 15.2 Ma
MEAN AGE = 46.6 ± 24.2 Ma

9414-11 Apatite

IRRADIATION wk140-12 COUNTED BY: Kao

No.	Ns	Ni	Na	RATIO	U(ppm)	RHOs	RHOi	F.T.AGE(Ma)
1	1	22	8	0.045	29.6	1.264E+05	2.781E+06	9.0 ± 9.2
2	2	13	6	0.154	23.3	3.370E+05	2.191E+06	30.5 ± 23.2
3	2	10	8	0.200	13.4	2.528E+05	1.264E+06	39.6 ± 30.7
4	23	53	20	0.434	28.5	1.163E+06	2.679E+06	85.6 ± 21.5
5	1	9	6	0.111	16.1	1.685E+05	1.517E+06	22.0 ± 23.2
6	16	41	28	0.390	15.8	5.778E+05	1.481E+06	77.0 ± 22.8
7	2	34	24	0.059	15.2	8.426E+04	1.432E+06	11.7 ± 8.5
8	1	21	18	0.048	12.6	5.617E+04	1.180E+06	9.4 ± 9.7
9	1	26	18	0.038	15.5	5.617E+04	1.461E+06	7.6 ± 7.8
10	3	21	10	0.143	22.6	3.033E+05	2.123E+06	28.3 ± 17.5
11	1	6	12	0.167	5.4	8.426E+04	5.056E+05	33.0 ± 35.7
12	6	101	12	0.059	90.6	5.056E+05	8.510E+06	11.8 ± 5.0
13	0	1	16	0.000	0.7	0.000E+00	6.320E+04	0.0 ± 0.0
14	0	16	6	0.000	28.7	0.000E+00	2.696E+06	0.0 ± 0.0
15	0	2	6	0.000	3.6	0.000E+00	3.370E+05	0.0 ± 0.0
16	1	30	18	0.033	17.9	5.617E+04	1.685E+06	6.6 ± 6.7
17	0	1	24	0.000	0.4	0.000E+00	4.213E+04	0.0 ± 0.0
18	1	23	12	0.043	20.6	8.426E+04	1.938E+06	8.6 ± 8.8
19	0	25	30	0.000	9.0	0.000E+00	8.426E+05	0.0 ± 0.0
20	1	64	12	0.016	57.4	8.426E+04	5.393E+06	3.1 ± 3.1
	62	519			19.0	2.132E+05	1.785E+06	

Area of basic unit = 9.89E-07 cm-2

CHI SQUARED = 35.22827 WITH 19 DEGREES OF FREEDOM
P(chi squared) = 0.000 %
CORRELATION COEFFICIENT = 0.460
VARIANCE OF SQR(Ns) = 1.589345
VARIANCE OF SQR(Ni) = 5.320508

Ns/Ni = 0.119 ± 0.016
MEAN RATIO = 0.097 ± 0.028

Pooled Age = 23.7 ± 3.2 Ma
Mean Age = 19.2 ± 5.5 Ma
Central Age = 20.0 ± 5.8Ma
% Rel. Error = 99.37
Ages calculated using a zeta of 348.4 ± 5.8 for SRM 612 glass
RHO D = 1.156E+06cm-2; ND = 2859

9414-12 APATITE Apatite

IRRADIATION wk140
SLIDE NUMBER 13
COUNTED BY: Kao

No.	Ns	Ni	Na	RATIO	U (ppm)	RHOs (E+06)	RHOi (E+06)	F.T.AGE (Ma)
1	3	33	8	0.091	47.3	0.379	4.171	18.0 ± 10.9
2	0	4	8	0.000	5.7	0.000	0.506	0.0 ± 0.0
3	4	29	40	0.138	8.3	0.101	0.733	27.3 ± 14.6
4	2	16	8	0.125	22.9	0.253	2.022	24.8 ± 18.6
	9	82			14.7	0.142	1.296	

AREA OF BASIC UNIT = 9.89E-07 cm
CHI SQUARED = .7513584 WITH 3 DEGREES OF FREEDOM
P(chi squared) = 86.1 %
CORRELATION COEFFICIENT = 0.926
VARIANCE OF SQR(Ns) = 0.79
VARIANCE OF SQR(Ni) = 2.88

Ns/Ni = 0.110 ± 0.039
MEAN RATIO = 0.088 ± 0.031

Ages calculated using a zeta of 348.4 ± 5.8 for SRM612 glass
RHO D = 1.156E+06 ; ND = 2859

POOLED AGE = 21.8 ± 7.7 Ma
MEAN AGE = 17.5 ± 6.2 Ma

9414-13 APATITE Apatite

IRRADIATION WK140
SLIDE NUMBER 14
COUNTED BY: Kao

No.	Ns	Ni	Na	RATIO	U (ppm)	RHOs (E+06)	RHOi (E+06)	F.T.AGE (Ma)
1	3	83	16	0.036	59.4	0.190	5.245	7.2 ± 4.2
2	1	37	8	0.027	53.0	0.126	4.676	5.4 ± 5.4
3	0	27	8	0.000	38.7	0.000	3.413	0.0 ± 0.0
	4	147			52.6	0.126	4.645	

AREA OF BASIC UNIT = 9.89E-07 cm
CHI SQUARED = .9696894 WITH 2 DEGREES OF FREEDOM
P(chi squared) = 61.6 %
CORRELATION COEFFICIENT = 0.986
VARIANCE OF SQR(Ns) = 0.76
VARIANCE OF SQR(Ni) = 4.21

Ns/Ni = 0.027 ± 0.014
MEAN RATIO = 0.021 ± 0.011

Ages calculated using a zeta of 348.4 ± 5.8 for SRM612 glass
RHO D = 1.156E+06 ; ND = 2859

POOLED AGE = 5.4 ± 2.7 Ma
MEAN AGE = 4.2 ± 2.2 Ma

9414-14 APATITE MARLBOROUGH

IRRADIATION WK140
SLIDE NUMBER 14
COUNTED BY: KAO

No.	Ns	Ni	Na	RATIO	U (ppm)	RHOs (E+06)	RHOi (E+06)	F.T.AGE (Ma)
1	3	20	4	0.150	59.1	0.758	5.056	29.2 ± 18.1
2	1	3	4	0.333	8.9	0.253	0.758	64.7 ± 74.7
	4	23			34.0	0.506	2.907	

AREA OF BASIC UNIT = 9.89E-07 cm
CHI SQUARED = .3859876 WITH 1 DEGREES OF FREEDOM
P(chi squared) = 53.4 %
CORRELATION COEFFICIENT = 1.000
VARIANCE OF SQR(Ns) = 0.27
VARIANCE OF SQR(Ni) = 3.75

Ns/Ni = 0.174 ± 0.094
MEAN RATIO = 0.242 ± 0.092

Ages calculated using a zeta of 348.4 ± 5.8 for SRM612 glass
RHO D = 1.120E+06 ; ND = 2768

POOLED AGE = 33.8 ± 18.4 Ma
MEAN AGE = 47.0 ± 17.9 Ma

9414-19 APATITE MARLBOROUGH

IRRADIATION WK140-19
SLIDE NUMBER 19
COUNTED BY: KAO

No.	Ns	Ni	Na	RATIO	U (ppm)	RHOs (E+06)	RHOi (E+06)	F.T.AGE (Ma)
1	1	32	12	0.031	31.5	0.084	2.696	6.1 ± 6.2
2	1	35	6	0.029	69.0	0.169	5.898	5.6 ± 5.7
3	0	6	6	0.000	11.8	0.000	1.011	0.0 ± 0.0
4	0	7	4	0.000	20.7	0.000	1.769	0.0 ± 0.0
5	0	8	4	0.000	23.7	0.000	2.022	0.0 ± 0.0
6	0	8	6	0.000	15.8	0.000	1.348	0.0 ± 0.0
7	0	54	9	0.000	71.0	0.000	6.067	0.0 ± 0.0
8	0	6	8	0.000	8.9	0.000	0.758	0.0 ± 0.0
9	0	11	10	0.000	13.0	0.000	1.112	0.0 ± 0.0
10	0	20	12	0.000	19.7	0.000	1.685	0.0 ± 0.0
	2	187			28.7	0.026	2.456	

AREA OF BASIC UNIT = 9.89E-07 cm
CHI SQUARED = 3.525948 WITH 9 DEGREES OF FREEDOM
P(chi squared) = 94.0 %
CORRELATION COEFFICIENT = 0.474
VARIANCE OF SQR(Ns) = 0.18
VARIANCE OF SQR(Ni) = 3.08

Ns/Ni = 0.011 ± 0.008
MEAN RATIO = 0.006 ± 0.004

Ages calculated using a zeta of 348.4 ± 5.8 for SRM612 glass
RHO D = 1.120E+06 ; ND = 2768

POOLED AGE = 2.1 ± 1.5 Ma
MEAN AGE = 1.2 ± 0.8 Ma

9414-20 APATITE MARLBOROUGH

IRRADIATION WK140-20
SLIDE NUMBER 20
COUNTED BY: KAO

No.	Ns	Ni	Na	RATIO	U (ppm)	RHOs (E+06)	RHOi (E+06)	F.T.AGE (Ma)
1	2	43	12	0.047	42.4	0.169	3.623	9.1 ± 6.6
2	1	45	6	0.022	88.7	0.169	7.583	4.3 ± 4.4
3	2	45	9	0.044	59.1	0.225	5.056	8.7 ± 6.3
4	1	22	4	0.045	65.0	0.253	5.561	8.9 ± 9.1
5	0	4	4	0.000	11.8	0.000	1.011	0.0 ± 0.0
6	0	9	6	0.000	17.7	0.000	1.517	0.0 ± 0.0
7	0	5	6	0.000	9.9	0.000	0.843	0.0 ± 0.0
8	0	46	9	0.000	60.4	0.000	5.168	0.0 ± 0.0
9	0	3	4	0.000	8.9	0.000	0.758	0.0 ± 0.0
	6	222			43.8	0.101	3.741	

AREA OF BASIC UNIT = 9.89E-07 cm
CHI SQUARED = 3.173596 WITH 8 DEGREES OF FREEDOM
P(chi squared) = 92.3 %
CORRELATION COEFFICIENT = 0.691
VARIANCE OF SQR(Ns) = 0.43
VARIANCE OF SQR(Ni) = 5.06

Ns/Ni = 0.027 ± 0.011
MEAN RATIO = 0.018 ± 0.007

Ages calculated using a zeta of 348.4 ± 5.8 for SRM612 glass
RHO D = 1.120E+06 ; ND = 2768

POOLED AGE = 5.3 ± 2.2 Ma
MEAN AGE = 3.4 ± 1.4 Ma

9414-21 APATITE MARLBOROUGH

IRRADIATION WK141-1
SLIDE NUMBER 1
COUNTED BY: KAO

No.	Ns	Ni	Na	RATIO	U (ppm)	RHOs (E+06)	RHOi (E+06)	F.T.AGE (Ma)
1	1	18	4	0.056	47.5	0.253	4.550	12.1 ± 12.5
2	0	5	6	0.000	8.8	0.000	0.843	0.0 ± 0.0
	1	23			24.3	0.101	2.326	

AREA OF BASIC UNIT = 9.89E-07 cm
CHI SQUARED = .2745996 WITH 1 DEGREES OF FREEDOM
P(chi squared) = 60.0 %
CORRELATION COEFFICIENT = 1.000
VARIANCE OF SQR(Ns) = 0.50
VARIANCE OF SQR(Ni) = 2.01

Ns/Ni = 0.043 ± 0.044
MEAN RATIO = 0.028 ± 0.028

Ages calculated using a zeta of 348.4 ± 5.8 for SRM612 glass
RHO D = 1.256E+06 ; ND = 3105

POOLED AGE = 9.5 ± 9.7 Ma
MEAN AGE = 6.1 ± 6.1 Ma

9414-23 Apatite

IRRADIATION wk141-03 COUNTED BY: Kao

No.	Ns	Ni	Na	RATIO	U(ppm)	RHOs	RHOi	F.T.AGE(Ma)
1	4	188	40	0.021	50.9	1.054E+05	4.953E+06	4.4 ± 2.2
2	0	3	12	0.000	2.7	0.000E+00	2.634E+05	0.0 ± 0.0
3	1	12	16	0.083	8.1	6.586E+04	7.903E+05	17.1 ± 17.8
4	0	1	12	0.000	0.9	0.000E+00	8.781E+04	0.0 ± 0.0
5	1	31	18	0.032	18.7	5.854E+04	1.815E+06	6.6 ± 6.7
6	5	249	36	0.020	75.0	1.464E+05	7.288E+06	4.1 ± 1.9
7	1	51	24	0.020	23.0	4.391E+04	2.239E+06	4.0 ± 4.1
8	2	185	32	0.011	62.7	6.586E+04	6.092E+06	2.2 ± 1.6
9	0	6	18	0.000	3.6	0.000E+00	3.512E+05	0.0 ± 0.0
10	1	57	9	0.018	68.6	1.171E+05	6.674E+06	3.6 ± 3.6
11	0	38	12	0.000	34.3	0.000E+00	3.337E+06	0.0 ± 0.0
	15	821			38.9	6.902E+04	3.778E+06	

Area of basic unit = 9.49E-07 cm-2

CHI SQUARED = 2.231909 WITH 10 DEGREES OF FREEDOM
P(chi squared) = 92.4 %
CORRELATION COEFFICIENT = 0.933
VARIANCE OF SQR(Ns) = .6533826
VARIANCE OF SQR(Ni) = 26.5615

Ns/Ni = 0.018 ± 0.005
MEAN RATIO = 0.019 ± 0.007

Pooled Age = 3.8 ± 1.0 Ma
Mean Age = 3.8 ± 1.5 Ma
Central Age = 3.8 ± 1.0Ma
% Rel. Error = 0.00
Ages calculated using a zeta of 348.4 ± 5.8 for SRM 612 glass
RHO D = 1.196E+06cm-2; ND = 2958

9414-25 APATITE MARLBOROUGH

IRRADIATION FT:WK141
SLIDE NUMBER 5
COUNTED BY: KAO

No.	Ns	Ni	Na	RATIO	U (ppm)	RHOs (E+06)	RHOI (E+06)	F.T.AGE (Ma)
1	1	19	4	0.053	48.7	0.253	4.803	11.8 ± 12.1
2	1	10	4	0.100	25.6	0.253	2.528	22.4 ± 23.6
3	1	20	4	0.050	51.3	0.253	5.056	11.2 ± 11.5
4	0	36	9	0.000	41.0	0.000	4.044	0.0 ± 0.0
	3	85			41.5	0.144	4.093	

AREA OF BASIC UNIT = 9.89E-07 cm
CHI SQUARED = 2.619458 WITH 3 DEGREES OF FREEDOM
P(chi squared) = 45.4 %
CORRELATION COEFFICIENT = -0.909
VARIANCE OF SQR(Ns) = 0.25
VARIANCE OF SQR(Ni) = 1.35

Ns/Ni = 0.035 ± 0.021
MEAN RATIO = 0.051 ± 0.020

Ages calculated using a zeta of 348.4 ± 5.8 for SRM612 glass
RHO D = 1.291E+06 ; ND = 3193

POOLED AGE = 7.9 ± 4.7 Ma
MEAN AGE = 11.4 ± 4.6 Ma

9414-31 Apatite

IRRADIATION Wk141-9 COUNTED BY: Kao

No.	Ns	Ni	Na	RATIO	U(ppm)	RHOs	RHOi	F.T.AGE(Ma)
1	0	52	16	0.000	32.3	0.000E+00	3.286E+06	0.0 ± 0.0
2	12	107	25	0.112	42.5	4.853E+05	4.328E+06	24.1 ± 7.3
3	0	13	6	0.000	21.5	0.000E+00	2.191E+06	0.0 ± 0.0
4	38	250	48	0.152	51.8	8.005E+05	5.266E+06	32.6 ± 5.7
5	11	56	16	0.196	34.8	6.951E+05	3.539E+06	42.1 ± 13.9
6	5	68	16	0.074	42.3	3.160E+05	4.297E+06	15.8 ± 7.3
7	8	37	9	0.216	40.9	8.988E+05	4.157E+06	46.3 ± 18.1
	74	583			42.6	5.502E+05	4.334E+06	

Area of basic unit = 9.89E-07 cm-2

CHI SQUARED = 7.302752 WITH 6 DEGREES OF FREEDOM
P(chi squared) = 2.4 %
CORRELATION COEFFICIENT = 0.953
VARIANCE OF SQR(Ns) = 4.610788
VARIANCE OF SQR(Ni) = 14.8903

Ns/Ni = 0.127 ± 0.016
MEAN RATIO = 0.107 ± 0.033

Pooled Age = 27.2 ± 3.4 Ma
Mean Age = 23.0 ± 7.1 Ma
Central Age = 24.7 ± 5.5Ma
% Rel. Error = 42.93
Ages calculated using a zeta of 348.4 ± 5.8 for SRM 612 glass
RHO D = 1.251E+06cm-2; ND = 3093

9414-33 APATITE Apatite

IRRADIATION WK141
SLIDE NUMBER 9
COUNTED BY: Kao

No.	Ns	Ni	Na	RATIO	U (ppm)	RHOs (E+06)	RHOi (E+06)	F.T.AGE (Ma)
1	0	4	18	0.000	2.4	0.000	0.225	0.0 ± 0.0
2	2	25	24	0.080	11.0	0.084	1.053	17.2 ± 12.6
3	0	19	8	0.000	25.1	0.000	2.401	0.0 ± 0.0
4	3	35	16	0.086	23.2	0.190	2.212	18.4 ± 11.1
5	1	17	16	0.059	11.2	0.063	1.074	12.6 ± 13.0
6	0	37	36	0.000	10.9	0.000	1.039	0.0 ± 0.0
7	0	16	12	0.000	14.1	0.000	1.348	0.0 ± 0.0
8	5	90	32	0.056	29.8	0.158	2.844	11.9 ± 5.5
	11	243			15.9	0.069	1.517	

AREA OF BASIC UNIT = 9.89E-07 cm
CHI SQUARED = 5.486774 WITH 7 DEGREES OF FREEDOM
P(chi squared) = 60.1 %
CORRELATION COEFFICIENT = 0.845
VARIANCE OF SQR(Ns) = 0.84
VARIANCE OF SQR(Ni) = 4.74

Ns/Ni = 0.045 ± 0.014
MEAN RATIO = 0.035 ± 0.014

Ages calculated using a zeta of 348.4 ± 5.8 for SRM612 glass
RHO D = 1.251E+06 ; ND = 3093

POOLED AGE = 9.7 ± 3.0 Ma
MEAN AGE = 7.5 ± 2.9 Ma

9414-34 APATITE MARLBOROUGH

IRRADIATION WK141-10
SLIDE NUMBER 10
COUNTED BY: KAO

No.	Ns	Ni	Na	RATIO	U (ppm)	RHOs (E+06)	RHOi (E+06)	F.T.AGE (Ma)
1	1	27	4	0.037	67.0	0.253	6.825	8.6 ± 8.8
2	3	18	8	0.167	22.3	0.379	2.275	38.6 ± 24.1
3	3	36	8	0.083	44.6	0.379	4.550	19.4 ± 11.6
4	3	22	4	0.136	54.6	0.758	5.561	31.6 ± 19.5
5	2	13	4	0.154	32.2	0.506	3.286	35.7 ± 27.1
	12	116			41.1	0.433	4.189	

AREA OF BASIC UNIT = 9.89E-07 cm
CHI SQUARED = 2.315435 WITH 4 DEGREES OF FREEDOM
P(chi squared) = 67.8 %
CORRELATION COEFFICIENT = 0.082
VARIANCE OF SQR(Ns) = 0.10
VARIANCE OF SQR(Ni) = 0.83

Ns/Ni = 0.103 ± 0.031
MEAN RATIO = 0.115 ± 0.024

Ages calculated using a zeta of 348.4 ± 5.8 for SRM612 glass
RHO D = 1.335E+06 ; ND = 3303

POOLED AGE = 24.0 ± 7.3 Ma
MEAN AGE = 26.8 ± 5.7 Ma

9414-35 APATITE MARLBOROUGH

IRRADIATION WK141-11
SLIDE NUMBER 11
COUNTED BY: KAO

No.	Ns	Ni	Na	RATIO	U (ppm)	RHOs (E+06)	RHOi (E+06)	F.T.AGE (Ma)
1	8	42	9	0.190	46.0	0.899	4.719	44.4 ± 17.2
2	5	45	18	0.111	24.6	0.281	2.528	26.0 ± 12.3
3	3	15	6	0.200	24.6	0.506	2.528	46.7 ± 29.5
4	3	53	9	0.057	58.0	0.337	5.954	13.2 ± 7.9
5	9	34	6	0.265	55.8	1.517	5.730	61.7 ± 23.2
6	3	21	9	0.143	23.0	0.337	2.359	33.4 ± 20.6
7	9	39	24	0.231	16.0	0.379	1.643	53.8 ± 19.9
8	34	260	70	0.131	36.6	0.491	3.756	30.5 ± 5.6
9	0	9	5	0.000	17.7	0.000	1.820	0.0 ± 0.0
10	2	14	8	0.143	17.2	0.253	1.769	33.4 ± 25.2
	76	532			32.0	0.469	3.280	

AREA OF BASIC UNIT = 9.89E-07 cm
CHI SQUARED = 9.772872 WITH 9 DEGREES OF FREEDOM
P(chi squared) = 36.9 %
CORRELATION COEFFICIENT = 0.967
VARIANCE OF SQR(Ns) = 2.31
VARIANCE OF SQR(Ni) = 13.79

Ns/Ni = 0.143 ± 0.018
MEAN RATIO = 0.147 ± 0.025

Ages calculated using a zeta of 348.4 ± 5.8 for SRM612 glass
RHO D = 1.344E+06 ; ND = 3325

POOLED AGE = 33.4 ± 4.2 Ma
MEAN AGE = 34.3 ± 5.9 Ma

9414-36 APATITE MARLBOROUGH

IRRADIATION WK141-12
SLIDE NUMBER 12
COUNTED BY: KAO

No.	Ns	Ni	Na	RATIO	U (ppm)	RHOs (E+06)	RHOi (E+06)	F.T.AGE (Ma)
1	4	22	18	0.182	12.0	0.225	1.236	42.7 ± 23.2
2	2	12	4	0.167	29.4	0.506	3.033	39.2 ± 29.9
3	3	6	4	0.500	14.7	0.758	1.517	116.8 ± 82.6
4	1	5	4	0.200	12.2	0.253	1.264	47.0 ± 51.5
5	1	5	4	0.200	12.2	0.253	1.264	47.0 ± 51.5
	11	50			14.4	0.327	1.487	

AREA OF BASIC UNIT = 9.89E-07 cm
CHI SQUARED = 1.69695 WITH 4 DEGREES OF FREEDOM
P(chi squared) = 79.1 %
CORRELATION COEFFICIENT = 0.786
VARIANCE OF SQR(Ns) = 0.20
VARIANCE OF SQR(Ni) = 1.14

Ns/Ni = 0.220 ± 0.073
MEAN RATIO = 0.250 ± 0.063

Ages calculated using a zeta of 348.4 ± 5.8 for SRM612 glass
RHO D = 1.353E+06 ; ND = 3347

POOLED AGE = 51.6 ± 17.2 Ma
MEAN AGE = 58.6 ± 14.8 Ma

9414-37 APATITE MARLBOROUGH

IRRADIATION WK141-13
SLIDE NUMBER 3
COUNTED BY: KAO

No.	Ns	Ni	Na	RATIO	U (ppm)	RHOs (E+06)	RHOi (E+06)	F.T.AGE (Ma)
1	3	5	4	0.600	12.2	0.758	1.264	140.8 ± 102.9
2	2	18	6	0.111	29.2	0.337	3.033	26.3 ± 19.6
3	2	17	4	0.118	41.3	0.506	4.297	27.9 ± 20.8
	7	40			27.8	0.506	2.889	

AREA OF BASIC UNIT = 9.89E-07 cm
CHI SQUARED = 3.889206 WITH 2 DEGREES OF FREEDOM
P(chi squared) = 14.3 %
CORRELATION COEFFICIENT = -0.998
VARIANCE OF SQR(Ns) = 0.03
VARIANCE OF SQR(Ni) = 1.27

Ns/Ni = 0.175 ± 0.072
MEAN RATIO = 0.276 ± 0.162

Ages calculated using a zeta of 348.4 ± 5.8 for SRM612 glass
RHO D = 1.362E+06 ; ND = 3369

POOLED AGE = 41.4 ± 17.0 Ma
MEAN AGE = 65.2 ± 38.2 Ma

9414-38 Apatite

IRRADIATION wk141-14 COUNTED BY: Kao

No.	Ns	Ni	Na	RATIO	U(ppm)	RHOs	RHOi	F.T.AGE(Ma)
1	2	11	6	0.182	18.3	3.512E+05	1.932E+06	40.4 ± 31.0
2	15	32	24	0.469	13.3	6.586E+05	1.405E+06	103.6 ± 32.5
3	25	40	18	0.625	22.2	1.464E+06	2.342E+06	137.7 ± 35.2
4	13	47	16	0.277	29.4	8.562E+05	3.095E+06	61.3 ± 19.3
5	2	86	20	0.023	43.0	1.054E+05	4.531E+06	5.2 ± 3.7
	57	216			25.7	7.150E+05	2.710E+06	

Area of basic unit = 9.49E-07 cm-2

CHI SQUARED = 17.16532 WITH 4 DEGREES OF FREEDOM
P(chi squared) = 0.000 %
CORRELATION COEFFICIENT = -0.166
VARIANCE OF SQR(Ns) = 2.534847
VARIANCE OF SQR(Ni) = 4.616219

Ns/Ni = 0.264 ± 0.039
MEAN RATIO = 0.315 ± 0.106

Pooled Age = 58.5 ± 8.8 Ma
Mean Age = 69.8 ± 23.5 Ma
Central Age = 63.2 ± 22.4Ma
% Rel. Error = 70.57
Ages calculated using a zeta of 348.4 ± 5.8 for SRM 612 glass
RHO D = 1.297E+06cm-2; ND = 3206

9414-39 APATITE Apatite

IRRADIATION wk141
SLIDE NUMBER 15
COUNTED BY: Kao

No.	Ns	Ni	Na	RATIO	U (ppm)	RHOs (E+06)	RHOi (E+06)	F.T.AGE (Ma)
1	4	9	32	0.444	2.9	0.126	0.284	98.9 ± 59.5
2	3	6	24	0.500	2.5	0.126	0.253	111.2 ± 78.7
3	7	22	8	0.318	27.9	0.885	2.781	71.0 ± 30.8
4	5	6	12	0.833	5.1	0.421	0.506	184.3 ± 111.6
5	74	136	20	0.544	69.0	3.741	6.876	120.9 ± 17.7
6	1	2	30	0.500	0.7	0.034	0.067	111.2 ± 136.2
7	9	17	12	0.529	14.4	0.758	1.432	117.7 ± 48.6
8	4	10	16	0.400	6.3	0.253	0.632	89.1 ± 52.8
9	4	10	8	0.400	12.7	0.506	1.264	89.1 ± 52.8
	111	218			13.6	0.693	1.361	

AREA OF BASIC UNIT = 9.89E-07 cm
CHI SQUARED = 2.477789 WITH 8 DEGREES OF FREEDOM
P(chi squared) = 96.3 %
CORRELATION COEFFICIENT = 0.997
VARIANCE OF SQR(Ns) = 5.04
VARIANCE OF SQR(Ni) = 9.14

Ns/Ni = 0.509 ± 0.059
MEAN RATIO = 0.497 ± 0.049

Ages calculated using a zeta of 348.4 ± 5.8 for SRM612 glass
RHO D = 1.306E+06 ; ND = 3229

POOLED AGE = 113.2 ± 13.4 Ma
MEAN AGE = 110.4 ± 11.1 Ma

9414-40 APATITE Apatite

IRRADIATION WK141
SLIDE NUMBER 16
COUNTED BY: Kao

No.	Ns	Ni	Na	RATIO	U (ppm)	RHOs (E+06)	RHOi (E+06)	F.T.AGE (Ma)
1	3	13	9	0.231	14.5	0.337	1.461	51.9 ± 33.3
2	3	14	25	0.214	5.6	0.121	0.566	48.2 ± 30.7
3	1	6	16	0.167	3.8	0.063	0.379	37.5 ± 40.5
4	15	44	12	0.341	36.9	1.264	3.707	76.5 ± 22.9
5	1	25	18	0.040	14.0	0.056	1.404	9.0 ± 9.2
6	1	6	12	0.167	5.0	0.084	0.506	37.5 ± 40.5
7	4	7	16	0.571	4.4	0.253	0.442	127.8 ± 80.1
8	5	9	12	0.556	7.6	0.421	0.758	124.3 ± 69.4
9	6	16	30	0.375	5.4	0.202	0.539	84.1 ± 40.3
10	1	5	12	0.200	4.2	0.084	0.421	45.0 ± 49.3
11	7	20	12	-0.350	16.8	0.590	1.685	78.6 ± 34.5
12	1	22	60	0.045	3.7	0.017	0.371	10.3 ± 10.5
	48	187			8.0	0.207	0.808	

AREA OF BASIC UNIT = 9.89E-07 cm
CHI SQUARED = 14.31675 WITH 11 DEGREES OF FREEDOM
P(chi squared) = 21.6 %
CORRELATION COEFFICIENT = 0.731
VARIANCE OF SQR(Ns) = 0.81
VARIANCE OF SQR(Ni) = 1.71

Ns/Ni = 0.257 ± 0.042
MEAN RATIO = 0.271 ± 0.050

Ages calculated using a zeta of 348.4 ± 5.8 for SRM612 glass
RHO D = 1.315E+06 ; ND = 3251

POOLED AGE = 57.7 ± 9.4 Ma
MEAN AGE = 61.0 ± 11.3 Ma

9414-41 APATITE Marlborough

IRRADIATION FT:wk141
SLIDE NUMBER 17
COUNTED BY: Kao

No.	Ns	Ni	Na	RATIO	U (ppm)	RHOs (E+06)	RHOi (E+06)	F.T.AGE (Ma)
1	2	6	4	0.333	14.1	0.506	1.517	81.1 ± 66.3
2	8	15	14	0.533	10.1	0.578	1.083	129.3 ± 56.7
3	12	28	12	0.429	22.0	1.011	2.359	104.1 ± 36.0
4	7	15	4	0.467	35.3	1.769	3.792	113.3 ± 51.9
5	17	50	24	0.340	19.6	0.716	2.106	82.7 ± 23.3
6	8	21	4	0.381	49.5	2.022	5.308	92.6 ± 38.6
7	9	18	9	0.500	18.8	1.011	2.022	121.3 ± 49.6
8	3	8	9	0.375	8.4	0.337	0.899	91.2 ± 61.8
9	4	10	9	0.400	10.5	0.449	1.123	97.2 ± 57.6
10	4	9	4	0.444	21.2	1.011	2.275	107.9 ± 64.9
11	3	8	4	0.375	18.8	0.758	2.022	91.2 ± 61.8
12	6	12	9	0.500	12.6	0.674	1.348	121.3 ± 60.7
13	10	21	9	0.476	22.0	1.123	2.359	115.6 ± 44.5
14	13	31	4	0.419	73.0	3.286	7.836	101.9 ± 33.8
15	4	10	4	0.400	23.6	1.011	2.528	97.2 ± 57.6
16	9	21	9	0.429	22.0	1.011	2.359	104.1 ± 41.6
17	11	26	6	0.423	40.8	1.854	4.382	102.8 ± 37.1
18	18	41	16	0.439	24.1	1.138	2.591	106.6 ± 30.3
	148	350			21.4	0.972	2.298	

AREA OF BASIC UNIT = 9.89E-07 cm
CHI SQUARED = 1.568617 WITH 17 DEGREES OF FREEDOM
P(chi squared) = 100.0 %
CORRELATION COEFFICIENT = 0.971
VARIANCE OF SQR(Ns) = 0.68
VARIANCE OF SQR(Ni) = 1.68

Ns/Ni = 0.423 ± 0.041
MEAN RATIO = 0.426 ± 0.013

Ages calculated using a zeta of 348.4 ± 5.8 for SRM612 glass
RHO D = 1.406E+06 ; ND = 3479

POOLED AGE = 102.7 ± 10.4 Ma
MEAN AGE = 103.4 ± 4.0 Ma

9414-42 APATITE Apatite

IRRADIATION WK141
SLIDE NUMBER 18
COUNTED BY: Kao

No.	Ns	Ni	Na	RATIO	U (ppm)	RHOs (E+06)	RHOi (E+06)	F.T.AGE (Ma)
1	3	4	6	0.750	6.6	0.506	0.674	169.5 ± 129.5
2	11	51	12	0.216	42.2	0.927	4.297	49.2 ± 16.4
3	11	41	8	0.268	50.9	1.390	5.182	61.1 ± 20.8
4	10	15	18	0.667	8.3	0.562	0.843	150.8 ± 61.7
5	8	9	12	0.889	7.5	0.674	0.758	200.4 ± 97.5
6	10	31	16	0.323	19.3	0.632	1.959	73.4 ± 26.8
7	19	37	50	0.514	7.4	0.384	0.748	116.5 ± 33.0
8	49	115	16	0.426	71.4	3.097	7.267	96.8 ± 16.7
9	13	22	12	0.591	18.2	1.095	1.854	133.9 ± 46.9
10	5	9	8	0.556	11.2	0.632	1.138	126.0 ± 70.3
	139	334			21.0	0.890	2.137	

AREA OF BASIC UNIT = 9.89E-07 cm
CHI SQUARED = 12.63148 WITH 9 DEGREES OF FREEDOM
P(chi squared) = 18.0 %
CORRELATION COEFFICIENT = 0.934
VARIANCE OF SQR(Ns) = 2.05
VARIANCE OF SQR(Ni) = 6.51

Ns/Ni = 0.416 ± 0.042
MEAN RATIO = 0.520 ± 0.068

Ages calculated using a zeta of $\overline{348.4} \pm \overline{5.8}$ for SRM612 glass
RHO D = 1.333E+06 ; ND = 3296

POOLED AGE = 94.6 ± 9.8 Ma
MEAN AGE = 117.9 ± 15.7 Ma

9414-43 APATITE Apatite

IRRADIATION WK141
SLIDE NUMBER 19
COUNTED BY: Kao

No.	Ns	Ni	Na	RATIO	U (ppm)	RHOs (E+06)	RHOi (E+06)	F.T.AGE (Ma)
1	9	31	8	0.290	38.2	1.138	3.918	66.6 ± 25.2
2	28	86	12	0.326	70.7	2.359	7.246	74.6 ± 16.3
3	5	16	9	0.312	17.5	0.562	1.798	71.6 ± 36.7
4	6	8	12	0.750	6.6	0.506	0.674	170.6 ± 92.2
5	50	81	25	0.617	32.0	2.022	3.276	140.7 ± 25.5
6	2	5	6	0.400	8.2	0.337	0.843	91.5 ± 76.6
7	55	97	16	0.567	59.8	3.476	6.130	129.4 ± 22.0
8	23	57	24	0.404	23.4	0.969	2.401	92.3 ± 22.9
9	7	13	24	0.538	5.3	0.295	0.548	122.9 ± 57.7
10	11	38	16	0.289	23.4	0.695	2.401	66.4 ± 22.8
11	28	71	12	0.394	58.4	2.359	5.982	90.3 ± 20.2
12	1	16	16	0.062	9.9	0.063	1.011	14.4 ± 14.8
13	105	222	30	0.473	73.0	3.539	7.482	108.1 ± 13.0
14	4	9	16	0.444	5.6	0.253	0.569	101.6 ± 61.1
15	23	62	24	0.371	25.5	0.969	2.612	84.9 ± 20.8
16	15	32	6	0.469	52.6	2.528	5.393	107.1 ± 33.6
17	3	3	6	1.000	4.9	0.506	0.506	226.5 ± 185.0
18	10	12	6	0.833	19.7	1.685	2.022	189.3 ± 81.1
19	0	2	4	0.000	4.9	0.000	0.506	0.0 ± 0.0
20	15	52	18	0.288	28.5	0.843	2.921	66.1 ± 19.4
	400	913			31.1	1.395	3.183	

AREA OF BASIC UNIT = 9.89E-07 cm
CHI SQUARED = 24.70377 WITH 19 DEGREES OF FREEDOM
P(chi squared) = 17.1 %
CORRELATION COEFFICIENT = 0.972
VARIANCE OF SQR(Ns) = 6.01
VARIANCE OF SQR(Ni) = 11.56

Ns/Ni = 0.438 ± 0.026
MEAN RATIO = 0.441 ± 0.053

Ages calculated using a zeta of 348.4 ± 5.8 for SRM612 glass
RHO D = 1.342E+06 ; ND = 3319

POOLED AGE = 100.2 ± 6.4 Ma
MEAN AGE = 101.0 ± 12.3 Ma

9414-44 APATITE Apatite

IRRADIATION FT:wk141
SLIDE NUMBER 20
COUNTED BY: Kao

No.	Ns	Ni	Na	RATIO	U (ppm)	RHOs (E+06)	RHOi (E+06)	F.T.AGE (Ma)
1	8	17	9	0.471	18.5	0.899	1.910	108.3 ± 46.5
2	10	19	9	0.526	20.7	1.123	2.135	121.0 ± 47.3
3	4	8	12	0.500	6.5	0.337	0.674	115.0 ± 70.5
4	95	184	36	0.516	50.1	2.668	5.168	118.7 ± 15.2
5	3	12	24	0.250	4.9	0.126	0.506	57.7 ± 37.3
6	3	8	16	0.375	4.9	0.190	0.506	86.4 ± 58.5
7	54	69	24	0.783	28.2	2.275	2.907	179.1 ± 32.8
	177	317			23.9	1.377	2.466	

AREA OF BASIC UNIT = 9.89E-07 cm
CHI SQUARED = 6.070564 WITH 6 DEGREES OF FREEDOM
P(chi squared) = 41.5 %
CORRELATION COEFFICIENT = 0.980
VARIANCE OF SQR(Ns) = 10.09
VARIANCE OF SQR(Ni) = 15.73

Ns/Ni = 0.558 ± 0.052
MEAN RATIO = 0.489 ± 0.062

Ages calculated using a zeta of 348.4 ± 5.8 for SRM612 glass
RHO D = 1.351E+06 ; ND = 3341

POOLED AGE = 128.3 ± 12.4 Ma
MEAN AGE = 112.4 ± 14.4 Ma

9414-45 APATITE Apatite

IRRADIATION wk142
SLIDE NUMBER 1
COUNTED BY: Kao

No.	Ns	Ni	Na	RATIO	U (ppm)	RHOs (E+06)	RHOi (E+06)	F.T.AGE (Ma)
1	17	25	36	0.680	7.9	0.477	0.702	135.2 ± 42.6
2	24	51	16	0.471	36.1	1.517	3.223	93.9 ± 23.3
3	115	187	24	0.615	88.2	4.845	7.878	122.4 ± 14.8
4	1	4	12	0.250	3.8	0.084	0.337	50.0 ± 56.0
5	9	22	6	0.409	41.5	1.517	3.707	81.7 ± 32.4
6	4	8	8	0.500	11.3	0.506	1.011	99.7 ± 61.1
7	16	31	8	0.516	43.9	2.022	3.918	102.9 ± 31.8
8	1	3	12	0.333	2.8	0.084	0.253	66.6 ± 77.0
9	6	13	24	0.462	6.1	0.253	0.548	92.1 ± 45.5
10	5	18	12	0.278	17.0	0.421	1.517	55.6 ± 28.1
11	46	76	12	0.605	71.7	3.876	6.404	120.5 ± 22.7
12	41	71	20	0.577	40.2	2.073	3.589	115.0 ± 22.7
13	3	7	12	0.429	6.6	0.253	0.590	85.6 ± 59.1
14	6	8	12	0.750	7.5	0.506	0.674	149.0 ± 80.5
15	32	67	24	0.478	31.6	1.348	2.823	95.3 ± 20.6
16	31	54	12	0.574	50.9	2.612	4.550	114.3 ± 25.9
17	1	18	12	0.056	17.0	0.084	1.517	11.2 ± 11.5
18	15	22	16	0.682	15.6	0.948	1.390	135.6 ± 45.5
19	3	15	24	0.200	7.1	0.126	0.632	40.1 ± 25.4
20	3	5	12	0.600	4.7	0.253	0.421	119.5 ± 87.3
	379	705			25.4	1.220	2.270	

AREA OF BASIC UNIT = 9.89E-07 cm
CHI SQUARED = 17.14938 WITH 19 DEGREES OF FREEDOM
P(chi squared) = 58.0 %
CORRELATION COEFFICIENT = 0.992
VARIANCE OF SQR(Ns) = 6.17
VARIANCE OF SQR(Ni) = 8.82

Ns/Ni = 0.538 ± 0.034
MEAN RATIO = 0.473 ± 0.040

Ages calculated using a zeta of 348.4 ± 5.8 for SRM612 glass
RHO D = 1.170E+06 ; ND = 2894

POOLED AGE = 107.1 ± 7.2 Ma
MEAN AGE = 94.4 ± 8.2 Ma

9414-46 APATITE Apatite

IRRADIATION WK142
SLIDE NUMBER 2
COUNTED BY: Kao

No.	Ns	Ni	Na	RATIO	U (ppm)	RHOs (E+06)	RHOi (E+06)	F.T.AGE (Ma)
1	32	54	16	0.593	37.9	2.022	3.413	118.9 ± 26.7
2	1	1	24	1.000	0.5	0.042	0.042	199.4 ± 282.0
3	9	28	18	0.321	17.5	0.506	1.573	64.8 ± 24.9
4	16	29	24	0.552	13.6	0.674	1.222	110.8 ± 34.6
5	12	14	8	0.857	19.7	1.517	1.769	171.3 ± 67.5
6	3	10	24	0.300	4.7	0.126	0.421	60.5 ± 39.8
7	15	48	18	0.312	30.0	0.843	2.696	63.0 ± 18.7
8	16	36	60	0.444	6.7	0.270	0.607	89.4 ± 26.9
	104	220			12.9	0.548	1.159	

AREA OF BASIC UNIT = 9.89E-07 cm
CHI SQUARED = 7.467674 WITH 7 DEGREES OF FREEDOM
P(chi squared) = 38.2 %
CORRELATION COEFFICIENT = 0.870
VARIANCE OF SQR(Ns) = 2.10
VARIANCE OF SQR(Ni) = 4.47

Ns/Ni = 0.473 ± 0.056
MEAN RATIO = 0.547 ± 0.093

Ages calculated using a zeta of 348.4 ± 5.8 for SRM612 glass
RHO D = 1.179E+06 ; ND = 2914

POOLED AGE = 95.0 ± 11.5 Ma
MEAN AGE = 109.9 ± 18.8 Ma

9414-47 Apatite

IRRADIATION wk142-03 COUNTED BY: Kao

No.	Ns	Ni	Na	RATIO	U(ppm)	RHOs	RHOi	F.T.AGE(Ma)
1	13	34	9	0.382	41.2	1.522E+06	3.981E+06	77.5 ± 25.3
2	4	10	6	0.400	18.2	7.025E+05	1.756E+06	81.0 ± 48.0
3	0	2	4	0.000	5.5	0.000E+00	5.269E+05	0.0 ± 0.0
4	4	13	6	0.308	23.7	7.025E+05	2.283E+06	62.4 ± 35.7
5	6	14	12	0.429	12.7	5.269E+05	1.229E+06	86.8 ± 42.4
6	32	69	9	0.464	83.7	3.747E+06	8.079E+06	93.9 ± 20.2
7	10	13	12	0.769	11.8	8.781E+05	1.142E+06	154.9 ± 65.3
8	32	47	8	0.681	64.1	4.215E+06	6.191E+06	137.3 ± 31.6
9	10	12	24	0.833	5.5	4.391E+05	5.269E+05	167.7 ± 71.9
10	12	24	9	0.500	29.1	1.405E+06	2.810E+06	101.1 ± 35.8
11	7	7	9	1.000	8.5	8.196E+05	8.196E+05	200.7 ±107.4
	130	245			24.8	1.268E+06	2.390E+06	

Area of basic unit = 9.49E-07 cm-2

CHI SQUARED = 4.209989 WITH 10 DEGREES OF FREEDOM
P(chi squared) = 58.8 %
CORRELATION COEFFICIENT = 0.937
VARIANCE OF SQR(Ns) = 2.612241
VARIANCE OF SQR(Ni) = 3.961586

Ns/Ni = 0.531 ± 0.058
MEAN RATIO = 0.524 ± 0.084

Pooled Age = 107.3 ± 11.9 Ma
Mean Age = 106.0 ± 17.2 Ma
Central Age = 107.3 ± 11.8Ma
% Rel. Error = 0.55
Ages calculated using a zeta of 348.4 ± 5.8 for SRM 612 glass
RHO D = 1.187E+06cm-2; ND = 2934

9414-49 APATITE MARLBOROUGH

IRRADIATION WK142-5
SLIDE NUMBER 5
COUNTED BY: KAO

No.	Ns	Ni	Na	RATIO	U (ppm)	RHOs (E+06)	RHOi (E+06)	F.T.AGE (Ma)
1	7	18	6	0.389	31.8	1.180	3.033	84.1 ± 37.5
2	3	9	4	0.333	23.9	0.758	2.275	72.1 ± 48.1
3	13	42	10	0.310	44.5	1.314	4.247	67.0 ± 21.3
4	2	7	4	0.286	18.6	0.506	1.769	61.9 ± 49.6
5	5	16	4	0.312	42.4	1.264	4.044	67.6 ± 34.7
6	4	12	9	0.333	14.1	0.449	1.348	72.1 ± 41.7
	34	104			29.8	0.929	2.842	

AREA OF BASIC UNIT = 9.89E-07 cm
CHI SQUARED = .2199341 WITH 5 DEGREES OF FREEDOM
P(chi squared) = 99.9 %
CORRELATION COEFFICIENT = 0.990
VARIANCE OF SQR(Ns) = 0.60
VARIANCE OF SQR(Ni) = 1.87

Ns/NI = 0.327 ± 0.065
MEAN RATIO = 0.327 ± 0.014

Ages calculated using a zeta of 348.4 ± 5.8 for SRM612 glass
RHO D = 1.249E+06 ; ND = 2536

POOLED AGE = 70.7 ± 14.1 Ma
MEAN AGE = 70.8 ± 3.6 Ma

9414-50 Apatite

IRRADIATION wk142-06 COUNTED BY: Kao

No.	Ns	Ni	Na	RATIO	U(ppm)	RHOs	RHOi	F.T.AGE(Ma)
1	1	25	16	0.040	16.7	6.586E+04	1.646E+06	8.3 ± 8.5
2	1	33	6	0.030	58.9	1.756E+05	5.796E+06	6.3 ± 6.4
3	0	4	18	0.000	2.4	0.000E+00	2.342E+05	0.0 ± 0.0
4	0	12	6	0.000	21.4	0.000E+00	2.107E+06	0.0 ± 0.0
	2	74			17.2	4.581E+04	1.695E+06	

Area of basic unit = 9.49E-07 cm-2

CHI SQUARED = .2974196 WITH 3 DEGREES OF FREEDOM
P(chi squared) = 89.8 %
CORRELATION COEFFICIENT = 0.934
VARIANCE OF SQR(Ns) = .3333333
VARIANCE OF SQR(Ni) = 2.77327

Ns/Ni = 0.027 ± 0.019
MEAN RATIO = 0.018 ± 0.010

Pooled Age = 5.6 ± 4.0 Ma
Mean Age = 3.7 ± 2.2 Ma
Central Age = 5.6 ± 4.0Ma
% Rel. Error = 0.00
Ages calculated using a zeta of 348.4 ± 5.8 for SRM 612 glass
RHO D = 1.211E+06cm-2; ND = 2995

9414-51 Apatite

IRRADIATION wk142-07 COUNTED BY: Kao

No.	Ns	Ni	Na	RATIO	U(ppm)	RHOs	RHOi	F.T.AGE(Ma)
1	73	327	48	0.223	72.4	1.603E+06	7.179E+06	46.6 ± 6.1
2	6	24	36	0.250	7.1	1.756E+05	7.025E+05	52.1 ± 23.8
3	10	92	40	0.109	24.5	2.634E+05	2.424E+06	22.7 ± 7.6
4	0	5	25	0.000	2.1	0.000E+00	2.107E+05	0.0 ± 0.0
5	4	30	20	0.133	15.9	2.107E+05	1.581E+06	27.9 ± 14.8
6	0	3	30	0.000	1.1	0.000E+00	1.054E+05	0.0 ± 0.0
7	1	96	100	0.010	10.2	1.054E+04	1.012E+06	2.2 ± 2.2
8	3	62	25	0.048	26.4	1.264E+05	2.613E+06	10.1 ± 6.0
9	0	1	36	0.000	0.3	0.000E+00	2.927E+04	0.0 ± 0.0
	97	640			18.9	2.839E+05	1.873E+06	

Area of basic unit = 9.49E-07 cm-2

CHI SQUARED = 14.68004 WITH 8 DEGREES OF FREEDOM
P(chi squared) = 0.027 %
CORRELATION COEFFICIENT = 0.952
VARIANCE OF SQR(Ns) = 7.170142
VARIANCE OF SQR(Ni) = 28.84154

Ns/Ni = 0.152 ± 0.017
MEAN RATIO = 0.086 ± 0.033

Pooled Age = 31.7 ± 3.5 Ma
Mean Age = 18.0 ± 6.9 Ma
Central Age = 23.2 ± 7.0Ma
% Rel. Error = 65.11
Ages calculated using a zeta of 348.4 ± 5.8 for SRM 612 glass
RHO D = 1.219E+06cm-2; ND = 3015

9414-52 APATITE MARLBOROUGH

IRRADIATION WK142-8
SLIDE NUMBER 8
COUNTED BY: KAO

No.	Ns	Ni	Na	RATIO	U (ppm)	RHOs (E+06)	RHOi (E+06)	F.T.AGE (Ma)
1	10	23	4	0.435	59.5	2.528	5.814	96.1 ± 36.5
2	17	35	6	0.486	60.4	2.865	5.898	107.3 ± 31.8
3	3	6	6	0.500	10.4	0.506	1.011	110.4 ± 78.1
4	1	3	4	0.333	7.8	0.253	0.758	73.8 ± 85.3
5	12	30	9	0.400	34.5	1.348	3.370	88.5 ± 30.3
6	5	10	9	0.500	11.5	0.562	1.123	110.4 ± 60.6
7	3	8	6	0.375	13.8	0.506	1.348	83.0 ± 56.2
8	7	14	8	0.500	18.1	0.885	1.769	110.4 ± 51.2
9	5	11	6	0.455	19.0	0.843	1.854	100.5 ± 54.3
10	7	20	8	0.350	25.9	0.885	2.528	77.5 ± 34.1
11	3	6	9	0.500	6.9	0.337	0.674	110.4 ± 78.1
12	1	2	4	0.500	5.2	0.253	0.506	110.4 ± 135.3
13	2	4	6	0.500	6.9	0.337	0.674	110.4 ± 95.7
14	5	17	6	0.294	29.3	0.843	2.865	65.2 ± 33.2
15	9	18	9	0.500	20.7	1.011	2.022	110.4 ± 45.2
16	9	31	18	0.290	17.8	0.506	1.741	64.4 ± 24.4
17	18	36	18	0.500	20.7	1.011	2.022	110.4 ± 32.0
18	8	28	6	0.286	48.3	1.348	4.719	63.3 ± 25.4
19	3	8	6	0.375	13.8	0.506	1.348	83.0 ± 56.2
20	3	6	4	0.500	15.5	0.758	1.517	110.4 ± 78.1
	131	316			21.5	0.871	2.102	

AREA OF BASIC UNIT = 9.89E-07 cm
CHI SQUARED = 3.996024 WITH 19 DEGREES OF FREEDOM
P(chi squared) = 100.0 %
CORRELATION COEFFICIENT = 0.936
VARIANCE OF SQR(Ns) = 0.86
VARIANCE OF SQR(Ni) = 2.12

Ns/Ni = 0.415 ± 0.043
MEAN RATIO = 0.429 ± 0.018

Ages calculated using a zeta of 348.4 ± 5.8 for SRM612 glass
RHO D = 1.279E+06 ; ND = 2720

POOLED AGE = 91.7 ± 9.8 Ma
MEAN AGE = 94.9 ± 4.7 Ma

9414-53 APATITE Apatite

IRRADIATION wk142
SLIDE NUMBER 9
COUNTED BY: Kao

No.	Ns	Ni	Na	RATIO	U (ppm)	RHOs (E+06)	RHOi (E+06)	F.T.AGE (Ma)
1	21	40	20	0.525	21.4	1.062	2.022	110.5 ± 29.9
2	2	12	36	0.167	3.6	0.056	0.337	35.3 ± 27.0
3	0	1	36	0.000	0.3	0.000	0.028	0.0 ± 0.0
4	0	1	16	0.000	0.7	0.000	0.063	0.0 ± 0.0
5	12	14	36	0.857	4.2	0.337	0.393	179.4 ± 70.7
6	0	1	36	0.000	0.3	0.000	0.028	0.0 ± 0.0
7	2	10	16	0.200	6.7	0.126	0.632	42.3 ± 32.8
8	1	26	36	0.038	7.7	0.028	0.730	8.2 ± 8.3
9	17	51	60	0.333	9.1	0.286	0.859	70.4 ± 19.8
10	0	1	40	0.000	0.3	0.000	0.025	0.0 ± 0.0
11	1	8	24	0.125	3.6	0.042	0.337	26.5 ± 28.1
12	17	61	36	0.279	18.2	0.477	1.713	58.9 ± 16.2
13	1	4	25	0.250	1.7	0.040	0.162	52.9 ± 59.1
14	3	9	25	0.333	3.9	0.121	0.364	70.4 ± 46.9
15	1	1	12	1.000	0.9	0.084	0.084	208.9 ± 295.4
16	4	14	24	0.286	6.3	0.169	0.590	60.4 ± 34.3
17	5	19	12	0.263	17.0	0.421	1.601	55.6 ± 28.0
	87	273			6.0	0.180	0.563	

AREA OF BASIC UNIT = 9.89E-07 cm
CHI SQUARED = 20.9853 WITH 16 DEGREES OF FREEDOM
P(chi squared) = 17.9 %
CORRELATION COEFFICIENT = 0.867
VARIANCE OF SQR(Ns) = 2.33
VARIANCE OF SQR(Ni) = 4.83

Ns/Ni = 0.319 ± 0.039
MEAN RATIO = 0.274 ± 0.070

Ages calculated using a zeta of $\overline{348.4 \pm 5.8}$ for SRM612 glass
RHO D = 1.236E+06 ; $\overline{ND}$ = 3055

POOLED AGE = 67.3 ± 8.4 Ma
MEAN AGE = 57.9 ± 14.8 Ma

9414-54 APATITE Apatite

IRRADIATION FT:WK142
SLIDE NUMBER 10
COUNTED BY: Kao

No.	Ns	Ni	Na	RATIO	U (ppm)	RHOs (E+06)	RHOi (E+06)	F.T.AGE (Ma)
1	2	40	12	0.050	35.5	0.169	3.370	10.7 ± 7.7
2	4	92	24	0.043	40.8	0.169	3.876	9.3 ± 4.7
	6	132			39.0	0.169	3.707	

AREA OF BASIC UNIT = 9.89E-07 cm
CHI SQUARED = 2.489183E-02 WITH 1 DEGREES OF FREEDOM
P(chi squared) = 87.5 %
CORRELATION COEFFICIENT = 1.000
VARIANCE OF SQR(Ns) = 0.17
VARIANCE OF SQR(Ni) = 5.34

Ns/Ni = 0.045 ± 0.019
MEAN RATIO = 0.047 ± 0.003

Ages calculated using a zeta of $\overline{348.4 \pm 5.8}$ for SRM612 glass
RHO D = 1.244E+06 ; $\overline{ND}$ = 3075

POOLED AGE = 9.7 ± 4.1 Ma
MEAN AGE = 10.0 ± 0.7 Ma

9414-55 APATITE Apatite

IRRADIATION WK142
SLIDE NUMBER 11
COUNTED BY: Kao

No.	Ns	Ni	Na	RATIO	U (ppm)	RHOs (E+06)	RHOi (E+06)	F.T.AGE (Ma)
1	1	18	20	0.056	9.5	0.051	0.910	11.9 ± 12.3
2	0	20	12	0.000	17.6	0.000	1.685	0.0 ± 0.0
3	0	14	16	0.000	9.3	0.000	0.885	0.0 ± 0.0
4	3	98	24	0.031	43.2	0.126	4.129	6.6 ± 3.9
5	3	56	8	0.054	74.1	0.379	7.078	11.5 ± 6.8
6	1	67	36	0.015	19.7	0.028	1.882	3.2 ± 3.2
7	0	2	16	0.000	1.3	0.000	0.126	0.0 ± 0.0
8	7	113	24	0.062	49.8	0.295	4.761	13.3 ± 5.2
9	0	25	12	0.000	22.0	0.000	2.106	0.0 ± 0.0
10	1	17	24	0.059	7.5	0.042	0.716	12.6 ± 13.0
11	5	113	36	0.044	33.2	0.140	3.174	9.5 ± 4.4
	21	543			25.2	0.093	2.408	

AREA OF BASIC UNIT = 9.89E-07 cm
CHI SQUARED = 5.65803 WITH 10 DEGREES OF FREEDOM
P(chi squared) = 84.3 %
CORRELATION COEFFICIENT = 0.894
VARIANCE OF SQR(Ns) = 0.93
VARIANCE OF SQR(Ni) = 9.98

Ns/Ni = 0.039 ± 0.009
MEAN RATIO = 0.029 ± 0.008

Ages calculated using a zeta of 348.4 ± 5.8 for SRM612 glass
RHO D = 1.252E+06 ; ND = 3095

POOLED AGE = 8.3 ± 1.9 Ma
MEAN AGE = 6.2 ± 1.7 Ma

9414-56 APATITE Marlborough

IRRADIATION FT:wk142
SLIDE NUMBER 12
COUNTED BY: IJL

No.	Ns	Ni	Na	RATIO	U (ppm)	RHOs (E+06)	RHOi (E+06)	F.T.AGE (Ma)
1	0	5	25	0.000	2.1	0.000	0.202	0.0 ± 0.0
2	0	25	48	0.000	5.5	0.000	0.527	0.0 ± 0.0
3	2	60	40	0.033	15.8	0.051	1.517	7.2 ± 5.2
4	0	3	18	0.000	1.8	0.000	0.169	0.0 ± 0.0
5	0	12	36	0.000	3.5	0.000	0.337	0.0 ± 0.0
6	0	2	40	0.000	0.5	0.000	0.051	0.0 ± 0.0
7	12	155	60	0.077	27.2	0.202	2.612	16.7 ± 5.0
8	0	10	36	0.000	2.9	0.000	0.281	0.0 ± 0.0
9	2	32	60	0.062	5.6	0.034	0.539	13.5 ± 9.9
10	1	23	60	0.043	4.0	0.017	0.388	9.4 ± 9.6
11	0	1	24	0.000	0.4	0.000	0.042	0.0 ± 0.0
	17	328			7.7	0.038	0.742	

AREA OF BASIC UNIT = 9.89E-07 cm
CHI SQUARED = 5.302848 WITH 10 DEGREES OF FREEDOM
P(chi squared) = 87.0 %
CORRELATION COEFFICIENT = 0.973
VARIANCE OF SQR(Ns) = 1.22
VARIANCE OF SQR(Ni) = 11.28

Ns/Ni = 0.052 ± 0.013
MEAN RATIO = 0.020 ± 0.009

Ages calculated using a zeta of 343.5 ± 4.5 for SRM612 glass
RHO D = 1.260E+06 ; ND = 3115

POOLED AGE = 11.2 ± 2.8 Ma
MEAN AGE = 4.3 ± 1.9 Ma

9414-58 Apatite

IRRADIATION wk142-14 COUNTED BY: Kao

No.	Ns	Ni	Na	RATIO	U(ppm)	RHOs	RHOi	F.T.AGE(Ma)
1	0	57	36	0.000	15.4	0.000E+00	1.601E+06	0.0 ± 0.0
2	47	102	60	0.461	16.6	7.920E+05	1.719E+06	100.2 ± 17.8
3	1	10	24	0.100	4.1	4.213E+04	4.213E+05	21.9 ± 23.0
	48	169			13.7	4.044E+05	1.424E+06	

Area of basic unit = 9.89E-07 cm-2

CHI SQUARED = 12.47725 WITH 2 DEGREES OF FREEDOM
P(chi squared) = 0.000 %
CORRELATION COEFFICIENT = 0.850
VARIANCE OF SQR(Ns) = 13.71478
VARIANCE OF SQR(Ni) = 12.31278

Ns/Ni = 0.284 ± 0.046
MEAN RATIO = 0.187 ± 0.140

Pooled Age = 61.9 ± 10.2 Ma
Mean Age = 40.8 ± 30.6 Ma
Central Age = 36.7 ± 25.2Ma
% Rel. Error = %109.02
Ages calculated using a zeta of 348.4 ± 5.8 for SRM 612 glass
RHO D = 1.276E+06cm-2; ND = 3155

9414-60 APATITE Apatite

IRRADIATION WK142
SLIDE NUMBER 16
COUNTED BY: Kao

No.	Ns	Ni	Na	RATIO	U (ppm)	RHOs (E+06)	RHOi (E+06)	F.T.AGE (Ma)
1	0	15	12	0.000	12.8	0.000	1.264	0.0 ± 0.0
2	0	5	6	0.000	8.5	0.000	0.843	0.0 ± 0.0
3	0	9	16	0.000	5.8	0.000	0.569	0.0 ± 0.0
4	1	26	16	0.038	16.6	0.063	1.643	8.5 ± 8.7
5	0	18	30	0.000	6.1	0.000	0.607	0.0 ± 0.0
6	2	15	40	0.133	3.8	0.051	0.379	29.5 ± 22.2
7	0	13	36	0.000	3.7	0.000	0.365	0.0 ± 0.0
8	0	25	16	0.000	16.0	0.000	1.580	0.0 ± 0.0
9	0	5	24	0.000	2.1	0.000	0.211	0.0 ± 0.0
10	0	14	36	0.000	4.0	0.000	0.393	0.0 ± 0.0
11	1	31	24	0.032	13.2	0.042	1.306	7.2 ± 7.3
12	0	2	16	0.000	1.3	0.000	0.126	0.0 ± 0.0
13	6	231	40	0.026	59.2	0.152	5.839	5.8 ± 2.4
14	0	2	20	0.000	1.0	0.000	0.101	0.0 ± 0.0
15	1	78	36	0.013	22.2	0.028	2.191	2.8 ± 2.9
16	0	3	16	0.000	1.9	0.000	0.190	0.0 ± 0.0
17	0	7	12	0.000	6.0	0.000	0.590	0.0 ± 0.0
	11	499			12.9	0.028	1.274	

AREA OF BASIC UNIT = 9.89E-07 cm
CHI SQUARED = 10.94056 WITH 16 DEGREES OF FREEDOM
P(chi squared) = 81.3 %
CORRELATION COEFFICIENT = 0.932
VARIANCE OF SQR(Ns) = 0.51
VARIANCE OF SQR(Ni) = 11.21

Ns/Ni = 0.022 ± 0.007
MEAN RATIO = 0.014 ± 0.008

Ages calculated using a zeta of 348.4 ± 5.8 for SRM612 glass
RHO D = 1.293E+06 ; ND = 3196

POOLED AGE = 4.9 ± 1.5 Ma
MEAN AGE = 3.2 ± 1.8 Ma

9414-61 Apatite

IRRADIATION WK142-17 COUNTED BY: KAO

No.	Ns	Ni	Na	RATIO	U(ppm)	RHOs	RHOi	F.T.AGE(Ma)
1	11	19	16	0.579	10.8	6.951E+05	1.201E+06	136.6 ± 51.9
2	11	18	28	0.611	5.8	3.972E+05	6.500E+05	144.1 ± 55.3
3	16	28	40	0.571	6.4	4.044E+05	7.078E+05	134.9 ± 42.4
4	43	200	70	0.215	26.0	6.211E+05	2.889E+06	51.1 ± 8.7
5	14	28	32	0.500	7.9	4.424E+05	8.847E+05	118.2 ± 38.8
6	31	40	50	0.775	7.3	6.269E+05	8.089E+05	182.2 ± 43.8
7	5	18	20	0.278	8.2	2.528E+05	9.100E+05	65.9 ± 33.4
8	25	61	70	0.410	7.9	3.611E+05	8.811E+05	97.0 ± 23.2
9	19	45	30	0.422	13.6	6.404E+05	1.517E+06	99.9 ± 27.4
10	11	21	20	0.524	9.5	5.561E+05	1.062E+06	123.7 ± 46.1
11	18	47	30	0.383	14.2	6.067E+05	1.584E+06	90.7 ± 25.2
12	16	34	50	0.471	6.2	3.236E+05	6.876E+05	111.3 ± 33.8
13	12	21	20	0.571	9.5	6.067E+05	1.062E+06	134.9 ± 48.9
14	17	43	42	0.395	9.3	4.093E+05	1.035E+06	93.6 ± 26.9
15	27	50	81	0.540	5.6	3.370E+05	6.241E+05	127.5 ± 30.6
16	11	28	24	0.393	10.6	4.634E+05	1.180E+06	93.0 ± 33.2
17	20	27	40	0.741	6.1	5.056E+05	6.825E+05	174.3 ± 51.6
18	12	24	27	0.500	8.1	4.494E+05	8.988E+05	118.2 ± 41.9
19	11	17	24	0.647	6.4	4.634E+05	7.162E+05	152.5 ± 59.1
20	12	29	28	0.414	9.4	4.333E+05	1.047E+06	97.9 ± 33.7
	342	798			9.8	4.660E+05	1.087E+06	

Area of basic unit = 9.89E-07 cm-2

CHI SQUARED = 17.16764 WITH 19 DEGREES OF FREEDOM
P(chi squared) = 1.7 %
CORRELATION COEFFICIENT = 0.838
VARIANCE OF SQR(Ns) = .9588735
VARIANCE OF SQR(Ni) = 4.86719

Ns/Ni = 0.429 ± 0.028
MEAN RATIO = 0.497 ± 0.031

Pooled Age = 101.4 ± 7.0 Ma
Mean Age = 117.4 ± 7.9 Ma
Central Age = 110.2 ± 9.6Ma
% Rel. Error = 22.99
Ages calculated using a zeta of 348.4 ± 5.8 for SRM 612 glass
RHO D = 1.369E+06cm-2; ND = 3274

9414-62 Apatite

IRRADIATION wk142-18 COUNTED BY: Kao

No.	Ns	Ni	Na	RATIO	U(ppm)	RHOs	RHOi	F.T.AGE(Ma)
1	16	28	25	0.571	11.1	6.744E+05	1.180E+06	127.2 ± 40.0
2	10	28	12	0.357	23.1	8.781E+05	2.459E+06	79.8 ± 29.4
3	15	58	32	0.259	17.9	4.939E+05	1.910E+06	57.9 ± 16.8
4	3	18	36	0.167	5.0	8.781E+04	5.269E+05	37.4 ± 23.3
5	28	82	12	0.341	67.7	2.459E+06	7.201E+06	76.3 ± 16.8
6	28	66	24	0.424	27.2	1.229E+06	2.898E+06	94.7 ± 21.5
7	33	75	16	0.440	46.4	2.173E+06	4.939E+06	98.2 ± 20.6
8	51	123	12	0.415	101.5	4.478E+06	1.080E+07	92.6 ± 15.5
9	47	65	18	0.723	35.8	2.751E+06	3.805E+06	160.5 ± 30.9
10	9	21	18	0.429	11.6	5.269E+05	1.229E+06	95.6 ± 38.2
11	21	35	40	0.600	8.7	5.532E+05	9.220E+05	133.5 ± 37.0
12	6	11	3	0.545	36.3	2.107E+06	3.864E+06	121.5 ± 61.7
13	4	7	8	0.571	8.7	5.269E+05	9.220E+05	127.2 ± 79.8
14	23	42	24	0.548	17.3	1.010E+06	1.844E+06	122.0 ± 31.7
15	35	124	50	0.282	24.6	7.376E+05	2.613E+06	63.1 ± 12.2
16	25	82	60	0.305	13.5	4.391E+05	1.440E+06	68.2 ± 15.6
17	12	19	24	0.632	7.8	5.269E+05	8.342E+05	140.5 ± 51.9
18	2	5	6	0.400	8.3	3.512E+05	8.781E+05	89.3 ± 74.7
19	2	5	25	0.400	2.0	8.430E+04	2.107E+05	89.3 ± 74.7
20	2	5	18	0.400	2.8	1.171E+05	2.927E+05	89.3 ± 74.7
	372	899			19.2	8.466E+05	2.046E+06	

Area of basic unit = 9.49E-07 cm-2

CHI SQUARED = 13.27319 WITH 19 DEGREES OF FREEDOM
P(chi squared) = 11.6 %
CORRELATION COEFFICIENT = 0.887
VARIANCE OF SQR(Ns) = 3.34486
VARIANCE OF SQR(Ni) = 8.382231

Ns/Ni = 0.414 ± 0.026
MEAN RATIO = 0.440 ± 0.031

Pooled Age = 92.4 ± 6.0 Ma
Mean Age = 98.3 ± 7.3 Ma
Central Age = 93.8 ± 7.8Ma
% Rel. Error = 19.83
Ages calculated using a zeta of 348.4 ± 5.8 for SRM 612 glass
RHO D = 1.309E+06cm-2; ND = 3236

9414-63 Apatite

IRRADIATION wk142-19 COUNTED BY: Kao

No.	Ns	Ni	Na	RATIO	U(ppm)	RHOs	RHOi	F.T.AGE(Ma)
1	5	13	50	0.385	2.6	1.054E+05	2.740E+05	86.4 ± 45.5
2	9	28	60	0.321	4.6	1.581E+05	4.917E+05	72.3 ± 27.7
3	19	24	80	0.792	3.0	2.503E+05	3.161E+05	176.6 ± 54.4
4	6	6	9	1.000	6.6	7.025E+05	7.025E+05	222.3 ±128.4
5	6	20	80	0.300	2.5	7.903E+04	2.634E+05	67.5 ± 31.5
6	7	7	48	1.000	1.4	1.537E+05	1.537E+05	222.3 ±118.9
7	31	60	12	0.517	49.2	2.722E+06	5.269E+06	115.8 ± 25.7
8	8	34	60	0.235	5.6	1.405E+05	5.971E+05	53.0 ± 20.9
9	11	18	18	0.611	9.8	6.440E+05	1.054E+06	136.8 ± 52.4
10	16	17	50	0.941	3.3	3.372E+05	3.583E+05	209.4 ± 73.1
11	4	4	36	1.000	1.1	1.171E+05	1.171E+05	222.3 ±157.3
12	39	71	24	0.549	29.1	1.712E+06	3.117E+06	123.1 ± 24.7
13	5	10	40	0.500	2.5	1.317E+05	2.634E+05	112.1 ± 61.5
14	26	58	36	0.448	15.9	7.610E+05	1.698E+06	100.6 ± 23.8
15	3	6	18	0.500	3.3	1.756E+05	3.512E+05	112.1 ± 79.3
16	6	11	36	0.545	3.0	1.756E+05	3.220E+05	122.2 ± 62.1
17	11	18	48	0.611	3.7	2.415E+05	3.952E+05	136.8 ± 52.4
18	8	19	40	0.421	4.7	2.107E+05	5.005E+05	94.5 ± 39.9
19	7	25	30	0.280	8.2	2.459E+05	8.781E+05	63.0 ± 27.0
20	6	12	48	0.500	2.5	1.317E+05	2.634E+05	112.1 ± 56.1
	233	461			5.5	2.983E+05	5.902E+05	

Area of basic unit = 9.49E-07 cm-2

CHI SQUARED = 9.818299 WITH 19 DEGREES OF FREEDOM
P(chi squared) = 41.7 %
CORRELATION COEFFICIENT = 0.911
VARIANCE OF SQR(Ns) = 1.533189
VARIANCE OF SQR(Ni) = 3.257905

Ns/Ni = 0.505 ± 0.041
MEAN RATIO = 0.573 ± 0.055

Pooled Age = 113.3 ± 9.4 Ma
Mean Age = 128.3 ± 12.7 Ma
Central Age = 113.3 ± 9.5Ma
% Rel. Error = 5.00
Ages calculated using a zeta of 348.4 ± 5.8 for SRM 612 glass
RHO D = 1.317E+06cm-2; ND = 3256

9414-64 Apatite

IRRADIATION wk142-20 COUNTED BY: Kao

No.	Ns	Ni	Na	RATIO	U(ppm)	RHOs	RHOi	F.T.AGE(Ma)
1	53	141	32	0.376	43.1	1.745E+06	4.643E+06	85.0 ± 13.8
2	25	70	36	0.357	19.0	7.318E+05	2.049E+06	80.8 ± 18.9
3	6	18	80	0.333	2.2	7.903E+04	2.371E+05	75.4 ± 35.6
4	13	40	16	0.325	24.5	8.562E+05	2.634E+06	73.5 ± 23.5
5	8	78	64	0.103	11.9	1.317E+05	1.284E+06	23.3 ± 8.7
6	13	20	36	0.650	5.4	3.805E+05	5.854E+05	146.2 ± 52.2
	118	367			13.6	4.710E+05	1.465E+06	

Area of basic unit = 9.49E-07 cm-2

CHI SQUARED = 7.884452 WITH 5 DEGREES OF FREEDOM
P(chi squared) = 0.754 %
CORRELATION COEFFICIENT = 0.862
VARIANCE OF SQR(Ns) = 3.149678
VARIANCE OF SQR(Ni) = 8.537628

Ns/Ni = 0.322 ± 0.034
MEAN RATIO = 0.357 ± 0.071

Pooled Age = 72.8 ± 7.9 Ma
Mean Age = 80.8 ± 16.2 Ma
Central Age = 73.6 ± 14.0Ma
% Rel. Error = 35.73
Ages calculated using a zeta of 348.4 ± 5.8 for SRM 612 glass
RHO D = 1.325E+06cm-2; ND = 3276

9414-65 Apatite

IRRADIATION wk143-01 COUNTED BY: Kao

No.	Ns	Ni	Na	RATIO	U(ppm)	RHOs	RHOi	F.T.AGE(Ma)
1	12	27	18	0.444	16.7	7.025E+05	1.581E+06	88.3 ± 30.7
2	3	47	40	0.064	13.1	7.903E+04	1.238E+06	12.8 ± 7.6
3	0	34	100	0.000	3.8	0.000E+00	3.583E+05	0.0 ± 0.0
4	0	8	40	0.000	2.2	0.000E+00	2.107E+05	0.0 ± 0.0
5	1	21	24	0.048	9.7	4.391E+04	9.220E+05	9.5 ± 9.7
6	0	9	60	0.000	1.7	0.000E+00	1.581E+05	0.0 ± 0.0
7	0	15	12	0.000	13.9	0.000E+00	1.317E+06	0.0 ± 0.0
	16	161			6.1	5.735E+04	5.770E+05	

Area of basic unit = 9.49E-07 cm-2

CHI SQUARED = 15.02864 WITH 6 DEGREES OF FREEDOM
P(chi squared) = 0.004 %
CORRELATION COEFFICIENT = 0.314
VARIANCE OF SQR(Ns) = 1.752564
VARIANCE OF SQR(Ni) = 2.197632

Ns/Ni = 0.099 ± 0.026
MEAN RATIO = 0.079 ± 0.062

Pooled Age = 19.9 ± 5.2 Ma
Mean Age = 15.9 ± 12.3 Ma
Central Age = 14.2 ± 9.9Ma
% Rel. Error = %161.48
Ages calculated using a zeta of 348.4 ± 5.8 for SRM 612 glass
RHO D = 1.165E+06cm-2; ND = 2880

9414-66 Apatite

IRRADIATION wk143-02 COUNTED BY: Kao

No.	Ns	Ni	Na	RATIO	U(ppm)	RHOs	RHOi	F.T.AGE(Ma)
1	0	1	16	0.000	0.7	0.000E+00	6.586E+04	0.0 ± 0.0
2	1	2	9	0.500	2.5	1.171E+05	2.342E+05	100.0 ±122.4
3	2	7	16	0.286	4.8	1.317E+05	4.610E+05	57.3 ± 46.0
4	8	23	24	0.348	10.6	3.512E+05	1.010E+06	69.7 ± 28.7
5	2	16	24	0.125	7.4	8.781E+04	7.025E+05	25.1 ± 18.9
6	0	1	16	0.000	0.7	0.000E+00	6.586E+04	0.0 ± 0.0
7	69	214	24	0.322	98.5	3.030E+06	9.396E+06	64.6 ± 9.1
8	3	12	60	0.250	2.2	5.269E+04	2.107E+05	50.2 ± 32.4
9	1	4	15	0.250	2.9	7.025E+04	2.810E+05	50.2 ± 56.1
10	4	11	16	0.364	7.6	2.634E+05	7.244E+05	72.8 ± 42.6
11	1	3	24	0.333	1.4	4.391E+04	1.317E+05	66.8 ± 77.2
12	1	6	32	0.167	2.1	3.293E+04	1.976E+05	33.5 ± 36.2
13	0	2	36	0.000	0.6	0.000E+00	5.854E+04	0.0 ± 0.0
14	0	5	36	0.000	1.5	0.000E+00	1.464E+05	0.0 ± 0.0
15	2	5	40	0.400	1.4	5.269E+04	1.317E+05	80.1 ± 67.0
16	5	109	30	0.046	40.1	1.756E+05	3.829E+06	9.2 ± 4.2
17	3	18	64	0.167	3.1	4.939E+04	2.964E+05	33.5 ± 20.9
18	5	21	60	0.238	3.9	8.781E+04	3.688E+05	47.8 ± 23.8
19	4	17	49	0.235	3.8	8.602E+04	3.656E+05	47.2 ± 26.3
20	0	5	12	0.000	4.6	0.000E+00	4.391E+05	0.0 ± 0.0
21	9	51	60	0.176	9.4	1.581E+05	8.957E+05	35.5 ± 12.8
	120	533			8.9	1.907E+05	8.471E+05	

Area of basic unit = 9.49E-07 cm-2

CHI SQUARED = 14.62709 WITH 20 DEGREES OF FREEDOM
P(chi squared) = 8.3 %
CORRELATION COEFFICIENT = 0.911
VARIANCE OF SQR(Ns) = 3.196558
VARIANCE OF SQR(Ni) = 10.99025

Ns/Ni = 0.225 ± 0.023
MEAN RATIO = 0.200 ± 0.033

Pooled Age = 45.2 ± 4.7 Ma
Mean Age = 40.2 ± 6.7 Ma
Central Age = 41.7 ± 7.0Ma
% Rel. Error = 38.31
Ages calculated using a zeta of 348.4 ± 5.8 for SRM 612 glass
RHO D = 1.173E+06cm-2; ND = 2900

9414-67 Apatite

IRRADIATION wk143-3 COUNTED BY: Kao

No.	Ns	Ni	Na	RATIO	U(ppm)	RHOs	RHOi	F.T.AGE(Ma)
1	16	16	48	1.000	3.5	3.370E+05	3.370E+05	199.7 ± 70.8
2	1	5	12	0.200	4.4	8.426E+04	4.213E+05	40.4 ± 44.3
3	0	6	12	0.000	5.3	0.000E+00	5.056E+05	0.0 ± 0.0
4	3	5	12	0.600	4.4	2.528E+05	4.213E+05	120.6 ± 88.1
5	15	17	40	0.882	4.5	3.792E+05	4.297E+05	176.5 ± 62.7
6	4	14	30	0.286	4.9	1.348E+05	4.719E+05	57.7 ± 32.7
7	17	31	20	0.548	16.3	8.595E+05	1.567E+06	110.3 ± 33.4
8	5	16	36	0.312	4.7	1.404E+05	4.494E+05	63.1 ± 32.3
9	1	20	24	0.050	8.8	4.213E+04	8.426E+05	10.1 ± 10.4
10	54	89	24	0.607	39.1	2.275E+06	3.750E+06	121.9 ± 21.2
11	5	54	110	0.093	5.2	4.596E+04	4.964E+05	18.8 ± 8.8
12	1	6	24	0.167	2.6	4.213E+04	2.528E+05	33.7 ± 36.4
13	2	27	8	0.074	35.5	2.528E+05	3.413E+06	15.0 ± 11.0
14	4	13	24	0.308	5.7	1.685E+05	5.477E+05	62.1 ± 35.5
15	8	14	18	0.571	8.2	4.494E+05	7.864E+05	114.9 ± 51.0
16	0	5	12	0.000	4.4	0.000E+00	4.213E+05	0.0 ± 0.0
17	5	11	30	0.455	3.9	1.685E+05	3.707E+05	91.5 ± 49.4
18	18	45	40	0.400	11.8	4.550E+05	1.138E+06	80.6 ± 22.6
19	2	17	40	0.118	4.5	5.056E+04	4.297E+05	23.8 ± 17.8
20	1	13	30	0.077	4.6	3.370E+04	4.382E+05	15.6 ± 16.2
	162	424			7.5	2.758E+05	7.217E+05	

Area of basic unit = 9.89E-07 cm-2

CHI SQUARED = 29.04491 WITH 19 DEGREES OF FREEDOM
P(chi squared) = 0.001 %
CORRELATION COEFFICIENT = 0.828
VARIANCE OF SQR(Ns) = 3.034063
VARIANCE OF SQR(Ni) = 3.485099

Ns/Ni = 0.382 ± 0.035
MEAN RATIO = 0.337 ± 0.065

Pooled Age = 77.0 ± 7.3 Ma
Mean Age = 68.1 ± 13.2 Ma
Central Age = 64.1 ± 12.1Ma
% Rel. Error = 66.03
Ages calculated using a zeta of 348.4 ± 5.8 for SRM 612 glass
RHO D = 1.181E+06cm-2; ND = 2920

9414-68 Apatite

IRRADIATION wk143-4 COUNTED BY: Kao

No.	Ns	Ni	Na	RATIO	U(ppm)	RHOs	RHOi	F.T.AGE(Ma)
1	7	83	25	0.084	34.7	2.831E+05	3.357E+06	17.2 ± 6.8
2	0	13	12	0.000	11.3	0.000E+00	1.095E+06	0.0 ± 0.0
3	7	27	24	0.259	11.8	2.949E+05	1.138E+06	52.7 ± 22.4
	14	123			21.1	2.321E+05	2.039E+06	

Area of basic unit = 9.89E-07 cm-2

CHI SQUARED = 3.024425 WITH 2 DEGREES OF FREEDOM
P(chi squared) = 4.9 %
CORRELATION COEFFICIENT = 0.655
VARIANCE OF SQR(Ns) = 2.333333
VARIANCE OF SQR(Ni) = 8.025898

Ns/Ni = 0.114 ± 0.032
MEAN RATIO = 0.115 ± 0.076

Pooled Age = 23.2 ± 6.6 Ma
Mean Age = 23.3 ± 15.6 Ma
Central Age = 24.2 ± 10.2Ma
% Rel. Error = 48.90
Ages calculated using a zeta of 348.4 ± 5.8 for SRM 612 glass
RHO D = 1.189E+06cm-2; ND = 2940

9414-69 APATITE MARLBOROUGH

IRRADIATION WK143-5
SLIDE NUMBER 5
COUNTED BY: KAO

No.	Ns	Ni	Na	RATIO	U (ppm)	RHOs (E+06)	RHOi (E+06)	F.T.AGE (Ma)
1	6	16	6	0.375	27.6	1.011	2.696	83.2 ± 39.9
2	16	35	8	0.457	45.2	2.022	4.424	101.3 ± 30.7
3	8	21	12	0.381	18.1	0.674	1.769	84.5 ± 35.2
4	3	6	8	0.500	7.7	0.379	0.758	110.7 ± 78.3
5	30	60	42	0.500	14.8	0.722	1.444	110.7 ± 24.9
6	51	116	16	0.440	74.9	3.223	7.331	97.4 ± 16.5
7	2	4	6	0.500	6.9	0.337	0.674	110.7 ± 95.9
8	4	9	24	0.444	3.9	0.169	0.379	98.5 ± 59.2
9	30	74	4.	0.405	191.1	7.583	18.706	89.9 ± 19.6
10	16	34	9	0.471	39.0	1.798	3.820	104.2 ± 31.7
	166	375			28.7	1.243	2.809	

AREA OF BASIC UNIT = 9.89E-07 cm
CHI SQUARED = .8166641 WITH 9 DEGREES OF FREEDOM
P(chi squared) = 100.0 %
CORRELATION COEFFICIENT = 0.995
VARIANCE OF SQR(Ns) = 3.63
VARIANCE OF SQR(Ni) = 8.18

Ns/Ni = 0.443 ± 0.041
MEAN RATIO = 0.447 ± 0.015

Ages calculated using a zeta of 348.4 ± 5.8 for SRM612 glass
RHO D = 1.282E+06 ; ND = 3169

POOLED AGE = 98.1 ± 9.5 Ma
MEAN AGE = 99.1 ± 4.1 Ma

9414-70 APATITE Apatite

IRRADIATION WK143
SLIDE NUMBER 6
COUNTED BY: Kao

No.	Ns	Ni	Na	RATIO	U (ppm)	RHOs (E+06)	RHOi (E+06)	F.T.AGE (Ma)
1	6	12	20	0.500	6.6	0.303	0.607	102.7 ± 51.4
2	38	44	24	0.864	20.2	1.601	1.854	176.3 ± 39.2
3	6	14	12	0.429	12.8	0.506	1.180	88.1 ± 43.0
4	4	9	8	0.444	12.4	0.506	1.138	91.3 ± 54.9
5	2	1	36	2.000	0.3	0.056	0.028	401.2 ± 491.4
6	5	10	8	0.500	13.7	0.632	1.264	102.7 ± 56.3
7	17	25	30	0.680	9.2	0.573	0.843	139.2 ± 43.9
8	14	49	12	0.286	44.9	1.180	4.129	58.9 ± 17.9
9	11	19	36	0.579	5.8	0.309	0.534	118.7 ± 45.1
10	7	8	24	0.875	3.7	0.295	0.337	178.6 ± 92.5
11	16	17	36	0.941	5.2	0.449	0.477	191.9 ± 67.0
12	12	25	36	0.480	7.6	0.337	0.702	98.6 ± 34.7
13	7	29	30	0.241	10.6	0.236	0.977	49.8 ± 21.0
14	12	31	16	0.387	21.3	0.758	1.959	79.6 ± 27.1
15	11	24	36	0.458	7.3	0.309	0.674	94.2 ± 34.4
	168	317			9.6	0.467	0.881	

AREA OF BASIC UNIT = 9.89E-07 cm
CHI SQUARED = 20.12033 WITH 14 DEGREES OF FREEDOM
P(chi squared) = 12.6 %
CORRELATION COEFFICIENT = 0.712
VARIANCE OF SQR(Ns) = 1.29
VARIANCE OF SQR(Ni) = 2.42

Ns/Ni = 0.530 ± 0.051
MEAN RATIO = 0.644 ± 0.111

Ages calculated using a zeta of 348.4 ± 5.8 for SRM612 glass
RHO D = 1.205E+06 ; ND = 2980

POOLED AGE = 108.8 ± 10.7 Ma
MEAN AGE = 132.0 ± 22.9 Ma

9414-72 Apatite

IRRADIATION wk143-8 COUNTED BY: Kao

No.	Ns	Ni	Na	RATIO	U(ppm)	RHOs	RHOi	F.T.AGE(Ma)
1	7	38	12	0.184	32.3	5.898E+05	3.202E+06	38.5 ± 15.9
2	1	12	16	0.083	7.6	6.320E+04	7.583E+05	17.5 ± 18.2
3	0	8	16	0.000	5.1	0.000E+00	5.056E+05	0.0 ± 0.0
4	9	66	80	0.136	8.4	1.138E+05	8.342E+05	28.5 ± 10.2
5	4	10	12	0.400	8.5	3.370E+05	8.426E+05	83.3 ± 49.3
6	2	7	25	0.286	2.9	8.089E+04	2.831E+05	59.6 ± 47.8
7	0	22	24	0.000	9.3	0.000E+00	9.269E+05	0.0 ± 0.0
8	2	41	18	0.049	23.2	1.123E+05	2.303E+06	10.2 ± 7.4
9	0	27	32	0.000	8.6	0.000E+00	8.531E+05	0.0 ± 0.0
10	2	43	24	0.047	18.2	8.426E+04	1.812E+06	9.7 ± 7.1
11	1	40	16	0.025	25.5	6.320E+04	2.528E+06	5.2 ± 5.3
12	1	13	12	0.077	11.0	8.426E+04	1.095E+06	16.1 ± 16.7
13	77	269	40	0.286	68.5	1.946E+06	6.800E+06	59.7 ± 7.8
14	0	8	12	0.000	6.8	0.000E+00	6.741E+05	0.0 ± 0.0
15	2	30	36	0.067	8.5	5.617E+04	8.426E+05	14.0 ± 10.2
16	0	8	12	0.000	6.8	0.000E+00	6.741E+05	0.0 ± 0.0
17	1	6	25	0.167	2.4	4.044E+04	2.427E+05	34.9 ± 37.7
18	10	179	24	0.056	76.0	4.213E+05	7.541E+06	11.7 ± 3.8
19	3	55	16	0.055	35.0	1.896E+05	3.476E+06	11.4 ± 6.8
20	3	42	8	0.071	53.5	3.792E+05	5.308E+06	15.0 ± 8.9
	125	924			20.5	2.748E+05	2.031E+06	

Area of basic unit = 9.89E-07 cm-2

CHI SQUARED = 35.74481 WITH 19 DEGREES OF FREEDOM
P(chi squared) = 0.000 %
CORRELATION COEFFICIENT = 0.873
VARIANCE OF SQR(Ns) = 3.764347
VARIANCE OF SQR(Ni) = 12.95984

Ns/Ni = 0.135 ± 0.013
MEAN RATIO = 0.099 ± 0.025

Pooled Age = 28.3 ± 2.8 Ma
Mean Age = 20.8 ± 5.3 Ma
Central Age = 19.4 ± 4.5Ma
% Rel. Error = 76.80
Ages calculated using a zeta of 348.4 ± 5.8 for SRM 612 glass
RHO D = 1.221E+06cm-2; ND = 3020

9414-73 Apatite

IRRADIATION wk143-9 COUNTED BY: Kao

No.	Ns	Ni	Na	RATIO	U(ppm)	RHOs	RHOi	F.T.AGE(Ma)
1	8	21	36	0.381	5.9	2.247E+05	5.898E+05	80.0 ± 33.3
2	9	16	70	0.562	2.3	1.300E+05	2.311E+05	117.7 ± 49.1
3	32	96	56	0.333	17.3	5.778E+05	1.733E+06	70.0 ± 14.4
4	8	24	25	0.333	9.7	3.236E+05	9.707E+05	70.0 ± 28.6
5	2	33	24	0.061	13.9	8.426E+04	1.390E+06	12.8 ± 9.3
6	27	82	48	0.329	17.3	5.688E+05	1.727E+06	69.2 ± 15.4
7	18	30	24	0.600	12.6	7.583E+05	1.264E+06	125.5 ± 37.5
8	6	31	36	0.194	8.7	1.685E+05	8.707E+05	40.8 ± 18.2
9	17	26	24	0.654	11.0	7.162E+05	1.095E+06	136.7 ± 42.7
10	6	13	9	0.462	14.6	6.741E+05	1.461E+06	96.8 ± 47.8
11	7	19	36	0.368	5.3	1.966E+05	5.336E+05	77.4 ± 34.2
12	9	23	16	0.391	14.5	5.688E+05	1.453E+06	82.1 ± 32.3
13	14	51	24	0.274	21.5	5.898E+05	2.149E+06	57.7 ± 17.5
14	3	23	24	0.130	9.7	1.264E+05	9.690E+05	27.5 ± 16.9
15	0	17	12	0.000	14.3	0.000E+00	1.432E+06	0.0 ± 0.0
16	1	10	24	0.100	4.2	4.213E+04	4.213E+05	21.1 ± 22.1
17	4	36	8	0.111	45.5	5.056E+05	4.550E+06	23.4 ± 12.4
18	5	13	16	0.385	8.2	3.160E+05	8.215E+05	80.7 ± 42.5
19	0	5	12	0.000	4.2	0.000E+00	4.213E+05	0.0 ± 0.0
20	18	49	36	0.367	13.8	5.056E+05	1.376E+06	77.1 ± 21.3
	194	618			11.2	3.503E+05	1.116E+06	

Area of basic unit = 9.89E-07 cm-2

CHI SQUARED = 18.50896 WITH 19 DEGREES OF FREEDOM
P(chi squared) = 0.789 %
CORRELATION COEFFICIENT = 0.860
VARIANCE OF SQR(Ns) = 2.311548
VARIANCE OF SQR(Ni) = 3.48662

Ns/Ni = 0.314 ± 0.026
MEAN RATIO = 0.302 ± 0.043

Pooled Age = 66.0 ± 5.6 Ma
Mean Age = 63.4 ± 9.1 Ma
Central Age = 63.5 ± 7.9Ma
% Rel. Error = 37.24
Ages calculated using a zeta of 348.4 ± 5.8 for SRM 612 glass
RHO D = 1.230E+06cm-2; ND = 3040

9414-74 Apatite

IRRADIATION wk143-10 COUNTED BY: Kao

No.	Ns	Ni	Na	RATIO	U(ppm)	RHOs	RHOi	F.T.AGE(Ma)
1	4	18	12	0.222	15.2	3.512E+05	1.581E+06	48.8 ± 27.0
2	6	18	18	0.333	10.1	3.512E+05	1.054E+06	73.0 ± 34.5
3	13	34	18	0.382	19.1	7.610E+05	1.990E+06	83.7 ± 27.4
4	22	35	28	0.629	12.6	8.279E+05	1.317E+06	137.0 ± 37.4
	45	105			14.0	6.239E+05	1.456E+06	

Area of basic unit = 9.49E-07 cm-2

CHI SQUARED = 1.93868 WITH 3 DEGREES OF FREEDOM
P(chi squared) = 27.5 %
CORRELATION-COEFFICIENT = 0.905
VARIANCE OF SQR(Ns) = 1.46278
VARIANCE OF SQR(Ni) = .8877996

Ns/Ni = 0.429 ± 0.076
MEAN RATIO = 0.392 ± 0.086

Pooled Age = 93.8 ± 16.8 Ma
Mean Age = 85.7 ± 18.9 Ma
Central Age = 93.0 ± 17.4Ma
% Rel. Error = 9.80
Ages calculated using a zeta of 348.4 ± 5.8 for SRM 612 glass
RHO D = 1.283E+06cm-2; ND = 3060

9414-75 APATITE MARLBOROUGH

IRRADIATION WK143-11
SLIDE NUMBER 11
COUNTED BY: KAO

No.	Ns	Ni	Na	RATIO	U (ppm)	RHOs (E+06)	RHOi (E+06)	F.T.AGE (Ma)
1	2	5	4	0.400	12.1	0.506	1.264	94.6 ± 79.2
2	2	4	4	0.500	9.7	0.506	1.011	118.1 ± 102.3
3	1	4	4	0.250	9.7	0.253	1.011	59.3 ± 66.3
4	4	15	4	0.267	36.3	1.011	3.792	63.2 ± 35.6
	9	28			16.9	0.569	1.769	

AREA OF BASIC UNIT = 9.89E-07 cm
CHI SQUARED = .4944224 WITH 3 DEGREES OF FREEDOM
P(chi squared) = 92.0 %
CORRELATION COEFFICIENT = 0.940
VARIANCE OF SQR(Ns) = 0.17
VARIANCE OF SQR(Ni) = 0.82

Ns/Ni = 0.321 ± 0.123
MEAN RATIO = 0.354 ± 0.059

Ages calculated using a zeta of 348.4 ± 5.8 for SRM612 glass
RHO D = 1.368E+06 ; ND = 3383

POOLED AGE = 76.1 ± 29.2 Ma
MEAN AGE = 83.9 ± 14.1 Ma

9414-76 APATITE MARLBOROUGH

IRRADIATION WK143-12
SLIDE NUMBER 12
COUNTED BY: KAO

No.	Ns	Ni	Na	RATIO	U (ppm)	RHOs (E+06)	RHOi (E+06)	F.T.AGE (Ma)
1	6	28	9	0.214	29.8	0.674	3.146	51.4 ± 23.1
2	2	12	4	0.167	28.8	0.506	3.033	40.0 ± 30.6
3	1	5	4	0.200	12.0	0.253	1.264	48.0 ± 52.6
4	2	30	4	0.067	71.9	0.506	7.583	16.0 ± 11.7
5	1	5	4	0.200	12.0	0.253	1.264	48.0 ± 52.6
6	1	14	4	0.071	33.5	0.253	3.539	17.2 ± 17.8
	13	94			31.1	0.453	3.277	

AREA OF BASIC UNIT = 9.89E-07 cm
CHI SQUARED = 2.717953 WITH 5 DEGREES OF FREEDOM
P(chi squared) = 74.3 %
CORRELATION COEFFICIENT = 0.680
VARIANCE OF SQR(Ns) = 0.32
VARIANCE OF SQR(Ni) = 2.00

Ns/Ni = 0.138 ± 0.041
MEAN RATIO = 0.153 ± 0.027

Ages calculated using a zeta of 348.4 ± 5.8 for SRM612 glass
RHO D = 1.382E+06 ; ND = 3419

POOLED AGE = 33.2 ± 9.9 Ma
MEAN AGE = 36.8 ± 6.6 Ma

9414-77 Apatite

IRRADIATION wk143-13 COUNTED BY: Kao

No.	Ns	Ni	Na	RATIO	U(ppm)	RHOs	RHOi	F.T.AGE(Ma)
1	1	25	12	0.040	21.4	8.781E+04	2.195E+06	8.7 ± 8.8
2	0	10	16	0.000	6.4	0.000E+00	6.586E+05	0.0 ± 0.0
3	2	149	30	0.013	51.0	7.025E+04	5.234E+06	2.9 ± 2.1
	3	184			32.6	5.450E+04	3.343E+06	

Area of basic unit = 9.49E-07 cm-2

CHI SQUARED = .5328737 WITH 2 DEGREES OF FREEDOM
P(chi squared) = 58.7 %
CORRELATION COEFFICIENT = 0.911
VARIANCE OF SQR(Ns) = .5285954
VARIANCE OF SQR(Ni) = 22.85177

Ns/Ni = 0.016 ± 0.009
MEAN RATIO = 0.018 ± 0.012

Pooled Age = 3.5 ± 2.1 Ma
Mean Age = 3.9 ± 2.5 Ma
Central Age = 3.5 ± 2.1Ma
% Rel. Error = 0.00
Ages calculated using a zeta of 348.4 ± 5.8 for SRM 612 glass
RHO D = 1.261E+06cm-2; ND = 3119

9414-78 Apatite

IRRADIATION wk143-14 COUNTED BY: Kao

No.	Ns	Ni	Na	RATIO	U(ppm)	RHOs	RHOi	F.T.AGE(Ma)
1	6	332	36	0.018	94.1	1.756E+05	9.718E+06	3.9 ± 1.6
2	0	5	36	0.000	1.4	0.000E+00	1.464E+05	0.0 ± 0.0
3	0	10	18	0.000	5.7	0.000E+00	5.854E+05	0.0 ± 0.0
	6	347			39.3	7.025E+04	4.063E+06	

Area of basic unit = 9.49E-07 cm-2

CHI SQUARED = .1354382 WITH 2 DEGREES OF FREEDOM
P(chi squared) = 87.3 %
CORRELATION COEFFICIENT = 1.000
VARIANCE OF SQR(Ns) = 2
VARIANCE OF SQR(Ni) = 80.52213

Ns/Ni = 0.017 ± 0.007
MEAN RATIO = 0.006 ± 0.006

Pooled Age = 3.8 ± 1.6 Ma
Mean Age = 1.3 ± 1.3 Ma
Central Age = 3.8 ± 1.6Ma
% Rel. Error = 0.00
Ages calculated using a zeta of 348.4 ± 5.8 for SRM 612 glass
RHO D = 1.270E+06cm-2; ND = 3139

9414-79 Apatite

IRRADIATION wk143-15 COUNTED BY: Kao

No.	Ns	Ni	Na	RATIO	U(ppm)	RHOs	RHOi	F.T.AGE(Ma)
1	0	8	36	0.000	2.3	0.000E+00	2.342E+05	0.0 ± 0.0
2	0	5	18	0.000	2.8	0.000E+00	2.927E+05	0.0 ± 0.0
3	0	4	16	0.000	2.5	0.000E+00	2.634E+05	0.0 ± 0.0
4	0	36	24	0.000	15.2	0.000E+00	1.581E+06	0.0 ± 0.0
5	0	2	12	0.000	1.7	0.000E+00	1.756E+05	0.0 ± 0.0
6	1	10	18	0.100	5.6	5.854E+04	5.854E+05	21.9 ± 23.0
7	1	69	12	0.014	58.3	8.781E+04	6.059E+06	3.2 ± 3.2
8	2	36	27	0.056	13.5	7.805E+04	1.405E+06	12.2 ± 8.9
	4	170			10.6	2.586E+04	1.099E+06	

Area of basic unit = 9.49E-07 cm-2

CHI SQUARED = 2.638107 WITH 7 DEGREES OF FREEDOM
P(chi squared) = 62.6 %
CORRELATION COEFFICIENT = 0.525
VARIANCE OF SQR(Ns) = .3632705
VARIANCE OF SQR(Ni) = 6.059826

Ns/Ni = 0.024 ± 0.012
MEAN RATIO = 0.021 ± 0.013

Pooled Age = 5.2 ± 2.6 Ma
Mean Age = 4.7 ± 2.9 Ma
Central Age = 5.2 ± 2.6Ma
% Rel. Error = 2.39
Ages calculated using a zeta of 348.4 ± 5.8 for SRM 612 glass
RHO D = 1.278E+06cm-2; ND = 3159

9414-81 Apatite

IRRADIATION wk143-17 COUNTED BY: Kao

No.	Ns	Ni	Na	RATIO	U(ppm)	RHOs	RHOi	F.T.AGE(Ma)
1	0	33	9	0.000	36.7	0.000E+00	3.864E+06	0.0 ± 0.0
2	0	3	12	0.000	2.5	0.000E+00	2.634E+05	0.0 ± 0.0
3	1	29	24	0.034	12.1	4.391E+04	1.273E+06	7.7 ± 7.8
4	2	33	16	0.061	20.7	1.317E+05	2.173E+06	13.5 ± 9.8
5	1	13	30	0.077	4.3	3.512E+04	4.566E+05	17.1 ± 17.7
6	1	13	16	0.077	8.1	6.586E+04	8.562E+05	17.1 ± 17.7
7	1	43	24	0.023	17.9	4.391E+04	1.888E+06	5.2 ± 5.2
8	0	7	18	0.000	3.9	0.000E+00	4.098E+05	0.0 ± 0.0
9	3	63	12	0.048	52.6	2.634E+05	5.532E+06	10.6 ± 6.3
10	3	56	16	0.054	35.1	1.976E+05	3.688E+06	11.9 ± 7.1
	12	293			16.6	7.144E+04	1.744E+06	

Area of basic unit = 9.49E-07 cm-2

CHI SQUARED = 1.719458 WITH 9 DEGREES OF FREEDOM
P(chi squared) = 94.4 %
CORRELATION COEFFICIENT = 0.809
VARIANCE OF SQR(Ns) = .4575058
VARIANCE OF SQR(Ni) = 4.285392

Ns/Ni = 0.041 ± 0.012
MEAN RATIO = 0.037 ± 0.010

Pooled Age = 9.1 ± 2.7 Ma
Mean Age = 8.3 ± 2.2 Ma
Central Age = 9.1 ± 2.7Ma
% Rel. Error = 0.00
Ages calculated using a zeta of 348.4 ± 5.8 for SRM 612 glass
RHO D = 1.294E+06cm-2; ND = 3199

9414-82 Apatite

IRRADIATION wk143-18 COUNTED BY: Kao

No.	Ns	Ni	Na	RATIO	U(ppm)	RHOs	RHOi	F.T.AGE(Ma)
1	1	45	40	0.022	11.2	2.634E+04	1.185E+06	5.0 ± 5.0
2	0	3	12	0.000	2.5	0.000E+00	2.634E+05	0.0 ± 0.0
3	0	16	12	0.000	13.3	0.000E+00	1.405E+06	0.0 ± 0.0
4	0	4	8	0.000	5.0	0.000E+00	5.269E+05	0.0 ± 0.0
5	0	3	12	0.000	2.5	0.000E+00	2.634E+05	0.0 ± 0.0
6	0	19	36	0.000	5.3	0.000E+00	5.561E+05	0.0 ± 0.0
7	2	23	36	0.087	6.4	5.854E+04	6.732E+05	19.4 ± 14.3
8	0	16	24	0.000	6.6	0.000E+00	7.025E+05	0.0 ± 0.0
9	0	19	36	0.000	5.3	0.000E+00	5.561E+05	0.0 ± 0.0
10	0	18	16	0.000	11.2	0.000E+00	1.185E+06	0.0 ± 0.0
11	0	36	24	0.000	14.9	0.000E+00	1.581E+06	0.0 ± 0.0
12	1	53	40	0.019	13.2	2.634E+04	1.396E+06	4.2 ± 4.3
13	0	1	24	0.000	0.4	0.000E+00	4.391E+04	0.0 ± 0.0
	4	256			8.0	1.317E+04	8.430E+05	

Area of basic unit = 9.49E-07 cm-2

CHI SQUARED = 4.578816 WITH 12 DEGREES OF FREEDOM
P(chi squared) = 68.9 %
CORRELATION COEFFICIENT = 0.527
VARIANCE OF SQR(Ns) = .2586099
VARIANCE OF SQR(Ni) = 3.860596

Ns/Ni = 0.016 ± 0.008
MEAN RATIO = 0.010 ± 0.007

Pooled Age = 3.5 ± 1.8 Ma
Mean Age = 2.2 ± 1.5 Ma
Central Age = 3.5 ± 1.8Ma
% Rel. Error = 11.18
Ages calculated using a zeta of 348.4 ± 5.8 for SRM 612 glass
RHO D = 1.302E+06cm-2; ND = 3219

9414-83 APATITE Apatite

IRRADIATION wk143
SLIDE NUMBER 19
COUNTED BY: Kao

No.	Ns	Ni	Na	RATIO	U (ppm)	RHOs (E+06)	RHOi (E+06)	F.T.AGE (Ma)
1	8	33	24	0.242	13.9	0.337	1.390	54.3 ± 21.4
2	8	16	15	0.500	10.8	0.539	1.079	111.5 ± 48.4
3	1	2	9	0.500	2.2	0.112	0.225	111.5 ± 136.6
4	2	3	9	0.667	3.4	0.225	0.337	148.3 ± 135.4
5	0	1	18	0.000	0.6	0.000	0.056	0.0 ± 0.0
6	6	8	9	0.750	9.0	0.674	0.899	166.6 ± 90.0
7	1	2	12	0.500	1.7	0.084	0.169	111.5 ± 136.6
8	3	8	12	0.375	6.7	0.253	0.674	83.8 ± 56.8
9	2	6	8	0.333	7.6	0.253	0.758	74.6 ± 60.9
10	46	102	12	0.451	85.9	3.876	8.595	100.7 ± 18.0
11	2	3	6	0.667	5.1	0.337	0.506	148.3 ± 135.4
12	3	4	10	0.750	4.0	0.303	0.404	166.6 ± 127.3
13	4	3	12	1.333	2.5	0.337	0.253	293.2 ± 224.0
14	3	5	24	0.600	2.1	0.126	0.211	133.6 ± 97.6
15	4	18	32	0.222	5.7	0.126	0.569	49.8 ± 27.6
16	5	5	16	1.000	3.2	0.316	0.316	221.2 ± 140.0
17	64	214	24	0.299	90.2	2.696	9.016	66.9 ± 9.6
18	0	2	6	0.000	3.4	0.000	0.337	0.0 ± 0.0
19	9	32	36	0.281	9.0	0.253	0.899	63.0 ± 23.8
20	0	1	16	0.000	0.6	0.000	0.063	0.0 ± 0.0
	171	468			15.3	0.558	1.526	

AREA OF BASIC UNIT = 9.89E-07 cm
CHI SQUARED = 18.13217 WITH 19 DEGREES OF FREEDOM
P(chi squared) = 51.4 %
CORRELATION COEFFICIENT = 0.977
VARIANCE OF SQR(Ns) = 4.01
VARIANCE OF SQR(Ni) = 11.59

Ns/Ni = 0.365 ± 0.033
MEAN RATIO = 0.474 ± 0.075

Ages calculated using a zeta of 348.4 ± 5.8 for SRM612 glass
RHO D = 1.310E+06 ; ND = 3239

POOLED AGE = 81.7 ± 7.5 Ma
MEAN AGE = 105.7 ± 16.9 Ma

9414-84 APATITE Apatite

IRRADIATION WK143
SLIDE NUMBER 20
COUNTED BY: Kao

No.	Ns	Ni	Na	RATIO	U (ppm)	RHOs (E+06)	RHOi (E+06)	F.T.AGE (Ma)
1	20	25	24	0.800	10.5	0.843	1.053	178.6 ± 53.7
2	5	11	12	0.455	9.2	0.421	0.927	102.1 ± 55.1
3	39	47	24	0.830	19.7	1.643	1.980	185.2 ± 40.3
4	37	71	32	0.521	22.3	1.169	2.243	116.9 ± 23.8
5	1	5	24	0.200	2.1	0.042	0.211	45.1 ± 49.4
6	71	126	40	0.563	31.7	1.795	3.185	126.3 ± 18.9
7	6	11	16	0.545	6.9	0.379	0.695	122.3 ± 62.1
8	23	49	12	0.469	41.0	1.938	4.129	105.4 ± 26.7
9	21	38	12	0.553	31.8	1.769	3.202	123.9 ± 33.8
10	7	16	16	0.438	10.0	0.442	1.011	98.3 ± 44.6
11	3	4	10	0.750	4.0	0.303	0.404	167.6 ± 128.0
12	1	1	16	1.000	0.6	0.063	0.063	222.5 ± 314.7
13	4	7	16	0.571	4.4	0.253	0.442	128.1 ± 80.3
14	10	15	24	0.667	6.3	0.421	0.632	149.2 ± 61.0
15	7	13	24	0.538	5.4	0.295	0.548	120.8 ± 56.7
16	26	47	36	0.553	13.1	0.730	1.320	124.0 ± 30.4
17	0	1	8	0.000	1.3	0.000	0.126	0.0 ± 0.0
18	2	3	15	0.667	2.0	0.135	0.202	149.2 ± 136.2
19	0	1	16	0.000	0.6	0.000	0.063	0.0 ± 0.0
20	2	4	8	0.500	5.0	0.253	0.506	112.2 ± 97.2
	285	495			12.9	0.748	1.300	

AREA OF BASIC UNIT = 9.89E-07 cm
CHI SQUARED = 8.285906 WITH 19 DEGREES OF FREEDOM
P(chi squared) = 98.4 %
CORRELATION COEFFICIENT = 0.981
VARIANCE OF SQR(Ns) = 5.08
VARIANCE OF SQR(Ni) = 7.81

Ns/Ni = 0.576 ± 0.043
MEAN RATIO = 0.531 ± 0.055

Ages calculated using a zeta of 348.4 ± 5.8 for SRM612 glass
RHO D = 1.318E+06 ; ND = 3259

POOLED AGE = 129.0 ± 10.0 Ma
MEAN AGE = 119.1 ± 12.7 Ma

9414-86 Apatite

IRRADIATION wk144-2 COUNTED BY: Kao

No.	Ns	Ni	Na	RATIO	U(ppm)	RHOs	RHOi	F.T.AGE(Ma)
1	7	124	24	0.056	52.2	2.949E+05	5.224E+06	11.9 ± 4.6
2	13	237	36	0.055	66.5	3.651E+05	6.657E+06	11.6 ± 3.3
3	0	1	12	0.000	0.8	0.000E+00	8.426E+04	0.0 ± 0.0
4	3	68	36	0.044	19.1	8.426E+04	1.910E+06	9.3 ± 5.5
5	4	16	36	0.250	4.5	1.123E+05	4.494E+05	52.6 ± 29.4
6	5	20	40	0.250	5.1	1.264E+05	5.056E+05	52.6 ± 26.3
7	3	24	50	0.125	4.8	6.067E+04	4.853E+05	26.4 ± 16.2
	35	490			21.2	1.512E+05	2.117E+06	

Area of basic unit = 9.89E-07 cm-2

CHI SQUARED = 7.849338 WITH 6 DEGREES OF FREEDOM
P(chi squared) = 1.5 %
CORRELATION COEFFICIENT = 0.925
VARIANCE OF SQR(Ns) = 1.198962
VARIANCE OF SQR(Ni) = 24.15494

Ns/Ni = 0.071 ± 0.012
MEAN RATIO = 0.111 ± 0.038

Pooled Age = 15.1 ± 2.7 Ma
Mean Age = 23.5 ± 8.1 Ma
Central Age = 19.5 ± 5.3Ma
% Rel. Error = 46.75
Ages calculated using a zeta of 348.4 ± 5.8 for SRM 612 glass
RHO D = 1.231E+06cm-2; ND = 3043

9414-87 APATITE Apatite

IRRADIATION FT:WK144
SLIDE NUMBER 3
COUNTED BY: Kao

No.	Ns	Ni	Na	RATIO	U (ppm)	RHOs (E+06)	RHOi (E+06)	F.T.AGE (Ma)
1	20	48	24	0.417	21.4	0.843	2.022	87.8 ± 23.4
2	11	44	36	0.250	13.1	0.309	1.236	52.8 ± 17.8
3	2	16	25	0.125	6.9	0.081	0.647	26.5 ± 19.9
4	4	30	60	0.133	5.4	0.067	0.506	28.2 ± 15.0
5	10	43	90	0.233	5.1	0.112	0.483	49.1 ± 17.3
6	27	94	30	0.287	33.6	0.910	3.168	60.6 ± 13.3
7	2	10	24	0.200	4.5	0.084	0.421	42.3 ± 32.8
8	10	20	48	0.500	4.5	0.211	0.421	105.2 ± 40.8
9	5	20	24	0.250	8.9	0.211	0.843	52.8 ± 26.4
10	2	22	15	0.091	15.7	0.135	1.483	19.3 ± 14.2
11	0	7	12	0.000	6.3	0.000	0.590	0.0 ± 0.0
12	2	10	24	0.200	4.5	0.084	0.421	42.3 ± 32.8
13	2	12	24	0.167	5.4	0.084	0.506	35.3 ± 26.9
14	7	16	30	0.438	5.7	0.236	0.539	92.1 ± 41.8
15	2	15	36	0.133	4.5	0.056	0.421	28.2 ± 21.3
16	4	31	24	0.129	13.9	0.169	1.306	27.3 ± 14.5
17	0	1	50	0.000	0.2	0.000	0.020	0.0 ± 0.0
18	1	11	20	0.091	5.9	0.051	0.556	19.3 ± 20.1
19	13	49	24	0.265	21.9	0.548	2.064	56.0 ± 17.5
20	2	8	8	0.250	10.7	0.253	1.011	52.8 ± 41.8
	126	507			8.7	0.203	0.816	

AREA OF BASIC UNIT = 9.89E-07 cm
CHI SQUARED = 19.38509 WITH 19 DEGREES OF FREEDOM
P(chi squared) = 43.2 %
CORRELATION COEFFICIENT = 0.925
VARIANCE OF SQR(Ns) = 1.83
VARIANCE OF SQR(Ni) = 3.95

Ns/Ni = 0.249 ± 0.025
MEAN RATIO = 0.208 ± 0.030

Ages calculated using a zeta of 348.4 ± 5.8 for SRM612 glass
RHO D = 1.235E+06 ; ND = 3053

POOLED AGE = 52.5 ± 5.4 Ma
MEAN AGE = 44.0 ± 6.4 Ma

9414-88 APATITE Apatite

IRRADIATION FT:WK144
SLIDE NUMBER 4
COUNTED BY: Kao

No.	Ns	Ni	Na	RATIO	U (ppm)	RHOs (E+06)	RHOi (E+06)	F.T.AGE (Ma)
1	2	5	18	0.400	3.0	0.112	0.281	84.6 ± 70.8
2	3	6	12	0.500	5.3	0.253	0.506	105.5 ± 74.7
3	7	20	12	0.350	17.8	0.590	1.685	74.1 ± 32.6
4	19	37	18	0.514	22.0	1.067	2.078	108.4 ± 30.7
5	6	12	12	0.500	10.7	0.506	1.011	105.5 ± 52.8
6	3	4	9	0.750	4.8	0.337	0.449	157.7 ± 120.5
7	41	125	24	0.328	55.7	1.727	5.266	69.4 ± 12.6
8	8	32	9	0.250	38.0	0.899	3.595	53.0 ± 21.0
	89	241			22.6	0.789	2.138	

AREA OF BASIC UNIT = 9.89E-07 cm
CHI SQUARED = 4.274267 WITH 7 DEGREES OF FREEDOM
P(chi squared) = 74.8 %
CORRELATION COEFFICIENT = 0.980
VARIANCE OF SQR(Ns) = 2.80
VARIANCE OF SQR(Ni) = 9.26

Ns/Ni = 0.369 ± 0.046
MEAN RATIO = 0.449 ± 0.055

Ages calculated using a zeta of 348.4 ± 5.8 for SRM612 glass
RHO D = 1.239E+06 ; ND = 3063

POOLED AGE = 78.1 ± 9.8 Ma
MEAN AGE = 94.8 ± 11.7 Ma

9414-90 Apatite

IRRADIATION wk144-05 COUNTED BY: Kao

No.	Ns	Ni	Na	RATIO	U(ppm)	RHOs	RHOi	F.T.AGE(Ma)
1	0	9	30	0.000	3.1	0.000E+00	3.161E+05	0.0 ± 0.0
2	1	25	16	0.040	16.3	6.586E+04	1.646E+06	8.5 ± 8.7
3	1	12	24	0.083	5.2	4.391E+04	5.269E+05	17.8 ± 18.5
4	7	81	120	0.086	7.0	6.147E+04	7.113E+05	18.4 ± 7.3
5	0	6	18	0.000	3.5	0.000E+00	3.512E+05	0.0 ± 0.0
	9	133			6.7	4.559E+04	6.738E+05	

Area of basic unit = 9.49E-07 cm-2

CHI SQUARED = .857267 WITH 4 DEGREES OF FREEDOM
P(chi squared) = 78.8 %
CORRELATION COEFFICIENT = 0.989
VARIANCE OF SQR(Ns) = 1.17085
VARIANCE OF SQR(Ni) = 6.998367

Ns/Ni = 0.068 ± 0.023
MEAN RATIO = 0.042 ± 0.019

Pooled Age = 14.4 ± 5.0 Ma
Mean Age = 8.9 ± 4.1 Ma
Central Age = 14.4 ± 5.0Ma
% Rel. Error = 0.00
Ages calculated using a zeta of 348.4 ± 5.8 for SRM 612 glass
RHO D = 1.243E+06cm-2; ND = 3074

9414-91 Apatite

IRRADIATION wk144-06 COUNTED BY: Kao

No.	Ns	Ni	Na	RATIO	U(ppm)	RHOs	RHOi	F.T.AGE(Ma)
1	1	3	9	0.333	3.5	1.171E+05	3.512E+05	71.0 ± 82.0
2	3	20	48	0.150	4.3	6.586E+04	4.391E+05	32.0 ± 19.9
3	1	9	30	0.111	3.1	3.512E+04	3.161E+05	23.8 ± 25.0
4	1	16	70	0.062	2.4	1.505E+04	2.409E+05	13.4 ± 13.8
5	2	26	48	0.077	5.6	4.391E+04	5.708E+05	16.5 ± 12.1
6	0	2	24	0.000	0.9	0.000E+00	8.781E+04	0.0 ± 0.0
7	0	6	24	0.000	2.6	0.000E+00	2.634E+05	0.0 ± 0.0
8	2	22	60	0.091	3.8	3.512E+04	3.864E+05	19.4 ± 14.4
9	4	28	80	0.143	3.6	5.269E+04	3.688E+05	30.5 ± 16.3
10	0	6	24	0.000	2.6	0.000E+00	2.634E+05	0.0 ± 0.0
11	1	5	18	0.200	2.9	5.854E+04	2.927E+05	42.7 ± 46.8
12	0	1	18	0.000	0.6	0.000E+00	5.854E+04	0.0 ± 0.0
13	1	21	36	0.048	6.1	2.927E+04	6.147E+05	10.2 ± 10.4
14	0	2	12	0.000	1.7	0.000E+00	1.756E+05	0.0 ± 0.0
15	1	3	24	0.333	1.3	4.391E+04	1.317E+05	71.0 ± 82.0
16	1	4	24	0.250	1.7	4.391E+04	1.756E+05	53.3 ± 59.6
17	1	7	32	0.143	2.3	3.293E+04	2.305E+05	30.5 ± 32.6
18	2	5	16	0.400	3.2	1.317E+05	3.293E+05	85.1 ± 71.2
19	2	19	60	0.105	3.3	3.512E+04	3.337E+05	22.5 ± 16.7
20	3	14	30	0.214	4.8	1.054E+05	4.917E+05	45.7 ± 29.1
	26	219			3.3	3.988E+04	3.359E+05	

Area of basic unit = 9.49E-07 cm-2

CHI SQUARED = 4.896168 WITH 19 DEGREES OF FREEDOM
P(chi squared) = 95.8 %
CORRELATION COEFFICIENT = 0.743
VARIANCE OF SQR(Ns) = .4062869
VARIANCE OF SQR(Ni) = 1.879552

Ns/Ni = 0.119 ± 0.025
MEAN RATIO = 0.133 ± 0.027

Pooled Age = 25.4 ± 5.3 Ma
Mean Age = 28.4 ± 5.9 Ma
Central Age = 25.4 ± 5.3Ma
% Rel. Error = 0.00
Ages calculated using a zeta of 348.4 ± 5.8 for SRM 612 glass
RHO D = 1.247E+06cm-2; ND = 3084

9414-92 APATITE MARLBOROUGH

IRRADIATION WK144-7
SLIDE NUMBER 7
COUNTED BY: KAO

No.	Ns	Ni	Na	RATIO	U (ppm)	RHOs (E+06)	RHOi (E+06)	F.T.AGE (Ma)
1	1	2	4	0.500	4.7	0.253	0.506	120.8 ± 148.0
2	2	5	4	0.400	11.8	0.506	1.264	96.8 ± 81.0
3	1	3	4	0.333	7.1	0.253	0.758	80.8 ± 93.3
4	2	3	4	0.667	7.1	0.506	0.758	160.6 ± 146.6
5	1	3	4	0.333	7.1	0.253	0.758	80.8 ± 93.3
	7	16			7.6	0.354	0.809	

AREA OF BASIC UNIT = 9.89E-07 cm
CHI SQUARED = .351063 WITH 4 DEGREES OF FREEDOM
P(chi squared) = 98.6 %
CORRELATION COEFFICIENT = 0.667
VARIANCE OF SQR(Ns) = 0.05
VARIANCE OF SQR(Ni) = 0.09

Ns/Ni = 0.438 ± 0.198
MEAN RATIO = 0.447 ± 0.063

Ages calculated using a zeta of 348.4 ± 5.8 for SRM612 glass
RHO D = 1.400E+06 ; ND = 3461

POOLED AGE = 105.8 ± 48.0 Ma
MEAN AGE = 108.0 ± 15.4 Ma

9414-93 APATITE MARLBOROUGH

IRRADIATION WK144-8
SLIDE NUMBER 8
COUNTED BY: KAO

No.	Ns	Ni	Na	RATIO	U (ppm)	RHOs (E+06)	RHOi (E+06)	F.T.AGE (Ma)
1	2	3	4	0.667	7.1	0.506	0.758	160.9 ± 146.9
2	2	4	8	0.500	4.7	0.253	0.506	121.1 ± 104.9
3	5	10	8	0.500	11.8	0.632	1.264	121.1 ± 66.4
4	4	8	9	0.500	8.4	0.449	0.899	121.1 ± 74.2
5	2	4	6	0.500	6.3	0.337	0.674	121.1 ± 104.9
6	2	3	4	0.667	7.1	0.506	0.758	160.9 ± 146.9
7	2	5	4	0.400	11.8	0.506	1.264	97.0 ± 81.2
	19	37			8.1	0.447	0.870	

AREA OF BASIC UNIT = 9.89E-07 cm
CHI SQUARED = .260218 WITH 6 DEGREES OF FREEDOM
P(chi squared) = 100.0 %
CORRELATION COEFFICIENT = 0.967
VARIANCE OF SQR(Ns) = 0.12
VARIANCE OF SQR(Ni) = 0.30

Ns/Ni = 0.514 ± 0.145
MEAN RATIO = 0.533 ± 0.037

Ages calculated using a zeta of 348.4 ± 5.8 for SRM612 glass
RHO D = 1.403E+06 ; ND = 3469

POOLED AGE = 124.3 ± 35.2 Ma
MEAN AGE = 129.0 ± 9.5 Ma

9414-94 APATITE MARLBOROUGH

IRRADIATION WK144-9
SLIDE NUMBER 9
COUNTED BY: KAO

No.	Ns	Ni	Na	RATIO	U (ppm)	RHOs (E+06)	RHOi (E+06)	F.T.AGE (Ma)
1	1	4	4	0.250	9.4	0.253	1.011	61.0 ± 68.2
2	3	6	4	0.500	14.1	0.758	1.517	121.4 ± 85.9
3	8	21	12	0.381	16.5	0.674	1.769	92.7 ± 38.6
4	1	3	4	0.333	7.1	0.253	0.758	81.2 ± 93.8
5	2	3	4	0.667	7.1	0.506	0.758	161.4 ± 147.4
6	1	4	4	0.250	9.4	0.253	1.011	61.0 ± 68.2
7	2	4	4	0.500	9.4	0.506	1.011	121.4 ± 105.2
8	3	8	8	0.375	9.4	0.379	1.011	91.3 ± 61.8
9	1	4	4	0.250	9.4	0.253	1.011	61.0 ± 68.2
10	1	3	4	0.333	7.1	0.253	0.758	81.2 ± 93.8
	23	60			10.9	0.447	1.167	

AREA OF BASIC UNIT = 9.89E-07 cm
CHI SQUARED = 1.089515 WITH 9 DEGREES OF FREEDOM
P(chi squared) = 99.9 %
CORRELATION COEFFICIENT = 0.972
VARIANCE OF SQR(Ns) = 0.34
VARIANCE OF SQR(Ni) = 0.76

Ns/Ni = 0.383 ± 0.094
MEAN RATIO = 0.384 ± 0.043

Ages calculated using a zeta of 348.4 ± 5.4 for SRM612 glass
RHO D = 1.407E+06 ; ND = 3486

POOLED AGE = 93.3 ± 23.0 Ma
MEAN AGE = 93.4 ± 10.7 Ma

9414-95 APATITE MARLBOROUGH

IRRADIATION WK144-10
SLIDE NUMBER 10
COUNTED BY: KAO

No.	Ns	Ni	Na	RATIO	U (ppm)	RHOs (E+06)	RHOi (E+06)	F.T.AGE (Ma)
1	2	4	4	0.500	9.4	0.506	1.011	121.7 ± 105.4
2	5	10	12	0.500	7.8	0.421	0.843	121.7 ± 66.7
3	4	11	4	0.364	25.8	1.011	2.781	88.7 ± 51.8
	11	25			11.7	0.556	1.264	

AREA OF BASIC UNIT = 9.89E-07 cm
CHI SQUARED = .1832727 WITH 2 DEGREES OF FREEDOM
P(chi squared) = 91.2 %
CORRELATION COEFFICIENT = 0.893
VARIANCE OF SQR(Ns) = 0.18
VARIANCE OF SQR(Ni) = 0.52

Ns/Ni = 0.440 ± 0.159
MEAN RATIO = 0.455 ± 0.045

Ages calculated using a zeta of 348.4 ± 5.8 for SRM612 glass
RHO D = 1.410E+06 ; ND = 3486

POOLED AGE = 107.2 ± 38.9 Ma
MEAN AGE = 110.7 ± 11.4 Ma

9414-96 Apatite

IRRADIATION wk144-11 COUNTED BY: Kao

No.	Ns	Ni	Na	RATIO	U(ppm)	RHOs	RHOi	F.T.AGE(Ma)
1	2	9	30	0.222	3.1	7.025E+04	3.161E+05	48.2 ± 37.7
2	6	43	18	0.140	24.4	3.512E+05	2.517E+06	30.3 ± 13.2
3	61	177	50	0.345	36.2	1.286E+06	3.730E+06	74.6 ± 11.2
4	4	28	80	0.143	3.6	5.269E+04	3.688E+05	31.0 ± 16.6
5	3	6	24	0.500	2.6	1.317E+05	2.634E+05	108.0 ± 76.4
	76	263			13.3	3.965E+05	1.372E+06	

Area of basic unit = 9.49E-07 cm-2

CHI SQUARED = 3.433704 WITH 4 DEGREES OF FREEDOM
P(chi squared) = 14.3 %
CORRELATION COEFFICIENT = 0.987
VARIANCE OF SQR(Ns) = 7.132754
VARIANCE OF SQR(Ni) = 18.92416

Ns/Ni = 0.289 ± 0.038
MEAN RATIO = 0.270 ± 0.069

Pooled Age = 62.6 ± 8.3 Ma
Mean Age = 58.5 ± 14.9 Ma
Central Age = 54.8 ± 11.9Ma
% Rel. Error = 27.63
Ages calculated using a zeta of 348.4 ± 5.8 for SRM 612 glass
RHO D = 1.268E+06cm-2; ND = 3135

9414-97 Apatite

IRRADIATION wk144-12 COUNTED BY: Kao

No.	Ns	Ni	Na	RATIO	U(ppm)	RHOs	RHOi	F.T.AGE(Ma)
1	2	4	20	0.500	2.0	1.054E+05	2.107E+05	108.3 ± 93.8
2	3	16	30	0.188	5.4	1.054E+05	5.620E+05	40.8 ± 25.7
3	3	12	36	0.250	3.4	8.781E+04	3.512E+05	54.4 ± 35.1
	8	32			3.8	9.802E+04	3.921E+05	

Area of basic unit = 9.49E-07 cm-2

CHI SQUARED = .4385965 WITH 2 DEGREES OF FREEDOM
P(chi squared) = 64.5 %
CORRELATION COEFFICIENT = 0.945
VARIANCE OF SQR(Ns) = 3.367305E-02
VARIANCE OF SQR(Ni) = 1.071796

Ns/Ni = 0.250 ± 0.099
MEAN RATIO = 0.312 ± 0.095

Pooled Age = 54.4 ± 21.5 Ma
Mean Age = 67.9 ± 20.8 Ma
Central Age = 54.4 ± 21.5Ma
% Rel. Error = 0.00
Ages calculated using a zeta of 348.4 ± 5.8 for SRM 612 glass
RHO D = 1.272E+06cm-2; ND = 3145

9414-98 Apatite

IRRADIATION wk144-13 COUNTED BY: Kao

No.	Ns	Ni	Na	RATIO	U(ppm)	RHOs	RHOi	F.T.AGE(Ma)
1	3	12	24	0.250	5.1	1.317E+05	5.269E+05	54.6 ± 35.2
2	45	142	30	0.317	48.1	1.581E+06	4.988E+06	69.1 ± 11.9
	48	154			29.0	9.367E+05	3.005E+06	

Area of basic unit = 9.49E-07 cm-2

CHI SQUARED = 6.330469E-02 WITH 1 DEGREES OF FREEDOM
P(chi squared) = 72.2 %
CORRELATION COEFFICIENT = 1.000
VARIANCE OF SQR(Ns) = 12.38105
VARIANCE OF SQR(Ni) = 35.72047

Ns/Ni = 0.312 ± 0.052
MEAN RATIO = 0.283 ± 0.033

Pooled Age = 67.9 ± 11.3 Ma
Mean Age = 61.8 ± 7.4 Ma
Central Age = 67.9 ± 11.3Ma
% Rel. Error = 0.00
Ages calculated using a zeta of 348.4 ± 5.8 for SRM 612 glass
RHO D = 1.276E+06cm-2; ND = 3155

9414-99 Apatite

IRRADIATION wk144-14 COUNTED BY: Kao

No.	Ns	Ni	Na	RATIO	U(ppm)	RHOs	RHOi	F.T.AGE(Ma)
1	6	25	50	0.240	5.1	1.264E+05	5.269E+05	52.5 ± 23.9
2	1	4	9	0.250	4.5	1.171E+05	4.683E+05	54.7 ± 61.2
3	4	28	36	0.143	7.9	1.171E+05	8.196E+05	31.3 ± 16.8
4	3	11	18	0.273	6.2	1.756E+05	6.440E+05	59.7 ± 38.9
5	7	21	30	0.333	7.1	2.459E+05	7.376E+05	72.9 ± 31.8
6	9	24	40	0.375	6.1	2.371E+05	6.322E+05	81.9 ± 32.1
7	3	7	12	0.429	5.9	2.634E+05	6.147E+05	93.5 ± 64.6
8	3	5	30	0.600	1.7	1.054E+05	1.756E+05	130.6 ± 95.4
9	3	21	40	0.143	5.3	7.903E+04	5.532E+05	31.3 ± 19.3
	39	146			5.6	1.551E+05	5.806E+05	

Area of basic unit = 9.49E-07 cm-2

CHI SQUARED = 2.665965 WITH 8 DEGREES OF FREEDOM
P(chi squared) = 72.2 %
CORRELATION COEFFICIENT = 0.681
VARIANCE OF SQR(Ns) = .3632698
VARIANCE OF SQR(Ni) = 1.666885

Ns/Ni = 0.267 ± 0.048
MEAN RATIO = 0.309 ± 0.048

Pooled Age = 58.5 ± 10.6 Ma
Mean Age = 67.7 ± 10.7 Ma
Central Age = 58.5 ± 10.6Ma
% Rel. Error = 0.26
Ages calculated using a zeta of 348.4 ± 5.8 for SRM 612 glass
RHO D = 1.280E+06cm-2; ND = 3165

9414-100 Apatite

IRRADIATION wk144-15 COUNTED BY: Kao

No.	Ns	Ni	Na	RATIO	U(ppm)	RHOs	RHOi	F.T.AGE(Ma)
1	4	10	30	0.400	3.4	1.405E+05	3.512E+05	87.6 ± 51.9
2	0	1	56	0.000	0.2	0.000E+00	1.882E+04	0.0 ± 0.0
3	0	1	6	0.000	1.7	0.000E+00	1.756E+05	0.0 ± 0.0
4	7	29	60	0.241	4.9	1.229E+05	5.093E+05	53.0 ± 22.4
	11	41			2.7	7.626E+04	2.842E+05	

Area of basic unit = 9.49E-07 cm-2

CHI SQUARED = .5307429 WITH 3 DEGREES OF FREEDOM
P(chi squared) = 78.6 %
CORRELATION COEFFICIENT = 0.966
VARIANCE OF SQR(Ns) = 1.868083
VARIANCE OF SQR(Ni) = 4.395955

Ns/Ni = 0.268 ± 0.091
MEAN RATIO = 0.160 ± 0.098

Pooled Age = 58.9 ± 20.0 Ma
Mean Age = 35.3 ± 21.6 Ma
Central Age = 58.9 ± 20.0Ma
% Rel. Error = 0.00
Ages calculated using a zeta of 348.4 ± 5.8 for SRM 612 glass
RHO D = 1.284E+06cm-2; ND = 3175

9414-101 Apatite

IRRADIATION wk144-16 COUNTED BY: Kao

No.	Ns	Ni	Na	RATIO	U(ppm)	RHOs	RHOi	F.T.AGE(Ma)
1	1	7	9	0.143	7.8	1.171E+05	8.196E+05	31.5 ± 33.7
2	1	12	30	0.083	4.0	3.512E+04	4.215E+05	18.4 ± 19.2
3	16	47	24	0.340	19.7	7.025E+05	2.064E+06	74.9 ± 21.7
	18	66			10.5	3.011E+05	1.104E+06	

Area of basic unit = 9.49E-07 cm-2

CHI SQUARED = 1.212445 WITH 2 DEGREES OF FREEDOM
P(chi squared) = 29.7 %
CORRELATION COEFFICIENT = 0.993
VARIANCE OF SQR(Ns) = 3
VARIANCE OF SQR(Ni) = 4.982603

Ns/Ni = 0.273 ± 0.073
MEAN RATIO = 0.189 ± 0.078

Pooled Age = 60.0 ± 16.0 Ma
Mean Age = 41.6 ± 17.2 Ma
Central Age = 60.0 ± 16.0Ma
% Rel. Error = 0.96
Ages calculated using a zeta of 348.4 ± 5.8 for SRM 612 glass
RHO D = 1.288E+06cm-2; ND = 3185

9414-104 Apatite

IRRADIATION wk144-19 COUNTED BY: Kao

No.	Ns	Ni	Na	RATIO	U(ppm)	RHOs	RHOi	F.T.AGE(Ma)
1	0	8	24	0.000	3.3	0.000E+00	3.512E+05	0.0 ± 0.0
2	0	2	16	0.000	1.2	0.000E+00	1.317E+05	0.0 ± 0.0
3	0	1	18	0.000	0.6	0.000E+00	5.854E+04	0.0 ± 0.0
4	0	5	16	0.000	3.1	0.000E+00	3.293E+05	0.0 ± 0.0
5	3	62	110	0.048	5.6	2.874E+04	5.939E+05	10.8 ± 6.4
6	0	12	24	0.000	5.0	0.000E+00	5.269E+05	0.0 ± 0.0
7	0	14	30	0.000	4.6	0.000E+00	4.917E+05	0.0 ± 0.0
8	1	12	12	0.083	10.0	8.781E+04	1.054E+06	18.6 ± 19.4
9	1	14	30	0.071	4.6	3.512E+04	4.917E+05	15.9 ± 16.5
10	0	9	24	0.000	3.7	0.000E+00	3.952E+05	0.0 ± 0.0
11	0	8	18	0.000	4.4	0.000E+00	4.683E+05	0.0 ± 0.0
12	0	21	60	0.000	3.5	0.000E+00	3.688E+05	0.0 ± 0.0
13	1	15	20	0.067	7.5	5.269E+04	7.903E+05	14.9 ± 15.4
14	1	6	18	0.167	3.3	5.854E+04	3.512E+05	37.1 ± 40.1
15	1	40	50	0.025	8.0	2.107E+04	8.430E+05	5.6 ± 5.7
16	0	16	40	0.000	4.0	0.000E+00	4.215E+05	0.0 ± 0.0
17	1	26	50	0.038	5.2	2.107E+04	5.479E+05	8.6 ± 8.8
18	3	43	60	0.070	7.1	5.269E+04	7.552E+05	15.6 ± 9.3
19	0	16	36	0.000	4.4	0.000E+00	4.683E+05	0.0 ± 0.0
20	0	8	16	0.000	5.0	0.000E+00	5.269E+05	0.0 ± 0.0
	12	338			5.0	1.882E+04	5.300E+05	

Area of basic unit = 9.49E-07 cm-2

CHI SQUARED = 5.029557 WITH 19 DEGREES OF FREEDOM
P(chi squared) = 95.1 %
CORRELATION COEFFICIENT = 0.823
VARIANCE OF SQR(Ns) = .3958705
VARIANCE OF SQR(Ni) = 2.865353

Ns/Ni = 0.036 ± 0.010
MEAN RATIO = 0.028 ± 0.010

Pooled Age = 7.9 ± 2.3 Ma
Mean Age = 6.4 ± 2.2 Ma
Central Age = 7.9 ± 2.3Ma
% Rel. Error = 0.05
Ages calculated using a zeta of 348.4 ± 5.8 for SRM 612 glass
RHO D = 1.301E+06cm-2; ND = 3216

9414-105 Apatite

IRRADIATION wk144-20 COUNTED BY: Kao

No.	Ns	Ni	Na	RATIO	U(ppm)	RHOs	RHOi	F.T.AGE(Ma)
1	4	24	60	0.167	4.0	7.025E+04	4.215E+05	37.2 ± 20.1
2	0	6	36	0.000	1.7	0.000E+00	1.756E+05	0.0 ± 0.0
3	3	3	18	1.000	1.7	1.756E+05	1.756E+05	220.3 ±180.0
4	0	17	36	0.000	4.7	0.000E+00	4.976E+05	0.0 ± 0.0
5	3	10	18	0.300	5.5	1.756E+05	5.854E+05	66.9 ± 44.1
6	3	26	40	0.115	6.5	7.903E+04	6.849E+05	25.8 ± 15.7
7	1	12	40	0.083	3.0	2.634E+04	3.161E+05	18.6 ± 19.4
8	2	14	24	0.143	5.8	8.781E+04	6.147E+05	31.9 ± 24.2
9	1	28	50	0.036	5.6	2.107E+04	5.901E+05	8.0 ± 8.1
10	1	14	32	0.071	4.3	3.293E+04	4.610E+05	16.0 ± 16.6
11	3	16	32	0.188	5.0	9.879E+04	5.269E+05	41.9 ± 26.4
12	1	11	32	0.091	3.4	3.293E+04	3.622E+05	20.3 ± 21.3
13	1	18	30	0.056	6.0	3.512E+04	6.322E+05	12.4 ± 12.8
14	0	12	24	0.000	5.0	0.000E+00	5.269E+05	0.0 ± 0.0
15	1	20	36	0.050	5.5	2.927E+04	5.854E+05	11.2 ± 11.5
16	0	8	16	0.000	5.0	0.000E+00	5.269E+05	0.0 ± 0.0
17	2	16	40	0.125	4.0	5.269E+04	4.215E+05	28.0 ± 21.0
18	1	16	24	0.062	6.6	4.391E+04	7.025E+05	14.0 ± 14.4
19	0	7	8	0.000	8.7	0.000E+00	9.220E+05	0.0 ± 0.0
20	2	14	16	0.143	8.7	1.317E+05	9.220E+05	31.9 ± 24.2
	29	292			4.7	4.993E+04	5.028E+05	

Area of basic unit = 9.49E-07 cm-2

CHI SQUARED = 12.59739 WITH 19 DEGREES OF FREEDOM
P(chi squared) = 15.4 %
CORRELATION COEFFICIENT = 0.291
VARIANCE OF SQR(Ns) = .4556239
VARIANCE OF SQR(Ni) = .7957426

Ns/Ni = 0.099 ± 0.019
MEAN RATIO = 0.131 ± 0.049

Pooled Age = 22.2 ± 4.4 Ma
Mean Age = 29.4 ± 11.0 Ma
Central Age = 22.2 ± 4.4Ma
% Rel. Error = 8.38
Ages calculated using a zeta of 348.4 ± 5.8 for SRM 612 glass
RHO D = 1.305E+06cm-2; ND = 3226

9414-107 Apatite

IRRADIATION WK154-2 COUNTED BY: KAO

No.	Ns	Ni	Na	RATIO	U(ppm)	RHOs	RHOi	F.T.AGE(Ma)
1	5	20	4	0.250	50.2	1.264E+06	5.056E+06	53.7 ± 26.9
2	3	12	4	0.250	30.1	7.583E+05	3.033E+06	53.7 ± 34.7
3	0	35	4	0.000	87.8	0.000E+00	8.847E+06	0.0 ± 0.0
	8	67			56.0	6.741E+05	5.645E+06	

Area of basic unit = 9.89E-07 cm-2

CHI SQUARED = 3.917911 WITH 2 DEGREES OF FREEDOM
P(chi squared) = 2.0 %
CORRELATION COEFFICIENT = -0.726
VARIANCE OF SQR(Ns) = 1.375672
VARIANCE OF SQR(Ni) = 1.518885

Ns/Ni = 0.119 ± 0.045
MEAN RATIO = 0.167 ± 0.083

Pooled Age = 25.7 ± 9.6 Ma
Mean Age = 35.9 ± 18.0 Ma
Central Age = 30.0 ± 16.3Ma
% Rel. Error = 71.27
Ages calculated using a zeta of 348.4 ± 5.8 for SRM 612 glass
RHO D = 1.239E+06cm-2; ND = 3065

9414-111 APATITE MARLBOROUGH

IRRADIATION WK154:WK154
SLIDE NUMBER 6
COUNTED BY: KAO

No.	Ns	Ni	Na	RATIO	U (ppm)	RHOs (E+06)	RHOi (E+06)	F.T.AGE (Ma)
1	2	5	6	0.400	8.6	0.337	0.843	88.6 ± 74.2
2	14	50	4	0.280	129.3	3.539	12.639	62.2 ± 18.9
	16	55			56.9	1.618	5.561	

AREA OF BASIC UNIT = 9.89E-07 cm
CHI SQUARED = .1620839 WITH 1 DEGREES OF FREEDOM
P(chi squared) = 68.7 %
CORRELATION COEFFICIENT = 1.000
VARIANCE OF SQR(Ns) = 2.71
VARIANCE OF SQR(Ni) = 11.69

Ns/Ni = 0.291 ± 0.083
MEAN RATIO = 0.340 ± 0.060

Ages calculated using a zeta of 348.4 ± 5.8 for SRM612 glass
RHO D = 1.281E+06 ; ND = 3167

POOLED AGE = 64.6 ± 18.4 Ma
MEAN AGE = 75.4 ± 13.4 Ma

9414-112 APATITE MARLBOROUGH

IRRADIATION WK154:WK154
SLIDE NUMBER 7
COUNTED BY: KAO

No.	Ns	Ni	Na	RATIO	U (ppm)	RHOs (E+06)	RHOI (E+06)	F.T.AGE (Ma)
1	9	43	9	0.209	49.0	1.011	4.831	46.9 ± 17.2
2	3	8	16	0.375	5.1	0.190	0.506	83.8 ± 56.8
3	5	28	4	0.179	71.8	1.264	7.078	40.0 ± 19.5
	17	79			27.9	0.593	2.754	

AREA OF BASIC UNIT = 9.89E-07 cm
CHI SQUARED = .8442847 WITH 2 DEGREES OF FREEDOM
P(chi squared) = 65.6 %
CORRELATION COEFFICIENT = 0.963
VARIANCE OF SQR(Ns) = 0.41
VARIANCE OF SQR(Ni) = 3.60

Ns/Ni = 0.215 ± 0.058
MEAN RATIO = 0.254 ± 0.061

Ages calculated using a zeta of 348.4 ± 5.8 for SRM612 glass
RHO D = 1.291E+06 ; ND = 3193

POOLED AGE = 48.2 ± 12.9 Ma
MEAN AGE = 56.9 ± 13.7 Ma

9414-1

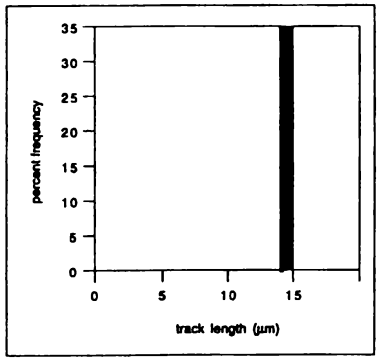

n = 2
Mean = 14.72 µm
Sample std. dev. = 0.10 µm

9414-2

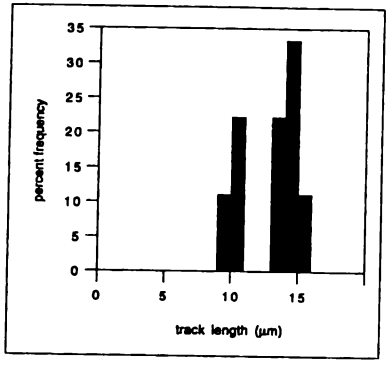

n = 9
Mean = 12.89 µm
Sample std. dev. = 2.00 µm

9414-5

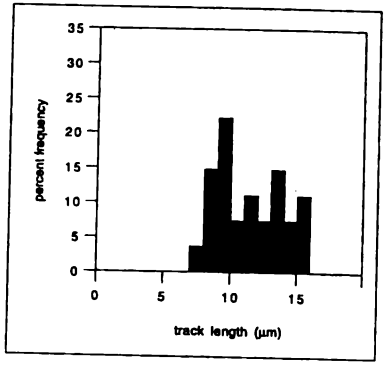

n = 27
Mean = 11.43 µm
Sample std. dev. = 2.40 µm

9414-6

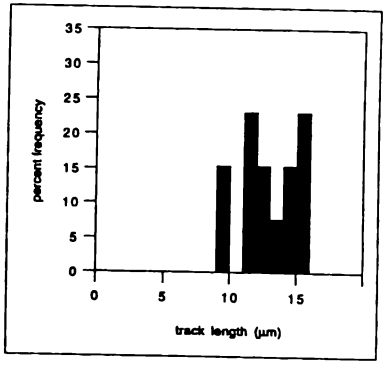

n = 13
Mean = 12.80 µm
Sample std. dev. = 1.95 µm

9414-9

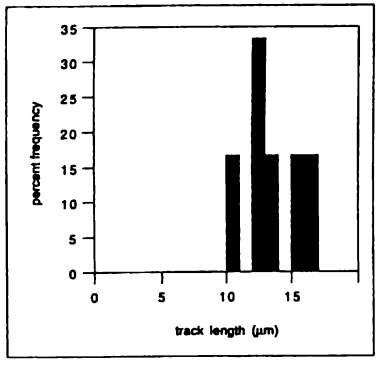

n = 6
Mean = 13.56 µm
Sample std. dev. = 2.02 µm

9414-11

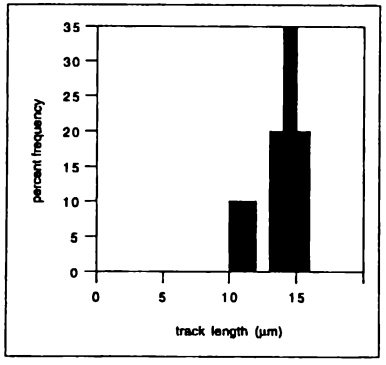

n = 10
Mean = 13.93 µm
Sample std. dev. = 1.65 µm

9414-31

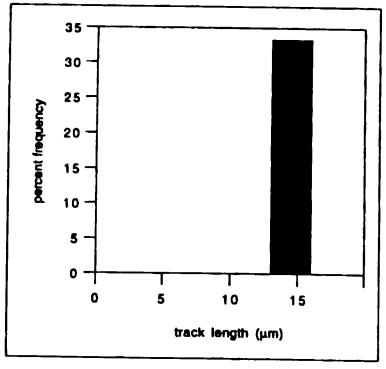

n = 3
Mean = 14.43 µm
Sample std. dev. = 0.99 µm

9414-33

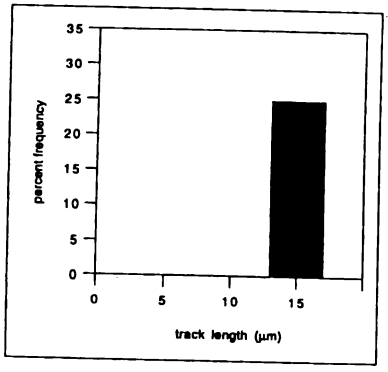

n = 4
Mean = 15.19 µm
Sample std. dev. = 1.15 µm

9414-35

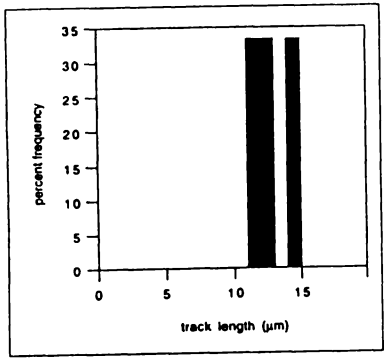

n = 3
Mean = 13.15 µm
Sample std. dev. = 1.34 µm

9414-39

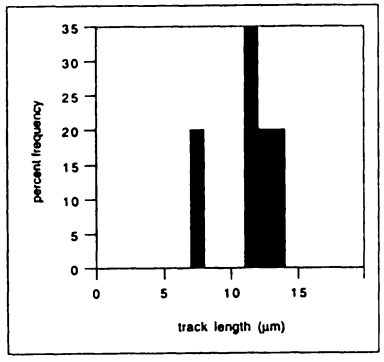

n = 5
Mean = 11.43 µm
Sample std. dev. = 2.22 µm

9414-40

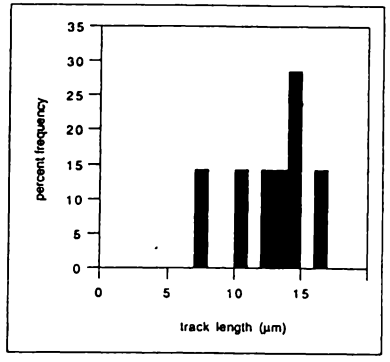

n = 7
Mean = 12.69 µm
Sample std. dev. = 2.75 µm

9414-42

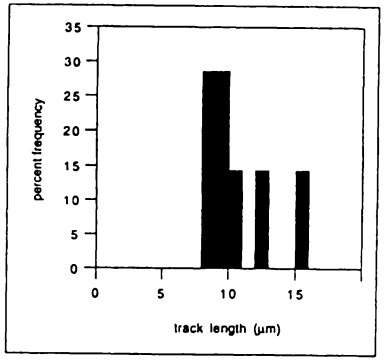

n = 7
Mean = 10.62 µm
Sample std. dev. = 2.28 µm

9414-43

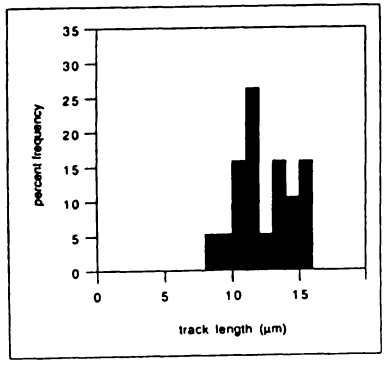

n = 19
Mean = 12.43 µm
Sample std. dev. = 1.97 µm

9414-44

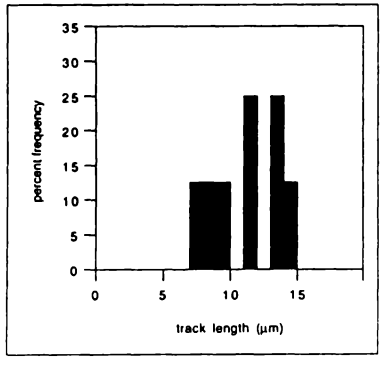

n = 8
Mean = 11.34 µm
Sample std. dev. = 2.28 µm

9414-45

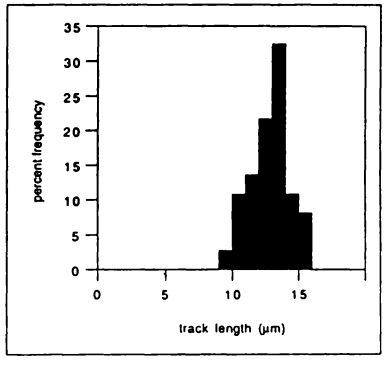

n = 37
Mean = 12.84 µm
Sample std. dev. = 1.46 µm

9414-46

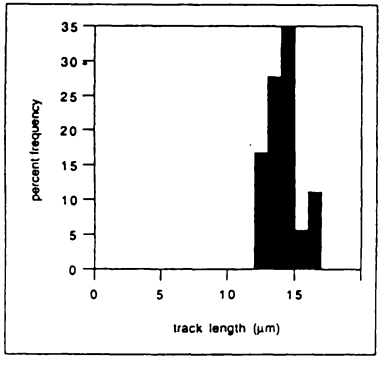

n = 18
Mean = 14.12 µm
Sample std. dev. = 1.09 µm

9414-47

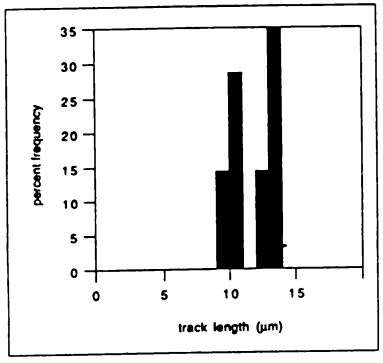

n = 7
Mean = 12.02 µm
Sample std. dev. = 1.53 µm

9414-51

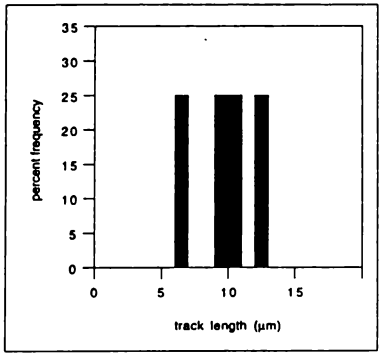

n = 4
Mean = 9.89 µm
Sample std. dev. = 2.02 µm

9414-53

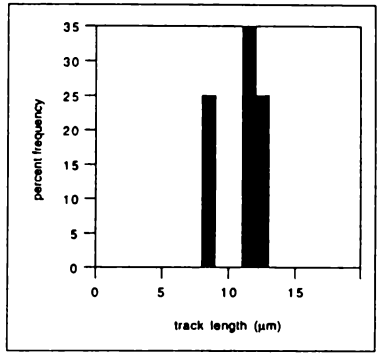

n = 4
Mean = 10.89 µm
Sample std. dev. = 1.40 µm

9414-60

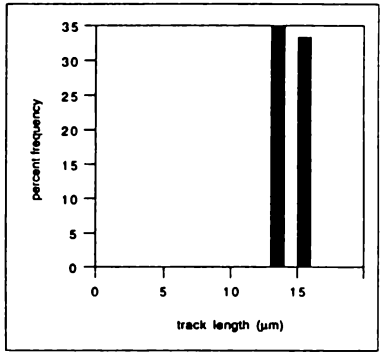

n = 3
Mean = 14.43 µm
Sample std. dev. = 1.08 µm

9414-61

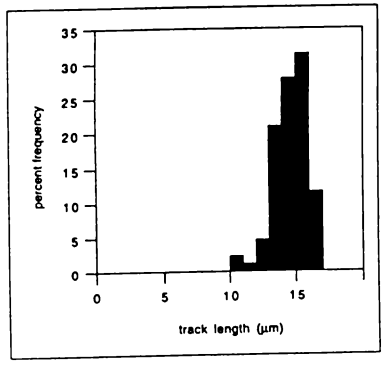

n = 86
Mean = 14.62 µm
Sample std. dev. = 1.28 µm

9414-62

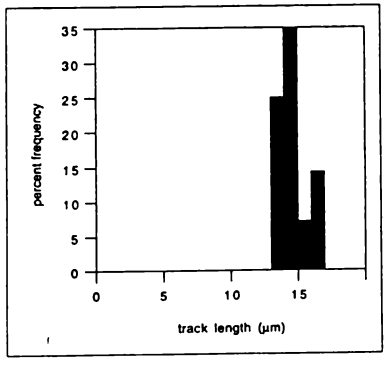

n = 28
Mean = 14.56 µm
Sample std. dev. = 0.87 µm

9414-63

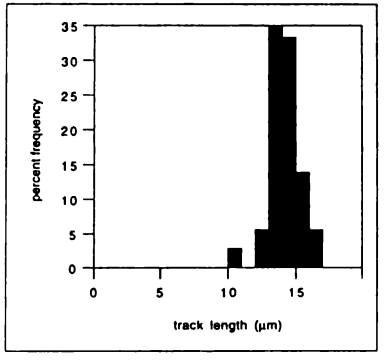

n = 36
Mean = 14.17 µm
Sample std. dev. = 1.15 µm

9414-64

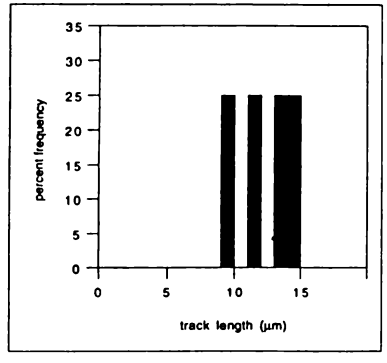

n = 4
Mean = 12.26 µm
Sample std. dev. = 2.00 µm

9414-67

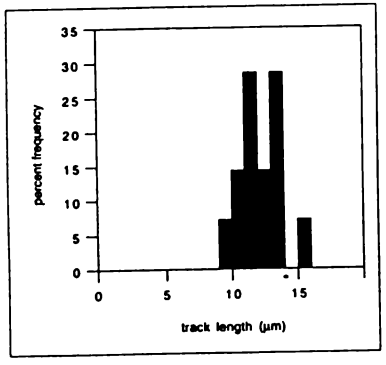

n = 14
Mean = 12.17 μm
Sample std. dev. = 1.38 μm

9414-70

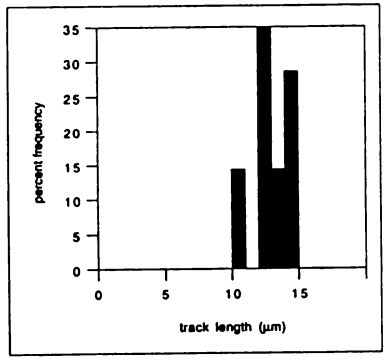

n = 7
Mean = 13.01 μm
Sample std. dev. = 1.39 μm

9414-72

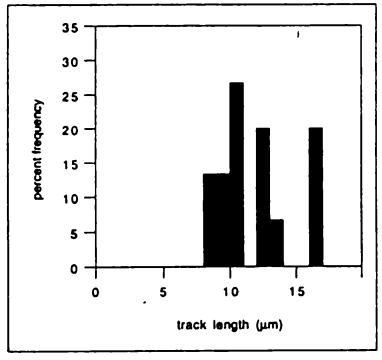

n = 15
Mean = 11.74 μm
Sample std. dev. = 2.52 μm

9414-73

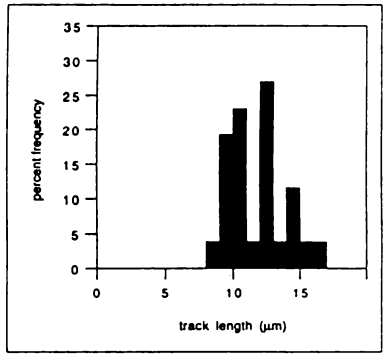

n = 26
Mean = 11.74 μm
Sample std. dev. = 2.09 μm

9414-81

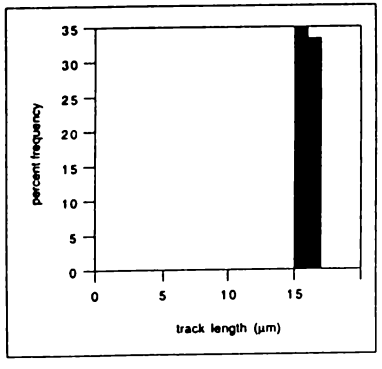

n = 3
Mean = 15.70 μm
Sample std. dev. = 0.46 μm

9414-83

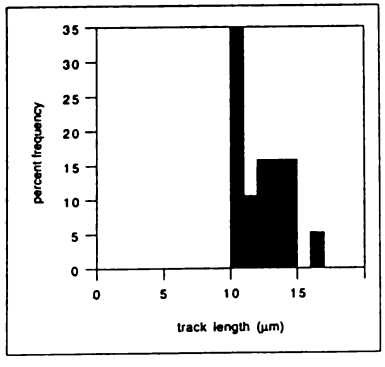

n = 19
Mean = 12.31 μm
Sample std. dev. = 1.78 μm

9414-84

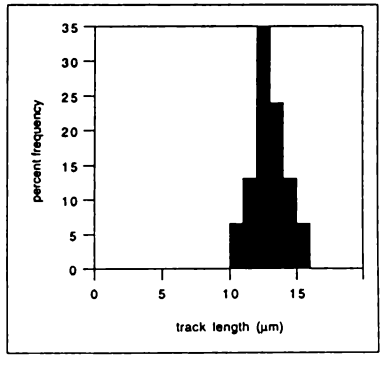

n = 46
Mean = 12.98 μm
Sample std. dev. = 1.25 μm

9414-87

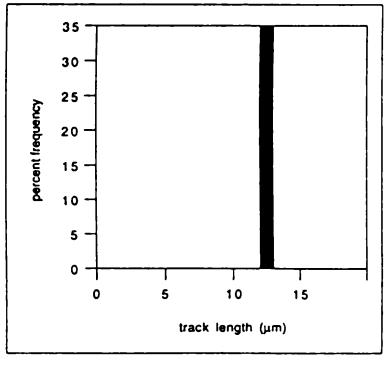

n = 5
Mean = 12.40 μm
Sample std. dev. = 0.22 μm

9414-96

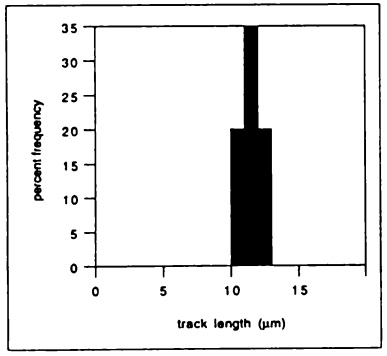

n = 5
Mean = 11.37 µm
Sample std. dev. = 0.84 µm

9414-98

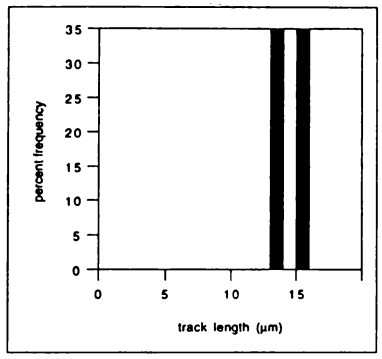

n = 2
Mean = 14.27 µm
Sample std. dev. = 0.88 µm

9414-88

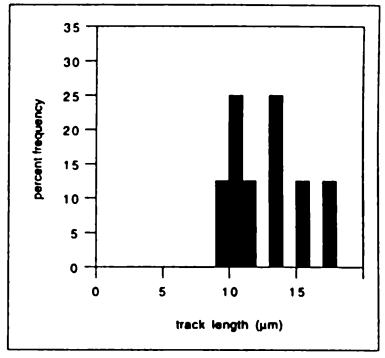

n = 8
Mean = 12.70 µm
Sample std. dev. = 2.68 µm

9414-99

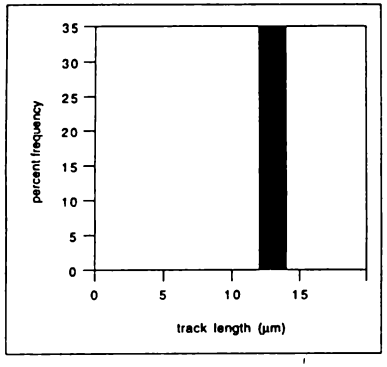

n = 2
Mean = 13.22 µm
Sample std. dev. = 0.37 µm

9414-104

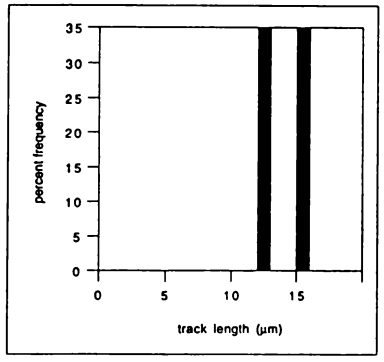

n = 2
Mean = 14.01 µm
Sample std. dev. = 1.01 µm

9414-1 Zircon

IRRADIATION WK145-1 COUNTED BY: KAO

No.	Ns	Ni	Na	RATIO	U(ppm)	RHOs	RHOi	F.T.AGE(Ma)
1	83	32	4	2.594	271.7	2.098E+07	8.089E+06	213.0 ± 44.8
2	150	46	9	3.261	173.6	1.685E+07	5.168E+06	266.7 ± 45.7
3	101	16	4	6.312	135.8	2.553E+07	4.044E+06	506.6 ±137.3
4	63	55	9	1.145	207.5	7.078E+06	6.179E+06	94.9 ± 17.8
5	115	27	9	4.259	101.9	1.292E+07	3.033E+06	346.1 ± 74.8
6	230	32	16	7.188	67.9	1.453E+07	2.022E+06	573.8 ±109.8
7	140	20	9	7.000	75.5	1.573E+07	2.247E+06	559.4 ±134.9
8	180	39	9	4.615	147.2	2.022E+07	4.382E+06	374.3 ± 67.2
9	230	46	9	5.000	173.6	2.584E+07	5.168E+06	404.5 ± 66.6
10	206	43	9	4.791	162.2	2.314E+07	4.831E+06	388.1 ± 66.2
11	106	20	4	5.300	169.8	2.679E+07	5.056E+06	428.0 ±105.2
12	182	52	9	3.500	196.2	2.045E+07	5.842E+06	285.8 ± 45.9
13	85	15	9	5.667	56.6	9.549E+06	1.685E+06	456.5 ±128.7
14	66	12	4	5.500	101.9	1.668E+07	3.033E+06	443.6 ±139.9
15	71	15	4	4.733	127.3	1.795E+07	3.792E+06	383.5 ±109.7
	2008	470			136.4	1.735E+07	4.062E+06	

Area of basic unit = 9.89E-07 cm-2

CHI SQUARED = 43.59871 WITH 14 DEGREES OF FREEDOM
P(chi squared) = 0.000 %
CORRELATION COEFFICIENT = 0.504
VARIANCE OF SQR(Ns) = 6.524728
VARIANCE OF SQR(Ni) = 1.818442

Ns/Ni = 4.272 ± 0.219
MEAN RATIO = 4.724 ± 0.419

Pooled Age = 347.2 ± 21.0 Ma
Mean Age = 382.8 ± 36.1 Ma
Central Age = 336.2 ± 45.3Ma
% Rel. Error = 47.33
Ages calculated using a zeta of 140.2 ± 3.6 for CN 1 glass
RHO D = 1.191E+06cm-2; ND = 2711

9414-2 Zircon

IRRADIATION WK145-3 COUNTED BY: KAO

No.	Ns	Ni	Na	RATIO	U(ppm)	RHOs	RHOi	F.T.AGE(Ma)
1	131	42	9	3.119	15.6	1.472E+06	4.719E+05	258.4 ± 46.6
2	70	32	9	2.188	11.9	7.864E+05	3.595E+05	182.3 ± 39.3
3	137	54	9	2.537	20.1	1.539E+06	6.067E+05	211.0 ± 34.6
4	57	36	16	1.583	7.5	3.602E+05	2.275E+05	132.5 ± 28.5
5	109	40	8	2.725	16.8	1.378E+06	5.056E+05	226.4 ± 42.5
6	140	58	9	2.414	21.6	1.573E+06	6.516E+05	200.9 ± 32.0
7	58	54	12	1.074	15.1	4.887E+05	4.550E+05	90.2 ± 17.3
8	124	76	16	1.632	15.9	7.836E+05	4.803E+05	136.5 ± 20.4
9	111	38	9	2.921	14.2	1.247E+06	4.269E+05	242.3 ± 46.2
10	157	66	9	2.379	24.6	1.764E+06	7.415E+05	198.0 ± 29.7
11	139	50	9	2.780	18.6	1.562E+06	5.617E+05	230.8 ± 38.8
12	104	58	16	1.793	12.2	6.572E+05	3.665E+05	149.8 ± 25.0
13	65	36	9	1.806	13.4	7.303E+05	4.044E+05	150.9 ± 31.7
14	128	75	9	1.707	27.9	1.438E+06	8.426E+05	142.7 ± 21.2
15	93	47	9	1.979	17.5	1.045E+06	5.280E+05	165.1 ± 30.0
16	78	30	9	2.600	11.2	8.763E+05	3.370E+05	216.1 ± 46.9
	1701	792			15.9	1.030E+06	4.795E+05	

Area of basic unit = 9.89E-06 cm-2

CHI SQUARED = 19.24408 WITH 15 DEGREES OF FREEDOM
P(chi squared) = 0.076 %
CORRELATION COEFFICIENT = 0.599
VARIANCE OF SQR(Ns) = 2.702279
VARIANCE OF SQR(Ni) = 1.035107

Ns/Ni = 2.148 ± 0.092
MEAN RATIO = 2.202 ± 0.143

Pooled Age = 179.1 ± 9.6 Ma
Mean Age = 183.5 ± 13.3 Ma
Central Age = 177.0 ± 12.4Ma
% Rel. Error = 20.66
Ages calculated using a zeta of 140.2 ± 3.6 for CN 1 glass
RHO D = 1.206E+06cm-2; ND = 2760

9414-3 Zircon

IRRADIATION WK145-4 COUNTED BY: KAO

No.	Ns	Ni	Na	RATIO	U(ppm)	RHOs	RHOi	F.T.AGE(Ma)
1	148	54	4	2.741	452.7	3.741E+07	1.365E+07	227.6 ± 36.9
2	97	42	4	2.310	352.1	2.452E+07	1.062E+07	192.4 ± 36.1
3	126	73	4	1.726	612.0	3.185E+07	1.845E+07	144.3 ± 21.7
4	94	25	4	3.760	209.6	2.376E+07	6.320E+06	310.3 ± 70.5
5	84	59	4	1.424	494.7	2.123E+07	1.491E+07	119.3 ± 20.6
	549	253			424.2	2.776E+07	1.279E+07	

Area of basic unit = 9.89E-07 cm-2

CHI SQUARED = 8.539709 WITH 4 DEGREES OF FREEDOM
P(chi squared) = 0.187 %
CORRELATION COEFFICIENT = 0.412
VARIANCE OF SQR(Ns) = 1.530197
VARIANCE OF SQR(Ni) = 1.809597

Ns/Ni = 2.170 ± 0.165
MEAN RATIO = 2.392 ± 0.411

Pooled Age = 180.9 ± 14.9 Ma
Mean Age = 199.1 ± 34.8 Ma
Central Age = 182.9 ± 26.7Ma
% Rel. Error = 27.44
Ages calculated using a zeta of 140.2 ± 3.6 for CN 1 glass
RHO D = 1.206E+06cm-2; ND = 2784

9414-4 ZIRCON MARLBOROUGH

IRRADIATION WK145-5
SLIDE NUMBER 5
COUNTED BY: KAO

No.	Ns	Ni	Na	RATIO	U (ppm)	RHOs (E+06)	RHOi (E+06)	F.T.AGE (Ma)
1	114	31	6	3.677	0.0	19.211	5.224	304.9 ± 62.5
2	170	59	9	2.881	0.0	19.099	6.628	240.1 ± 37.1
3	61	30	6	2.033	0.0	10.280	5.056	170.3 ± 38.4
4	80	34	9	2.353	0.0	8.988	3.820	196.7 ± 40.8
5	185	42	9	4.405	0.0	20.784	4.719	363.5 ± 63.2
6	58	21	9	2.762	0.0	6.516	2.359	230.3 ± 59.1
7	60	16	9	3.750	0.0	6.741	1.798	310.7 ± 88.0
8	166	63	9	2.635	0.0	18.650	7.078	219.9 ± 33.3
9	130	44	9	2.955	0.0	14.605	4.943	246.1 ± 43.6
10	48	13	4	3.692	0.0	12.133	3.286	306.1 ± 96.2
11	125	31	9	4.032	0.0	14.043	3.483	333.5 ± 67.8
12	131	31	9	4.226	0.0	14.717	3.483	349.1 ± 70.6
13	157	49	9	3.204	0.0	17.638	5.505	266.4 ± 44.4
14	70	18	4	3.889	0.0	17.695	4.550	322.0 ± 85.7
15	178	66	24	2.697	0.0	7.499	2.781	225.0 ± 33.2
16	62	17	4	3.647	0.0	15.672	4.297	302.4 ± 83.3
17	160	53	9	3.019	0.0	17.976	5.954	251.3 ± 40.6
18	98	45	9	2.178	0.0	11.010	5.056	182.3 ± 33.3
19	101	32	9	3.156	0.0	11.347	3.595	262.5 ± 53.9
20	100	31	9	3.226	0.0	11.235	3.483	268.2 ± 55.8
	2254	726			0.0	13.098	4.219	

AREA OF BASIC UNIT = 9.89E-07 cm
CHI SQUARED = 23.12983 WITH 19 DEGREES OF FREEDOM
P(chi squared) = 23.2 %
CORRELATION COEFFICIENT = 0.872
VARIANCE OF SQR(Ns) = 4.80
VARIANCE OF SQR(Ni) = 1.79

Ns/Ni = 3.105 ± 0.132
MEAN RATIO = 3.221 ± 0.151

Ages calculated using a zeta of 140.2 ± 3.6 for CN1 glass
RHO D = 1.211E+06 ; ND = 2809

POOLED AGE = 258.3 ± 13.8 Ma
MEAN AGE = 267.8 ± 15.2 Ma

9414-5 ZIRCON MARLBOROUGH

IRRADIATION WK145-6
SLIDE NUMBER 6
COUNTED BY: KAO

No.	Ns	Ni	Na	RATIO	U (ppm)	RHOs (E+06)	RHOi (E+06)	F.T.AGE (Ma)
1	55	11	4	5.000	0.0	13.903	2.781	412.7 ± 136.9
2	220	71	9	3.099	0.0	24.716	7.977	258.9 ± 36.3
3	165	48	9	3.438	0.0	18.537	5.393	286.6 ± 47.9
4	46	18	9	2.556	0.0	5.168	2.022	214.2 ± 60.0
5	88	26	9	3.385	0.0	9.887	2.921	282.2 ± 63.6
6	89	27	9	3.296	0.0	9.999	3.033	275.0 ± 61.1
7	85	24	6	3.542	0.0	14.324	4.044	295.0 ± 68.8
8	195	66	16	2.955	0.0	12.323	4.171	247.1 ± 36.0
9	109	26	9	4.192	0.0	12.246	2.921	347.8 ± 76.7
10	192	43	25	4.465	0.0	7.765	1.739	369.8 ± 63.5
11	83	22	9	3.773	0.0	9.325	2.472	313.8 ± 75.9
12	200	35	9	5.714	0.0	22.469	3.932	469.6 ± 87.3
13	165	40	9	4.125	0.0	18.537	4.494	342.4 ± 61.3
14	81	26	8	3.115	0.0	10.238	3.286	260.2 ± 59.2
15	77	21	10	3.667	0.0	7.786	2.123	305.2 ± 75.8
16	119	32	9	3.719	0.0	13.369	3.595	309.4 ± 62.4
17	111	36	9	3.083	0.0	12.471	4.044	257.6 ± 50.1
18	85	25	9	3.400	0.0	9.549	2.809	283.5 ± 65.1
19	172	52	9	3.308	0.0	19.324	5.842	276.0 ± 44.5
20	58	18	4	3.222	0.0	14.661	4.550	269.0 ± 73.1
	2395	667			0.0	12.745	3.550	

AREA OF BASIC UNIT = 9.89E-07 cm
CHI SQUARED = 16.81603 WITH 19 DEGREES OF FREEDOM
P(chi squared) = 60.2 %
CORRELATION COEFFICIENT = 0.898
VARIANCE OF SQR(Ns) = 6.17
VARIANCE OF SQR(Ni) = 1.73

Ns/Ni = 3.591 ± 0.157
MEAN RATIO = 3.653 ± 0.166

Ages calculated using a zeta of 140.2 ± 3.6 for CN1 glass
RHO D = 1.216E+06 ; ND = 2834

POOLED AGE = 299.0 ± 16.2 Ma
MEAN AGE = 304.1 ± 16.9 Ma

9414-6 Zircon

IRRADIATION WK145-7 COUNTED BY: KAO

No.	Ns	Ni	Na	RATIO	U(ppm)	RHOs	RHOi	F.T.AGE(Ma)
1	54	40	6	1.350	220.8	9.100E+06	6.741E+06	114.5 ± 24.2
2	61	24	6	2.542	132.5	1.028E+07	4.044E+06	214.0 ± 52.0
3	87	34	4	2.559	281.6	2.199E+07	8.595E+06	215.4 ± 44.1
4	76	21	4	3.619	173.9	1.921E+07	5.308E+06	302.5 ± 75.2
5	51	23	6	2.217	127.0	8.595E+06	3.876E+06	187.1 ± 47.4
6	74	23	6	3.217	127.0	1.247E+07	3.876E+06	269.7 ± 64.9
7	79	28	12	2.821	77.3	6.657E+06	2.359E+06	237.1 ± 52.7
8	109	26	12	4.192	71.8	9.184E+06	2.191E+06	349.2 ± 77.0
9	51	17	6	3.000	93.9	8.595E+06	2.865E+06	251.8 ± 71.0
10	118	31	6	3.806	171.1	1.989E+07	5.224E+06	317.8 ± 64.9
11	48	15	4	3.200	124.2	1.213E+07	3.792E+06	268.2 ± 79.8
12	121	28	9	4.321	103.1	1.359E+07	3.146E+06	359.7 ± 76.3
13	33	12	8	2.750	49.7	4.171E+06	1.517E+06	231.2 ± 78.3
14	42	16	9	2.625	58.9	4.719E+06	1.798E+06	220.9 ± 65.3
15	127	26	9	4.885	95.7	1.427E+07	2.921E+06	405.1 ± 88.1
16	137	43	8	3.186	178.0	1.732E+07	5.435E+06	267.1 ± 47.5
17	99	29	6	3.414	160.1	1.668E+07	4.887E+06	285.8 ± 61.0
18	97	35	9	2.771	128.8	1.090E+07	3.932E+06	233.0 ± 46.5
19	46	12	4	3.833	99.4	1.163E+07	3.033E+06	320.0 ±104.2
20	102	25	16	4.080	51.8	6.446E+06	1.580E+06	340.1 ± 76.7
	1612	508			112.2	1.087E+07	3.424E+06	

Area of basic unit = 9.89E-07 cm-2

CHI SQUARED = 17.00874 WITH 19 DEGREES OF FREEDOM
P(chi squared) = 1.8 %
CORRELATION COEFFICIENT = 0.657
VARIANCE OF SQR(Ns) = 3.244276
VARIANCE OF SQR(Ni) = .7565581

Ns/Ni = 3.173 ± 0.161
MEAN RATIO = 3.220 ± 0.185

Pooled Age = 266.0 ± 16.0 Ma
Mean Age = 269.8 ± 17.7 Ma
Central Age = 261.5 ± 18.3Ma
% Rel. Error = 19.34
Ages calculated using a zeta of 140.2 ± 3.6 for CN 1 glass
RHO D = 1.221E+06cm-2; ND = 2859

9414-7 ZIRCON MARLBOROUGH

IRRADIATION WK145-8
SLIDE NUMBER 8
COUNTED BY: KAO

No.	Ns	Ni	Na	RATIO	U (ppm)	RHOs (E+06)	RHOi (E+06)	F.T.AGE (Ma)
1	63	19	4	3.316	0.0	15.925	4.803	278.8 ± 73.5
2	48	15	4	3.200	0.0	12.133	3.792	269.3 ± 80.1
3	68	30	9	2.267	0.0	7.640	3.370	191.9 ± 42.5
4	57	19	8	3.000	0.0	7.204	2.401	252.8 ± 67.4
5	79	25	6	3.160	0.0	13.313	4.213	266.0 ± 61.6
6	70	23	8	3.043	0.0	8.847	2.907	256.4 ± 62.2
7	67	18	6	3.722	0.0	11.291	3.033	312.2 ± 83.5
8	62	13	6	4.769	0.0	10.448	2.191	397.4 ± 121.9
9	71	28	8	2.536	0.0	8.974	3.539	214.3 ± 48.3
10	39	11	4	3.545	0.0	9.858	2.781	297.7 ± 102.1
11	114	25	4	4.560	0.0	28.817	6.320	380.4 ± 84.9
12	25	7	4	3.571	0.0	6.320	1.769	299.9 ± 128.6
13	95	23	6	4.130	0.0	16.009	3.876	345.6 ± 81.0
14	114	38	6	3.000	0.0	19.211	6.404	252.8 ± 48.0
15	114	34	9	3.353	0.0	12.808	3.820	281.9 ± 55.8
16	129	41	9	3.146	0.0	14.493	4.606	264.9 ± 48.2
17	105	28	6	3.750	0.0	17.695	4.719	314.5 ± 67.6
18	103	38	9	2.711	0.0	11.572	4.269	228.8 ± 44.0
19	108	29	6	3.724	0.0	18.200	4.887	312.4 ± 66.1
20	69	33	6	2.091	0.0	11.628	5.561	177.2 ± 37.9
	1600	497			0.0	12.639	3.926	

AREA OF BASIC UNIT = 9.89E-07 cm
CHI SQUARED = 15.91953 WITH 19 DEGREES OF FREEDOM
P(chi squared) = 66.3 %
CORRELATION COEFFICIENT = 0.832
VARIANCE OF SQR(Ns) = 2.81
VARIANCE OF SQR(Ni) = 1.02

Ns/Ni = 3.219 ± 0.165
MEAN RATIO = 3.330 ± 0.153

Ages calculated using a zeta of 140.2 ± 3.6 for CN1 glass
RHO D = 1.226E+06 ; ND = 2883

POOLED AGE = 270.9 ± 16.4 Ma
MEAN AGE = 280.0 ± 15.6 Ma

9414-8 ZIRCON MARLBOROUGH

IRRADIATION WK145-9
SLIDE NUMBER 9
COUNTED BY: KAO

No.	Ns	Ni	Na	RATIO	U (ppm)	RHOs (E+06)	RHOi (E+06)	F.T.AGE (Ma)
1	140	44	9	3.182	0.0	15.729	4.943	268.9 ± 47.2
2	99	37	9	2.676	0.0	11.122	4.157	226.9 ± 44.3
3	100	37	6	2.703	0.0	16.852	6.235	229.1 ± 44.7
4	143	50	9	2.860	0.0	16.066	5.617	242.2 ± 40.5
5	138	39	9	3.538	0.0	15.504	4.382	298.3 ± 54.9
6	136	23	8	5.913	0.0	17.189	2.907	491.1 ± 111.8
7	109	29	8	3.759	0.0	13.777	3.665	316.4 ± 66.9
8	98	29	4	3.379	0.0	24.772	7.331	285.2 ± 61.0
9	70	22	4	3.182	0.0	17.695	5.561	268.9 ± 66.3
10	73	29	8	2.517	0.0	9.226	3.665	213.6 ± 47.4
11	49	18	4	2.722	0.0	12.386	4.550	230.7 ± 64.0
12	94	25	6	3.760	0.0	15.841	4.213	316.6 ± 71.9
13	134	28	6	4.786	0.0	22.582	4.719	400.3 ± 84.1
14	150	25	9	6.000	0.0	16.852	2.809	498.0 ± 108.7
15	173	58	9	2.983	0.0	19.436	6.516	252.4 ± 39.1
16	74	26	9	2.846	0.0	8.314	2.921	241.0 ± 55.5
17	92	34	16	2.706	0.0	5.814	2.149	229.4 ± 46.6
18	34	11	4	3.091	0.0	8.595	2.781	261.4 ± 91.0
19	42	17	6	2.471	0.0	7.078	2.865	209.7 ± 60.7
20	51	18	9	2.833	0.0	5.730	2.022	240.0 ± 66.2
	1999	599			0.0	13.298	3.985	

AREA OF BASIC UNIT = 9.89E-07 cm
CHI SQUARED = 27.33278 WITH 19 DEGREES OF FREEDOM
P(chi squared) = 9.7 %
CORRELATION COEFFICIENT = 0.768
VARIANCE OF SQR(Ns) = 4.41
VARIANCE OF SQR(Ni) = 1.10

Ns/Ni = 3.337 ± 0.155
MEAN RATIO = 3.395 ± 0.230

Ages calculated using a zeta of 140.2 ± 3.6 for CN1 glass
RHO D = 1.231E+06 ; ND = 2908

POOLED AGE = 281.7 ± 15.9 Ma
MEAN AGE = 286.5 ± 21.4 Ma

9414-9 Zircon

IRRADIATION WK145-10 COUNTED BY: KAO

No.	Ns	Ni	Na	RATIO	U(ppm)	RHOs	RHOi	F.T.AGE(Ma)
1	87	50	6	1.740	27.3	1.466E+06	8.426E+05	149.0 ± 26.9
2	65	29	6	2.241	15.8	1.095E+06	4.887E+05	191.3 ± 43.2
3	44	39	6	1.128	21.3	7.415E+05	6.572E+05	97.0 ± 21.6
4	79	49	9	1.612	17.8	8.875E+05	5.505E+05	138.2 ± 25.5
5	104	27	9	3.852	9.8	1.168E+06	3.033E+05	325.4 ± 71.0
6	144	63	9	2.286	22.9	1.618E+06	7.078E+05	195.1 ± 30.1
7	183	65	9	2.815	23.6	2.056E+06	7.303E+05	239.4 ± 35.4
8	124	61	9	2.033	22.2	1.393E+06	6.853E+05	173.8 ± 27.7
9	92	28	6	3.286	15.3	1.550E+06	4.719E+05	278.6 ± 60.8
10	132	71	9	1.859	25.8	1.483E+06	7.977E+05	159.1 ± 24.0
11	72	31	9	2.323	11.3	8.089E+05	3.483E+05	198.2 ± 43.0
12	118	38	9	3.105	13.8	1.326E+06	4.269E+05	263.6 ± 49.9
13	149	98	9	1.520	35.6	1.674E+06	1.101E+06	130.4 ± 17.5
14	56	16	9	3.500	5.8	6.291E+05	1.798E+05	296.3 ± 84.5
15	55	17	9	3.235	6.2	6.179E+05	1.910E+05	274.4 ± 76.6
16	152	40	9	3.800	14.5	1.708E+06	4.494E+05	321.1 ± 58.0
17	120	47	9	2.553	17.1	1.348E+06	5.280E+05	217.5 ± 38.1
18	100	35	9	2.857	12.7	1.123E+06	3.932E+05	242.9 ± 48.3
19	60	27	9	2.222	9.8	6.741E+05	3.033E+05	189.7 ± 44.4
20	87	50	9	1.740	18.2	9.774E+05	5.617E+05	149.0 ± 26.9
	2023	881			17.2	1.218E+06	5.302E+05	

Area of basic unit = 9.89E-06 cm-2

CHI SQUARED = 29.71644 WITH 19 DEGREES OF FREEDOM
P(chi squared) = 0.000 %
CORRELATION COEFFICIENT = 0.705
VARIANCE OF SQR(Ns) = 3.65519
VARIANCE OF SQR(Ni) = 2.206832

Ns/Ni = 2.296 ± 0.093
MEAN RATIO = 2.485 ± 0.177

Pooled Age = 195.9 ± 10.0 Ma
Mean Age = 211.8 ± 16.5 Ma
Central Age = 197.0 ± 14.5Ma
% Rel. Error = 25.63
Ages calculated using a zeta of 140.2 ± 3.6 for CN 1 glass
RHO D = 1.236E+06cm-2; ND = 2932

9414-10 Zircon

IRRADIATION WK145-12 COUNTED BY: KAO

No.	Ns	Ni	Na	RATIO	U(ppm)	RHOs	RHOi	F.T.AGE(Ma)
1	71	14	16	5.071	28.5	4.487E+06	8.847E+05	426.7 ±125.5
2	56	34	9	1.647	123.1	6.291E+06	3.820E+06	141.7 ± 31.1
3	109	28	9	3.893	101.4	1.225E+07	3.146E+06	330.1 ± 70.7
4	67	34	12	1.971	92.3	5.645E+06	2.865E+06	169.2 ± 36.0
5	141	42	10	3.357	136.9	1.426E+07	4.247E+06	285.6 ± 51.0
6	59	44	6	1.341	239.0	9.943E+06	7.415E+06	115.6 ± 23.3
7	120	80	9	1.500	289.7	1.348E+07	8.988E+06	129.2 ± 19.1
8	134	42	8	3.190	171.1	1.694E+07	5.308E+06	271.7 ± 48.8
9	105	68	16	1.544	138.5	6.635E+06	4.297E+06	132.9 ± 21.1
10	129	73	9	1.767	264.3	1.449E+07	8.201E+06	151.9 ± 22.8
11	60	45	6	1.333	244.4	1.011E+07	7.583E+06	115.0 ± 23.0
12	73	43	9	1.698	155.7	8.201E+06	4.831E+06	146.0 ± 28.4
13	81	25	9	3.240	90.5	9.100E+06	2.809E+06	275.9 ± 63.7
14	19	6	4	3.167	48.9	4.803E+06	1.517E+06	269.8 ±126.6
15	65	33	9	1.970	119.5	7.303E+06	3.707E+06	169.1 ± 36.5
16	115	51	9	2.255	184.7	1.292E+07	5.730E+06	193.2 ± 33.1
17	43	25	9	1.720	90.5	4.831E+06	2.809E+06	147.9 ± 37.5
18	105	41	9	2.561	148.5	1.180E+07	4.606E+06	219.0 ± 40.9
19	95	42	9	2.262	152.1	1.067E+07	4.719E+06	193.8 ± 36.4
20	78	56	8	1.393	228.1	9.858E+06	7.078E+06	120.0 ± 21.4
	1725	826			145.5	9.428E+06	4.515E+06	

Area of basic unit = 9.89E-07 cm-2

CHI SQUARED = 33.70186 WITH 19 DEGREES OF FREEDOM
P(chi squared) = 0.000 %
CORRELATION COEFFICIENT = 0.612
VARIANCE OF SQR(Ns) = 3.579359
VARIANCE OF SQR(Ni) = 2.360146

Ns/Ni = 2.088 ± 0.088
MEAN RATIO = 2.344 ± 0.225

Pooled Age = 179.2 ± 9.5 Ma
Mean Age = 200.8 ± 20.3 Ma
Central Age = 179.7 ± 14.7Ma
% Rel. Error = 29.53
Ages calculated using a zeta of 140.2 ± 3.6 for CN 1 glass
RHO D = 1.241E+06cm-2; ND = 2957

9414-11 Zircon

IRRADIATION WK145-13 COUNTED BY: KAO

No.	Ns	Ni	Na	RATIO	U(ppm)	RHOs	RHOi	F.T.AGE(Ma)
1	79	20	6	3.950	107.8	1.331E+07	3.370E+06	337.4 ± 85.1
2	19	10	9	1.900	35.9	2.135E+06	1.123E+06	164.5 ± 64.5
3	42	21	4	2.000	169.7	1.062E+07	5.308E+06	173.0 ± 46.6
4	69	47	9	1.468	168.8	7.752E+06	5.280E+06	127.5 ± 24.4
5	50	25	6	2.000	134.7	8.426E+06	4.213E+06	173.0 ± 42.7
6	112	70	9	1.600	251.5	1.258E+07	7.864E+06	138.8 ± 21.6
7	79	46	9	1.717	165.2	8.875E+06	5.168E+06	148.9 ± 28.0
8	113	34	6	3.324	183.2	1.904E+07	5.730E+06	285.1 ± 56.5
9	107	34	9	3.147	122.1	1.202E+07	3.820E+06	270.2 ± 53.9
10	121	78	9	1.551	280.2	1.359E+07	8.763E+06	134.6 ± 20.0
11	89	56	6	1.589	301.7	1.500E+07	9.437E+06	137.9 ± 23.9
12	70	24	6	2.917	129.3	1.180E+07	4.044E+06	250.8 ± 59.9
13	60	28	6	2.143	150.9	1.011E+07	4.719E+06	185.2 ± 42.8
14	129	42	9	3.071	150.9	1.449E+07	4.719E+06	263.9 ± 47.6
15	92	50	9	1.840	179.6	1.034E+07	5.617E+06	159.4 ± 28.4
16	48	25	4	1.920	202.1	1.213E+07	6.320E+06	166.2 ± 41.3
17	77	33	6	2.333	177.8	1.298E+07	5.561E+06	201.4 ± 42.4
18	102	73	9	1.397	262.2	1.146E+07	8.201E+06	121.4 ± 19.0
19	66	43	4	1.535	347.5	1.668E+07	1.087E+07	133.2 ± 26.4
20	57	45	6	1.267	242.5	9.606E+06	7.583E+06	110.1 ± 22.2
	1581	804			184.4	1.134E+07	5.766E+06	

Area of basic unit = 9.89E-07 cm-2

CHI SQUARED = 26.02791 WITH 19 DEGREES OF FREEDOM
P(chi squared) = 0.006 %
CORRELATION COEFFICIENT = 0.676
VARIANCE OF SQR(Ns) = 3.056685
VARIANCE OF SQR(Ni) = 2.181512

Ns/Ni = 1.966 ± 0.085
MEAN RATIO = 2.133 ± 0.168

Pooled Age = 170.2 ± 9.1 Ma
Mean Age = 184.4 ± 15.6 Ma
Central Age = 171.7 ± 12.6Ma
% Rel. Error = 24.60
Ages calculated using a zeta of 140.2 ± 3.6 for CN 1 glass
RHO D = 1.251E+06cm-2; ND = 3006

9414-12 ZIRCON MARLBOROUGH

IRRADIATION WK145-14
SLIDE NUMBER 14
COUNTED BY: KAO

No.	Ns	Ni	Na	RATIO	U (ppm)	RHOs (E+06)	RHOi (E+06)	F.T.AGE (Ma)
1	74	22	4	3.364	0.0	18.706	5.561	289.6 ± 70.9
2	62	25	4	2.480	0.0	15.672	6.320	214.7 ± 51.3
3	89	35	6	2.543	0.0	14.998	5.898	220.1 ± 44.5
4	42	15	4	2.800	0.0	10.617	3.792	241.9 ± 73.2
5	52	31	4	1.677	0.0	13.145	7.836	146.0 ± 33.5
6	43	20	4	2.150	0.0	10.870	5.056	186.6 ± 50.8
	362	148			0.0	14.078	5.756	

AREA OF BASIC UNIT = 9.89E-07 cm
CHI SQUARED = 5.002738 WITH 5 DEGREES OF FREEDOM
P(chi squared) = 41.6 %
CORRELATION COEFFICIENT = 0.685
VARIANCE OF SQR(Ns) = 1.38
VARIANCE OF SQR(Ni) = 0.55

Ns/Ni = 2.446 ± 0.239
MEAN RATIO = 2.502 ± 0.234

Ages calculated using a zeta of 140.2 ± 3.6 for CN1 glass
RHO D = 1.256E+06 ; ND = 3031

POOLED AGE = 211.8 ± 21.7 Ma
MEAN AGE = 216.6 ± 21.3 Ma

9414-14 ZIRCON MARLBOROUGH

IRRADIATION WK145-16
SLIDE NUMBER 16
COUNTED BY: KAO

No.	Ns	Ni	Na	RATIO	U (ppm)	RHOs (E+06)	RHOi (E+06)	F.T.AGE (Ma)
1	179	58	9	3.086	0.0	20.110	6.516	268.2 ± 41.4
2	210	55	9	3.818	0.0	23.593	6.179	330.2 ± 51.1
3	158	58	9	2.724	0.0	17.751	6.516	237.3 ± 37.2
4	108	32	9	3.375	0.0	12.133	3.595	292.8 ± 59.6
5	69	28	4	2.464	0.0	17.442	7.078	215.1 ± 48.7
6	179	52	9	3.442	0.0	20.110	5.842	298.5 ± 47.9
7	79	34	9	2.324	0.0	8.875	3.820	203.0 ± 42.1
8	67	30	6	2.233	0.0	11.291	5.056	195.2 ± 43.3
9	137	39	9	3.513	0.0	15.392	4.382	304.4 ± 56.1
10	143	70	9	2.043	0.0	16.066	7.864	178.8 ± 26.7
11	157	74	9	2.122	0.0	17.638	8.314	185.6 ± 26.8
12	128	51	9	2.510	0.0	14.380	5.730	219.0 ± 36.9
13	132	45	9	2.933	0.0	14.830	5.056	255.2 ± 44.8
14	141	54	9	2.611	0.0	15.841	6.067	227.7 ± 37.1
15	76	29	9	2.621	0.0	8.538	3.258	228.5 ± 50.4
16	96	33	9	2.909	0.0	10.785	3.707	253.1 ± 51.7
17	93	30	6	3.100	0.0	15.672	5.056	269.4 ± 57.2
18	117	51	9	2.294	0.0	13.145	5.730	200.4 ± 34.2
19	68	27	6	2.519	0.0	11.459	4.550	219.7 ± 50.5
20	152	45	9	3.378	0.0	17.077	5.056	293.0 ± 50.6
	2489	895			0.0	15.161	5.452	

AREA OF BASIC UNIT = 9.89E-07 cm
CHI SQUARED = 23.47018 WITH 19 DEGREES OF FREEDOM
P(chi squared) = 21.7 %
CORRELATION COEFFICIENT = 0.789
VARIANCE OF SQR(Ns) = 3.62
VARIANCE OF SQR(Ni) = 1.13

Ns/Ni = 2.781 ± 0.108
MEAN RATIO = 2.801 ± 0.115

Ages calculated using a zeta of 140.2 ± 3.6 for CN1 glass
RHO D = 1.266E+06 ; ND = 3080

POOLED AGE = 242.2 ± 12.1 Ma
MEAN AGE = 243.9 ± 12.6 Ma

9414-15 Zircon

IRRADIATION WK145-17 COUNTED BY: KAO

No.	Ns	Ni	Na	RATIO	U(ppm)	RHOs	RHOi	F.T.AGE(Ma)
1	149	37	9	4.027	130.8	1.674E+07	4.157E+06	349.2 ± 65.1
2	155	106	9	1.462	374.8	1.741E+07	1.191E+07	129.0 ± 16.8
3	103	38	6	2.711	201.5	1.736E+07	6.404E+06	237.1 ± 45.6
4	103	38	6	2.711	201.5	1.736E+07	6.404E+06	237.1 ± 45.6
5	65	37	6	1.757	196.2	1.095E+07	6.235E+06	154.7 ± 32.2
6	76	35	4	2.171	278.4	1.921E+07	8.847E+06	190.6 ± 39.4
7	81	27	4	3.000	214.8	2.048E+07	6.825E+06	261.9 ± 58.8
8	65	33	8	1.970	131.3	8.215E+06	4.171E+06	173.1 ± 37.4
9	93	31	6	3.000	164.4	1.567E+07	5.224E+06	261.9 ± 54.9
10	85	29	6	2.931	153.8	1.432E+07	4.887E+06	256.0 ± 55.6
11	157	41	9	3.829	145.0	1.764E+07	4.606E+06	332.5 ± 59.2
12	42	25	4	1.680	198.9	1.062E+07	6.320E+06	148.0 ± 37.7
	1174	477			197.1	1.542E+07	6.264E+06	

Area of basic unit = 9.89E-07 cm-2

CHI SQUARED = 20.30912 WITH 11 DEGREES OF FREEDOM
P(chi squared) = 0.003 %
CORRELATION COEFFICIENT = 0.600
VARIANCE OF SQR(Ns) = 3.606101
VARIANCE OF SQR(Ni) = 1.875621

Ns/Ni = 2.461 ± 0.134
MEAN RATIO = 2.604 ± 0.237

Pooled Age = 215.6 ± 13.5 Ma
Mean Age = 227.9 ± 22.0 Ma
Central Age = 215.6 ± 20.9Ma
% Rel. Error = 26.73
Ages calculated using a zeta of 140.2 ± 3.6 for CN 1 glass
RHO D = 1.271E+06cm-2; ND = 3105

9414-16 ZIRCON MARLBOROUGH

IRRADIATION WK145-18
SLIDE NUMBER 18
COUNTED BY: KAO

No.	Ns	Ni	Na	RATIO	U (ppm)	RHOs (E+06)	RHOi (E+06)	F.T.AGE (Ma)
1	180	52	9	3.462	0.0	20.222	5.842	302.4 ± 48.5
2	156	48	8	3.250	0.0	19.717	6.067	284.3 ± 47.8
3	94	22	9	4.273	0.0	10.561	2.472	371.3 ± 88.7
4	44	21	6	2.095	0.0	7.415	3.539	184.7 ± 49.3
5	68	26	8	2.615	0.0	8.595	3.286	229.8 ± 53.5
6	25	7	4	3.571	0.0	6.320	1.769	311.8 ± 133.7
7	78	24	8	3.250	0.0	9.858	3.033	284.3 ± 67.0
8	106	28	8	3.786	0.0	13.397	3.539	330.0 ± 70.9
9	61	23	4	2.652	0.0	15.420	5.814	233.0 ± 57.5
10	45	14	4	3.214	0.0	11.375	3.539	281.3 ± 86.5
11	69	27	4	2.556	0.0	17.442	6.825	224.6 ± 51.5
12	118	54	8	2.185	0.0	14.914	6.825	192.6 ± 32.2
13	96	45	4	2.133	0.0	24.267	11.375	188.1 ± 34.5
14	59	17	6	3.471	0.0	9.943	2.865	303.2 ± 84.0
15	65	38	6	1.711	0.0	10.954	6.404	151.2 ± 31.2
16	55	15	9	3.667	0.0	6.179	1.685	319.9 ± 93.7
17	104	55	8	1.891	0.0	13.145	6.951	167.0 ± 28.3
18	100	40	8	2.500	0.0	12.639	5.056	219.8 ± 41.7
19	58	22	4	2.636	0.0	14.661	5.561	231.6 ± 58.4
20	114	44	6	2.591	0.0	19.211	7.415	227.7 ± 41.0
	1695	622			0.0	13.083	4.801	

AREA OF BASIC UNIT = 9.89E-07 cm
CHI SQUARED = 27.8658 WITH 19 DEGREES OF FREEDOM
P(chi squared) = 8.6 %
CORRELATION COEFFICIENT = 0.825
VARIANCE OF SQR(Ns) = 4.19
VARIANCE OF SQR(Ni) = 1.84

Ns/Ni = 2.725 ± 0.128
MEAN RATIO = 2.875 ± 0.158

Ages calculated using a zeta of 140.2 ± 3.6 for CN1 glass
RHO D = 1.276E+06 ; ND = 3129

POOLED AGE = 239.3 ± 13.5 Ma
MEAN AGE = 252.2 ± 15.9 Ma

9414-17 ZIRCON MARLBOROUGH

IRRADIATION WK145-19
SLIDE NUMBER 19
COUNTED BY: KAO

No.	Ns	Ni	Na	RATIO	U (ppm)	RHOs (E+06)	RHOi (E+06)	F.T.AGE (Ma)
1	86	34	9	2.529	0.0	9.662	3.820	223.2 ± 45.8
2	47	12	4	3.917	0.0	11.881	3.033	342.4 ± 111.3
3	37	12	4	3.083	0.0	9.353	3.033	271.1 ± 90.5
4	69	27	6	2.556	0.0	11.628	4.550	225.5 ± 51.7
5	25	10	4	2.500	0.0	6.320	2.528	220.7 ± 82.9
6	48	16	4	3.000	0.0	12.133	4.044	263.9 ± 76.6
7	94	29	4	3.241	0.0	23.761	7.331	284.7 ± 61.1
8	74	28	4	2.643	0.0	18.706	7.078	233.1 ± 52.2
9	56	18	4	3.111	0.0	14.156	4.550	273.5 ± 74.6
10	18	6	4	3.000	0.0	4.550	1.517	263.9 ± 124.7
11	66	41	4	1.610	0.0	16.684	10.364	143.0 ± 28.8
12	75	31	8	2.419	0.0	9.479	3.918	213.7 ± 46.1
	695	264			0.0	11.911	4.524	

AREA OF BASIC UNIT = 9.89E-07 cm
CHI SQUARED = 9.856169 WITH 11 DEGREES OF FREEDOM
P(chi squared) = 54.3 %
CORRELATION COEFFICIENT = 0.856
VARIANCE OF SQR(Ns) = 2.83
VARIANCE OF SQR(Ni) = 1.53

Ns/Ni = 2.633 ± 0.190
MEAN RATIO = 2.801 ± 0.163

Ages calculated using a zeta of 140.2 ± 3.6 for CN1 glass
RHO D = 1.281E+06 ; ND = 3154

POOLED AGE = 232.2 ± 18.3 Ma
MEAN AGE = 246.7 ± 16.3 Ma

9414-19 Zircon

IRRADIATION WK146-1 COUNTED BY: KAO

No.	Ns	Ni	Na	RATIO	U(ppm)	RHOs	RHOi	F.T.AGE(Ma)
1	27	127	10	0.213	679.4	2.730E+06	1.284E+07	11.3 ± 2.4
2	18	90	6	0.200	802.5	3.033E+06	1.517E+07	10.6 ± 2.8
3	6	22	4	0.273	294.2	1.517E+06	5.561E+06	14.4 ± 6.7
4	25	108	10	0.231	577.8	2.528E+06	1.092E+07	12.3 ± 2.8
5	15	116	8	0.129	775.7	1.896E+06	1.466E+07	6.8 ± 1.9
6	19	111	4	0.171	%1484.6	4.803E+06	2.806E+07	9.1 ± 2.3
7	8	50	9	0.160	297.2	8.988E+05	5.617E+06	8.5 ± 3.2
8	18	91	9	0.198	540.9	2.022E+06	1.022E+07	10.5 ± 2.7
9	18	106	9	0.170	630.1	2.022E+06	1.191E+07	9.0 ± 2.3
10	4	54	9	0.074	321.0	4.494E+05	6.067E+06	3.9 ± 2.0
11	15	62	8	0.242	414.6	1.896E+06	7.836E+06	12.8 ± 3.7
12	14	83	9	0.169	493.4	1.573E+06	9.325E+06	8.9 ± 2.6
13	15	64	6	0.234	570.7	2.528E+06	1.079E+07	12.4 ± 3.6
14	4	64	8	0.062	428.0	5.056E+05	8.089E+06	3.3 ± 1.7
15	38	79	12	0.481	352.2	3.202E+06	6.657E+06	25.4 ± 5.1
16	36	190	8	0.189	%1270.6	4.550E+06	2.401E+07	10.0 ± 1.9
17	12	128	9	0.094	760.9	1.348E+06	1.438E+07	5.0 ± 1.5
18	19	90	8	0.211	601.9	2.401E+06	1.138E+07	11.2 ± 2.8
19	22	104	9	0.212	618.2	2.472E+06	1.168E+07	11.2 ± 2.7
20	15	96	9	0.156	570.7	1.685E+06	1.079E+07	8.3 ± 2.3
	348	1835			598.6	2.146E+06	1.131E+07	

Area of basic unit = 9.89E-07 cm-2

CHI SQUARED = 22.43726 WITH 19 DEGREES OF FREEDOM
P(chi squared) = 0.071 %
CORRELATION COEFFICIENT = 0.655
VARIANCE OF SQR(Ns) = 1.274233
VARIANCE OF SQR(Ni) = 3.714086

Ns/Ni = 0.190 ± 0.011
MEAN RATIO = 0.193 ± 0.020

Pooled Age = 10.0 ± 0.7 Ma
Mean Age = 10.2 ± 1.1 Ma
Central Age = 10.0 ± 0.9Ma
% Rel. Error = 30.01
Ages calculated using a zeta of 140.2 ± 3.6 for CN 1 glass
RHO D = 7.560E+05cm-2; ND = 1870

9414-20 ZIRCON MARLBOROUGH

IRRADIATION WK146-2
SLIDE NUMBER 2
COUNTED BY: KAO

No.	Ns	Ni	Na	RATIO	U (ppm)	RHOs (E+06)	RHOi (E+06)	F.T.AGE (Ma)
1	7	69	12	0.101	0.0	0.590	5.814	5.6 ± 2.2
2	11	84	12	0.131	0.0	0.927	7.078	7.2 ± 2.3
3	11	130	12	0.085	0.0	0.927	10.954	4.6 ± 1.5
4	17	44	6	0.386	0.0	2.865	7.415	21.2 ± 6.1
5	17	142	12	0.120	0.0	1.432	11.965	6.6 ± 1.7
6	30	162	9	0.185	0.0	3.370	18.200	10.2 ± 2.0
7	17	154	9	0.110	0.0	1.910	17.301	6.1 ± 1.6
8	22	158	10	0.139	0.0	2.224	15.976	7.6 ± 1.8
9	9	88	9	0.102	0.0	1.011	9.887	5.6 ± 2.0
10	11	115	9	0.096	0.0	1.236	12.920	5.2 ± 1.7
11	10	117	9	0.085	0.0	1.123	13.145	4.7 ± 1.6
12	19	125	12	0.152	0.0	1.601	10.533	8.3 ± 2.1
13	24	149	12	0.161	0.0	2.022	12.555	8.8 ± 2.0
14	8	54	4	0.148	0.0	2.022	13.650	8.1 ± 3.1
15	11	79	9	0.139	0.0	1.236	8.875	7.6 ± 2.5
16	7	61	6	0.115	0.0	1.180	10.280	6.3 ± 2.5
17	12	118	9	0.102	0.0	1.348	13.257	5.6 ± 1.7
18	21	148	12	0.142	0.0	1.769	12.471	7.8 ± 1.8
19	11	56	4	0.196	0.0	2.781	14.156	10.8 ± 3.6
20	7	73	4	0.096	0.0	1.769	18.453	5.3 ± 2.1
	282	2126			0.0	1.575	11.876	

AREA OF BASIC UNIT = 9.89E-07 cm
CHI SQUARED = 29.26193 WITH 19 DEGREES OF FREEDOM
P(chi squared) = 6.2 %
CORRELATION COEFFICIENT = 0.731
VARIANCE OF SQR(Ns) = 0.68
VARIANCE OF SQR(Ni) = 3.94

Ns/Ni = 0.133 ± 0.008
MEAN RATIO = 0.140 ± 0.015

Ages calculated using a zeta of 140.2 ± 3.6 for CN1 glass
RHO D = 7.830E+05 ; ND = 1939

POOLED AGE = 7.3 ± 0.5 Ma
MEAN AGE = 7.7 ± 0.9 Ma

9414-21 ZIRCON MARLBOROUGH

IRRADIATION WK146-4
SLIDE NUMBER 4
COUNTED BY: KAO

No.	Ns	Ni	Na	RATIO	U (ppm)	RHOs (E+06)	RHOi (E+06)	F.T.AGE (Ma)
1	7	70	9	0.100	0.0	0.786	7.864	5.9 ± 2.3
2	24	148	9	0.162	0.0	2.696	16.627	9.5 ± 2.1
3	11	139	9	0.079	0.0	1.236	15.616	4.6 ± 1.5
4	11	104	8	0.106	0.0	1.390	13.145	6.2 ± 2.0
5	6	37	4	0.162	0.0	1.517	9.353	9.5 ± 4.2
6	6	107	4	0.056	0.0	1.517	27.048	3.3 ± 1.4
7	6	53	9	0.113	0.0	0.674	5.954	6.6 ± 2.9
8	12	74	8	0.162	0.0	1.517	9.353	9.5 ± 3.0
9	9	120	9	0.075	0.0	1.011	13.482	4.4 ± 1.5
10	17	159	9	0.107	0.0	1.910	17.863	6.3 ± 1.6
11	22	162	9	0.136	0.0	2.472	18.200	8.0 ± 1.8
12	23	147	9	0.156	0.0	2.584	16.515	9.2 ± 2.1
13	12	88	8	0.136	0.0	1.517	11.122	8.0 ± 2.5
14	7	38	6	0.184	0.0	1.180	6.404	10.8 ± 4.5
15	16	197	9	0.081	0.0	1.798	22.132	4.8 ± 1.2
16	8	92	8	0.087	0.0	1.011	11.628	5.1 ± 1.9
17	14	67	6	0.209	0.0	2.359	11.291	12.2 ± 3.6
18	15	119	10	0.126	0.0	1.517	12.032	7.4 ± 2.0
19	17	159	9	0.107	0.0	1.910	17.863	6.3 ± 1.6
20	9	82	9	0.110	0.0	1.011	9.212	6.4 ± 2.3
	252	2162			0.0	1.583	13.578	

AREA OF BASIC UNIT = 9.89E-07 cm
CHI SQUARED = 21.30423 WITH 19 DEGREES OF FREEDOM
P(chi squared) = 32.0 %
CORRELATION COEFFICIENT = 0.735
VARIANCE OF SQR(Ns) = 0.63
VARIANCE OF SQR(Ni) = 5.16

Ns/Ni = 0.117 ± 0.008
MEAN RATIO = 0.123 ± 0.009

Ages calculated using a zeta of 140.2 ± 3.6 for CN1 glass
RHO D = 8.360E+05 ; ND = 2070

POOLED AGE = 6.8 ± 0.5 Ma
MEAN AGE = 7.2 ± 0.6 Ma

9414-25 ZIRCON MARLBOROUGH

IRRADIATION WK146-5
SLIDE NUMBER 5
COUNTED BY: KAO

No.	Ns	Ni	Na	RATIO	U (ppm)	RHOs (E+06)	RHOi (E+06)	F.T.AGE (Ma)
1	18	104	12	0.173	0.0	1.517	8.763	10.4 ± 2.7
2	21	150	9	0.140	0.0	2.359	16.852	8.5 ± 2.0
3	14	106	9	0.132	0.0	1.573	11.909	8.0 ± 2.3
4	10	76	9	0.132	0.0	1.123	8.538	7.9 ± 2.7
5	12	68	9	0.176	0.0	1.348	7.640	10.7 ± 3.4
6	14	102	8	0.137	0.0	1.769	12.892	8.3 ± 2.4
7	19	98	9	0.194	0.0	2.135	11.010	11.7 ± 3.0
8	25	107	9	0.234	0.0	2.809	12.021	14.1 ± 3.2
9	16	79	9	0.203	0.0	1.798	8.875	12.2 ± 3.4
10	25	196	9	0.128	0.0	2.809	22.020	7.7 ± 1.7
11	26	206	9	0.126	0.0	2.921	23.143	7.6 ± 1.6
12	12	111	9	0.108	0.0	1.348	12.471	6.5 ± 2.0
13	11	61	9	0.180	0.0	1.236	6.853	10.9 ± 3.6
14	9	82	10	0.110	0.0	0.910	8.291	6.6 ± 2.3
15	13	85	9	0.153	0.0	1.461	9.549	9.2 ± 2.8
16	23	117	9	0.197	0.0	2.584	13.145	11.9 ± 2.7
17	26	135	9	0.193	0.0	2.921	15.167	11.6 ± 2.5
18	13	92	10	0.141	0.0	1.314	9.302	8.5 ± 2.5
19	13	82	9	0.159	0.0	1.461	9.212	9.6 ± 2.9
20	16	77	9	0.208	0.0	1.798	8.651	12.5 ± 3.5
	336	2134			0.0	1.846	11.727	

AREA OF BASIC UNIT = 9.89E-07 cm
CHI SQUARED = 14.08061 WITH 19 DEGREES OF FREEDOM
P(chi squared) = 77.9 %
CORRELATION COEFFICIENT = 0.775
VARIANCE OF SQR(Ns) = 0.47
VARIANCE OF SQR(Ni) = 3.05

Ns/Ni = 0.157 ± 0.009
MEAN RATIO = 0.161 ± 0.008

Ages calculated using a zeta of 140.2 ± 3.6 for CN1 glass
RHO D = 8.620E+05 ; ND = 2136

POOLED AGE = 9.5 ± 0.6 Ma
MEAN AGE = 9.7 ± 0.6 Ma

9414-31 ZIRCON MARLBOROUGH

IRRADIATION WK146-13
SLIDE NUMBER 13
COUNTED BY: KAO

No.	Ns	Ni	Na	RATIO	U (ppm)	RHOs (E+06)	RHOi (E+06)	F.T.AGE (Ma)
1	126	22	4	5.727	0.0	31.850	5.561	418.1 ± 97.5
2	75	18	4	4.167	0.0	18.959	4.550	306.9 ± 81.1
3	91	36	4	2.528	0.0	23.003	9.100	187.9 ± 37.5
4	260	79	9	3.291	0.0	29.210	8.875	243.6 ± 32.3
5	79	24	4	3.292	0.0	19.970	6.067	243.6 ± 57.3
6	122	37	4	3.297	0.0	30.839	9.353	244.0 ± 46.5
7	103	34	4	3.029	0.0	26.036	8.595	224.5 ± 45.0
8	151	61	9	2.475	0.0	16.964	6.853	184.1 ± 28.5
9	77	18	4	4.278	0.0	19.464	4.550	314.8 ± 83.0
10	92	22	4	4.182	0.0	23.256	5.561	308.0 ± 73.8
	1176	351			0.0	23.782	7.098	

AREA OF BASIC UNIT = 9.89E-07 cm
CHI SQUARED = 14.32247 WITH 9 DEGREES OF FREEDOM
P(chi squared) = 11.1 %
CORRELATION COEFFICIENT = 0.909
VARIANCE OF SQR(Ns) = 5.15
VARIANCE OF SQR(Ni) = 2.42

Ns/Ni = 3.350 ± 0.204
MEAN RATIO = 3.627 ± 0.310

Ages calculated using a zeta of 140.2 ± 3.6 for CN1 glass
RHO D = 1.076E+06 ; ND = 2662

POOLED AGE = 247.9 ± 17.1 Ma
MEAN AGE = 267.9 ± 24.5 Ma

9414-32 ZIRCON MARLBOROUGH

IRRADIATION WK146-14
SLIDE NUMBER 14
COUNTED BY: KAO

No.	Ns	Ni	Na	RATIO	U (ppm)	RHOs (E+06)	RHOi (E+06)	F.T.AGE (Ma)
1	103	40	9	2.575	0.0	11.572	4.494	195.9 ± 37.0
2	120	43	6	2.791	0.0	20.222	7.246	212.1 ± 38.3
3	110	51	9	2.157	0.0	12.358	5.730	164.5 ± 28.4
4	45	26	9	1.731	0.0	5.056	2.921	132.3 ± 32.9
5	65	31	9	2.097	0.0	7.303	3.483	160.0 ± 35.3
6	97	34	9	2.853	0.0	10.898	3.820	216.7 ± 43.7
7	123	73	9	1.685	0.0	13.819	8.201	128.9 ± 19.5
8	84	27	4	3.111	0.0	21.234	6.825	236.0 ± 52.7
9	200	71	9	2.817	0.0	22.469	7.977	214.0 ± 30.3
10	92	53	6	1.736	0.0	15.504	8.932	132.7 ± 23.3
	1039	449			0.0	13.298	5.747	

AREA OF BASIC UNIT = 9.89E-07 cm
CHI SQUARED = 15.61165 WITH 9 DEGREES OF FREEDOM
P(chi squared) = 7.5 %
CORRELATION COEFFICIENT = 0.797
VARIANCE OF SQR(Ns) = 3.89
VARIANCE OF SQR(Ni) = 1.54

Ns/Ni = 2.314 ± 0.131
MEAN RATIO = 2.355 ± 0.170

Ages calculated using a zeta of 140.2 ± 3.6 for CN1 glass
RHO D = 1.102E+06 ; ND = 2728

POOLED AGE = 176.3 ± 11.4 Ma
MEAN AGE = 179.4 ± 14.2 Ma

9414-33 ZIRCON MARLBOROUGH

IRRADIATION WK146-15
SLIDE NUMBER 15
COUNTED BY: KAO

No.	Ns	Ni	Na	RATIO	U (ppm)	RHOs (E+06)	RHOi (E+06)	F.T.AGE (Ma)
1	189	110	9	1.718	0.0	21.234	12.358	134.6 ± 16.7
2	98	36	4	2.722	0.0	24.772	9.100	211.9 ± 41.8
3	75	33	4	2.273	0.0	18.959	8.342	177.4 ± 37.5
4	29	14	6	2.071	0.0	4.887	2.359	161.9 ± 52.9
5	57	29	4	1.966	0.0	14.408	7.331	153.7 ± 35.4
6	79	42	4	1.881	0.0	19.970	10.617	147.2 ± 28.5
7	136	50	10	2.720	0.0	13.751	5.056	211.8 ± 35.7
8	72	38	9	1.895	0.0	8.089	4.269	148.2 ± 30.1
9	138	63	9	2.190	0.0	15.504	7.078	171.1 ± 26.6
10	66	32	6	2.062	0.0	11.122	5.393	161.2 ± 35.1
11	71	32	6	2.219	0.0	11.965	5.393	173.2 ± 37.3
12	98	54	9	1.815	0.0	11.010	6.067	142.1 ± 24.5
13	122	39	6	3.128	0.0	20.559	6.572	242.9 ± 45.4
14	70	41	9	1.707	0.0	7.864	4.606	133.7 ± 26.6
15	76	34	9	2.235	0.0	8.538	3.820	174.5 ± 36.4
16	80	36	4	2.222	0.0	20.222	9.100	173.5 ± 35.3
17	62	34	6	1.824	0.0	10.448	5.730	142.7 ± 30.8
18	33	17	9	1.941	0.0	3.707	1.910	151.8 ± 45.6
19	111	43	9	2.581	0.0	12.471	4.831	201.1 ± 36.7
20	77	38	9	2.026	0.0	8.651	4.269	158.4 ± 31.8
	1739	815			0.0	12.471	5.844	

AREA OF BASIC UNIT = 9.89E-07 cm
CHI SQUARED = 16.63015 WITH 19 DEGREES OF FREEDOM
P(chi squared) = 61.5 %
CORRELATION COEFFICIENT = 0.901
VARIANCE OF SQR(Ns) = 3.90
VARIANCE OF SQR(Ni) = 1.89

Ns/Ni = 2.134 ± 0.091
MEAN RATIO = 2.160 ± 0.084

Ages calculated using a zeta of 140.2 ± 3.6 for CN1 glass
RHO D = 1.129E+06 ; ND = 2794

POOLED AGE = 166.7 ± 8.9 Ma
MEAN AGE = 168.7 ± 8.5 Ma

9414-34 ZIRCON MARLBOROUGH

IRRADIATION WK146-16
SLIDE NUMBER 16
COUNTED BY: KAO

No.	Ns	Ni	Na	RATIO	U (ppm)	RHOs (E+06)	RHOi (E+06)	F.T.AGE (Ma)
1	52	16	4	3.250	0.0	13.145	4.044	257.9 ± 74.2
2	62	43	4	1.442	0.0	15.672	10.870	115.7 ± 23.3
3	65	16	4	4.062	0.0	16.431	4.044	320.8 ± 90.1
4	69	35	4	1.971	0.0	17.442	8.847	157.7 ± 33.1
5	72	35	4	2.057	0.0	18.200	8.847	164.4 ± 34.3
6	121	56	8	2.161	0.0	15.293	7.078	172.6 ± 28.4
7	51	29	4	1.759	0.0	12.892	7.331	140.8 ± 33.1
8	66	19	4	3.474	0.0	16.684	4.803	275.3 ± 72.2
9	120	64	8	1.875	0.0	15.167	8.089	150.0 ± 23.7
10	61	37	8	1.649	0.0	7.710	4.676	132.1 ± 27.8
11	63	39	6	1.615	0.0	10.617	6.572	129.5 ± 26.7
12	79	46	4	1.717	0.0	19.970	11.628	137.6 ± 25.9
13	58	26	4	2.231	0.0	14.661	6.572	178.1 ± 42.4
14	85	55	4	1.545	0.0	21.486	13.903	123.9 ± 21.8
15	63	31	4	2.032	0.0	15.925	7.836	162.5 ± 36.0
	1087	547			0.0	14.853	7.474	

AREA OF BASIC UNIT = 9.89E-07 cm
CHI SQUARED = 22.77985 WITH 14 DEGREES OF FREEDOM
P(chi squared) = 6.4 %
CORRELATION COEFFICIENT = 0.803
VARIANCE OF SQR(Ns) = 1.36
VARIANCE OF SQR(Ni) = 1.51

Ns/Ni = 1.987 ± 0.104
MEAN RATIO = 2.189 ± 0.201

Ages calculated using a zeta of 140.2 ± 3.6 for CN1 glass
RHO D = 1.155E+06 ; ND = 2860

POOLED AGE = 158.9 ± 9.7 Ma
MEAN AGE = 174.9 ± 17.0 Ma

9414-35 ZIRCON MARLBOROUGH

IRRADIATION WK146-17
SLIDE NUMBER 17
COUNTED BY: KAO

No.	Ns	Ni	Na	RATIO	U (ppm)	RHOs (E+06)	RHOi (E+06)	F.T.AGE (Ma)
1	76	18	4	4.222	0.0	19.211	4.550	340.7 ± 90.0
2	62	32	6	1.938	0.0	10.448	5.393	158.6 ± 34.9
3	91	37	4	2.459	0.0	23.003	9.353	200.6 ± 39.6
4	90	38	4	2.368	0.0	22.750	9.606	193.3 ± 37.9
5	131	53	9	2.472	0.0	14.717	5.954	201.6 ± 33.4
6	111	36	9	3.083	0.0	12.471	4.044	250.5 ± 48.7
7	63	24	4	2.625	0.0	15.925	6.067	213.9 ± 51.8
8	130	36	9	3.611	0.0	14.605	4.044	292.5 ± 55.9
9	115	47	9	2.447	0.0	12.920	5.280	199.6 ± 35.1
10	105	37	4	2.838	0.0	26.542	9.353	231.0 ± 44.8
11	99	35	9	2.829	0.0	11.122	3.932	230.2 ± 45.9
	1073	393			0.0	15.281	5.597	

AREA OF BASIC UNIT = 9.89E-07 cm
CHI SQUARED = 9.64241 WITH 10 DEGREES OF FREEDOM
P(chi squared) = 47.2 %
CORRELATION COEFFICIENT = 0.744
VARIANCE OF SQR(Ns) = 1.54
VARIANCE OF SQR(Ni) = 0.68

Ns/Ni = 2.730 ± 0.161
MEAN RATIO = 2.808 ± 0.192

Ages calculated using a zeta of 140.2 ± 3.6 for CN1 glass
RHO D = 1.182E+06 ; ND = 2926

POOLED AGE = 222.3 ± 14.9 Ma
MEAN AGE = 228.6 ± 17.2 Ma

9414-36 Zircon

IRRADIATION WK146-18 COUNTED BY: KAO

No.	Ns	Ni	Na	RATIO	U(ppm)	RHOs	RHOi	F.T.AGE(Ma)
1	56	13	4	4.308	108.7	1.416E+07	3.286E+06	355.1 ±109.9
2	92	30	6	3.067	167.3	1.550E+07	5.056E+06	254.8 ± 54.2
3	98	28	4	3.500	234.2	2.477E+07	7.078E+06	290.0 ± 62.8
4	63	26	4	2.423	217.4	1.593E+07	6.572E+06	202.2 ± 47.6
5	69	26	4	2.654	217.4	1.744E+07	6.572E+06	221.1 ± 51.3
6	71	69	4	1.029	577.1	1.795E+07	1.744E+07	86.6 ± 14.9
7	42	13	4	3.231	108.7	1.062E+07	3.286E+06	268.2 ± 85.5
8	59	27	4	2.185	225.8	1.491E+07	6.825E+06	182.6 ± 42.8
9	72	24	6	3.000	133.8	1.213E+07	4.044E+06	249.4 ± 59.3
10	105	16	6	6.562	89.2	1.769E+07	2.696E+06	533.5 ±144.2
11	130	18	4	7.222	150.5	3.286E+07	4.550E+06	584.7 ±148.2
	857	290			194.0	1.733E+07	5.865E+06	

Area of basic unit = 9.89E-07 cm-2

CHI SQUARED = 35.20123 WITH 10 DEGREES OF FREEDOM
P(chi squared) = 0.000 %
CORRELATION COEFFICIENT = -0.036
VARIANCE OF SQR(Ns) = 2.022229
VARIANCE OF SQR(Ni) = 1.677444

Ns/Ni = 2.955 ± 0.201
MEAN RATIO = 3.562 ± 0.556

Pooled Age = 245.7 ± 18.4 Ma
Mean Age = 295.0 ± 47.0 Ma
Central Age = 246.6 ± 39.7Ma
% Rel. Error = 47.95
Ages calculated using a zeta of 140.2 ± 3.6 for CN 1 glass
RHO D = 1.209E+06cm-2; ND = 2992

9414-37 Zircon

IRRADIATION WK146-19 COUNTED BY: KAO

No.	Ns	Ni	Na	RATIO	U(ppm)	RHOs	RHOi	F.T.AGE(Ma)
1	53	22	4	2.409	18.0	1.340E+06	5.561E+05	205.3 ± 52.5
2	53	35	4	1.514	28.7	1.340E+06	8.847E+05	129.8 ± 28.6
3	47	36	4	1.306	29.5	1.188E+06	9.100E+05	112.0 ± 25.1
4	54	10	4	5.400	8.2	1.365E+06	2.528E+05	451.3 ±156.0
5	31	9	4	3.444	7.4	7.836E+05	2.275E+05	291.5 ±110.8
	238	112			18.3	1.203E+06	5.662E+05	

Area of basic unit = 9.89E-06 cm-2

CHI SQUARED = 8.583975 WITH 4 DEGREES OF FREEDOM
P(chi squared) = 0.179 %
CORRELATION COEFFICIENT = 0.398
VARIANCE OF SQR(Ns) = .5653191
VARIANCE OF SQR(Ni) = 2.079151

Ns/Ni = 2.125 ± 0.243
MEAN RATIO = 2.815 ± 0.749

Pooled Age = 181.4 ± 21.6 Ma
Mean Age = 239.2 ± 64.1 Ma
Central Age = 192.6 ± 42.5Ma
% Rel. Error = 41.71
Ages calculated using a zeta of 140.2 ± 3.6 for CN 1 glass
RHO D = 1.235E+06cm-2; ND = 3057

9414-38 Zircon

IRRADIATION WK146-20 COUNTED BY: KAO

No.	Ns	Ni	Na	RATIO	U(ppm)	RHOs	RHOi	F.T.AGE(Ma)
1	123	29	9	4.241	103.3	1.382E+07	3.258E+06	364.7 ± 76.1
2	107	34	9	3.147	121.1	1.202E+07	3.820E+06	272.6 ± 54.3
3	61	21	9	2.905	74.8	6.853E+06	2.359E+06	252.0 ± 64.2
4	105	98	9	1.071	349.0	1.180E+07	1.101E+07	94.1 ± 13.5
5	100	73	8	1.370	292.4	1.264E+07	9.226E+06	120.1 ± 18.9
6	63	40	6	1.575	213.7	1.062E+07	6.741E+06	137.8 ± 28.2
7	131	94	16	1.394	188.3	8.279E+06	5.940E+06	122.1 ± 16.9
8	93	48	4	1.938	384.6	2.351E+07	1.213E+07	169.2 ± 30.5
9	42	18	6	2.333	96.1	7.078E+06	3.033E+06	203.2 ± 57.6
10	78	54	6	1.444	288.4	1.314E+07	9.100E+06	126.5 ± 22.7
11	76	62	8	1.226	248.4	9.606E+06	7.836E+06	107.5 ± 18.7
12	76	28	6	2.714	149.6	1.281E+07	4.719E+06	235.8 ± 52.6
13	72	57	9	1.263	203.0	8.089E+06	6.404E+06	110.8 ± 19.9
14	88	78	20	1.128	125.0	4.449E+06	3.943E+06	99.0 ± 15.7
15	111	29	9	3.828	103.3	1.247E+07	3.258E+06	330.0 ± 69.6
16	101	34	9	2.971	121.1	1.135E+07	3.820E+06	257.6 ± 51.7
17	76	49	9	1.551	174.5	8.538E+06	5.505E+06	135.8 ± 25.2
18	76	39	9	1.949	138.9	8.538E+06	4.382E+06	170.1 ± 33.9
19	74	32	4	2.312	256.4	1.871E+07	8.089E+06	201.4 ± 43.1
20	40	24	4	1.667	192.3	1.011E+07	6.067E+06	145.8 ± 37.9
	1693	941			178.4	1.013E+07	5.630E+06	

Area of basic unit = 9.89E-07 cm-2

CHI SQUARED = 49.16979 WITH 19 DEGREES OF FREEDOM
P(chi squared) = 0.000 %
CORRELATION COEFFICIENT = 0.473
VARIANCE OF SQR(Ns) = 1.859767
VARIANCE OF SQR(Ni) = 2.734179

Ns/Ni = 1.799 ± 0.073
MEAN RATIO = 2.101 ± 0.207

Pooled Age = 157.2 ± 8.1 Ma
Mean Age = 183.3 ± 18.9 Ma
Central Age = 162.8 ± 14.8Ma
% Rel. Error = 35.26
Ages calculated using a zeta of 140.2 ± 3.6 for CN 1 glass
RHO D = 1.262E+06cm-2; ND = 3120

9414-39 Zircon

IRRADIATION WK147-2 COUNTED BY: KAO

No.	Ns	Ni	Na	RATIO	U(ppm)	RHOs	RHOi	F.T.AGE(Ma)
1	90	53	6	1.698	%2878.1	1.354E+08	7.972E+07	130.6 ± 23.0
2	37	11	8	3.364	448.0	4.174E+07	1.241E+07	256.1 ± 88.3
3	146	45	9	3.244	%1629.1	1.464E+08	4.513E+07	247.2 ± 42.9
4	116	38	8	3.053	%1547.7	1.309E+08	4.287E+07	232.8 ± 44.2
5	121	55	9	2.200	%1991.1	1.213E+08	5.515E+07	168.6 ± 28.0
6	104	68	10	1.529	%2215.6	9.386E+07	6.137E+07	117.7 ± 18.7
7	91	27	9	3.370	977.5	9.126E+07	2.708E+07	256.6 ± 56.8
8	124	34	9	3.647	%1230.9	1.243E+08	3.410E+07	277.2 ± 54.4
9	99	49	9	2.020	%1773.9	9.928E+07	4.914E+07	155.0 ± 27.5
10	39	30	4	1.300	%2443.7	8.800E+07	6.769E+07	100.2 ± 24.5
11	29	8	9	3.625	289.6	2.908E+07	8.022E+06	275.6 ±110.4
12	42	22	4	1.909	%1792.0	9.477E+07	4.964E+07	146.6 ± 38.9
13	70	18	4	3.889	%1466.2	1.579E+08	4.061E+07	295.2 ± 78.6
14	26	18	4	1.444	%1466.2	5.866E+07	4.061E+07	111.2 ± 34.3
15	57	52	9	1.096	%1882.5	5.716E+07	5.215E+07	84.6 ± 16.4
16	67	35	9	1.914	%1267.1	6.719E+07	3.510E+07	147.0 ± 31.0
17	65	47	9	1.383	%1701.5	6.518E+07	4.713E+07	106.5 ± 20.7
18	121	68	9	1.779	%2461.8	1.213E+08	6.819E+07	136.7 ± 21.2
	1444	678			%1600.8	9.444E+07	4.434E+07	

Area of basic unit = 1.108E-07 cm-2

CHI SQUARED = 31.48453 WITH 17 DEGREES OF FREEDOM
P(chi squared) = 0.000 %
CORRELATION COEFFICIENT = 0.663
VARIANCE OF SQR(Ns) = 4.7786
VARIANCE OF SQR(Ni) = 2.558705

Ns/Ni = 2.130 ± 0.099
MEAN RATIO = 2.359 ± 0.224

Pooled Age = 163.3 ± 9.2 Ma
Mean Age = 180.7 ± 18.1 Ma
Central Age = 162.0 ± 14.9Ma
% Rel. Error = 31.94
Ages calculated using a zeta of 140.2 ± 3.6 for CN 1 glass
RHO D = 1.108E+06cm-2; ND = 2738

9414-40 ZIRCON MARLBOROUGH

IRRADIATION WK147-3
SLIDE NUMBER 3
COUNTED BY: KAO

No.	Ns	Ni	Na	RATIO	U (ppm)	RHOs (E+06)	RHOi (E+06)	F.T.AGE (Ma)
1	119	33	9	3.606	0.0	13.369	3.707	276.4 ± 55.1
2	21	8	9	2.625	0.0	2.359	0.899	202.3 ± 84.3
3	38	22	4	1.727	0.0	9.606	5.561	133.8 ± 36.1
4	120	38	9	3.158	0.0	13.482	4.269	242.6 ± 45.8
5	34	15	4	2.267	0.0	8.595	3.792	175.1 ± 54.6
6	40	20	4	2.000	0.0	10.111	5.056	154.7 ± 42.7
	372	136			0.0	9.645	3.526	

AREA OF BASIC UNIT = 9.89E-07 cm
CHI SQUARED = 7.275556 WITH 5 DEGREES OF FREEDOM
P(chi squared) = 20.1 %
CORRELATION COEFFICIENT = 0.942
VARIANCE OF SQR(Ns) = 7.60
VARIANCE OF SQR(Ni) = 1.49

Ns/Ni = 2.735 ± 0.274
MEAN RATIO = 2.564 ± 0.291

Ages calculated using a zeta of 140.2 ± 3.6 for CN1 glass
RHO D = 1.117E+06 ; ND = 2761

POOLED AGE = 210.7 ± 22.2 Ma
MEAN AGE = 197.7 ± 23.3 Ma

9414-41 Zircon

IRRADIATION WK147-4 COUNTED BY: KAO

No.	Ns	Ni	Na	RATIO	U(ppm)	RHOs	RHOi	F.T.AGE(Ma)
1	55	14	6	3.929	83.7	9.269E+06	2.359E+06	303.1 ± 91.3
2	99	38	6	2.605	227.3	1.668E+07	6.404E+06	202.6 ± 39.2
3	53	31	4	1.710	278.1	1.340E+07	7.836E+06	133.7 ± 30.5
4	127	39	9	3.256	155.5	1.427E+07	4.382E+06	252.3 ± 46.9
5	45	14	6	3.214	83.7	7.583E+06	2.359E+06	249.1 ± 76.6
6	107	30	8	3.567	134.6	1.352E+07	3.792E+06	275.8 ± 57.7
7	35	30	8	1.167	134.6	4.424E+06	3.792E+06	91.5 ± 23.0
8	25	9	4	2.778	80.7	6.320E+06	2.275E+06	215.8 ± 84.2
9	44	26	4	1.692	233.3	1.112E+07	6.572E+06	132.3 ± 33.0
10	46	13	4	3.538	116.6	1.163E+07	3.286E+06	273.7 ± 86.4
	636	244	.		148.4	1.090E+07	4.182E+06	

Area of basic unit = 9.89E-07 cm-2

CHI SQUARED = 12.40251 WITH 9 DEGREES OF FREEDOM
P(chi squared) = 0.319 %
CORRELATION COEFFICIENT = 0.722
VARIANCE OF SQR(Ns) = 4.275309
VARIANCE OF SQR(Ni) = 1.383469

Ns/Ni = 2.607 ± 0.196
MEAN RATIO = 2.746 ± 0.296

Pooled Age = 202.7 ± 16.6 Ma
Mean Age = 213.3 ± 24.0 Ma
Central Age = 196.3 ± 24.5Ma
% Rel. Error = 30.03
Ages calculated using a zeta of 140.2 ± 3.6 for CN 1 glass
RHO D = 1.127E+06cm-2; ND = 2785

9414-42 Zircon

IRRADIATION WK147-5 COUNTED BY: KAO

No.	Ns	Ni	Na	RATIO	U(ppm)	RHOs	RHOi	F.T.AGE(Ma)
1	76	56	9	1.357	221.5	8.538E+06	6.291E+06	107.2 ± 19.2
2	98	71	14	1.380	180.6	7.078E+06	5.128E+06	109.0 ± 17.3
3	49	18	8	2.722	80.1	6.193E+06	2.275E+06	213.2 ± 59.2
4	50	50	9	1.000	197.8	5.617E+06	5.617E+06	79.1 ± 16.0
5	77	48	9	1.604	189.9	8.651E+06	5.393E+06	126.5 ± 23.6
6	46	32	9	1.438	126.6	5.168E+06	3.595E+06	113.5 ± 26.4
7	32	17	9	1.882	67.2	3.595E+06	1.910E+06	148.2 ± 44.7
8	101	64	9	1.578	253.2	1.135E+07	7.190E+06	124.5 ± 20.3
9	42	38	9	1.105	150.3	4.719E+06	4.269E+06	87.4 ± 19.8
10	123	85	9	1.447	336.2	1.382E+07	9.549E+06	114.2 ± 16.5
11	94	61	9	1.541	241.3	1.056E+07	6.853E+06	121.6 ± 20.4
12	70	23	8	3.043	102.4	8.847E+06	2.907E+06	237.9 ± 57.7
13	144	70	9	2.057	276.9	1.618E+07	7.864E+06	161.8 ± 24.1
14	108	48	8	2.250	213.6	1.365E+07	6.067E+06	176.7 ± 31.2
15	74	21	9	3.524	83.1	8.314E+06	2.359E+06	274.7 ± 68.5
16	36	25	8	1.440	111.3	4.550E+06	3.160E+06	113.7 ± 29.8
17	55	38	9	1.447	150.3	6.179E+06	4.269E+06	114.2 ± 24.4
18	71	27	10	2.630	96.1	7.179E+06	2.730E+06	206.1 ± 47.1
19	121	78	9	1.551	308.6	1.359E+07	8.763E+06	122.4 ± 18.2
20	48	16	6	3.000	94.9	8.089E+06	2.696E+06	234.6 ± 68.1
	1515	886			176.2	8.558E+06	5.005E+06	

Area of basic unit = 9.89E-07 cm-2

CHI SQUARED = 24.33389 WITH 19 DEGREES OF FREEDOM
P(chi squared) = 0.021 %
CORRELATION COEFFICIENT = 0.819
VARIANCE OF SQR(Ns) = 3.370014
VARIANCE OF SQR(Ni) = 2.845533

Ns/Ni = 1.710 ± 0.072
MEAN RATIO = 1.900 ± 0.161

Pooled Age = 134.7 ± 7.1 Ma
Mean Age = 149.5 ± 13.5 Ma
Central Age = 136.7 ± 9.9Ma
% Rel. Error = 23.95
Ages calculated using a zeta of 140.2 ± 3.6 for CN 1 glass
RHO D = 1.136E+06cm-2; ND = 2809

9414-43 Zircon

IRRADIATION WK147-6 COUNTED BY: KAO

No.	Ns	Ni	Na	RATIO	U(ppm)	RHOs	RHOi	F.T.AGE(Ma)
1	52	21	6	2.476	123.5	8.763E+06	3.539E+06	195.9 ± 51.0
2	37	13	6	2.846	76.5	6.235E+06	2.191E+06	224.7 ± 72.8
3	143	43	9	3.326	168.6	1.607E+07	4.831E+06	261.8 ± 46.3
4	54	50	9	1.080	196.1	6.067E+06	5.617E+06	86.2 ± 17.1
5	29	8	4	3.625	70.6	7.331E+06	2.022E+06	284.8 ±114.1
6	41	20	8	2.050	88.2	5.182E+06	2.528E+06	162.6 ± 44.7
7	52	39	8	1.333	172.0	6.572E+06	4.929E+06	106.2 ± 22.8
8	60	20	8	3.000	88.2	7.583E+06	2.528E+06	236.6 ± 61.6
9	75	25	6	3.000	147.1	1.264E+07	4.213E+06	236.6 ± 55.2
10	52	38	9	1.368	149.0	5.842E+06	4.269E+06	109.0 ± 23.5
	595	277	-		133.9	8.241E+06	3.837E+06	

Area of basic unit = 9.89E-07 cm-2

CHI SQUARED = 17.77209 WITH 9 DEGREES OF FREEDOM
P(chi squared) = 0.005 %
CORRELATION COEFFICIENT = 0.518
VARIANCE OF SQR(Ns) = 3.24842
VARIANCE OF SQR(Ni) = 1.879205

Ns/Ni = 2.148 ± 0.156
MEAN RATIO = 2.410 ± 0.286

Pooled Age = 170.3 ± 13.5 Ma
Mean Age = 190.8 ± 23.4 Ma
Central Age = 169.4 ± 23.3Ma
% Rel. Error = 35.64
Ages calculated using a zeta of 140.2 ± 3.6 for CN 1 glass
RHO D = 1.146E+06cm-2; ND = 2833

9414-44 ZIRCON MARLBOROUGH

IRRADIATION WK147-7
SLIDE NUMBER 7
COUNTED BY: KAO

No.	Ns	Ni	Na	RATIO	U (ppm)	RHOs (E+06)	RHOi (E+06)	F.T.AGE (Ma)
1	54	34	9	1.588	0.0	6.067	3.820	127.4 ± 28.2
2	36	23	6	1.565	0.0	6.067	3.876	125.6 ± 33.8
3	52	25	6	2.080	0.0	8.763	4.213	166.4 ± 40.8
4	21	10	4	2.100	0.0	5.308	2.528	168.0 ± 64.8
5	53	36	4	1.472	0.0	13.397	9.100	118.2 ± 25.8
6	50	32	6	1.562	0.0	8.426	5.393	125.4 ± 28.7
7	32	13	4	2.462	0.0	8.089	3.286	196.4 ± 64.9
8	136	51	8	2.667	0.0	17.189	6.446	212.6 ± 35.5
9	47	24	4	1.958	0.0	11.881	6.067	156.8 ± 39.6
10	41	35	9	1.171	0.0	4.606	3.932	94.2 ± 21.9
11	21	12	6	1.750	0.0	3.539	2.022	140.3 ± 51.0
12	121	68	9	1.779	0.0	13.594	7.640	142.6 ± 22.1
13	19	12	4	1.583	0.0	4.803	3.033	127.0 ± 47.0
14	50	37	4	1.351	0.0	12.639	9.353	108.6 ± 23.8
15	53	23	8	2.304	0.0	6.699	2.907	184.1 ± 46.3
16	50	19	6	2.632	0.0	8.426	3.202	209.8 ± 56.9
17	34	17	4	2.000	0.0	8.595	4.297	160.1 ± 47.8
18	46	32	6	1.438	0.0	7.752	5.393	115.4 ± 26.8
19	59	38	4	1.553	0.0	14.914	9.606	124.6 ± 26.2
20	19	9	4	2.111	0.0	4.803	2.275	168.8 ± 68.5
	994	550			0.0	8.740	4.836	

AREA OF BASIC UNIT = 9.89E-07 cm
CHI SQUARED = 19.39411 WITH 19 DEGREES OF FREEDOM
P(chi squared) = 43.2 %
CORRELATION COEFFICIENT = 0.882
VARIANCE OF SQR(Ns) = 3.58
VARIANCE OF SQR(Ni) = 1.91

Ns/Ni = 1.807 ± 0.096
MEAN RATIO = 1.856 ± 0.096

Ages calculated using a zeta of 140.2 ± 3.6 for CN1 glass
RHO D = 1.156E+06 ; ND = 2856

POOLED AGE = 144.8 ± 9.0 Ma
MEAN AGE = 148.7 ± 9.0 Ma

9414-45 Zircon

IRRADIATION WK147-8 COUNTED BY: KAO

No.	Ns	Ni	Na	RATIO	U(ppm)	RHOs	RHOi	F.T.AGE(Ma)
1	116	32	9	3.625	123.3	1.303E+07	3.595E+06	289.7 ± 58.6
2	87	54	9	1.611	208.1	9.774E+06	6.067E+06	130.4 ± 23.0
3	35	18	9	1.944	69.4	3.932E+06	2.022E+06	157.0 ± 45.8
4	78	47	6	1.660	271.7	1.314E+07	7.920E+06	134.2 ± 25.2
5	64	64	9	1.000	246.7	7.190E+06	7.190E+06	81.2 ± 14.6
6	97	24	6	4.042	138.7	1.635E+07	4.044E+06	322.2 ± 74.2
7	39	35	4	1.114	303.5	9.858E+06	8.847E+06	90.4 ± 21.3
8	32	29	9	1.103	111.8	3.595E+06	3.258E+06	89.6 ± 23.1
9	79	52	9	1.519	200.4	8.875E+06	5.842E+06	123.0 ± 22.3
10	68	45	9	1.511	173.4	7.640E+06	5.056E+06	122.3 ± 23.8
11	74	47	4	1.574	407.6	1.871E+07	1.188E+07	127.4 ± 24.1
12	67	24	9	2.792	92.5	7.527E+06	2.696E+06	224.2 ± 53.8
13	62	37	9	1.676	142.6	6.966E+06	4.157E+06	135.5 ± 28.5
14	97	60	9	1.617	231.2	1.090E+07	6.741E+06	130.8 ± 21.9
15	63	48	12	1.312	138.7	5.308E+06	4.044E+06	106.4 ± 20.7
16	65	27	9	2.407	104.1	7.303E+06	3.033E+06	193.8 ± 44.8
17	103	42	8	2.452	182.1	1.302E+07	5.308E+06	197.4 ± 36.7
18	91	54	9	1.685	208.1	1.022E+07	6.067E+06	136.3 ± 23.8
19	40	34	9	1.176	131.0	4.494E+06	3.820E+06	95.4 ± 22.5
20	61	27	4	2.259	234.1	1.542E+07	6.825E+06	182.1 ± 42.5
	1418	800			172.4	8.905E+06	5.024E+06	

Area of basic unit = 9.89E-07 cm-2

CHI SQUARED = 31.88738 WITH 19 DEGREES OF FREEDOM
P(chi squared) = 0.000 %
CORRELATION COEFFICIENT = 0.359
VARIANCE OF SQR(Ns) = 2.060026
VARIANCE OF SQR(Ni) = 1.126744

Ns/Ni = 1.772 ± 0.078
MEAN RATIO = 1.904 ± 0.183

Pooled Age = 143.3 ± 7.8 Ma
Mean Age = 153.8 ± 15.6 Ma
Central Age = 141.3 ± 11.5Ma
% Rel. Error = 29.20
Ages calculated using a zeta of 140.2 ± 3.6 for CN 1 glass
RHO D = 1.166E+06cm-2; ND = 2880

9414-47 Zircon

IRRADIATION WK147-10 COUNTED BY: KAO

No.	Ns	Ni	Na	RATIO	U(ppm)	RHOs	RHOi	F.T.AGE(Ma)
1	85	38	6	2.237	216.2	1.432E+07	6.404E+06	183.2 ± 36.2
2	60	36	8	1.667	153.6	7.583E+06	4.550E+06	137.0 ± 29.2
3	93	51	9	1.824	193.4	1.045E+07	5.730E+06	149.7 ± 26.5
4	145	45	9	3.222	170.7	1.629E+07	5.056E+06	262.3 ± 45.5
5	78	63	9	1.238	238.9	8.763E+06	7.078E+06	102.0 ± 17.6
6	91	65	9	1.400	246.5	1.022E+07	7.303E+06	115.3 ± 19.1
7	109	81	9	1.346	307.2	1.225E+07	9.100E+06	110.8 ± 16.6
8	100	70	9	1.429	265.5	1.123E+07	7.864E+06	117.6 ± 18.7
9	65	67	9	0.970	254.1	7.303E+06	7.527E+06	80.1 ± 14.2
10	169	93	9	1.817	352.7	1.899E+07	1.045E+07	149.2 ± 19.8
	995	609			241.7	1.170E+07	7.160E+06	

Area of basic unit = 9.89E-07 cm-2

CHI SQUARED = 17.71398 WITH 9 DEGREES OF FREEDOM
P(chi squared) = 0.005 %
CORRELATION COEFFICIENT = 0.491
VARIANCE OF SQR(Ns) = 2.699198
VARIANCE OF SQR(Ni) = 1.430522

Ns/Ni = 1.634 ± 0.084
MEAN RATIO = 1.715 ± 0.202

Pooled Age = 134.3 ± 8.1 Ma
Mean Age = 140.9 ± 17.2 Ma
Central Age = 132.5 ± 13.1Ma
% Rel. Error = 25.97
Ages calculated using a zeta of 140.2 ± 3.6 for CN 1 glass
RHO D = 1.185E+06cm-2; ND = 2927

9414-48 Zircon

IRRADIATION WK147-11 COUNTED BY: KAO

No.	Ns	Ni	Na	RATIO	U(ppm)	RHOs	RHOi	F.T.AGE(Ma)
1	73	36	6	2.028	203.1	1.230E+07	6.067E+06	167.7 ± 34.6
2	29	23	6	1.261	129.7	4.887E+06	3.876E+06	104.8 ± 29.4
3	36	18	6	2.000	101.5	6.067E+06	3.033E+06	165.4 ± 48.0
4	31	14	4	2.214	118.5	7.836E+06	3.539E+06	182.9 ± 59.2
5	86	46	8	1.870	194.6	1.087E+07	5.814E+06	154.7 ± 28.7
6	50	9	4	5.556	76.2	1.264E+07	2.275E+06	449.4 ±163.3
7	58	56	6	1.036	315.9	9.774E+06	9.437E+06	86.2 ± 16.4
8	57	15	6	3.800	84.6	9.606E+06	2.528E+06	310.7 ± 90.7
9	62	23	5	2.696	155.7	1.254E+07	4.651E+06	221.9 ± 54.6
10	95	13	6	7.308	73.3	1.601E+07	2.191E+06	584.8 ±173.9
11	36	25	6	1.440	141.0	6.067E+06	4.213E+06	119.5 ± 31.3
12	54	12	4	4.500	101.5	1.365E+07	3.033E+06	366.4 ±117.5
	667	290			146.5	1.007E+07	4.376E+06	

Area of basic unit = 9.89E-07 cm-2

CHI SQUARED = 30.2855 WITH 11 DEGREES OF FREEDOM
P(chi squared) = 0.000 %
CORRELATION COEFFICIENT = 0.286
VARIANCE OF SQR(Ns) = 2.001026
VARIANCE OF SQR(Ni) = 1.935985

Ns/Ni = 2.300 ± 0.162
MEAN RATIO = 2.976 ± 0.559

Pooled Age = 189.8 ± 14.6 Ma
Mean Age = 244.6 ± 46.6 Ma
Central Age = 192.6 ± 30.4Ma
% Rel. Error = 48.20
Ages calculated using a zeta of 140.2 ± 3.6 for CN 1 glass
RHO D = 1.195E+06cm-2; ND = 2951

9414-49 Zircon

IRRADIATION WK147-12 COUNTED BY: KAO

No.	Ns	Ni	Na	RATIO	U(ppm)	RHOs	RHOi	F.T.AGE(Ma)
1	83	45	12	1.844	125.9	6.994E+06	3.792E+06	153.9 ± 28.9
2	91	51	9	1.784	190.2	1.022E+07	5.730E+06	149.0 ± 26.5
3	26	6	9	4.333	22.4	2.921E+06	6.741E+05	356.0 ±161.6
4	77	47	9	1.638	175.3	8.651E+06	5.280E+06	136.9 ± 25.7
5	58	32	9	1.812	119.3	6.516E+06	3.595E+06	151.3 ± 33.7
6	81	53	9	1.528	197.7	9.100E+06	5.954E+06	127.8 ± 22.9
7	94	58	9	1.621	216.3	1.056E+07	6.516E+06	135.5 ± 23.0
8	137	38	9	3.605	141.7	1.539E+07	4.269E+06	297.6 ± 55.4
9	71	40	9	1.775	149.2	7.977E+06	4.494E+06	148.2 ± 29.7
10	128	71	9	1.803	264.8	1.438E+07	7.977E+06	150.5 ± 22.8
11	70	20	6	3.500	111.9	1.180E+07	3.370E+06	289.1 ± 73.9
12	123	67	9	1.836	249.9	1.382E+07	7.527E+06	153.2 ± 23.8
13	102	21	4	4.857	176.2	2.578E+07	5.308E+06	397.8 ± 96.1
14	120	50	9	2.400	186.5	1.348E+07	5.617E+06	199.6 ± 34.2
15	70	52	9	1.346	193.9	7.864E+06	5.842E+06	112.7 ± 20.9
16	102	30	9	3.400	111.9	1.146E+07	3.370E+06	281.0 ± 59.0
17	120	86	9	1.395	320.7	1.348E+07	9.662E+06	116.8 ± 16.9
18	83	42	4	1.976	352.4	2.098E+07	1.062E+07	164.8 ± 31.6
19	93	47	6	1.979	262.9	1.567E+07	7.920E+06	165.0 ± 30.0
20	75	31	9	2.419	115.6	8.426E+06	3.483E+06	201.2 ± 43.4
	1804	887			178.3	1.092E+07	5.370E+06	

Area of basic unit = 9.89E-07 cm-2

CHI SQUARED = 30.27434 WITH 19 DEGREES OF FREEDOM
P(chi squared) = 0.000 %
CORRELATION COEFFICIENT = 0.617
VARIANCE OF SQR(Ns) = 2.307065
VARIANCE OF SQR(Ni) = 2.347358

Ns/Ni = 2.034 ± 0.083
MEAN RATIO = 2.343 ± 0.229

Pooled Age = 169.5 ± 8.8 Ma
Mean Age = 194.9 ± 20.0 Ma
Central Age = 172.7 ± 13.0Ma
% Rel. Error = 26.54
Ages calculated using a zeta of 140.2 ± 3.6 for CN 1 glass
RHO D = 1.205E+06cm-2; ND = 2974

9414-50 Zircon

IRRADIATION WK147-13 COUNTED BY: KAO

No.	Ns	Ni	Na	RATIO	U(ppm)	RHOs	RHOi	F.T.AGE(Ma)
1	144	32	9	4.500	118.4	1.618E+07	3.595E+06	372.3 ± 73.7
2	68	50	9	1.360	184.9	7.640E+06	5.617E+06	114.8 ± 21.7
3	131	53	9	2.472	196.0	1.472E+07	5.954E+06	207.2 ± 34.3
4	65	45	9	1.444	166.4	7.303E+06	5.056E+06	121.9 ± 23.9
5	113	82	9	1.378	303.3	1.270E+07	9.212E+06	116.3 ± 17.3
6	102	42	6	2.429	233.0	1.719E+07	7.078E+06	203.6 ± 37.9
7	31	35	9	0.886	129.5	3.483E+06	3.932E+06	75.0 ± 18.6
8	94	38	9	2.474	140.5	1.056E+07	4.269E+06	207.3 ± 40.4
9	112	101	9	1.109	373.6	1.258E+07	1.135E+07	93.8 ± 13.2
10	79	31	4	2.548	258.0	1.997E+07	7.836E+06	213.5 ± 45.7
11	151	56	9	2.696	207.1	1.696E+07	6.291E+06	225.7 ± 36.0
12	76	51	9	1.490	188.6	8.538E+06	5.730E+06	125.7 ± 23.1
13	75	90	9	0.833	332.9	8.426E+06	1.011E+07	70.6 ± 11.3
14	72	52	9	1.385	192.3	8.089E+06	5.842E+06	116.9 ± 21.6
15	40	20	6	2.000	111.0	6.741E+06	3.370E+06	168.1 ± 46.3
16	75	32	6	2.344	177.5	1.264E+07	5.393E+06	196.6 ± 42.0
17	67	31	9	2.161	114.7	7.527E+06	3.483E+06	181.5 ± 39.8
18	72	44	9	1.636	162.7	8.089E+06	4.943E+06	137.9 ± 26.7
19	53	35	9	1.514	129.5	5.954E+06	3.932E+06	127.7 ± 28.1
20	55	28	9	1.964	103.6	6.179E+06	3.146E+06	165.2 ± 38.7
	1675	948			190.1	1.020E+07	5.774E+06	

Area of basic unit = 9.89E-07 cm-2

CHI SQUARED = 51.00234 WITH 19 DEGREES OF FREEDOM
P(chi squared) = 0.000 %
CORRELATION COEFFICIENT = 0.386
VARIANCE OF SQR(Ns) = 3.158627
VARIANCE OF SQR(Ni) = 2.068587

Ns/Ni = 1.767 ± 0.072
MEAN RATIO = 1.931 ± 0.187

Pooled Age = 148.8 ± 7.6 Ma
Mean Age = 162.4 ± 16.5 Ma
Central Age = 147.5 ± 13.4Ma
% Rel. Error = 34.99
Ages calculated using a zeta of 140.2 ± 3.6 for CN 1 glass
RHO D = 1.215E+06cm-2; ND = 2998

9414-51 Zircon

IRRADIATION WK147-14 COUNTED BY: KAO

No.	Ns	Ni	Na	RATIO	U(ppm)	RHOs	RHOi	F.T.AGE(Ma)
1	60	40	9	1.500	146.9	6.741E+06	4.494E+06	127.4 ± 26.3
2	80	44	9	1.818	161.5	8.988E+06	4.943E+06	154.1 ± 29.3
3	115	53	8	2.170	218.9	1.453E+07	6.699E+06	183.5 ± 31.0
4	96	37	9	2.595	135.8	1.079E+07	4.157E+06	218.9 ± 42.9
5	93	34	9	2.735	124.8	1.045E+07	3.820E+06	230.5 ± 46.8
6	70	42	9	1.667	154.2	7.864E+06	4.719E+06	141.4 ± 28.0
7	62	42	9	1.476	154.2	6.966E+06	4.719E+06	125.4 ± 25.4
8	95	65	8	1.462	268.5	1.201E+07	8.215E+06	124.2 ± 20.4
9	73	41	6	1.780	225.8	1.230E+07	6.909E+06	151.0 ± 29.8
10	73	64	9	1.141	235.0	8.201E+06	7.190E+06	97.1 ± 16.9
11	82	35	9	2.343	128.5	9.212E+06	3.932E+06	198.0 ± 40.4
12	115	79	9	1.456	290.0	1.292E+07	8.875E+06	123.7 ± 18.5
13	103	41	9	2.512	150.5	1.157E+07	4.606E+06	212.0 ± 39.7
14	88	41	9	2.146	150.5	9.887E+06	4.606E+06	181.6 ± 34.8
15	65	49	9	1.327	179.9	7.303E+06	5.505E+06	112.8 ± 21.6
16	95	61	9	1.557	224.0	1.067E+07	6.853E+06	132.3 ± 22.1
17	115	74	8	1.554	305.6	1.453E+07	9.353E+06	132.0 ± 20.1
18	86	26	9	3.308	95.5	9.662E+06	2.921E+06	277.7 ± 62.8
19	100	60	9	1.667	220.3	1.123E+07	6.741E+06	141.4 ± 23.5
20	72	45	9	1.600	165.2	8.089E+06	5.056E+06	135.8 ± 26.2
	1738	973			184.8	1.010E+07	5.654E+06	

Area of basic unit = 9.89E-07 cm-2

CHI SQUARED = 20.31361 WITH 19 DEGREES OF FREEDOM
P(chi squared) = 0.270 %
CORRELATION COEFFICIENT = 0.491
VARIANCE OF SQR(Ns) = .8894235
VARIANCE OF SQR(Ni) = .9822645

Ns/Ni = 1.786 ± 0.072
MEAN RATIO = 1.891 ± 0.125

Pooled Age = 151.5 ± 7.7 Ma
Mean Age = 160.2 ± 11.7 Ma
Central Age = 152.2 ± 9.2Ma
% Rel. Error = 18.36
Ages calculated using a zeta of 140.2 ± 3.6 for CN 1 glass
RHO D = 1.224E+06cm-2; ND = 3022

9414-52 ZIRCON MARLBOROUGH

IRRADIATION WK147-15
SLIDE NUMBER 15
COUNTED BY: KAO

No.	Ns	Ni	Na	RATIO	U (ppm)	RHOs (E+06)	RHOi (E+06)	F.T.AGE (Ma)
1	49	32	9	1.531	0.0	5.505	3.595	131.1 ± 30.1
2	59	30	4	1.967	0.0	14.914	7.583	167.9 ± 38.0
3	48	36	6	1.333	0.0	8.089	6.067	114.3 ± 25.5
4	92	60	6	1.533	0.0	15.504	10.111	131.3 ± 22.2
5	37	20	9	1.850	0.0	4.157	2.247	158.1 ± 44.2
6	51	20	4	2.550	0.0	12.892	5.056	216.9 ± 57.6
7	25	17	4	1.471	0.0	6.320	4.297	126.0 ± 39.8
	361	215			0.0	8.691	5.176	

AREA OF BASIC UNIT = 9.89E-07 cm
CHI SQUARED = 4.905914 WITH 6 DEGREES OF FREEDOM
P(chi squared) = 55.6 %
CORRELATION COEFFICIENT = 0.909
VARIANCE OF SQR(Ns) = 2.00
VARIANCE OF SQR(Ni) = 1.55

Ns/Ni = 1.679 ± 0.145
MEAN RATIO = 1.748 ± 0.158

Ages calculated using a zeta of 140.2 ± 3.6 for CN1 glass
RHO D = 1.234E+06 ; ND = 3046

POOLED AGE = 143.6 ± 13.2 Ma
MEAN AGE = 149.5 ± 14.3 Ma

9414-53 Zircon

IRRADIATION WK147-16 COUNTED BY: KAO

No.	Ns	Ni	Na	RATIO	U(ppm)	RHOs	RHOi	F.T.AGE(Ma)
1	70	31	9	2.258	112.1	7.864E+06	3.483E+06	193.8 ± 42.3
2	31	13	10	2.385	42.3	3.134E+06	1.314E+06	204.5 ± 67.9
3	87	68	9	1.279	245.8	9.774E+06	7.640E+06	110.5 ± 18.2
4	51	42	6	1.214	227.8	8.595E+06	7.078E+06	104.9 ± 22.1
5	56	25	9	2.240	90.4	6.291E+06	2.809E+06	192.3 ± 46.6
6	40	37	9	1.081	133.8	4.494E+06	4.157E+06	93.5 ± 21.5
7	77	13	4	5.923	105.7	1.946E+07	3.286E+06	496.5 ±149.7
8	114	35	9	3.257	126.5	1.281E+07	3.932E+06	277.7 ± 54.4
9	55	24	6	2.292	130.2	9.269E+06	4.044E+06	196.7 ± 48.5
10	131	59	9	2.220	213.3	1.472E+07	6.628E+06	190.6 ± 30.5
	712	347			141.1	8.999E+06	4.386E+06	

Area of basic unit = 9.89E-07 cm-2

CHI SQUARED = 21.92862 WITH 9 DEGREES OF FREEDOM
P(chi squared) = 0.000 %
CORRELATION COEFFICIENT = 0.549
VARIANCE OF SQR(Ns) = 3.440619
VARIANCE OF SQR(Ni) = 2.348087

Ns/Ni = 2.052 ± 0.134
MEAN RATIO = 2.415 ± 0.443

Pooled Age = 176.4 ± 12.8 Ma
Mean Age = 207.1 ± 38.5 Ma
Central Age = 176.3 ± 25.1Ma
% Rel. Error = 39.11
Ages calculated using a zeta of 140.2 ± 3.6 for CN 1 glass
RHO D = 1.243E+06cm-2; ND = 3070

9414-54 Zircon

IRRADIATION WK147-17 COUNTED BY: KAO

No.	Ns	Ni	Na	RATIO	U(ppm)	RHOs	RHOi	F.T.AGE(Ma)
1	115	30	4	3.833	242.1	2.907E+07	7.583E+06	328.2 ± 68.1
2	140	38	9	3.684	136.3	1.573E+07	4.269E+06	315.7 ± 58.6
3	87	47	9	1.851	168.6	9.774E+06	5.280E+06	160.6 ± 29.5
4	122	41	9	2.976	147.0	1.371E+07	4.606E+06	256.2 ± 46.9
5	91	35	9	2.600	125.5	1.022E+07	3.932E+06	224.4 ± 45.2
6	87	45	8	1.933	181.6	1.100E+07	5.688E+06	167.6 ± 31.2
7	96	21	9	4.571	75.3	1.079E+07	2.359E+06	389.5 ± 94.6
8	105	22	6	4.773	118.4	1.769E+07	3.707E+06	406.1 ± 96.1
9	118	53	9	2.226	190.1	1.326E+07	5.954E+06	192.6 ± 32.4
10	152	60	9	2.533	215.2	1.708E+07	6.741E+06	218.8 ± 34.1
11	102	39	6	2.615	209.8	1.719E+07	6.572E+06	225.7 ± 43.1
12	61	32	6	1.906	172.2	1.028E+07	5.393E+06	165.3 ± 36.4
13	69	39	9	1.769	139.9	7.752E+06	4.382E+06	153.6 ± 31.1
14	148	65	9	2.277	233.1	1.663E+07	7.303E+06	197.0 ± 30.0
15	90	46	8	1.957	185.6	1.138E+07	5.814E+06	169.6 ± 31.2
16	37	15	6	2.467	80.7	6.235E+06	2.528E+06	213.1 ± 65.6
	1620	628			162.2	1.310E+07	5.080E+06	

Area of basic unit = 9.89E-07 cm-2

CHI SQUARED = 18.21413 WITH 15 DEGREES OF FREEDOM
P(chi squared) = 0.153 %
CORRELATION COEFFICIENT = 0.627
VARIANCE OF SQR(Ns) = 2.684391
VARIANCE OF SQR(Ni) = 1.286007

Ns/Ni = 2.580 ± 0.121
MEAN RATIO = 2.748 ± 0.241

Pooled Age = 222.7 ± 12.6 Ma
Mean Age = 237.0 ± 22.1 Ma
Central Age = 221.8 ± 16.5Ma
% Rel. Error = 21.71
Ages calculated using a zeta of 140.2 ± 3.6 for CN 1 glass
RHO D = 1.253E+06cm-2; ND = 3093

9414-55 Zircon

IRRADIATION WK147-18 COUNTED BY: KAO

No.	Ns	Ni	Na	RATIO	U(ppm)	RHOs	RHOi	F.T.AGE(Ma)
1	95	37	9	2.568	131.6	1.067E+07	4.157E+06	223.4 ± 43.9
2	90	24	9	3.750	85.4	1.011E+07	2.696E+06	323.7 ± 75.1
3	127	69	9	1.841	245.5	1.427E+07	7.752E+06	160.9 ± 24.6
4	119	36	9	3.306	128.1	1.337E+07	4.044E+06	286.2 ± 55.2
5	89	30	9	2.967	106.7	9.999E+06	3.370E+06	257.4 ± 54.9
6	92	32	9	2.875	113.9	1.034E+07	3.595E+06	249.6 ± 51.8
7	127	28	9	4.536	99.6	1.427E+07	3.146E+06	389.6 ± 82.2
8	122	41	9	2.976	145.9	1.371E+07	4.606E+06	258.2 ± 47.3
9	67	24	9	2.792	85.4	7.527E+06	2.696E+06	242.5 ± 58.2
10	119	50	9	2.380	177.9	1.337E+07	5.617E+06	207.3 ± 35.5
11	87	35	9	2.486	124.5	9.774E+06	3.932E+06	216.4 ± 43.8
12	65	15	9	4.333	53.4	7.303E+06	1.685E+06	372.7 ±107.4
13	85	21	9	4.048	74.7	9.549E+06	2.359E+06	348.8 ± 85.7
	1284	442			121.0	1.110E+07	3.820E+06	

Area of basic unit = 9.89E-07 cm-2

CHI SQUARED = 11.06414 WITH 12 DEGREES OF FREEDOM
P(chi squared) = 3.6 %
CORRELATION COEFFICIENT = 0.716
VARIANCE OF SQR(Ns) = 1.225637
VARIANCE OF SQR(Ni) = 1.2942

Ns/Ni = 2.905 ± 0.160
MEAN RATIO = 3.143 ± 0.225

Pooled Age = 252.2 ± 16.0 Ma
Mean Age = 272.4 ± 21.2 Ma
Central Age = 255.7 ± 19.3Ma
% Rel. Error = 17.22
Ages calculated using a zeta of 140.2 ± 3.6 for CN 1 glass
RHO D = 1.263E+06cm-2; ND = 3117

9414-56 Zircon

IRRADIATION WK147-19 COUNTED BY: KAO

No.	Ns	Ni	Na	RATIO	U(ppm)	RHOs	RHOi	F.T.AGE(Ma)
1	73	46	9	1.587	162.5	8.201E+06	5.168E+06	140.0 ± 26.7
2	101	60	9	1.683	212.0	1.135E+07	6.741E+06	148.4 ± 24.6
3	50	24	12	2.083	63.6	4.213E+06	2.022E+06	183.1 ± 45.8
4	51	33	9	1.545	116.6	5.730E+06	3.707E+06	136.4 ± 30.8
5	130	65	9	2.000	229.6	1.461E+07	7.303E+06	175.9 ± 27.3
6	66	23	8	2.870	91.4	8.342E+06	2.907E+06	250.9 ± 61.3
7	92	73	8	1.260	290.1	1.163E+07	9.226E+06	111.4 ± 17.8
8	99	33	9	3.000	116.6	1.112E+07	3.707E+06	262.1 ± 53.3
9	92	41	9	2.244	144.8	1.034E+07	4.606E+06	197.0 ± 37.5
10	49	14	9	3.500	49.5	5.505E+06	1.573E+06	304.8 ± 92.8
	803	412			144.0	8.922E+06	4.578E+06	

Area of basic unit = 9.89E-07 cm-2

CHI SQUARED = 11.35717 WITH 9 DEGREES OF FREEDOM
P(chi squared) = 0.687 %
CORRELATION COEFFICIENT = 0.763
VARIANCE OF SQR(Ns) = 2.265333
VARIANCE OF SQR(Ni) = 2.425991

Ns/Ni = 1.949 ± 0.118
MEAN RATIO = 2.177 ± 0.231

Pooled Age = 171.5 ± 11.7 Ma
Mean Age = 191.3 ± 21.1 Ma
Central Age = 175.4 ± 16.7Ma
% Rel. Error = 22.07
Ages calculated using a zeta of 140.2 ± 3.6 for CN 1 glass
RHO D = 1.272E+06cm-2; ND = 3141

9414-57 ZIRCON MARLBOROUGH

IRRADIATION WK147-20
SLIDE NUMBER 20
COUNTED BY: KAO

No.	Ns	Ni	Na	RATIO	U (ppm)	RHOs (E+06)	RHOi (E+06)	F.T.AGE (Ma)
1	78	54	9	1.444	0.0	8.763	6.067	128.3 ± 23.1
2	115	85	9	1.353	0.0	12.920	9.549	120.3 ± 17.6
3	98	51	12	1.922	0.0	8.257	4.297	170.2 ± 29.9
4	127	76	9	1.671	0.0	14.268	8.538	148.2 ± 22.0
5	66	53	9	1.245	0.0	7.415	5.954	110.8 ± 20.7
6	74	32	6	2.312	0.0	12.471	5.393	204.2 ± 43.7
7	108	80	9	1.350	0.0	12.133	8.988	120.0 ± 18.1
8	55	39	12	1.410	0.0	4.634	3.286	125.3 ± 26.5
9	149	77	8	1.935	0.0	18.832	9.732	171.3 ± 24.6
10	52	47	8	1.106	0.0	6.572	5.940	98.5 ± 20.1
	922	594			0.0	10.245	6.600	

AREA OF BASIC UNIT = 9.89E-07 cm
CHI SQUARED = 14.35405 WITH 9 DEGREES OF FREEDOM
P(chi squared) = 11.0 %
CORRELATION COEFFICIENT = 0.816
VARIANCE OF SQR(Ns) = 2.85
VARIANCE OF SQR(Ni) = 1.51

Ns/Ni = 1.552 ± 0.082
MEAN RATIO = 1.575 ± 0.119

Ages calculated using a zeta of 140.2 ± 3.6 for CN1 glass
RHO D = 1.280E+06 ; ND = 3165

POOLED AGE = 137.8 ± 8.4 Ma
MEAN AGE = 139.8 ± 11.4 Ma

9414-58 Zircon

IRRADIATION WK148-1 COUNTED BY: KAO

No.	Ns	Ni	Na	RATIO	U(ppm)	RHOs	RHOi	F.T.AGE(Ma)
1	78	38	9	2.053	16.3	8.763E+05	4.269E+05	149.3 ± 29.9
2	27	9	4	3.000	8.7	6.825E+05	2.275E+05	217.1 ± 83.9
3	73	38	9	1.921	16.3	8.201E+05	4.269E+05	139.9 ± 28.3
4	48	31	12	1.548	10.0	4.044E+05	2.612E+05	113.0 ± 26.3
5	134	45	9	2.978	19.3	1.505E+06	5.056E+05	215.5 ± 37.8
6	53	40	8	1.325	19.3	6.699E+05	5.056E+05	96.8 ± 20.5
7	61	20	9	3.050	8.6	6.853E+05	2.247E+05	220.7 ± 57.3
8	33	22	9	1.500	9.4	3.707E+05	2.472E+05	109.5 ± 30.3
9	98	32	9	3.062	13.7	1.101E+06	3.595E+05	221.6 ± 45.7
10	38	31	9	1.226	13.3	4.269E+05	3.483E+05	89.6 ± 21.9
11	79	40	9	1.975	17.1	8.875E+05	4.494E+05	143.8 ± 28.3
12	62	26	9	2.385	11.1	6.966E+05	2.921E+05	173.2 ± 40.8
13	127	43	9	2.953	18.4	1.427E+06	4.831E+05	213.8 ± 38.4
14	100	19	9	5.263	8.1	1.123E+06	2.135E+05	376.2 ± 94.9
15	62	18	9	3.444	7.7	6.966E+05	2.022E+05	248.7 ± 67.1
16	52	24	6	2.167	15.4	8.763E+05	4.044E+05	157.5 ± 39.2
	1125	476			13.3	8.243E+05	3.488E+05	

Area of basic unit = 9.89E-06 cm-2

CHI SQUARED = 21.72235 WITH 15 DEGREES OF FREEDOM
P(chi squared) = 0.013 %
CORRELATION COEFFICIENT = 0.590
VARIANCE OF SQR(Ns) = 3.395874
VARIANCE OF SQR(Ni) = 1.061228

Ns/Ni = 2.363 ± 0.129
MEAN RATIO = 2.491 ± 0.256

Pooled Age = 171.7 ± 10.9 Ma
Mean Age = 180.8 ± 19.4 Ma
Central Age = 166.0 ± 15.6Ma
% Rel. Error = 28.94
Ages calculated using a zeta of 140.2 ± 3.6 for CN 1 glass
RHO D = 1.050E+06cm-2; ND = 2595

9414-59 Zircon

IRRADIATION WK148-2 COUNTED BY: KAO

No.	Ns	Ni	Na	RATIO	U(ppm)	RHOs	RHOi	F.T.AGE(Ma)
1	132	45	9	2.933	191.9	1.483E+07	5.056E+06	213.2 ± 37.4
2	98	36	12	2.722	115.1	8.257E+06	3.033E+06	198.1 ± 39.1
3	22	5	12	4.400	16.0	1.854E+06	4.213E+05	317.2 ±157.5
4	71	26	9	2.731	110.9	7.977E+06	2.921E+06	198.7 ± 46.0
5	41	19	9	2.158	81.0	4.606E+06	2.135E+06	157.5 ± 44.0
6	129	20	9	6.450	85.3	1.449E+07	2.247E+06	459.8 ±111.5
7	25	27	16	0.926	64.8	1.580E+06	1.706E+06	68.1 ± 19.0
8	48	29	9	1.655	123.6	5.393E+06	3.258E+06	121.1 ± 28.8
9	92	57	9	1.614	243.0	1.034E+07	6.404E+06	118.2 ± 20.3
10	40	14	9	2.857	59.7	4.494E+06	1.573E+06	207.7 ± 64.8
11	118	42	8	2.810	201.5	1.491E+07	5.308E+06	204.3 ± 37.3
12	52	10	9	5.200	42.6	5.842E+06	1.123E+06	373.2 ±129.4
13	96	68	16	1.412	163.1	6.067E+06	4.297E+06	103.5 ± 16.7
14	60	29	9	2.069	123.6	6.741E+06	3.258E+06	151.1 ± 34.5
15	58	53	9	1.094	226.0	6.516E+06	5.954E+06	80.4 ± 15.5
16	22	18	9	1.222	76.7	2.472E+06	2.022E+06	89.7 ± 28.6
17	36	24	12	1.500	76.7	3.033E+06	2.022E+06	109.9 ± 29.2
18	127	45	9	2.822	191.9	1.427E+07	5.056E+06	205.2 ± 36.2
	1267	567			118.2	6.962E+06	3.116E+06	

Area of basic unit = 9.89E-07 cm-2

CHI SQUARED = 41.79457 WITH 17 DEGREES OF FREEDOM
P(chi squared) = 0.000 %
CORRELATION COEFFICIENT = 0.580
VARIANCE OF SQR(Ns) = 5.531903
VARIANCE OF SQR(Ni) = 2.508476

Ns/Ni = 2.235 ± 0.113
MEAN RATIO = 2.588 ± 0.348

Pooled Age = 163.0 ± 9.8 Ma
Mean Age = 188.4 ± 26.1 Ma
Central Age = 157.5 ± 17.9Ma
% Rel. Error = 41.49
Ages calculated using a zeta of 140.2 ± 3.6 for CN 1 glass
RHO D = 1.054E+06cm-2; ND = 2605

9414-60 Zircon

IRRADIATION WK148-3 COUNTED BY: KAO

No.	Ns	Ni	Na	RATIO	U(ppm)	RHOs	RHOi	F.T.AGE(Ma)
1	111	38	9	2.921	161.4	1.247E+07	4.269E+06	213.1 ± 40.6
2	76	31	9	2.452	131.7	8.538E+06	3.483E+06	179.3 ± 38.6
3	163	63	9	2.587	267.6	1.831E+07	7.078E+06	189.1 ± 28.7
4	193	63	9	3.063	267.6	2.168E+07	7.078E+06	223.3 ± 33.2
5	30	24	12	1.250	76.5	2.528E+06	2.022E+06	92.0 ± 25.4
6	113	78	9	1.449	331.3	1.270E+07	8.763E+06	106.6 ± 16.1
7	66	31	4	2.129	296.3	1.668E+07	7.836E+06	156.0 ± 34.3
8	115	31	9	3.710	131.7	1.292E+07	3.483E+06	269.4 ± 55.2
9	78	32	9	2.438	135.9	8.763E+06	3.595E+06	178.3 ± 37.9
10	140	78	8	1.795	372.7	1.769E+07	9.858E+06	131.8 ± 19.1
11	106	44	9	2.409	186.9	1.191E+07	4.943E+06	176.2 ± 32.1
12	137	82	9	1.671	348.3	1.539E+07	9.212E+06	122.7 ± 17.6
13	65	42	9	1.548	178.4	7.303E+06	4.719E+06	113.8 ± 22.8
14	81	22	9	3.682	93.4	9.100E+06	2.472E+06	267.4 ± 64.9
15	71	20	8	3.550	95.6	8.974E+06	2.528E+06	258.1 ± 65.9
16	102	51	18	2.000	108.3	5.730E+06	2.865E+06	146.6 ± 25.6
	1647	730			187.3	1.118E+07	4.954E+06	

Area of basic unit = 9.89E-07 cm-2

CHI SQUARED = 23.41611 WITH 15 DEGREES OF FREEDOM
P(chi squared) = 0.004 %
CORRELATION COEFFICIENT = 0.726
VARIANCE OF SQR(Ns) = 4.302897
VARIANCE OF SQR(Ni) = 2.347827

Ns/Ni = 2.256 ± 0.100
MEAN RATIO = 2.416 ± 0.199

Pooled Age = 165.2 ± 9.1 Ma
Mean Age = 176.7 ± 15.6 Ma
Central Age = 165.5 ± 13.2Ma
% Rel. Error = 24.85
Ages calculated using a zeta of 140.2 ± 3.6 for CN 1 glass
RHO D = 1.058E+06cm-2; ND = 2615

9414-61 Zircon

IRRADIATION WK148-4 COUNTED BY: KAO

No.	Ns	Ni	Na	RATIO	U(ppm)	RHOs	RHOi	F.T.AGE(Ma)
1	61	31	8	1.968	147.6	7.710E+06	3.918E+06	144.9 ± 32.3
2	153	113	16	1.354	269.0	9.669E+06	7.141E+06	100.0 ± 12.8
3	92	60	9	1.533	253.9	1.034E+07	6.741E+06	113.2 ± 19.1
4	70	49	9	1.429	207.3	7.864E+06	5.505E+06	105.5 ± 19.9
5	45	49	9	0.918	207.3	5.056E+06	5.505E+06	68.0 ± 14.2
6	83	26	9	3.192	110.0	9.325E+06	2.921E+06	233.4 ± 53.0
7	214	56	9	3.821	237.0	2.404E+07	6.291E+06	278.4 ± 42.7
8	135	35	9	3.857	148.1	1.517E+07	3.932E+06	280.9 ± 54.1
9	91	48	9	1.896	203.1	1.022E+07	5.393E+06	139.6 ± 25.3
10	63	55	12	1.145	174.6	5.308E+06	4.634E+06	84.7 ± 15.9
11	180	77	9	2.338	325.8	2.022E+07	8.651E+06	171.7 ± 24.0
12	58	49	9	1.184	207.3	6.516E+06	5.505E+06	87.5 ± 17.2
13	63	57	9	1.105	241.2	7.078E+06	6.404E+06	81.8 ± 15.2
14	84	70	9	1.200	296.2	9.437E+06	7.864E+06	88.7 ± 14.6
15	103	80	9	1.288	338.5	1.157E+07	8.988E+06	95.1 ± 14.5
16	55	33	9	1.667	139.6	6.179E+06	3.707E+06	122.9 ± 27.4
17	85	25	9	3.400	105.8	9.549E+06	2.809E+06	248.3 ± 57.1
18	111	51	9	2.176	215.8	1.247E+07	5.730E+06	160.0 ± 27.6
19	58	41	9	1.415	173.5	6.516E+06	4.606E+06	104.5 ± 21.6
20	137	59	9	2.322	249.7	1.539E+07	6.628E+06	170.6 ± 27.1
	1941	1064			214.4	1.038E+07	5.692E+06	

Area of basic unit = 9.89E-07 cm-2

CHI SQUARED = 58.10157 WITH 19 DEGREES OF FREEDOM
P(chi squared) = 0.000 %
CORRELATION COEFFICIENT = 0.458
VARIANCE OF SQR(Ns) = 4.685874
VARIANCE OF SQR(Ni) = 1.890953

Ns/Ni = 1.824 ± 0.070
MEAN RATIO = 1.960 ± 0.207

Pooled Age = 134.4 ± 6.7 Ma
Mean Age = 144.3 ± 15.9 Ma
Central Age = 129.0 ± 12.0Ma
% Rel. Error = 36.58
Ages calculated using a zeta of 140.2 ± 3.6 for CN 1 glass
RHO D = 1.062E+06cm-2; ND = 2624

9414-62 Zircon

IRRADIATION WK148-5 COUNTED BY: KAO

No.	Ns	Ni	Na	RATIO	U(ppm)	RHOs	RHOi	F.T.AGE(Ma)
1	179	42	9	4.262	177.1	2.011E+07	4.719E+06	310.9 ± 54.2
2	129	34	10	3.794	129.0	1.304E+07	3.438E+06	277.5 ± 54.2
3	101	36	12	2.806	113.8	8.510E+06	3.033E+06	206.3 ± 40.6
4	65	31	12	2.097	98.0	5.477E+06	2.612E+06	154.8 ± 34.2
5	182	42	9	4.333	177.1	2.045E+07	4.719E+06	315.9 ± 55.0
6	168	34	9	4.941	143.3	1.887E+07	3.820E+06	359.0 ± 68.5
7	139	18	9	7.722	75.9	1.562E+07	2.022E+06	552.7 ±139.6
8	59	23	9	2.565	97.0	6.628E+06	2.584E+06	188.9 ± 46.8
9	105	26	9	4.038	109.6	1.180E+07	2.921E+06	294.9 ± 65.3
10	83	30	6	2.767	189.7	1.399E+07	5.056E+06	203.5 ± 43.8
	1210	316			127.5	1.302E+07	3.399E+06	

Area of basic unit = 9.89E-07 cm-2

CHI SQUARED = 13.23219 WITH 9 DEGREES OF FREEDOM
P(chi squared) = 0.171 %
CORRELATION COEFFICIENT = 0.551
VARIANCE OF SQR(Ns) = 4.533203
VARIANCE OF SQR(Ni) = .5078362

Ns/Ni = 3.829 ± 0.242
MEAN RATIO = 3.933 ± 0.512

Pooled Age = 280.0 ± 19.9 Ma
Mean Age = 287.4 ± 38.5 Ma
Central Age = 267.9 ± 28.4Ma
% Rel. Error = 26.00
Ages calculated using a zeta of 140.2 ± 3.6 for CN 1 glass
RHO D = 1.066E+06cm-2; ND = 2634

9414-63 Zircon

IRRADIATION WK148-6 COUNTED BY: KAO

No.	Ns	Ni	Na	RATIO	U(ppm)	RHOs	RHOi	F.T.AGE(Ma)
1	90	42	9	2.143	176.4	1.011E+07	4.719E+06	158.8 ± 30.1
2	77	19	16	4.053	44.9	4.866E+06	1.201E+06	297.0 ± 76.7
3	109	48	9	2.271	201.6	1.225E+07	5.393E+06	168.1 ± 29.6
4	39	26	9	1.500	109.2	4.382E+06	2.921E+06	111.5 ± 28.5
5	116	44	9	2.636	184.8	1.303E+07	4.943E+06	194.8 ± 35.1
6	164	34	8	4.824	160.6	2.073E+07	4.297E+06	352.0 ± 67.3
7	97	56	9	1.732	235.2	1.090E+07	6.291E+06	128.6 ± 22.0
8	69	23	9	3.000	96.6	7.752E+06	2.584E+06	221.2 ± 53.7
9	188	43	12	4.372	135.4	1.584E+07	3.623E+06	319.9 ± 55.0
10	32	14	6	2.286	88.2	5.393E+06	2.359E+06	169.2 ± 54.5
11	86	40	9	2.150	168.0	9.662E+06	4.494E+06	159.3 ± 30.9
12	72	34	6	2.118	214.2	1.213E+07	5.730E+06	156.9 ± 33.0
13	54	34	6	1.588	214.2	9.100E+06	5.730E+06	118.0 ± 26.1
14	76	50	6	1.520	315.0	1.281E+07	8.426E+06	113.0 ± 20.9
15	129	31	6	4.161	195.3	2.174E+07	5.224E+06	304.8 ± 61.8
16	76	18	6	4.222	113.4	1.281E+07	3.033E+06	309.2 ± 81.7
17	34	26	12	1.308	81.9	2.865E+06	2.191E+06	97.3 ± 25.6
18	52	28	9	1.857	117.6	5.842E+06	3.146E+06	137.8 ± 32.6
19	62	26	9	2.385	109.2	6.966E+06	2.921E+06	176.4 ± 41.6
20	62	16	9	3.875	67.2	6.966E+06	1.798E+06	284.3 ± 80.2
	1684	652			141.6	9.786E+06	3.789E+06	

Area of basic unit = 9.89E-07 cm-2

CHI SQUARED = 36.61738 WITH 19 DEGREES OF FREEDOM
P(chi squared) = 0.000 %
CORRELATION COEFFICIENT = 0.499
VARIANCE OF SQR(Ns) = 4.559634
VARIANCE OF SQR(Ni) = 1.14783

Ns/Ni = 2.583 ± 0.119
MEAN RATIO = 2.700 ± 0.252

Pooled Age = 190.9 ± 10.7 Ma
Mean Age = 199.4 ± 19.7 Ma
Central Age = 181.6 ± 16.1Ma
% Rel. Error = 32.41
Ages calculated using a zeta of 140.2 ± 3.6 for CN 1 glass
RHO D = 1.070E+06cm-2; ND = 2644

9414-64 Zircon

IRRADIATION WK148-7 COUNTED BY: KAO

No.	Ns	Ni	Na	RATIO	U(ppm)	RHOs	RHOi	F.T.AGE(Ma)
1	54	20	9	2.700	83.8	6.067E+06	2.247E+06	200.0 ± 52.7
2	90	40	9	2.250	167.5	1.011E+07	4.494E+06	167.1 ± 32.2
3	70	39	9	1.795	163.3	7.864E+06	4.382E+06	133.6 ± 27.0
4	77	25	9	3.080	104.7	8.651E+06	2.809E+06	227.6 ± 52.9
5	74	37	9	2.000	155.0	8.314E+06	4.157E+06	148.7 ± 30.3
6	77	45	9	1.711	188.5	8.651E+06	5.056E+06	127.4 ± 24.3
7	76	50	9	1.520	209.4	8.538E+06	5.617E+06	113.3 ± 21.0
8	76	33	9	2.303	138.2	8.538E+06	3.707E+06	170.9 ± 36.1
9	76	34	9	2.235	142.4	8.538E+06	3.820E+06	166.0 ± 34.7
10	74	23	9	3.217	96.3	8.314E+06	2.584E+06	237.6 ± 57.2
11	70	27	9	2.593	113.1	7.864E+06	3.033E+06	192.1 ± 44.0
12	55	13	9	4.231	54.4	6.179E+06	1.461E+06	310.6 ± 96.3
13	34	12	6	2.833	75.4	5.730E+06	2.022E+06	209.7 ± 70.7
14	59	32	9	1.844	134.0	6.628E+06	3.595E+06	137.2 ± 30.4
15	90	54	12	1.667	169.6	7.583E+06	4.550E+06	124.2 ± 21.7
16	51	21	9	2.429	88.0	5.730E+06	2.359E+06	180.1 ± 47.1
17	108	27	9	4.000	113.1	1.213E+07	3.033E+06	294.1 ± 64.0
18	79	52	9	1.519	217.8	8.875E+06	5.842E+06	113.3 ± 20.6
19	123	42	9	2.929	175.9	1.382E+07	4.719E+06	216.6 ± 39.3
20	113	70	9	1.614	293.2	1.270E+07	7.864E+06	120.3 ± 18.7
	1526	696			145.7	8.572E+06	3.910E+06	

Area of basic unit = 9.89E-07 cm-2

CHI SQUARED = 20.40557 WITH 19 DEGREES OF FREEDOM
P(chi squared) = 0.256 %
CORRELATION COEFFICIENT = 0.662
VARIANCE OF SQR(Ns) = 1.524125
VARIANCE OF SQR(Ni) = 1.596522

Ns/Ni = 2.193 ± 0.100
MEAN RATIO = 2.423 ± 0.175

Pooled Age = 162.8 ± 9.1 Ma
Mean Age = 179.8 ± 14.2 Ma
Central Age = 165.5 ± 11.5Ma
% Rel. Error = 21.14
Ages calculated using a zeta of 140.2 ± 3.6 for CN 1 glass
RHO D = 1.073E+06cm-2; ND = 2654

9414-65 Zircon

IRRADIATION WK148-8 COUNTED BY: KAO

No.	Ns	Ni	Na	RATIO	U(ppm)	RHOs	RHOi	F.T.AGE(Ma)
1	142	69	9	2.058	287.9	1.595E+07	7.752E+06	153.5 ± 23.1
2	80	44	9	1.818	183.6	8.988E+06	4.943E+06	135.8 ± 25.9
3	33	23	10	1.435	86.4	3.337E+06	2.326E+06	107.4 ± 29.4
4	131	28	9	4.679	116.8	1.472E+07	3.146E+06	343.9 ± 72.4
5	86	35	9	2.457	146.0	9.662E+06	3.932E+06	182.9 ± 37.1
6	120	67	12	1.791	209.7	1.011E+07	5.645E+06	133.8 ± 20.9
7	118	30	9	3.933	125.2	1.326E+07	3.370E+06	290.3 ± 60.1
8	103	18	9	5.722	75.1	1.157E+07	2.022E+06	418.2 ±107.7
9	156	70	9	2.229	292.1	1.753E+07	7.864E+06	166.1 ± 24.5
10	113	26	9	4.346	108.5	1.270E+07	2.921E+06	320.0 ± 70.4
11	124	33	9	3.758	137.7	1.393E+07	3.707E+06	277.6 ± 55.1
12	85	34	9	2.500	141.9	9.549E+06	3.820E+06	186.0 ± 38.2
13	53	19	9	2.789	79.3	5.954E+06	2.135E+06	207.2 ± 55.8
14	75	36	12	2.083	112.7	6.320E+06	3.033E+06	155.4 ± 31.9
15	113	33	9	3.424	137.7	1.270E+07	3.707E+06	253.5 ± 50.8
16	92	19	6	4.842	118.9	1.550E+07	3.202E+06	355.6 ± 90.3
17	163	50	9	3.260	208.6	1.831E+07	5.617E+06	241.5 ± 39.8
18	84	31	9	2.710	129.4	9.437E+06	3.483E+06	201.4 ± 42.8
19	133	41	12	3.244	128.3	1.121E+07	3.455E+06	240.4 ± 43.6
20	116	20	9	5.800	83.5	1.303E+07	2.247E+06	423.7 ±103.5
	2120	726			145.8	1.146E+07	3.926E+06	

Area of basic unit = 9.89E-07 cm-2

CHI SQUARED = 35.6146 WITH 19 DEGREES OF FREEDOM
P(chi squared) = 0.000 %
CORRELATION COEFFICIENT = 0.567
VARIANCE OF SQR(Ns) = 2.959986
VARIANCE OF SQR(Ni) = 1.651544

Ns/Ni = 2.920 ± 0.126
MEAN RATIO = 3.244 ± 0.291

Pooled Age = 216.8 ± 11.6 Ma
Mean Age = 240.4 ± 22.9 Ma
Central Age = 217.0 ± 18.5Ma
% Rel. Error = 31.38
Ages calculated using a zeta of 140.2 ± 3.6 for CN 1 glass
RHO D = 1.077E+06cm-2; ND = 2664

9414-66 ZIRCON MARLBOROUGH

IRRADIATION WK148-9
SLIDE NUMBER 9
COUNTED BY: KAO

No.	Ns	Ni	Na	RATIO	U (ppm)	RHOs (E+06)	RHOi (E+06)	F.T.AGE (Ma)
1	84	46	9	1.826	0.0	9.437	5.168	136.9 ± 25.5
2	109	46	9	2.370	0.0	12.246	5.168	177.1 ± 31.7
3	59	34	9	1.735	0.0	6.628	3.820	130.2 ± 28.3
4	48	25	6	1.920	0.0	8.089	4.213	143.9 ± 35.8
5	129	56	9	2.304	0.0	14.493	6.291	172.2 ± 28.1
6	45	19	9	2.368	0.0	5.056	2.135	177.0 ± 48.8
7	77	48	8	1.604	0.0	9.732	6.067	120.4 ± 22.5
8	111	65	9	1.708	0.0	12.471	7.303	128.1 ± 20.4
9	73	57	9	1.281	0.0	8.201	6.404	96.3 ± 17.3
10	92	40	9	2.300	0.0	10.336	4.494	172.0 ± 33.0
11	74	41	9	1.805	0.0	8.314	4.606	135.3 ± 26.7
12	85	49	16	1.735	0.0	5.372	3.097	130.1 ± 23.7
13	52	34	9	1.529	0.0	5.842	3.820	114.9 ± 25.6
14	84	43	9	1.953	0.0	9.437	4.831	146.4 ± 27.8
15	49	27	16	1.815	0.0	3.097	1.706	136.1 ± 32.9
16	58	40	6	1.450	0.0	9.774	6.741	109.0 ± 22.7
17	59	45	9	1.311	0.0	6.628	5.056	98.6 ± 19.8
18	87	54	9	1.611	0.0	9.774	6.067	120.9 ± 21.3
19	50	31	6	1.613	0.0	8.426	5.224	121.1 ± 28.0
20	51	35	6	1.457	0.0	8.595	5.898	109.5 ± 24.3
	1476	835			0.0	8.245	4.665	

AREA OF BASIC UNIT = 9.89E-07 cm
CHI SQUARED = 17.68153 WITH 19 DEGREES OF FREEDOM
P(chi squared) = 54.4 %
CORRELATION COEFFICIENT = 0.795
VARIANCE OF SQR(Ns) = 1.84
VARIANCE OF SQR(Ni) = 0.86

Ns/Ni = 1.768 ± 0.077
MEAN RATIO = 1.785 ± 0.075

Ages calculated using a zeta of 140.2 ± 3.6 for CN1 glass
RHO D = 1.081E+06 ; ND = 2674

POOLED AGE = 132.6 ± 7.1 Ma
MEAN AGE = 133.8 ± 7.1 Ma

9414-67 Zircon

IRRADIATION WK148-10 COUNTED BY: KAO

No.	Ns	Ni	Na	RATIO	U(ppm)	RHOs	RHOi	F.T.AGE(Ma)
1	87	22	9	3.955	91.1	9.774E+06	2.472E+06	294.0 ± 70.8
2	48	42	6	1.143	260.9	8.089E+06	7.078E+06	86.3 ± 18.5
3	29	15	9	1.933	62.1	3.258E+06	1.685E+06	145.4 ± 46.5
4	116	48	9	2.417	198.8	1.303E+07	5.393E+06	181.2 ± 31.6
5	95	66	9	1.439	273.4	1.067E+07	7.415E+06	108.6 ± 17.7
6	166	64	9	2.594	265.1	1.865E+07	7.190E+06	194.3 ± 29.3
7	110	61	9	1.803	252.7	1.236E+07	6.853E+06	135.7 ± 22.1
8	106	73	9	1.452	302.4	1.191E+07	8.201E+06	109.5 ± 17.0
9	75	60	9	1.250	248.5	8.426E+06	6.741E+06	94.4 ± 16.6
10	93	22	9	4.227	91.1	1.045E+07	2.472E+06	313.8 ± 75.1
11	81	49	9	1.653	202.9	9.100E+06	5.505E+06	124.5 ± 22.9
12	101	75	8	1.347	349.5	1.277E+07	9.479E+06	101.6 ± 15.8
13	138	66	9	2.091	273.4	1.550E+07	7.415E+06	157.1 ± 24.0
14	134	55	9	2.436	227.8	1.505E+07	6.179E+06	182.7 ± 29.8
15	86	39	9	2.205	161.5	9.662E+06	4.382E+06	165.6 ± 32.4
16	163	54	9	3.019	223.7	1.831E+07	6.067E+06	225.6 ± 36.2
17	141	92	16	1.533	214.3	8.911E+06	5.814E+06	115.5 ± 15.9
18	157	69	9	2.275	285.8	1.764E+07	7.752E+06	170.8 ± 25.3
19	117	58	9	2.017	240.2	1.314E+07	6.516E+06	151.6 ± 24.8
20	57	47	9	1.213	194.7	6.404E+06	5.280E+06	91.6 ± 18.3
	2100	1077			219.4	1.160E+07	5.951E+06	

Area of basic unit = 9.89E-07 cm-2

CHI SQUARED = 37.08789 WITH 19 DEGREES OF FREEDOM
P(chi squared) = 0.000 %
CORRELATION COEFFICIENT = 0.594
VARIANCE OF SQR(Ns) = 3.875251
VARIANCE OF SQR(Ni) = 2.077367

Ns/Ni = 1.950 ± 0.073
MEAN RATIO = 2.100 ± 0.191

Pooled Age = 146.6 ± 7.2 Ma
Mean Age = 157.8 ± 15.2 Ma
Central Age = 144.9 ± 11.3Ma
% Rel. Error = 28.80
Ages calculated using a zeta of 140.2 ± 3.6 for CN 1 glass
RHO D = 1.085E+06cm-2; ND = 2683

9414-68 ZIRCON MARLBOROUGH

IRRADIATION WK148-11
SLIDE NUMBER 11
COUNTED BY: KAO

No.	Ns	Ni	Na	RATIO	U (ppm)	RHOs (E+06)	RHOi (E+06)	F.T.AGE (Ma)
1	60	34	9	1.765	0.0	6.741	3.820	133.3 ± 28.9
2	69	45	6	1.533	0.0	11.628	7.583	116.0 ± 22.5
3	133	81	9	1.642	0.0	14.942	9.100	124.1 ± 17.9
4	145	56	9	2.589	0.0	16.290	6.291	194.7 ± 31.3
5	85	30	9	2.833	0.0	9.549	3.370	212.7 ± 45.7
6	98	59	9	1.661	0.0	11.010	6.628	125.6 ± 21.1
7	98	50	9	1.960	0.0	11.010	5.617	147.9 ± 26.1
8	105	54	6	1.944	0.0	17.695	9.100	146.8 ± 25.0
9	113	68	9	1.662	0.0	12.695	7.640	125.6 ± 19.7
10	125	60	9	2.083	0.0	14.043	6.741	157.1 ± 25.2
11	152	64	9	2.375	0.0	17.077	7.190	178.8 ± 27.3
12	84	62	9	1.355	0.0	9.437	6.966	102.6 ± 17.5
13	120	60	9	2.000	0.0	13.482	6.741	150.9 ± 24.3
14	80	38	9	2.105	0.0	8.988	4.269	158.7 ± 31.7
15	106	65	9	1.631	0.0	11.909	7.303	123.3 ± 19.8
	1573	826			0.0	12.329	6.474	

AREA OF BASIC UNIT = 9.89E-07 cm
CHI SQUARED = 19.46464 WITH 14 DEGREES OF FREEDOM
P(chi squared) = 14.8 %
CORRELATION COEFFICIENT = 0.691
VARIANCE OF SQR(Ns) = 1.77
VARIANCE OF SQR(Ni) = 0.92

Ns/Ni = 1.904 ± 0.082
MEAN RATIO = 1.943 ± 0.106

Ages calculated using a zeta of 140.2 ± 3.6 for CN1 glass
RHO D = 1.089E+06 ; ND = 2693

POOLED AGE = 143.8 ± 7.7 Ma
MEAN AGE = 146.6 ± 9.3 Ma

9414-69 Zircon

IRRADIATION WK148-12 COUNTED BY: KAO

No.	Ns	Ni	Na	RATIO	U(ppm)	RHOs	RHOi	F.T.AGE(Ma)
1	165	81	9	2.037	333.0	1.854E+07	9.100E+06	154.2 ± 21.5
2	87	27	6	3.222	166.5	1.466E+07	4.550E+06	242.3 ± 53.9
3	68	31	9	2.194	127.5	7.640E+06	3.483E+06	165.9 ± 36.3
4	90	65	9	1.385	267.2	1.011E+07	7.303E+06	105.2 ± 17.5
5	148	37	9	4.000	152.1	1.663E+07	4.157E+06	299.4 ± 55.9
6	80	56	9	1.429	230.2	8.988E+06	6.291E+06	108.5 ± 19.2
7	73	45	6	1.622	277.5	1.230E+07	7.583E+06	123.1 ± 23.7
8	46	32	6	1.438	197.4	7.752E+06	5.393E+06	109.2 ± 25.4
9	91	65	16	1.400	150.3	5.751E+06	4.108E+06	106.4 ± 17.6
10	108	65	9	1.662	267.2	1.213E+07	7.303E+06	126.1 ± 20.2
11	112	64	9	1.750	263.1	1.258E+07	7.190E+06	132.7 ± 21.2
12	34	22	9	1.545	90.5	3.820E+06	2.472E+06	117.3 ± 32.3
13	105	58	9	1.810	238.5	1.180E+07	6.516E+06	137.2 ± 22.9
14	109	47	9	2.319	193.2	1.225E+07	5.280E+06	175.3 ± 31.1
15	111	51	9	2.176	209.7	1.247E+07	5.730E+06	164.6 ± 28.3
16	85	39	8	2.179	180.4	1.074E+07	4.929E+06	164.9 ± 32.3
17	79	54	9	1.463	222.0	8.875E+06	6.067E+06	111.1 ± 19.9
18	69	45	9	1.533	185.0	7.752E+06	5.056E+06	116.4 ± 22.6
19	92	38	4	2.421	351.5	2.326E+07	9.606E+06	182.9 ± 35.8
20	123	55	9	2.236	226.1	1.382E+07	6.179E+06	169.1 ± 28.0
	1875	977			210.2	1.102E+07	5.743E+06	

Area of basic unit = 9.89E-07 cm-2

CHI SQUARED = 23.13784 WITH 19 DEGREES OF FREEDOM
P(chi squared) = 0.045 %
CORRELATION COEFFICIENT = 0.608
VARIANCE OF SQR(Ns) = 2.67465
VARIANCE OF SQR(Ni) = 1.256322

Ns/Ni = 1.919 ± 0.076
MEAN RATIO = 1.991 ± 0.148

Pooled Age = 145.4 ± 7.4 Ma
Mean Age = 150.8 ± 12.2 Ma
Central Age = 144.0 ± 9.1Ma
% Rel. Error = 20.24
Ages calculated using a zeta of 140.2 ± 3.6 for CN 1 glass
RHO D = 1.093E+06cm-2; ND = 2703

9414-70 Zircon

IRRADIATION WK148-13 COUNTED BY: KAO

No.	Ns	Ni	Na	RATIO	U(ppm)	RHOs	RHOi	F.T.AGE(Ma)
1	55	35	9	1.571	143.4	6.179E+06	3.932E+06	119.7 ± 26.2
2	111	55	10	2.018	202.8	1.122E+07	5.561E+06	153.4 ± 25.8
3	108	32	9	3.375	131.1	1.213E+07	3.595E+06	254.4 ± 51.9
4	102	61	9	1.672	249.9	1.146E+07	6.853E+06	127.3 ± 21.0
5	66	41	9	1.610	168.0	7.415E+06	4.606E+06	122.6 ± 24.7
6	191	25	9	7.640	102.4	2.146E+07	2.809E+06	562.3 ±120.9
7	96	57	9	1.684	233.5	1.079E+07	6.404E+06	128.2 ± 21.8
8	55	22	9	2.500	90.1	6.179E+06	2.472E+06	189.4 ± 48.2
9	88	50	6	1.760	307.2	1.483E+07	8.426E+06	133.9 ± 24.1
10	64	34	9	1.882	139.3	7.190E+06	3.820E+06	143.2 ± 30.7
11	99	60	10	1.650	221.2	1.001E+07	6.067E+06	125.7 ± 20.9
12	77	35	9	2.200	143.4	8.651E+06	3.932E+06	167.0 ± 34.5
13	93	59	9	1.576	241.7	1.045E+07	6.628E+06	120.1 ± 20.4
14	48	24	6	2.000	147.5	8.089E+06	4.044E+06	152.0 ± 38.3
15	78	63	6	1.238	387.1	1.314E+07	1.062E+07	94.5 ± 16.3
	1331	653			188.1	1.051E+07	5.158E+06	

Area of basic unit = 9.89E-07 cm-2

CHI SQUARED = 35.59381 WITH 14 DEGREES OF FREEDOM
P(chi squared) = 0.000 %
CORRELATION COEFFICIENT = 0.095
VARIANCE OF SQR(Ns) = 2.919111
VARIANCE OF SQR(Ni) = 1.352526

Ns/Ni = 2.038 ± 0.097
MEAN RATIO = 2.292 ± 0.404

Pooled Age = 154.9 ± 8.9 Ma
Mean Age = 173.9 ± 31.1 Ma
Central Age = 150.6 ± 14.7Ma
% Rel. Error = 31.91
Ages calculated using a zeta of 140.2 ± 3.6 for CN 1 glass
RHO D = 1.097E+06cm-2; ND = 2713

9414-71 Zircon

IRRADIATION WK148-14 COUNTED BY: KAO

No.	Ns	Ni	Na	RATIO	U(ppm)	RHOs	RHOi	F.T.AGE(Ma)
1	73	25	4	2.920	229.6	1.845E+07	6.320E+06	221.5 ± 51.8
2	85	16	4	5.312	146.9	2.149E+07	4.044E+06	397.5 ±109.1
3	63	36	9	1.750	146.9	7.078E+06	4.044E+06	133.7 ± 28.3
	221	77			166.4	1.314E+07	4.580E+06	

Area of basic unit = 9.89E-07 cm-2

CHI SQUARED = 5.498105 WITH 2 DEGREES OF FREEDOM
P(chi squared) = 0.409 %
CORRELATION COEFFICIENT = -0.994
VARIANCE OF SQR(Ns) = .4114456
VARIANCE OF SQR(Ni) = 1

Ns/Ni = 2.870 ± 0.380
MEAN RATIO = 3.328 ± 1.048

Pooled Age = 217.8 ± 29.7 Ma
Mean Age = 251.8 ± 79.8 Ma
Central Age = 217.3 ± 55.1Ma
% Rel. Error = 37.48
Ages calculated using a zeta of 140.2 ± 3.6 for CN 1 glass
RHO D = 1.101E+06cm-2; ND = 2723

9414-72 Zircon

IRRADIATION WK148-15 COUNTED BY: KAO

No.	Ns	Ni	Na	RATIO	U(ppm)	RHOs	RHOi	F.T.AGE(Ma)
1	143	68	9	2.103	276.5	1.607E+07	7.640E+06	160.9 ± 24.2
2	78	23	6	3.391	140.3	1.314E+07	3.876E+06	257.5 ± 61.6
3	107	38	10	2.816	139.1	1.082E+07	3.842E+06	214.5 ± 41.1
4	64	24	12	2.667	73.2	5.393E+06	2.022E+06	203.3 ± 49.1
5	140	41	9	3.415	166.7	1.573E+07	4.606E+06	259.2 ± 46.8
6	92	32	9	2.875	130.1	1.034E+07	3.595E+06	218.9 ± 45.5
7	67	51	4	1.314	466.7	1.694E+07	1.289E+07	101.0 ± 19.0
8	130	50	6	2.600	305.0	2.191E+07	8.426E+06	198.3 ± 33.6
9	99	56	9	1.768	227.7	1.112E+07	6.291E+06	135.5 ± 23.1
10	138	73	9	1.890	296.9	1.550E+07	8.201E+06	144.8 ± 21.5
11	109	53	9	2.057	215.5	1.225E+07	5.954E+06	157.4 ± 26.8
12	86	29	6	2.966	176.9	1.449E+07	4.887E+06	225.7 ± 49.0
13	102	58	9	1.759	235.9	1.146E+07	6.516E+06	134.8 ± 22.6
14	121	37	8	3.270	169.3	1.529E+07	4.676E+06	248.5 ± 47.4
15	156	32	9	4.875	130.1	1.753E+07	3.595E+06	367.0 ± 72.2
16	112	70	9	1.600	284.7	1.258E+07	7.864E+06	122.8 ± 19.1
17	80	40	9	2.000	162.7	8.988E+06	4.494E+06	153.1 ± 30.0
18	58	48	9	1.208	195.2	6.516E+06	5.393E+06	92.9 ± 18.4
19	74	70	9	1.057	284.7	8.314E+06	7.864E+06	81.4 ± 13.8
20	130	54	9	2.407	219.6	1.461E+07	6.067E+06	183.8 ± 30.3
	2086	947			205.1	1.248E+07	5.666E+06	

Area of basic unit = 9.89E-07 cm-2

CHI SQUARED = 43.29393 WITH 19 DEGREES OF FREEDOM
P(chi squared) = 0.000 %
CORRELATION COEFFICIENT = 0.260
VARIANCE OF SQR(Ns) = 2.099025
VARIANCE OF SQR(Ni) = 1.339844

Ns/Ni = 2.203 ± 0.086
MEAN RATIO = 2.402 ± 0.206

Pooled Age = 168.4 ± 8.5 Ma
Mean Age = 183.4 ± 16.8 Ma
Central Age = 167.2 ± 14.2Ma
% Rel. Error = 32.50
Ages calculated using a zeta of 140.2 ± 3.6 for CN 1 glass
RHO D = 1.105E+06cm-2; ND = 2732

9414-73 Zircon

IRRADIATION WK148-16 COUNTED BY: KAO

No.	Ns	Ni	Na	RATIO	U(ppm)	RHOs	RHOi	F.T.AGE(Ma)
1	105	86	25	1.221	125.5	4.247E+06	3.478E+06	94.2 ± 14.0
2	101	42	4	2.405	382.9	2.553E+07	1.062E+07	184.3 ± 34.3
3	50	23	4	2.174	209.7	1.264E+07	5.814E+06	166.8 ± 42.4
4	55	24	4	2.292	218.8	1.390E+07	6.067E+06	175.7 ± 43.4
5	60	28	9	2.143	113.5	6.741E+06	3.146E+06	164.5 ± 38.0
6	99	53	9	1.868	214.8	1.112E+07	5.954E+06	143.6 ± 24.9
7	123	72	9	1.708	291.8	1.382E+07	8.089E+06	131.5 ± 20.0
8	129	86	9	1.500	348.5	1.449E+07	9.662E+06	115.6 ± 16.5
9	162	84	9	1.929	340.4	1.820E+07	9.437E+06	148.2 ± 20.5
10	95	76	25	1.250	110.9	3.842E+06	3.074E+06	96.5 ± 15.2
11	74	52	9	1.423	210.7	8.314E+06	5.842E+06	109.7 ± 20.2
12	110	36	9	3.056	145.9	1.236E+07	4.044E+06	233.3 ± 45.4
13	205	125	21	1.640	217.1	9.870E+06	6.019E+06	126.2 ± 14.9
14	124	77	12	1.610	234.0	1.045E+07	6.488E+06	124.0 ± 18.4
15	94	30	9	3.133	121.6	1.056E+07	3.370E+06	239.1 ± 50.7
16	52	45	8	1.156	205.1	6.572E+06	5.688E+06	89.2 ± 18.4
17	93	66	9	1.409	267.4	1.045E+07	7.415E+06	108.6 ± 17.8
18	26	15	12	1.733	45.6	2.191E+06	1.264E+06	133.4 ± 43.4
19	88	59	9	1.492	239.1	9.887E+06	6.628E+06	114.9 ± 19.7
20	106	51	9	2.078	206.7	1.191E+07	5.730E+06	159.6 ± 27.7
	1951	1130			192.6	9.218E+06	5.339E+06	

Area of basic unit = 9.89E-07 cm-2

CHI SQUARED = 22.46684 WITH 19 DEGREES OF FREEDOM
P(chi squared) = 0.070 %
CORRELATION COEFFICIENT = 0.860
VARIANCE OF SQR(Ns) = 4.38368
VARIANCE OF SQR(Ni) = 3.506399

Ns/Ni = 1.727 ± 0.065
MEAN RATIO = 1.861 ± 0.124

Pooled Age = 132.8 ± 6.5 Ma
Mean Age = 143.1 ± 10.6 Ma
Central Age = 134.6 ± 8.3Ma
% Rel. Error = 19.53
Ages calculated using a zeta of 140.2 ± 3.6 for CN 1 glass
RHO D = 1.109E+06cm-2; ND = 2742

9414-74 ZIRCON MARLBOROUGH

IRRADIATION WK148-17
SLIDE NUMBER 17
COUNTED BY: KAO

No.	Ns	Ni	Na	RATIO	U (ppm)	RHOs (E+06)	RHOi (E+06)	F.T.AGE (Ma)
1	159	99	15	1.606	0.0	10.718	6.673	124.0 ± 16.4
2	86	47	9	1.830	0.0	9.662	5.280	141.1 ± 26.0
3	53	15	6	3.533	0.0	8.932	2.528	269.7 ± 79.3
4	47	29	6	1.621	0.0	7.920	4.887	125.1 ± 29.8
5	43	34	9	1.265	0.0	4.831	3.820	97.8 ± 22.7
6	51	30	10	1.700	0.0	5.157	3.033	131.2 ± 30.5
7	93	44	9	2.114	0.0	10.448	4.943	162.7 ± 30.2
8	42	14	6	3.000	0.0	7.078	2.359	229.7 ± 71.3
9	50	24	6	2.083	0.0	8.426	4.044	160.4 ± 40.2
10	76	38	8	2.000	0.0	9.606	4.803	154.0 ± 31.0
11	42	20	4	2.100	0.0	10.617	5.056	161.7 ± 44.2
12	51	23	6	2.217	0.0	8.595	3.876	170.6 ± 43.2
13	67	55	6	1.218	0.0	11.291	9.269	94.3 ± 17.4
14	130	84	9	1.548	0.0	14.605	9.437	119.5 ± 17.2
15	58	39	6	1.487	0.0	9.774	6.572	114.9 ± 24.1
	1048	595			0.0	9.214	5.231	

AREA OF BASIC UNIT = 9.89E-07 cm
CHI SQUARED = 20.56717 WITH 14 DEGREES OF FREEDOM
P(chi squared) = 11.3 %
CORRELATION COEFFICIENT = 0.939
VARIANCE OF SQR(Ns) = 3.45
VARIANCE OF SQR(Ni) = 3.15

Ns/Ni = 1.761 ± 0.090
MEAN RATIO = 1.955 ± 0.161

Ages calculated using a zeta of 140.2 ± 3.6 for CN1 glass
RHO D = 1.112E+06 ; ND = 2752

POOLED AGE = 135.9 ± 8.2 Ma
MEAN AGE = 150.6 ± 13.3 Ma

9414-75 Zircon

IRRADIATION WK148-18 COUNTED BY: KAO

No.	Ns	Ni	Na	RATIO	U(ppm)	RHOs	RHOi	F.T.AGE(Ma)
1	101	85	9	1.188	342.3	1.135E+07	9.549E+06	92.3 ± 13.9
2	158	106	9	1.491	426.8	1.775E+07	1.191E+07	115.6 ± 15.0
3	109	30	9	3.633	120.8	1.225E+07	3.370E+06	278.2 ± 58.0
4	157	115	9	1.365	463.1	1.764E+07	1.292E+07	105.9 ± 13.4
5	232	67	9	3.463	269.8	2.606E+07	7.527E+06	265.4 ± 37.8
6	105	31	10	3.387	112.3	1.062E+07	3.134E+06	259.7 ± 53.7
7	129	28	9	4.607	112.7	1.449E+07	3.146E+06	350.7 ± 74.0
8	56	26	4	2.154	235.6	1.416E+07	6.572E+06	166.3 ± 39.8
9	59	77	12	0.766	232.5	4.971E+06	6.488E+06	59.7 ± 10.5
10	88	71	8	1.239	321.6	1.112E+07	8.974E+06	96.2 ± 15.7
11	94	90	9	1.044	362.4	1.056E+07	1.011E+07	81.2 ± 12.3
12	138	64	9	2.156	257.7	1.550E+07	7.190E+06	166.5 ± 25.7
13	95	47	9	2.021	189.3	1.067E+07	5.280E+06	156.2 ± 28.3
14	127	40	9	3.175	161.1	1.427E+07	4.494E+06	243.7 ± 44.9
15	54	21	4	2.571	190.3	1.365E+07	5.308E+06	198.1 ± 51.3
16	126	33	6	3.818	199.3	2.123E+07	5.561E+06	292.0 ± 57.9
17	137	70	8	1.957	317.1	1.732E+07	8.847E+06	151.3 ± 22.8
18	70	44	9	1.591	177.2	7.864E+06	4.943E+06	123.3 ± 24.0
19	79	48	9	1.646	193.3	8.875E+06	5.393E+06	127.5 ± 23.7
20	70	38	9	1.842	153.0	7.864E+06	4.269E+06	142.5 ± 29.1
	2184	1131			242.5	1.307E+07	6.767E+06	

Area of basic unit = 9.89E-07 cm-2

CHI SQUARED = 79.14261 WITH 19 DEGREES OF FREEDOM
P(chi squared) = 0.000 %
CORRELATION COEFFICIENT = 0.397
VARIANCE OF SQR(Ns) = 3.998946
VARIANCE OF SQR(Ni) = 3.318102

Ns/Ni = 1.931 ± 0.071
MEAN RATIO = 2.256 ± 0.240

Pooled Age = 149.3 ± 7.3 Ma
Mean Age = 174.1 ± 19.4 Ma
Central Age = 150.6 ± 15.9Ma
% Rel. Error = 43.18
Ages calculated using a zeta of 140.2 ± 3.6 for CN 1 glass
RHO D = 1.116E+06cm-2; ND = 2762

9414-76 Zircon

IRRADIATION WK148-19 COUNTED BY: KAO

No.	Ns	Ni	Na	RATIO	U(ppm)	RHOs	RHOi	F.T.AGE(Ma)
1	107	76	8	1.408	34.3	1.352E+06	9.606E+05	109.6 ± 16.8
2	169	50	9	3.380	20.1	1.899E+06	5.617E+05	260.1 ± 42.7
3	220	82	16	2.683	18.5	1.390E+06	5.182E+05	207.3 ± 27.6
4	47	17	6	2.765	10.2	7.920E+05	2.865E+05	213.5 ± 60.8
5	185	68	9	2.721	27.3	2.078E+06	7.640E+05	210.1 ± 30.5
6	82	26	4	3.154	23.5	2.073E+06	6.572E+05	243.0 ± 55.2
7	90	57	12	1.579	17.2	7.583E+05	4.803E+05	122.8 ± 21.2
8	87	42	8	2.071	19.0	1.100E+06	5.308E+05	160.6 ± 30.6
9	72	47	9	1.532	18.9	8.089E+05	5.280E+05	119.2 ± 22.7
10	200	57	9	3.509	22.9	2.247E+06	6.404E+05	269.8 ± 41.4
11	143	36	9	3.972	14.4	1.607E+06	4.044E+05	304.6 ± 57.6
12	101	25	8	4.040	11.3	1.277E+06	3.160E+05	309.6 ± 69.9
13	208	90	9	2.311	36.1	2.337E+06	1.011E+06	178.9 ± 23.3
14	155	50	8	3.100	22.6	1.959E+06	6.320E+05	238.9 ± 39.6
15	139	71	9	1.958	28.5	1.562E+06	7.977E+05	151.9 ± 22.7
16	92	39	16	2.359	8.8	5.814E+05	2.465E+05	182.6 ± 35.4
17	96	41	9	2.341	16.4	1.079E+06	4.606E+05	181.3 ± 34.3
18	78	55	9	1.418	22.1	8.763E+05	6.179E+05	110.4 ± 19.8
19	49	34	6	1.441	20.5	8.257E+05	5.730E+05	112.2 ± 25.3
20	153	87	9	1.759	34.9	1.719E+06	9.774E+05	136.6 ± 18.9
	2473	1050			20.8	1.374E+06	5.833E+05	

Area of basic unit = 9.89E-06 cm-2

CHI SQUARED = 38.25002 WITH 19 DEGREES OF FREEDOM
P(chi squared) = 0.000 %
CORRELATION COEFFICIENT = 0.690
VARIANCE OF SQR(Ns) = 5.792108
VARIANCE OF SQR(Ni) = 2.233379

Ns/Ni = 2.355 ± 0.087
MEAN RATIO = 2.475 ± 0.189

Pooled Age = 182.3 ± 8.9 Ma
Mean Age = 191.4 ± 15.9 Ma
Central Age = 178.3 ± 13.7Ma
% Rel. Error = 28.44
Ages calculated using a zeta of 140.2 ± 3.6 for CN 1 glass
RHO D = 1.120E+06cm-2; ND = 2772

9414-77 Zircon

IRRADIATION WK148-20 COUNTED BY: KAO

No.	Ns	Ni	Na	RATIO	U(ppm)	RHOs	RHOi	F.T.AGE(Ma)
1	163	52	9	3.135	207.7	1.831E+07	5.842E+06	242.6 ± 39.4
2	158	55	9	2.873	219.7	1.775E+07	6.179E+06	222.7 ± 35.6
3	27	32	6	0.844	191.7	4.550E+06	5.393E+06	66.2 ± 17.4
4	118	31	4	3.806	278.6	2.983E+07	7.836E+06	293.4 ± 60.0
5	144	63	9	2.286	251.7	1.618E+07	7.078E+06	177.8 ± 27.4
6	60	24	6	2.500	143.8	1.011E+07	4.044E+06	194.2 ± 47.3
7	88	53	9	1.660	211.7	9.887E+06	5.954E+06	129.6 ± 22.9
8	109	36	8	3.028	161.8	1.378E+07	4.550E+06	234.5 ± 45.7
9	91	146	9	0.623	583.2	1.022E+07	1.640E+07	49.0 ± 6.7
10	162	65	9	2.492	259.6	1.820E+07	7.303E+06	193.6 ± 29.1
11	139	26	9	5.346	103.9	1.562E+07	2.921E+06	408.4 ± 88.2
12	193	154	9	1.253	615.2	2.168E+07	1.730E+07	98.1 ± 11.0
	1452	737			276.0	1.529E+07	7.762E+06	

Area of basic unit = 9.89E-07 cm-2

CHI SQUARED = 85.82807 WITH 11 DEGREES OF FREEDOM
P(chi squared) = 0.000 %
CORRELATION COEFFICIENT = 0.378
VARIANCE OF SQR(Ns) = 6.102661
VARIANCE OF SQR(Ni) = 6.150385

Ns/Ni = 1.970 ± 0.089
MEAN RATIO = 2.487 ± 0.381

Pooled Age = 153.5 ± 8.5 Ma
Mean Age = 193.2 ± 30.3 Ma
Central Age = 158.4 ± 27.4Ma
% Rel. Error = 57.25
Ages calculated using a zeta of 140.2 ± 3.6 for CN 1 glass
RHO D = 1.125E+06cm-2; ND = 2781

9414-78 Zircon

IRRADIATION WK149-1 COUNTED BY: KAO

No.	Ns	Ni	Na	RATIO	U(ppm)	RHOs	RHOi	F.T.AGE(Ma)
1	109	51	9	2.137	231.9	1.225E+07	5.730E+06	146.4 ± 25.3
2	121	22	9	5.500	100.1	1.359E+07	2.472E+06	370.1 ± 86.6
3	100	49	9	2.041	222.9	1.123E+07	5.505E+06	139.8 ± 24.8
4	144	46	9	3.130	209.2	1.618E+07	5.168E+06	213.3 ± 36.8
5	99	36	8	2.750	184.2	1.251E+07	4.550E+06	187.7 ± 37.0
6	136	52	9	2.615	236.5	1.528E+07	5.842E+06	178.7 ± 29.7
7	58	32	9	1.812	145.5	6.516E+06	3.595E+06	124.3 ± 27.7
8	86	46	9	1.870	209.2	9.662E+06	5.168E+06	128.2 ± 23.8
9	81	26	12	3.115	88.7	6.825E+06	2.191E+06	212.3 ± 48.3
10	21	8	9	2.625	36.4	2.359E+06	8.988E+05	179.3 ± 74.7
11	86	33	9	2.606	150.1	9.662E+06	3.707E+06	178.0 ± 36.9
12	44	24	9	1.833	109.2	4.943E+06	2.696E+06	125.8 ± 32.2
13	79	35	12	2.257	119.4	6.657E+06	2.949E+06	154.5 ± 31.8
14	111	29	9	3.828	131.9	1.247E+07	3.258E+06	259.8 ± 54.8
15	166	52	16	3.192	133.0	1.049E+07	3.286E+06	217.4 ± 35.3
16	97	27	9	3.593	122.8	1.090E+07	3.033E+06	244.2 ± 53.7
17	48	17	9	2.824	77.3	5.393E+06	1.910E+06	192.7 ± 54.7
18	119	24	9	4.958	109.2	1.337E+07	2.696E+06	334.6 ± 75.7
19	73	34	9	2.147	154.6	8.201E+06	3.820E+06	147.0 ± 30.9
20	67	39	6	1.718	266.1	1.129E+07	6.572E+06	117.9 ± 24.1
	1845	682			147.7	9.870E+06	3.649E+06	

Area of basic unit = 9.89E-07 cm-2

CHI SQUARED = 22.91331 WITH 19 DEGREES OF FREEDOM
P(chi squared) = 0.052 %
CORRELATION COEFFICIENT = 0.646
VARIANCE OF SQR(Ns) = 3.942312
VARIANCE OF SQR(Ni) = 1.308472

Ns/Ni = 2.705 ± 0.121
MEAN RATIO = 2.828 ± 0.228

Pooled Age = 184.7 ± 10.2 Ma
Mean Age = 192.9 ± 16.8 Ma
Central Age = 181.5 ± 13.1Ma
% Rel. Error = 23.06
Ages calculated using a zeta of 140.2 ± 3.6 for CN 1 glass
RHO D = 9.881E+05cm-2; ND = 2443

9414-79 ZIRCON Marlborough

IRRADIATION wk149-2
SLIDE NUMBER 2
COUNTED BY: Kao

No.	Ns	NI	Na	RATIO	U (ppm)	RHOs (E+06)	RHOI (E+06)	F.T.AGE (Ma)
1	149	88	16	1.693	0.0	9.416	5.561	117.7 ± 16.3
2	117	48	9	2.438	0.0	13.145	5.393	168.8 ± 29.5
3	61	34	9	1.794	0.0	6.853	3.820	124.7 ± 27.0
4	46	33	4	1.394	0.0	11.628	8.342	97.1 ± 22.4
5	69	34	9	2.029	0.0	7.752	3.820	140.9 ± 29.9
	442	237			0.0	9.509	5.099	

AREA OF BASIC UNIT = 9.89E-07 cm
CHI SQUARED = 4.806754 WITH 4 DEGREES OF FREEDOM
P(chi squared) = 30.8 %
CORRELATION COEFFICIENT = 0.917
VARIANCE OF SQR(Ns) = 5.06
VARIANCE OF SQR(Ni) = 2.41

Ns/Ni = 1.865 ± 0.150
MEAN RATIO = 1.870 ± 0.175

Ages calculated using a zeta of 140.2 ± 3.6 for CN1 glass
RHO D = 1.001E+06 ; ND = 2476

POOLED AGE = 129.6 ± 11.3 Ma
MEAN AGE = 129.9 ± 12.9 Ma

9414-80 Zircon

IRRADIATION WK149-3 COUNTED BY: KAO

No.	Ns	Ni	Na	RATIO	U(ppm)	RHOs	RHOi	F.T.AGE(Ma)
1	172	67	9	2.567	296.9	1.932E+07	7.527E+06	179.9 ± 26.6
2	76	34	6	2.235	226.0	1.281E+07	5.730E+06	157.0 ± 32.8
3	56	51	10	1.098	203.4	5.662E+06	5.157E+06	77.6 ± 15.2
4	121	32	8	3.781	159.5	1.529E+07	4.044E+06	263.3 ± 53.0
5	70	34	9	2.059	150.7	7.864E+06	3.820E+06	144.7 ± 30.6
6	66	41	9	1.610	181.7	7.415E+06	4.606E+06	113.4 ± 22.9
7	36	23	9	1.565	101.9	4.044E+06	2.584E+06	110.3 ± 29.7
8	62	34	6	1.824	226.0	1.045E+07	5.730E+06	128.3 ± 27.7
9	35	34	6	1.029	226.0	5.898E+06	5.730E+06	72.8 ± 17.7
10	69	50	9	1.380	221.6	7.752E+06	5.617E+06	97.4 ± 18.4
11	81	38	9	2.132	168.4	9.100E+06	4.269E+06	149.8 ± 29.8
12	82	24	9	3.417	106.4	9.212E+06	2.696E+06	238.4 ± 55.9
13	148	69	9	2.145	305.8	1.663E+07	7.752E+06	150.7 ± 22.5
14	58	18	6	3.222	119.7	9.774E+06	3.033E+06	225.1 ± 61.2
15	69	43	9	1.605	190.6	7.752E+06	4.831E+06	113.1 ± 22.3
16	99	35	9	2.829	155.1	1.112E+07	3.932E+06	198.0 ± 39.5
17	108	47	9	2.298	208.3	1.213E+07	5.280E+06	161.3 ± 28.7
	1408	674			190.7	1.010E+07	4.833E+06	

Area of basic unit = 9.89E-07 cm-2

CHI SQUARED = 25.96762 WITH 16 DEGREES OF FREEDOM
P(chi squared) = 0.001 %
CORRELATION COEFFICIENT = 0.668
VARIANCE OF SQR(Ns) = 3.740532
VARIANCE OF SQR(Ni) = 1.189999

Ns/Ni = 2.089 ± 0.098
MEAN RATIO = 2.164 ± 0.192

Pooled Age = 146.8 ± 8.4 Ma
Mean Age = 152.0 ± 14.4 Ma
Central Age = 141.9 ± 12.3Ma
% Rel. Error = 28.50
Ages calculated using a zeta of 140.2 ± 3.6 for CN 1 glass
RHO D = 1.014E+06cm-2; ND = 2508

9414-81 Zircon

IRRADIATION WK149-4 COUNTED BY: KAO

No.	Ns	Ni	Na	RATIO	U(ppm)	RHOs	RHOi	F.T.AGE(Ma)
1	48	36	9	1.333	157.5	5.393E+06	4.044E+06	95.3 ± 21.2
2	111	28	9	3.964	122.5	1.247E+07	3.146E+06	279.3 ± 59.7
3	159	114	9	1.395	498.8	1.786E+07	1.281E+07	99.6 ± 12.6
4	117	64	9	1.828	280.0	1.314E+07	7.190E+06	130.3 ± 20.7
5	89	58	12	1.534	190.3	7.499E+06	4.887E+06	109.5 ± 18.8
6	70	51	9	1.373	223.2	7.864E+06	5.730E+06	98.1 ± 18.3
7	128	67	16	1.910	164.9	8.089E+06	4.234E+06	136.1 ± 21.0
8	95	46	9	2.065	201.3	1.067E+07	5.168E+06	147.0 ± 26.8
9	41	11	9	3.727	48.1	4.606E+06	1.236E+06	262.9 ± 89.7
10	121	67	9	1.806	293.2	1.359E+07	7.527E+06	128.7 ± 20.0
11	84	35	9	2.400	153.2	9.437E+06	3.932E+06	170.5 ± 34.7
12	154	119	9	1.294	520.7	1.730E+07	1.337E+07	92.5 ± 11.7
13	90	65	9	1.385	284.4	1.011E+07	7.303E+06	98.9 ± 16.4
14	93	61	9	1.525	266.9	1.045E+07	6.853E+06	108.8 ± 18.3
15	90	42	9	2.143	183.8	1.011E+07	4.719E+06	152.5 ± 28.9
16	96	62	9	1.548	271.3	1.079E+07	6.966E+06	110.5 ± 18.4
17	112	58	9	1.931	253.8	1.258E+07	6.516E+06	137.5 ± 22.7
18	86	45	18	1.911	98.5	4.831E+06	2.528E+06	136.1 ± 25.4
19	44	28	9	1.571	122.5	4.943E+06	3.146E+06	112.2 ± 27.4
20	57	44	9	1.295	192.5	6.404E+06	4.943E+06	92.6 ± 18.8
	1885	1101			217.9	9.578E+06	5.594E+06	

Area of basic unit = 9.89E-07 cm-2

CHI SQUARED = 22.63334 WITH 19 DEGREES OF FREEDOM
P(chi squared) = 0.063 %
CORRELATION COEFFICIENT = 0.837
VARIANCE OF SQR(Ns) = 3.022789
VARIANCE OF SQR(Ni) = 3.002223

Ns/Ni = 1.712 ± 0.065
MEAN RATIO = 1.897 ± 0.165

Pooled Age = 122.1 ± 6.1 Ma
Mean Age = 135.1 ± 12.5 Ma
Central Age = 124.3 ± 7.6Ma
% Rel. Error = 19.18
Ages calculated using a zeta of 140.2 ± 3.6 for CN 1 glass
RHO D = 1.027E+06cm-2; ND = 2541

9414-82 ZIRCON MARLBOROUGH

IRRADIATION WK149-5
SLIDE NUMBER 5
COUNTED BY: KAO

No.	Ns	Ni	Na	RATIO	U (ppm)	RHOs (E+06)	RHOi (E+06)	F.T.AGE (Ma)
1	148	43	9	3.442	0.0	16.627	4.831	246.4 ± 43.4
2	97	29	9	3.345	0.0	10.898	3.258	239.6 ± 51.3
3	60	25	9	2.400	0.0	6.741	2.809	172.8 ± 41.5
4	105	36	9	2.917	0.0	11.796	4.044	209.4 ± 41.0
5	63	37	9	1.703	0.0	7.078	4.157	123.1 ± 25.8
6	117	58	9	2.017	0.0	13.145	6.516	145.6 ± 23.8
7	66	26	9	2.538	0.0	7.415	2.921	182.6 ± 42.7
8	130	57	9	2.281	0.0	14.605	6.404	164.3 ± 26.6
9	84	36	6	2.333	0.0	14.156	6.067	168.1 ± 33.9
10	114	60	9	1.900	0.0	12.808	6.741	137.2 ± 22.3
11	91	42	9	2.167	0.0	10.224	4.719	156.2 ± 29.6
12	39	14	6	2.786	0.0	6.572	2.359	200.1 ± 62.7
	1114	463			0.0	11.043	4.590	

AREA OF BASIC UNIT = 9.89E-07 cm
CHI SQUARED = 14.7105 WITH 11 DEGREES OF FREEDOM
P(chi squared) = 19.6 %
CORRELATION COEFFICIENT = 0.782
VARIANCE OF SQR(Ns) = 2.97
VARIANCE OF SQR(Ni) = 1.43

Ns/Ni = 2.406 ± 0.133
MEAN RATIO = 2.486 ± 0.158

Ages calculated using a zeta of 140.2 ± 3.6 for CN1 glass
RHO D = 1.041E+06 ; ND = 2574

POOLED AGE = 173.2 ± 11.1 Ma
MEAN AGE = 178.9 ± 12.7 Ma

9414-83 ZIRCON Marlborough

IRRADIATION wk149-6
SLIDE NUMBER 6
COUNTED BY: Kao

No.	Ns	Ni	Na	RATIO	U (ppm)	RHOs (E+06)	RHOi (E+06)	F.T.AGE (Ma)
1	92	69	8	1.333	0.0	11.628	8.721	97.8 ± 15.9
2	20	11	6	1.818	0.0	3.370	1.854	133.0 ± 50.1
3	128	50	9	2.560	0.0	14.380	5.617	186.4 ± 31.7
4	97	61	6	1.590	0.0	16.346	10.280	116.4 ± 19.4
5	91	40	8	2.275	0.0	11.502	5.056	165.9 ± 31.9
6	26	18	6	1.444	0.0	4.382	3.033	105.8 ± 32.6
7	54	33	9	1.636	0.0	6.067	3.707	119.8 ± 26.7
	508	282			0.0	9.878	5.483	

AREA OF BASIC UNIT = 9.89E-07 cm
CHI SQUARED = 10.89813 WITH 6 DEGREES OF FREEDOM
P(chi squared) = 9.2 %
CORRELATION COEFFICIENT = 0.835
VARIANCE OF SQR(Ns) = 6.73
VARIANCE OF SQR(Ni) = 3.35

Ns/Ni = 1.801 ± 0.134
MEAN RATIO = 1.808 ± 0.170

Ages calculated using a zeta of 140.2 ± 3.6 for CN1 glass
RHO D = 1.054E+06 ; ND = 2607

POOLED AGE = 131.7 ± 10.7 Ma
MEAN AGE = 132.2 ± 13.2 Ma

9414-84 ZIRCON MARLBOROUGH

IRRADIATION WK149-7
SLIDE NUMBER 7
COUNTED BY: KAO

No.	Ns	Ni	Na	RATIO	U (ppm)	RHOs (E+06)	RHOi (E+06)	F.T.AGE (Ma)
1	28	13	4	2.154	0.0	7.078	3.286	159.1 ± 53.6
2	83	31	9	2.677	0.0	9.325	3.483	197.2 ± 42.0
3	55	19	4	2.895	0.0	13.903	4.803	213.0 ± 57.1
4	53	19	4	2.789	0.0	13.397	4.803	205.3 ± 55.3
5	86	27	4	3.185	0.0	21.739	6.825	233.9 ± 52.2
6	100	21	4	4.762	0.0	25.278	5.308	346.7 ± 84.0
7	102	36	9	2.833	0.0	11.459	4.044	208.5 ± 41.0
8	43	12	4	3.583	0.0	10.870	3.033	262.6 ± 86.2
9	61	19	4	3.211	0.0	15.420	4.803	235.8 ± 62.4
10	51	23	9	2.217	0.0	5.730	2.584	163.8 ± 41.5
11	80	21	4	3.810	0.0	20.222	5.308	278.8 ± 69.0
12	75	22	4	3.409	0.0	18.959	5.561	250.1 ± 61.2
13	34	11	4	3.091	0.0	8.595	2.781	227.1 ± 79.1
14	81	18	4	4.500	0.0	20.475	4.550	328.1 ± 86.1
15	49	26	4	1.885	0.0	12.386	6.572	139.4 ± 34.1
16	85	20	4	4.250	0.0	21.486	5.056	310.3 ± 77.8
17	106	22	4	4.818	0.0	26.795	5.561	350.7 ± 82.9
18	33	16	4	2.062	0.0	8.342	4.044	152.4 ± 46.7
19	74	22	4	3.364	0.0	18.706	5.561	246.8 ± 60.5
20	66	16	4	4.125	0.0	16.684	4.044	301.4 ± 84.5
	1345	414			0.0	14.315	4.406	

AREA OF BASIC UNIT = 9.89E-07 cm
CHI SQUARED = 22.67669 WITH 19 DEGREES OF FREEDOM
P(chi squared) = 25.2 %
CORRELATION COEFFICIENT = 0.647
VARIANCE OF SQR(Ns) = 2.24
VARIANCE OF SQR(Ni) = 0.44

Ns/Ni = 3.249 ± 0.183
MEAN RATIO = 3.281 ± 0.198

Ages calculated using a zeta of 140.2 ± 3.6 for CN1 glass
RHO D = 1.067E+06 ; ND = 2639

POOLED AGE = 238.5 ± 15.5 Ma
MEAN AGE = 240.9 ± 16.5 Ma

9414-85 Zircon

IRRADIATION WK149-8 COUNTED BY: KAO

No.	Ns	Ni	Na	RATIO	U(ppm)	RHOs	RHOi	F.T.AGE(Ma)
1	162	41	9	3.951	170.6	1.820E+07	4.606E+06	292.4 ± 52.0
2	64	37	9	1.730	154.0	7.190E+06	4.157E+06	129.6 ± 27.1
3	115	42	8	2.738	196.6	1.453E+07	5.308E+06	204.0 ± 37.4
4	68	32	9	2.125	133.2	7.640E+06	3.595E+06	158.9 ± 34.4
5	76	29	12	2.621	90.5	6.404E+06	2.444E+06	195.4 ± 43.1
6	71	38	12	1.868	118.6	5.982E+06	3.202E+06	139.9 ± 28.5
7	90	25	9	3.600	104.0	1.011E+07	2.809E+06	266.9 ± 61.0
8	162	42	9	3.857	174.8	1.820E+07	4.719E+06	285.6 ± 50.3
9	102	88	9	1.159	366.2	1.146E+07	9.887E+06	87.2 ± 13.0
10	140	59	9	2.373	245.5	1.573E+07	6.628E+06	177.2 ± 28.1
11	138	64	9	2.156	266.3	1.550E+07	7.190E+06	161.2 ± 24.9
12	93	58	9	1.603	241.3	1.045E+07	6.516E+06	120.3 ± 20.5
13	73	55	9	1.327	228.9	8.201E+06	6.179E+06	99.7 ± 18.1
14	84	33	9	2.545	137.3	9.437E+06	3.707E+06	189.9 ± 39.5
15	84	68	8	1.235	318.3	1.062E+07	8.595E+06	92.8 ± 15.4
16	60	28	9	2.143	116.5	6.741E+06	3.146E+06	160.2 ± 37.0
17	123	61	9	2.016	253.8	1.382E+07	6.853E+06	150.9 ± 24.1
18	65	23	9	2.826	95.7	7.303E+06	2.584E+06	210.5 ± 51.5
19	53	23	8	2.304	107.7	6.699E+06	2.907E+06	172.1 ± 43.3
20	61	33	9	1.848	137.3	6.853E+06	3.707E+06	138.4 ± 30.2
	1884	879			179.9	1.041E+07	4.857E+06	

Area of basic unit = 9.89E-07 cm-2

CHI SQUARED = 38.87934 WITH 19 DEGREES OF FREEDOM
P(chi squared) = 0.000 %
CORRELATION COEFFICIENT = 0.436
VARIANCE OF SQR(Ns) = 2.911152
VARIANCE OF SQR(Ni) = 1.668643

Ns/Ni = 2.143 ± 0.088
MEAN RATIO = 2.301 ± 0.179

Pooled Age = 160.3 ± 8.3 Ma
Mean Age = 171.9 ± 14.5 Ma
Central Age = 159.3 ± 12.9Ma
% Rel. Error = 29.59
Ages calculated using a zeta of 140.2 ± 3.6 for CN 1 glass
RHO D = 1.080E+06cm-2; ND = 2672

9414-86 Zircon

IRRADIATION WK149-9 COUNTED BY: KAO

No.	Ns	Ni	Na	RATIO	U(ppm)	RHOs	RHOi	F.T.AGE(Ma)
1	219	51	9	4.294	209.7	2.460E+07	5.730E+06	320.9 ± 50.9
2	174	98	9	1.776	402.9	1.955E+07	1.101E+07	134.6 ± 17.5
3	78	60	8	1.300	277.5	9.858E+06	7.583E+06	98.8 ± 17.3
4	64	28	10	2.286	103.6	6.471E+06	2.831E+06	172.8 ± 39.5
5	97	47	6	2.064	289.9	1.635E+07	7.920E+06	156.2 ± 28.2
6	204	40	9	5.100	164.5	2.292E+07	4.494E+06	379.4 ± 66.7
7	82	41	6	2.000	252.9	1.382E+07	6.909E+06	151.4 ± 29.4
8	93	68	9	1.368	279.6	1.045E+07	7.640E+06	103.9 ± 16.9
9	122	71	9	1.718	291.9	1.371E+07	7.977E+06	130.3 ± 19.9
10	141	45	6	3.133	277.5	2.376E+07	7.583E+06	235.7 ± 41.1
11	235	79	9	2.975	324.8	2.640E+07	8.875E+06	224.0 ± 30.0
12	62	44	6	1.409	271.4	1.045E+07	7.415E+06	107.1 ± 21.4
13	83	64	12	1.297	197.4	6.994E+06	5.393E+06	98.6 ± 16.7
14	81	79	9	1.025	324.8	9.100E+06	8.875E+06	78.1 ± 12.6
15	157	132	9	1.189	542.7	1.764E+07	1.483E+07	90.5 ± 11.1
16	193	115	9	1.678	472.8	2.168E+07	1.292E+07	127.3 ± 15.5
17	204	55	9	3.709	226.1	2.292E+07	6.179E+06	278.1 ± 43.2
18	139	137	9	1.015	563.3	1.562E+07	1.539E+07	77.3 ± 9.6
19	115	55	9	2.091	226.1	1.292E+07	6.179E+06	158.2 ± 26.4
20	59	27	9	2.185	111.0	6.628E+06	3.033E+06	165.3 ± 38.8
	2602	1336			289.1	1.539E+07	7.900E+06	

Area of basic unit = 9.89E-07 cm-2

CHI SQUARED = 93.20418 WITH 19 DEGREES OF FREEDOM
P(chi squared) = 0.000 %
CORRELATION COEFFICIENT = 0.356
VARIANCE OF SQR(Ns) = 6.332686
VARIANCE OF SQR(Ni) = 3.453292

Ns/Ni = 1.948 ± 0.066
MEAN RATIO = 2.181 ± 0.252

Pooled Age = 147.5 ± 6.9 Ma
Mean Age = 164.9 ± 19.8 Ma
Central Age = 143.8 ± 14.3Ma
% Rel. Error = 40.56
Ages calculated using a zeta of 140.2 ± 3.6 for CN 1 glass
RHO D = 1.093E+06cm-2; ND = 2705

9414-87 Zircon

IRRADIATION WK149-10 COUNTED BY: KAO

No.	Ns	Ni	Na	RATIO	U(ppm)	RHOs	RHOi	F.T.AGE(Ma)
1	153	107	12	1.430	101.8	1.289E+07	9.016E+06	110.0 ± 14.3
2	61	37	6	1.649	70.4	1.028E+07	6.235E+06	126.7 ± 26.7
3	61	32	9	1.906	40.6	6.853E+06	3.595E+06	146.3 ± 32.3
4	65	65	9	1.000	82.5	7.303E+06	7.303E+06	77.1 ± 13.8
5	105	43	9	2.442	54.5	1.180E+07	4.831E+06	186.8 ± 34.3
6	120	84	9	1.429	106.6	1.348E+07	9.437E+06	109.9 ± 16.0
7	144	52	10	2.769	59.4	1.456E+07	5.258E+06	211.4 ± 34.9
8	88	31	9	2.839	39.3	9.887E+06	3.483E+06	216.6 ± 45.8
9	76	54	9	1.407	68.5	8.538E+06	6.067E+06	108.3 ± 19.6
10	62	33	6	1.879	62.8	1.045E+07	5.561E+06	144.2 ± 31.4
	935	538			69.8	1.074E+07	6.182E+06	

Area of basic unit = 9.89E-07 cm-2

CHI SQUARED = 16.95576 WITH 9 DEGREES OF FREEDOM
P(chi squared) = 0.009 %
CORRELATION COEFFICIENT = 0.685
VARIANCE OF SQR(Ns) = 3.133213
VARIANCE OF SQR(Ni) = 2.592333

Ns/Ni = 1.738 ± 0.094
MEAN RATIO = 1.875 ± 0.197

Pooled Age = 133.5 ± 8.4 Ma
Mean Age = 143.9 ± 15.8 Ma
Central Age = 134.7 ± 13.9Ma
% Rel. Error = 26.59
Ages calculated using a zeta of 140.2 ± 3.6 for CN 1 glass
RHO D = 1.107E+06cm-2; ND = 2737

9414-88 Zircon

IRRADIATION WK149-11 COUNTED BY: KAO

No.	Ns	Ni	Na	RATIO	U(ppm)	RHOs	RHOi	F.T.AGE(Ma)
1	58	56	9	1.036	224.7	6.516E+06	6.291E+06	80.8 ± 15.4
2	88	42	6	2.095	252.8	1.483E+07	7.078E+06	162.4 ± 30.9
3	62	35	9	1.771	140.4	6.966E+06	3.932E+06	137.6 ± 29.4
4	60	21	6	2.857	126.4	1.011E+07	3.539E+06	220.5 ± 56.4
5	64	38	6	1.684	228.7	1.079E+07	6.404E+06	130.9 ± 27.1
6	67	20	6	3.350	120.4	1.129E+07	3.370E+06	257.8 ± 66.2
7	30	15	6	2.000	90.3	5.056E+06	2.528E+06	155.1 ± 49.3
8	114	45	9	2.533	180.6	1.281E+07	5.056E+06	195.9 ± 35.0
9	107	33	9	3.242	132.4	1.202E+07	3.707E+06	249.7 ± 50.4
10	36	15	9	2.400	60.2	4.044E+06	1.685E+06	185.7 ± 57.4
	686	320	-		154.1	9.248E+06	4.314E+06	

Area of basic unit = 9.89E-07 cm-2

CHI SQUARED = 13.92932 WITH 9 DEGREES OF FREEDOM
P(chi squared) = 0.101 %
CORRELATION COEFFICIENT = 0.541
VARIANCE OF SQR(Ns) = 2.780653
VARIANCE OF SQR(Ni) = 1.579254

Ns/Ni = 2.144 ± 0.145
MEAN RATIO = 2.297 ± 0.230

Pooled Age = 166.2 ± 12.4 Ma
Mean Age = 177.9 ± 18.7 Ma
Central Age = 165.7 ± 19.2Ma
% Rel. Error = 28.55
Ages calculated using a zeta of 140.2 ± 3.6 for CN 1 glass
RHO D = 1.120E+06cm-2; ND = 2770

9414-89 Zircon

IRRADIATION WK149-12 COUNTED BY: KAO

No.	Ns	Ni	Na	RATIO	U(ppm)	RHOs	RHOi	F.T.AGE(Ma)
1	35	35	4	1.000	312.4	8.847E+06	8.847E+06	78.9 ± 19.0
2	184	53	9	3.472	210.2	2.067E+07	5.954E+06	270.0 ± 43.0
	219	88			241.6	1.703E+07	6.845E+06	

Area of basic unit = 9.89E-07 cm-2

CHI SQUARED = 10.09285 WITH 1 DEGREES OF FREEDOM
P(chi squared) = 0.001 %
CORRELATION COEFFICIENT = 1.000
VARIANCE OF SQR(Ns) = 29.2504
VARIANCE OF SQR(Ni) = .9302826

Ns/Ni = 2.489 ± 0.314
MEAN RATIO = 2.236 ± 1.236

Pooled Age = 194.7 ± 25.3 Ma
Mean Age = 175.2 ± 97.0 Ma
Central Age = 143.3 ± 61.1Ma
% Rel. Error = 57.14
Ages calculated using a zeta of 140.2 ± 3.6 for CN 1 glass
RHO D = 1.133E+06cm-2; ND = 2803

9414-90 ZIRCON MARLBOROUGH

IRRADIATION WK149-13
SLIDE NUMBER 13
COUNTED BY: KAO

No.	Ns	Ni	Na	RATIO	U (ppm)	RHOs (E+06)	RHOi (E+06)	F.T.AGE (Ma)
1	162	60	9	2.700	0.0	18.200	6.741	213.3 ± 32.9
2	90	20	4	4.500	0.0	22.750	5.056	351.7 ± 87.7
3	112	50	6	2.240	0.0	18.874	8.426	177.5 ± 30.7
4	96	46	9	2.087	0.0	10.785	5.168	165.5 ± 30.1
5	115	39	6	2.949	0.0	19.380	6.572	232.6 ± 43.7
	575	215			0.0	17.100	6.394	

AREA OF BASIC UNIT = 9.89E-07 cm
CHI SQUARED = 7.825177 WITH 4 DEGREES OF FREEDOM
P(chi squared) = 9.8 %
CORRELATION COEFFICIENT = 0.767
VARIANCE OF SQR(Ns) = 1.60
VARIANCE OF SQR(Ni) = 1.53

Ns/Ni = 2.674 ± 0.214
MEAN RATIO = 2.895 ± 0.430

Ages calculated using a zeta of 140.2 ± 3.6 for CN1 glass
RHO D = 1.146E+06 ; ND = 2835

POOLED AGE = 211.3 ± 18.2 Ma
MEAN AGE = 228.5 ± 34.7 Ma

9414-91 Zircon

IRRADIATION WK149-14 COUNTED BY: KAO

No.	Ns	Ni	Na	RATIO	U(ppm)	RHOs	RHOi	F.T.AGE(Ma)
1	68	24	4	2.833	209.4	1.719E+07	6.067E+06	226.2 ± 54.2
2	120	40	4	3.000	349.0	3.033E+07	1.011E+07	239.2 ± 44.3
3	62	35	9	1.771	135.7	6.966E+06	3.932E+06	142.3 ± 30.4
4	43	12	9	3.583	46.5	4.831E+06	1.348E+06	284.7 ± 93.4
5	126	40	9	3.150	155.1	1.416E+07	4.494E+06	251.0 ± 46.2
6	35	17	6	2.059	98.9	5.898E+06	2.865E+06	165.1 ± 49.1
7	53	26	6	2.038	151.2	8.932E+06	4.382E+06	163.5 ± 39.5
8	101	55	6	1.836	319.9	1.702E+07	9.269E+06	147.5 ± 25.2
9	131	26	9	5.038	100.8	1.472E+07	2.921E+06	396.9 ± 86.1
10	75	32	9	2.344	124.1	8.426E+06	3.595E+06	187.7 ± 40.1
11	92	53	8	1.736	231.2	1.163E+07	6.699E+06	139.5 ± 24.5
12	65	21	6	3.095	122.1	1.095E+07	3.539E+06	246.7 ± 62.4
13	156	62	9	2.516	240.4	1.753E+07	6.966E+06	201.2 ± 30.9
	1127	443			164.5	1.212E+07	4.765E+06	

Area of basic unit = 9.89E-07 cm-2

CHI SQUARED = 13.97683 WITH 12 DEGREES OF FREEDOM
P(chi squared) = 0.562 %
CORRELATION COEFFICIENT = 0.722
VARIANCE OF SQR(Ns) = 4.125681
VARIANCE OF SQR(Ni) = 1.757957

Ns/Ni = 2.544 ± 0.143
MEAN RATIO = 2.692 ± 0.256

Pooled Age = 203.4 ± 13.1 Ma
Mean Age = 215.1 ± 21.6 Ma
Central Age = 202.0 ± 17.4Ma
% Rel. Error = 21.85
Ages calculated using a zeta of 140.2 ± 3.6 for CN 1 glass
RHO D = 1.159E+06cm-2; ND = 2868

9414-92 ZIRCON MARLBOROUGH

IRRADIATION WK149-15
SLIDE NUMBER 15
COUNTED BY: KAO

No.	Ns	Ni	Na	RATIO	U (ppm)	RHOs (E+06)	RHOi (E+06)	F.T.AGE (Ma)
1	101	37	15	2.730	0.0	6.808	2.494	220.6 ± 43.0
2	135	38	9	3.553	0.0	15.167	4.269	285.7 ± 53.2
3	181	49	9	3.694	0.0	20.335	5.505	296.8 ± 48.7
4	54	18	9	3.000	0.0	6.067	2.022	242.1 ± 66.3
5	269	102	50	2.637	0.0	5.440	2.063	213.3 ± 25.7
6	74	30	9	2.467	0.0	8.314	3.370	199.7 ± 43.7
7	81	43	6	1.884	0.0	13.650	7.246	153.1 ± 29.3
8	58	28	9	2.071	0.0	6.516	3.146	168.1 ± 39.1
9	81	34	20	2.382	0.0	4.095	1.719	193.0 ± 39.9
10	82	38	9	2.158	0.0	9.212	4.269	175.0 ± 34.8
11	46	12	9	3.833	0.0	5.168	1.348	307.7 ± 100.2
12	118	50	6	2.360	0.0	19.885	8.426	191.2 ± 32.8
13	87	38	9	2.289	0.0	9.774	4.269	185.6 ± 36.6
14	122	44	10	2.773	0.0	12.336	4.449	224.1 ± 40.0
15	86	33	9	2.606	0.0	9.662	3.707	210.8 ± 43.7
16	104	53	9	1.962	0.0	11.684	5.954	159.4 ± 27.4
17	96	60	12	1.600	0.0	8.089	5.056	130.2 ± 21.8
18	66	30	12	2.200	0.0	5.561	2.528	178.4 ± 39.7
19	38	19	12	2.000	0.0	3.202	1.601	162.4 ± 45.9
20	87	42	16	2.071	0.0	5.498	2.654	168.1 ± 32.0
	1966	798			0.0	7.983	3.240	

AREA OF BASIC UNIT = 9.89E-07 cm
CHI SQUARED = 27.78143 WITH 19 DEGREES OF FREEDOM
P(chi squared) = 8.8 %
CORRELATION COEFFICIENT = 0.885
VARIANCE OF SQR(Ns) = 5.40
VARIANCE OF SQR(Ni) = 1.97

Ns/Ni = 2.464 ± 0.103
MEAN RATIO = 2.514 ± 0.137

Ages calculated using a zeta of 140.2 ± 3.6 for CN1 glass
RHO D = 1.173E+06 ; ND = 2900

POOLED AGE = 199.5 ± 10.5 Ma
MEAN AGE = 203.4 ± 12.8 Ma

9414-93 Zircon

IRRADIATION WK149-16 COUNTED BY: KAO

No.	Ns	Ni	Na	RATIO	U(ppm)	RHOs	RHOi	F.T.AGE(Ma)
1	131	30	4	4.367	255.8	3.311E+07	7.583E+06	353.2 ± 72.4
2	122	62	9	1.968	234.9	1.371E+07	6.966E+06	161.6 ± 25.7
3	61	27	9	2.259	102.3	6.853E+06	3.033E+06	185.1 ± 43.2
4	159	67	9	2.373	253.9	1.786E+07	7.527E+06	194.3 ± 29.0
5	117	41	9	2.854	155.4	1.314E+07	4.606E+06	233.0 ± 42.9
6	54	28	9	1.929	106.1	6.067E+06	3.146E+06	158.4 ± 37.2
7	73	30	8	2.433	127.9	9.226E+06	3.792E+06	199.2 ± 43.7
8	75	32	4	2.344	272.8	1.896E+07	8.089E+06	192.0 ± 41.0
9	53	21	4	2.524	179.0	1.340E+07	5.308E+06	206.5 ± 53.6
10	146	37	9	3.946	140.2	1.640E+07	4.157E+06	320.0 ± 59.8
11	48	31	4	1.548	264.3	1.213E+07	7.836E+06	127.5 ± 29.6
12	119	29	8	4.103	123.6	1.504E+07	3.665E+06	332.4 ± 69.6
13	113	33	9	3.424	125.0	1.270E+07	3.707E+06	278.6 ± 55.8
14	66	14	6	4.714	79.6	1.112E+07	2.359E+06	380.5 ±112.6
	1337	482			162.7	1.338E+07	4.825E+06	

Area of basic unit = 9.89E-07 cm-2

CHI SQUARED = 16.97413 WITH 13 DEGREES OF FREEDOM
P(chi squared) = 0.123 %
CORRELATION COEFFICIENT = 0.678
VARIANCE OF SQR(Ns) = 3.841496
VARIANCE OF SQR(Ni) = 1.324212

Ns/Ni = 2.774 ± 0.147
MEAN RATIO = 2.913 ± 0.270

Pooled Age = 226.6 ± 14.0 Ma
Mean Age = 237.8 ± 23.3 Ma
Central Age = 223.3 ± 19.2Ma
% Rel. Error = 23.75
Ages calculated using a zeta of 140.2 ± 3.6 for CN 1 glass
RHO D = 1.186E+06cm-2; ND = 2933

9414-94 ZIRCON MARLBOROUGH

IRRADIATION WK149-18
SLIDE NUMBER 18
COUNTED BY: KAO

No.	Ns	Ni	Na	RATIO	U (ppm)	RHOs (E+06)	RHOi (E+06)	F.T.AGE (Ma)
1	73	22	6	3.318	0.0	12.302	3.707	275.9 ± 67.7
2	113	29	9	3.897	0.0	12.695	3.258	322.8 ± 68.0
3	51	9	6	5.667	0.0	8.595	1.517	464.3 ± 168.5
4	64	22	9	2.909	0.0	7.190	2.472	242.5 ± 60.4
5	56	27	9	2.074	0.0	6.291	3.033	173.8 ± 41.1
	357	109			0.0	9.256	2.826	

AREA OF BASIC UNIT = 9.89E-07 cm
CHI SQUARED = 7.157634 WITH 4 DEGREES OF FREEDOM
P(chi squared) = 12.8 %
CORRELATION COEFFICIENT = 0.623
VARIANCE OF SQR(Ns) = 1.89
VARIANCE OF SQR(Ni) = 0.89

Ns/Ni = 3.275 ± 0.358
MEAN RATIO = 3.573 ± 0.602

Ages calculated using a zeta of 140.2 ± 3.6 for CN1 glass
RHO D = 1.212E+06 ; ND = 2999

POOLED AGE = 272.4 ± 31.0 Ma
MEAN AGE = 296.6 ± 50.8 Ma

9414-95 ZIRCON MARLBOROUGH

IRRADIATION WK149-20
SLIDE NUMBER 20
COUNTED BY: KAO

No.	Ns	Ni	Na	RATIO	U (ppm)	RHOs (E+06)	RHOi (E+06)	F.T.AGE (Ma)
1	133	47	9	2.830	0.0	14.942	5.280	241.2 ± 41.6
2	82	43	16	1.907	0.0	5.182	2.717	163.5 ± 31.2
3	32	13	4	2.462	0.0	8.089	3.286	210.3 ± 69.5
	247	103			0.0	8.612	3.591	

AREA OF BASIC UNIT = 9.89E-07 cm
CHI SQUARED = 2.447733 WITH 2 DEGREES OF FREEDOM
P(chi squared) = 29.4 %
CORRELATION COEFFICIENT = 0.912
VARIANCE OF SQR(Ns) = 8.70
VARIANCE OF SQR(Ni) = 3.23

Ns/Ni = 2.398 ± 0.281
MEAN RATIO = 2.399 ± 0.268

Ages calculated using a zeta of 140.2 ± 3.6 for CN1 glass
RHO D = 1.239E+06 ; ND = 3064

POOLED AGE = 205.0 ± 24.9 Ma
MEAN AGE = 205.1 ± 23.8 Ma

9414-96 Zircon

IRRADIATION WK150-1 COUNTED BY: KAO

No.	Ns	Ni	Na	RATIO	U(ppm)	RHOs	RHOi	F.T.AGE(Ma)
1	162	40	9	4.050	161.6	1.820E+07	4.494E+06	308.2 ± 55.3
2	122	40	9	3.050	161.6	1.371E+07	4.494E+06	233.5 ± 43.2
3	71	42	9	1.690	169.7	7.977E+06	4.719E+06	130.4 ± 25.7
4	90	37	9	2.432	149.5	1.011E+07	4.157E+06	186.9 ± 37.0
5	49	18	8	2.722	81.8	6.193E+06	2.275E+06	208.8 ± 57.9
6	50	20	9	2.500	80.8	5.617E+06	2.247E+06	192.0 ± 51.2
7	35	11	9	3.182	44.5	3.932E+06	1.236E+06	243.4 ± 84.5
8	111	37	9	3.000	149.5	1.247E+07	4.157E+06	229.7 ± 44.2
9	122	25	9	4.880	101.0	1.371E+07	2.809E+06	369.6 ± 82.0
10	57	24	9	2.375	97.0	6.404E+06	2.696E+06	182.5 ± 44.8
	869	294			120.1	9.873E+06	3.340E+06	

Area of basic unit = 9.89E-07 cm-2

CHI SQUARED = 9.68623 WITH 9 DEGREES OF FREEDOM
P(chi squared) = 2.2 %
CORRELATION COEFFICIENT = 0.708
VARIANCE OF SQR(Ns) = 4.939847
VARIANCE OF SQR(Ni) = 1.189097

Ns/Ni = 2.956 ± 0.199
MEAN RATIO = 2.988 ± 0.287

Pooled Age = 226.4 ± 16.9 Ma
Mean Age = 228.8 ± 23.2 Ma
Central Age = 220.4 ± 21.6Ma
% Rel. Error = 20.99
Ages calculated using a zeta of 140.2 ± 3.6 for CN 1 glass
RHO D = 1.112E+06cm-2; ND = 2749

9414-97 Zircon

IRRADIATION WK150-2 COUNTED BY: KAO

No.	Ns	Ni	Na	RATIO	U(ppm)	RHOs	RHOi	F.T.AGE(Ma)
1	134	55	12	2.436	164.5	1.129E+07	4.634E+06	189.7 ± 31.0
2	56	17	12	3.294	50.8	4.719E+06	1.432E+06	255.1 ± 71.1
3	137	31	12	4.419	92.7	1.154E+07	2.612E+06	340.0 ± 68.5
4	82	20	12	4.100	59.8	6.909E+06	1.685E+06	316.0 ± 79.5
5	71	25	9	2.840	99.7	7.977E+06	2.809E+06	220.6 ± 51.8
6	84	29	9	2.897	115.6	9.437E+06	3.258E+06	224.9 ± 49.0
7	40	16	4	2.500	143.5	1.011E+07	4.044E+06	194.5 ± 57.9
8	46	16	9	2.875	63.8	5.168E+06	1.798E+06	223.2 ± 65.2
9	138	58	9	2.379	231.3	1.550E+07	6.516E+06	185.3 ± 29.6
10	28	15	9	1.867	59.8	3.146E+06	1.685E+06	145.8 ± 46.9
11	86	42	15	2.048	100.5	5.797E+06	2.831E+06	159.8 ± 30.5
12	128	36	12	3.556	107.7	1.079E+07	3.033E+06	275.0 ± 52.6
13	153	59	9	2.593	235.3	1.719E+07	6.628E+06	201.7 ± 31.6
14	94	32	9	2.938	127.6	1.056E+07	3.595E+06	228.0 ± 47.2
15	102	37	9	2.757	147.5	1.146E+07	4.157E+06	214.2 ± 41.7
16	149	24	9	6.208	95.7	1.674E+07	2.696E+06	472.7 ±105.1
17	109	39	9	2.795	155.5	1.225E+07	4.382E+06	217.1 ± 41.1
18	65	16	6	4.062	95.7	1.095E+07	2.696E+06	313.2 ± 88.0
19	78	38	9	2.053	151.5	8.763E+06	4.269E+06	160.2 ± 32.1
20	179	32	9	5.594	127.6	2.011E+07	3.595E+06	427.4 ± 83.2
	1959	637			118.4	1.026E+07	3.337E+06	

Area of basic unit = 9.89E-07 cm-2

CHI SQUARED = 22.94538 WITH 19 DEGREES OF FREEDOM
P(chi squared) = 0.051 %
CORRELATION COEFFICIENT = 0.668
VARIANCE OF SQR(Ns) = 4.850117
VARIANCE OF SQR(Ni) = 1.49876

Ns/Ni = 3.075 ± 0.140
MEAN RATIO = 3.210 ± 0.258

Pooled Age = 238.5 ± 13.3 Ma
Mean Age = 248.8 ± 21.5 Ma
Central Age = 235.0 ± 16.9Ma
% Rel. Error = 22.73
Ages calculated using a zeta of 140.2 ± 3.6 for CN 1 glass
RHO D = 1.127E+06cm-2; ND = 2787

9414-99 ZIRCON MARLBOROUGH

IRRADIATION WK150-5
SLIDE NUMBER 5
COUNTED BY: KAO

No.	Ns	Ni	Na	RATIO	U (ppm)	RHOs (E+06)	RHOi (E+06)	F.T.AGE (Ma)
1	63	20	4	3.150	0.0	15.925	5.056	249.5 ± 64.5
2	51	21	4	2.429	0.0	12.892	5.308	193.2 ± 50.5
3	48	15	4	3.200	0.0	12.133	3.792	253.4 ± 75.4
	162	56			0.0	13.650	4.719	

AREA OF BASIC UNIT = 9.89E-07 cm
CHI SQUARED = .6830242 WITH 2 DEGREES OF FREEDOM
P(chi squared) = 71.1 %
CORRELATION COEFFICIENT = 0.529
VARIANCE OF SQR(Ns) = 0.28
VARIANCE OF SQR(Ni) = 0.15

Ns/Ni = 2.893 ± 0.448
MEAN RATIO = 2.926 ± 0.249

Ages calculated using a zeta of 140.2 ± 3.6 for CN1 glass
RHO D = 1.152E+06 ; ND = 2848

POOLED AGE = 229.5 ± 36.3 Ma
MEAN AGE = 232.1 ± 21.1 Ma

9414-100 ZIRCON MARLBOROUGH

IRRADIATION WK150-6
SLIDE NUMBER 6
COUNTED BY: KAO

No.	Ns	Ni	Na	RATIO	U (ppm)	RHOs (E+06)	RHOi (E+06)	F.T.AGE (Ma)
1	80	29	16	2.759	0.0	5.056	1.833	220.9 ± 48.4
2	42	13	9	3.231	0.0	4.719	1.461	257.9 ± 82.3
3	161	56	9	2.875	0.0	18.088	6.291	230.0 ± 36.4
4	50	17	9	2.941	0.0	5.617	1.910	235.2 ± 66.5
5	96	47	8	2.043	0.0	12.133	5.940	164.3 ± 29.7
6	79	29	9	2.724	0.0	8.875	3.258	218.2 ± 47.9
7	33	11	15	3.000	0.0	2.224	0.741	239.8 ± 83.9
8	46	20	10	2.300	0.0	4.651	2.022	184.7 ± 49.8
9	55	29	9	1.897	0.0	6.179	3.258	152.7 ± 35.4
10	92	20	9	4.600	0.0	10.336	2.247	364.2 ± 90.6
11	61	24	9	2.542	0.0	6.853	2.696	203.8 ± 49.5
12	62	20	9	3.100	0.0	6.966	2.247	247.7 ± 64.2
13	82	27	9	3.037	0.0	9.212	3.033	242.8 ± 54.4
14	76	24	12	3.167	0.0	6.404	2.022	252.9 ± 59.8
15	101	35	9	2.886	0.0	11.347	3.932	230.9 ± 45.9
16	95	40	16	2.375	0.0	6.004	2.528	190.6 ± 36.4
17	66	18	9	3.667	0.0	7.415	2.022	292.0 ± 78.2
18	54	26	9	2.077	0.0	6.067	2.921	167.0 ± 40.2
19	65	20	9	3.250	0.0	7.303	2.247	259.4 ± 66.8
20	102	36	9	2.833	0.0	11.459	4.044	226.8 ± 44.5
	1498	541			0.0	7.461	2.695	

AREA OF BASIC UNIT = 9.89E-07 cm
CHI SQUARED = 15.42405 WITH 19 DEGREES OF FREEDOM
P(chi squared) = 69.5 %
CORRELATION COEFFICIENT = 0.872
VARIANCE OF SQR(Ns) = 2.53
VARIANCE OF SQR(Ni) = 1.09

Ns/Ni = 2.769 ± 0.139
MEAN RATIO = 2.865 ± 0.136

Ages calculated using a zeta of 140.2 ± 3.6 for CN1 glass
RHO D = 1.162E+06 ; ND = 2873

POOLED AGE = 221.7 ± 13.2 Ma
MEAN AGE = 229.3 ± 13.1 Ma

9414-101 ZIRCON MARLBOROUGH

IRRADIATION WK150-7
SLIDE NUMBER 8
COUNTED BY: KAO

No.	Ns	Ni	Na	RATIO	U (ppm)	RHOs (E+06)	RHOi (E+06)	F.T.AGE (Ma)
1	102	42	20	2.429	0.0	5.157	2.123	196.5 ± 36.6
2	95	32	6	2.969	0.0	16.009	5.393	239.4 ± 49.5
3	56	28	9	2.000	0.0	6.291	3.146	162.3 ± 37.9
4	95	37	9	2.568	0.0	10.673	4.157	207.6 ± 40.8
5	60	31	9	1.935	0.0	6.741	3.483	157.1 ± 35.1
6	100	53	9	1.887	0.0	11.235	5.954	153.2 ± 26.5
7	123	56	9	2.196	0.0	13.819	6.291	178.0 ± 29.2
8	83	59	9	1.407	0.0	9.325	6.628	114.6 ± 19.8
9	64	25	30	2.560	0.0	2.157	0.843	207.0 ± 49.3
10	364	173	50	2.104	0.0	7.361	3.498	170.6 ± 16.7
11	158	62	18	2.548	0.0	8.875	3.483	206.0 ± 31.6
12	32	19	9	1.684	0.0	3.595	2.135	136.9 ± 39.9
13	102	48	9	2.125	0.0	11.459	5.393	172.3 ± 30.6
14	84	44	9	1.909	0.0	9.437	4.943	155.0 ± 29.3
15	62	48	10	1.292	0.0	6.269	4.853	105.3 ± 20.5
	1580	757			0.0	7.431	3.560	

AREA OF BASIC UNIT = 9.89E-07 cm
CHI SQUARED = 20.55648 WITH 14 DEGREES OF FREEDOM
P(chi squared) = 11.4 %
CORRELATION COEFFICIENT = 0.966
VARIANCE OF SQR(Ns) = 9.30
VARIANCE OF SQR(Ni) = 4.14

Ns/Ni = 2.087 ± 0.092
MEAN RATIO = 2.108 ± 0.118

Ages calculated using a zeta of 140.2 ± 3.6 for CN1 glass
RHO D = 1.172E+06 ; ND = 2897

POOLED AGE = 169.2 ± 9.2 Ma
MEAN AGE = 170.9 ± 11.0 Ma

9414-102 ZIRCON MARLBOROUGH

IRRADIATION WK150-8
SLIDE NUMBER 8
COUNTED BY: KAO

No.	Ns	Ni	Na	RATIO	U (ppm)	RHOs (E+06)	RHOI (E+06)	F.T.AGE (Ma)
1	70	26	9	2.692	0.0	7.864	2.921	219.3 ± 50.8
2	106	47	9	2.255	0.0	11.909	5.280	184.2 ± 32.8
3	30	14	4	2.143	0.0	7.583	3.539	175.2 ± 57.0
4	91	39	9	2.333	0.0	10.224	4.382	190.5 ± 37.0
5	69	31	6	2.226	0.0	11.628	5.224	181.8 ± 39.7
6	43	20	6	2.150	0.0	7.246	3.370	175.7 ± 47.9
7	55	21	10	2.619	0.0	5.561	2.123	213.4 ± 55.2
8	123	49	9	2.510	0.0	13.819	5.505	204.7 ± 35.2
9	51	19	4	2.684	0.0	12.892	4.803	218.7 ± 59.2
10	54	18	6	3.000	0.0	9.100	3.033	243.9 ± 66.8
	692	284			0.0	9.718	3.988	

AREA OF BASIC UNIT = 9.89E-07 cm
CHI SQUARED = 1.808228 WITH 9 DEGREES OF FREEDOM
P(chi squared) = 99.4 %
CORRELATION COEFFICIENT = 0.978
VARIANCE OF SQR(Ns) = 3.01
VARIANCE OF SQR(Ni) = 1.32

Ns/Ni = 2.437 ± 0.172
MEAN RATIO = 2.461 ± 0.090

Ages calculated using a zeta of 140.2 ± 3.6 for CN1 glass
RHO D = 1.182E+06 ; ND = 2922

POOLED AGE = 198.8 ± 15.4 Ma
MEAN AGE = 200.8 ± 9.7 Ma

9414-103 ZIRCON MARLBOROUGH

IRRADIATION WK150-9
SLIDE NUMBER 9
COUNTED BY: KAO

No.	Ns	Ni	Na	RATIO	U (ppm)	RHOs (E+06)	RHOi (E+06)	F.T.AGE (Ma)
1	75	30	12	2.500	0.0	6.320	2.528	205.6 ± 44.9
2	125	42	9	2.976	0.0	14.043	4.719	244.0 ± 44.2
3	190	53	40	3.585	0.0	4.803	1.340	292.8 ± 46.4
4	118	63	12	1.873	0.0	9.943	5.308	154.6 ± 24.6
5	91	31	9	2.935	0.0	10.224	3.483	240.7 ± 50.6
6	53	18	9	2.944	0.0	5.954	2.022	241.5 ± 66.3
7	61	18	6	3.389	0.0	10.280	3.033	277.1 ± 74.8
8	36	10	4	3.600	0.0	9.100	2.528	294.0 ± 105.5
9	64	25	9	2.560	0.0	7.190	2.809	210.4 ± 50.1
10	208	58	9	3.586	0.0	23.368	6.516	292.9 ± 44.5
11	61	25	6	2.440	0.0	10.280	4.213	200.7 ± 48.1
12	32	16	6	2.000	0.0	5.393	2.696	165.0 ± 50.8
	1114	389			0.0	8.598	3.002	

AREA OF BASIC UNIT = 9.89E-07 cm
CHI SQUARED = 15.26514 WITH 11 DEGREES OF FREEDOM
P(chi squared) = 17.1 %
CORRELATION COEFFICIENT = 0.886
VARIANCE OF SQR(Ns) = 7.92
VARIANCE OF SQR(Ni) = 2.36

Ns/Ni = 2.864 ± 0.169
MEAN RATIO = 2.866 ± 0.174

Ages calculated using a zeta of 140.2 ± 3.6 for CN1 glass
RHO D = 1.192E+06 ; ND = 2947

POOLED AGE = 235.0 ± 15.7 Ma
MEAN AGE = 235.1 ± 16.1 Ma

9414-104 ZIRCON Marlborough

IRRADIATION wk150-10
SLIDE NUMBER 10
COUNTED BY: Kao

No.	Ns	Ni	Na	RATIO	U (ppm)	RHOs (E+06)	RHOi (E+06)	F.T.AGE (Ma)
1	85	64	6	1.328	0.0	14.324	10.785	110.9 ± 18.7
2	173	127	20	1.362	0.0	8.746	6.421	113.8 ± 13.8
3	71	26	9	2.731	0.0	7.977	2.921	226.1 ± 52.3
4	109	74	9	1.473	0.0	12.246	8.314	122.9 ± 18.9
5	80	64	9	1.250	0.0	8.988	7.190	104.5 ± 17.8
6	92	75	9	1.227	0.0	10.336	8.426	102.5 ± 16.3
7	30	22	4	1.364	0.0	7.583	5.561	113.9 ± 32.2
8	41	28	4	1.464	0.0	10.364	7.078	122.2 ± 30.2
9	130	89	12	1.461	0.0	10.954	7.499	121.9 ± 17.2
	811	569			0.0	10.000	7.016	

AREA OF BASIC UNIT = 9.89E-07 cm
CHI SQUARED = 10.32741 WITH 8 DEGREES OF FREEDOM
P(chi squared) = 24.3 %
CORRELATION COEFFICIENT = 0.958
VARIANCE OF SQR(Ns) = 5.56
VARIANCE OF SQR(Ni) = 4.91

Ns/Ni = 1.425 ± 0.078
MEAN RATIO = 1.518 ± 0.155

Ages calculated using a zeta of 140.2 ± 3.6 for CN1 glass
RHO D = 1.202E+06 ; ND = 2971

POOLED AGE = 119.0 ± 7.5 Ma
MEAN AGE = 126.6 ± 13.5 Ma

9414-105 ZIRCON MARLBOROUGH

IRRADIATION WK150-11
SLIDE NUMBER 11
COUNTED BY: KAO

No.	Ns	Ni	Na	RATIO	U (ppm)	RHOs (E+06)	RHOi (E+06)	F.T.AGE (Ma)
1	41	24	4	1.708	0.0	10.364	6.067	143.5 ± 37.2
2	11	5	1	2.200	0.0	11.122	5.056	184.3 ± 99.5
	52	29			0.0	10.516	5.865	

AREA OF BASIC UNIT = 9.89E-07 cm
CHI SQUARED = .1797854 WITH 1 DEGREES OF FREEDOM
P(chi squared) = 67.2 %
CORRELATION COEFFICIENT = 1.000
VARIANCE OF SQR(Ns) = 4.76
VARIANCE OF SQR(Ni) = 3.55

Ns/Ni = 1.793 ± 0.416
MEAN RATIO = 1.954 ± 0.246

Ages calculated using a zeta of 140.2 ± 3.6 for CN1 glass
RHO D = 1.212E+06 ; ND = 2996

POOLED AGE = 150.6 ± 35.2 Ma
MEAN AGE = 163.9 ± 21.3 Ma

9414-107 Zircon

IRRADIATION WK150-12 COUNTED BY: KAO

No.	Ns	Ni	Na	RATIO	U(ppm)	RHOs	RHOi	F.T.AGE(Ma)
1	53	18	6	2.944	99.3	8.932E+06	3.033E+06	247.4 ± 67.9
2	63	27	9	2.333	99.3	7.078E+06	3.033E+06	196.8 ± 45.7
3	64	38	12	1.684	104.8	5.393E+06	3.202E+06	142.7 ± 29.6
4	95	51	9	1.863	187.6	1.067E+07	5.730E+06	157.6 ± 27.8
5	109	47	9	2.319	172.8	1.225E+07	5.280E+06	195.7 ± 34.7
6	202	32	9	6.312	117.7	2.269E+07	3.595E+06	519.3 ±100.1
7	108	47	9	2.298	172.8	1.213E+07	5.280E+06	193.9 ± 34.4
8	44	32	9	1.375	117.7	4.943E+06	3.595E+06	116.7 ± 27.4
9	51	19	9	2.684	69.9	5.730E+06	2.135E+06	225.9 ± 61.1
10	73	20	9	3.650	73.5	8.201E+06	2.247E+06	305.3 ± 77.7
11	88	24	9	3.667	88.3	9.887E+06	2.696E+06	306.7 ± 71.3
	950	355			118.7	9.703E+06	3.626E+06	

Area of basic unit = 9.89E-07 cm-2

CHI SQUARED = 22.53984 WITH 10 DEGREES OF FREEDOM
P(chi squared) = 0.000 %
CORRELATION COEFFICIENT = 0.352
VARIANCE OF SQR(Ns) = 4.61933
VARIANCE OF SQR(Ni) = 1.116284

Ns/Ni = 2.676 ± 0.166
MEAN RATIO = 2.830 ± 0.412

Pooled Age = 225.3 ± 15.7 Ma
Mean Age = 238.0 ± 35.5 Ma
Central Age = 213.7 ± 25.5Ma
% Rel. Error = 32.90
Ages calculated using a zeta of 140.2 ± 3.6 for CN 1 glass
RHO D = 1.222E+06cm-2; ND = 3021

9414-108 ZIRCON MARLBOROUGH

IRRADIATION WK150-13
SLIDE NUMBER 13
COUNTED BY: KAO

No.	Ns	Ni	Na	RATIO	U (ppm)	RHOs (E+06)	RHOi (E+06)	F.T.AGE (Ma)
1	123	79	9	1.557	0.0	13.819	8.875	133.1 ± 19.6
2	87	66	9	1.318	0.0	9.774	7.415	112.8 ± 18.8
3	124	58	9	2.138	0.0	13.931	6.516	182.0 ± 29.5
4	104	64	8	1.625	0.0	13.145	8.089	138.8 ± 22.5
5	30	21	6	1.429	0.0	5.056	3.539	122.2 ± 35.0
6	92	46	6	2.000	0.0	15.504	7.752	170.5 ± 31.2
7	41	32	9	1.281	0.0	4.606	3.595	109.7 ± 26.1
	601	366			0.0	10.852	6.608	

AREA OF BASIC UNIT = 9.89E-07 cm
CHI SQUARED = 7.27561 WITH 6 DEGREES OF FREEDOM
P(chi squared) = 29.6 %
CORRELATION COEFFICIENT = 0.889
VARIANCE OF SQR(Ns) = 4.99
VARIANCE OF SQR(Ni) = 2.31

Ns/Ni = 1.642 ± 0.109
MEAN RATIO = 1.621 ± 0.125

Ages calculated using a zeta of 140.2 ± 3.6 for CN1 glass
RHO D = 1.232E+06 ; ND = 3045

POOLED AGE = 140.3 ± 10.3 Ma
MEAN AGE = 138.5 ± 11.6 Ma

9414-109 ZIRCON MARLBOROUGH

IRRADIATION WK150-14
SLIDE NUMBER 14
COUNTED BY: KAO

No.	Ns	Ni	Na	RATIO	U (ppm)	RHOs (E+06)	RHOi (E+06)	F.T.AGE (Ma)
1	125	81	9	1.543	0.0	14.043	9.100	133.0 ± 19.4
2	83	37	9	2.243	0.0	9.325	4.157	192.4 ± 38.5
3	54	28	9	1.929	0.0	6.067	3.146	165.8 ± 39.0
4	131	46	9	2.848	0.0	14.717	5.168	243.3 ± 42.4
5	38	28	6	1.357	0.0	6.404	4.719	117.1 ± 29.4
6	67	28	12	2.393	0.0	5.645	2.359	205.0 ± 46.6
7	106	52	9	2.038	0.0	11.909	5.842	175.1 ± 30.1
8	38	23	8	1.652	0.0	4.803	2.907	142.3 ± 37.8
9	54	23	6	2.348	0.0	9.100	3.876	201.2 ± 50.5
10	58	20	9	2.900	0.0	6.516	2.247	247.7 ± 64.7
	754	366			0.0	8.865	4.303	

AREA OF BASIC UNIT = 9.89E-07 cm
CHI SQUARED = 14.02686 WITH 9 DEGREES OF FREEDOM
P(chi squared) = 12.1 %
CORRELATION COEFFICIENT = 0.839
VARIANCE OF SQR(Ns) = 3.77
VARIANCE OF SQR(Ni) = 1.97

Ns/Ni = 2.060 ± 0.131
MEAN RATIO = 2.125 ± 0.165

Ages calculated using a zeta of 140.2 ± 3.6 for CN1 glass
RHO D = 1.242E+06 ; ND = 3070

POOLED AGE = 176.9 ± 12.6 Ma
MEAN AGE = 182.4 ± 15.3 Ma

9414-110 Zircon

IRRADIATION WK150-15 COUNTED BY: KAO

No.	Ns	Ni	Na	RATIO	U(ppm)	RHOs	RHOi	F.T.AGE(Ma)
1	118	62	9	1.903	222.5	1.326E+07	6.966E+06	164.9 ± 26.4
2	143	59	9	2.424	211.8	1.607E+07	6.628E+06	209.3 ± 33.0
3	121	16	9	7.562	57.4	1.359E+07	1.798E+06	631.7 ±169.2
4	107	36	5	2.972	232.6	2.164E+07	7.280E+06	255.7 ± 49.9
5	143	86	12	1.663	231.5	1.205E+07	7.246E+06	144.3 ± 20.2
6	106	36	9	2.944	129.2	1.191E+07	4.044E+06	253.4 ± 49.5
7	198	98	18	2.020	175.9	1.112E+07	5.505E+06	174.9 ± 22.3
8	107	45	9	2.378	161.5	1.202E+07	5.056E+06	205.4 ± 37.1
9	79	32	10	2.469	103.4	7.988E+06	3.236E+06	213.1 ± 45.2
10	126	70	16	1.800	141.3	7.963E+06	4.424E+06	156.1 ± 23.8
11	74	34	8	2.176	137.3	9.353E+06	4.297E+06	188.2 ± 39.4
12	107	63	9	1.698	226.1	1.202E+07	7.078E+06	147.4 ± 23.9
13	83	30	9	2.767	107.7	9.325E+06	3.370E+06	238.4 ± 51.3
14	112	71	16	1.577	143.4	7.078E+06	4.487E+06	137.0 ± 21.2
15	67	43	9	1.558	154.3	7.527E+06	4.831E+06	135.3 ± 26.8
16	116	65	16	1.785	131.2	7.331E+06	4.108E+06	154.8 ± 24.5
17	39	19	9	2.053	68.2	4.382E+06	2.135E+06	177.7 ± 50.0
18	100	42	9	2.381	150.8	1.123E+07	4.719E+06	205.6 ± 38.4
19	104	48	9	2.167	172.3	1.168E+07	5.393E+06	187.4 ± 33.2
20	120	48	9	2.500	172.3	1.348E+07	5.393E+06	215.8 ± 37.5
	2170	1003			155.0	1.050E+07	4.852E+06	

Area of basic unit = 9.89E-07 cm-2

CHI SQUARED = 25.71062 WITH 19 DEGREES OF FREEDOM
P(chi squared) = 0.008 %
CORRELATION COEFFICIENT = 0.764
VARIANCE OF SQR(Ns) = 2.601344
VARIANCE OF SQR(Ni) = 2.348305

Ns/Ni = 2.164 ± 0.083
MEAN RATIO = 2.440 ± 0.286

Pooled Age = 187.1 ± 9.2 Ma
Mean Age = 210.7 ± 25.6 Ma
Central Age = 190.2 ± 12.5Ma
% Rel. Error = 22.17
Ages calculated using a zeta of 140.2 ± 3.6 for CN 1 glass
RHO D = 1.252E+06cm-2; ND = 3095

9414-111 ZIRCON MARLBOROUGH

IRRADIATION WK150-16
SLIDE NUMBER 16
COUNTED BY: KAO

No.	Ns	Ni	Na	RATIO	U (ppm)	RHOs (E+06)	RHOI (E+06)	F.T.AGE (Ma)
1	165	75	60	2.200	0.0	2.781	1.264	191.7 ± 27.4
2	86	45	8	1.911	0.0	10.870	5.688	166.9 ± 31.1
3	109	50	12	2.180	0.0	9.184	4.213	190.0 ± 33.0
4	43	25	6	1.720	0.0	7.246	4.213	150.4 ± 38.1
5	129	56	9	2.304	0.0	14.493	6.291	200.6 ± 32.7
6	45	25	4	1.800	0.0	11.375	6.320	157.3 ± 39.5
7	130	46	24	2.826	0.0	5.477	1.938	245.3 ± 42.8
8	74	49	9	1.510	0.0	8.314	5.505	132.2 ± 24.7
9	78	34	6	2.294	0.0	13.145	5.730	199.8 ± 41.5
10	52	36	9	1.444	0.0	5.842	4.044	126.5 ± 27.7
11	123	63	9	1.952	0.0	13.819	7.078	170.4 ± 26.9
12	80	50	10	1.600	0.0	8.089	5.056	140.0 ± 25.6
13	86	49	16	1.755	0.0	5.435	3.097	153.4 ± 27.9
14	76	26	8	2.923	0.0	9.606	3.286	253.5 ± 58.1
15	51	36	9	1.417	0.0	5.730	4.044	124.1 ± 27.3
16	44	18	6	2.444	0.0	7.415	3.033	212.7 ± 59.9
17	54	31	6	1.742	0.0	9.100	5.224	152.3 ± 34.6
18	80	48	9	1.667	0.0	8.988	5.393	145.8 ± 27.0
19	51	24	6	2.125	0.0	8.595	4.044	185.3 ± 46.2
20	57	20	4	2.850	0.0	14.408	5.056	247.3 ± 64.7
	1613	806			0.0	7.091	3.543	

AREA OF BASIC UNIT = 9.89E-07 cm
CHI SQUARED = 22.55505 WITH 19 DEGREES OF FREEDOM
P(chi squared) = 25.8 %
CORRELATION COEFFICIENT = 0.870
VARIANCE OF SQR(Ns) = 3.37
VARIANCE OF SQR(NI) = 1.46

Ns/Ni = 2.001 ± 0.086
MEAN RATIO = 2.033 ± 0.104

Ages calculated using a zeta of 140.2 ± 3.6 for CN1 glass
RHO D = 1.262E+06 ; ND = 3120

POOLED AGE = 174.7 ± 9.3 Ma
MEAN AGE = 177.4 ± 10.6 Ma

9414-112 ZIRCON MARLBOROUGH

IRRADIATION WK150-17
SLIDE NUMBER 17
COUNTED BY: KAO

No.	Ns	Ni	Na	RATIO	U (ppm)	RHOs (E+06)	RHOi (E+06)	F.T.AGE (Ma)
1	53	33	6	1.606	0.0	8.932	5.561	141.6 ± 31.7
2	104	34	9	3.059	0.0	11.684	3.820	267.1 ± 53.4
3	44	27	9	1.630	0.0	4.943	3.033	143.7 ± 35.4
4	62	43	9	1.442	0.0	6.966	4.831	127.3 ± 25.6
5	85	43	9	1.977	0.0	9.549	4.831	173.9 ± 33.0
6	67	28	9	2.393	0.0	7.527	3.146	209.9 ± 47.7
7	32	11	4	2.909	0.0	8.089	2.781	254.3 ± 89.2
8	43	22	4	1.955	0.0	10.870	5.561	172.0 ± 45.4
9	32	15	4	2.133	0.0	8.089	3.792	187.5 ± 59.0
10	30	14	9-	2.143	0.0	3.370	1.573	188.3 ± 61.2
	552	270			0.0	7.752	3.792	

AREA OF BASIC UNIT = 9.89E-07 cm
CHI SQUARED = 11.01854 WITH 9 DEGREES OF FREEDOM
P(chi squared) = 27.4 %
CORRELATION COEFFICIENT = 0.771
VARIANCE OF SQR(Ns) = 2.55
VARIANCE OF SQR(Ni) = 1.33

Ns/Ni = 2.044 ± 0.152
MEAN RATIO = 2.125 ± 0.170

Ages calculated using a zeta of 140.2 ± 3.6 for CN1 glass
RHO D = 1.272E+06 ; ND = 3144

POOLED AGE = 179.8 ± 14.5 Ma
MEAN AGE = 186.7 ± 16.0 Ma